frontiers | Research Topics

Adaptive immune resistance in cancer therapy

Edited by
Lin Qi, Zhigang Liu, Ouyang Chen and Hongzhou Cai

Published in
Frontiers in Pharmacology
Frontiers in Oncology

ISSN 1664-8714
ISBN 978-2-8325-4489-1
DOI 10.3389/978-2-8325-4489-1

About Frontiers

Frontiers is more than just an open access publisher of scholarly articles: it is a pioneering approach to the world of academia, radically improving the way scholarly research is managed. The grand vision of Frontiers is a world where all people have an equal opportunity to seek, share and generate knowledge. Frontiers provides immediate and permanent online open access to all its publications, but this alone is not enough to realize our grand goals.

Frontiers journal series

The Frontiers journal series is a multi-tier and interdisciplinary set of open-access, online journals, promising a paradigm shift from the current review, selection and dissemination processes in academic publishing. All Frontiers journals are driven by researchers for researchers; therefore, they constitute a service to the scholarly community. At the same time, the *Frontiers journal series* operates on a revolutionary invention, the tiered publishing system, initially addressing specific communities of scholars, and gradually climbing up to broader public understanding, thus serving the interests of the lay society, too.

Dedication to quality

Each Frontiers article is a landmark of the highest quality, thanks to genuinely collaborative interactions between authors and review editors, who include some of the world's best academicians. Research must be certified by peers before entering a stream of knowledge that may eventually reach the public - and shape society; therefore, Frontiers only applies the most rigorous and unbiased reviews. Frontiers revolutionizes research publishing by freely delivering the most outstanding research, evaluated with no bias from both the academic and social point of view. By applying the most advanced information technologies, Frontiers is catapulting scholarly publishing into a new generation.

What are Frontiers Research Topics?

Frontiers Research Topics are very popular trademarks of the *Frontiers journals series*: they are collections of at least ten articles, all centered on a particular subject. With their unique mix of varied contributions from Original Research to Review Articles, Frontiers Research Topics unify the most influential researchers, the latest key findings and historical advances in a hot research area.

Find out more on how to host your own Frontiers Research Topic or contribute to one as an author by contacting the Frontiers editorial office: frontiersin.org/about/contact

Adaptive immune resistance in cancer therapy

Topic editors

Lin Qi – Central South University, China

Zhigang Liu – The Fifth Affiliated Hospital of Sun Yat-sen University, China

Ouyang Chen – Duke University, United States

Hongzhou Cai – Nanjing Medical University, China

Citation

Qi, L., Liu, Z., Chen, O., Cai, H., eds. (2024). *Adaptive immune resistance in cancer therapy*. Lausanne: Frontiers Media SA. doi: 10.3389/978-2-8325-4489-1

Table of contents

frontiers | Frontiers in Pharmacology

TYPE Editorial
PUBLISHED 25 August 2023
DOI 10.3389/fphar.2023.1277902

OPEN ACCESS

EDITED AND REVIEWED BY
Olivier Feron,
Université catholique de Louvain,
Belgium

*CORRESPONDENCE
Linhui Wang,
wanglinhui@smmu.edu.cn
Lin Qi,
qi.lin@csu.edu.cn

RECEIVED 15 August 2023
ACCEPTED 21 August 2023
PUBLISHED 25 August 2023

CITATION
Jiang A, Chen O, Liu Z, Cai H, Wang L and Qi L (2023), Editorial: Adaptive immune resistance in cancer therapy.
Front. Pharmacol. 14:1277902.
doi: 10.3389/fphar.2023.1277902

Editorial: Adaptive immune resistance in cancer therapy

Aimin Jiang[1], Ouyang Chen[2], Zhigang Liu[3], Hongzhou Cai[4], Linhui Wang[1]* and Lin Qi[5,6]*

[1]Department of Urology, Changhai Hospital, Naval Medical University, Shanghai, China, [2]Department of Cell Biology, Duke University Medical Center, Durham, NC, United States, [3]Dongguan Key Laboratory of Precision Diagnosis and Treatment for Tumors, Dongguan, Guangdong, China, [4]Department of Urology, Jiangsu Cancer Hospital and The Affiliated Cancer Hospital of Nanjing Medical University and Jiangsu Institute of Cancer Research, Nanjing, Jiangsu, China, [5]Department of Orthopedics, The Second Xiangya Hospital, Central South University, Changsha, Hunan, China, [6]Hunan Key Laboratory of Tumor Models and Individualized Medicine, The Second Xiangya Hospital, Changsha, Hunan, China

KEYWORDS

adaptive immune resistance, tumour microenvironment (TME), immunotherapy, biomarker, prognosis

Editorial on the Research Topic
Adaptive immune resistance in cancer therapy

Tumours employ various strategies to adapt and ultimately evade the immune system's attack, collectively known as the adaptive immune resistance (AIR) (Morad et al., 2021). The initial AIR mechanism to be defined and validated therapeutically is the targeted induction of programmed cell death 1 ligand 1 (PDL1) by interferon-γ within the tumour. The use of antibodies to block the binding of PDL1 to its receptor, PD1 (referred to as anti-PD therapy), has led to remission in a notable subset of patients with advanced-stage cancer, particularly in solid tumours (Vasan et al., 2019; Sharma et al., 2021). However, several clinical trials investigating the combination of anti-PD therapy with other anti-tumour drugs, without a strong mechanistic rationale, have failed to identify a synergistic or additive effect (Hegde and Chen, 2020). Given the aforementioned concerns, it is imperative to identify specific AIR mechanisms that hold significant importance in the development of novel drugs and the enhancement of cancer treatment efficacy.

To address this pressing issue, a comprehensive analysis of AIR is conducted through an examination of 3 literature reviews and 11 original research papers authored by a total of 92 individuals. These collective studies bring forth valuable insights into the mechanisms and interconnectedness between AIR and the tumour microenvironment (TME).

Inhibitors targeting PD-1 and PD-L1 have become extensively utilized in the treatment of various types of cancer. To gain a comprehensive understanding of the current research landscape and pinpoint promising areas of investigation in the realm of PD-1/PD-L1 inhibitors, Lai et al. conducted an in-depth analysis utilizing bibliometric and visualized techniques. Their findings revealed that the United States is leading the country in this field, contributing a significant 42.03% of the total publications. Notably, the journal "Value in Health" emerged as the most productive journal in terms of publications. Moreover, the journal "New England Journal of Medicine" played a prominent role in the research network. The study also sheds light on active collaborations between countries and research institutes, highlighting the collaborative nature of this field. Bristol Myers Squibb was identified as the top productive institute, reinforcing the leading role of the United States in this area. Additionally, Wan XM was

recognized as the most productive author. Analysing the global trend in this research area, the study identified the cost-effectiveness of PD-1/PD-L1 inhibitors and the comparative analysis of their economic impact in relation to other drugs as the prevailing hot topics. Thus, it is advisable for pharmaceutical companies involved in the development of novel PD-1/PD-L1 inhibitors to explore overseas markets to capitalize on this growing field. Finally, the study noted that developing countries engaged in health economics research on PD-1/PD-L1 inhibitors should prioritize the expansion of medical insurance coverage and expedite the marketing process of new drugs. These measures are essential in ensuring access to novel treatments and promoting advancements in healthcare systems.

Platelets, an essential component of blood responsible for clotting and stopping bleeding, have been found to display an important role in the invasion and spread of tumours. In a study conducted by Deng et al., the researchers conducted a comprehensive analysis of platelets in bladder cancer using data from multiple real-world cohorts. Their findings revealed two distinct patterns of platelet expression, named as Cluster 1 and Cluster 2, respectively. The first pattern, Cluster 1, was characterized with an inferior clinical outcome and showed a significant presence of cytokines, chemokines, and T-cell-related pathways. This suggests that Cluster 1 may represent a specific subgroup of bladder cancer with an immune-activated phenotype, making it potentially responsive to immune checkpoint inhibitor (ICI) therapy. To further support their findings, the researchers developed a robust risk score system known as the platelet risk score (PRS). This system consisted of 13 platelet-related genes and was validated using data from the GSE32894 and Xiangya cohorts. The PRS demonstrated satisfactory performance in predicting both prognosis and therapy response. Patients with bladder cancer divided into the high-risk group based on their PRS had a poorer prognosis but were found to be more sensitive to immunotherapy. This implies that patients in the high-risk group may benefit from targeted immunotherapy approaches. In conclusion, this study highlighted the significant impact of platelets on cancer progression and metastasis in bladder cancer. The identification of distinct platelet expression patterns and the development of the PRS provide valuable insights for predicting prognosis and guiding therapy decisions, particularly regarding the use of immune checkpoint inhibitors. Liposomal coenzyme A synthetase is an essential enzyme responsible for activating fatty acids and initiating the initial step of fatty acid metabolism. This metabolic process is categorized into four distinct groups, with medium-chain acyl-CoA synthetase (ACSM) being one of them. Interestingly, a study conducted by Li et al. indicated that ACSM6 might serve as a promising target for immunotherapy in bladder cancer. To gain deeper insights, they investigated the relationship between ACSM6 and the TME in BLCA. Astonishingly, their findings shed light on the role of ACSM6 in shaping the noninflammatory TME in BLCA while also providing the ability to predict the molecular subtypes of BLCA. Moreover, patients displaying low ACSM6 expression also showed a higher likelihood of responding positively to multiple therapies, including adjuvant therapy, neoadjuvant chemotherapy, and ERBB treatment.

Emerging evidence suggests a strong link between cell death and the development of tumors, as well as the response to ICI in various types of cancers. A recent study conducted by Li et al. aimed to construct a prognostic model for bladder cancer patients by examining genes related to both cuproptosis and ferroptosis (CFRGs). Utilizing a total of 5 CFRGs, the researchers constructed proportional hazards regression models. Remarkably, the high-risk groups identified in both the training and validation sets exhibited significantly poorer survival rates. Furthermore, the risk score was found to have a positive correlation with the tumor mutational burden (TMB), indicating its potential as a predictive marker. Conversely, the risk score showed an inverse relationship with tumor immune dysfunction and exclusion values, as well as tumor purity. Notably, the infiltration levels of antitumour immune cells and the expression of immune checkpoints were noticeably lower in the high-risk group. Additionally, the study observed a correlation between the risk scores and various pathway signals, including ErbB, MAPK, PI3K/AKT, mTOR, Hif-1 and TGF-β, suggesting their involvement in disease progression.

Immunogenic cell death (ICD) is an emerging mechanism of cellular death that triggers immune system activation and regulation against cancer. This unique process involves the release of various substances and antigens from deceased cells, which engage with antigen-presenting cells and other immune cells. In a study conducted by Su et al. applied several analytical techniques, to evaluate the prognostic significance of genes associated with ICD in patients with liver cancer. Through rigorous investigation, the researchers identified three genes, including PRNP, DNM1L and CASP8, as crucial prognostic markers for ICD. Subsequently, these genes were employed to construct a risk system that could categorize patients with liver cancer into high- and low-risk subgroups based on their ICD-related profile. To facilitate clinical application, a prognostic nomogram encompassing both the patients' clinical characteristics and risk scores was devised, offering a comprehensive tool for personalized prognostication. In conclusion, this ground-breaking study highlights the importance of ICD-related genes and their potential for guiding patient management in liver cancer. The identified risk signature not only holds promise as a prognostic marker but also serves as a valuable resource for developing immunotherapeutic interventions targeting ICD in liver cancer patients.

In recent years, non-small cell lung cancer (NSCLC) has seen significant progress in immune and targeted therapies. However, the development of precision therapy has been hindered by the prevalence of cisplatin and ICI resistance in clinical settings. To address this issue, Li et al. conducted an in-depth analysis of public databases (GSE21656 and GSE108214) and identified protocadherin 7 (PCDH7) as a potential player in cisplatin resistance in lung cancer. They then conducted a series of *in vitro* experiments, confirming the oncogenic role of PCDH7 in NSCLC. Furthermore, the results of IC50 detection indicated a potential association between PCDH7 and cisplatin resistance in NSCLC. Interestingly, patients with high PCDH7 expression may exhibit increased sensitivity to bortezomib, docetaxel, and gemcitabine while showing resistance to immunotherapy. Finally, based on three genes correlated with PCDH7, the researchers developed a prognosis model that demonstrated a strong predictive ability for NSCLC patient survival. In conclusion, this study sheds light on the role of PCDH7 in cisplatin resistance in NSCLC and provides valuable insights into potential treatment strategies for patients with high PCDH7 expression. The findings also underscore the

importance of personalized medicine in managing NSCLC and offer a promising prognostic model for predicting patient survival.

There has been a significant shift in the treatment strategy for NSCLC with the emergence of molecularly targeted therapies that focus on specific gene abnormalities. These targeted drugs have revolutionized the field; however, a major challenge remains in the form of tumor resistance to these therapies. To address this issue, Zhou et al. employed ESTIMATE algorithm to investigate the immune score. By analysing the immune score, the researchers were able to divide the patients into two distinct groups based on an optimal threshold. This division allowed them to identify differential genes that were associated with prognosis. Through a rigorous series of statistical analyses, they established a gene signature that could predict patient outcomes. To validate the accuracy of their findings, they conducted external validation using datasets GSE37745 and GSE31210, which further supported the prognostic model. These analyses revealed that pathways such as epithelial mesenchymal transition and immune-associated pathways were predominantly implicated in this group. Additionally, the researchers conducted somatic mutation and immune analyses to compare the differences between the two patient groups. This comparison provided valuable insights into potential drug sensitivity, which could serve as a basis for clinical treatment decisions. Further investigation led to the identification of two key prognostic genes: EREG and ADH1C. In summary, this research has shed light on the importance of the immune score in predicting survival outcomes for NSCLC patients. By identifying differentially expressed genes and understanding their involvement in key pathways, this study has provided valuable insights into potential treatments and prognostic markers for this challenging disease. With the continuous advancements in technology used for the detection of circulating tumor DNA (ctDNA), the importance of liquid biopsy as a valuable tool for prognostication and evaluating treatment response in patients diagnosed with NSCLC is increasingly acknowledged. A clinical trial conducted by Dong et al. included the participation of 90 individuals diagnosed with stage I-IIIA NSCLC. The aim of this trial was to evaluate the relationship between molecular residual disease (MRD) and various clinicopathological features, gene mutations, the tumor immune microenvironment, and treatment outcomes. Specifically, they discovered that the presence of ctDNA-MRD after surgery in NSCLC patients correlated with several factors, including primary tumor size, lymph node metastasis state, pathological subtype, presence of vascular invasion, and PD-L1 expression. Additionally, they observed that adjuvant EGFR-TKI targeted therapy was more effective than chemotherapy in eliminating ctDNA in postoperative patients with MRD.

TME plays a vital role in immunotherapy resistance, making it a significant factor to consider when examining lung cancer. Nanomedicine has emerged as a promising approach to enhance immunotherapy in this context. In Zhang et al. review, the authors shed light on the interplay between TME and immunotherapy, emphasizing the crucial role of TME in lung cancer immunotherapy (Zhang et al.). Additionally, they explored the potential of nanoparticles in regulating the TME to improve the effectiveness of immunotherapy. The authors also concluded that nanoparticle-based targeting of the TME could be a valuable strategy for solving resistance to PD-1/PD-L1 blockade in lung cancer.

NSCLC has emerged as a prime example of precision medicine, with the identification of multiple subtypes characterized by specific oncogenic driver mutations, leading to the development of targeted therapies at a molecular level. In recent years, significant strides have been made in the field of immunotherapy, particularly in the form of ICI, which involve the use of antagonistic antibodies to target the PD-L1-PD-1 axis for the treatment of NSCLC. In a study by Wang et al., the authors delved into the correlation between the types of immune cells within the TME and the effectiveness of immunotherapy in lung cancer. Additionally, they explored the efficacy of immunotherapy in the context of various gene mutations found in lung cancer, such as KRAS, TP53 and EGFR. Ultimately, the authors emphasize the potential of modulating immune cell populations within the TME as a promising strategy to enhance adaptive immune resistance in lung cancer.

Skin cutaneous melanoma, SKCM, known as one of the most lethal forms of cancer with a high likelihood of metastasis, poses considerable challenges for treatment. Current options such as chemotherapy, immunotherapy, and molecular therapy have not significantly improved the prognosis for SKCM patients, who face an alarmingly short median survival time. Recognizing the urgency of this issue, Sun et al. conducted an in-depth analysis of cuproptosis related signatures over-expressed in SKCM. Through their research, they developed an innovative risk stratification system that holds the potential to revolutionize the management of SKCM patients by enabling precise and targeted interventions. ROC values signify the robustness of the risk classification system in predicting the disease prognosis accurately. Furthermore, the study uncovered notable discrepancies between the low-risk and high-risk groups in terms of tumor burden mutational and immunology function, cell stemness characteristics, and drug sensitivity. These findings highlight the potential impact of the risk stratification system on tailoring personalized treatment plans for SKCM patients, ensuring optimum therapeutic outcomes. These findings further emphasize the potential of the risk stratification system in identifying gene expression patterns that correlate with disease progression and prognosis. In conclusion, the study conducted by Sun et al. sheds light on the pressing issue of SKCM and its poor prognosis. By thoroughly analysing cuproptosis-related differential genes, the researchers developed a novel risk stratification system that demonstrates efficacy in predicting disease outcomes. This system holds immense potential for guiding precise management and treatment decisions for SKCM patients, ultimately improving their overall prognosis.

Over the past decade, there has been significant research focused on unravelling the underlying mechanisms responsible for the development of acute myeloid leukaemia (AML). This increased attention has greatly enhanced our understanding of this disease. However, despite these advancements, the primary barriers to successful treatment remain resistance to chemotherapy and recurrence of the disease. Conventional cytotoxic chemotherapy often leads to acute and chronic side effects, making consolidation chemotherapy impractical, particularly in elderly patients. As a result, there has been a surge of interest in finding alternative

approaches to address this issue. A comprehensive review conducted by Chen et al. has provided a thorough summary of various immunotherapies for the treatment of acute myeloid leukaemia. These therapies include immune checkpoint inhibitors such as CTLA-4 and PD-1/PD-L1, monoclonal antibody therapy targeting anti-CD33, anti-CD123, and anti-CD3/CD33 or CD3/CD123 bispecific antibodies. Presenting the recent progress in immunotherapy for AML, the authors also highlight the most effective therapies and major challenges in their implementation. In a related study, Li et al. conducted a comprehensive investigation into the clinical implications of genes involved in iron-associated cell death and apoptotic pathways in individuals with AML. The researchers developed a robust risk model based on four specific genes, which demonstrated promising prognostic value in both the training and validation cohorts. This model holds potential for aiding clinical decision-making and facilitating risk stratification in AML patients. To validate their findings, Western blot analysis was performed, indicating a significant decrease in the expression levels of C-Myc and Cyclin D1 after inhibiting CD4 expression levels. This result underscores the potential of iron-related cell death pathways as prognostic biomarkers and therapeutic targets in AML. Furthermore, this study emphasizes the importance of further exploration into the molecular mechanisms underlying iron balance, apoptosis regulation, and immune modulation within the bone marrow microenvironment. By shedding light on these interconnected processes, future research has the potential to significantly advance our understanding of AML and pave the way for innovative therapeutic approaches.

Liver metastasis from colorectal cancer is a significant risk factor that often leads to poor outcomes. Therefore, it is crucial to implement proactive interventions and treatments. Cancer-associated fibroblasts (CAFs) play a crucial role in the metastasis process, particularly through their involvement in metabolic reprogramming. However, the understanding of the relationship between CAF metabolic phenotypes and immune cells is currently limited. Wu et al. utilized both single-cell and bulk transcriptomics data to unravel the contributions of CAFs and immune cells in liver metastasis. They specifically focused on the metabolic subtype of CAFs and its impact. By decoding the roles of metabolism-related CAF subtypes and immune cells, the researchers developed a prognostic model that could effectively predict the outcomes of colorectal cancer patients with liver metastases. An intriguing finding of the study was the distinct interaction patterns observed between CAFs with different metabolic states and various immune cell types. Significantly, the researchers discovered that CAFs with varying metabolic profiles exhibited divergent communication patterns with different immune cell populations. This finding shed new light on the complex interplay between CAFs and immune cells during liver metastasis. Moreover, the study established that the prognostic features derived from CAF signature scores can serve as valuable indicators of the prognostic status of colorectal cancer patients. Samples with high CAF signature scores demonstrated elevated immune activity and an enrichment of tumor-related pathways. This suggests that a strong immune response and the activation of tumor-related pathways are associated with better outcomes in patients with liver metastases. Furthermore, the CAF signature score has shown practical utility in guiding the selection of chemotherapeutic agents with greater sensitivity. By considering this signature, clinicians can make more informed decisions regarding precision therapy for colorectal cancer with liver metastases. Therefore, this innovative approach has promising clinical implications for the management and treatment of such patients.

The discovery of AIR mechanisms and the development of therapeutic strategies to selectively inhibit AIR have proven to be effective in treating cancer patients, as demonstrated by the success of anti-PD therapy. Extensive efforts have been made to dissect, analyse, and classify the human tumour microenvironment (TME), leading to the identification of additional complex and diverse AIR mechanisms. However, it is pivotal to note that we have only just scratched the surface of this vast landscape. Nevertheless, it is possible to identify a few predominant or dominant AIR mechanisms that operate within the TME, which can guide the development of more targeted treatment approaches. By understanding and targeting these newly discovered AIR mechanisms, we can expect to achieve more efficient and effective treatment outcomes for a larger proportion of human cancers soon.

Author contributions

AJ: Writing–original draft. OC: Investigation, Supervision, Writing–review and editing. ZL: Formal Analysis, Investigation, Writing–review and editing. HC: Conceptualization, Writing–review and editing. LW: Investigation, Writing–review and editing. LQ: Conceptualization, Writing–original draft, Writing–review and editing.

Funding

The author(s) declare financial support was received for the research, authorship, and/or publication of this article. This study was supported by the National Natural Science Foundation of China (81902560, 81730073 and 81872074) and the Fundamental Research Funds for the Central Universities of Central South University (2023ZZTS0024).

Acknowledgments

We deeply thank all the authors and reviewers who have participated in this Research Topic.

Conflict of interest

The authors declare that the research was conducted in the absence of any commercial or financial relationships that could be construed as a potential conflict of interest.

The author(s) declared that they were an editorial board member of Frontiers, at the time of submission. This had no impact on the peer review process and the final decision.

Publisher's note

References

Hegde, P. S., and Chen, D. S. (2020). Top 10 challenges in cancer immunotherapy. *Immunity* 52, 17–35. doi:10.1016/j.immuni.2019.12.011

Morad, G., Helmink, B. A., Sharma, P., and Wargo, J. A. (2021). Hallmarks of response, resistance, and toxicity to immune checkpoint blockade. *Cell* 184, 5309–5337. doi:10.1016/j.cell.2021.09.020

Sharma, P., Siddiqui, B. A., Anandhan, S., Yadav, S. S., Subudhi, S. K., Gao, J., et al. (2021). The next decade of immune checkpoint therapy. *Cancer Discov.* 11, 838–857. doi:10.1158/2159-8290.CD-20-1680

Vasan, N., Baselga, J., and Hyman, D. M. (2019). A view on drug resistance in cancer. *Nat. Nov.* 575, 299–309. doi:10.1038/s41586-019-1730-1

frontiers | Frontiers in Pharmacology

TYPE Review
PUBLISHED 15 February 2023
DOI 10.3389/fphar.2023.1132158

OPEN ACCESS

EDITED BY
Lin Qi,
Second Xiangya Hospital, Central South University, China

REVIEWED BY
Xin Cheng,
Dana–Farber Cancer Institute, United States
Changli Wang,
Tianjin Medical University Cancer Institute and Hospital, China

*CORRESPONDENCE
Ying Tang,
tang_ying@jlu.edu.cn

SPECIALTY SECTION
This article was submitted to Pharmacology of Anti-Cancer Drugs, a section of the journal Frontiers in Pharmacology

RECEIVED 26 December 2022
ACCEPTED 06 February 2023
PUBLISHED 15 February 2023

CITATION
Wang M, Zhu L, Yang X, Li J, Liu Y and Tang Y (2023), Targeting immune cell types of tumor microenvironment to overcome resistance to PD-1/PD-L1 blockade in lung cancer.
Front. Pharmacol. 14:1132158.
doi: 10.3389/fphar.2023.1132158

Targeting immune cell types of tumor microenvironment to overcome resistance to PD-1/PD-L1 blockade in lung cancer

Man Wang[1], Lijie Zhu[1], Xiaoxu Yang[1], Jiahui Li[1], Yu'e Liu[2] and Ying Tang[1]*

[1]Department of Respiratory Medicine, The First Hospital of Jilin University, Changchun, Jilin, China, [2]Tongji University Cancer Center, Shanghai Tenth People's Hospital of Tongji University, School of Medicine, Tongji University, Shanghai, China

Lung cancer is the common malignant tumor with the highest mortality rate. Lung cancer patients have achieved benefits from immunotherapy, including immune checkpoint inhibitors (ICIs) therapy. Unfortunately, cancer patients acquire adaptive immune resistance, leading to poor prognosis. Tumor microenvironment (TME) has been demonstrated to play a critical role in participating in acquired adaptive immune resistance. TME is associated with molecular heterogeneity of immunotherapy efficacy in lung cancer. In this article, we discuss how immune cell types of TME are correlated with immunotherapy in lung cancer. Moreover, we describe the efficacy of immunotherapy in driven gene mutations in lung cancer, including KRAS, TP53, EGFR, ALK, ROS1, KEAP1, ZFHX3, PTCH1, PAK7, UBE3A, TNF-α, NOTCH, LRP1B, FBXW7, and STK11. We also emphasize that modulation of immune cell types of TME could be a promising strategy for improving adaptive immune resistance in lung cancer.

KEYWORDS

TME, PD-L1, PD-1, time, immunotherapy, resistance

Introduction

Lung cancer is the common malignant tumor and displays the highest mortality rate (Chen P. et al., 2022; Choi and Mazzone, 2022). Lung cancer had 1.8 million deaths (18% of the total cancer-related deaths) worldwide in 2020 (Sung et al., 2021). Lung cancer is the most frequently occurring tumor in males and the third commonly diagnosed tumor in females. Lung cancer is the first cause of tumor death in males and the second leading cause

Abbreviations: ALK, anaplastic lymphoma kinase; BRAF, v-Raf murine sarcoma viral oncogene homolog B; CNV, copy number variation; CTLA-4, cytotoxic T-lymphocyte antigen 4; DDR, DNA damage response and repair; EGFR, epidermal growth factor receptor; FBXW7, F-box and WD-40 domain protein 7; ICIs, immune checkpoint inhibitors; KRAS, Kirsten rat sarcoma; LRP1B, low-density lipoprotein receptor-related protein 1B; mTOR, mammalian target of rapamycin; NSCLC, non-small cell lung carcinoma; OS, overall survival; PD-1, programmed cell death-1; PD-L1, programmed cell death ligand-1; PFS, progression-free survival; ROS1, receptor tyrosine kinase c-ros oncogene 1; TMB, tumor mutational burden; TME, tumor microenvironment; TIME, tumor immune microenvironment; TNFα, tumor necrosis factor α; ZFHX3, zinc finger homeobox 3.

of cancer mortality in women (Sung et al., 2021). In the United States, there are 2,36,740 new lung cancer cases and 1,30,180 lung cancer-related deaths (Siegel et al., 2022). The 5-year survival rate of lung cancer is only 10%–20% in some countries (Sung et al., 2021).

Lung cancer has three-type categories, including small cell lung cancer (SCLC, 14%), non-small cell lung cancer (NSCLC, 82%) and unspecified histology (3%) (Miller et al., 2022). The NSCLC includes large cell carcinoma, adenocarcinoma, and squamous cell carcinoma (Mengoli et al., 2018). The global lung cancer occurrence could be due to outdoor ambient PM2.5 and tobacco (Guo et al., 2020; Turner et al., 2020; Frazer et al., 2022). Multiple gene mutations have been found in NSCLC patient, including epidermal growth factor receptor (EGFR) (Zhao D. et al., 2022; Castaneda-Gonzalez et al., 2022), Kirsten rat sarcoma viral oncogene homolog (KRAS) (Desage et al., 2022; Garcia-Robledo et al., 2022), anaplastic lymphoma kinase (ALK) (Cognigni et al., 2022; Xiang et al., 2022), Erb-B2 Receptor Tyrosine Kinase 2 (ERBB2) (Ni and Zhang, 2021; Vathiotis et al., 2021; Yu X. et al., 2022), B-Raf proto-oncogene (BRAF) (Abdayem and Planchard, 2022; Riudavets et al., 2022; Sforza et al., 2022), phosphatidylinositol-4,5-bisphosphate 3-kinase catalytic subunit alpha (PIK3CA), AKT serine/threonine kinase 1 (AKT1), mitogen-activated protein kinase kinase 1 (MAP2K1) (Kim and Giaccone, 2018; Han et al., 2021), c-ros oncogene 1 (ROS1) (Guaitoli et al., 2021; Yu Z. Q. et al., 2022), neurotrophic tyrosine receptor kinase (NTRK) (Liu C. et al., 2022; Qin and Patel, 2022), and mesenchymal-epithelial transition factor (MET) (Pao and Girard, 2011; Olmedo et al., 2022) (Figure 1). In SCLC patients, gene mutations often include retinoblastoma (Rb), TP53, PTEN, FBXW7, VHL mutations (Cardona et al., 2019; Guan et al., 2022). In addition, targeted therapy, immunotherapy, antiangiogenic therapy and combination therapy have been used in the clinic for lung cancer patients (Luo et al., 2021; Wang et al., 2021; Guo et al., 2022) (Figure 1). NSCLC patients with KRAS mutation or EGFR often have a worse benefit from immunotherapy (Di Nicolantonio et al., 2021).

Immunotherapy has improved the therapeutic outcomes in lung cancer patients (Caliman et al., 2022; Catalano et al., 2022; Martin and Enrico, 2022; Tartarone et al., 2022; Yang et al., 2022). Immune checkpoint inhibitors (ICIs) have been used for the cancer therapy, including anti-PD-1, anti-PD-L1 and anti-CTLA-4. Anti-PD-1 drugs in NSCLC have cemiplimab, pembrolizumab, and nivolumab (Bote et al., 2022; Mussafi et al., 2022). The anti-PD-L1 monoclonal antibodies have durvalumab and atezolizumab in NSCLC. Anti-CTLA-4 (ipilimumab) is also be used in lung cancer because of CTLA-4 as a checkpoint on lymphocytes (Ackermann et al., 2019; Dawe et al., 2020; Peng et al., 2022). However, PD-1/PD-L1 monoclonal antibodies and anti-CTLA-3 treatment obtain a

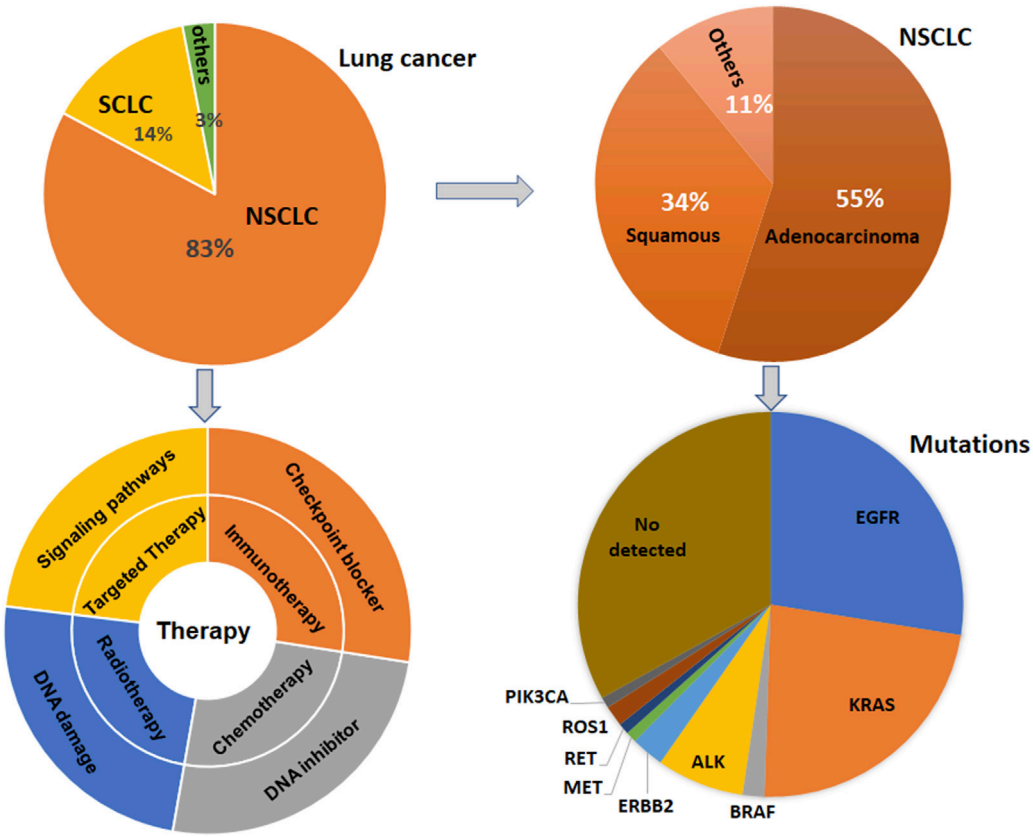

FIGURE 1
Gene Mutations and therapies are illustrated in lung cancer. Lung cancer has three-type categories, including SCLC, NSCLC, and unspecified histology. NSCLC patients have multiple gene mutations. Targeted therapy, immunotherapy, antiangiogenic therapy and combination therapy have been used in the clinic for lung cancer patients.

TABLE 1 The association of gene mutations and TME, immunotherapy in lung cancer.

Gene mutation	TME	Mechanism	Therapy	Ref
KRAS-G12D	Reduction of $CD8^+$ TILs and an immunosuppressive TIME	Targeted P70S6K/PI3K/AKT, decreased CXCL10/CXCL11, inhibition of HMGA2	Resistance to anti-PD-1/PD-L1 therapy	Liu F. et al. (2022)
EGFR	ILT4 increases TAMs recruitment and M2-like polarization, impairing proliferation and cytotoxicity of T cells	Targeting ERK and AKT pathways	Inhibition of ILT4 increased the efficacy of immunotherapy	Chen K. et al. (2021)
ALK	Low proportion of PD-L1+/CD8+, activated memory $CD4^+$ T cells	Targeting PD-L1 pathway	Shows a poor response to ICIs	Liu et al. (2018)
ROS1	TME is active and plasma inflammatory factors is upregulated	High expression level of PD-L1 expression	Not correlated with therapy response	Lee et al. (2019), Yue et al. (2021), Bahnassy et al. (2022)
PTCH1	Associates with $CD8^+$ TILs density	High PD-L1 expression	Associated with survival	Cheng P. et al. (2022)
TP53	Enriches IFN-γ signatures and TME composition; promotes suppressor immune cells, M2 Macrophage and Neutrophils	Associates with PD-L1 expression	Associates with response to ICIs treatment	Assoun et al. (2019), Sun et al. (2020), Wang S. et al. (2022)
ZFHX3	Correlates with TILs	Correlates with immune-related gene expression	Longer survival of NSCLC patients after ICIs treatment	Zhang L. et al. (2021)
PAK7	Associated with TMB, neoantigen load, copy number variation, $CD8^+$ TILs	DNA damage response-related pathways	Prediction of the immunotherapy efficacy	Zeng et al. (2022)
UBE3A	Higher TILs	High expression of immune checkpoint biomarkers	Promotes the immunotherapy efficacy	Zhang N. et al. (2022)
TNF-alpha	Related with TMB, infiltrating immune cells, neoantigen load	DNA damage response signaling	Associates with immunotherapy	Lin et al. (2021)

good response in a subgroup of lung cancer patients. Moreover, adaptive immune resistance is observed in lung cancer patients and attenuated the immunotherapeutic benefits (Gkountakos et al., 2021; Gemelli et al., 2022). Furthermore, immunotherapy often causes side-effects, such as endocrinopathy, colitis, pneumonitis, nephritis in lung cancer patients (Bredin and Naidoo, 2022; Hao et al., 2022).

Tumor microenvironment (TME) is a unique environment and composed of many other types of cells, such as stromal, endothelial and immune cells, which has shown to participate in tumor development, initiation and progression as well as metastasis (Eulberg et al., 2022; Nallasamy et al., 2022). The TME cellular components consist of MDSCs, Treg cells, M1 macrophages, M2 macrophages, cytotoxic $CD8^+$ T cells and NK cells (Gajewski et al., 2013; Cao et al., 2022). It has been known that tumor cells inhibit the anticancer functions of TME and promote pro-tumorigenic functions of TME (Faraj et al., 2022; Tiwari et al., 2022). Tumor immune microenvironment (TIME) consists of tumor cells, different cell types of the immune system and their interactions in the TME niche (Binnewies et al., 2018).

In this review article, we described the association between immune cell types in TME and immunotherapy in lung cancer. Moreover, we discussed the efficacy of immunotherapy in driven gene mutations in lung cancer, including KRAS, TP53, EGFR, ALK, ROS1, KEAP1, ZFHX3, PTCH1, and STK11. Furthermore, we concluded that targeting TME could be helpful to overcome resistance to PD-1/PD-L1 blockade in lung cancer.

Immunotherapy, driven gene mutations, and TME

TME has been identified to take part in tumorigenesis and cancer metastasis. Several adverse conditions in TME, such as acidity, hypoxia, and nutrient restriction, have been unraveled to affect the responses of immunotherapy (Li and Qiao, 2022). Moreover, TME governs immune cell functions *via* regulation of immune cells activation (Ahluwalia et al., 2021; Genova et al., 2021). In this section, the relationship of TME, driven gene mutations and immunotherapy will be summarized. Evidence dissects that immune therapy benefit is associated with driven gene mutations and smoking status in NSCLC patients. These driven genes include EGFR, KRAS, ALK, and BRAF (Skoulidis and Heymach, 2019). One study identified that the most frequently mutated genes included TP53, KRAS, ERBB2, SMAD4, ERBB4, EGFR, BRAF, and MET (Cinausero et al., 2019). In the following sections, we will describe how these driven gene mutations modulate the TIME and affect the anti-PD-1/PD-L1 therapy in NSCLC patients (Table 1). We highlight that the efficacy of immunotherapy is modulated by these key gene mutations in NSCLC patients.

The efficacy of immunotherapy in KRAS-mutant NSCLC

KRAS oncogenic pathway affected TME *via* modulation of cancer-associated fibroblasts and immune cells (Dias Carvalho et al., 2018; Ceddia et al., 2022). KRAS-mutant cancer cells

govern immune responses through regulation of immune cell recruitment, activation, and differentiation, leading to enhancement of protumorigenic ability and promotion of tumor cell evasion (Dias Carvalho et al., 2018). KRAS pathway controls populations of myeloid cells, T cells, fibroblasts, endothelial cells, ECM composition. In KRAS-mutant lung cancer patients, M2 macrophages, MDSCs, CD4+FoxP3+ Treg cells, IL-17-producing T helper cells displayed a pro-tumorigenic TME (Cullis et al., 2018). Studies have shown that the efficacy of anti-PD-1 and anti-PD-L1 immunotherapy was associated with promotion of immunogenicity and an inflammatory TME (Liu et al., 2020; Ceddia et al., 2022). Kirsten rat sarcoma viral oncogene homolog (KRAS) mutations are linked to superior patient response to PD-1/PD-L1 inhibitors. KRAS mutations are associated with treatment efficacy and prognosis in NSCLC (Wood et al., 2016; Ferrer et al., 2018; Roman et al., 2018). Targeting KRAS variant has be shown to have potential treatment applications in NSCLC (Ricciuti et al., 2016; Uras et al., 2020; Li J. X. et al., 2022). Notably, KRAS mutations are linked to immune therapy resistance in NSCLC patients (Kim et al., 2017; Adderley et al., 2019).

In clinic study, NSCLC patients with KRAS mutation obtained treatment benefit from immunotherapy *via* anti-PD-1 and anti-PD-L1 approaches (Liu et al., 2020). Interestingly, suppression of PD-L1 in combination with docetaxel failed to enhance an anti-tumor response in a KRAS-mutant lung adenocarcinoma mouse model (Liu et al., 2020). This study indicated that the combination of immunotherapy and chemotherapy need to be revaluated in NSCLC patients with KRAS mutations (Liu et al., 2020). Moreover, evidence has demonstrated resistance to ICIs in NSCLC with KRAS mutation *via* modulation of tumor metabolism and TME functions (Li W. et al., 2022). KRAS-G12D mutation induced immune suppression and caused the resistance to anti-PD-1/PD-L1 therapy in NSCLC. KRAS-G12D point mutation was negatively associated with PD-L1 expression level and CXCL10/CXCL11, resulting in a reduction of $CD8^+$ TILs and an immunosuppressive TIME (Liu F. et al., 2022). KRAS-G12D mutation reduced PD-L1 expression through P70S6K/PI3K/AKT pathway and decreased CXCL10/CXCL11 expression *via* inhibition of HMGA2 in lung cancer cells. Paclitaxel plus PD-L1 blockade treatments promoted $CD8^+$ TILs recruitment due to CXCL10/CXCL11 upregulation (Liu J. et al., 2022). This study suggested that chemotherapy plus ICIs are effective in NSCLC patients with KRAS-G12D mutation (Liu C. et al., 2022).

The efficacy of immunotherapy in EGFR-mutant NSCLC

EGFR-mutant lung cancer patients exhibit therapy resistance (Passaro et al., 2021; Girard, 2022). Activation of EGFR has been reported to establish an immunosuppressive TME in NSCLC cells, including promotion of suppressive TAMs, Tregs, blockade of T cell infiltration and cytotoxicity, and induction of inhibitory cytokines, which impair the immunotherapy (Lin et al., 2019). About 50% of NSCLC patients with EGFR mutations acquired EGFR-tyrosine kinase inhibitor (TKI) resistance. EGFR pathway has been reported to regulate PD-L1 in NSCLC (Hsu et al., 2019). EGFR-TKI resistance upregulated PD-L1 expression and caused immune escape in lung cancer *via* activation of phosphatidylinositol-3 kinase (PI3K), mitogen-activated protein kinase (MAPK) and NF-kappa B (NF-κB) pathways (Peng et al., 2019). One study found that hypoxia-inducible factor 1α (HIF-1α) and NF-κB are critical to modulate the expression of PD-L1 in EGFR-mutant NSCLC cells (Guo et al., 2019). Another group suggested that TGF-β/Smad pathway participated in PD-L1-mediated EGFR-TKIs resistance in NSCLC with EGFR mutations (Zhang et al., 2019). Overexpression of PD-L1 increased gefitinib resistance in EGFR-mutant NSCLC cells, while depletion of PD-L1 reduced gefitinib resistance (Zhang et al., 2019). Activation of OPN/integrin αVβ3/FAK pathway is important for regulation of EGFR-TKI resistance in NSCLC with EGFR mutations (Fu et al., 2020). PD-L1 expression is correlated with TKIs response and prognosis in lung cancer patients with EGFR mutations (Lin et al., 2015).

Immunoglobulin-like transcript 4 (ILT4) belongs to the immunoglobulin superfamily and often expressed in myeloids, which can promote the proliferation, migration and invasion in human cancers. ILT4 induced immunosuppressive T cell infiltration and led to poor prognosis in lung cancer. ILT4 stimulated T cell senescence and reduced tumor immunity in the TME in human cancer (Gao et al., 2021; Yang et al., 2021). Moreover, ILT4 acts as a useful checkpoint molecule for immunotherapy (Gao et al., 2018). One group showed that ILT4 expression can be elevated after EGFR activation in NSCLC cells, which was mediated by activated ERK and AKT cellular signaling pathways (Chen K. et al., 2021). Moreover, ILT4 increased recruitment of TAMs and M2-like polarization in NSCLC cells with EGFR activation, leading to impairing proliferation and cytotoxicity of T cells (Chen X. et al., 2021). Furthermore, inhibition of ILT4 promoted the efficacy of PD-L1 inhibitors and abrogated TAMs- and T cell-involved immunosuppression in NSCLC cells with EGFR activation. *In vivo* study showed that knockdown of ILT4 and PD-L1 blockade synergistically retarded mouse tumor growth and inhibited immune escape (Chen K. et al., 2021). Animal study data further showed that inhibition of ILT4 alone repressed tumor progression and immune evasion in EGFR mutant NSCLC. This work implied that inhibition of ILT4 increased the efficacy of immunotherapy in EGFR-mutant NSCLC (Chen X. et al., 2021). One retrospective study determined the association between PD-L1, TILs and immunotherapy response in uncommon EGFR-mutant NSCLC patients (Chen et al., 2020). Among 600 NSCLC cases with EGFR mutations, 49 cases were borne with uncommon alterations, such as Ex20, L861Q, S7681, G719X. Uncommon EGFR-mutant NSCLC patients had a high PD-L1 expression and $CD8^+$ TILs and displayed a favorable response to anti-PD-1 therapy (Chen et al., 2020). Therefore, like in common EGFR-mutant NSCLC patients, combination of $CD8^+$ TILs and PD-L1 level in TME can determine the anti-PD-1/PD-L1 therapy efficacy for NSCLC patients with uncommon EGFR mutations (Chen et al., 2020). Anti-CD73 in combination with anti-PD-L1 therapy enhanced T cell response *via* upregulation of the number of $CD8^+$ T cells and promotion of TNF-α and IFN-γ production in EGFR-mutant NSCLC, leading to inhibition of tumor growth (Tu et al., 2022).

ERBB-family genetic alterations and KRAS mutations regulated response to anti-PD-1 inhibitors in NSCLC with metastasis (Cinausero et al., 2019). NSCLC patients with KRAS mutations had a better anti-PD-1 therapy efficacy and a longer PFS and OS. NSCLC patients with EGFR mutation, ERBB2 mutation and

ERBB4 mutations had a worse response to anti-PD-1 therapy (Cinausero et al., 2019). STK11/LKB1 mutations were linked to resistance of PD-1 blockade in KRAS-mutant lung cancer (Skoulidis et al., 2018). Biton et al. (2018) also reported that TP53, STK11, and EGFR mutations represented the anti-PD-1 treatment efficacy in lung adenocarcinoma. NSCLC patients with STK11 mutation displayed chemotherapy resistance, while co-mutations with KRAS or TP53 modulated TIME of STK11-mutant NSCLC tumors and affected immunotherapy response (Malhotra et al., 2022). Additionally, NSCLC patients with EGFR/HER2 exon 20 insertions had a higher expression of PD-L1 and exhibited the sensitive to anti-PD-1/PD-L1 therapy (Chen X. et al., 2021).

The efficacy of immunotherapy in ALK-rearranged NSCLC

ALK-rearranged tumors exhibited more resting memory $CD4^+$ T cells and less activated memory $CD4^+$ T cells and $CD8^+$ T cells (Jin et al., 2020). Anti-PD-1/PD-L1 therapy is useful for the treatment of ALK-translocated NSCLC patients (Bylicki et al., 2017). ALK positivity and EGFR mutations have been reported to be adverse predictors for NSCLC patients (Bahnassy et al., 2022). A retrospective analysis showed that ALK rearrangement and EGFR mutations were involved in poor response to blockade of PD-1 pathway in NSCLC (Gainor et al., 2016). This could be due to low rates of PD-L1 expression and $CD8^+$ TILS in the TME in NSCLC patients (Gainor et al., 2016). Similarly, PD-L1 expression and $CD8^+$ T cells infiltration have a clinical relationship in lung cancer patients with ALK-rearranged and EGFR-mutated tumors (Liu et al., 2018). Lung cancer patients with ALK-rearrangement or EGFR mutations had lowest proportion of PD-L1+/CD8+ tumors and the shortest overall survival. Lung cancer patients with ALK-rearrangement or EGFR mutations showed a poor response to ICIs (Liu et al., 2018). Strikingly, PD-L1 expression and CD8 expression are biomarkers for prediction of prognosis with poor prognosis in patients with EGFR mutations or ALK rearrangement (Liu et al., 2018). Interestingly, a retrospectively study indicated that cytotoxic chemotherapy affected the TIME in NSCLC patients with wild type of ALK and EGFR (Sakai et al., 2019). Platinum-based adjuvant chemotherapy modulated PD-L1 expression, $CD8^+$ TIL density and tumor mutation burden (TMB) in NSCLC patients (Sakai et al., 2019).

The efficacy of immunotherapy in ROS1-rearrangement NSCLC

One research group reported that expression of ROS1 and ROS1-rearrangement was observed in 18.57% and 15.71% of the 70 NSCLC patients, respectively (Bahnassy et al., 2022). ROS1 expression was not correlated with PD-1, PD-L1, survival and therapy response (Bahnassy et al., 2022). Another research simultaneous genotypic screening of three gene mutations, including ROS1, ALK and EGFR, to measure the prevalence and clinicopathologic features of ROS1 mutations and immunotherapy efficacy in NSCLC patients (Lee et al., 2019). This study found that among 407 NSCLC cause, there were 14 ROS1 and 19 ALK rearrangements and 106 EGFR mutations. Among 130 NSCLC tumors, 29 samples had high expression of PD-L1. Among 14 cases with ROS1 mutations, 12 samples exhibited PD-L1 expression and 5 cases displayed high expression level of PD-L1 expression (Lee et al., 2019). This work indicated that ROS1 rearrangement was overlapped with high expression of PD-L1 in NSCLC patients (Lee et al., 2019). Similarly, the correlation among oncogenic mutations in ROS1, ALK, EGFR and PD-L1 had been reported in lung adenocarcinoma (Rangachari et al., 2017). This retrospective work explored 71 cases of lung cancer and found that 29.6% cases had a PD-L1 TPS of high than 50%. Of 19 cases with ALK, ROS1, or EGFR mutations, 18 cases had a PD-L1 TPS less than 50%. Moreover, lung cancer with a PD-L1 TPS of high than 50% was correlated with smoking status (Rangachari et al., 2017). In addition, it has been compared with ALK, ROS1, EGFR, and PD-L1 between cytological tumors and surgical tumors in NSCLC to explore the adequacy of PD-L1 expression by a retrospective study (Ekin et al., 2021). Among 220 NSCLC cases, there were 64 small histology biopsies, 90 surgical biopsies and 66 cytology samples. However, there was no difference between two types of samples (154 histological plus surgical and 66 cytology samples) in cellular adequacy for EGFR, ROS1, ALK, and PD-L1. There was no change in the expression positivity rates for these four biomarkers between two types of samples (Ekin et al., 2021). ROS1-rearranged lung adenocarcinoma patient had active TME and increased plasma inflammatory factors when the patient received immune therapy and ceritinib chemotherapy. PD-L1 expression was elevated in tumor samples during treatment, suggesting that the patient obtained a limited benefit from combination therapies (Yue et al., 2021).

The efficacy of immunotherapy in TP53-mutant NSCLC

An immunohistochemical work illustrated that PD-L1 expression was associated with poor overall survival and PFS in NSCLC patients. $CD8^+$ TILs were correlated with therapy response and a good PFS and overall survival. P53 expression was observed in most of NSCLC samples, but was not correlated with PD-L1 expression (Rashed et al., 2017). Serra et al. (2018) found that RAS/TP53 mutations were associated with PD-L1 expression in lung adenocarcinoma. Moreover, Dong et al. (2017) uncovered that TP53 mutation and KRAS mutation can predict the response to anti-PD-1 immunotherapy in lung adenocarcinoma. Zhang L. et al. (2021) reported that 219 cases from 350 NSCLC patients harbored TP53 mutations. Coexisting TP53 and ZFHX3 mutations were correlated with prognosis, indicating that TP53 and ZFHX3 mutations could be prognostic factors for late-stage NSCLC cases undergoing anti-PD-1/PD-L1 therapy. Another study also clarified that TP53 mutations were associated with response to ICIs treatment and a longer survival in advanced NSCLC patients (Assoun et al., 2019). Notably, NSCLC patients with TP53 plus KEAP1 mutations had a better PFS after treatment with PD-1/PD-L1 monotherapy (Wang S. et al., 2022). Strikingly, the TP53-missense mutation patients displayed enriched IFN-γ signatures and TME composition compared with TP53 wild-type patients (Sun et al., 2020). TP53 non-sense mutation patients

exhibited promotion of suppressor immune cells, such as M2 Macrophage and Neutrophils. Upregulation of TMB and neoantigen levels were observed in both TP53 non-sense and missense mutations. TP53 missense was linked to better benefit of anti-PD-1/PD-L1 therapy (Sun et al., 2020).

The efficacy of immunotherapy in PTCH1-mutant NSCLC

Patched 1 (PTCH1) is one component of hedgehog pathway, which has been correlated with tumor malignancies (Sigafoos et al., 2021). In NSCLC patients, PTCH1 was underexpressed in the tumor specimens compared with normal lung samples (Herreros-Pomares et al., 2022). NSCLC patients with overexpression of PTCH1 displayed a better outcome (Herreros-Pomares et al., 2022). Moreover, PTCH1 expression was found to be correlated with NSCLC development (Barbirou et al., 2022). One circulating tumor cell NGS assay in early-stage lung cancer patients showed that more than 50% of lung cancer patients presented four common mutations, including Notch1, EGFR, IGF2, and PTCH1 (Wan et al., 2021). Genetic mutation analysis demonstrated that 147 mutant genes were discovered in small cell lung cancer patients, including TP53, RB1, KMT2D, PTCH1, APC, LRRK2, ARID2, and BRCA1 (Jin et al., 2021). In addition, elevated mutations of six genes were linked to advanced clinical stages II and III, such as SETD2, WT1, EPHA3, ACVR1B, NOTCH1 and KDM6A (Jin et al., 2021). Similarly, TP53 and RB1 mutations are two most frequently mutations in SCLC, while FGFR1, KIT, PTCH1, RICTOR, and RET mutations are low-frequency mutations (Dowlati et al., 2016). One retrospective study used the data from 180 lung squamous cell carcinoma and reported that patched receptor 1 (PTCH1) gene mutation was linked to $CD8^+$ TILs density (Cheng et al., 2022). $CD8^+$ TILs and high expression of PD-L1 were correlated with better disease-free survival in lung squamous cell carcinoma patients (Cheng et al., 2022). Serial sequencing of circulating tumor DNA (ctDNA) showed that PTCH1 mutation and β2 microglobulin (B2M) mutations were observed in NSCLC patients with anti-PD-1 treatment. Moreover, PTCH1 and B2M mutations were associated with distant metastasis in NSCLC patients (Li et al., 2019).

The efficacy of immunotherapy in ZFHX3-mutant NSCLC

ZFHX3 was reported to suppress alpha-fetoprotein expression. ZFHX3 mRNA expression in tumor tissues was linked to overall survival rate in 140 NSCLC patients. Low expression of ZFHX3 in NSCLC patients was associated with LNM and poor prognosis (Minamiya et al., 2012). Song et al. (2021) reported genomic profiles and TIME of lung cancer with brain metastasis. High-frequent ZFHX3 was found in 40% lung tumors and 28% brain tumors. A majority of lung cancer patients had lesions-shared mutations, such as EGFR mutation. Zhou et al. (2020) reported that 19% ZFHX3 mutation frequency was identified in lung cancer patients by next-generation sequencing. Another study also identified that the mutation of ZFHX3 in NSCLC patients could have benefit from ICIs treatment (Principe, 2022). ZFHX3 was identified as a genomic mutation for prediction of immunotherapy in NSCLC patients (Wang Z. et al., 2022). ZFHX3 mutation in NSCLC patients was correlated with TILs, immune-related gene expression and tumor mutation burden. ZFHX3 mutation was also linked to longer overall survival of NSCLC patients after treatment with ICIs (Zhang J. et al., 2021).

The efficacy of immunotherapy in PAK7-mutant NSCLC

Evidence has shown that p21-activated kinase (PAK7) regulates carcinogenesis in a variety of malignancies (Gu et al., 2013; Han et al., 2014; Quan et al., 2020; Wang et al., 2020). Suppression of PAK7 increased radio-sensitivity in hepatocellular carcinoma (HCC) (Gu and Kong, 2021). Depletion of PAK7 by shRNA transfection induced apoptosis and G2/M phase arrest, decreased clone formation and elevated γ-H2AX expression in HCC cells (Gu and Kong, 2021). PAK7 expression was upregulated in breast tumor samples and associated with differentiation and TNM stage in breast cancer patients. PAK7 activated Wnt/β-Catenin pathway and caused promotion of proliferation and migration as well as inhibition of apoptosis in breast cancer (Li et al., 2018). In esophageal squamous cell cancers (ESCC), high expression of PAK7 was correlated with LNM (He et al., 2016). Moreover, PAK7 was regulated by Aurora-A *via* binding with E2F1 in ESCC cells. PAK7 induced cisplatin resistance of ESCC with Aurora-A overexpression (He et al., 2016). One group revealed that PAK7 could be related to gemcitabine resistance in NSCLC cells (Zhang et al., 2013). PAK7 mutations were found to be associated with tumor mutation burden, neoantigen load, copy number variation, $CD8^+$ TILs, mutation rate in the DDR-related pathways, suggesting that PAK7 mutations could be a helpful biomarker for prediction of the immunotherapy efficacy in NSCLC patients (Zeng et al., 2022).

The efficacy of immunotherapy in UBE3A-mutant NSCLC

UBE3A, also known as E6AP, acts as an E3 ligase and critically involves in carcinogenesis (Owais et al., 2020; Zheng et al., 2021). For example, UBE3A promoted tumor progression *via* disruption of ZNF185 in ESCC (Zheng et al., 2021). UBE3A targeted SIRT6 and regulated liver tumorigenesis, which was dependent on ANXA2 (Kohli et al., 2018). Downregulation of E6AP led to decreased expression of p15, p16 and p19 in NSCLC. E6AP represses the expression of CDC6 *via* inhibiting its E2F1 transcription (Gamell et al., 2017). UBE3A deletion promoted the immunotherapy efficacy in NSCLC patients (Zhang L. X. et al., 2022). NSCLC patients with UBE3A deletion had higher TILs and higher expression of immune checkpoint biomarkers (Zhang N. et al., 2022).

The efficacy of immunotherapy in TNF-α-mutant NSCLC

A mutated human tumor necrosis factor alpha (TNF-α) has been reported to improve the therapeutic index in the mouse fibroblast cell line L929 and mice (Yan et al., 2006). Similarly,

TNF-α mutant was also found to promote cytotoxicity and receptor binding affinity (Shin et al., 1998). Pharmacokinetics of the recombinant mutated human TNF-α (rmhTNF-α) displayed that rmhTNF-α has a low systemic toxicity and high anticancer ability (Li et al., 2010). Phase II multicenter, randomized, double-blind trial showed that rmhTNF-α plus chemotherapies displayed higher response rate compared with chemotherapy alone group in multiple types of cancers. 11.39% patients had a response in the chemotherapy alone, while 27.47% patients had a response in the chemotherapy plus rmhTNF-α treatment. In lung cancer patients, the combination treatment caused 48.89% patients a response (Li et al., 2012). Moreover, a randomized phase III trial in stage IIIB/IV NSCLC patients showed that rmhTNF-α potentiated the efficacy of chemotherapy in advanced NSCLC patients (Ma et al., 2015). TNF-α alternation was uncovered for prediction of survival of ICIs in NSCLC patients. TNF-α mutations were linked to prolonged overall survival in NSCLC patients undergoing immunotherapy (Lin et al., 2021). TNF-α mutations were also related with TMB, DDR mutations and neoantigen load, and infiltrating immune cells (Lin et al., 2021).

The efficacy of immunotherapy in NOTCH-mutant NSCLC

Notch signaling pathway is critically involved in tumorigenesis, which consists of four receptors, Notch1, Notch2, Notch 3, Notch4, and several ligands, such as delta-like proteins (DLL1, DLL3, DLL4), Jagged-1 and Jagged-2 (Gao et al., 2020; Majumder et al., 2021). In general, 20%–25% of SCLC patients exhibited Notch mutations with loss-of-function (LOF). Notch can act as a tumor suppressor in SCLC and also enhance non-neuroendocrine plasticity to facilitate tumor growth in SCLC (Hong et al., 2022). Mice with genetic loss of Nocth1 or Nocth2 facilitated SCLC tumorigenesis and formed non-neuroendocrine populations *via* regulation of RUNX2/REST pathway and STING (stimulator of interferon genes) (Hong et al., 2022). Li Y. et al. (2022) reported that Notch pathway was correlated with TIME in SCLC. Notch1 gene mutation was negatively linked to PD-L1 expression in SCLC patients. Higher expression of DLL3 was found in SCLC patients and associated with PD-L1 levels. Hence, SCLC patients with positive DLL3 expression and Notch1 wild type had PD-L1 overexpression, which could be likely to have good immunotherapy efficacy. Notch2 mutation was a prognostic factor in NSCLC patients and could be provide a new treatment option for patients without EGFR mutations (Niu et al., 2021).

The high-mutated NOTCH pathway could act as a biomarker for predicting the prognosis of ICIs-treated NSCLC patients because NSCLC patients with high-mutated NOTCH pathway had a better PFS and OS (Li et al., 2021). Zhang et al. (2020) also identified that Notch mutation acted as a new predictor for efficacious immunotherapy in NSCLC patients. Notch1/2/3 mutation had a correlation with better ICI treatment outcomes, including PFS and overall survival due to regulation of transcription of genes that were related to immune activation and DNA damage response (Zhang et al., 2020). Notch4 mutation was also a potential response biomarker for ICIs therapy in several cancer types, including NSCLC (Long et al., 2021). Cancer patients with Notch4 mutation displayed better responses for ICI therapy, including ORR, DCB, PFS and overall survival. Notch4 mutation was linked to increased immunogenicity, high TMB, anticancer immunity and activation of the antigen-processing machinery (Long et al., 2021).

The efficacy of immunotherapy in LRP1B-mutant NSCLC

LRP1B has been reported to be frequently mutated in numerous types of cancers, including lung cancer (Principe et al., 2021). The bioinformatics analysis showed that LRP1B mutation was linked to age and MUC16 and TP53 mutation status in gastric cancer patients (Hu et al., 2021). The next-generation sequencing (NGS) data showed that 13.98% of NSCLC patients had LRP1B mutation (Xu et al., 2023). LRP1B mutation was correlated with high TMB in NSCLC. Moreover, NSCLC patients with LRP1B mutation had a high infiltrating levels of immune cells and immune molecules. Additionally, LRP1B mutations were linked to several pathways in the immune system, including cell cycle, Notch, mTOR and insulin pathways (Xu et al., 2023). LRP1B mutation was associated with TMB and outcomes in NSCLC patients with immunotherapy (Chen et al., 2019). LRP1B mutation was correlated with a better survival in NSCLC patients. Moreover, LRP1B mutations was also associated with immunocytes and enriched pathways, such as cell cycle mitotic, antigen processing and presentation pathways (Chen et al., 2019). Another group reported that LRP1B mutation was correlated with better outcomes to ICIs in combination with chemotherapy in NSCLC patients (Zhou J. et al., 2022). Hence, LRP1B mutations could be critical in promoting immunotherapy and might be a biomarker for judgement of treatment responsiveness.

The efficacy of immunotherapy in FBXW7-mutant NSCLC

FBXW7, one of F-box proteins, has been identified to regulate carcinogenesis and progression (Wang et al., 2014; Yan et al., 2020; Liu F. et al., 2022). FBXW7 mutation caused drug resistance *via* targeting several downstream substrates for ubiquitination and degradation, including Mcl-1, mTOR, snail and CCDC6 in NSCLC (Peng and Chen, 2019). Several compounds displayed an effective treatment efficacy in NSCLC patients with FBXW7 mutation, such as rabdosia, MS-275 and rapamycin (Peng and Chen, 2019). By analysis of TCGA data, 30.9% of lung adenocarcinoma presents FBXW7 deletion, and 63.5% of lung squamous cell carcinoma exhibited FBXW7 deletion. FBXW7 deletion led to lung oncogenesis and contributed to gefitinib resistance (Xiao et al., 2018). One study revealed that 5.6% of NSCLC patients (7 cases) had FBXW7 truncating mutations in 125 NSCLC cases. In these seven patients with FBXW7 mutation after they obtained immunotherapy, four cases presented partial response, two cases showed stable disease, and one case displayed progressive disease (Liu J. et al., 2022). FBXW7-mutant NSCLC patients had 13 months for median progression-free survival (PFS), while FBXW7 wild type patients had 4 months for PFS. FBXW7-mutant patients had a higher TMB and the activation

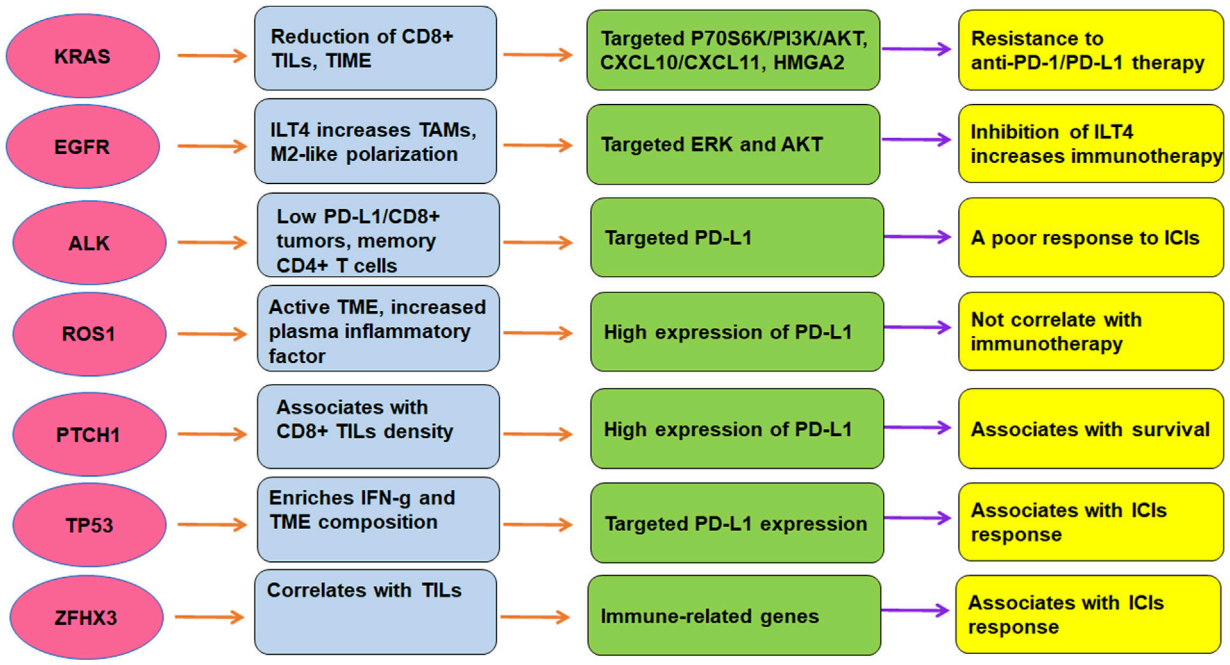

FIGURE 2
The role of gene mutations in regulation of TME and immunotherapy in lung cancer. The efficacy of immunotherapy was regulated by driven gene mutations in lung cancer, including KRAS, TP53, EGFR, ALK, ROS1, ZFHX3, and PTCH1.

of T cells. Moreover, FBXW7 mutation was linked to upregulation of $CD8^+$ T cell infiltration and M1 macrophages. FBXW7 gene mutation could predict the prognosis of immunotherapy in patients with NSCLC (Liu C. et al., 2022).

LncRNAs and circRNAs regulate TME and immunotherapy in lung cancer

Besides these gene mutations, non-coding RNAs have been reported to involve in regulating TME and immunotherapy in lung cancer. Non-coding RNAs have been reported to involved in human cancer development and progression (Ghafouri-Fard et al., 2020; Yan and Bu, 2021; Chen T. et al., 2022; Liu and Shang, 2022). Evidence has shown that lncRNAs play an essential role in NSCLC initiation, development and progression (Osielska and Jagodzinski, 2018; Wang et al., 2018; Hu et al., 2022). Moreover, non-coding RNAs are critically involved in cancer drug resistance in human cancers (Jiang et al., 2020; Zhou X. et al., 2022; Xie et al., 2022). LncRNAs and exosomal lncRNAs regulate tumor progression, drug sensitivity and TME remodeling in lung cancer (Entezari et al., 2022). The role of lncRNAs in the regulation of PD-1 and PD-L1 pathways and TME in cancer immunotherapy has been discussed (Jiang W. et al., 2021; Dai et al., 2021; Zhang P. et al., 2022). For example, lncRNA C5orf64 was characterized as a potential indicator for TME and mutation pattern remodeling in lung cancer (Pang et al., 2021). LncRNA C5orf64 expression was positively associated with neutrophils, monocytes, M2 macrophages and eosinophils, and negatively linked to Tregs and plasma cells (Pang et al., 2021). High expression of C5orf64 was linked to upregulation of PD-1, PD-L1 and CTLA-4 expression. Interestingly, lung adenocarcinoma patients with high expression of C5orf64 had a low frequency of TP53 mutation (Pang et al., 2021). Together, lncRNA C5orf64 could be a useful indicator for TME modulation and immunotherapy in lung cancer. Jiang Y. et al. (2021) found that cancer-associated fibroblasts (CAFs)-derived exosomes can regulate lncRNA OIP5-AS1 and modulate miR-142-5p and control the expression of PD-L1, leading to promotion of lung cancer progression. Moreover, N6-methyladenosin (m6A) related lncRNA signatures with TME have been defined to predict the immunotherapy in lung cancer (Weng et al., 2021; Zhao et al., 2021; Zhang W. et al., 2022; Yan et al., 2022). Recently, the circular RNA circHMGB2 was uncovered to promote immunosuppression and resistance to anti-PD-1 therapy *via* targeting miR-181a-5p and upregulating CARM1 in lung cancer, suggesting that circHMGB2 reshaped the TME and governed immunotherapy in lung cancer (Zhang L. X. et al., 2022).

Conclusion and perspectives

TME is critically involved in immunotherapy in lung cancer. The efficacy of immunotherapy was regulated by driven gene mutations in lung cancer, including KRAS, TP53, EGFR, ALK, ROS1, ZFHX3, and PTCH1 (Figure 2). Targeting TME could abolish immune resistance of anti-PD-1/PD-L1 treatment in lung cancer. It has been suggested that PD-1/PD-L1 blockade should be combined with other therapy such as chemotherapy to improve the anticancer efficacy in human cancer (Wu et al., 2022).

Several issues need to be clarified regarding the TME and immunotherapy in NSCLC. For example, several reports showed that mRNA vaccine could be applied for cancer treatment *via* regulation of TME (Zhong et al., 2021; Zhao W. et al., 2022; Huang et al., 2022). Proteomics, genomics, and metabolomics might be good approaches to explore the mechanism of gene mutation-driven lung cancer and TME (Zhou et al., 2019; Bourbonne et al., 2022). Recently, several studies used the single-cell profiling of lung cancer to determine the TME and immunotherapy (Maynard et al., 2020; Wu et al., 2021; Hui et al., 2022). Hui et al. (2022) reported single-cell profiling of immune cells after chemotherapy and pembrolizumab in advanced NSCLC. This study found the synergistical increase of $CD4^+$ cells and B cells were positively correlated with chemoimmunotherapy. Moreover, this work identified several positive outcomes, such as promotion of TNFRSF4+ Tregs, LAMP3+ DCs, intratumoral $CD4^+$ T clones and $CD8^+$ T clones (Hui et al., 2022). In addition, single-cell RNA sequencing was used to evaluate therapy-induced evolution in lung cancer patients, including TN (patients before initiating systemic therapy, TKI naive), RD (residual disease) and PD (on-therapy progressive disease) (Maynard et al., 2020). Transcriptional differences between RD and TN tumor cells suggested cell-state-specific programs, while transcriptional differences between PD and TN tumor cells indicated that immune modulation and invasion are critical for cancer progression. RD patients displayed active T-lymphocytes and reduced macrophages, while PD patients displayed immunosuppressive cell states (Maynard et al., 2020). Wu et al. also reported single-cell profiling of tumor heterogeneity and TME in advanced NSCLC. This work identified not only common cell types but also rare cell types in tumors including T helper 17 cells and follicular dendritic cells. Different NSCLC patients exhibited larger heterogeneity in chromosomal structure, intercellular signaling network and cellular composition and so on (194). Further investigations are necessary to determine the underlying molecular mechanisms of TME in regulation of immunotherapy resistance. In addition, besides TME, immunotherapy resistance could be caused by other factors in lung cancer, which should be explored in the future.

Author contributions

MW wrote the manuscript; LZ, XY, and JL searched the literatures, made the tables and figures. YT edited and revised the manuscript. All authors have approved for the final submission of the manuscript.

Funding

This work is supported by the National Natural Science Foundation of China (grant No. 81900037).

Conflict of interest

The authors declare that the research was conducted in the absence of any commercial or financial relationships that could be construed as a potential conflict of interest.

Publisher's note

All claims expressed in this article are solely those of the authors and do not necessarily represent those of their affiliated organizations, or those of the publisher, the editors and the reviewers. Any product that may be evaluated in this article, or claim that may be made by its manufacturer, is not guaranteed or endorsed by the publisher.

References

Abdayem, P., and Planchard, D. (2022). Ongoing progress in BRAF-mutated non-small cell lung cancer. *Clin. Adv. Hematol. Oncol.* 20 (11), 662–672. Cited in: Pubmed; PMID 36331404.

Ackermann, C. J., Reck, M., Paz-Ares, L., Barlesi, F., and Califano, R. (2019). First-line immune checkpoint blockade for advanced non-small-cell lung cancer: Travelling at the speed of light. *Lung Cancer* 134, 245–253. Epub 20190619Cited in: Pubmed; PMID 31319988. doi:10.1016/j.lungcan.2019.06.007

Adderley, H., Blackhall, F. H., and Lindsay, C. R. (2019). KRAS-mutant non-small cell lung cancer: Converging small molecules and immune checkpoint inhibition. *EBioMedicine* 41, 711–716. Epub 20190307Cited in: Pubmed; PMID 30852159. doi:10.1016/j.ebiom.2019.02.049

Ahluwalia, P., Ahluwalia, M., Mondal, A. K., Sahajpal, N. S., Kota, V., Rojiani, M. V., et al. (2021). Natural killer cells and dendritic cells: Expanding clinical relevance in the non-small cell lung cancer (NSCLC) tumor microenvironment. *Cancers (Basel)* 13 (16), 4037. Epub 20210811. doi:10.3390/cancers13164037

Assoun, S., Theou-Anton, N., Nguenang, M., Cazes, A., Danel, C., Abbar, B., et al. (2019). Association of TP53 mutations with response and longer survival under immune checkpoint inhibitors in advanced non-small-cell lung cancer. *Lung Cancer* 132, 65–71. Epub 20190408Cited in: Pubmed; PMID 31097096. doi:10.1016/j.lungcan.2019.04.005

Bahnassy, A. A., Ismail, H., Mohanad, M., El-Bastawisy, A., and Yousef, H. F. (2022). The prognostic role of PD-1, PD-L1, ALK, and ROS1 proteins expression in non-small cell lung carcinoma patients from Egypt. *J. Egypt Natl. Canc Inst.* 34 (1), 23. Epub 20220530Cited in: Pubmed; PMID 35644823. doi:10.1186/s43046-022-00121-8

Barbirou, M., Miller, A., Manjunath, Y., Ramirez, A. B., Ericson, N. G., Staveley-O'Carroll, K. F., et al. (2022). Single circulating-tumor-cell-targeted sequencing to identify somatic variants in liquid biopsies in non-small-cell lung cancer patients. *Curr. Issues Mol. Biol.* 44 (2), 750–763. Epub 20220202. doi:10.3390/cimb44020052

Binnewies, M., Roberts, E. W., Kersten, K., Chan, V., Fearon, D. F., Merad, M., et al. (2018). Understanding the tumor immune microenvironment (TIME) for effective therapy. *Nat. Med.* 24 (5), 541–550. Epub 20180423Cited in: Pubmed; PMID 29686425. doi:10.1038/s41591-018-0014-x

Biton, J., Mansuet-Lupo, A., Pecuchet, N., Alifano, M., Ouakrim, H., Arrondeau, J., et al. (2018). TP53, STK11, and EGFR mutations predict tumor immune profile and the response to anti-PD-1 in lung adenocarcinoma. *Clin. Cancer Res.* 24 (22), 5710–5723. Epub 20180515Cited in: Pubmed; PMID 29764856. doi:10.1158/1078-0432.CCR-18-0163

Bote, H., Mesas, A., Baena, J., Herrera, M., and Paz-Ares, L. (2022). Emerging immune checkpoint inhibitors for the treatment of non-small cell lung cancer. *Expert Opin. Emerg. Drugs* 27 (3), 289–300. Epub 20221006. doi:10.1080/14728214.2022.2113377

Bourbonne, V., Geier, M., Schick, U., and Lucia, F. (2022). Multi-omics approaches for the prediction of clinical endpoints after immunotherapy in non-small cell lung cancer: A comprehensive review. *Biomedicines* 10 (6), 1237. Epub 20220526. doi:10.3390/biomedicines10061237

Bredin, P., and Naidoo, J. (2022). The gut microbiome, immune check point inhibition and immune-related adverse events in non-small cell lung cancer. *Cancer Metastasis Rev.* 41 (2), 347–366. Epub 20220725Cited in: Pubmed; PMID 35876944. doi:10.1007/s10555-022-10039-1

Bylicki, O., Paleiron, N., Margery, J., Guisier, F., Vergnenegre, A., Robinet, G., et al. (2017). Targeting the PD-1/PD-L1 immune checkpoint in EGFR-mutated or ALK-translocated non-small-cell lung cancer. *Target Oncol.* 12 (5), 563–569. Cited in: Pubmed; PMID 28624922. doi:10.1007/s11523-017-0510-9

Caliman, E., Fancelli, S., Petroni, G., Gatta Michelet, M. R., Cosso, F., Ottanelli, C., et al. (2022). Challenges in the treatment of small cell lung cancer in the era of immunotherapy and molecular classification. *Lung Cancer* 175, 88–100. Epub 20221123Cited in: Pubmed; PMID 36493578. doi:10.1016/j.lungcan.2022.11.014

Cao, H., Gao, S., Jogani, R., and Sugimura, R. (2022). The tumor microenvironment reprograms immune cells. *Cell Reprogr.* 24 (6), 343–352. Epub 20221026. doi:10.1089/cell.2022.0047

Cardona, A. F., Rojas, L., Zatarain-Barron, Z. L., Ruiz-Patino, A., Ricaurte, L., Corrales, L., et al. (2019). Multigene mutation profiling and clinical characteristics of small-cell lung cancer in never-smokers vs. Heavy smokers (Geno1.3-CLICaP). *Front. Oncol.* 9, 254. Epub 20190417. doi:10.3389/fonc.2019.00254

Castaneda-Gonzalez, J. P., Chaves, J. J., and Parra-Medina, R. (2022). Multiple mutations in the EGFR gene in lung cancer: A systematic review. *Transl. Lung Cancer Res.* 11 (10), 2148–2163. Cited in: Pubmed; PMID 36386461. doi:10.21037/tlcr-22-235

Catalano, M., Shabani, S., Venturini, J., Ottanelli, C., Voltolini, L., and Roviello, G. (2022). Lung cancer immunotherapy: Beyond common immune checkpoints inhibitors. *Cancers (Basel)* 14 (24), 6145. Epub 20221213. doi:10.3390/cancers14246145

Ceddia, S., Landi, L., and Cappuzzo, F. (2022). KRAS-mutant non-small-cell lung cancer: From past efforts to future challenges. *Int. J. Mol. Sci.* 23 (16), 9391. Epub 20220820. doi:10.3390/ijms23169391

Chen, H., Chong, W., Wu, Q., Yao, Y., Mao, M., and Wang, X. (2019). Association of LRP1B mutation with tumor mutation burden and outcomes in melanoma and non-small cell lung cancer patients treated with immune check-point blockades. *Front. Immunol.* 10, 1113. Epub 20190521. doi:10.3389/fimmu.2019.01113

Chen, K., Cheng, G., Zhang, F., Zhu, G., Xu, Y., Yu, X., et al. (2020). PD-L1 expression and T cells infiltration in patients with uncommon EGFR-mutant non-small cell lung cancer and the response to immunotherapy. *Lung Cancer* 142, 98–105. Epub 20200219Cited in: Pubmed; PMID 32120230. doi:10.1016/j.lungcan.2020.02.010

Chen, K., Pan, G., Cheng, G., Zhang, F., Xu, Y., Huang, Z., et al. (2021). Immune microenvironment features and efficacy of PD-1/PD-L1 blockade in non-small cell lung cancer patients with EGFR or HER2 exon 20 insertions. *Thorac. Cancer* 12 (2), 218–226. Epub 20201118. doi:10.1111/1759-7714.13748

Chen, X., Gao, A., Zhang, F., Yang, Z., Wang, S., Fang, Y., et al. (2021). ILT4 inhibition prevents TAM- and dysfunctional T cell-mediated immunosuppression and enhances the efficacy of anti-PD-L1 therapy in NSCLC with EGFR activation. *Theranostics* 11 (7), 3392–3416. Epub 20210119. doi:10.7150/thno.52435

Chen, P., Liu, Y., Wen, Y., and Zhou, C. (2022). Non-small cell lung cancer in China. *Cancer Commun. (Lond)* 42 (10), 937–970. Epub 20220908. doi:10.1002/cac2.12359

Chen, T., Liu, J., Zhang, H., Li, J., and Shang, G. (2022). Long intergenic noncoding RNA00265 enhances cell viability and metastasis via targeting miR-485-5p/USP22 Axis in osteosarcoma. *Front. Oncol.* 12, 907472. Epub 20220526. doi:10.3389/fonc.2022.907472

Cheng, X., Wang, L., and Zhang, Z. (2022). Prognostic significance of PD-L1 expression and CD8(+) TILs density for disease-free survival in surgically resected lung squamous cell carcinoma: A retrospective study. *J. Thorac. Dis.* 14 (6), 2224–2234. Cited in: Pubmed; PMID 35813758. doi:10.21037/jtd-22-630

Choi, H. K., and Mazzone, P. J. (2022). Lung cancer screening. *Med. Clin. North Am.* 106 (6), 1041–1053. Epub 20221004Cited in: Pubmed; PMID 36280331. doi:10.1016/j.mcna.2022.07.007

Cinausero, M., Laprovitera, N., De Maglio, G., Gerratana, L., Riefolo, M., Macerelli, M., et al. (2019). KRAS and ERBB-family genetic alterations affect response to PD-1 inhibitors in metastatic nonsquamous NSCLC. *Ther. Adv. Med. Oncol.* 11, 1758835919885540. Epub 20191114. doi:10.1177/1758835919885540

Cognigni, V., Pecci, F., Lupi, A., Pinterpe, G., De Filippis, C., Felicetti, C., et al. (2022). The landscape of ALK-rearranged non-small cell lung cancer: A comprehensive review of clinicopathologic, genomic characteristics, and therapeutic perspectives. *Cancers (Basel)* 14 (19), 4765. Epub 20220929. doi:10.3390/cancers14194765

Cullis, J., Das, S., and Bar-Sagi, D. (2018). Kras and tumor immunity: Friend or foe? *Cold Spring Harb. Perspect. Med.* 8 (9), a031849. Epub 20180904. doi:10.1101/cshperspect.a031849

Dai, S., Liu, T., Liu, Y. Y., He, Y., Liu, T., Xu, Z., et al. (2021). Long non-coding RNAs in lung cancer: The role in tumor microenvironment. *Front. Cell Dev. Biol.* 9, 795874. Epub 20220103. doi:10.3389/fcell.2021.795874

Dawe, D. E., Harlos, C. H., and Juergens, R. A. (2020). Immuno-oncology-the new paradigm of lung cancer treatment. *Curr. Oncol.* 27, S78–S86. Epub 20200401. doi:10.3747/co.27.5183

Desage, A. L., Leonce, C., Swalduz, A., and Ortiz-Cuaran, S. (2022). Targeting KRAS mutant in non-small cell lung cancer: Novel insights into therapeutic strategies. *Front. Oncol.* 12, 796832. Epub 20220216. doi:10.3389/fonc.2022.796832

Di Nicolantonio, F., Vitiello, P. P., Marsoni, S., Siena, S., Tabernero, J., Trusolino, L., et al. (2021). Precision oncology in metastatic colorectal cancer - from biology to medicine. *Nat. Rev. Clin. Oncol.* 18 (8), 506–525. Epub 20210416Cited in: Pubmed; PMID 33864051. doi:10.1038/s41571-021-00495-z

Dias Carvalho, P., Guimaraes, C. F., Cardoso, A. P., Mendonca, S., Costa, A. M., Oliveira, M. J., et al. (2018). KRAS oncogenic signaling extends beyond cancer cells to orchestrate the microenvironment. *Cancer Res.* 78 (1), 7–14. Epub 20171220. doi:10.1158/0008-5472.CAN-17-2084

Dong, Z. Y., Zhong, W. Z., Zhang, X. C., Su, J., Xie, Z., Liu, S. Y., et al. (2017). Potential predictive value of TP53 and KRAS mutation status for response to PD-1 blockade immunotherapy in lung adenocarcinoma. *Clin. Cancer Res.* 23 (12), 3012–3024. Epub 20161230. doi:10.1158/1078-0432.CCR-16-2554

Dowlati, A., Lipka, M. B., McColl, K., Dabir, S., Behtaj, M., Kresak, A., et al. (2016). Clinical correlation of extensive-stage small-cell lung cancer genomics. *Ann. Oncol.* 27 (4), 642–647. Epub 20160122. doi:10.1093/annonc/mdw005

Ekin, Z., Nart, D., Savas, P., and Veral, A. (2021). Comparison of PD-L1, EGFR, ALK, and ROS1 status between surgical samples and cytological samples in non-small cell lung carcinoma. *Balk. Med. J.* 38 (5), 287–295. in: Pubmed; PMID 34558414. doi:10.5152/balkanmedj.2021.20086

Entezari, M., Ghanbarirad, M., Taheriazam, A., Sadrkhanloo, M., Zabolian, A., Goharrizi, M., et al. (2022). Long non-coding RNAs and exosomal lncRNAs: Potential functions in lung cancer progression, drug resistance and tumor microenvironment remodeling. *Biomed. Pharmacother.* 150, 112963. Epub 20220422. doi:10.1016/j.biopha.2022.112963

Eulberg, D., Fromming, A., Lapid, K., Mangasarian, A., and Barak, A. (2022). The prospect of tumor microenvironment-modulating therapeutical strategies. *Front. Oncol.* 12, 1070243. Epub 20221208. doi:10.3389/fonc.2022.1070243

Faraj, J. A., Al-Athari, A. J. H., Mohie, S. E. D., Kadhim, I. K., Jawad, N. M., Abbas, W. J., et al. (2022). Reprogramming the tumor microenvironment to improve the efficacy of cancer immunotherapies. *Med. Oncol.* 39 (12), 239. Epub 20220929Cited in: Pubmed; PMID 36175691. doi:10.1007/s12032-022-01842-5

Ferrer, I., Zugazagoitia, J., Herbertz, S., John, W., Paz-Ares, L., and Schmid-Bindert, G. (2018). KRAS-Mutant non-small cell lung cancer: From biology to therapy. *Lung Cancer* 124, 53–64. Epub 20180719Cited in: Pubmed; PMID 30268480. doi:10.1016/j.lungcan.2018.07.013

Frazer, K., Bhardwaj, N., Fox, P., Stokes, D., Niranjan, V., Quinn, S., et al. (2022). Systematic review of smoking cessation inventions for smokers diagnosed with cancer. *Int. J. Environ. Res. Public Health* 19 (24), 17010. Epub 20221218. doi:10.3390/ijerph192417010

Fu, Y., Zhang, Y., Lei, Z., Liu, T., Cai, T., Wang, A., et al. (2020). Abnormally activated OPN/integrin αVβ3/FAK signalling is responsible for EGFR-TKI resistance in EGFR mutant non-small-cell lung cancer. *J. Hematol. Oncol.* 13 (1), 169. Epub 20201207Cited in: Pubmed; PMID 33287873. doi:10.1186/s13045-020-01009-7

Gainor, J. F., Shaw, A. T., Sequist, L. V., Fu, X., Azzoli, C. G., Piotrowska, Z., et al. (2016). EGFR mutations and ALK rearrangements are associated with low response rates to PD-1 pathway blockade in non-small cell lung cancer: A retrospective analysis. *Clin. Cancer Res.* 22 (18), 4585–4593. Epub 20160525. doi:10.1158/1078-0432.CCR-15-3101

Gajewski, T. F., Schreiber, H., and Fu, Y. X. (2013). Innate and adaptive immune cells in the tumor microenvironment. *Nat. Immunol.* 14 (10), 1014–1022. . Cited in: Pubmed; PMID 24048123. doi:10.1038/ni.2703

Gamell, C., Gulati, T., Levav-Cohen, Y., Young, R. J., Do, H., Pilling, P., et al. (2017). Reduced abundance of the E3 ubiquitin ligase E6AP contributes to decreased expression of the INK4/ARF locus in non-small cell lung cancer. *Sci. Signal* 10 (461), eaaf8223. Epub 20170110. doi:10.1126/scisignal.aaf8223

Gao, A., Liu, X., Lin, W., Wang, J., Wang, S., Si, F., et al. (2021). Tumor-derived ILT4 induces T cell senescence and suppresses tumor immunity. *J. Immunother. Cancer* 9 (3), e001536. Cited in: Pubmed; PMID 33653799. doi:10.1136/jitc-2020-001536

Gao, A., Sun, Y., and Peng, G. (2018). ILT4 functions as a potential checkpoint molecule for tumor immunotherapy. *Biochim. Biophys. Acta Rev. Cancer* 1869 (2), 278–285. Epub 20180410Cited in: Pubmed; PMID 29649510. doi:10.1016/j.bbcan.2018.04.001

Gao, Y., Bai, L., and Shang, G. (2020). Notch-1 promotes the malignant progression of osteosarcoma through the activation of cell division cycle 20. *Aging (Albany NY)* 13 (2), 2668–2680. Epub 20201219. doi:10.18632/aging.202314

Garcia-Robledo, J. E., Rosell, R., Ruiz-Patino, A., Sotelo, C., Arrieta, O., Zatarain-Barron, L., et al. (2022). KRAS and MET in non-small-cell lung cancer: Two of the new kids on the 'drivers' block. *Ther. Adv. Respir. Dis.* 16, 17534666211066064. in: Pubmed; PMID 35098800. doi:10.1177/17534666211066064

Gemelli, M., Noonan, D. M., Carlini, V., Pelosi, G., Barberis, M., Ricotta, R., et al. (2022). Overcoming resistance to checkpoint inhibitors: Natural killer cells in non-small cell lung cancer. *Front. Oncol.* 12, 886440. Epub 20220531. doi:10.3389/fonc.2022.886440

Genova, C., Dellepiane, C., Carrega, P., Sommariva, S., Ferlazzo, G., Pronzato, P., et al. (2021). Therapeutic implications of tumor microenvironment in lung cancer: Focus on immune checkpoint blockade. *Front. Immunol.* 12, 799455. Epub 20220107. doi:10.3389/fimmu.2021.799455

Ghafouri-Fard, S., Shoorei, H., Branicki, W., and Taheri, M. (2020). Non-coding RNA profile in lung cancer. *Exp. Mol. Pathol.* 114, 104411. Epub 20200226. doi:10.1016/j.yexmp.2020.104411

Girard, N. (2022). New strategies and novel combinations in EGFR TKI-resistant non-small cell lung cancer. *Curr. Treat. Options Oncol.* 23 (11), 1626–1644. Epub 20221015Cited in: Pubmed; PMID 36242712. doi:10.1007/s11864-022-01022-7

Gkountakos, A., Delfino, P., Lawlor, R. T., Scarpa, A., Corbo, V., and Bria, E. (2021). Harnessing the epigenome to boost immunotherapy response in non-small cell lung cancer patients. *Ther. Adv. Med. Oncol.* 13, 17588359211006947. Epub 20210525. doi:10.1177/17588359211006947

Gu, J., Li, K., Li, M., Wu, X., Zhang, L., Ding, Q., et al. (2013). A role for p21-activated kinase 7 in the development of gastric cancer. *FEBS J.* 280 (1), 46–55. Epub 20121123. doi:10.1111/febs.12048

Gu, Y. F., and Kong, L. T. (2021). Inhibiting p21-activated kinase (PAK7) enhances radiosensitivity in hepatocellular carcinoma. *Hum. Exp. Toxicol.* 40 (12), 2202–2214. Epub 20210624. doi:10.1177/09603271211027948

Guaitoli, G., Bertolini, F., Bettelli, S., Manfredini, S., Maur, M., Trudu, L., et al. (2021). Deepening the knowledge of ROS1 rearrangements in non-small cell lung cancer: Diagnosis, treatment, resistance and concomitant alterations. *Int. J. Mol. Sci.* 22 (23), 12867. Epub 20211128. doi:10.3390/ijms222312867

Guan, X., Bao, G., Liang, J., Yao, Y., Xiang, Y., and Zhong, X. (2022). Evolution of small cell lung cancer tumor mutation: From molecular mechanisms to novel viewpoints. *Semin. Cancer Biol.* 86, 346–355. Epub 20220330Cited in: Pubmed; PMID 35367118. doi:10.1016/j.semcancer.2022.03.015

Guo, H., Li, W., and Wu, J. (2020). Ambient PM2.5 and annual lung cancer incidence: A nationwide study in 295 Chinese counties. *Int. J. Environ. Res. Public Health* 17 (5), 1481. Epub 20200225. doi:10.3390/ijerph17051481

Guo, Q., Liu, L., Chen, Z., Fan, Y., Zhou, Y., Yuan, Z., et al. (2022). Current treatments for non-small cell lung cancer. *Front. Oncol.* 12, 945102. Epub 20220811. doi:10.3389/fonc.2022.945102

Guo, R., Li, Y., Wang, Z., Bai, H., Duan, J., Wang, S., et al. (2019). Hypoxia-inducible factor-1α and nuclear factor-κB play important roles in regulating programmed cell death ligand 1 expression by epidermal growth factor receptor mutants in non-small-cell lung cancer cells. *Cancer Sci.* 110 (5), 1665–1675. Epub 20190323. doi:10.1111/cas.13989

Han, J., Liu, Y., Yang, S., Wu, X., Li, H., and Wang, Q. (2021). MEK inhibitors for the treatment of non-small cell lung cancer. *J. Hematol. Oncol.* 14 (1), 1. Epub 20210105Cited in: Pubmed; PMID 33402199. doi:10.1186/s13045-020-01025-7

Han, K., Zhou, Y., Gan, Z. H., Qi, W. X., Zhang, J. J., Fen, T., et al. (2014). p21-activated kinase 7 is an oncogene in human osteosarcoma. *Cell Biol. Int.* 38 (12), 1394–1402. Epub 20140806. doi:10.1002/cbin.10351

Hao, Y., Zhang, X., and Yu, L. (2022). Immune checkpoint inhibitor-related pneumonitis in non-small cell lung cancer: A review. *Front. Oncol.* 12, 911906. Epub 20220816Cited in: Pubmed; PMID 36052257. doi:10.3389/fonc.2022.911906

He, S., Liu, M., Zhang, W., Xu, N., and Zhu, H. (2016). Over expression of p21-activated kinase 7 associates with lymph node metastasis in esophageal squamous cell cancers. *Cancer Biomark.* 16 (2), 203–209. . Cited in: Pubmed; PMID 26682509. doi:10.3233/CBM-150557

Herreros-Pomares, A., Doria, P., Gallach, S., Meri-Abad, M., Guijarro, R., Calabuig-Farinas, S., et al. (2022). A sonic hedgehog pathway score to predict the outcome of resected non-small cell lung cancer patients. *Ann. Surg. Oncol.* 30, 1225–1235. Epub 20220921Cited in: Pubmed; PMID 36131117. doi:10.1245/s10434-022-12565-2

Hong, D., Knelson, E. H., Li, Y., Durmaz, Y. T., Gao, W., Walton, E., et al. (2022). Plasticity in the absence of NOTCH uncovers a RUNX2-dependent pathway in small cell lung cancer. *Cancer Res.* 82 (2), 248–263. Epub 20211122. doi:10.1158/0008-5472.CAN-21-1991

Hsu, P. C., Jablons, D. M., Yang, C. T., and You, L. (2019). Epidermal growth factor receptor (EGFR) pathway, yes-associated protein (YAP) and the regulation of programmed death-ligand 1 (PD-L1) in non-small cell lung cancer (NSCLC). *Int. J. Mol. Sci.* 20 (15), 3821. Epub 20190805. doi:10.3390/ijms20153821

Hu, Q., Ma, H., Chen, H., Zhang, Z., and Xue, Q. (2022). LncRNA in tumorigenesis of non-small-cell lung cancer: From bench to bedside. *Cell Death Discov.* 8 (1), 359. Epub 20220813Cited in: Pubmed; PMID 35963868. doi:10.1038/s41420-022-01157-4

Hu, S., Zhao, X., Qian, F., Jin, C., and Hou, K. (2021). Correlation between LRP1B mutations and tumor mutation burden in gastric cancer. *Comput. Math. Methods Med.* 2021, 1522250. Epub 20210921. doi:10.1155/2021/1522250

Huang, T., Peng, L., Han, Y., Wang, D., He, X., Wang, J., et al. (2022). Lipid nanoparticle-based mRNA vaccines in cancers: Current advances and future prospects. *Front. Immunol.* 13, 922301. Epub 20220826. doi:10.3389/fimmu.2022.922301

Hui, Z., Zhang, J., Ren, Y., Li, X., Yan, C., Yu, W., et al. (2022). Single-cell profiling of immune cells after neoadjuvant pembrolizumab and chemotherapy in IIIA non-small cell lung cancer (NSCLC). *Cell Death Dis.* 13 (7), 607. Epub 20220713Cited in: Pubmed; PMID 35831283. doi:10.1038/s41419-022-05057-4

Jiang, W., Pan, S., Chen, X., Wang, Z. W., and Zhu, X. (2021). The role of lncRNAs and circRNAs in the PD-1/PD-L1 pathway in cancer immunotherapy. *Mol. Cancer* 20 (1), 116. Epub 20210908Cited in: Pubmed; PMID 34496886. doi:10.1186/s12943-021-01406-7

Jiang, Y., Wang, K., Lu, X., Wang, Y., and Chen, J. (2021). Cancer-associated fibroblasts-derived exosomes promote lung cancer progression by OIP5-AS1/miR-142-5p/PD-L1 axis. *Mol. Immunol.* 140, 47–58. Epub 20211013Cited in: Pubmed; PMID 34653794. doi:10.1016/j.molimm.2021.10.002

Jiang, W., Xia, J., Xie, S., Zou, R., Pan, S., Wang, Z. W., et al. (2020). Long non-coding RNAs as a determinant of cancer drug resistance: Towards the overcoming of chemoresistance via modulation of lncRNAs. *Drug Resist Updat* 50, 100683. Epub 20200225. doi:10.1016/j.drup.2020.100683

Jin, R., Liu, C., Zheng, S., Wang, X., Feng, X., Li, H., et al. (2020). Molecular heterogeneity of anti-PD-1/PD-L1 immunotherapy efficacy is correlated with tumor immune microenvironment in East Asian patients with non-small cell lung cancer. *Cancer Biol. Med.* 17 (3), 768–781. Cited in: Pubmed; PMID 32944405. doi:10.20892/j.issn.2095-3941.2020.0121

Jin, W., Lei, Z., Xu, S., Fachen, Z., Yixiang, Z., Shilei, Z., et al. (2021). Genetic mutation analysis in small cell lung cancer by a novel NGS-based targeted resequencing gene panel and relation with clinical features. *Biomed. Res. Int.* 2021, 3609028. Epub 20210405. doi:10.1155/2021/3609028

Kim, C., and Giaccone, G. (2018). MEK inhibitors under development for treatment of non-small-cell lung cancer. *Expert Opin. Investig. Drugs* 27 (1), 17–30. Epub 20171213. doi:10.1080/13543784.2018.1415324

Kim, J. H., Kim, H. S., and Kim, B. J. (2017). Prognostic value of KRAS mutation in advanced non-small-cell lung cancer treated with immune checkpoint inhibitors: A meta-analysis and review. *Oncotarget* 8 (29), 48248–48252. in: Pubmed; PMID 28525386. doi:10.18632/oncotarget.17594

Kohli, S., Bhardwaj, A., Kumari, R., and Das, S. (2018). SIRT6 is a target of regulation by UBE3A that contributes to liver tumorigenesis in an ANXA2-dependent manner. *Cancer Res.* 78 (3), 645–658. Epub 20171207. doi:10.1158/0008-5472.CAN-17-1692

Lee, J., Park, C. K., Yoon, H. K., Sa, Y. J., Woo, I. S., Kim, H. R., et al. (2019). PD-L1 expression in ROS1-rearranged non-small cell lung cancer: A study using simultaneous genotypic screening of EGFR, ALK, and ROS1. *Thorac. Cancer* 10 (1), 103–110. Epub 20181126. doi:10.1111/1759-7714.12917

Li, W., Ye, L., Huang, Y., Zhou, F., Wu, C., Wu, F., et al. (2022). Characteristics of Notch signaling pathway and its correlation with immune microenvironment in SCLC. *Lung Cancer* 167, 25–33. Epub 20220329Cited in: Pubmed; PMID 35381444. doi:10.1016/j.lungcan.2022.03.019

Li, J. X., Li, R. Z., Ma, L. R., Wang, P., Xu, D. H., Huang, J., et al. (2022). Targeting mutant kirsten rat sarcoma viral oncogene homolog in non-small cell lung cancer: Current difficulties, integrative treatments and future perspectives. *Front. Pharmacol.* 13, 875330. Epub 20220420. doi:10.3389/fphar.2022.875330

Li, Y., Hu, L., Peng, X., Xu, H., Tang, B., and Xu, C. (2022). Resistance to immune checkpoint inhibitors in KRAS-mutant non-small cell lung cancer. *Cancer Drug Resist* 5 (1), 129–146. Epub 20220208. doi:10.20517/cdr.2021.102

Li, K., Xu, X., He, Y., Tian, Y., Pan, W., Xu, L., et al. (2018). P21-activated kinase 7 (PAK7) interacts with and activates Wnt/β-catenin signaling pathway in breast cancer. *J. Cancer* 9 (10), 1821–1835. Epub 20180422. doi:10.7150/jca.24934

Li, L., Wang, Y., Shi, W., Zhu, M., Liu, Z., Luo, N., et al. (2019). Serial ultra-deep sequencing of circulating tumor DNA reveals the clonal evolution in non-small cell lung cancer patients treated with anti-PD1 immunotherapy. *Cancer Med.* 8 (18), 7669–7678. Epub 20191106. doi:10.1002/cam4.2632

Li, M., Qin, X., Xue, X., Zhang, C., Yan, Z., Han, W., et al. (2010). Safety evaluation and pharmacokinetics of a novel human tumor necrosis factor-alpha exhibited a higher antitumor activity and a lower systemic toxicity. *Anticancer Drugs* 21 (3), 243–251. . Cited in: Pubmed; PMID 20166241. doi:10.1097/cad.0b013e328333d5ce

Li, M., Xu, T., Zhang, Z., Xue, X., Zhang, C., Qin, X., et al. (2012). Phase II multicenter, randomized, double-blind study of recombinant mutated human tumor necrosis factor-alpha in combination with chemotherapies in cancer patients. *Cancer Sci.* 103 (2), 288–295. Epub 20120109. doi:10.1111/j.1349-7006.2011.02153.x

Li, T., and Qiao, T. (2022). Unraveling tumor microenvironment of small-cell lung cancer: Implications for immunotherapy. *Semin. Cancer Biol.* 86 (2), 117–125. Epub 20220929Cited in: Pubmed; PMID 36183998. doi:10.1016/j.semcancer.2022.09.005

Li, X., Wang, Y., Li, X., Feng, G., Hu, S., and Bai, Y. (2021). The impact of NOTCH pathway alteration on tumor microenvironment and clinical survival of immune checkpoint inhibitors in NSCLC. *Front. Immunol.* 12, 638763. Epub 20210709. doi:10.3389/fimmu.2021.638763

Lin, A., Wei, T., Meng, H., Luo, P., and Zhang, J. (2019). Role of the dynamic tumor microenvironment in controversies regarding immune checkpoint inhibitors for the treatment of non-small cell lung cancer (NSCLC) with EGFR mutations. *Mol. Cancer* 18 (1), 139. Epub 20190916Cited in: Pubmed; PMID 31526368. doi:10.1186/s12943-019-1062-7

Lin, A., Zhang, H., Meng, H., Deng, Z., Gu, T., Luo, P., et al. (2021). TNF-alpha pathway alternation predicts survival of immune checkpoint inhibitors in non-small cell lung cancer. *Front. Immunol.* 12, 667875. Epub 20210916. doi:10.3389/fimmu.2021.667875

Lin, C., Chen, X., Li, M., Liu, J., Qi, X., Yang, W., et al. (2015). Programmed death-ligand 1 expression predicts tyrosine kinase inhibitor response and better prognosis in a cohort of patients with epidermal growth factor receptor mutation-positive lung

adenocarcinoma. *Clin. Lung Cancer* 16 (5), e25–e35. Epub 20150219Cited in: Pubmed; PMID 25801750. doi:10.1016/j.cllc.2015.02.002

Liu, C., Zheng, S., Jin, R., Wang, X., Wang, F., Zang, R., et al. (2020). The superior efficacy of anti-PD-1/PD-L1 immunotherapy in KRAS-mutant non-small cell lung cancer that correlates with an inflammatory phenotype and increased immunogenicity. *Cancer Lett.* 470, 95–105. Epub 20191020Cited in: Pubmed; PMID 31644929. doi:10.1016/j.canlet.2019.10.027

Liu, C., Zheng, S., Wang, Z., Wang, S., Wang, X., Yang, L., et al. (2022). KRAS-G12D mutation drives immune suppression and the primary resistance of anti-PD-1/PD-L1 immunotherapy in non-small cell lung cancer. *Cancer Commun. (Lond)* 42 (9), 828–847. Epub 20220711. doi:10.1002/cac2.12327

Liu, F., Wei, Y., Zhang, H., Jiang, J., Zhang, P., and Chu, Q. (2022). NTRK fusion in non-small cell lung cancer: Diagnosis, therapy, and TRK inhibitor resistance. *Front. Oncol.* 12, 864666. Epub 20220317. doi:10.3389/fonc.2022.864666

Liu, J., Chen, T., Li, S., Liu, W., Wang, P., and Shang, G. (2022). Targeting matrix metalloproteinases by E3 ubiquitin ligases as a way to regulate the tumor microenvironment for cancer therapy. *Semin. Cancer Biol.* 86 (2), 259–268. Epub 20220618Cited in: Pubmed; PMID 35724822. doi:10.1016/j.semcancer.2022.06.004

Liu, J., and Shang, G. (2022). The roles of noncoding RNAs in the development of osteosarcoma stem cells and potential therapeutic targets. *Front. Cell Dev. Biol.* 10, 773038. Epub 20220216. doi:10.3389/fcell.2022.773038

Liu, S. Y., Dong, Z. Y., Wu, S. P., Xie, Z., Yan, L. X., Li, Y. F., et al. (2018). Clinical relevance of PD-L1 expression and CD8+ T cells infiltration in patients with EGFR-mutated and ALK-rearranged lung cancer. *Lung Cancer* 125, 86–92. Epub 20180914Cited in: Pubmed; PMID 30429043. doi:10.1016/j.lungcan.2018.09.010

Liu, X. Y., Cui, Y. N., Li, J., Zhang, Z., and Guo, R. H. (2022). Effect of FBXW7 gene mutation on the prognosis of immunotherapy in patients with non-small cell lung cancer. *Zhonghua Yi Xue Za Zhi* 102 (13), 914–921. Cited in: Pubmed; PMID 35385962. doi:10.3760/cma.j.cn112137-20211021-02332

Long, J., Wang, D., Yang, X., Wang, A., Lin, Y., Zheng, M., et al. (2021). Identification of NOTCH4 mutation as a response biomarker for immune checkpoint inhibitor therapy. *BMC Med.* 19 (1), 154. Epub 20210721Cited in: Pubmed; PMID 34284787. doi:10.1186/s12916-021-02031-3

Luo, W., Wang, Z., Zhang, T., Yang, L., Xian, J., Li, Y., et al. (2021). Immunotherapy in non-small cell lung cancer: Rationale, recent advances and future perspectives. *Precis. Clin. Med.* 4 (4), 258–270. Epub 20211202. doi:10.1093/pcmedi/pbab027

Ma, X., Song, Y., Zhang, K., Shang, L., Gao, Y., Zhang, W., et al. (2015). Recombinant mutated human TNF in combination with chemotherapy for stage IIIB/IV non-small cell lung cancer: A randomized, phase III study. *Sci. Rep.* 4, 9918. Epub 20150421. doi:10.1038/srep09918

Majumder, S., Crabtree, J. S., Golde, T. E., Minter, L. M., Osborne, B. A., and Miele, L. (2021). Targeting Notch in oncology: The path forward. *Nat. Rev. Drug Discov.* 20 (2), 125–144. Epub 20201208Cited in: Pubmed; PMID 33293690. doi:10.1038/s41573-020-00091-3

Malhotra, J., Ryan, B., Patel, M., Chan, N., Guo, Y., Aisner, J., et al. (2022). Clinical outcomes and immune phenotypes associated with STK11 co-occurring mutations in non-small cell lung cancer. *J. Thorac. Dis.* 14 (6), 1772–1783. Cited in: Pubmed; PMID 35813711. doi:10.21037/jtd-21-1377

Martin, C., and Enrico, D. (2022). Current and novel therapeutic strategies for optimizing immunotherapy outcomes in advanced non-small cell lung cancer. *Front. Oncol.* 12, 962947. Epub 20221208. doi:10.3389/fonc.2022.962947

Maynard, A., McCoach, C. E., Rotow, J. K., Harris, L., Haderk, F., Kerr, D. L., et al. (2020). Therapy-induced evolution of human lung cancer revealed by single-cell RNA sequencing. *Cell* 182 (5), 1232–1251.e22. e22 Epub 20200820Cited in: Pubmed; PMID 32822576. doi:10.1016/j.cell.2020.07.017

Mengoli, M. C., Longo, F. R., Fraggetta, F., Cavazza, A., Dubini, A., Ali, G., et al. (2018). The 2015 world health organization classification of lung tumors: New entities since the 2004 classification. *Pathologica* 110 (1), 39–67. Cited in: Pubmed; PMID 30259912.

Miller, K. D., Nogueira, L., Devasia, T., Mariotto, A. B., Yabroff, K. R., Jemal, A., et al. (2022). Cancer treatment and survivorship statistics. *CA Cancer J. Clin.* 72 (5), 409–436. Epub 20220623. doi:10.3322/caac.21731

Minamiya, Y., Saito, H., Ito, M., Imai, K., Konno, H., Takahashi, N., et al. (2012). Suppression of Zinc Finger Homeobox 3 expression in tumor cells decreases the survival rate among non-small cell lung cancer patients. *Cancer Biomark.* 11 (4), 139–146. . Cited in: Pubmed; PMID 23144151. doi:10.3233/CBM-2012-00272

Mussafi, O., Mei, J., Mao, W., and Wan, Y. (2022). Immune checkpoint inhibitors for PD-1/PD-L1 axis in combination with other immunotherapies and targeted therapies for non-small cell lung cancer. *Front. Oncol.* 12, 948405. Epub 20220817. doi:10.3389/fonc.2022.948405

Nallasamy, P., Nimmakayala, R. K., Parte, S., Are, A. C., Batra, S. K., and Ponnusamy, M. P. (2022). Tumor microenvironment enriches the stemness features: The architectural event of therapy resistance and metastasis. *Mol. Cancer* 21 (1), 225. Epub 20221222Cited in: Pubmed; PMID 36550571. doi:10.1186/s12943-022-01682-x

Ni, J., and Zhang, L. (2021). Progress in treatment of non-small cell lung cancer harboring HER2 aberrations. *Onco Targets Ther.* 14, 4087–4098. Epub 20210706. doi:10.2147/OTT.S312820

Niu, L., Dang, C., Li, L., Guo, N., Xu, Y., Li, X., et al. (2021). Next-generation sequencing-based identification of EGFR and NOTCH2 complementary mutations in non-small cell lung cancer. *Oncol. Lett.* 22 (2), 594. Epub 20210607. doi:10.3892/ol.2021.12855

Olmedo, M. E., Cervera, R., Cabezon-Gutierrez, L., Lage, Y., Corral de la Fuente, E., Gomez Rueda, A., et al. (2022). New horizons for uncommon mutations in non-small cell lung cancer: BRAF, KRAS, RET, MET, NTRK, HER2. *World J. Clin. Oncol.* 13 (4), 276–286. in: Pubmed; PMID 35582653. doi:10.5306/wjco.v13.i4.276

Osielska, M. A., and Jagodzinski, P. P. (2018). Long non-coding RNA as potential biomarkers in non-small-cell lung cancer: What do we know so far? *Biomed. Pharmacother.* 101, 322–333. Epub 20180322Cited in: Pubmed; PMID 29499406. doi:10.1016/j.biopha.2018.02.099

Owais, A., Mishra, R. K., and Kiyokawa, H. (2020). The HECT E3 ligase e6ap/ube3a as a therapeutic target in cancer and neurological disorders. *Cancers (Basel)* 12 (8), 2108. Epub 20200729. doi:10.3390/cancers12082108

Pang, Z., Chen, X., Wang, Y., Wang, Y., Yan, T., Wan, J., et al. (2021). Long non-coding RNA C5orf64 is a potential indicator for tumor microenvironment and mutation pattern remodeling in lung adenocarcinoma. *Genomics* 113, 291–304. Epub 20201210Cited in: Pubmed; PMID 33309768. doi:10.1016/j.ygeno.2020.12.010

Pao, W., and Girard, N. (2011). New driver mutations in non-small-cell lung cancer. *Lancet Oncol.* 12 (2), 175–180. Cited in: Pubmed; PMID 21277552. doi:10.1016/S1470-2045(10)70087-5

Passaro, A., Janne, P. A., Mok, T., and Peters, S. (2021). Overcoming therapy resistance in EGFR-mutant lung cancer. *Nat. Cancer* 2 (4), 377–391. Epub 20210415Cited in: Pubmed; PMID 35122001. doi:10.1038/s43018-021-00195-8

Peng, L., Wang, Z., Stebbing, J., and Yu, Z. (2022). Novel immunotherapeutic drugs for the treatment of lung cancer. *Curr. Opin. Oncol.* 34 (1), 89–94. . Cited in: Pubmed; PMID 34636350. doi:10.1097/CCO.0000000000000800

Peng, S., Wang, R., Zhang, X., Ma, Y., Zhong, L., Li, K., et al. (2019). EGFR-TKI resistance promotes immune escape in lung cancer via increased PD-L1 expression. *Mol. Cancer* 18 (1), 165. Epub 20191120Cited in: Pubmed; PMID 31747941. doi:10.1186/s12943-019-1073-4

Peng, Z., and Chen, Q. (2019). Research progress in the role of FBXW7 in drug resistance against non-small cell lung cancer. *Zhong Nan Da Xue Xue Bao Yi Xue Ban.* 44 (4), 444–448. Cited in: Pubmed; PMID 31113922. doi:10.11817/j.issn.1672-7347.2019.04.016

Principe, C., Dionisio de Sousa, I. J., Prazeres, H., Soares, P., and Lima, R. T. (2021). LRP1B: A giant lost in cancer translation. *Pharm. (Basel)* 14 (9), 836. Epub 20210824. doi:10.3390/ph14090836

Principe, D. R. (2022). Patients deriving long-term benefit from immune checkpoint inhibitors demonstrate conserved patterns of site-specific mutations. *Sci. Rep.* 12 (1), 11490. Epub 20220707Cited in: Pubmed; PMID 35798829. doi:10.1038/s41598-022-15714-5

Qin, H., and Patel, M. R. (2022). The challenge and opportunity of NTRK inhibitors in non-small cell lung cancer. *Int. J. Mol. Sci.* 23 (6), 2916. Epub 20220308. doi:10.3390/ijms23062916

Quan, L., Cheng, Z., Dai, Y., Jiao, Y., Shi, J., and Fu, L. (2020). Prognostic significance of PAK family kinases in acute myeloid leukemia. *Cancer Gene Ther.* 27 (1-2), 30–37. Epub 20190320Cited in: Pubmed; PMID 30890765. doi:10.1038/s41417-019-0090-1

Rangachari, D., VanderLaan, P. A., Shea, M., Le, X., Huberman, M. S., Kobayashi, S. S., et al. (2017). Correlation between classic driver oncogene mutations in EGFR, ALK, or ROS1 and 22C3-PD-L1 ≥50% expression in lung adenocarcinoma. *J. Thorac. Oncol.* 12 (5), 878–883. Epub 20170116. doi:10.1016/j.jtho.2016.12.026

Rashed, H. E., Abdelrahman, A. E., Abdelgawad, M., Balata, S., and Shabrawy, M. E. (2017). Prognostic significance of programmed cell death ligand 1 (PD-L1), CD8+ tumor-infiltrating lymphocytes and p53 in non-small cell lung cancer: An immunohistochemical study. *Turk Patoloji Derg.* 1 (1), 211–222. Cited in: Pubmed; PMID 28832075. doi:10.5146/tjpath.2017.01398

Ricciuti, B., Leonardi, G. C., Metro, G., Grignani, F., Paglialunga, L., Bellezza, G., et al. (2016). Targeting the KRAS variant for treatment of non-small cell lung cancer: Potential therapeutic applications. *Expert Rev. Respir. Med.* 10 (1), 53–68. Epub 20151117. doi:10.1586/17476348.2016.1115349

Riudavets, M., Cascetta, P., and Planchard, D. (2022). Targeting BRAF-mutant non-small cell lung cancer: Current status and future directions. *Lung Cancer* 169, 102–114. Epub 20220526Cited in: Pubmed; PMID 35696864. doi:10.1016/j.lungcan.2022.05.014

Roman, M., Baraibar, I., Lopez, I., Nadal, E., Rolfo, C., Vicent, S., et al. (2018). KRAS oncogene in non-small cell lung cancer: Clinical perspectives on the treatment of an old target. *Mol. Cancer* 17 (1), 33. Epub 20180219Cited in: Pubmed; PMID 29455666. doi:10.1186/s12943-018-0789-x

Sakai, H., Takeda, M., Sakai, K., Nakamura, Y., Ito, A., Hayashi, H., et al. (2019). Impact of cytotoxic chemotherapy on PD-L1 expression in patients with non-small cell lung cancer negative for EGFR mutation and ALK fusion. *Lung Cancer* 127, 59–65. Epub 20181123Cited in: Pubmed; PMID 30642552. doi:10.1016/j.lungcan.2018.11.025

Serra, P., Petat, A., Maury, J. M., Thivolet-Bejui, F., Chalabreysse, L., Barritault, M., et al. (2018). Programmed cell death-ligand 1 (PD-L1) expression is associated with

RAS/TP53 mutations in lung adenocarcinoma. *Lung Cancer* 118, 62–68. Epub 20180206Cited in: Pubmed; PMID 29572005. doi:10.1016/j.lungcan.2018.02.005

Sforza, V., Palumbo, G., Cascetta, P., Carillio, G., Manzo, A., Montanino, A., et al. (2022). BRAF inhibitors in non-small cell lung cancer. *Cancers (Basel)* 14 (19), 4863. Epub 20221005. doi:10.3390/cancers14194863

Shin, N. K., Lee, I., Chang, S. G., and Shin, H. C. (1998). A novel tumor necrosis factor-alpha mutant with significantly enhanced cytotoxicity and receptor binding affinity. *Biochem. Mol. Biol. Int.* 44 (6), 1075–1082. in: Pubmed; PMID 9623760. doi:10.1080/15216549800202142

Siegel, R. L., Miller, K. D., Fuchs, H. E., and Jemal, A. (2022). Cancer statistics, 2022. *CA Cancer J. Clin.* 72 (1), 7–33. Epub 20220112. doi:10.3322/caac.21708

Sigafoos, A. N., Paradise, B. D., and Fernandez-Zapico, M. E. (2021). Hedgehog/GLI signaling pathway: Transduction, regulation, and implications for disease. *Cancers (Basel)* 13 (14), 3410. Epub 20210707. doi:10.3390/cancers13143410

Skoulidis, F., Goldberg, M. E., Greenawalt, D. M., Hellmann, M. D., Awad, M. M., Gainor, J. F., et al. (2018). STK11/LKB1 mutations and PD-1 inhibitor resistance in KRAS-mutant lung adenocarcinoma. *Cancer Discov.* 8 (7), 822–835. Epub 20180517Cited in: Pubmed; PMID 29773717. doi:10.1158/2159-8290.CD-18-0099

Skoulidis, F., and Heymach, J. V. (2019). Co-occurring genomic alterations in non-small-cell lung cancer biology and therapy. *Nat. Rev. Cancer* 19 (9), 495–509. Epub 20190812Cited in: Pubmed; PMID 31406302. doi:10.1038/s41568-019-0179-8

Song, Z., Yang, L., Zhou, Z., Li, P., Wang, W., Cheng, G., et al. (2021). Genomic profiles and tumor immune microenvironment of primary lung carcinoma and brain oligo-metastasis. *Cell Death Dis.* 12 (1), 106. Epub 20210121Cited in: Pubmed; PMID 33479213. doi:10.1038/s41419-021-03410-7

Sun, H., Liu, S. Y., Zhou, J. Y., Xu, J. T., Zhang, H. K., Yan, H. H., et al. (2020). Specific TP53 subtype as biomarker for immune checkpoint inhibitors in lung adenocarcinoma. *EBioMedicine* 60, 102990. Epub 20200911Cited in: Pubmed; PMID 32927274. doi:10.1016/j.ebiom.2020.102990

Sung, H., Ferlay, J., Siegel, R. L., Laversanne, M., Soerjomataram, I., Jemal, A., et al. (2021). Global cancer statistics 2020: GLOBOCAN estimates of incidence and mortality worldwide for 36 cancers in 185 countries. *CA Cancer J. Clin.* 71 (3), 209–249. Epub 20210204. doi:10.3322/caac.21660

Tartarone, A., Lerose, R., Tartarone, M., and Aieta, M. (2022). Potential role of tumor-derived exosomes in non-small-cell lung cancer in the era of immunotherapy. *Life (Basel)* 12 (12), 2104. Epub 20221214. doi:10.3390/life12122104

Tiwari, A., Trivedi, R., and Lin, S. Y. (2022). Tumor microenvironment: Barrier or opportunity towards effective cancer therapy. *J. Biomed. Sci.* 29 (1), 83. Epub 20221017Cited in: Pubmed; PMID 36253762. doi:10.1186/s12929-022-00866-3

Tu, E., McGlinchey, K., Wang, J., Martin, P., Ching, S. L., Floc'h, N., et al. (2022). Anti-PD-L1 and anti-CD73 combination therapy promotes T cell response to EGFR-mutated NSCLC. *JCI Insight* 7 (3), e142843. Epub 20220208Cited in: Pubmed; PMID 35132961. doi:10.1172/jci.insight.142843

Turner, M. C., Andersen, Z. J., Baccarelli, A., Diver, W. R., Gapstur, S. M., Pope, C. A., 3rd, et al. (2020). Outdoor air pollution and cancer: An overview of the current evidence and public health recommendations. *CA Cancer J. Clin.* 70, 460–479. Epub 20200825. doi:10.3322/caac.21632

Uras, I. Z., Moll, H. P., and Casanova, E. (2020). Targeting KRAS mutant non-small-cell lung cancer: Past, present and future. *Int. J. Mol. Sci.* 21 (12), 4325. Epub 20200617. doi:10.3390/ijms21124325

Vathiotis, I. A., Charpidou, A., Gavrielatou, N., and Syrigos, K. N. (2021). HER2 aberrations in non-small cell lung cancer: From pathophysiology to targeted therapy. *Pharm. (Basel)* 14 (12), 1300. Epub 20211214. doi:10.3390/ph14121300

Wan, L., Liu, Q., Liang, D., Guo, Y., Liu, G., Ren, J., et al. (2021). Circulating tumor cell and metabolites as novel biomarkers for early-stage lung cancer diagnosis. *Front. Oncol.* 11, 630672. Epub 20210531. doi:10.3389/fonc.2021.630672

Wang, L., Ma, L., Xu, F., Zhai, W., Dong, S., Yin, L., et al. (2018). Role of long non-coding RNA in drug resistance in non-small cell lung cancer. *Thorac. Cancer* 9 (7), 761–768. Epub 20180503. doi:10.1111/1759-7714.12652

Wang, M., Herbst, R. S., and Boshoff, C. (2021). Toward personalized treatment approaches for non-small-cell lung cancer. *Nat. Med.* 27 (8), 1345–1356. Epub 20210812Cited in: Pubmed; PMID 34385702. doi:10.1038/s41591-021-01450-2

Wang, S., Jiang, M., Yang, Z., Huang, X., and Li, N. (2022). The role of distinct co-mutation patterns with TP53 mutation in immunotherapy for NSCLC. *Genes Dis.* 9 (1), 245–251. Epub 20200409Cited in: Pubmed; PMID 35005121. doi:10.1016/j.gendis.2020.04.001

Wang, Z., Ge, Y., Li, H., Fei, G., Wang, S., and Wei, P. (2022). Identification and validation of a genomic mutation signature as a predictor for immunotherapy in NSCLC. *Biosci. Rep.* (11), 42. in: Pubmed; PMID 36305643. doi:10.1042/BSR20220892

Wang, X., Liu, S., Shao, Z., and Zhang, P. (2020). Bioinformatic analysis of the potential molecular mechanism of PAK7 expression in glioblastoma. *Mol. Med. Rep.* 22 (2), 1362–1372. Epub 20200603. doi:10.3892/mmr.2020.11206

Wang, Z., Liu, P., Inuzuka, H., and Wei, W. (2014). Roles of F-box proteins in cancer. *Nat. Rev. Cancer* 14 (4), 233–247. in: Pubmed; PMID 24658274. doi:10.1038/nrc3700

Weng, C., Wang, L., Liu, G., Guan, M., and Lu, L. (2021). Identification of a N6-methyladenosine (m6A)-Related lncRNA signature for predicting the prognosis and immune landscape of lung squamous cell carcinoma. *Front. Oncol.* 11, 763027. Epub 20211118. doi:10.3389/fonc.2021.763027

Wood, K., Hensing, T., Malik, R., and Salgia, R. (2016). Prognostic and predictive value in KRAS in non-small-cell lung cancer: A review. *JAMA Oncol.* 2 (6), 805–812. Cited in: Pubmed; PMID 27100819. doi:10.1001/jamaoncol.2016.0405

Wu, F., Fan, J., He, Y., Xiong, A., Yu, J., Li, Y., et al. (2021). Single-cell profiling of tumor heterogeneity and the microenvironment in advanced non-small cell lung cancer. *Nat. Commun.* 12 (1), 2540. Epub 20210505Cited in: Pubmed; PMID 33953163. doi:10.1038/s41467-021-22801-0

Wu, M., Huang, Q., Xie, Y., Wu, X., Ma, H., Zhang, Y., et al. (2022). Improvement of the anticancer efficacy of PD-1/PD-L1 blockade via combination therapy and PD-L1 regulation. *J. Hematol. Oncol.* 15 (1), 24. Epub 20220312Cited in: Pubmed; PMID 35279217. doi:10.1186/s13045-022-01242-2

Xiang, Y., Zhang, S., Fang, X., Jiang, Y., Fang, T., Liu, J., et al. (2022). Therapeutic advances of rare ALK fusions in non-small cell lung cancer. *Curr. Oncol.* 29 (10), 7816–7831. Epub 20221016. doi:10.3390/curroncol29100618

Xiao, Y., Yin, C., Wang, Y., Lv, H., Wang, W., Huang, Y., et al. (2018). FBXW7 deletion contributes to lung tumor development and confers resistance to gefitinib therapy. *Mol. Oncol.* 12 (6), 883–895. Epub 20180509. doi:10.1002/1878-0261.12200

Xie, W., Chu, M., Song, G., Zuo, Z., Han, Z., Chen, C., et al. (2022). Emerging roles of long noncoding RNAs in chemoresistance of pancreatic cancer. *Semin. Cancer Biol.* 83, 303–318. Epub 20201115Cited in: Pubmed; PMID 33207266. doi:10.1016/j.semcancer.2020.11.004

Xu, F., Cui, W. Q., Liu, C., Feng, F., Liu, R., Zhang, J., et al. (2023). Prognostic biomarkers correlated with immune infiltration in non-small cell lung cancer. *FEBS Open Bio* 13 (1), 72–88. Epub 20221128. doi:10.1002/2211-5463.13501

Yan, H., and Bu, P. (2021). Non-coding RNA in cancer. *Essays Biochem.* 65 (4), 625–639. in: Pubmed; PMID 33860799. doi:10.1042/ebc20200032

Yan, L., Lin, M., Pan, S., Assaraf, Y. G., Wang, Z. W., and Zhu, X. (2020). Emerging roles of F-box proteins in cancer drug resistance. *Drug Resist Updat* 49, 100673. Epub 20191217. doi:10.1016/j.drup.2019.100673

Yan, Q., Hu, B., Chen, H., Zhu, L., Lyu, Y., Qian, D., et al. (2022). A novel algorithm for lung adenocarcinoma based on N6 methyladenosine-related immune long noncoding RNAs as a reliable biomarker for predicting survival outcomes and selecting sensitive anti-tumor therapies. *J. Clin. Lab. Anal.* 36 (9), e24636. Epub 20220810. doi:10.1002/jcla.24636

Yan, Z., Zhao, N., Wang, Z., Li, B., Bao, C., Shi, J., et al. (2006). A mutated human tumor necrosis factor-alpha improves the therapeutic index *in vitro* and *in vivo*. *Cytotherapy* 8 (4), 415–423. in: Pubmed; PMID 16923618. doi:10.1080/14653240600845278

Yang, T., Xiong, Y., Zeng, Y., Wang, Y., Zeng, J., Liu, J., et al. (2022). Current status of immunotherapy for non-small cell lung cancer. *Front. Pharmacol.* 13, 989461. Epub 20221013. doi:10.3389/fphar.2022.989461

Yang, Z., Gao, A., Shi, W., Wang, J., Zhang, X., Xu, Z., et al. (2021). ILT4 in colorectal cancer cells induces suppressive T cell contexture and disease progression. *Onco Targets Ther.* 14, 4239–4254. Epub 20210720. doi:10.2147/OTT.S290348

Yu, X., Ji, X., and Su, C. (2022). HER2-Altered non-small cell lung cancer: Biology, clinicopathologic features, and emerging therapies. *Front. Oncol.* 12, 860313. Epub 20220329. doi:10.3389/fonc.2022.860313

Yu, Z. Q., Wang, M., Zhou, W., Mao, M. X., Chen, Y. Y., Li, N., et al. (2022). ROS1-positive non-small cell lung cancer (NSCLC): Biology, diagnostics, therapeutics and resistance. *J. Drug Target* 30 (8), 845–857. Epub 20220614. doi:10.1080/1061186X.2022.2085730

Yue, D., Qian, J., Chen, Z., Zhang, B., Chen, P., Zhang, L., et al. (2021). Short-term response to immune-chemotherapy and immune features of a ceritinib-resistant patient with ROS1-rearranged lung adenocarcinoma. *J. Immunother. Cancer* 9 (2), e001967. Cited in: Pubmed; PMID 33558279. doi:10.1136/jitc-2020-001967

Zeng, H., Tong, F., Bin, Y., Peng, L., Gao, X., Xia, X., et al. (2022). The predictive value of PAK7 mutation for immune checkpoint inhibitors therapy in non-small cell cancer. *Front. Immunol.* 13, 834142. Epub 20220203. doi:10.3389/fimmu.2022.834142

Zhang, H. H., Zhang, Z. Y., Che, C. L., Mei, Y. F., and Shi, Y. Z. (2013). Array analysis for potential biomarker of gemcitabine identification in non-small cell lung cancer cell lines. *Int. J. Clin. Exp. Pathol.* 6 (9), 1734–1746. Epub 20130815. Cited in: Pubmed; PMID 24040438.

Zhang, J., Zhou, N., Lin, A., Luo, P., Chen, X., Deng, H., et al. (2021). ZFHX3 mutation as a protective biomarker for immune checkpoint blockade in non-small cell lung cancer. *Cancer Immunol. Immunother.* 70 (1), 137–151. Epub 20200711Cited in: Pubmed; PMID 32653938. doi:10.1007/s00262-020-02668-8

Zhang, L., Zhang, T., Shang, B., Li, Y., Cao, Z., and Wang, H. (2021). Prognostic effect of coexisting TP53 and ZFHX3 mutations in non-small cell lung cancer patients treated with immune checkpoint inhibitors. *Scand. J. Immunol.* 94 (3), e13087. Epub 20210613. doi:10.1111/sji.13087

Zhang, K., Hong, X., Song, Z., Xu, Y., Li, C., Wang, G., et al. (2020). Identification of deleterious NOTCH mutation as novel predictor to efficacious immunotherapy in NSCLC. *Clin. Cancer Res.* 26 (14), 3649–3661. Epub 20200402Cited in: Pubmed; PMID 32241817. doi:10.1158/1078-0432.CCR-19-3976

Zhang, L. X., Gao, J., Long, X., Zhang, P. F., Yang, X., Zhu, S. Q., et al. (2022). The circular RNA circHMGB2 drives immunosuppression and anti-PD-1 resistance in lung adenocarcinomas and squamous cell carcinomas via the miR-181a-5p/CARM1 axis. *Mol. Cancer* 21 (1), 110. Epub 20220507Cited in: Pubmed; PMID 35525959. doi:10.1186/s12943-022-01586-w

Zhang, N., Shen, J., Gou, L., Cao, M., Ding, W., Luo, P., et al. (2022). UBE3A deletion enhances the efficiency of immunotherapy in non-small-cell lung cancer. *Bioengineered* 13 (5), 11577–11592. in: Pubmed; PMID 35531878. doi:10.1080/21655979.2022.2069328

Zhang, P., Li, H., Cheng, X., and Wang, W. (2022). Comprehensive analysis of immune cell infiltration of m6a-related lncRNA in lung squamous cell carcinoma and construction of relevant prognostic models. *Biomed. Res. Int.* 2022, 9139823. Epub 20220714. doi:10.1155/2022/9139823

Zhang, W., Zhang, Q., Xie, Z., Che, L., Xia, T., Cai, X., et al. (2022). N^6-Methyladenosine-Related long non-coding RNAs are identified as a potential prognostic biomarker for lung squamous cell carcinoma and validated by real-time PCR. *Front. Genet.* 13, 839957. Epub 20220603. doi:10.3389/fgene.2022.839957

Zhang, Y., Zeng, Y., Liu, T., Du, W., Zhu, J., Liu, Z., et al. (2019). The canonical TGF-β/Smad signalling pathway is involved in PD-L1-induced primary resistance to EGFR-TKIs in EGFR-mutant non-small-cell lung cancer. *Respir. Res.* 20 (1), 164. Epub 20190722Cited in: Pubmed; PMID 31331328. doi:10.1186/s12931-019-1137-4

Zhao, D., Liu, X., Shan, Y., Li, J., Cui, W., Wang, J., et al. (2022). Recognition of immune-related tumor antigens and immune subtypes for mRNA vaccine development in lung adenocarcinoma. *Comput. Struct. Biotechnol. J.* 20, 5001–5013. Epub 20220905Cited in: Pubmed; PMID 36187916. doi:10.1016/j.csbj.2022.08.066

Zhao, W., Zhou, W., Rong, L., Sun, M., Lin, X., Wang, L., et al. (2022). Epidermal growth factor receptor mutations and brain metastases in non-small cell lung cancer. *Front. Oncol.* 12, 912505. Epub 20221115. doi:10.3389/fonc.2022.912505

Zhao, J., Lin, X., Zhuang, J., and He, F. (2021). Relationships of N6-methyladenosine-related long non-coding RNAs with tumor immune microenvironment and clinical prognosis in lung adenocarcinoma. *Front. Genet.* 12, 714697. Epub 20211020. doi:10.3389/fgene.2021.714697

Zheng, Z., Zhang, B., Yu, H., Li, S., Song, N., Jin, X., et al. (2021). UBE3A activates the NOTCH pathway and promotes esophageal cancer progression by degradation of ZNF185. *Int. J. Biol. Sci.* 17 (12), 3024–3035. Epub 20210713. doi:10.7150/ijbs.61117

Zhong, H., Liu, S., Cao, F., Zhao, Y., Zhou, J., Tang, F., et al. (2021). Dissecting tumor antigens and immune subtypes of glioma to develop mRNA vaccine. *Front. Immunol.* 12, 709986. Epub 20210827. doi:10.3389/fimmu.2021.709986

Zhou, J., Bao, M., Gao, G., Cai, Y., Wu, L., Lei, L., et al. (2022). Increased blood-based intratumor heterogeneity (bITH) is associated with unfavorable outcomes of immune checkpoint inhibitors plus chemotherapy in non-small cell lung cancer. *BMC Med.* 20 (1), 256. Epub 20220729Cited in: Pubmed; PMID 35902848. doi:10.1186/s12916-022-02444-8

Zhou, X., Ao, X., Jia, Z., Li, Y., Kuang, S., Du, C., et al. (2022). Non-coding RNA in cancer drug resistance: Underlying mechanisms and clinical applications. *Front. Oncol.* 12, 951864. Epub 20220817. doi:10.3389/fonc.2022.951864

Zhou, J. G., Zhong, H., Zhang, J., Jin, S. H., Roudi, R., and Ma, H. (2019). Development and validation of a prognostic signature for malignant pleural mesothelioma. *Front. Oncol.* 9, 78. Epub 20190215. doi:10.3389/fonc.2019.00078

Zhou, X., Xu, X., Tian, Z., Xu, W. Y., and Cui, Y. (2020). Mutational profiling of lung adenocarcinoma in China detected by next-generation sequencing. *J. Cancer Res. Clin. Oncol.* 146 (9), 2277–2287. Epub 20200622Cited in: Pubmed; PMID 32572558. doi:10.1007/s00432-020-03284-w

frontiers | Frontiers in Pharmacology

TYPE Original Research
PUBLISHED 22 March 2023
DOI 10.3389/fphar.2023.1141075

OPEN ACCESS

EDITED BY
Ouyang Chen,
Duke University, United States

REVIEWED BY
Wu Lanxiang,
Chongqing Medical University, China
Mingzhu Yin,
Chongqing University Three Gorges Hospital, Chongqing University, China
Liu Yang,
Huazhong University of Science and Technology, China
Ran Guo,
Duke University, United States

*CORRESPONDENCE
Wangqing Chen,
✉ Lanchen2008@163.com
Kai Huang,
✉ kaiserhuang@csu.edu.cn

†These authors have contributed equally to this work

SPECIALTY SECTION
This article was submitted to Pharmacology of Anti-Cancer Drugs, a section of the journal Frontiers in Pharmacology

RECEIVED 09 January 2023
ACCEPTED 01 March 2023
PUBLISHED 22 March 2023

CITATION
Lai S, Xu L, Zhang L, Peng L, Li Y, Liu Y, Yu N, Chen W and Huang K (2023), Global trends in the health economics field of PD-1/PD-L1 inhibitors: A bibliometric and visualized study.
Front. Pharmacol. 14:1141075.
doi: 10.3389/fphar.2023.1141075

Global trends in the health economics field of PD-1/PD-L1 inhibitors: A bibliometric and visualized study

Sicen Lai[1,2,3,4†], Licong Xu[1,2,3,5†], Liang Zhang[6†], Lanyuan Peng[1,2,3,5], Yixin Li[1,2,3,5], Yuancheng Liu[1,2,3,5], Nianzhou Yu[1,2,3,5], Wangqing Chen[1,2,3,5*] and Kai Huang[1,2,3,5*]

[1]Department of Dermatology, Xiangya Hospital, Central South University, Changsha, China, [2]Hunan Engineering Research Center of Skin Health and Disease, Central South University, Changsha, China, [3]Hunan Key Laboratory of Skin Cancer and Psoriasis, Xiangya Hospital, Central South University, Changsha, China, [4]XiangYa School of Medicine, Central South University, Changsha, China, [5]National Clinical Research Center for Geriatric Disorders, Xiangya Hospital, Central South University, Changsha, China, [6]Department of Dermatology, Wuhan No. 1 Hospital, Wuhan, China

Inhibitors of programmed cell death protein 1 and its associated ligand (PD-L1) are widely used in cancer treatment. However, medical costs and benefits of PD-1/PD-L1 inhibitors need attention owing to differences in response rates among individuals. This study explored global trends in the health economics field of PD-1/PD-L1 inhibitors to enhance their worldwide development. Bibliometric analysis of all documents currently indexed in Web of Science Core Collection from inception to 2022 was performed. Publication year, authors, countries, institutes, and journals were analyzed by Bibliometrix package (version 3.2.1) in R (version 4.1.3). CiteSpace (version 6.1.R6) and VOSviewer (version 1.6.18) were used to analyze burst words, co-authorship of institutes, co-cited journals, and co-cited references, while figures were mainly drawn by Ggplot2 package (version 3.3.5) in R (version 4.1.3) and SCImago Graphica Beta (version 1.0.23). A total of 2020 documents related to the health economics of PD-1/PD-L1 inhibitors were identified, and 1,204 documents met the selection criteria for inclusion in the study. A rapid increase in the number of publications since 2019 was observed, but this increase stopped in 2022, revealing research saturation in the field. *Value in Health* (166 publications, 13.79% of total documents) had the most publications, while *New England Journal of Medicine* (2,890 co-citations) was the most co-cited journal. The United States was the leading contributor in this field with 506 publications and the top two productive institutes globally. The main hot topics included the cost-effectiveness of treatment with PD-1 and/or PD-L1 inhibitors, and the comparison between the cost-effectiveness of PD-/PD-L1 inhibitors and other drugs. There were substantial differences between developed and developing countries in the health economics field of PD-1 and/or PD-L1 inhibitors. The cost-effectiveness analysis of combined treatment with PD-1/PD-L1 inhibitors and other drugs warrants further attention. Findings from this study may provide governments and pharmaceutical companies with a strong reference for future research.

KEYWORDS

PD-1, PD-L1, the health economic, cancer immunotherapy, bibliometric analysis, future trends

Introduction

Cancer is one of the top three causes of death before the age of 70 years in 177 countries according to the World Health Organization (Bray et al., 2021; World Health Organization, 2022). Inhibitors of programmed cell death protein 1 (PD-1) and its associated ligand (PD-L1) as medicines of immunotherapy, the most promising treatment for cancers (Tang J, 2018; Cancer Research Institute, 2022), have been used for non-small-cell lung cancer (Brahmer et al., 2015; Jia et al., 2018; Gao et al., 2019), Hodgkin's lymphoma (Ansell et al., 2015; Jia et al., 2018; Gao et al., 2019), and others in recent years. However, some disadvantages of PD-1/PD-L1 inhibitors have emerged, such as marked differences in effective response rate among different people (Su et al., 2019; Daassi et al., 2020; Beaver and Pazdur, 2022) and the high cost of the inhibitors (Tarhini et al., 2019; Cheng et al., 2022).

Use of PD-1/PD-L1 inhibitors is uneven worldwide. Attested by Frost and Sullivan in 2019 (Frost & Sullivan, 2022), the size of the global market for PD-1/PD-L1 inhibitors exceeded $16 billion in 2018, with the Chinese and North American markets accounting for approximately 6.25% and 60% of the global market size, respectively. Factors confining the development of health economics research of PD-1/PD-L1 inhibitors include, but are not limited to, the time research commenced, the efficiency of the development, etc. (Wagstaff and Culyer, 2012). Thus, starting the experiment earlier and developing the drugs faster results in larger ownership of the markets. For instance, as early as 2015, the United States, who occupies the largest share of the global market for PD-1 inhibitors and PD-L1 inhibitors, first published a document about the health economics of Pembrolizumab after finishing clinical trials for the drug and starting to use it for the treatment of the metastatic melanoma (Tan and Quintal, 2015). Furthermore, six kinds of PD-1 inhibitors and PD-L1 inhibitors developed by the United States were in use in different countries before 2021 (National Medical Products Administration, 2022; U.S. Food & Drug Administration, 2022). Research in health economics can help in clinical drug selection to maximize patient benefit and can also help develop an optimization strategey suitable for the market and clinical practice of PD-1/PD-L1 inhibitors (Wagstaff and Culyer, 2012; Husereau et al., 2022). Therefore, research on the health economics of PD-1/PD-L1 inhibitors is essential.

Bibliometrics may be a prominent approach to reveal the research status and development trend of health economics on PD-1/PDL-1 inhibitors by visualization and statistical analysis. Previous bibliometric analysis was conducted to research the PD-1/PD-L1 inhibitors in the cancer field (Cancer Research Institute, 2022). However, there is currently an absence of bibliometric research on the health economics of PD-1 and PD-L1 inhibitors. Thus, in this study, a bibliometric analysis was conducted to 1) comprehensively understand the global trend of health economics of PD-1 inhibitors and PD-L1 inhibitors; 2) make suggestions for the future development of PD-1 inhibitors and PD-L1 inhibitors by pharmaceutical companies; 3) and help developing and developed countries to improve care to reduce the burden of patients' treatment.

Materials and methods

Search strategy and criteria

The Web of Science Core Collection database was fully searched from its inception to 31 December 2022. The search query included two main terms: "PD-1" and "the health economic". An additional file shows more details about the search strategy. There were no restrictions on the language, document type, data category, or year of publication. Subsequently, a preliminary selection was completed by the title, keywords, and the abstract of the document. For records that could not be clearly judged by reading these three components, a secondary screening was conducted by reading the content of the identified records. The selection of records and flow chart of the research framework are shown in Figure 1. In addition, a more detailed searching strategy is demonstrated in Supplementary Table S1.

Analysis method

The preliminary search found 2020 documents, which were then further analyzed to select those suitable for inclusion in the study. First, 32 documents relating to electrochemistry research, including some documents about catalysts like palladium (Pd), were excluded, then excluded 781 documents that only covered topics about economics or PD-1/PD-L1, which referred to two types of documents unrelated to the research, one is documents that analyzed economic effectiveness but the objects of documents were not PD-1/PD-L1 inhibitors; another type is documents working on PD-1/PD-L1 inhibitors, but the research content had nothing to do with the health economics.

After selection and removal of duplicates, 1,204 documents were retained, and countries, authors, journals, affiliations, and keywords of those documents were subsequently analyzed.

Bibliometrix package (version 3.2.1) in R software (version 4.1.3) was used to analyze the documents. SCImago Graphica Beta (version 1.0.23) was used to present the networks of co-authorship of countries and main authors. The network map, and the density map for keywords were created using VOSviewer WPS Office (version 11.1.0.13703). CiteSpace (version 6.1.R6) was then used to create the figure of keywords bursts. Data aggregation and analysis were conducted in WPS Office (version 11.1.0.13703), the pie chart of document types was generated by OriginPro (Version 2023 OriginLab Corporation, Northampton, MA, USA), and the remaining figures were drawn with Ggplot2 package (version 3.3.5) in R software (version 4.1.3).

Results

Document types and publication outputs

A total of 1,204 records were selected for inclusion in the study and were divided into seven categories (Figure 2A). Articles accounted for the largest part (54.82%), followed by meeting abstracts (23.01%) and reviews (17.03%), which are close in number. Figure 2B shows the publication output trends from

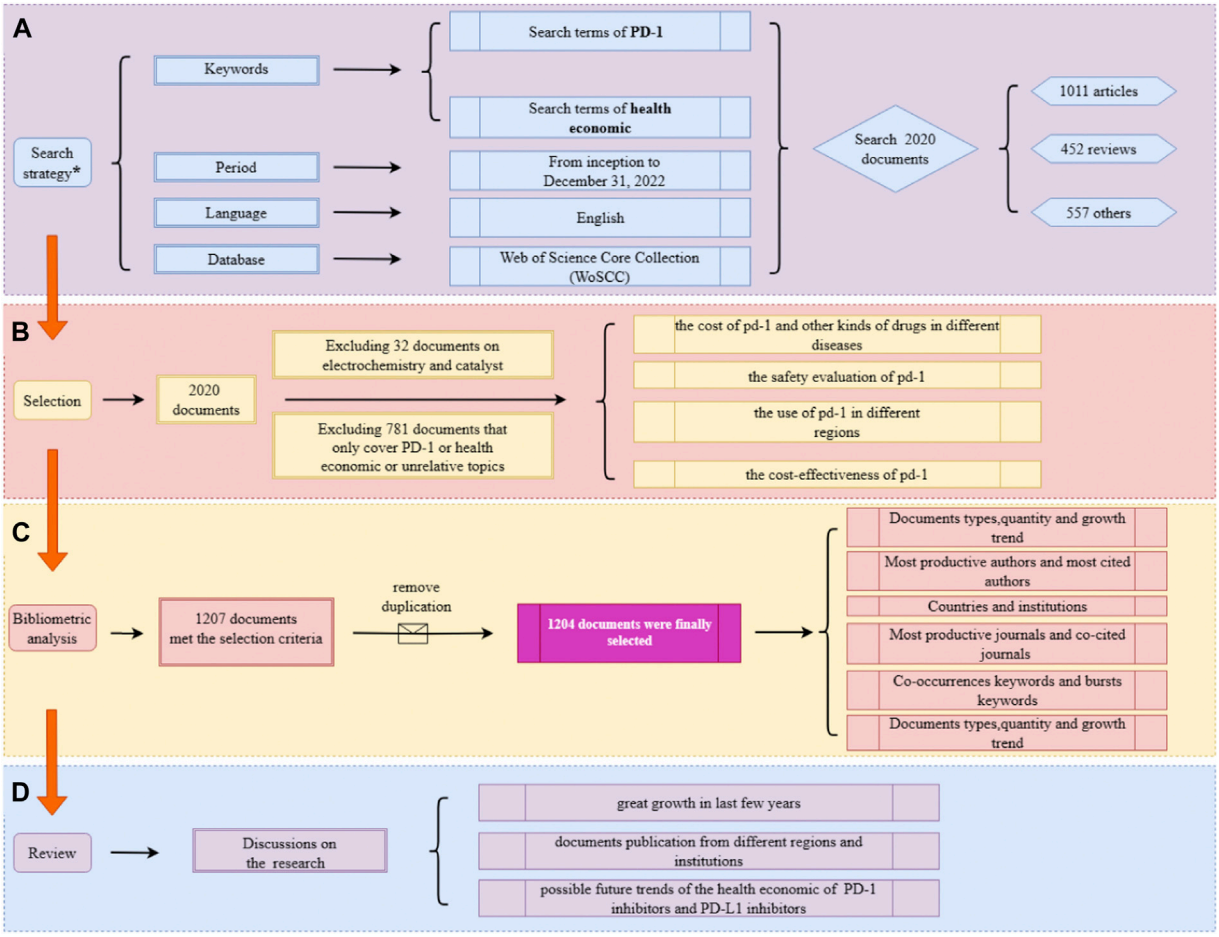

FIGURE 1
Overview of the study flow diagram. **(A)** The search strategy. **(B)** The selection process. **(C)** The process of bibliometric analysis. **(D)** Results of the analysis.

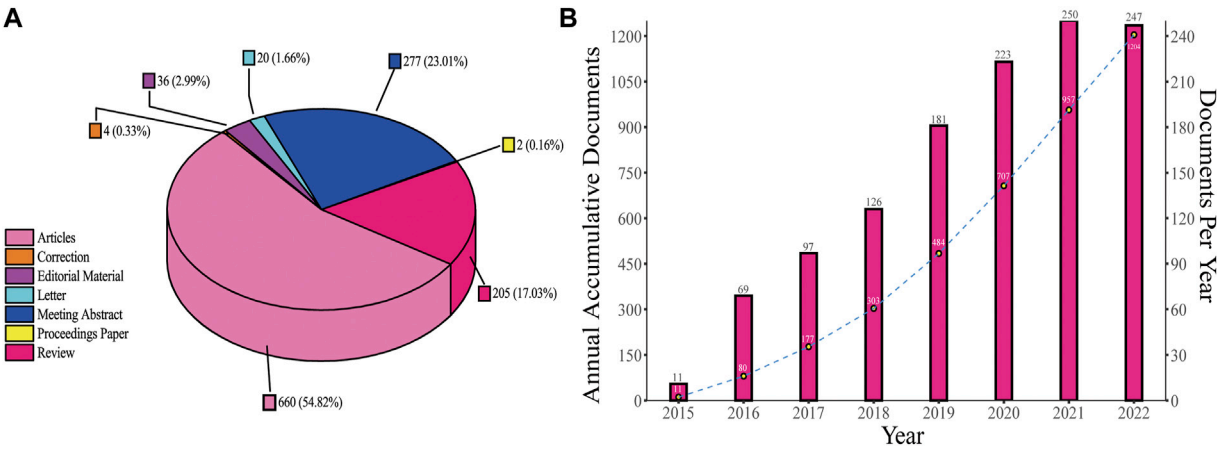

FIGURE 2
Document types and publication outputs. **(A)** Percentage of each type of document. **(B)** Publications number per year and annual accumulative number.

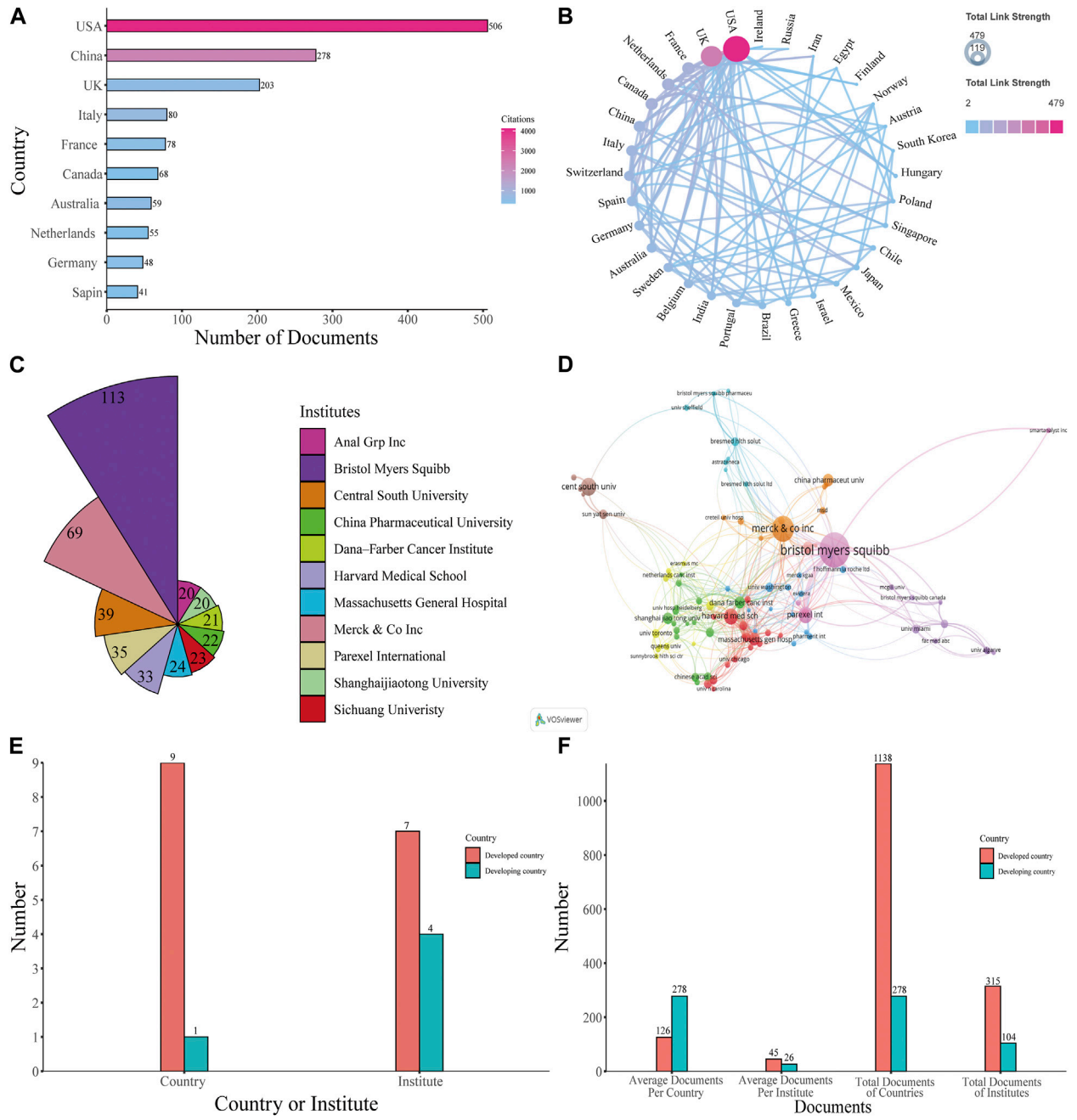

FIGURE 3
Analysis of countries and institutes. **(A)** The number of articles and citations among the 10 most productive countries with the number of total papers and total citations. **(B)** Filled map of the cooperation between various countries. The color reflects the total link strengths of different countries, while the arrow demonstrates cooperation between the corresponding two countries. **(C)** The top 11 institutes with the most contributions. **(D)** Visualized map of co-authorship of the institutes. **(E)** The number of developed and developing countries among the top 10 productive countries, and the number of institutes from developed and developing countries among the top 11 productive institutes. **(F)** The total number and average number of developed countries and developing countries among the top 10 productive countries, the total number and average number of documents of institutes from developed countries and developing countries among the top productive institutes.

2015 to 2022. The first study was published in 2015, and since then, the number of publications continuously increased to the year 2021. However, the number of documents in 2022 was almost the same as that in 2021; there were only three fewer publications in 2022 compared with 2021. Annual outputs were less than 100 in the first three years. After 2018, the number of annual publications showed more significant growth, gradually increasing from 126 in 2018 to the maximum of 250 in 2021. From 2018 to 2021, a total of 780 documents were published, accounting for 64.78% of all the documents included in the study.

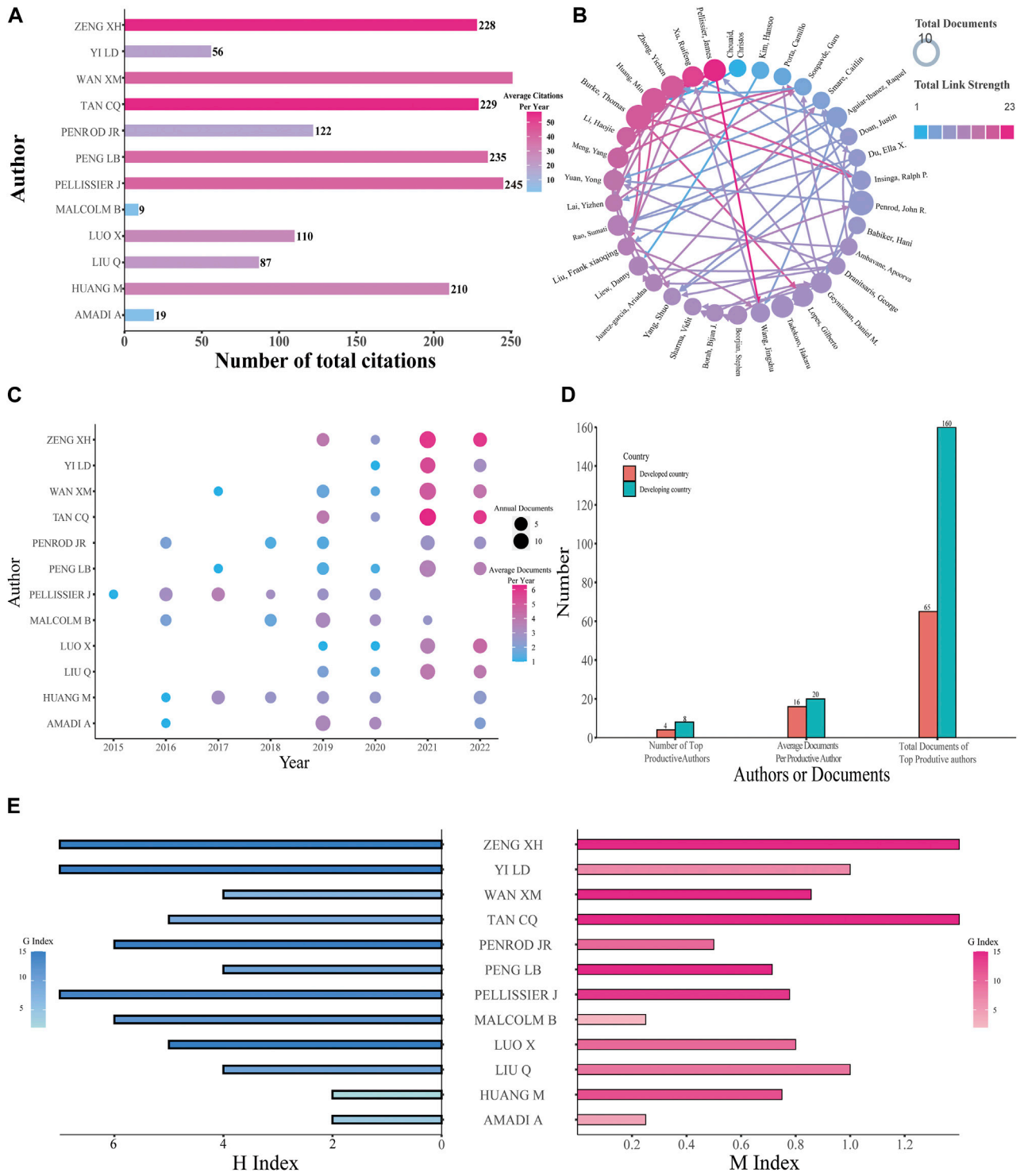

FIGURE 4
Analysis of authors. **(A)** Total citations and annual citations of the top 12 productive authors. **(B)** The co-authorship of productive authors. **(C)** Annual publications and annual average publications of the top 12 productive authors. **(D)** Number of authors and their documents among the top 12 productive authors. **(E)** G-index, H-index, and M-index of the top 12 productive authors.

Publication distribution of countries, institutes, and authors

The publications included in the study originated from 64 countries. The United States published the highest number of papers at 506, accounting for 42.03% of all papers, and had the highest number of total citations (4,119). This was followed by China (278 papers, 23.09%, 2,252 citations) and the United Kingdom (203 papers, 16.86%, 597 citations), while other countries with less than or equal to 80 publications (Figure 3A). The

cooperation between various countries is reflected in the filled map in Figure 3B. Cooperation partnerships among different countries were strong. The United States and the United Kingdom were the top two countries that had the most cooperation with other countries.

Among the 1850 institutes around the world that were responsible for the selected publication, Bristol Myers Squibb ranked first, with 113 published papers, accounting for 9.39% of all publications. Merck and Co., Inc. was the second institute (69 papers, 5.73%), followed by Central South University (39 papers, 3.24%), Parexel International (35 papers, 2.91%), Harvard Medical School (33 papers, 2.74%), and then other institutes that published less than 30 papers (Figure 3C). Anal Grp Inc. and Shanghaijiaotong University both published 20 papers, so tied in tenth place. Collaborative relationships between diverse institutes with more than 5 published papers are shown in Figure 3D. The results indicated close cooperation between global institutes.

As shown in Figure 3E, most countries among the top 10 productive countries are developed countries and most institutes among the top 11 productive institutes are in developed countries. To better reflect difference among developed countries and developing countries, we made Figure 3F. Among the top 10 productive countries, Developed countries produced significantly more documents compared with developing countries, but on average, a developing country own more documents than a developed country does. For institutes, institutions in developed countries produce more documents, both in terms of total and average publications, than institutes in developing countries do.

Analysis of authors

In total, 6,033 authors were involved in the study, and the 12 most productive authors were analyzed (the final three authors were tied for tenth place). The United States and China were the main countries with the largest number of authors. Among the most productive authors, the one who has the most citations is Wan XM (Figure 4A). For cooperation of authors with more than five published papers, Pellissier J has a total link strength of 23, ranking first, followed by Xu RF (a total link strength of 21) (Figure 4B). The top three productive authors all came from China; Wan XM published the highest number of papers at 25, while Tan CQ and Zeng XH both ranked second with 24 papers (Figure 4C). The developing countries contain two-thirds of the top 12 productive authors and own 71.11% of the entire documents of the top 12 productive authors. In addition, among the 12 productive authors, developing countries have four more articles per author compared with developed countries (Figure 4D). To analyze authors' productivity more comprehensively, H-index, M-index, and G-index were used (Figure 4E). Papers from Pellissier J, Tan CQ, and Zeng XH had the highest H-index 7). The G-index of papers from Peng LB, Tan CQ, Wan XM, and Zeng XH was 15, sharing first position. For the M-index of papers, Tan CQ (1.4) and Zeng XH (1.4) both ranked first, followed by Liu Q (1.0) and Yi LD (1.0). Tan CQ and Zeng XH have identical values in these three different indexes. More information about the top productive authors including the number of publications and their corresponding H-index, M-index, and G-index is encompassed in Table 1.

Distribution of journals, co-cited journals, and co-cited references

Research on the health economics of PD-1 inhibitors and PD-L1 inhibitors has been published in 362 journals. The journal with the most published papers was *Value in Health*, which published 166 papers, accounting for 13.79% of the total papers included in the study (Figure 5A), although this journal only had 132 citations in the papers included in the study. This was followed by *Journal of Clinical Oncology* with 58 papers and 357 total citations in the selected journals. Half of the top 10 journals were in the United States, while the United Kingdom had two journals and Switzerland had three journals. The numbers of annual documents are shown in Figure 5B. More detailed information is provided in Supplementary Table S2.

Figure 5C presents the co-citation map of various journals. *New England Journal of Medicine* had 2,890 co-citations, ranking first, while *Journal of Clinical Medicine* (2,562 co-citations) and *Lancet Oncology* (1,151 co-citations) ranked second and third, respectively. A summary of the top 10 co-cited references according to the total number of citations is presented in Table 2, and Figure 5D is the map of co-cited references that had more than 30 citations, which can directly reflect researchers' attention according to the number of citations. Two references in the map had been co-cited more than 100 times, including papers published by Reck, Martin et al. (2016), Borghaei, H et al. (2015).

Co-occurrence keywords analysis

The study selected 120 keywords that had no less than 10 occurrences. These words include cost-effectiveness of therapy, different drugs, therapy mechanisms, and specific cancers treated with immunotherapy. The keywords with red nodes were grouped into one category in Figure 6A. Keywords with red nodes have a strong connection with nodes of other colors, which means most documents focused their research on keywords with red nodes. Thus, we put keywords with red nodes into the cluster named "Common topics cluster". This cluster predominantly relates to immunotherapy and its mechanism and includes the key terms "PD-1", "PD-L1", "inhibitors", "cancer", and "biomarker". The remaining keywords indicate the health economics study in following three aspects: 1) in different kinds of drugs that are widely used in immunotherapy and chemotherapy; 2) in different periods of clinical treatments; and 3) in more specific cancers, such as melanoma.

Figure 6B shows how the frequency of keywords changes with time. Most keywords have emerged from 2018, which may be related to the awarding of the Nobel Prize in Physiology or Medicine in 2018 for work on PD-1 as a target in cancer therapy. The keywords with the highest density are pembrolizumab, cost-effectiveness, nivolumab, immunotherapy, and chemotherapy. The importance and frequency of different keywords is demonstrated by the destiny visualization map (Figure 6C).

TABLE 1 More details of top 12 most productive authors for the research (n%).

Rank	Author	Country	N (%)	H-index	G-index	M-index
1	Wan, XM	China	25 (2.08%)	6	15	0.86
2	Tan, CQ	China	24 (1.99%)	7	15	1.4
3	Zeng, XH	China	24 (1.99%)	7	15	1.4
4	Peng, LB	China	22 (1.83%)	5	15	0.71
5	Luo, X	China	18 (1.50%)	4	10	0.8
6	Huang, M	China	17 (1.42%)	6	12	0.75
7	Penrod, JR	United States	17 (1.42%)	4	10	0.5
8	Liu, Q	China	16 (1.33%)	5	9	1
9	Malcolm, B	Australia	16 (1.33%)	2	2	0.25
10	Amadi, A	United Kingdom	15 (1.25%)	2	4	0.25
11	Pellissier, J	United States	15 (1.25%)	7	14	0.78
12	Yi, LD	China	15 (1.25%)	4	7	1

N (%), the number of published documents of every journal and the percentages show their proportions of total 1,201 documents.

Burst analysis of keywords

According to Figure 6D, during the early years, the hot topics of this field concerned melanoma and some typical anti-cancer drugs. This may indicate that the health economics study of inhibitors of PD-1 and PD-L1 for the treatment of melanoma had been extensively investigated, while relevant research on other kinds of tumor was not sufficiently mature at that time. During the intervening years, the hot topics were predominantly about the mechanism of immunotherapy with PD-1. In recent years, the emergence of keywords such as "efficacy" and "combined Nivolumab" suggests that research on boosting the effectiveness of PD-1 inhibitor therapy is becoming popular.

Network visualization maps of keywords of documents from China (Figure 6E) and documents from the United States (Figure 6F) were created. The research in developing countries is more in-depth than it in developed countries

Discussion

This study presented a bibliometric and visualized analysis to summarize the current research status and predict promising research fields of PD-1/PD-L1 inhibitors. To the best of our best knowledge, this is the first study to systematically evaluate this field in regard to contributing countries, institutions, journals, authors, and research hot spots. Moreover, substantial differences between developed and developing countries were revealed. This study provides information that can accurately guide scholars, governments, and pharmaceutical companies on relative study, policy making, and promotion of PD-1/PD-L1 inhibitors.

Research on PD-1/PD-L1 inhibitors in the health economics field is in an uneven situation currently. From Figure 3, the total numbers of documents from different countries and different institutes and the frequency of cooperation between different countries all reflect the unbalanced development in the health economics field of PD-1/PD-L1 inhibitors. According to the analysis of authors in Figure 4, it is obvious how lopsided the productivity and influence of different authors are. Figure 5 demonstrates the discrepancy between different journals; some influential journals published more documents, over 30 documents per year in some cases. In summary, there is markedly uneven development in the research of PD-1/PD-L1 inhibitors in the health economics field in terms of countries, institutes, authors, and journals. Furthermore, the uneven development of the relative research may originate from the gap between the developed countries and the developing countries. Thus, to better identify the reason behind this situation, it is essential to analyze how the differences of the developed and developing countries are formed.

Among all the countries selected in the study, the United States and China are top among the developed and the developing countries, respectively. Consequently, the network visualization maps of keywords of documents from these two countries were analyzed to identify the potential differences and the future trends in the health economics field of PD-1/PD-L1 inhibitors for developed and developing countries. The circle clusters in Figures 6E, F highlight the research hot spots in the health economics field of PD-1/PD-L1 inhibitors for each of the two countries. The hot spots of the United States are more detailed than those of China; besides cost-effectiveness, the United States has gradually started to analyze more specific problems including the economic burden (Nesline et al., 2020; Morgans et al., 2021). This suggests that researchers need to be more precise in their research issues when conducting studies in the health economics field of PD-1/PD-L1 inhibitors if they want to make more progress and have more outputs in the future. Additionally, to elucidate how governments influence the research in the health economics field of PD-1/PD-L1 inhibitors, several factors affecting the new drug marketing process have to be compared (Lanthier et al., 2013; Eder et al., 2014; Darrow et al., 2020; Wang et al., 2022), and the results of this analysis are listed in Table 3. Here are the results after comparing strategies in the

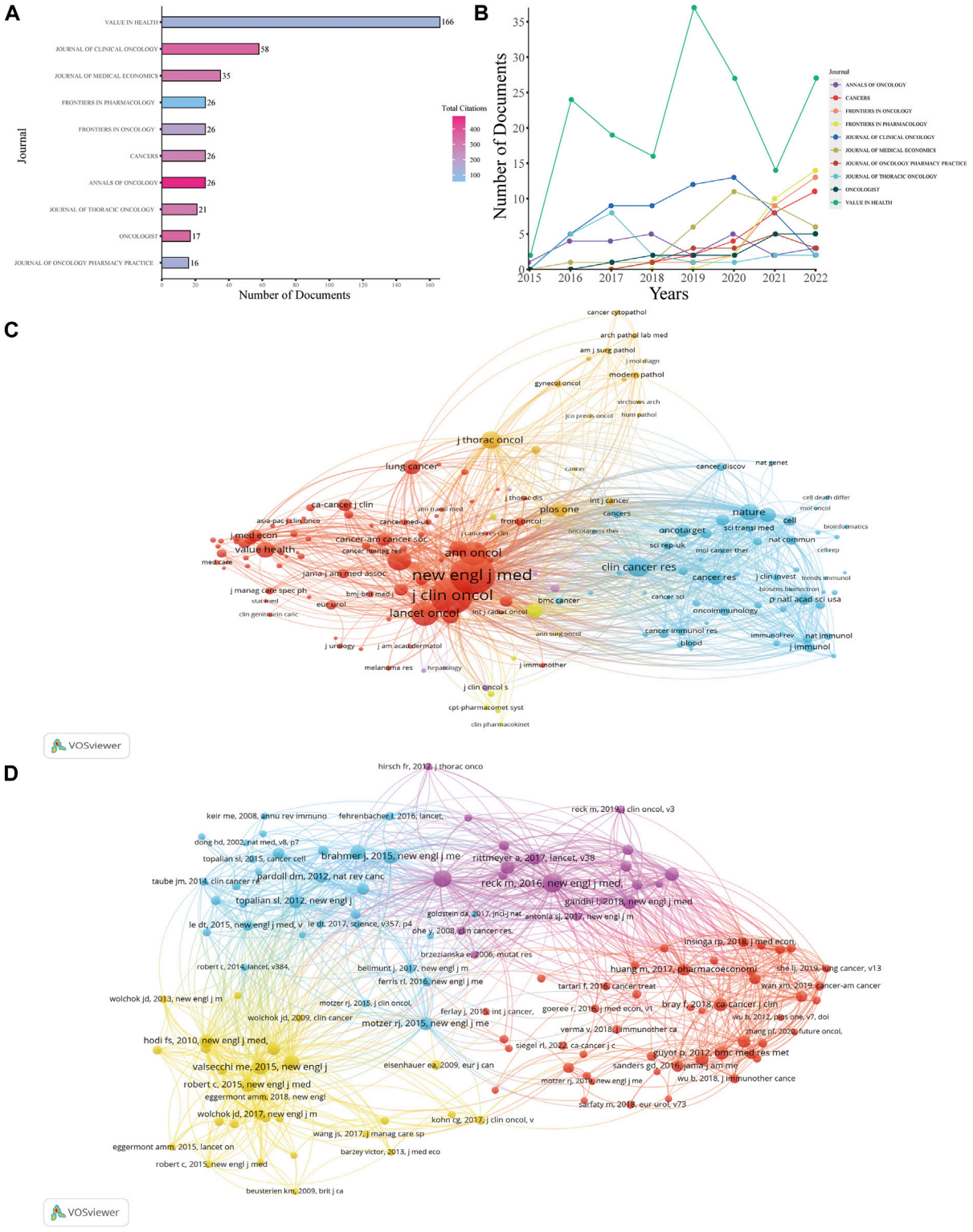

FIGURE 5
Analysis of journals and references. **(A)** Number of total documents and citations of the top 10 productive journals. **(B)** Number of documents produced annually by the top 10 productive journals. **(C)** Network map of co-cited journals. **(D)** Network map of co-cited references.

United States and China (Center For Drug Evaluation, NMPA, 2022; National Medical Products Administration, 2022; U.S. Food & Drug Administration, 2022; U.S. Department of Health & Human Services, 2022). The application process of new drugs is more efficient in the United States, probably because the United States puts more manpower into examination and approval for marketing.

TABLE 2 The top cited references and citations.

Rank	Cited references	Citations
1	Reck M, et al., 2016, Pembrolizumab *versus* Chemotherapy for PD-L1-Positive Non-Small-Cell Lung Cancer. N Engl J Med.	142
2	Borghaei H, et al., 2015, Nivolumab *versus* Docetaxel in Advanced Non-squamous Non-Small-Cell Lung Cancer. N Engl J Med.	118
3	Brahmer J, et al., 2015, Nivolumab *versus* Docetaxel in Advanced Squamous-Cell Non-Small-Cell Lung Cancer. N Engl J Med.	95
4	Valsecchi Me, et al., 2015, Combined Nivolumab and Ipilimumab or Monotherapy in Untreated Melanoma REPLY.	95
5	Robert C, et al., 2015, Pembrolizumab *versus* Ipilimumab in Advanced Melanoma. N Engl J Med.	89
6	Garon EB, et al., 2015, Pembrolizumab for the treatment of non-small-cell lung cancer. N Engl J Med.	84
7	Robert C, et al., 2015, Nivolumab in previously untreated melanoma without BRAF mutation. N Engl J Med.	80
8	Gandhi L, et al., 2018, Pembrolizumab plus Chemotherapy in Metastatic Non-Small-Cell Lung Cancer. N Engl J Med.	80
9	Topalian SL, et al., 2012, Safety, activity, and immune correlates of anti-PD-1 antibody in cancer. N Engl J Med.	76
10	Herbst RS, et al., 2016, Pembrolizumab *versus* docetaxel for previously treated, PD-L1-positive, advanced non-small-cell lung cancer (KEYNOTE-010): a randomised controlled trial. Lancet.	73

China has relatively strict requirements on the process of data submitted by pharmaceutical companies, while the United States has additional requirements in the quality and comprehensiveness of the clinical research. Furthermore, compared with the United States, China, the prices of drugs in China were generally lower, including Pembrolizumab, Nivolumab, Atezolizumab and Durvalumab. In addition, among these four drugs, Pembrolizumab, Nivolumab and Atezolizumabwhich in China were almost half the prices than in the United States (Huang et al., 2022). To summarize, compared with the United States, the marketing process of new drugs in China is more conservative. Moreover, in both countries, the comprehensive coverage of medical care has certain influencing factors in the marketing of PD-1/PD-L1 inhibitors. Overall, for the governments, if they want to propel the research in the health economics field of PD-1/PD-L1 inhibitors, they can: 1) accelerate to include the relevant drugs in national insurance so that these inhibitors can be more affordable, thereby expanding the markets for PD-1/PD-L1 inhibitors; 2) optimize the approval process for new drugs to reduce unnecessary time and effort; and 3) solve the lack of talented people in the field of new drugs approval process as soon as possible to improve the efficiency of the approval process.

Besides the differences between the developed countries and the developing countries, the analysis also revealed information that would be helpful for developing countries. The rectangular box in Figure 6E reveals the current possible development trend of the developing countries in the health economics field of PD-1/PD-L1 inhibitors. Camrelizumab is the third drug officially developed and successfully marketed in China. In terms of marketing time, this drug is not as advantageous as the previous two domestic drugs, however, the health economics research of this kind of drug is more than that of the previous two domestic drugs. According to those previous bibliometric analyses, there are two options for a country like China that were relatively late in developing the research in this field: 1) focus on other kinds of chemical drugs for co-treatment with PD-1/PD-L1 inhibitors to improve the efficacy of inhibitors; 2) continue to develop novel PD-1/PD-L1 inhibitors and attempt to enter the overseas markets. Clearly, the first option far exceeds the second option in terms of economic benefits. Excessive research in the development of PD-1/PD-L1 inhibitors may cause wastage of clinical materials and scientific research funds after prolonged research without results. Furthermore, the drug market is highly competitive given the global economic downturn in recent years (The World Bank, 2022). However, the bibliometric analysis of the health economics of Camrelizumab has already revealed that even with the impact of the global great economic downturn, for countries that are still developing in this field, the second option—that is, applying money, manpower, and time for the development of new drugs—is a possible but necessary path.

Our results reveal the potential trends of the health economics field of PD-1 inhibitors and PD-L1 inhibitors. The bursts words shows that "phase III trial" emerged in 2017, which means clinical trials of these two inhibitors have appeared for at least five years. Furthermore, the overlay visualization map of the keywords also contains some noticeable labels including "Docetaxel", "Cisplatin", "Dabrafenib", and "Ipilimumab", and although none of these drugs are PD-1 inhibitors or PD-L1 inhibitors, their emergence is related to the shift of the research hot spot. In the last few years, much related research of this health economics field has focused on the comparison of the curative effect of PD-1 inhibitors, PD-L1 inhibitors, and other kinds of chemical drugs. However, since 2018, the proportion of clinical trials of single-drug immunotherapy has begun to decrease and is being replaced by combined immunotherapy, which uses both PD-1/PD-L1 inhibitors and other types of chemical drugs to increase the curative effect of the immunotherapy. Meanwhile, not only are combination therapy trials accounting for a large part of the research, but drug combinations are also shifting from using chemotherapy and anti-CTLA4 combinations to other targeted methods to bypass drug resistance mechanisms and thus achieve greater efficacy of PD-1/PD-L1 inhibitors.

In 2022, the number of published documents in the health economics field of PD-1 inhibitors and PD-L1 inhibitors stopped increasing, which indicates saturation of the research areas. For the researchers who continue to study in this field, we suggest a number of further analyses for the future: 1) a more specific comparison of analysis of the health economics of different kinds of PD-1 inhibitors and PD-L1 inhibitors, such as Nivolumab and Pembrolizumab. This kind of comparison can help to demonstrate the economic development of different kinds of PD-1 inhibitors and PD-L1 inhibitors and provide more detailed information for future research in the health economics

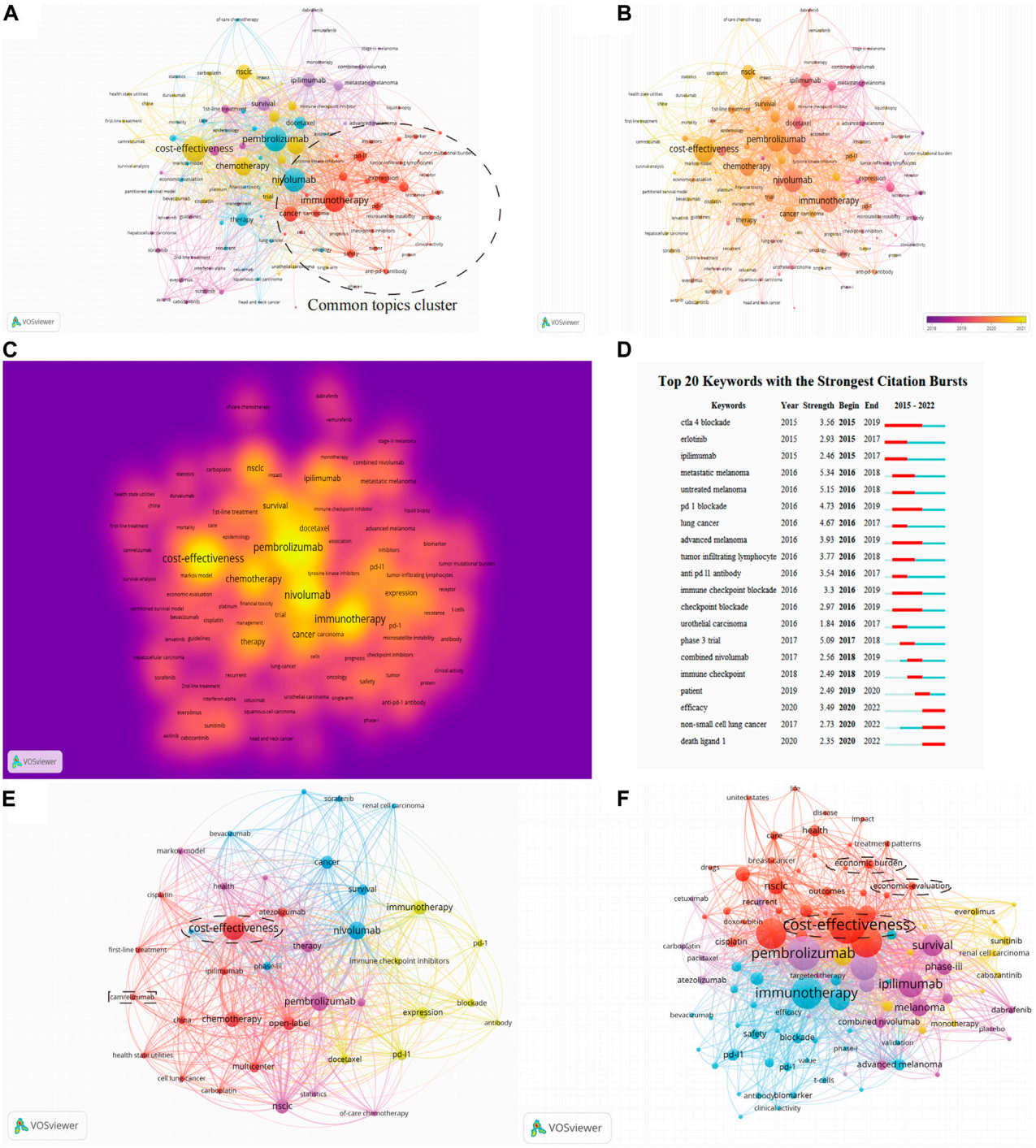

FIGURE 6
Analysis of keywords. **(A)** Clusters network visualization map of keywords. **(B)** Overlay visualization map of keywords. **(C)** Destiny visualization map of keywords. **(D)** The strongest citation bursts. **(E)** Network visualization map of keywords of documents from China. **(F)** Network visualization map of keywords of documents from the United States.

of PD-1/PD-L1 inhibitors; 2) developing appropriate biomarkers to increase the precision when using targeted and differentiated PD-1/PD-L1 inhibitors; 3) exploration of the economic benefits of PD-1/PD-L1 inhibitors in other cancers that have not been studied previously; 4) a comparison of research output trends in the health economics of other kinds of drugs that are widely used for immunotherapy, which may help to explain some of the situations that have occurred in the health economics field of PD-1 inhibitors and PD-L1 inhibitors; 5) to confirm the optimal dose of PD-1 inhibitors and PD-L1 inhibitors for treatment; and 6) periodic repetition of such analyses to observe the potential trends in research outputs and finally to encourage collaborations of different scientific research teams.

TABLE 3 Factors affecting the new drugs marketing process.

Item	United States (developed country)	China (developing country)
Review procedure and application process	One declaration and direct review	Repeated declarations and hierarchical approval
Number of approved anticancer drugs in China and the United States from 2012 to 2021	118	87
Price information of drugs in China and the United States	Pembrolizumab: $ 5,102	Pembrolizumab: $ 2,818
	:Nivolumab: $ 3,697	:Nivolumab: $ 1,456
	Atezolizumab: $ 9,411	Atezolizumab: $ 5,158
	Durvalumab: $ 3,697	Durvalumab: $ 2,844
Policy to accelerate process	PR, AA, FTD, BTD	PR, BTD, CA, SRA
Insurance coverage in 2022	92%	>95%

PR: Priority Review; AA: Accelerated Approval; FTD: Fast Track Designation; BTD: Breakthrough Therapy Designation; CM: Conditional Approval; SRA: Special Review and Approval.

Similar to all other bibliometric analyses (Gao et al., 2019; Liu et al., 2022), there are limitations in our study. Final results of the study are affected by the choice of database (Web of Science Core Collection) and the search queries used. The selected documents included a few articles that focused on the efficacy of PD-1 inhibitors but pointed out that their conclusions were helpful to the study of health economics, and this is where the major limitation lies. This also emphasizes the need not only for skill in data searches and analysis, but also for expertise in the selected field to ensure the accuracy of the criteria for the process of selecting documents.

This study found that the United States led in this research field by contributing 42.03% of the total publications. The top productive journal is *Value in Health*. The top co-cited journal is *New England Journal of Medicine*, and active collaborations among countries and institutes can be observed. The top productive institute is Bristol Myers Squibb, which is in the United States. The most productive author is Wan XM. For the global trend of this field, the cost effectiveness of PD-1/PD-L1 inhibitors and comparative analysis of the economic effects of PD-1/PD-L1 inhibitors and other drugs are the predominant hot topics. For pharmaceutical companies that are developing PD-1/PD-L1 inhibitors, we suggest they should exploit overseas markets. Finally, for developing countries who continue to study the health economics field of the PD-1/PD-L1 inhibitors, the expansion of medical insurance coverage and acceleration of the marketing process of new drugs are needed.

Data availability statement

The raw data supporting the conclusion of this article will be made available by the authors, without undue reservation.

Author contributions

SL carried out the literature search, data acquisition, data analysis and manuscript preparation. LX carried out the manuscript preparation, collected important background information and data analysis. LZ carried out the manuscript preparation and collected important background information. YL, LP, YL and NY provided assistance for data acquisition, data analysis and statistical analysis. WC and KH carried out the concepts, design, definition of intellectual content and made substantial contributions to the revision of manuscript.

Funding

This work was financially supported by the science and technology innovation Program of Hunan Province (grant no. 2020RC3059), National Key Research and Development Program of China (grant no. 2021YFF1201205).

Conflict of interest

The authors declare that the research was conducted in the absence of any commercial or financial relationships that could be construed as a potential conflict of interest.

The reviewer MY declared a past co-authorship with the author NY to the handling editor.

Publisher's note

All claims expressed in this article are solely those of the authors and do not necessarily represent those of their affiliated organizations, or those of the publisher, the editors and the reviewers. Any product that may be evaluated in this article, or claim that may be made by its manufacturer, is not guaranteed or endorsed by the publisher.

Supplementary material

The Supplementary Material for this article can be found online at: https://www.frontiersin.org/articles/10.3389/fphar.2023.1141075/full#supplementary-material

References

Ansell, S. M., Lesokhin, A. M., Borrello, I., Halwani, A., Scott, E. C., Gutierrez, M., et al. (2015). PD-1 blockade with nivolumab in relapsed or refractory Hodgkin's lymphoma. *N. Engl. J. Med.* 372, 311–319. doi:10.1056/NEJMoa1411087

Beaver, J. A., and Pazdur, R. (2022). The wild west of checkpoint inhibitor development. *N. Engl. J. Med.* 386, 1297–1301. doi:10.1056/NEJMp2116863

Borghaei, H., Paz-Ares, L., Horn, L., Spigel, D. R., Steins, M., Ready, N. E., et al. (2015). Nivolumab versus docetaxel in advanced nonsquamous non-small-cell lung cancer. *N. Engl. J. Med.* 373, 1627–1639. doi:10.1056/NEJMoa1507643

Brahmer, J., Reckamp, K. L., Baas, P., Crino, L., Eberhardt, W. E. E., Poddubskaya, E., et al. (2015). Nivolumab versus docetaxel in advanced squamous-cell non-small-cell lung cancer. *N. Engl. J. Med.* 373, 123–135. doi:10.1056/NEJMoa1504627

Bray, F., Laversanne, M., Weiderpass, E., and Soerjomataram, I. (2021). The ever-increasing importance of cancer as a leading cause of premature death worldwide. *Cancer* 127, 3029–3030. doi:10.1002/cncr.33587

Cancer Research Institute (2022). *Cancer Research Institute*. https://www.cancerresearch.org/news/2018/pd-1-l1-checkpoint-inhibitor-landscape-analysis (Accessed Jan 03, 2023).

Center For Drug Evaluation (2022). *Nmpa*. https://www.cde.org.cn/ (Accessed Feb 08, 2023).

Cheng, R. H., Zhou, Z., and Liu, Q. (2022). Cost-effectiveness of first-line versus second-line use of domestic anti-PD-1 antibody sintilimab in Chinese patients with advanced or metastatic squamous non-small cell lung cancer. *Cancer Med.* doi:10.1002/cam4.5440

Daassi, D., Mahoney, K. M., and Freeman, G. J. (2020). The importance of exosomal PDL1 in tumour immune evasion. *Nat. Rev. Immunol.* 20, 209–215. doi:10.1038/s41577-019-0264-y

Darrow, J. J., Avorn, J., and Kesselheim, A. S. (2020). FDA approval and regulation of pharmaceuticals, 1983-2018. *Jama-Journal Am. Med. Assoc.* 323, 164–176. doi:10.1001/jama.2019.20288

Eder, J., Sedrani, R., and Wiesmann, C. (2014). The discovery of first-in-class drugs: Origins and evolution. *Nat. Rev. Drug Discov.* 13, 577–587. doi:10.1038/nrd4336

Frost and Sullivan (2022). *China biological drug market research report*. https://img.frostchina.com/attachment/2022/08/11/scQBetjysMroniAuLscNk3.pdf (Accessed Jan 03, 2023).2019

Gao, Y., Shi, S. Z., Ma, W. J., Chen, J., Cai, Y. T., Ge, L., et al. (2019). Bibliometric analysis of global research on PD-1 and PD-L1 in the field of cancer. *Int. Immunopharmacol.* 72, 374–384. doi:10.1016/j.intimp.2019.03.045

Huang, H., Zhu, Q., Ga, M., Wu, D., Meng, X., Wang, S., et al. (2022). Availability and affordability of Oncology drugs in 2012-2021 in China and the United States. *Front. Oncol.* 12, 930846. doi:10.3389/fonc.2022.930846

Husereau, D., Drummond, M., Augustovski, F., De Bekker-Grob, E., Briggs, A. H., Carswell, C., et al. (2022). Consolidated health economic evaluation reporting standards 2022 (CHEERS 2022) statement: Updated reporting guidance for health economic evaluations. *Appl. Health Econ. Health Policy* 20, 213–221. doi:10.1007/s40258-021-00704-x

Jia, L., Zhang, Q., and Zhang, R. X. (2018). PD-1/PD-L1 pathway blockade works as an effective and practical therapy for cancer immunotherapy. *Cancer Biol. Med.* 15, 116–123. doi:10.20892/j.issn.2095-3941.2017.0086

Lanthier, M., Miller, K. L., Nardinelli, C., and Woodcock, J. (2013). An improved approach to measuring drug innovation finds steady rates of first-in-class pharmaceuticals, 1987-2011. *Health Aff.* 32, 1433–1439. doi:10.1377/hlthaff.2012.0541

Liu, Y. H., Xu, Y., Cheng, X., Lin, Y. R., Jiang, S., Yu, H. M., et al. (2022). Research trends and most influential clinical studies on anti-PD1/PDL1 immunotherapy for cancers: A bibliometric analysis. *Front. Immunol.* 13, 862084. doi:10.3389/fimmu.2022.862084

Morgans, A. K., Hepp, Z., Shah, S. N., Shah, A., Petrilla, A., Small, M., et al. (2021). Real-world burden of illness and unmet need in locally advanced or metastatic urothelial carcinoma following discontinuation of PD-1/L1 inhibitor therapy: A medicare claims database analysis. *Urologic Oncology-Seminars Orig. Investigations* 39, 733.e1–733733.e10. doi:10.1016/j.urolonc.2021.05.001

National Medical Products Administration (2022). *National medical products administration*. https://www.nmpa.gov.cn/ (Accessed Jan 03, 2023).

Nesline, M. K., Knight, T., Colman, S., and Patel, K. (2020). Economic burden of checkpoint inhibitor immunotherapy for the treatment of non-small cell lung cancer in US clinical practice. *Clin. Ther.* 42, 1682–1698. doi:10.1016/j.clinthera.2020.06.018

Reck, M., Rodriguez-Abreu, D., Robinson, A. G., Hui, R., Csoszi, T., Fulop, A., et al. (2016). Pembrolizumab versus chemotherapy for PD-L1-positive non-small-cell lung cancer. *N. Engl. J. Med.* 375, 1823–1833. doi:10.1056/NEJMoa1606774

Su, Q., Zhu, E. C., Wu, J. B., Li, T., Hou, Y. L., Wang, D. Y., et al. (2019). Risk of pneumonitis and pneumonia associated with immune checkpoint inhibitors for solid tumors: A systematic review and meta-analysis. *Front. Immunol.* 10, 108. doi:10.3389/fimmu.2019.00108

Tan, M., and Quintal, L. (2015). Pembrolizumab: A novel antiprogrammed death 1 (PD-1) monoclonal antibody for treatment of metastatic melanoma. *J. Clin. Pharm. Ther.* 40, 504–507. doi:10.1111/jcpt.12304

Tang J, Y. J., Hubbard-Lucey, Vm, Neftelinov, St, Hodge, Jp, and Lin, Y. (2018). Trial watch: The clinical trial landscape for PD1/PDL1 immune checkpoint inhibitors. *Nat. Rev. Drug Discov.* 17, 854–855. doi:10.1038/nrd.2018.210

Tarhini, A., Mcdermott, D., Ambavane, A., Gupte-Singh, K., Aponte-Ribero, V., Ritchings, C., et al. (2019). Clinical and economic outcomes associated with treatment sequences in patients with BRAF-mutant advanced melanoma. *Immunotherapy* 11, 283–295. doi:10.2217/imt-2018-0168

The World Bank (2022). *The World Bank*. https://www.worldbank.org (Accessed Jan 03, 2023).

U.S. Department of Health and Human Services (2022). *Department of health and human Services*. https://www.hhs.gov/ (Accessed Feb 05, 2023).

U.S. Food and Drug Administration (2022). *Food and drug administration*. https://www.fda.gov/ (Accessed Jan 03, 2023).

Wagstaff, A., and Culyer, A. J. (2012). Four decades of health economics through a bibliometric lens. *J. Health Econ.* 31, 406–439. doi:10.1016/j.jhealeco.2012.03.002

Wang, S., Yang, Q., Deng, L., Lei, Q., Yang, Y., Ma, P., et al. (2022). An overview of cancer drugs approved through expedited approval programs and orphan medicine designation globally between 2011 and 2020. *Drug Discov. Today* 27, 1236–1250. doi:10.1016/j.drudis.2021.12.021

World Health Organization (2022). *World Health Organization*. http://who.int/data/gho/data/themes/mortality-and-global-health-estimates/ghe-leading-causes-of-death (Accessed Jan 03, 2023).

frontiers | Frontiers in Pharmacology

TYPE Review
PUBLISHED 24 March 2023
DOI 10.3389/fphar.2023.1130937

OPEN ACCESS

EDITED BY
Hongzhou Cai,
Nanjing Medical University, China

REVIEWED BY
Lizhi Zhang,
Mayo Clinic, United States
Hong Shu,
Guangxi Medical University Cancer Hospital, China

*CORRESPONDENCE
Xueju Wang,
xueju@jlu.edu.cn

†These authors have contributed equally to this work

SPECIALTY SECTION
This article was submitted to Pharmacology of Anti-Cancer Drugs, a section of the journal Frontiers in Pharmacology

RECEIVED 23 December 2022
ACCEPTED 16 March 2023
PUBLISHED 24 March 2023

CITATION
Zhang X, Wang X, Hou L, Xu Z, Liu Y and Wang X (2023), Nanoparticles overcome adaptive immune resistance and enhance immunotherapy *via* targeting tumor microenvironment in lung cancer. *Front. Pharmacol.* 14:1130937. doi: 10.3389/fphar.2023.1130937

Nanoparticles overcome adaptive immune resistance and enhance immunotherapy *via* targeting tumor microenvironment in lung cancer

Xin Zhang[1†], Xuemei Wang[1†], Lijian Hou[1], Zheng Xu[1], Yu'e Liu[2] and Xueju Wang[1*]

[1]Department of Pathology, China-Japan Union Hospital, Jilin University, Changchun, China, [2]School of Medicine, Tongji University Cancer Center, Shanghai Tenth People's Hospital of Tongji University, Tongji University, Shanghai, China

Lung cancer is one of the common malignant cancers worldwide. Immune checkpoint inhibitor (ICI) therapy has improved survival of lung cancer patients. However, ICI therapy leads to adaptive immune resistance and displays resistance to PD-1/PD-L1 blockade in lung cancer, leading to less immune response of lung cancer patients. Tumor microenvironment (TME) is an integral tumor microenvironment, which is involved in immunotherapy resistance. Nanomedicine has been used to enhance the immunotherapy in lung cancer. In this review article, we described the association between TME and immunotherapy in lung cancer. We also highlighted the importance of TME in immunotherapy in lung cancer. Moreover, we discussed how nanoparticles are involved in regulation of TME to improve the efficacy of immunotherapy, including Nanomedicine SGT-53, AZD1080, Nanomodulator NRF2, Cisplatin nanoparticles, Au@PG, DPAICP@ME, SPIO NP@M-P, NBTXR3 nanoparticles, ARAC nanoparticles, Nano-DOX, MS NPs, Nab-paclitaxel, GNPs-hPD-L1 siRNA. Furthermore, we concluded that targeting TME by nanoparticles could be helpful to overcome resistance to PD-1/PD-L1 blockade in lung cancer.

KEYWORDS

nanoparticles improve immunotherapy TME, PD-L1, PD-1, nanoparticles, immunotherapy, resistance

Introduction

Lung cancer is one of the common malignant cancers worldwide (Lee and Kazerooni, 2022). There are about 236,740 new cases of lung cancer and about 130,180 deaths from this disease in the United States (Siegel et al., 2022). In the United States, the 5-year relative survival rates for lung cancer is 22% (Siegel et al., 2022). Cigarette smoking is one key reason

Abbreviations: ALK, anaplastic lymphoma kinase; EGFR, epidermal growth factor receptor; GAB2, GRB2-associated-binding protein 2; ICAM1, intercellular adhesion molecule-1; ICIs, immune checkpoint inhibitors; KRAS, Kirsten rat sarcoma; mTOR, mammalian target of rapamycin; NSCLC, non-small cell lung carcinoma; OS, overall survival; PD-1, programmed cell death-1; PD-L1, programmed cell death ligand-1; ROS1, receptor tyrosine kinase c-ros oncogene 1; TME, tumor microenvironment; TIME, tumor immune microenvironment; YFCD, yellow fluorescent carbon dot.

for lung cancer development. Lung cancer has three types: non-small cell lung cancer (NSCLC, 82%), small cell lung cancer (SCLC, 14%) and unspecified histology (3%) (Miller et al., 2022). Patients with stage I or II lung cancer often undergo surgery, and patients with stage III lung cancer undergo surgery, chemotherapy and/or radiation (Guo et al., 2022a). However, the lung cancer patients often obtain drug resistance during targeted therapy, chemotherapy and radiotherapy (Wang et al., 2022a; Wu and Lin, 2022).

Immune checkpoints belong to the immune system, which prevent an immune reaction to impair healthy cells (Yu et al., 2022a; Johnson et al., 2022; Song et al., 2022). Immune checkpoint proteins often exist on the surface of T immune cells and tumor cells. After immune checkpoint proteins of T cells bind to other partner proteins of tumor cells, T cells are blocked from impairing the tumor cells (Ma et al., 2021; Hassanian et al., 2022; Korman et al., 2022). For example, immune checkpoint protein PD-1 of T cells can bind with PD-L1 of tumor cells, leading to impairment of killing tumor cells in the body (Hu et al., 2021a; Hou et al., 2023). Immune checkpoint blockade (ICB) with PD-1 antibody or PD-L1 antibody can block the binding between PD-1 and PD-L1, and allow the T cells to destroy tumor cells (Hu et al., 2021b; Jiang et al., 2021; Archilla-Ortega et al., 2022). Immune checkpoint inhibitors (ICIs) often impair the interaction between checkpoint proteins (such as PD-1) and their partner proteins (PD-L1), which allows the T cells to eradicate tumor cells (Havel et al., 2019). For example, one ICI ipilimumab blocks CTLA-4, pembrolizumab and nivolumab blocks PD-1, and atezolizumab, avelumab and durvalumab blocks PD-L1 (Huang and Zappasodi, 2022; Tison et al., 2022). Therefore, ICI therapy has been used in various cancer types, including lung cancer (Fang and Su, 2022; Hao et al., 2022; Mussafi et al., 2022; Punekar et al., 2022; Zulfiqar et al., 2022).

Tumor microenvironment (TME) is an integral tumor microenvironment, which is involved in tumorigenesis, malignant progression and drug resistance (Li and Qiao, 2022; Shi et al., 2022). TME includes complex cellular components, such as tumor-associated macrophages (TAMs), T cells and other immunocytes, blood vessels, fibroblast and extracellular matrix (Liu et al., 2022a). TAMs have been revealed to promote tumor initiation and progression *via* promotion of T cell dysfunction, invasive activity, migratory capacity and angiogenesis (Cao et al., 2022). TAMs can regulate tumor immune microenvironment (TIME) and suppress cytotoxic T lymphocyte (CTL) reaction, resulting in impeding activity of ICIs (Petroni et al., 2022).

Recently, nanomedicine has been widely used to enhance the immunotherapy in lung cancer (Cheng and Santos, 2022). In this review article, we discussed the relationship between TME and immunotherapy in lung cancer. Moreover, we discussed how nanoparticles are involved in regulation of TME to improve the efficacy of immunotherapy. Furthermore, we verified that

TABLE 1 Nanoparticles in regulation of TME and immunotherapy in lung cancer.

Nanoparticles	Functions	Immunotherapy	Ref.
SGT-53	Promotion of tumor immunogenicity, enhancement of innate and adaptive immune responses and inhibits immunosuppression	Sensitizes the efficacy of anti-PD1 antibody treatment	Kim et al. (2018)
AZD1080	Enhances delivery to tumor sites	Reduces expression of PD1 and releases $CD8^+$ T cells	Allen et al. (2021)
ZVI-NP	Enhances anti-tumor immunity *via* reduction of Treg cells and promotion of M2 macrophages to M1.	Repression of PD1 and CTLA4 in $CD8^+$ T cells, reduction of PD-L1 expression	Hsieh et al. (2021)
Cisplatin nanoparticle	Sustained upregulation of PD-L1 expression levels	Promotes the treatment efficacy of anti-PD1/PD-L1 blockade	Shen et al. (2021)
Au@PG nanoparticles	Make tumor remodeling from a cold TME to a hot TME, contributing to tumor suppression and cytotoxic T cell response promotion.	Plus anti-PD1 therapy enhanced tumor suppression and immunosuppression	Su et al. (2022)
DPAICP@ME	Elevates the p53 activation, causes T cell activation	Augments anti-PD1 immunotherapy	He et al. (2022)
SPIO NP@M-P	Maintains the longer half-life of the PD-L1 inhibitory peptides, leading to reactivation of T cells and inhibition of tumor growth	Targets TME for improving immunotherapy	Meng et al. (2021)
NBTXR3 nanoparticles	Modulated the TIME *via* regulation of the T cell receptor repertoire, elevating $CD8^+$ T cells and activation of immune signaling pathways	Overcomes anti-PD1 resistance	Hu et al. (2021c)
ARAC	Decreases effective concentrations of volasertib and PD-L1 antibody *via* modulation of $CD8^+$ T cells.	Increases the effect of PD-L1 inhibitors	Reda et al. (2022)
Nano-DOX	Enhances immunogenicity of tumor cells and reactivates the TAM into M1 phenotype *via* regulation of RAGE/NF-kappa B.	Induction of PD-L1 in the tumor cells and PD-1/PD-L1 in the TAMs. Improves immunotherapy.	Xu et al. (2021)
MS NPs	Retards tumor metastasis *via* increasing immune surveillance and modifying the extracellular matrix	Improves immunotherapy *via* suppression of PD-L1 expression level by metformin.	Cai et al. (2021)
GNPs-hPD-L1 siRNA)	Inhibit the expression of PD-L1 and serve as photothermal agent for theranostic functions	Improves immunotherapy	Liu et al. (2019)

nanoparticles might target TME to improve immunotherapy efficacy and overcome anti-PD1/PD-L1 therapeutic resistance in lung cancer (Table 1).

TME and immunotherapy

TME has been identified to be associated with lung cancer development and progression (Zhao et al., 2022a; Liu et al., 2022b; Madeddu et al., 2022; Mansouri et al., 2022; Peters et al., 2022). TIME is associated with molecular heterogeneity of immunotherapy efficacy in NSCLC patients (Graves et al., 2010; Jin et al., 2020; Belluomini et al., 2021; Genova et al., 2021). In this section, we discuss the association of TME and immunotherapy.

Signaling pathways and TME in immunotherapy

Cellular signaling pathways play a prominent role in regulation of TME in lung cancer. For example, depletion of Periostin modulated TME and suppressed bone metastasis *via* repressing integrin signaling pathway in lung cancer (Che et al., 2017). Vav1 was found to modulate TME in Ras-driven lung cancer (Shalom et al., 2022). Vav1 instigated TME by fibrosis enhancement and reduction in tumor infiltrating macrophage, which was due to cross-talking with colony-stimulating factor 1 (CSF1) pathway, favoring lung cancer growth (Sebban et al., 2014). Blockade of IL6 regulated TME and limited the lung cancer development and progression *via* inactivation of STAT3 pathway (Caetano et al., 2016). Indoleamine 2,3-dioxygenase (IDO) pathway governed antitumor immunity *via* metabolic reprogramming of immune cells in TME through regulating AMPK pathway in lung cancer (Schafer et al., 2016). TRAF4 facilitated lung cancer malignant aggressiveness by regulating TME in normal fibroblasts *via* NF-κB pathway-induced ICAM1 upregulation (Kim et al., 2017). One study showed that low dose of IFNγ endowed tumor stemness in TME of NSCLC *via* regulation of ICAM1/PI3K/AKT/Notch-1 pathway, whereas high dose of IFNγ induced apoptosis of NSCLC cells *via* activation of JAK1/STAT1/caspase pathway (Song et al., 2019). Fibronectin in TME activated inflammatory response *via* regulation of TLR4/NF-κB signaling pathway in lung cancer cells (Cho et al., 2020).

Cyclophosphamide, a cytotoxic agent for cancer treatment, modulated TME *via* TGF-β signaling pathway in a mouse model of Lewis lung cancer (Zhong et al., 2020). Low dose cyclophosphamide increased CD4 + /CD8 + T cells and reduced Treg cells as well as reduced myofibroblasts, which was accompanied with upregulation of E-cadherin and downregulation of N-cadherin (Zhong et al., 2020). Dietary restriction attenuated tumor growth and improved TME and inhibited angiogenesis in NSCLC xenografts through regulation of PI3K/AKT and NF-κB/COX2/iNOS pathways (Lin et al., 2013). The diffusible gas carbon monoxide altered TME and impeded tumor growth *via* regulating MAPK/Erk1/2 pathway, Notch-1 pathway, HO-1 and CD86 expressions in lung cancer (Nemeth et al., 2016). Neobavaisoflavone nanoemulsion was reported to block tumor progression *via* targeting TME of lung cancer through repressing TGF-β/SMADs pathway (Ye et al., 2020). A small nucleolar RNA SNORA38B was reported to promote oncogenesis and reduce immunotherapy effects *via* remodeling the TME through targeting GAB2/AKT/mTOR signaling pathway (Zhuo et al., 2022). SNORA38B recruited the CD4+FOXP3 + Treg cells in TME, contributing to poorer immune efficacy in NSCLC (Zhuo et al., 2022). Evidence has suggested that simultaneous targeting of tumor-initiating cells and signaling pathways in the TME led to effective immunotherapy in lung cancer (Dubinett and Sharma, 2009).

EGFR and ALK mutations affect TME in immunotherapy

EGFR-mutant tumors and ALK-rearranged tumors exhibited a poor response to anti-PD-1/PD-L1 immunotherapy (Jin et al., 2020). TIME was associated with oncogenic manners in NSCLC patients because KRAS mutations and EGFR L858R mutation play a critical role in inflammatory response and immune resistance in tumor microenvironment (Jin et al., 2020). In addition, EGFR-mutant and ALK-rearranged tumors displayed more resting memory $CD4^+$ T cells and less $CD8^+$ T cells and activated memory $CD4^+$ T cells (Jin et al., 2020). Another study also confirmed that targeting the PD-1/PD-L1 did not benefit the EGFR-mutant or ALK-translocated NSCLC patients (Bylicki et al., 2017).

One study reported that $CD25^+$; $CD4^+$ T cells with high expression of PD-L1 (PD-L1 high Treg) were increased in TME of NSCLC patients (Wu et al., 2018). PD-L1 high Treg was positively linked to PD-1 + CD8 in Treg in NSCLC. Moreover, PD-1/PD-L1 pathway promoted the effect of TILs by anti-PD-1/PD-L1 immunotherapy (Wu et al., 2018). These NSCLC patients with PD-L1 expression exhibited a better prognosis. Hence, the density of PD-L1 +; $CD4^+$; $CD25^+$ Tregs in TME could be a diagnostic predictor and immunotherapy response markers in NSCLC (Wu et al., 2018). Another study implied that lymphocyte activing 3 (LAG-3) expression was associated with TILs, PD-1, PD-L1 and survival in NSCLC (He et al., 2017). LAG-3 was expressed on TILs in NSCLC patients' tumor tissues, which was associated with the expression of PD-1 and PD-L1 in NSCLC. NSCLC patients with LAG-3 positivity or both PD-L1 and LAG-3 positivity had an early recurrence and poor prognosis (He et al., 2017).

Low expression of PD-1 in cytotoxic $CD8^+$ TILs indicated a privileged TIME in NSCLC, which suggested a predictive and prognostic values (Mazzaschi et al., 2018). NSCLC patients with low PD-1 expression in $CD8^+$ cells after nivolumab treatment displayed a prolonged survival, indicating that $CD8^+$; PD-1 low was a prediction factor for response to immunotherapy in NSCLC (Mazzaschi et al., 2018). Similarly, one tissue microarray showed that $CD8^+$ cells, especially PD-L1 negative tumors lacking PD-1 + TILs had a big prognostic value. PD-L1 positive tumors with $CD8^+$ lymphocytes can promote the survival in NSCLC (Munari et al., 2021). In addition, PD-L1 overexpression had an unfavorable prognosis and high $CD8^+$ TILs had a favorable prognosis in NSCLC patients (Rashed et al., 2017). Zhang et al. reported that PD-L1 plus $CD8^+$ TILs established an immunosuppressive TME

with high mutation burden in NSCLC (Zhang et al., 2021). NSCLC patients with high PD-L1+; $CD8^+$ TILs had a better response to the anti-PD-1 immunotherapy (Zhang et al., 2021). Consistently, differential TIME determined immunotherapy efficacy in NSCLC patients with advanced stages (Shirasawa et al., 2021).

Four types of groups from 228 NSCLC patients were identified: type I, 73 patients with PD-L1 high/TIL high; type II: 70 cases with PD-L1 low/TIL low; type III: 37 patients with PD-L1 high/TIL low; type IV: 48 cases with PD-L1 low/TIL high. Each type patients had a different survival: Type I tumors had good prognosis compared with type III tumors (Shirasawa et al., 2021). Yang et al. also observed that PD-L1 expression in combination with $CD8^+$ TILs showed a prognostic value in patients with NSCLC after surgery (Yang et al., 2018). A retrospective study defined that PD-L1 expression plus $CD8^+$ TILs density is useful for prediction of disease-free survival in lung squamous cell carcinoma after surgery (Cheng et al., 2022). In addition, PD-L1 expression and TIL infiltration appeared in brain metastasis of small cell lung cancer. PD-L1 TILs and CD45RO+ memory T cells were linked to favorable survival (Berghoff et al., 2016). Lung cancer patients with intracranial resection of brain metastases had a better outcomes if the patients had PD-L1 positivity and a high intraepithelial $CD8^+$ T cell infiltration (Li et al., 2022a). Zhou et al. discovered that paired primary NSCLC and brain metastatic lesions in NSCLC have a difference for PD-L1 expression and $CD8^+$ TILs (Zhou et al., 2018). There were a fewer $CD8^+$ TILs in brain metastatic tissues *versus* primary lung tumor samples, which was associated with shorter overall survival *versus* high $CD8^+$ TILs density (Zhou et al., 2018). However, Batur et al. found that PD-L1 expression and $CD8^+$ TIL intensity had a concordance between brain metastases and NSCLC (Batur et al., 2020). Hence, further investigation is required to determine the role of PD-L1, $CD8^+$ TIL and TIME in immunotherapy of NSCLC patients (Vilarino et al., 2020). Notably, seven randomized controlled trials had uncovered that PD-1/PD-L1 inhibitors exhibited a treatment efficacy in brain metastases of NSCLC, reducing risk of disease progression and death in NSCLC patients with brain metastases (Li et al., 2022b). Strikingly, TME, including spatial and temporal discordance of TILs and PD-L1 expression, was discovered between lung primary lesions and brain metastases in lung cancer (Mansfield et al., 2016). Together, PD-1, PD-L1 expression and TIL status can predict the response of anti-PD-1/PD-L1 treatment in NSCLC (Nakagawa and Kawakami, 2022).

TME and CCRT in NSCLC patients

TME has been known to affect concurrent chemoradiation therapy (CCRT) in NSCLC patients (Shirasawa et al., 2020). Next, we summarize how TME regulates CCRT *via* $CD8^+$ TILs and PD-L1 in NSCLC. A retrospective research showed that chemoradiation therapy can change the expression of PD-L1 and $CD8^+$ TILs (Choe et al., 2019). NSCLC patients with PD-L1 expression had a short survival after concurrent chemoradiation therapy (CCRT). Patients with an upregulation of $CD8^+$ TILs after CCRT displayed a longer overall survival (Choe et al., 2019). Moreover, Tokito et al. defined predictive relevance of PD-L1 plus $CD8^+$ TIL density in patients with stage III NSCLC after CCRT (Tokito et al., 2016). PD-L1+/CD8 low patients had the worst overall survival, whereas PD-L1-/CD8 high patients had the best prognosis (Tokito et al., 2016). PD-L1+ tumor cells were reduced after CCRT in NSCLC patients. Modulation of PD-L1 expression was linked to prognosis in locally advanced NSCLC patients after CCRT (Fujimoto et al., 2017). Similarly, evidence showed that PD-L1 expression was linked to high tumor grade and low density of CD8 TILs (El-Guindy et al., 2018). PD-L1-/CD8 high patients had a good overall survival, while PD-L1+/CD8 low patients often had advantage tumor stage and the poorest overall survival (El-Guindy et al., 2018).

One clinical trial also confirmed the alteration in tumoral PD-L1 expression and stromal $CD8^+$ TILs in NSCLC patients after CCRT (Yoneda et al., 2019). PD-L1 expression was increased in NSCLC patients after CCRT, and stromal $CD8^+$ TIL was elevated after CCRT. Higher $CD8^+$ TILs supported a favorable prognosis. CCRT-induced PD-L1 expression in NSCLC after CCRT suggested that PD-L1 blockade in combination with CCRT is necessary to improve survival in NSCLC (Yoneda et al., 2019). PD-L1-/CD8 low NSCLC patients after CCRT had the longest overall survival, while PD-L1+/CD8 low patients with locally advanced NSCLC after CCRT had the shortest overall survival (Gennen et al., 2020). One study also discovered that PD-L1 expression was changed after CCRT, the density of $CD8^+$ TILs was upregulated after CCRT. Moreover, locally advanced NSCLC patients after CCRT had a good response to anti-PD-1/PD-L1 therapy (Shirasawa et al., 2020).

In lung cancer mouse models

To better understand the role of TME in PD-1 blockade resistance in lung cancer, one group used genetically engineered lung cancer mouse models (Martinez-Usatorre et al., 2021). The mouse models included $Kras^{G12D/+}$; $p53^{-/-}$ (KP) mice, $Kras^{G12D/+}$; $p53^{-/-}$; $Msh2^{-/-}$ (KPM) mice and $Kras^{G12D/+}$; $p53^{-/-}$; ovalbumin (KPO) mice. Blockade of ANGPT2 and VEGFA by a bispecific antibody A2V retarded progression and metastasis of KP lung tumors *via* development of a favorable TME and modulation of the immune cell composition of KP tumors (Martinez-Usatorre et al., 2021). Specifically, A2V treatment was correlated with reprogramming of the TIME through increased T cells and decreased TAMs (Martinez-Usatorre et al., 2021). Interestingly, inhibition of PD-1 by its antibody failed to improve tumor response to A2V treatment in KP mice. However, the PD-1 antibody affected PD-1^+ Tregs in KP tumors (Martinez-Usatorre et al., 2021). Moreover, TAMs interacted with Tregs in KP tumors. Furthermore, CSF1R suppression in combination with cisplatin inhibited TAMs and enhanced the efficacy of anti-angiogenic immunotherapy (Martinez-Usatorre et al., 2021). Another study used the $Kras^{LSL-G12D}$/+$Tp53^{fl/fl}$ (KP) and the $Kras^{LSL-G12D}$/+$Lkb1^{fl/fl}$ (KL) NSCLC mouse models to determine the immunotherapy efficacy and TME of NSCLC (Zhang et al., 2020a). This work showed that CCL7 enhanced anti-PD-1 therapy in these mouse models *via* promoting conventional DC 1 into TME, leading to T cell expansion. In NSCLC tissues, CCL7 expression was elevated, and it was associated with conventional DC 1 infiltration and overall survival in NSCLC patients (Zhang et al., 2020a). In KP mouse model, depletion of CCL7 destroyed the conventional DC 1 infiltration in the TME and promoted expansion of $CD4^+$ and $CD8^+$ T cells in TME, resulting in tumor development. Upregulation

of CCL7 in lungs retarded tumor development and increased the survival of KP and KL mice. Thus, CCL7 could act a biomarker for anti-PD-1 therapy of NSCLC (Zhang et al., 2020a).

Nanomedicine

Nanomedicine is a novel unique branch of medicine using nano-size technology for exploration of underlying mechanisms of disease development and progression and for the prevention, diagnosis and therapy of various diseases (de Lazaro and Mooney, 2021; Stater et al., 2021). Nanomedicine has been used for cancer diagnosis and therapy *via* merging the physical, biological, chemical and digital technologies together (Ahmad et al., 2023; Li et al., 2023). In recent years, nanomedicine has exhibited a potent effect in immunotherapy for cancer patients (Irvine and Dane, 2020; Guo et al., 2022b; Wang et al., 2022b; Yang et al., 2023).

Nanomedicine enhances immunotherapy in lung cancer

Evidence has suggested that nanomedicine could enhance immunotherapy in NSCLC (Seshadri and Ramamurthi, 2018; Garcia-Fernandez et al., 2020; Pu et al., 2022). For example, TME component-targeted nanomedicine delivery facilitated the efficacy of immune checkpoint inhibitors (Kim et al., 2021). In addition, nanoparticle-based ICI therapy elevated the local dose of ICIs and reduced the side effects of ICIs, leading to boosting the anti-tumor immunity in several types of cancers, including lung cancer (Sanaei et al., 2021).

Nanomedicine SGT-53 enhances anti-PD1 antibody immunotherapy

One group designed SGT-53, a nanomedicine carrying a p53 plasmid, to detect whether SGT-53 can augment immune checkpoint inhibitor therapy (Kim et al., 2018). This group used three mouse models, including a glioblastoma, a NSCLC and a breast cancer. SGT-53 sensitized the efficacy of anti-PD1 antibody treatment *via* promotion of tumor immunogenicity, enhancement of innate and adaptive immune responses and inhibited immunosuppression in a breast tumor model (Kim et al., 2018). STG-53 in combination of an anti-PD1 antibody was stronger than each agent individually in suppression of tumor growth and metastasis. STG-53 blocked fatal xenogeneic hypersensitivity after anti-PD1 therapy in breast cancer model (Kim et al., 2018). This work indicated that nanomedicine SGT-53 restored p53 biological function and caused anti-tumor immunity to increase sensitization of anti-PD1 treatment in human cancer.

Nanoparticle AZD1080 enhances delivery to tumor sites

One study used the remote loading of GSK3 inhibitor AZD1080 into nanoparticles coated with a lipid bilayer. Intravenous injection of AZD1080 nanoparticles enhanced biodistribution and drug delivery to cancer site and reduced the expression of PD1 and released $CD8^+$ T cells (Allen et al., 2021). Encapsulated AZD1080 reduced tumor growth in CT26 colorectal tumor, KPC pancreatic cancer and LLC lung cancer models without treatment toxicity. Hence, nano drug delivery of AZD1080 could be used in combination with immunotherapy or chemotherapy in human cancer (Allen et al., 2021).

Nanomodulator NRF2 induces an immunostimulatory TME

It has been reported that zero-valent-iron nanoparticle (ZVI-NP) triggered anticancer immunity and cancer-specific cytotoxicity in lung cancer (Hsieh et al., 2021). ZVI-NP induced ferroptotic death *via* regulation of lipid peroxidation, mitochondria dysfunction and ROS in lung tumor cells. Furthermore, β-TrCP-induced NRF2 destruction *via* AMPK/mTOR pathway was increased in this kind of ferroptosis. ZVI-NP suppressed angiogenesis-associated genes and reduced the self-renewal capacity. ZVI-NP enhanced anti-tumor immunity *via* reduction of Treg cells and promotion of M2 macrophages to M1, and repression of PD1 and CTLA4 in $CD8^+$ T cells, as well as reduction of PD-L1 expression in tumor cells. Strikingly, ZVI-NP mainly stayed in lung tissues and tumor sites, resulting in inhibition of tumor metastasis and growth (Hsieh et al., 2021). Taken together, NRF2 nanomodulator stimulated lung cancer ferroptosis and maintained an immunostimulatory TME.

Cisplatin nanoparticles sensitize PD1/PD-L1 inhibitors

Cisplatin nanoparticles improved the PD1/PD-L1 inhibitor therapeutic outcomes because cisplatin nanoparticles increased the expression of PD-L1 levels (Shen et al., 2021). Cisplatin nanoparticles in combination with PD1/PD-L1 inhibitors, BMS-202 and anti-PD1 antibody, caused a superior inhibition of tumor growth. Cisplatin nanoparticles plus anti-PD1 antibody displayed a stronger tumor inhibition than cisplatin plus anti-PD1 antibody in the LLC tumor model. Altogether, cisplatin nanoparticle promoted the treatment efficacy of anti-PD1/PD-L1 blockade through sustained upregulation of PD-L1 expression levels (Shen et al., 2021).

Au@PG nanoparticles improve immunotherapy

Polyaniline-based glyco-condensation on Au nanoparticles have been found to promote immunotherapy in lung cancer (Su et al., 2022). Au@PG nanoparticles can make tumor remodeling from a cold TME to a hot TME, contributing to tumor suppression and cytotoxic T cell response promotion. Au@PG nanoparticles plus anti-PD1 therapy enhanced tumor suppression and immunosuppression and improved cytokine secretion (Su et al., 2022). Moreover, the size of Au@PG nanoparticles made a decision

for the switch from M2 to M1 macrophages: the smaller Au@PG nanoparticles exhibited better functions than larger ones. Au@PG nanoparticles caused endoplasmic reticulum stress and spleen tyrosine kinase activation and macrophage polarization in lung cancer (Su et al., 2022).

DPAICP@ME augments anti-PD1 immunotherapy

A chiral-peptide supramolecular (DPAICP) interacting with the membrane from milk-derived extracellular vesicles (ME) was constructed (He et al., 2022). DPAICP@ME was found to be stable in blood circulation after gastrointestinal absorption, and displayed tumor accumulation by oral medication. Oral DPAICP@ME elevated the p53 activation for treating cancer in LLC lung cancer orthotopic model and PDOX mice of colon cancer and B16F10 homograft melanoma model (He et al., 2022). Oral DPAICP@ME caused T cell activation and led to enhancement of anti-PD1 immunotherapy. Hence, DPAICP@ME could boost the anti-PD1 immunotherapy in human cancer (He et al., 2022).

SPIO NP@M-P targets TME for immunotherapy

Superparamagnetic iron oxide nanoparticles (SPIO NPs) were combined with lung cancer H460 cell membranes, PD-L1 inhibitory peptide (TPP1) and MMP2 substrate peptide (PLGLLG), which were named as SPIO NP@M-P (Meng et al., 2021). The TPP1 peptide with homotypic effect of cancer cell membrane was entered to the TME and digested by MMP2 enzyme. Therefore, SPIO NP@M-P maintained the longer half-life of the PD-L1 inhibitory peptides, leading to reactivation of T cells and inhibition of tumor growth (Meng et al., 2021). SPIO NP@M-P could be a useful platform for cancer therapy and tumor diagnosis.

NBTXR3 nanoparticles overcomes anti-PD1 resistance

To overcome anti-PD1 resistance in lung cancer, one group combined radiation with NBTXR3 nanoparticles and anti-PD1 therapy (Hu et al., 2021c). This group reported that the triple combination (anti-PD1, localized radiation and NBTXR3) reduced growth of irradiated and unirradiated tumors in 344SQP anti-PD1-sensitive lung cancer cells and 344SQR anti-PD1-resistant lung cancer cells (Hu et al., 2021c). Moreover, NBTXR3 modulated the TIME of unirradiated tumors *via* regulation of the T cell receptor repertoire, elevating $CD8^+$ T cells and activation of immune signaling pathways in 344SQR tumor model. NBTXR3 nanoparticles could be helpful for treating metastatic lung cancer patients regardless of immunotherapeutic resistance or sensitivity (Hu et al., 2021c). Later, this group combined NBTXR3 with three inhibitors of checkpoint receptors: PD1, TIGIT and LAG3 (Hu et al., 2022). The nanoparticle-involved combination treatment reduced the growth of irradiated and unirradiated tumors due to activation of the immune response and increased immune cells (Hu et al., 2022). Furthermore, a triple-combination therapy includes NBTXR3, high-dose radiation (HDXRT) for primary tumors and low-dose radiation (LDXRT) for a secondary tumor, and ICIs (Hu et al., 2021d). This triple-combination therapy displayed remarkable anticancer activity and improve the survival in mice of anti-PD1-resistant lung cancer. NBTXR3+HDXRT + LDXRT reduced the number of Treg cells and promoted CD8 T cell infiltration. NBTXR3 nanoparticle plus radioimmunotherapy enhance antitumor immune response and promote the survival (Hu et al., 2021d).

ARAC nanoparticles target PD-L1

A nanoparticle-based treatment named antigen release agent and checkpoint inhibitor (ARAC) was discovered to increase the effect of PD-L1 inhibitors (Reda et al., 2022). ARAC nanoparticle co-delivered PLK1 inhibitor (volasertib) and PD-L1 antibody. Because PLK1 was often upregulated in lung cancer and promoted tumor growth, suppression of PLK1 could reduce cancer growth. ARAC decreased effective concentrations of volasertib and PD-L1 antibody in LLC tumor model *via* modulation of $CD8^+$ T cells. ARAC exhibited therapy efficacy in KLN-205 lung tumor model (Reda et al., 2022).

Nano-DOX improve immunotherapy

Nanodiamond-doxorubicin conjugates (Nano-DOX) in combination with anti-PD-L1 agent BMS-1 synergistically enhanced tumor suppression (Xu et al., 2021). Nano-DOX enhanced immunogenicity of tumor cells and reactivated the TAM into M1 phenotype *via* regulation of RAGE/NF-κB pathway and induction of PD-L1 in the tumor cells and PD-1/PD-L1 in the TAMs. Nano-DOX increased the cytokine HMGB1 *via* targeting RAGE/NF-κB pathway (Xu et al., 2021). BMS-1 promoted M1 activation of TAMs that was induced by Nano-DOX *via* reducing PD-L1 in the TAMs and impairing the interaction between PD1 and PD-L1, contributing to inhibition of tumor growth due to killing tumor cells. Nano-DOX enhanced BMS-1 efficacy on tumor growth in a TAM-mediated manner (Xu et al., 2021).

MS NPs enhance chemo-immunotherapy

A nanodrug (MS NPs) was developed to combine immunoadjuvant metformin with 7-ethyl-10-hydroxycamptothecin (SN38) *via* electrostatic interactions (Cai et al., 2021). MS NPs improved immunotherapy *via* suppression of PD-L1 expression level by metformin. MS NPs were also found to retard tumor metastasis *via* increasing immune surveillance and modifying the extracellular matrix (Cai et al., 2021). Importantly, MS NPs increased mouse survival with no obvious toxicity. MS NPs increased the efficacy of ICIs, indicating that MS NPs could open a new window for the development of novel anti-PD1/PD-L1 therapy (Cai et al., 2021).

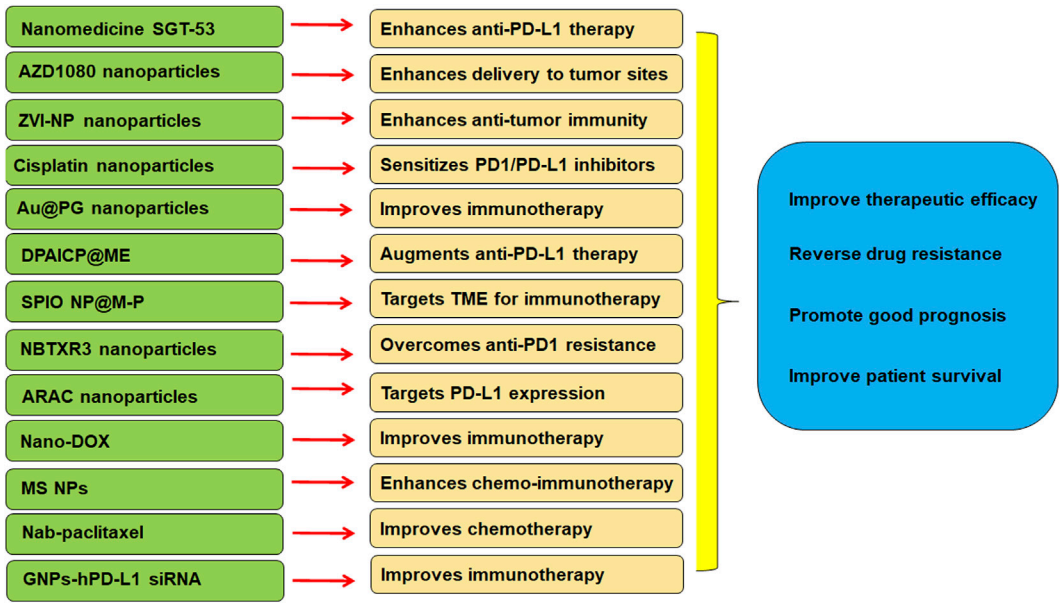

FIGURE 1
The role of nanoparticles in regulation of TME and immunotherapy in lung cancer.

Other nanoparticles improve immunotherapy

One group designed nanoarchitecture using anti-PD-L1 antibody and magnetic-nanoparticle-attached YFCD for the separation and identification of PD-L1-expressing exosomes (Pramanik et al., 2022). Different lung cancer cell lines had a different amount of PD-L1+ exosomes. H460 lung cancer cells expressed huge PD-L1+ exosomes, and A549 cancer cells expressed low PD-L1+ exosomes, while normal skin HaCaT cells did not express PD-L1+ exosomes (Pramanik et al., 2022). The nanoarchitectures with YFCDs and anti-PD-L1 antibody separated and tracked PD-L1+ exosomes, suggesting that this nanoarchitecture could be used for clinical application to analyze PD-L1+ exosomes, which can help immunotherapy (Pramanik et al., 2022). Nanoparticle albumin-bound (Nab)-paclitaxel had improved the survival of older patients with stage IV NSCLC after disease progression with platinum-based doublet chemotherapy (Weiss et al., 2020). A gold nanoprism-assisted human PD-L1 siRNA (GNPs-hPD-L1 siRNA) was designed to inhibit the expression of PD-L1 and serve as photothermal agent for theranostic functions in lung cancer (Liu et al., 2019).

Conclusion

In conclusion, there is a close association between TME and immunotherapy in lung cancer. Targeting TME could be a strategy for overcoming resistance to PD-1/PD-L1 blockade in lung cancer. ICIs have demonstrated the therapeutic benefits in NSCLC. But ICIs have several side effects, such as ICI-related pneumonitis (Conroy and Naidoo, 2022; Hao et al., 2022). Altogether, nanoparticle-based ICI therapy can boost the anti-tumor immunity in lung cancer (Figure 1).

Several issues need to be highlighted in lung cancer therapy. For example, mRNA vaccine development to recognize immune-associated tumor antigens and immune subtypes in lung cancer (Wang et al., 2021; Zhao et al., 2022b; Zhao et al., 2022c; Xu et al., 2022; Zhou et al., 2022). Similar mRNA vaccines have been reported in other cancers, such as glioma and melanoma (Zhong et al., 2021; Sittplangkoon et al., 2022). Moreover, lipid nanoparticle-based mRNA cancer vaccines displayed advantages in cancer therapy ((Persano et al., 2017; Chen et al., 2022a; Huang et al., 2022a)). In addition, non-coding RNAs have been revealed to participate in tumorigenesis in various cancer types ((Chen et al., 2022b; Yu et al., 2022b; Liu and Shang, 2022)). RNA nanotechnology has emerged in cancer therapy in recent years [(Guo, 2010), (Huang et al., 2022b)]. It is important to use nanomedicine to treat cancer cells *via* modulation of non-coding RNAs in lung cancer.

Recently, there is an association between lung cancer, COVID-19 and vaccines [(Trivanovic et al., 2022), (Mao et al., 2021)]. Lung cancer patients have an increased risk from COVID-19 infection and exhibit poor outcomes [(Oldani et al., 2022), (Aramini et al., 2022)]. In addition, genomics, transcriptomics, proteomics, lipidomics and metabolomics are important to be used to determine the mechanisms of disease development and carcinogenesis [(Zhou et al., 2019; Zhang et al., 2020b; Boys et al., 2022)]. The role of multi-omics has been described in lung cancer early detection and therapy [(Abbasian et al., 2022), (Ling et al., 2022)]. The multi-omics should be applied for exploration of TME and immunotherapy in lung cancer to overcome the immunotherapy resistance. Lastly, it must be mentioned that nanomaterials could have side-effects, such as toxicity, and delivery problems. The degradation byproducts from the

nanomaterials could have toxicity for host cells. Hence, it is critical to solve these disadvantages of nanomaterials when they are used for cancer therapy to improve immunotherapeutic efficacy in lung cancer.

Author contributions

XZ and XW wrote the manuscript; LH, ZX, and, YL edited manuscript and made the figures and tables. XW edited and revised the manuscript. All authors have read and approved for the final version of the manuscript.

Funding

This work is supported by the Young Scientists Fund of the National Natural Science Foundation of China (grant No. 81700198), the Science and Technology Development Project of Jilin Province (grant No. 20190701064GH).

Conflict of interest

The authors declare that the research was conducted in the absence of any commercial or financial relationships that could be construed as a potential conflict of interest.

Publisher's note

References

Abbasian, M. H., Ardekani, A. M., Sobhani, N., and Roudi, R. (2022). The role of genomics and proteomics in lung cancer early detection and treatment. *Cancers (Basel)* 14 (20), 5144. Epub 20221020. doi:10.3390/cancers14205144

Ahmad, A., Rashid, S., Chaudhary, A. A., Alawam, A. S., Alghonaim, M. I., Raza, S. S., et al. (2023). Nanomedicine as potential cancer therapy via targeting dysregulated transcription factors. *Semin. Cancer Biol.* 89, 38–60. Epub 20230118. doi:10.1016/j.semcancer.2023.01.002

Allen, S. D., Liu, X., Jiang, J., Liao, Y. P., Chang, C. H., Nel, A. E., et al. (2021). Immune checkpoint inhibition in syngeneic mouse cancer models by a silicasome nanocarrier delivering a GSK3 inhibitor. *Biomaterials* 269, 120635. Epub 20201228. doi:10.1016/j.biomaterials.2020.120635

Aramini, B., Masciale, V., Samarelli, A. V., Tonelli, R., Cerri, S., Clini, E., et al. (2022). Biological effects of COVID-19 on lung cancer: Can we drive our decisions. *Front. Oncol.* 12, 1029830. Epub 20221010. doi:10.3389/fonc.2022.1029830

Archilla-Ortega, A., Domuro, C., Martin-Liberal, J., and Munoz, P. (2022). Blockade of novel immune checkpoints and new therapeutic combinations to boost antitumor immunity. *J. Exp. Clin. Cancer Res.* 41 (1), 62. Epub 20220214. doi:10.1186/s13046-022-02264-x

Batur, S., Dulger, O., Durak, S., Yumuk, P. F., Caglar, H. B., Bozkurtlar, E., et al. (2020). Concordance of PD-L1 expression and CD8+ TIL intensity between NSCLC and synchronous brain metastases. *Bosn. J. Basic Med. Sci.* 20 (3), 329–335. Epub 20200803. doi:10.17305/bjbms.2019.4474

Belluomini, L., Dodi, A., Caldart, A., Kadrija, D., Sposito, M., Casali, M., et al. (2021). A narrative review on tumor microenvironment in oligometastatic and oligoprogressive non-small cell lung cancer: A lot remains to be done. *Transl. Lung Cancer Res.* 10 (7), 3369–3384. doi:10.21037/tlcr-20-1134

Berghoff, A. S., Ricken, G., Wilhelm, D., Rajky, O., Widhalm, G., Dieckmann, K., et al. (2016). Tumor infiltrating lymphocytes and PD-L1 expression in brain metastases of small cell lung cancer (SCLC). *J. Neurooncol* 130 (1), 19–29. Epub 20160719. doi:10.1007/s11060-016-2216-8

Boys, E. L., Liu, J., Robinson, P. J., and Reddel, R. R. (2022). Clinical applications of mass spectrometry-based proteomics in cancer: Where are we? *Proteomics*, e2200238. Epub 20220815. doi:10.1002/pmic.202200238

Bylicki, O., Paleiron, N., Margery, J., Guisier, F., Vergnenegre, A., Robinet, G., et al. (2017). Targeting the PD-1/PD-L1 immune checkpoint in EGFR-mutated or ALK-translocated non-small-cell lung cancer. *Target Oncol.* 12 (5), 563–569. doi:10.1007/s11523-017-0510-9

Caetano, M. S., Zhang, H., Cumpian, A. M., Gong, L., Unver, N., Ostrin, E. J., et al. (2016). IL6 blockade reprograms the lung tumor microenvironment to limit the development and progression of K-ras-Mutant lung cancer. *Cancer Res.* 76 (11), 3189–3199. Epub 20160401. doi:10.1158/0008-5472.CAN-15-2840

Cai, S., Chen, Z., Wang, Y., Wang, M., Wu, J., Tong, Y., et al. (2021). Reducing PD-L1 expression with a self-assembled nanodrug: An alternative to PD-L1 antibody for enhanced chemo-immunotherapy. *Theranostics* 11 (4), 1970–1981. Epub 20210101. doi:10.7150/thno.45777

Cao, H., Gao, S., Jogani, R., and Sugimura, R. (2022). The tumor microenvironment reprograms immune cells. *Cell Reprogr.* 24 (6), 343–352. Epub 20221026. doi:10.1089/cell.2022.0047

Che, J., Shen, W. Z., Deng, Y., Dai, Y. H., Liao, Y. D., Yuan, X. L., et al. (2017). Effects of lentivirus-mediated silencing of Periostin on tumor microenvironment and bone metastasis via the integrin-signaling pathway in lung cancer. *Life Sci.* 182, 10–21. 10.1016/j.lfs.2017.05.030.

Chen, J., Ye, Z., Huang, C., Qiu, M., Song, D., Li, Y., et al. (2022). Lipid nanoparticle-mediated lymph node-targeting delivery of mRNA cancer vaccine elicits robust CD8(+) T cell response. *Proc. Natl. Acad. Sci. U. S. A.* 119 (34), e2207841119. Epub 20220815. doi:10.1073/pnas.2207841119

Chen, T., Liu, J., Zhang, H., Li, J., and Shang, G. (2022). Long intergenic noncoding RNA00265 enhances cell viability and metastasis via targeting miR-485-5p/USP22 Axis in osteosarcoma. *Front. Oncol.* 12, 907472. Epub 20220526. doi:10.3389/fonc.2022.907472

Cheng, R., and Santos, H. A. (2022). Smart nanoparticle-based platforms for regulating tumor microenvironment and cancer immunotherapy. *Adv. Healthc. Mater* 2022, e2202063. Epub 20221207. doi:10.1002/adhm.202202063

Cheng, X., Wang, L., and Zhang, Z. (2022). Prognostic significance of PD-L1 expression and CD8(+) TILs density for disease-free survival in surgically resected lung squamous cell carcinoma: A retrospective study. *J. Thorac. Dis.* 14 (6), 2224–2234. doi:10.21037/jtd-22-630

Cho, C., Horzempa, C., Longo, C. M., Peters, D. M., Jones, D. M., and McKeown-Longo, P. J. (2020). Fibronectin in the tumor microenvironment activates a TLR4-dependent inflammatory response in lung cancer cells. *J. Cancer* 11 (11), 3099–3105. Epub 20200304. doi:10.7150/jca.39771

Choe, E. A., Cha, Y. J., Kim, J. H., Pyo, K. H., Hong, M. H., Park, S. Y., et al. (2019). Dynamic changes in PD-L1 expression and CD8(+) T cell infiltration in non-small cell lung cancer following chemoradiation therapy. *Lung Cancer* 136, 30–36. Epub 20190801. doi:10.1016/j.lungcan.2019.07.027

Conroy, M., and Naidoo, J. (2022). Immune-related adverse events and the balancing act of immunotherapy. *Nat. Commun.* 13 (1), 392. Epub 20220119. doi:10.1038/s41467-022-27960-2

de Lazaro, I., and Mooney, D. J. (2021). Obstacles and opportunities in a forward vision for cancer nanomedicine. *Nat. Mater* 20 (11), 1469–1479. Epub 20210705. doi:10.1038/s41563-021-01047-7

Dubinett, S., and Sharma, S. (2009). Towards effective immunotherapy for lung cancer: Simultaneous targeting of tumor-initiating cells and immune pathways in the tumor microenvironment. *Immunotherapy* 1 (5), 721–725. in: Pubmed; PMID 20636013. doi:10.2217/imt.09.56

El-Guindy, D. M., Helal, D. S., Sabry, N. M., and Abo El-Nasr, M. (2018). Programmed cell death ligand-1 (PD-L1) expression combined with CD8 tumor infiltrating lymphocytes density in non-small cell lung cancer patients. *J. Egypt Natl. Canc Inst.* 30 (4), 125–131. Epub 20181015. doi:10.1016/j.jnci.2018.08.003

Fang, Y., and Su, C. (2022). Research progress on the microenvironment and immunotherapy of advanced non-small cell lung cancer with liver metastases. *Front. Oncol.* 12, 893716. Epub 20220728. doi:10.3389/fonc.2022.893716

Fujimoto, D., Uehara, K., Sato, Y., Sakanoue, I., Ito, M., Teraoka, S., et al. (2017). Alteration of PD-L1 expression and its prognostic impact after concurrent chemoradiation therapy in non-small cell lung cancer patients. *Sci. Rep.* 7 (1), 11373. Epub 20170912. doi:10.1038/s41598-017-11949-9

Garcia-Fernandez, C., Fornaguera, C., and Borros, S. (2020). Nanomedicine in non-small cell lung cancer: From conventional treatments to immunotherapy. *Cancers (Basel)* 12 (6). doi:10.3390/cancers12061609

Gennen, K., Kasmann, L., Taugner, J., Eze, C., Karin, M., Roengvoraphoj, O., et al. (2020). Prognostic value of PD-L1 expression on tumor cells combined with CD8+ TIL density in patients with locally advanced non-small cell lung cancer treated with concurrent chemoradiotherapy. *Radiat. Oncol.* 15 (1), 5. Epub 20200102. doi:10.1186/s13014-019-1453-3

Genova, C., Dellepiane, C., Carrega, P., Sommariva, S., Ferlazzo, G., Pronzato, P., et al. (2021). Therapeutic implications of tumor microenvironment in lung cancer: Focus on immune checkpoint blockade. *Front. Immunol.* 12, 799455. Epub 20220107. doi:10.3389/fimmu.2021.799455

Graves, E. E., Maity, A., and Le, Q. T. (2010). The tumor microenvironment in non-small-cell lung cancer. *Semin. Radiat. Oncol.* 20 (3), 156–163. doi:10.1016/j.semradonc.2010.01.003

Guo, P. (2010). The emerging field of RNA nanotechnology. *Nat. Nanotechnol.* 5 (12), 833–842. Epub 20101121. doi:10.1038/nnano.2010.231

Guo, Q., Liu, L., Chen, Z., Fan, Y., Zhou, Y., Yuan, Z., et al. (2022). Current treatments for non-small cell lung cancer. *Front. Oncol.* 12, 945102. Epub 20220811. doi:10.3389/fonc.2022.945102

Guo, S., Feng, J., Li, Z., Yang, S., Qiu, X., Xu, Y., et al. (2022). *Improved cancer immunotherapy strategies by nanomedicine.* Wiley Interdiscip Rev Nanomed Nanobiotechnol, e1873. Epub 20221228. doi:10.1002/wnan.1873

Hao, Y., Zhang, X., and Yu, L. (2022). Immune checkpoint inhibitor-related pneumonitis in non-small cell lung cancer: A review. *Front. Oncol.* 12, 911906. Epub 20220816. doi:10.3389/fonc.2022.911906

Hassanian, H., Asadzadeh, Z., Baghbanzadeh, A., Derakhshani, A., Dufour, A., Rostami Khosroshahi, N., et al. (2022). The expression pattern of Immune checkpoints after chemo/radiotherapy in the tumor microenvironment. *Front. Immunol.* 13, 938063. Epub 20220728. doi:10.3389/fimmu.2022.938063

Havel, J. J., Chowell, D., and Chan, T. A. (2019). The evolving landscape of biomarkers for checkpoint inhibitor immunotherapy. *Nat. Rev. Cancer* 19 (3), 133–150. doi:10.1038/s41568-019-0116-x

He, W., Zhang, Z., Yang, W., Zheng, X., You, W., Yao, Y., et al. (2022). Turing milk into pro-apoptotic oral nanotherapeutic: De novo bionic chiral-peptide supramolecule for cancer targeted and immunological therapy. *Theranostics* 12 (5), 2322–2334. Epub 20220221. doi:10.7150/thno.70568

He, Y., Yu, H., Rozeboom, L., Rivard, C. J., Ellison, K., Dziadziuszko, R., et al. (2017). LAG-3 protein expression in non-small cell lung cancer and its relationship with PD-1/PD-L1 and tumor-infiltrating lymphocytes. *J. Thorac. Oncol.* 12 (5), 814–823. Epub 20170126. doi:10.1016/j.jtho.2017.01.019

Hou, B., Chen, T., Zhang, H., Li, J., Wang, P., and Shang, G. (2023). The E3 ubiquitin ligases regulate PD-1/PD-L1 protein levels in tumor microenvironment to improve immunotherapy. *Front. Immunol.* 14, 1123244. Epub 20230117. doi:10.3389/fimmu.2023.1123244

Hsieh, C. H., Hsieh, H. C., Shih, F. S., Wang, P. W., Yang, L. X., Shieh, D. B., et al. (2021). An innovative NRF2 nano-modulator induces lung cancer ferroptosis and elicits an immunostimulatory tumor microenvironment. *Theranostics* 11 (14), 7072–7091. Epub 20210513. doi:10.7150/thno.57803

Hu, X., Lin, Z., Wang, Z., and Zhou, Q. (2021). Emerging role of PD-L1 modification in cancer immunotherapy. *Am. J. Cancer Res.* 11 (8), 3832–3840.

Hu, X., Wang, J., Chu, M., Liu, Y., Wang, Z. W., and Zhu, X. (2021). Emerging role of ubiquitination in the regulation of PD-1/PD-L1 in cancer immunotherapy. *Mol. Ther.* 29 (3), 908–919. Epub 20210101. doi:10.1016/j.ymthe.2020.12.032

Hu, Y., Paris, S., Barsoumian, H., Abana, C. O., He, K., Sezen, D., et al. (2021). A radioenhancing nanoparticle mediated immunoradiation improves survival and generates long-term antitumor immune memory in an anti-PD1-resistant murine lung cancer model. *J. Nanobiotechnology* 19 (1), 416. Epub 20211211. doi:10.1186/s12951-021-01163-1

Hu, Y., Paris, S., Barsoumian, H., Abana, C. O., He, K., Wasley, M., et al. (2021). Radiation therapy enhanced by NBTXR3 nanoparticles overcomes anti-PD1 resistance and evokes abscopal effects. *Int. J. Radiat. Oncol. Biol. Phys.* 111 (3), 647–657. Epub 20210706. doi:10.1016/j.ijrobp.2021.06.041

Hu, Y., Paris, S., Bertolet, G., Barsoumian, H. B., He, K., Sezen, D., et al. (2022). Combining a nanoparticle-mediated immunoradiotherapy with dual blockade of LAG3 and TIGIT improves the treatment efficacy in anti-PD1 resistant lung cancer. *J. Nanobiotechnology* 20 (1), 417. Epub 20220919. doi:10.1186/s12951-022-01621-4

Huang, A. C., and Zappasodi, R. (2022). A decade of checkpoint blockade immunotherapy in melanoma: Understanding the molecular basis for immune sensitivity and resistance. *Nat. Immunol.* 23 (5), 660–670. Epub 20220303. doi:10.1038/s41590-022-01141-1

Huang, T., Peng, L., Han, Y., Wang, D., He, X., Wang, J., et al. (2022). Lipid nanoparticle-based mRNA vaccines in cancers: Current advances and future prospects. *Front. Immunol.* 13, 922301. Epub 20220826. doi:10.3389/fimmu.2022.922301

Huang, X., Kong, N., Zhang, X., Cao, Y., Langer, R., and Tao, W. (2022). The landscape of mRNA nanomedicine. *Nat. Med.* 28 (11), 2273–2287. Epub 20221110. doi:10.1038/s41591-022-02061-1

Irvine, D. J., and Dane, E. L. (2020). Enhancing cancer immunotherapy with nanomedicine. *Nat. Rev. Immunol.* 20 (5), 321–334. Epub 20200131. doi:10.1038/s41577-019-0269-6

Jiang, W., Pan, S., Chen, X., Wang, Z. W., and Zhu, X. (2021). The role of lncRNAs and circRNAs in the PD-1/PD-L1 pathway in cancer immunotherapy. *Mol. Cancer* 20 (1), 116. Epub 20210908. doi:10.1186/s12943-021-01406-7

Jin, R., Liu, C., Zheng, S., Wang, X., Feng, X., Li, H., et al. (2020). Molecular heterogeneity of anti-PD-1/PD-L1 immunotherapy efficacy is correlated with tumor immune microenvironment in East Asian patients with non-small cell lung cancer. *Cancer Biol. Med.* 17 (3), 768–781. doi:10.20892/j.issn.2095-3941.2020.0121

Johnson, D. B., Nebhan, C. A., Moslehi, J. J., and Balko, J. M. (2022). Immune-checkpoint inhibitors: Long-term implications of toxicity. *Nat. Rev. Clin. Oncol.* 19 (4), 254–267. Epub 20220126. doi:10.1038/s41571-022-00600-w

Kim, E., Kim, W., Lee, S., Chun, J., Kang, J., Park, G., et al. (2017). TRAF4 promotes lung cancer aggressiveness by modulating tumor microenvironment in normal fibroblasts. *Sci. Rep.* 7 (1), 8923. Epub 20170821. doi:10.1038/s41598-017-09447-z

Kim, J., Hong, J., Lee, J., Fakhraei Lahiji, S., and Kim, Y. H. (2021). Recent advances in tumor microenvironment-targeted nanomedicine delivery approaches to overcome limitations of immune checkpoint blockade-based immunotherapy. *J. Control Release* 332, 109–126. 10.1016/j.jconrel.2021.02.002.

Kim, S. S., Harford, J. B., Moghe, M., Rait, A., and Chang, E. H. (2018). Combination with SGT-53 overcomes tumor resistance to a checkpoint inhibitor. *Oncoimmunology* 7 (10), e1484982. Epub 20180801. doi:10.1080/2162402X.2018.1484982

Korman, A. J., Garrett-Thomson, S. C., and Lonberg, N. (2022). The foundations of immune checkpoint blockade and the ipilimumab approval decennial. *Nat. Rev. Drug Discov.* 21 (7), 509–528. Epub 20211222. doi:10.1038/s41573-021-00345-8

Lee, E., and Kazerooni, E. A. (2022). Lung cancer screening. *Semin. Respir. Crit. Care Med.* 43 (6), 839–850. Epub 20221128. doi:10.1055/s-0042-1757885

Li, H., Luo, Q., Zhang, H., Ma, X., Gu, Z., Gong, Q., et al. (2023). Nanomedicine embraces cancer radio-immunotherapy: Mechanism, design, recent advances, and clinical translation. *Chem. Soc. Rev.* 52 (1), 47–96. Epub 20230103. doi:10.1039/d2cs00437b

Li, L. L., Zhou, D. X., Lu, M., Zhou, D., Lin, X. F., Chen, Y., et al. (2022). An integrated biomarker of PD-L1 expression and intraepithelial CD8(+) T cell infiltration was associated with the prognosis of lung cancer patients after intracranial resection of brain metastases. *Thorac. Cancer* 13 (13), 1948–1960. Epub 20220520. doi:10.1111/1759-7714.14473

Li, T., and Qiao, T. (2022). Unraveling tumor microenvironment of small-cell lung cancer: Implications for immunotherapy. *Semin. Cancer Biol.* 86 (2), 117–125. doi:10.1016/j.semcancer.2022.09.005

Li, W., Jiang, J., Huang, L., and Long, F. (2022). Efficacy of PD-1/L1 inhibitors in brain metastases of non-small-cell lung cancer: Pooled analysis from seven randomized controlled trials. *Future Oncol.* 18 (3), 403–412. Epub 20211117. doi:10.2217/fon-2021-0795

Lin, B. Q., Zeng, Z. Y., Yang, S. S., and Zhuang, C. W. (2013). Dietary restriction suppresses tumor growth, reduces angiogenesis, and improves tumor microenvironment in human non-small-cell lung cancer xenografts. *Lung Cancer* 79 (2), 111–117. Epub 20121128. doi:10.1016/j.lungcan.2012.11.001

Ling, B., Zhang, Z., Xiang, Z., Cai, Y., Zhang, X., and Wu, J. (2022). Advances in the application of proteomics in lung cancer. *Front. Oncol.* 12, 993781. Epub 20220927. doi:10.3389/fonc.2022.993781

Liu, B., Cao, W., Qiao, G., Yao, S., Pan, S., Wang, L., et al. (2019). Effects of gold nanoprism-assisted human PD-L1 siRNA on both gene down-regulation and photothermal therapy on lung cancer. *Acta Biomater.* 99, 307–319. Epub 20190909. doi:10.1016/j.actbio.2019.08.046

Liu, J., Chen, T., Li, S., Liu, W., Wang, P., and Shang, G. (2022). Targeting matrix metalloproteinases by E3 ubiquitin ligases as a way to regulate the tumor microenvironment for cancer therapy. *Semin. Cancer Biol.* 86 (2), 259–268. 10.1016/j.semcancer.2022.06.004.

Liu, J., and Shang, G. (2022). The roles of noncoding RNAs in the development of osteosarcoma stem cells and potential therapeutic targets. *Front. Cell Dev. Biol.* 10, 773038. Epub 20220216. doi:10.3389/fcell.2022.773038

Liu, W., Powell, C. A., and Wang, Q. (2022). Tumor microenvironment in lung cancer-derived brain metastasis. *Chin. Med. J. Engl.* 135 (15), 1781–1791. Epub 20220805. doi:10.1097/CM9.0000000000002127

Ma, L. R., Li, J. X., Tang, L., Li, R. Z., Yang, J. S., Sun, A., et al. (2021). Immune checkpoints and immunotherapy in non-small cell lung cancer: Novel study progression, challenges and solutions. *Oncol. Lett.* 22 (5), 787. Epub 20210914. doi:10.3892/ol.2021.13048

Madeddu, C., Donisi, C., Liscia, N., Lai, E., Scartozzi, M., and Maccio, A. (2022). EGFR-mutated non-small cell lung cancer and resistance to immunotherapy: Role of the tumor microenvironment. *Int. J. Mol. Sci.* 23 (12), 6489. Epub 20220610. doi:10.3390/ijms23126489

Mansfield, A. S., Aubry, M. C., Moser, J. C., Harrington, S. M., Dronca, R. S., Park, S. S., et al. (2016). Temporal and spatial discordance of programmed cell death-ligand 1 expression and lymphocyte tumor infiltration between paired primary lesions and

brain metastases in lung cancer. *Ann. Oncol.* 27 (10), 1953–1958. Epub 20160808. doi:10.1093/annonc/mdw289

Mansouri, S., Heylmann, D., Stiewe, T., Kracht, M., and Savai, R. (2022). Cancer genome and tumor microenvironment: Reciprocal crosstalk shapes lung cancer plasticity. *Elife* 11, e79895. Epub 20220908. doi:10.7554/eLife.79895

Mao, K., Tan, Q., Ma, Y., Wang, S., Zhong, H., Liao, Y., et al. (2021). Proteomics of extracellular vesicles in plasma reveals the characteristics and residual traces of COVID-19 patients without underlying diseases after 3 months of recovery. *Cell Death Dis.* 12 (6), 541. 10.1038/s41419-021-03816-3.

Martinez-Usatorre, A., Kadioglu, E., Boivin, G., Cianciaruso, C., Guichard, A., Torchia, B., et al. (2021). Overcoming microenvironmental resistance to PD-1 blockade in genetically engineered lung cancer models. *Sci. Transl. Med.* 13 (606), eabd1616. doi:10.1126/scitranslmed.abd1616

Mazzaschi, G., Madeddu, D., Falco, A., Bocchialini, G., Goldoni, M., Sogni, F., et al. (2018). Low PD-1 expression in cytotoxic CD8(+) tumor-infiltrating lymphocytes confers an immune-privileged tissue microenvironment in NSCLC with a prognostic and predictive value. *Clin. Cancer Res.* 24 (2), 407–419. Epub 20171026. doi:10.1158/1078-0432.CCR-17-2156

Meng, X., Wang, J., Zhou, J., Tian, Q., Qie, B., Zhou, G., et al. (2021). Tumor cell membrane-based peptide delivery system targeting the tumor microenvironment for cancer immunotherapy and diagnosis. *Acta Biomater.* 127, 266–275. Epub 20210402. doi:10.1016/j.actbio.2021.03.056

Miller, K. D., Nogueira, L., Devasia, T., Mariotto, A. B., Yabroff, K. R., Jemal, A., et al. (2022). Cancer treatment and survivorship statistics. *CA Cancer J. Clin.* 72 (5), 409–436. Epub 20220623. doi:10.3322/caac.21731

Munari, E., Marconi, M., Querzoli, G., Lunardi, G., Bertoglio, P., Ciompi, F., et al. (2021). Impact of PD-L1 and PD-1 expression on the prognostic significance of CD8(+) tumor-infiltrating lymphocytes in non-small cell lung cancer. *Front. Immunol.* 12, 680973. Epub 20210526. doi:10.3389/fimmu.2021.680973

Mussafi, O., Mei, J., Mao, W., and Wan, Y. (2022). Immune checkpoint inhibitors for PD-1/PD-L1 axis in combination with other immunotherapies and targeted therapies for non-small cell lung cancer. *Front. Oncol.* 12, 948405. Epub 20220817. doi:10.3389/fonc.2022.948405

Nakagawa, N., and Kawakami, M. (2022). Choosing the optimal immunotherapeutic strategies for non-small cell lung cancer based on clinical factors. *Front. Oncol.* 12, 952393. Epub 20220812. doi:10.3389/fonc.2022.952393

Nemeth, Z., Csizmadia, E., Vikstrom, L., Li, M., Bisht, K., Feizi, A., et al. (2016). Alterations of tumor microenvironment by carbon monoxide impedes lung cancer growth. *Oncotarget* 7 (17), 23919–23932. in: Pubmed; PMID 26993595. doi:10.18632/oncotarget.8081

Oldani, S., Petrelli, F., Dognini, G., Borgonovo, K., Parati, M. C., Ghilardi, M., et al. (2022). COVID-19 and lung cancer survival: An updated systematic review and meta-analysis. *Cancers (Basel)* 14 (22). 10.3390/cancers14225706.

Persano, S., Guevara, M. L., Li, Z., Mai, J., Ferrari, M., Pompa, P. P., et al. (2017). Lipopolyplex potentiates anti-tumor immunity of mRNA-based vaccination. *Biomaterials* 125, 81–89. Epub 20170221. doi:10.1016/j.biomaterials.2017.02.019

Peters, S., Paz-Ares, L., Herbst, R. S., and Reck, M. (2022). Addressing CPI resistance in NSCLC: Targeting TAM receptors to modulate the tumor microenvironment and future prospects. *J. Immunother. Cancer* 10 (7), e004863. doi:10.1136/jitc-2022-004863

Petroni, G., Buque, A., Coussens, L. M., and Galluzzi, L. (2022). Targeting oncogene and non-oncogene addiction to inflame the tumour microenvironment. *Nat. Rev. Drug Discov.* 21 (6), 440–462. Epub 20220315. doi:10.1038/s41573-022-00415-5

Pramanik, A., Patibandla, S., Gao, Y., Corby, L. R., Rhaman, M. M., Sinha, S. S., et al. (2022). Bio-conjugated magnetic-fluorescence nanoarchitectures for the capture and identification of lung-tumor-derived programmed cell death lighand 1-positive exosomes. *ACS Omega* 7 (18), 16035–16042. Epub 20220425. doi:10.1021/acsomega.2c01210

Pu, Z., Wei, Y., Sun, Y., Wang, Y., and Zhu, S. (2022). Carbon nanotubes as carriers in drug delivery for non-small cell lung cancer, mechanistic analysis of their carcinogenic potential, safety profiling and identification of biomarkers. *Int. J. Nanomedicine* 17, 6157–6180. 10.2147/IJN.S384592.

Punekar, S. R., Shum, E., Grello, C. M., Lau, S. C., and Velcheti, V. (2022). Immunotherapy in non-small cell lung cancer: Past, present, and future directions. *Front. Oncol.* 12, 877594. Epub 20220802. doi:10.3389/fonc.2022.877594

Rashed, H. E., Abdelrahman, A. E., Abdelgawad, M., Balata, S., and Shabrawy, M. E. (2017). Prognostic significance of programmed cell death ligand 1 (PD-L1), CD8+ tumor-infiltrating lymphocytes and p53 in non-small cell lung cancer: An immunohistochemical study. *Turk Patoloji Derg.* 1 (1), 211–222. doi:10.5146/tjpath.2017.01398

Reda, M., Ngamcherdtrakul, W., Nelson, M. A., Siriwon, N., Wang, R., Zaidan, H. Y., et al. (2022). Development of a nanoparticle-based immunotherapy targeting PD-L1 and PLK1 for lung cancer treatment. *Nat. Commun.* 13 (1), 4261. Epub 20220723. doi:10.1038/s41467-022-31926-9

Sanaei, M. J., Pourbagheri-Sigaroodi, A., Kaveh, V., Abolghasemi, H., Ghaffari, S. H., Momeny, M., et al. (2021). Recent advances in immune checkpoint therapy in non-small cell lung cancer and opportunities for nanoparticle-based therapy. *Eur. J. Pharmacol.* 909, 174404. 10.1016/j.ejphar.2021.174404.

Schafer, C. C., Wang, Y., Hough, K. P., Sawant, A., Grant, S. C., Thannickal, V. J., et al. (2016). Indoleamine 2,3-dioxygenase regulates anti-tumor immunity in lung cancer by metabolic reprogramming of immune cells in the tumor microenvironment. *Oncotarget* 7 (46), 75407–75424. in: Pubmed; PMID 27705910. doi:10.18632/oncotarget.12249

Sebban, S., Farago, M., Rabinovich, S., Lazer, G., Idelchuck, Y., Ilan, L., et al. (2014). Vav1 promotes lung cancer growth by instigating tumor-microenvironment cross-talk via growth factor secretion. *Oncotarget* 5 (19), 9214–9226. in: Pubmed; PMID 25313137. doi:10.18632/oncotarget.2400

Seshadri, D. R., and Ramamurthi, A. (2018). Nanotherapeutics to modulate the compromised micro-environment for lung cancers and chronic obstructive pulmonary disease. *Front. Pharmacol.* 9, 759. 10.3389/fphar.2018.00759.

Shalom, B., Farago, M., Salaymeh, Y., Sebban, S., Risling, M., Pikarsky, E., et al. (2022). Vav1 accelerates Ras-driven lung cancer and modulates its tumor microenvironment. *Cell Signal* 97, 110395. Epub 20220623. doi:10.1016/j.cellsig.2022.110395

Shen, N., Yang, C., Zhang, X., Tang, Z., and Chen, X. (2021). Cisplatin nanoparticles possess stronger anti-tumor synergy with PD1/PD-L1 inhibitors than the parental drug. *Acta Biomater.* 135, 543–555. Epub 20210814. doi:10.1016/j.actbio.2021.08.013

Shi, S., Ye, L., Yu, X., Jin, K., and Wu, W. (2022). Focus on mast cells in the tumor microenvironment: Current knowledge and future directions. *Biochim. Biophys. Acta Rev. Cancer* 1878 (1), 188845. 10.1016/j.bbcan.2022.188845.

Shirasawa, M., Yoshida, T., Matsumoto, Y., Shinno, Y., Okuma, Y., Goto, Y., et al. (2020). Impact of chemoradiotherapy on the immune-related tumour microenvironment and efficacy of anti-PD-(L)1 therapy for recurrences after chemoradiotherapy in patients with unresectable locally advanced non-small cell lung cancer. *Eur. J. Cancer* 140, 28–36. Epub 20201008. doi:10.1016/j.ejca.2020.08.028

Shirasawa, M., Yoshida, T., Shimoda, Y., Takayanagi, D., Shiraishi, K., Kubo, T., et al. (2021). Differential immune-related microenvironment determines programmed cell death protein-1/programmed death-ligand 1 blockade efficacy in patients with advanced NSCLC. *J. Thorac. Oncol.* 16 (12), 2078–2090. Epub 20210820. doi:10.1016/j.jtho.2021.07.027

Siegel, R. L., Miller, K. D., Fuchs, H. E., and Jemal, A. (2022). Cancer statistics, 2022. *CA Cancer J. Clin.* 72 (1), 7–33. Epub 20220112. doi:10.3322/caac.21708

Sittplangkoon, C., Alameh, M. G., Weissman, D., Lin, P. J. C., Tam, Y. K., Prompetchara, E., et al. (2022). mRNA vaccine with unmodified uridine induces robust type I interferon-dependent anti-tumor immunity in a melanoma model. *Front. Immunol.* 13, 983000. Epub 20221014. doi:10.3389/fimmu.2022.983000

Song, M., Ping, Y., Zhang, K., Yang, L., Li, F., Zhang, C., et al. (2019). Low-dose IFNγ induces tumor cell stemness in tumor microenvironment of non-small cell lung cancer. *Cancer Res.* 79 (14), 3737–3748. Epub 20190513. doi:10.1158/0008-5472.CAN-19-0596

Song, Z., Wang, X., Chen, F., Chen, Q., Liu, W., Yang, X., et al. (2022). LncRNA MALAT1 regulates METTL3-mediated PD-L1 expression and immune infiltrates in pancreatic cancer. *Front. Oncol.* 12, 1004212. Epub 20220921. doi:10.3389/fonc.2022.1004212

Stater, E. P., Sonay, A. Y., Hart, C., and Grimm, J. (2021). The ancillary effects of nanoparticles and their implications for nanomedicine. *Nat. Nanotechnol.* 16 (11), 1180–1194. Epub 20211110. doi:10.1038/s41565-021-01017-9

Su, W. P., Chang, L. C., Song, W. H., Yang, L. X., Wang, L. C., Chia, Z. C., et al. (2022). Polyaniline-based glyco-condensation on Au nanoparticles enhances immunotherapy in lung cancer. *ACS Appl. Mater Interfaces* 14 (21), 24144–24159. Epub 20220517. doi:10.1021/acsami.2c03839

Tison, A., Garaud, S., Chiche, L., Cornec, D., and Kostine, M. (2022). Immune-checkpoint inhibitor use in patients with cancer and pre-existing autoimmune diseases. *Nat. Rev. Rheumatol.* 18 (11), 641–656. Epub 20221005. doi:10.1038/s41584-022-00841-0

Tokito, T., Azuma, K., Kawahara, A., Ishii, H., Yamada, K., Matsuo, N., et al. (2016). Predictive relevance of PD-L1 expression combined with CD8+ TIL density in stage III non-small cell lung cancer patients receiving concurrent chemoradiotherapy. *Eur. J. Cancer* 55, 7–14. Epub 20160106. doi:10.1016/j.ejca.2015.11.020

Trivanovic, D., Persuric, Z., Agaj, A., Jakopovic, M., Samarzija, M., Bitar, L., et al. (2022). *Int. J. Mol. Sci.* 23 (23). 10.3390/ijms232315067.

Vilarino, N., Bruna, J., Bosch-Barrera, J., Valiente, M., and Nadal, E. (2020). Immunotherapy in NSCLC patients with brain metastases. Understanding brain tumor microenvironment and dissecting outcomes from immune checkpoint blockade in the clinic. *Cancer Treat. Rev.* 89, 102067. Epub 20200707. doi:10.1016/j.ctrv.2020.102067

Wang, L., Xu, H., Weng, L., Sun, J., Jin, Y., and Xiao, C. (2022). Activation of cancer immunotherapy by nanomedicine. *Front. Pharmacol.* 13, 1041073. Epub 20221222. doi:10.3389/fphar.2022.1041073

Wang, Y., Tan, H., Yu, T., Chen, X., Jing, F., and Shi, H. (2021). Potential immune biomarker candidates and immune subtypes of lung adenocarcinoma for developing mRNA vaccines. *Front. Immunol.* 12, 755401. Epub 20211130. doi:10.3389/fimmu.2021.755401

Wang, Z., Xing, Y., Li, B., Li, X., Liu, B., and Wang, Y. (2022). Molecular pathways, resistance mechanisms and targeted interventions in non-small-cell lung cancer. *Mol. Biomed.* 3 (1), 42. Epub 20221212. doi:10.1186/s43556-022-00107-x

Weiss, J. M., Pennell, N., Deal, A. M., Morgensztern, D., Bradford, D. S., Crane, J., et al. (2020). Nab-paclitaxel in older patients with non-small cell lung cancer who have developed disease progression after platinum-based doublet chemotherapy. *Cancer* 126 (5), 1060–1067. Epub 20200114. doi:10.1002/cncr.32573

Wu, J., and Lin, Z. (2022). Non-small cell lung cancer targeted therapy: Drugs and mechanisms of drug resistance. *Int. J. Mol. Sci.* 23 (23), 15056. Epub 20221201. doi:10.3390/ijms232315056

Wu, S. P., Liao, R. Q., Tu, H. Y., Wang, W. J., Dong, Z. Y., Huang, S. M., et al. (2018). Stromal PD-L1-positive regulatory T cells and PD-1-positive CD8-positive T cells define the response of different subsets of non-small cell lung cancer to PD-1/PD-L1 blockade immunotherapy. *J. Thorac. Oncol.* 13 (4), 521–532. Epub 20171218. doi:10.1016/j.jtho.2017.11.132

Xu, H. Z., Li, T. F., Wang, C., Ma, Y., Liu, Y., Zheng, M. Y., et al. (2021). Synergy of nanodiamond-doxorubicin conjugates and PD-L1 blockade effectively turns tumor-associated macrophages against tumor cells. *J. Nanobiotechnology* 19 (1), 268. Epub 20210906. doi:10.1186/s12951-021-01017-w

Xu, R., Lu, T., Zhao, J., Wang, J., Peng, B., and Zhang, L. (2022). Identification of tumor antigens and immune subtypes in lung adenocarcinoma for mRNA vaccine development. *Front. Cell Dev. Biol.* 10, 815596. Epub 20220221. doi:10.3389/fcell.2022.815596

Yang, H., Shi, J., Lin, D., Li, X., Zhao, C., Wang, Q., et al. (2018). Prognostic value of PD-L1 expression in combination with CD8(+) TILs density in patients with surgically resected non-small cell lung cancer. *Cancer Med.* 7 (1), 32–45. Epub 20171123. doi:10.1002/cam4.1243

Yang, Z., Gao, D., Zhao, J., Yang, G., Guo, M., Wang, Y., et al. (2023). Thermal immuno-nanomedicine in cancer. *Nat. Rev. Clin. Oncol.* 20 (2), 116–134. Epub 20230105. doi:10.1038/s41571-022-00717-y

Ye, H., He, X., and Feng, X. (2020). Developing neobavaisoflavone nanoemulsion suppresses lung cancer progression by regulating tumor microenvironment. *Biomed. Pharmacother.* 129, 110369. Epub 20200618. doi:10.1016/j.biopha.2020.110369

Yoneda, K., Kuwata, T., Kanayama, M., Mori, M., Kawanami, T., Yatera, K., et al. (2019). Alteration in tumoural PD-L1 expression and stromal CD8-positive tumour-infiltrating lymphocytes after concurrent chemo-radiotherapy for non-small cell lung cancer. *Br. J. Cancer* 121 (6), 490–496. Epub 20190807. doi:10.1038/s41416-019-0541-3

Yu, L., Sun, M., Zhang, Q., Zhou, Q., and Wang, Y. (2022). Harnessing the immune system by targeting immune checkpoints: Providing new hope for Oncotherapy. *Front. Immunol.* 13, 982026. Epub 20220908. doi:10.3389/fimmu.2022.982026

Yu, P., He, X., Lu, F., Li, L., Song, H., and Bian, X. (2022). Research progress regarding long-chain non-coding RNA in lung cancer: A narrative review. *J. Thorac. Dis.* 14 (8), 3016–3029. doi:10.21037/jtd-22-897

Zhang, L., Chen, Y., Wang, H., Xu, Z., Wang, Y., Li, S., et al. (2021). Massive PD-L1 and CD8 double positive TILs characterize an immunosuppressive microenvironment with high mutational burden in lung cancer. *J. Immunother. Cancer* 9 (6), e002356. doi:10.1136/jitc-2021-002356

Zhang, M., Yang, W., Wang, P., Deng, Y., Dong, Y. T., Liu, F. F., et al. (2020). CCL7 recruits cDC1 to promote antitumor immunity and facilitate checkpoint immunotherapy to non-small cell lung cancer. *Nat. Commun.* 11 (1), 6119. Epub 20201130. doi:10.1038/s41467-020-19973-6

Zhang, Q., Zhong, H., Fan, Y., Liu, Q., Song, J., Yao, S., et al. (2020). Immune and clinical features of CD96 expression in glioma by *in silico* analysis. *Front. Bioeng. Biotechnol.* 8, 592. Epub 20200630. doi:10.3389/fbioe.2020.00592

Zhao, D., Liu, X., Shan, Y., Li, J., Cui, W., Wang, J., et al. (2022). Recognition of immune-related tumor antigens and immune subtypes for mRNA vaccine development in lung adenocarcinoma. *Comput. Struct. Biotechnol. J.* 20, 5001–5013. Epub 20220905. doi:10.1016/j.csbj.2022.08.066

Zhao, J., Xu, R., Lu, T., Wang, J., and Zhang, L. (2022). Identification of tumor antigens and immune subtypes in lung squamous cell carcinoma for mRNA vaccine development. *J. Thorac. Dis.* 14 (9), 3517–3530. doi:10.21037/jtd-22-1113

Zhao, Y., Guo, S., Deng, J., Shen, J., Du, F., Wu, X., et al. (2022). VEGF/VEGFR-targeted therapy and immunotherapy in non-small cell lung cancer: Targeting the tumor microenvironment. *Int. J. Biol. Sci.* 18 (9), 3845–3858. Epub 20220529. doi:10.7150/ijbs.70958

Zhong, H., Lai, Y., Zhang, R., Daoud, A., Feng, Q., Zhou, J., et al. (2020). Low dose cyclophosphamide modulates tumor microenvironment by TGF-beta signaling pathway. *Int. J. Mol. Sci.* 21 (3), 957. Epub 20200131. doi:10.3390/ijms21030957

Zhong, H., Liu, S., Cao, F., Zhao, Y., Zhou, J., Tang, F., et al. (2021). Dissecting tumor antigens and immune subtypes of glioma to develop mRNA vaccine. *Front. Immunol.* 12, 709986. Epub 20210827. doi:10.3389/fimmu.2021.709986

Zhou, B., Zang, R., Zhang, M., Song, P., Liu, L., Bie, F., et al. (2022). Identifying novel tumor-related antigens and immune phenotypes for developing mRNA vaccines in lung adenocarcinoma. *Int. Immunopharmacol.* 109, 108816. Epub 20220430. doi:10.1016/j.intimp.2022.108816

Zhou, J., Gong, Z., Jia, Q., Wu, Y., Yang, Z. Z., and Zhu, B. (2018). Programmed death ligand 1 expression and CD8(+) tumor-infiltrating lymphocyte density differences between paired primary and brain metastatic lesions in non-small cell lung cancer. *Biochem. Biophys. Res. Commun.* 498 (4), 751–757. Epub 20180317. doi:10.1016/j.bbrc.2018.03.053

Zhou, J. G., Zhong, H., Zhang, J., Jin, S. H., Roudi, R., and Ma, H. (2019). Development and validation of a prognostic signature for malignant pleural mesothelioma. *Front. Oncol.* 9, 78. Epub 20190215. doi:10.3389/fonc.2019.00078

Zhuo, Y., Li, S., Hu, W., Zhang, Y., Shi, Y., Zhang, F., et al. (2022). Targeting SNORA38B attenuates tumorigenesis and sensitizes immune checkpoint blockade in non-small cell lung cancer by remodeling the tumor microenvironment via regulation of GAB2/AKT/mTOR signaling pathway. *J. Immunother. Cancer* 10 (5), e004113. doi:10.1136/jitc-2021-004113

Zulfiqar, B., Farooq, A., Kanwal, S., and Asghar, K. (2022). Immunotherapy and targeted therapy for lung cancer: Current status and future perspectives. *Front. Pharmacol.* 13, 1035171. 10.3389/fphar.2022.1035171.

frontiers | Frontiers in Pharmacology

TYPE Original Research
PUBLISHED 03 April 2023
DOI 10.3389/fphar.2023.1153565

OPEN ACCESS

EDITED BY
Lin Qi,
Central South University, China

REVIEWED BY
Zheng Wu,
Central South University, China
Min Wu,
The Affiliated Hospital of Southwest Medical University, China
Yabing Cao,
Kiang Wu Hospital, Macao SAR, China

*CORRESPONDENCE
Rongzhi Xie,
xierzhi@mail.sysu.edu.cn
Hongyu Zhang,
zhhyu@mail.sysu.edu.cn

SPECIALTY SECTION
This article was submitted to Pharmacology of Anti-Cancer Drugs, a section of the journal Frontiers in Pharmacology

RECEIVED 29 January 2023
ACCEPTED 23 March 2023
PUBLISHED 03 April 2023

CITATION
Zhou J, Shi S, Qiu Y, Jin Z, Yu W, Xie R and Zhang H (2023), Integrative bioinformatics approaches to establish potential prognostic immune-related genes signature and drugs in the non-small cell lung cancer microenvironment. *Front. Pharmacol.* 14:1153565. doi: 10.3389/fphar.2023.1153565

Integrative bioinformatics approaches to establish potential prognostic immune-related genes signature and drugs in the non-small cell lung cancer microenvironment

Jiao Zhou[1,2], Shan Shi[1,2], Yeqing Qiu[1,2], Zhongwen Jin[1,2], Wenyan Yu[1,2], Rongzhi Xie[1,3]* and Hongyu Zhang[1,3]*

[1]The Fifth Affiliated Hospital of Sun Yat-sen University, Zhuhai, China, [2]Zhongshan School of Medicine, Sun Yat-sen University, Guangzhou, China, [3]Cancer Center, The Fifth Affiliated Hospital of Sun Yat-sen University, Zhuhai, China

Introduction: Research has revealed that the tumor microenvironment (TME) is associated with the progression of malignancy. The combination of meaningful prognostic biomarkers related to the TME is expected to be a reliable direction for improving the diagnosis and treatment of non-small cell lung cancer (NSCLC).

Method and Result: Therefore, to better understand the connection between the TME and survival outcomes of NSCLC, we used the "DESeq2" R package to mine the differentially expressed genes (DEGs) of two groups of NSCLC samples according to the optimal cutoff value of the immune score through the ESTIMATE algorithm. A total of 978 up-DEGs and 828 down-DEGs were eventually identified. A fifteen-gene prognostic signature was established *via* LASSO and Cox regression analysis and further divided the patients into two risk sets. The survival outcome of high-risk patients was significantly worse than that of low-risk patients in both the TCGA and two external validation sets (p-*value* < 0.05). The gene signature showed high predictive accuracy in TCGA (1-year area under the time-dependent ROC curve (AUC) = 0.722, 2-year AUC = 0.708, 3-year AUC = 0.686). The nomogram comprised of the risk score and related clinicopathological information was constructed, and calibration plots and ROC curves were applied, KEGG and GSEA analyses showed that the epithelial-mesenchymal transition (EMT) pathway, E2F target pathway and immune-associated pathway were mainly involved in the high-risk group. Further somatic mutation and immune analyses were conducted to compare the differences between the two groups. Drug sensitivity provides a potential treatment basis for clinical treatment. Finally, EREG and ADH1C were selected as the key prognostic genes of the two overlapping results from PPI and multiple Cox analyses. They were verified by comparing the mRNA expression in cell lines and protein expression in the HPA database, and clinical validation further confirmed the effectiveness of key genes.

Conclusion: In conclusion, we obtained an immune-related fifteen-gene prognostic signature and potential mechanism and sensitive drugs underling the prognosis model, which may provide accurate prognosis prediction and available strategies for NSCLC.

KEYWORDS

non-small cell lung cancer, tumor microenvironment, estimate, prognostic gene signature, drug sensitivity

Introduction

Lung cancer remains one of the most threatening malignancies to human health worldwide with relatively high incidence and mortality (Sung et al., 2021). NSCLC is the predominant histological subtype, comprising approximately 85% of lung cancer (Travis et al., 2015). Surgical resection is recommended for early-stage NSCLC, and adjuvant platinum-based chemotherapy confers a 5-year survival benefit rate, which increased by 5% for stage II-IIIA disease (Arriagada et al., 2010). Because of the concealed pathogenesis, approximately 60% of patients with NSCLC have locally advanced or metastatic disease, and conventional chemoradiotherapy has become the optimal treatment (Osmani et al., 2018). However, with a high recurrence rate after pulmonary resection, there was a significant sensitivity difference and clear toxic effects of chemoradiotherapy. Owing to the molecular heterogeneity of NSCLC, patients show various responses to conventional therapies, and even standard therapy according to the guidelines has major limitations. Therefore, precise individualized medicine gradually replaced the traditional one-size-fits-all toxic treatment (Herbst et al., 2018).

Over the past decade, molecularly targeted therapies targeting driver gene abnormalities have dramatically changed the treatment strategy for NSCLC; however, these new targeted drugs also present insufficient therapy due to the development of tumor resistance (Denisenko et al., 2018). Anti-PD-1/PD-L1 immunotherapy demonstrates an overall survival benefit in advanced NSCLC, but only 20% of patients benefit from immune checkpoint inhibitors (Huang et al., 2018). In conclusion, although substantial and promising achievements have been made in the therapeutic strategy of NSCLC, the prevention, early detection and treatment of NSCLC are still challenging. Therefore, it is particularly crucial to continue to identify new target genes and therapies to improve the curative effect and outcomes of NSCLC patients.

Malignant solid tumor tissue consists of not only cancer cells but also the TME, which contains extracellular matrix, stromal cells, and immune cells (Binnewies et al., 2018). Studies have certified that the TME influences the gene expression of tumor tissues in a variety of ways and then facilitates the occurrence, progression and metastasis of tumors (Hu and Polyak, 2008). Immune cells and adaptive immune cells in the TME act directly on cancer cells or through cytokine and chemokine signaling to influence tumor behavior and therapeutic reactions (Schulz et al., 2019). By taking advantage of the negative regulatory mechanism in the human immune system, malignant tumor cells can generate wholescale immune suppression in the TME to counteract the body's antitumor immune effect (Teng et al., 2015). The difference in individual efficacy in tumor immunotherapy is strongly associated with immunosuppression in the TME (Anari et al., 2018). Therefore, exploring new biomarkers related to the tumor microenvironment opens up new avenues for precise individualized therapy of NSCLC.

To understand the impact of the tumor genetic genome on clinical prognosis, comprehensive whole genome gene expression collections have been established (Blum et al., 2018). In addition, to predict the infiltration of non-tumor cells in tumor tissues, ESTIMATE algorithms have been designed to premeasure tumor purity utilizing gene expression information from The Cancer Genome Atlas (TCGA) database (Yoshihara et al., 2013). This algorithm was soon applied to ovarian cancer (Hornburg et al., 2021), renal cell carcinoma (Xu et al., 2019), and diffuse large B-cell lymphoma (Lou et al., 2022). Therefore, bioinformatics analysis based on TME-related prognostic signatures has become possible. In this study, the ESTIMATE algorithm and CIBERSORT algorithm in R language were utilized to explore the tumor microenvironment of patients with NSCLC in the TCGA database. First, we identified differentially expressed genes with prognostic and therapeutic value in the tumor microenvironment and predicted their regulatory network. Furthermore, we developed an innovative prognostic signature for risk stratification based on prognostic genes, and the potential biological mechanism and therapeutic drugs based on the prediction model were evaluated. This result provides additional prospective therapeutic interventions and personalized treatment strategies for NSCLC patients.

Materials and methods

Chip data acquisition and processing

We downloaded the gene expression data of NSCLC patients and related clinical materials meeting the study criteria from the TCGA databases (https://portal.gdc.cancer.gov/). Patients were enrolled when they met the following criteria: a) pathologically confirmed NSCLC; b) available detailed prognostic information; and c) complete mRNA expression data. A total of 955 NSCLC patients with stage I-IV disease were included through screening. The clinical information of patients included age, sex, survival status, overall survival, last follow-up time, T stage, N stage, M stage and clinical stage. The TCGA-NSCLC cohort was used as a training set to construct an immune score prognostic model. For further verification of the performance of immune scores in predicting survival, transcriptome sequencing profiles and corresponding clinical data of two other cohorts of NSCLC patients were obtained from the Gene Expression Omnibus (GEO) datasets (https://www.ncbi.nlm.nih.gov/), namely, GSE31210 and GSE37745. GSE31210 comprised 226 early-stage NSCLC patients, and GSE37745 included 196 NSCLC samples. GSE31210 and GSE37745 were downloaded based on Affymetrix U133 Plus 2.0.

ESTIMATE algorithm and identification of stromal and immune groups

Based on R statistical software (version 4.1.0; https://www.r-project.org/), the proportion of stromal and immune cells in each tumor tissue sample was calculated by the ESTIMATE algorithm, and the ratio was represented in the form of immune, stromal and ESTIMATE scores. The stromal score represented the percentage of

stromal cells in the TME, the immune score was used to assess the ratio of immune cells, and the ESTIMATE score represented the comprehensive level of the immune and matrix score. The Surv_cutpoint function was used to find the best cutoff values for the immune, stromal and ESTIMATE scores. NSCLC patients were categorized into high- and low-score groups based on the optimal cutoff value of the related score. The "survival" and "survminer" packages were utilized to evaluate the overall survival of NSCLC patients on the basis of the high-low score, which included the immune, stromal and ESTIMATE scores. Associations of the abovementioned scores with clinicopathologic characteristics were also further assessed by unpaired t-tests.

DEGs screening and functional enrichment analysis

The DEG screening between the high and low immune score groups was constructed through the "DESeq2" R package (version 4.1.0), and a false discovery rate (FDR) < 0.05 and | log2-fold change| (|log2FC|) ≥ 1 were set up to screen DEGs. A higher gene expression value was selected if multiple probes measured the same gene. The selected DEGs were visualized through the "ggplot2" package of R to generate scatter plots and heatmaps.

Functional enrichment analyses, including molecular function (MF), cell component (CC), and biological process (BP), were performed for the DEGs using the "cluster-Profiler" package. The "cluster-Profiler" package was used to analyze the Kyoto Encyclopedia of Genes and Genomes (KEGG), which was used to identify the crucial signal pathways between upregulated and downregulated DEGs. Terms were identified as statistically significantly enriched with the threshold of *p-value* < 0.05 for gene ontology (GO) and KEGG. In addition, GO and KEGG analyses were evaluated by fold enrichment scores to determine which genetic functions and cell signaling pathways may be relevant to DEGs.

Prognostic DEGs screening

First, univariate Cox analysis using the "survival" package was employed to screen prognostic DEGs that were significantly relevant to the overall survival (OS) of 936 NSCLC patients in the TCGA cohort. The candidate prognostic DEGs with *p-value* < 0.01 were used for the subsequent analysis. Subsequently, the candidate prognostic DEGs underwent least absolute shrinkage selection operator (LASSO) analysis. Eventually, multivariate Cox regression analysis was conducted to calculate the hazard ratios (HRs) with a 95% confidence interval (95% CI) and determine prognostic genes.

Establishment and evaluation of prognostic signature

Each NSCLC patient's survival risk score in the TCGA cohort was calculated according to the mRNA expression of optimal prognostic genes multiplied by the corresponding regression coefficients.

The computational formula is as follows: risk score

$$= \sum_{n=1}^{j} Coef\ j * Xj$$

$Coef\ j$ is the regression coefficient determined through multivariate Cox analysis, and Xj refers to the normalized mRNA expression level of optimal genes. NSCLC patients in the TCGA were separated into high- and low-risk subtypes according to the median threshold of the risk score.

The OS between the two risk groups was evaluated by Kaplan-Meier analysis with the log-rank test. In addition, external validation of the GSE31210 and GSE37745 datasets was performed to predict the accuracy of the prognostic DEG signature. The Time-dependent ROC curves were performed for confirmingthe prognostic DEG signatur e's prognosis capability by calculating the AUC of the 1-, 2-, and 3-year OS of NSCLC patients in TCGA. Finally, the GSE31210 and GSE37745 datasets were used for external validation to corroborate the results.

Construction of predictive nomogram

First, univariate and multivariate Cox regression analyses were utilized to evaluate the individual covariates, the risk score calculated above and the associated clinicopathological parameters, which clearly impacted the patient's survival outcome. A *p-value* < 0.05 was considered to be the significance threshold. Then, the nomogram was constructed through calibration plots to predict 1-, 3- and 5-year overall survival, using the concordance index (C-index) to test internal validation. The predictive value of the nomogram, risk score and other clinical parameters were compared by ROC curves.

Pathway enrichment analysis

KEGG was performed to explore signal pathways between the high- and low-risk groups. DEGs underwent gene set enrichment analysis (GSEA), which aimed to better confirm the molecular and biological mechanisms between the two groups.

The pathway enrichment of differences underlying gene sets in two risk score subgroups was calculated by the annotation file "hallmark gene sets" of the Molecular Signatures Database (MSigDB) (https://www.gseamsigdb.org/gsea/msigdb/).

Immune infiltration assessment

The CIBERSORT algorithm was applied to evaluate the relative infiltration abundance of various types of tumor-infiltrating immune cells. We utilized CIBERSORT through an online R script in the local R environment, and the algorithm was iterated with 1,000 permutations and based on the LM22 gene signature. Related results were filtered with a *p-value* < 0.05. Twenty-two

subtypes of immune cells between the two risk groups were subsequently compared. As supplementary, the mRNA expression of typical immune checkpoints between the two groups was further compared.

Mutation analysis and prediction of the sensitive drugs

Mutation information of NSCLC was retrieved from the TCGA database. The Mutation Annotation Format (MAF) form was used to reserve somatic variant data. Maftools of the R package was used to identify the top 30 most frequently mutated genes between the two risk cohorts. The "pRRophetic" R package was utilized to estimate the IC50 of common drugs between the patients in the two groups using the Wilcoxon signed-rank test to predict the drug sensitivity of the groups.

Exploration of hub genes in prognosis signature and experimental validation

We first built a protein-protein interaction (PPI) network to examine the interplay between the prognostic DEGs obtained from univariate Cox regression analysis. Then, the DEGs were uploaded to String (https://string-db.org/), and the PPI network was constructed and further visualized and analyzed by Cytoscape software (version 3.8.0).

Molecular Complex Detection (MCODE) screened the modules of the subnetwork, and the cutoff criterion was degree cutoff = 2, node score cutoff = 0.2, k-core = 2 and max depth = 100. The common gene, overlapping result from PPI and multiple cox analysis, was selected as the key prognosis gene. First, the protein expression levels of tumor or normal tissue were confirmed based on the HPA (The Human Protein Atlas) database (https://www.proteinatlas.org). The "Survival" package was used to assess the prognosis among the normalized mRNA expression of the prognostic hub genes. Kaplan-Meier analysis was used for evaluating the impact of quantities of gene expression on patient survival according to individual mRNA expression of particular prognostic genes (high versus low expression). Finally, PCR experiments were conducted to determine the mRNA expression of hub genes in normal lung epithelial cells and NSCLC cell lines.

Real-time RT-PCR

The total RNA of relative cell lines was extracted using the RNeasy mini kit following the manufacturer's protocol (Qiagen). RNA was eluted in 30 μL of RNase-free water and stored at −80 ℃. RNA (500 ng) was reverse-transcribed using the PrimeScript™ RT reagent kit (Takara Bio, Inc., Otsu, Japan). Then, PCR amplification of the cDNA was performed using TB Green® Premix Ex Taq™ II (Takara Bio, Inc.) according to the manufacturer's instructions. The sample volume was 10 μL, and the following reaction conditions were used: 95°C for 30 s (predenaturation), then 40 cycles at 95°C for 10 s (denaturation), 55°C for 30 s (annealing), 72°C for 30 s (extension) and the ultimate extension at 72°C. Relative mRNA expression levels were acquired by the $2^{-\Delta\Delta Cq}$ method.

TABLE 1 Primers sequences corresponding to prognostic genes and GAPDH.

Genes name		(5′to3′)
ADH1C	Forward primer	CTCGCCCCTGGAGAAAGTC
	Reverse primer	GGCCCCCAACTCTTTAGCC
EREG	Forward primer	GTGATTCCATCATGTATCCCAGG
	Reverse primer	GTGATTCCATCATGTATCCCAGG
GAPDH	Forward primer	GGAGCGAGATCCCTCCAAAAT
	Reverse primer	GGCTGTTGTCATACTTCTCATGG

Gene primer sequences were acquired from Generay Biotechnology (Shanghai, China). Table 1 describes the detailed sequences.

Statistical analysis

The distributional differences in clinical variables between the two risk sets were analyzed by the chi-square test. Univariate and multivariate Cox regression analyses were adopted to assess independent prognostic parameters, and HRs and 95% CIs were evaluated at the same time. The Kaplan-Meier method was applied to generate survival curves for prognosis analyses, and the log-rank test was used to define the significance of differences. Statistical analyses in the study were conducted by R software (version 4.1.0), IBM SPSS Statistics (version 25.0) or GraphPad Prism (version 8.0). If not mentioned above, a threshold of $p\text{-}value < 0.05$ was defined as statistical significance.

Results

Flow of data collection and analysis

In our research, we utilized ESTIMATE algorithms to calculate the immune, stromal and ESTIMATE scores in NSCLC patients after obtaining mRNA expression profiles and corresponding clinical characteristics from the TCGA cohort. By comparing the relationship between each score and survival outcome together with clinicopathological parameters, the immune score was shown to play a vital role in the prognosis of NSCLC patients. We identified the immune-related DEGs based on high- and low-immune score subtypes and predicted their potential biological functions and pathways. The DEGs associated with OS were analyzed and screened by univariate Cox analysis, and the genes with $p\text{-}value \leq 0.01$ were further analyzed by LASSO analysis and subsequent multivariate Cox analysis. A 15-gene prognostic signature was developed. A gene-based classifier was generated, and NSCLC samples in our study were classified into two risk cohorts based on the median risk score obtained from the risk score computational formula. OS

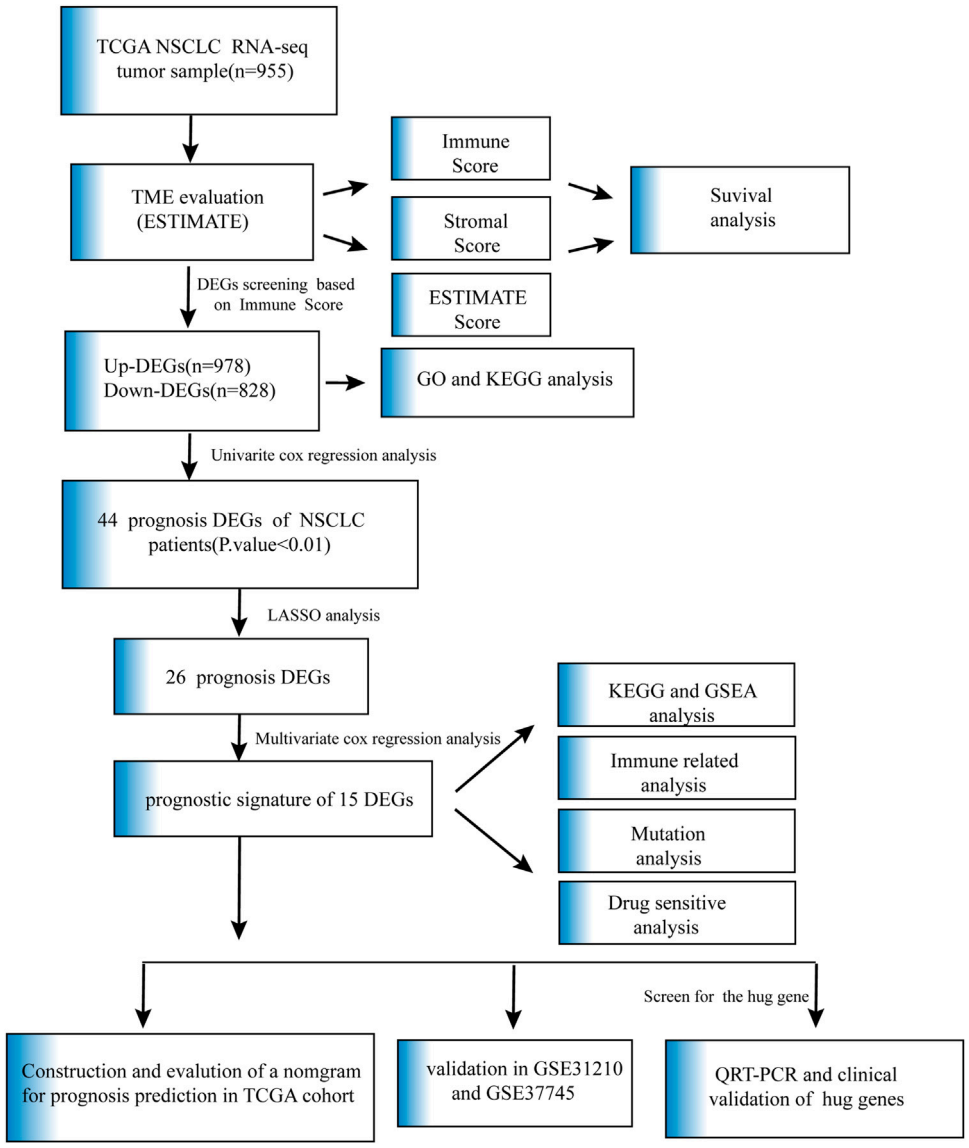

FIGURE 1
Flow chart of data collection and analysis.

was evaluated by Kaplan-Meier analysis between the two groups. The nomogram integrated risk score and related clinical information, and calibration plots and ROC curves were applied to verify prognosis accuracy. The GSE31210 and GSE37745 datasets, as external validations, also confirmed the high predictive efficiency of the 15-gene diagnostic model described above. KEGG and GSEA were performed to explore the molecular and biological differences, and further mutation and drug sensitivity analyses were also conducted between the patients in the two risk groups. In addition, immune-related analysis was performed to compare the proportions of immune cells in the high- and low-risk groups. Finally, the common gene, selected as the key prognostic gene of two overlapping results from PPI and multiple Cox analyses, was verified by comparing the mRNA expression of normal lung epithelial and NSCLC cell lines and protein expression in the HPA database. The clinical validation of the TCGA database further confirmed the effectiveness of key genes. Details are described in Figure 1.

Immune score was connected with the prognosis of NSCLC patients

Among 955 NSCLC cases enrolled in our study in the TCGA cohort, 489 were LUAD and 466 were LUSC patients. According to the ESTIMATE algorithm, the generated immune, stromal and ESTIMATE scores were utilized in the Kaplan–Meier survival analysis. The best demarcation values of the abovementioned thresholds for subsequent survival analysis were 698.1, −802.72 and 2,296.17, respectively (Figures 2A–C). The

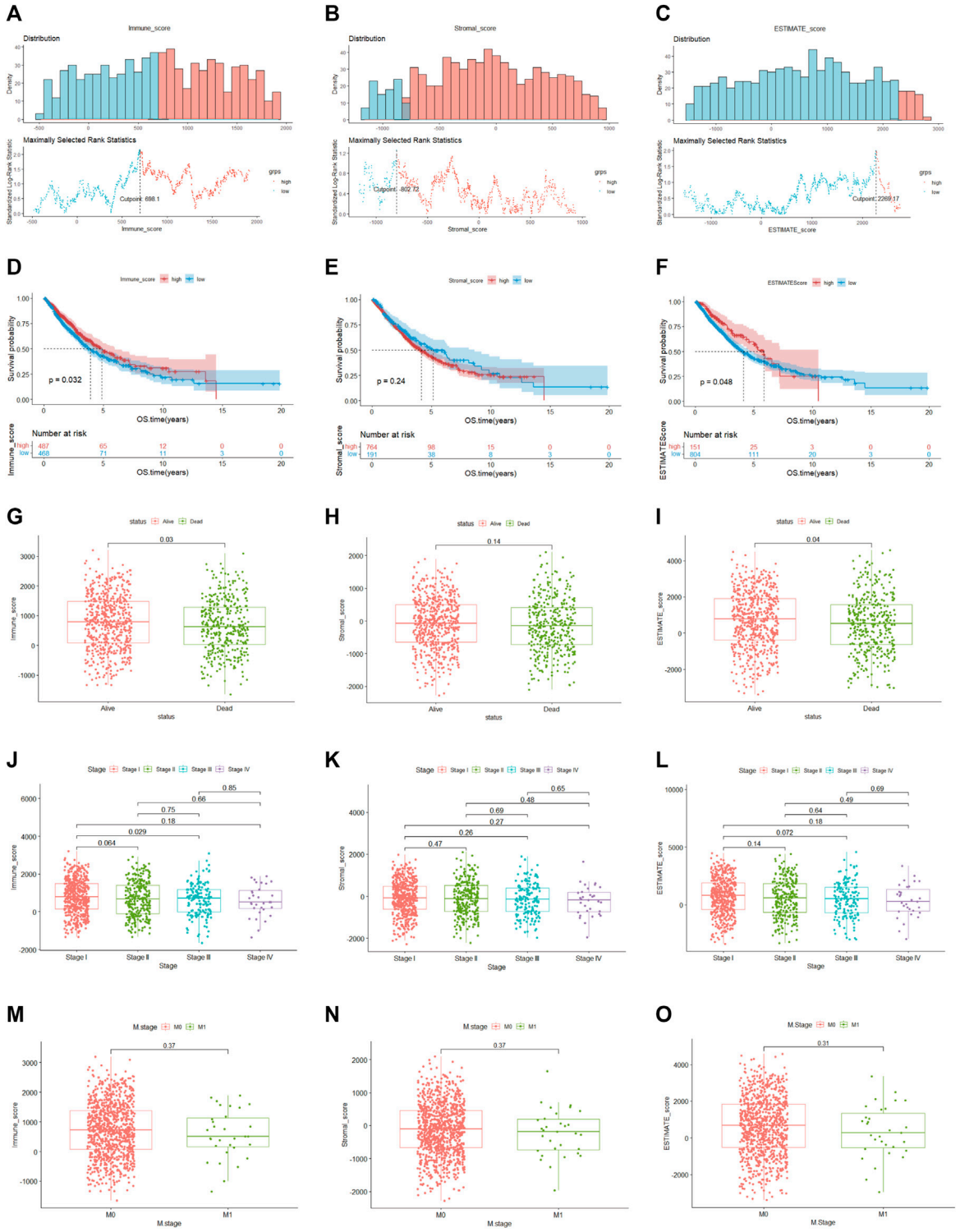

FIGURE 2
Relationship between clinical characteristics and immune, stromal and ESTIMATE scores **(A–C)**. The optimal cutoff values of the immune, stromal and ESTIMATE scores. **(D–F)**. **(K–M)** analysis of immune, stromal and ESTIMATE scores. **(G–I)**. Distribution of the three scores among patients with different statuses **(J–L)**. Distribution of immune, stromal and ESTIMATE scores among NSCLC stages **(M–O)**. Distribution of three scores between M-stage of NSCLC.

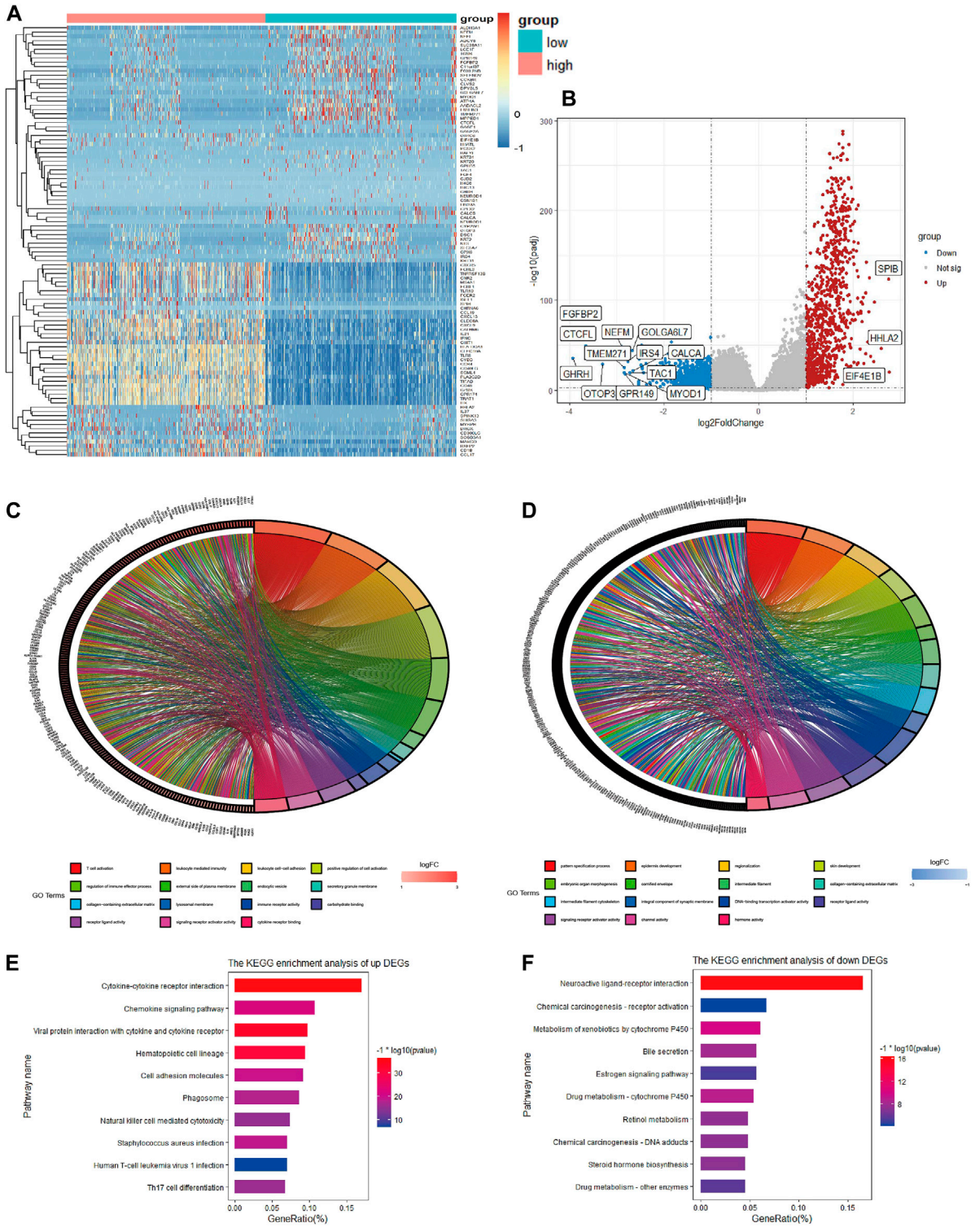

FIGURE 3
Heatmap, volcano plot and enrichment analysis of GO and KEGG for DEGs **(A)**. Heatmap of DEGs in TCGA **(B)**. Volcano plot of DEGs in TCGA **(C)**. Top 5 enriched biological processes, molecular functions, and cellular components of upregulated co-DEGs and **(D)** downregulated co-DEGs **(E)**. Top 10 KEGG pathways of upregulated co-DEGs and **(F)** downregulated co-DEGs.

results in our research demonstrated that a higher immune and ESTIMATE score was associated with a better prognosis ($p < 0.05$) (Figures 2D, F); however, there was no significant correlation with the stromal score ($p = 0.24$) (Figure 2E). The three scores were subsequently analyzed to evaluate the relationship with clinicopathologic characteristics (Figures

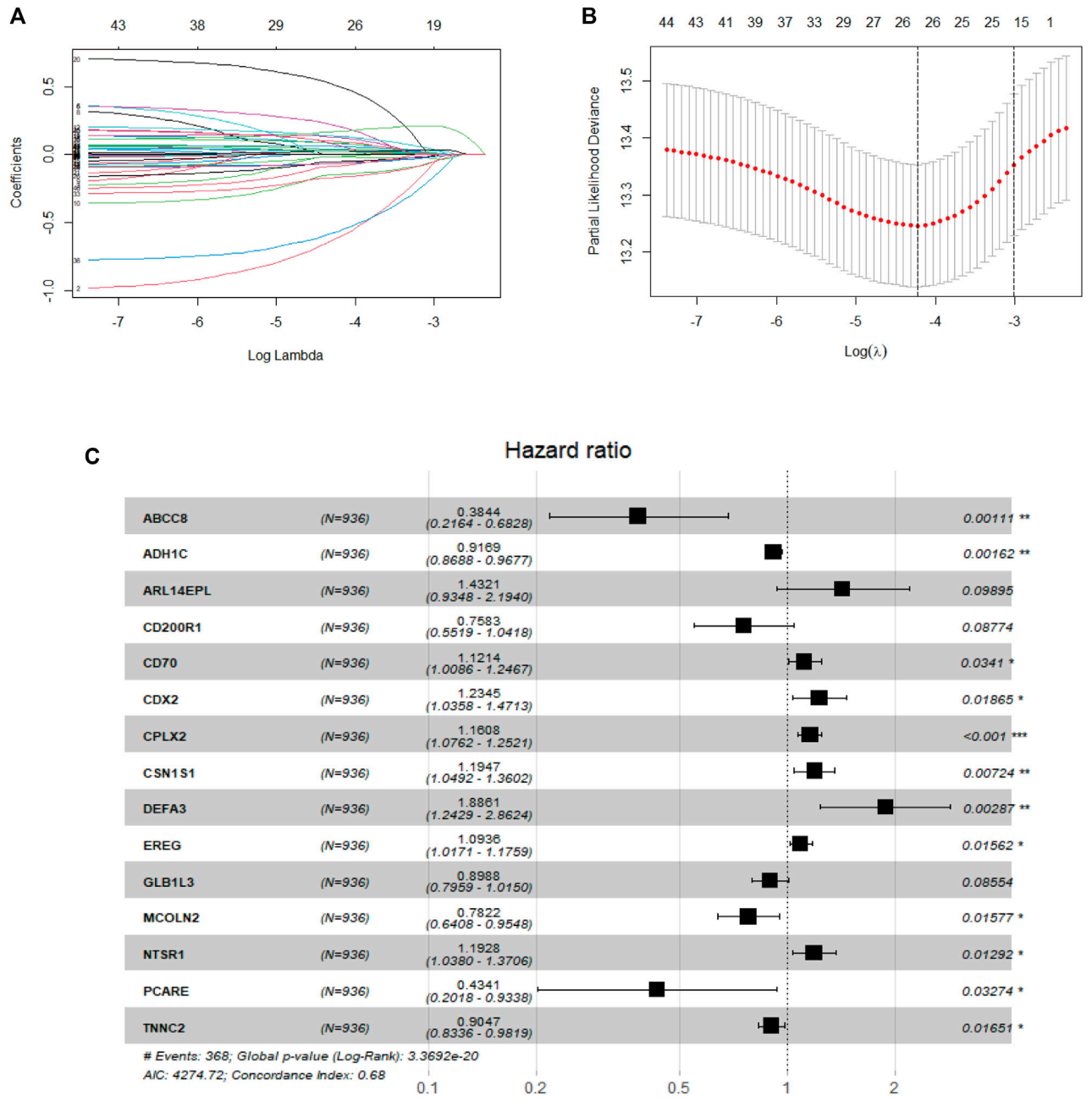

FIGURE 4
Development of the prognostic signature in the TCGA cohort **(A)**. Diagnostic model construction using a LASSO regression model **(B)**. Coefficient distribution plots to select the optimum lambda value **(C)**. Results of multivariate Cox regression analysis of OS in the TCGA cohort.

2G–O), showing that living NSCLC patients had notably higher immune and ESTIMATE scores ($p < 0.05$), and the immune score declined along with the progression of stage and M stage classification despite no striking difference. In contrast, the stromal score was not associated with the abovementioned clinical features. These findings clarified that the immune and ESTIMATE scores played a crucial role in the progression of NSCLC. Since the ESTIMATE score represents a combination of immune and stromal scores, the immune score seemed to be a better indicator of prognosis in NSCLC patients.

DEG screening and functional analysis between low- and high-immune score groups

To determine the global gene expression profiles in the high and low immune score groups, DEG analysis was further conducted. As a result, 1806 DEGs containing 978 upregulated and 828 downregulated genes were determined. The expression distribution of DEGs was visualized by volcano plots (Figure 3B), and the top 50 DEGs of the two groups are illustrated in the heatmap (Figure 3A). Moreover,

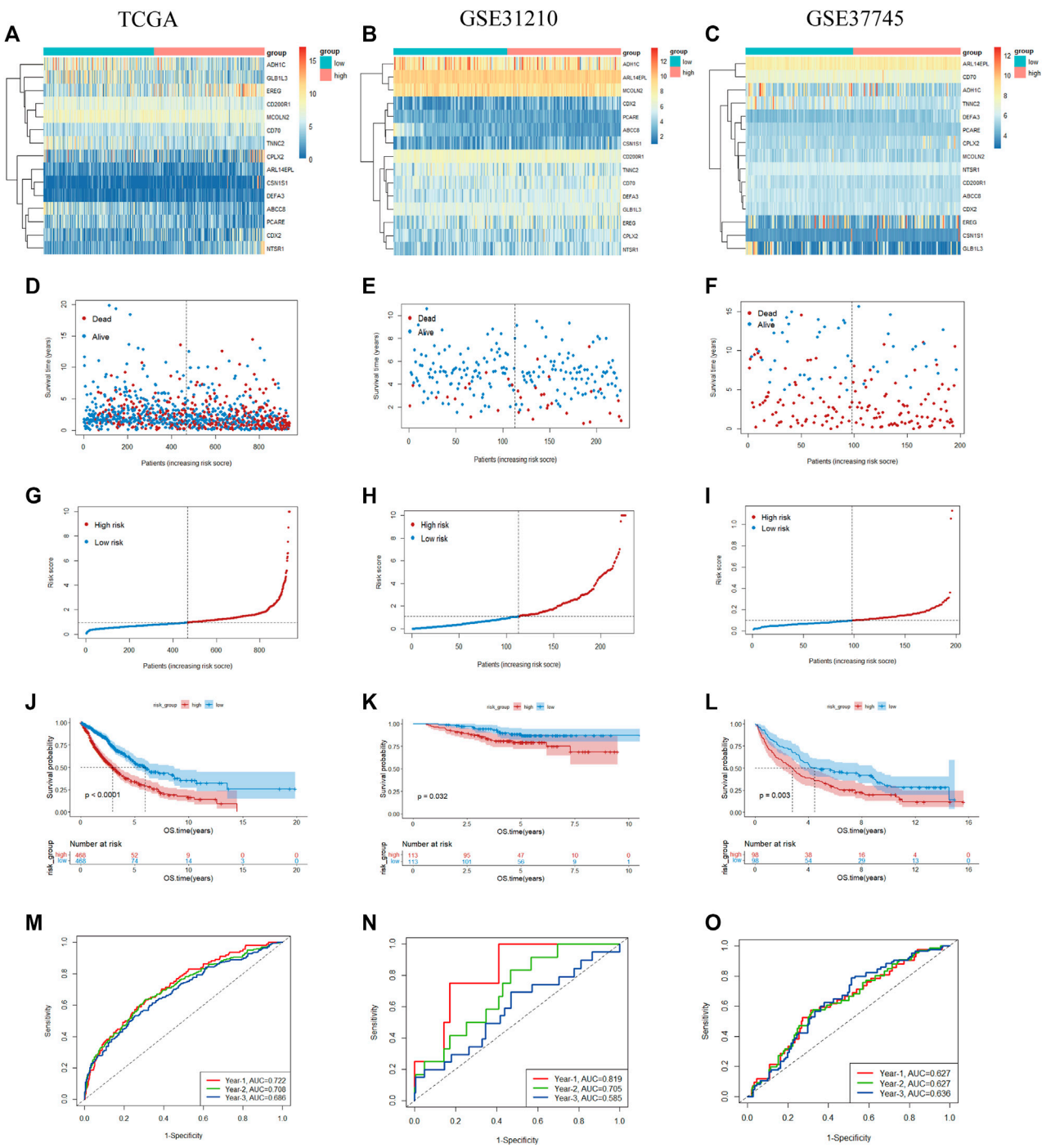

FIGURE 5
Prognostic value of the 15-gene prognostic model in the TCGA and validation cohorts **(A–C)**. Heatmap of fifteen genes between the two groups in the TCGA and validation sets **(D–F)**. Risk score scatter plot. Red dots indicate dead patients, and blue dots indicate alive patients **(G–I)**. Risk score curve plot. The dotted line indicates the individual distribution of the risk score, and the patients are categorized into low-risk (blue) and high-risk (red) groups **(J–L)**. Survival status and time of patients between the two groups in the TCGA and validation sets, respectively **(M–O)**. The time-dependent ROC curve of patients between the two groups in the TCGA and validation sets.

potential biological function analysis was conducted, and the top 5 GO annotations (BP, CC, MF) of up- and downregulated DEGs are described in the circle plot of Figures 3C, D. As shown, the upregulated DEGs were primarily linked to immune functions, including T cell activation, immune receptor activity and lymphocyte activation regulation, while pattern specification process, epidermis development and DNA-binding transcription activator activity were enriched in downregulated DEGs. Furthermore, KEGG analysis demonstrated that the upregulated DEGs were significantly associated with cytokine-cytokine receptor interactions, cell adhesion

molecules and chemokine signaling pathways (Figure 3E). However, the downregulated DEGs were enriched in neuroactive ligand-receptor interactions and chemical carcinogenesis-receptor activation (Figure 3F).

Screening of independent prognostic feature DEGs

In the beginning, univariate Cox analysis was utilized to analyze the 1806 DEGs selected from this study, and genes with a *p-value* < 0.01 were incorporated in survival-related analysis and used for subsequent LASSO and further multivariate Cox analysis. Twenty-six DEGs were screened through LASSO analysis and were significantly correlated with survival outcome (Figures 4A, B). After subsequent screening, the results of multivariate Cox analysis revealed that a prognostic signature of 15 genes was independently related to OS, including alcohol dehydrogenase 1C (ADH1C), complexin2 (CPLX2), casein alpha s1 (CSN1S1), neurotensin receptor 1 (NTSR1), caudal type homeobox 2 (CDX2), ATP binding cassette subfamily C member 8 (ABCC8), photoreceptor cilium actin regulator (PCARE), troponin C2, fast skeletal type (TNNC2), epiregulin (EREG), mucolipin TRP cation channel 2 (MCOLN2), CD70 molecule (CD70), galactosidase beta 1 like 3 (GLB1L3), CD200 receptor 1 (CD200R1), defensin alpha 3 (DEFA3), and ADP ribosylation factor like GTPase 14 effector protein like (ARL14EPL). These genes were represented by a forest map (Figure 4C). Supplementary information is described in Supplementary Table S1.

Establishment and validation of prognostic model

The prognostic signature was identified, and the risk score of each NSCLC patient was calculated using the following formula:

The risk score = (−0.08672) × *Exp*ADH1C + (0.14913) × *Exp* CPLX2 + (0.17786) × *Exp*CSN1S1 + (0.17628) × *Exp*NTSR1 + (0.21064) × *Exp*CDX2 + (−0.9561) × *Exp* ABCC8 + (−0.83455) × *Exp*PCARE + (−0.10013) × *Exp*TNNC2 + (0.08950) × *Exp* EREG + (−0.24566) × *Exp* MCOLN2 + (0.11454) × *Exp* CD70 + (−0.10665) × *Exp* GLB1L3 + (−0.27673) × *Exp* CD200R1 + (0.63454) × *Exp* DEFA3 + (0.35913) × *Exp* ARL14EPL.

Based on the demarcation point of the risk score, the NSCLC samples were divided into high- or low-risk categories. The mRNA expression of 15 genes in the two risk subtypes was presented in the form of a heatmap (Figure 5A). The patients had a higher risk of death with increasing risk score, as shown in the risk score curve and scatter plot (Figures 5D, G). Subsequently, the K-M analysis revealed that the prognosis of NSCLC samples in the low-risk subgroup was remarkably better than that in the high-risk subgroup ($p < 0.05$) (Figure 5J). For completeness, the time-dependent ROC curves predicted the OS of NSCLC patients (AUC of 1-year = 0.722, 2-year = 0.708, 3-year = 0.686) (Figure 5M).

To validate the reliability of our prognostic signature constructed from the TCGA cohort, the risk score was further calculated with the abovementioned formula for each patient in GSE31210 (226 LUADs) and GSE37745 (n = 196, 106 LUADs, 24 LCLCs, 66 LUSCs). Patients were also split into high- and low-risk subtypes according to the cutoff point of the risk score. The heatmap shows the expression of 15 prognostic genes in the two risk groups (Figures 5B, C). Similar to the results of TCGA, patients tended to have a higher probability of death in the high-risk group than in the low-risk group (Figures 5E, F, H, I). As a supplementary, we evaluated the prognostic value of prognostic features in LUAD and LUSC, validation in the NSCLC subtypes also demonstrated the similar result (Supplementary Figure S1). We also observed a significant OS difference in GSE31210 and GSE37745, which also implied the prognostic value of the gene signature ($p < 0.05$) (Figures 5K, L). As shown in Figures 5N, O**,** ROC curves also reached preferable AUC values in the two validation sets, demonstrating the potent capability of the 15-gene prognostic model.

Relationship between the risk score and clinical parameters

A total of 936 NSCLC patients (475 LUADs and 461 LUSCs) with complete clinical information were enrolled in our clinical prognostic analysis. Table 2 shows the association between the two risk groups and clinical factors, including age, sex, stage, T stage, smoking index, status and tumor type. Our study revealed that the high-risk group had a higher rate of males and LUSC patients and more advanced cases, while other clinical variables were not significantly associated with risk scores.

Similarly, as external validation, the results of GSE31210 indicated that the risk score was remarkably associated with EGFR mutation and had no association with other clinical parameters (Supplementary Table S2). In addition, GSE37745, also used for external validation, showed that the risk score was not associated with clinical parameters except tumor type (details are described in Supplementary Table S3).

Screening of independent prognostic parameters and establishment of nomogram

To assess whether the risk score and which clinical parameters could serve as independent predictive factors, subsequently, univariate and multivariate Cox analyses were conducted. A total of 936 NSCLC samples were enrolled from the TCGA cohort, as shown in Figures 6A, B. From the results of univariate Cox analysis, the stage ($p < 0.0001$) and risk score ($p < 0.0001$) were observably related to OS. We further chose the variable with a *p*-value < 0.1 for the multivariate Cox test, and the obtained results showed that the risk score (HR = 2.178; 95% CI, 1.760–2.697; $p < 0.0001$) remained significant for overall survival in NSCLC patients. In addition, stage (HR = 1.880; 95% CI, 1.496–2.363; $p < 0.0001$) and age (HR = 1.326; 95% CI, 1.075–1.637; $p = 0.009$) were also significant predictors of prognosis.

To demonstrate the accurate prediction efficiency of the prognostic signature that we established, univariate and multivariate Cox analyses were also performed in GSE31210 and GSE37745. The obtained results also indicated that the risk score (HR = 2.333; 95% CI, 1.156–4.708; $p = 0.018$) was correlated with survival in GSE31210 and could also be a good predictor in GSE37745 (HR = 1.571; 95% CI, 1.129–2.185; $p = 0.007$). The details are described in Figures 6C–F. Moreover, we constructed a nomogram based on three independent prognostic indices (age,

TABLE 2 Relationship between risk score and clinical characteristics of 936 patients in TCGA cohort.

Characteristics	Total *n* = 936 (%)	High-risk group *n* = 468 (%)	Low-risk group *n* = 468 (%)	χ^2	*p*-value
Age, year				0.852	0.356
≤ 65	408 (43.6%)	211 (45.1%)	197 (42.1%)		
>65	528 (56.4%)	257 (54.9%)	271 (57.9%)		
Gender				36.84	<0.001
Male	561 (59.9%)	326 (69.7%)	235 (50.2%)		
Female	375 (40.1%)	142 (30.3%)	233 (49.8%)		
Stage				6.816	0.009
Stage I/II	748 (79.9%)	358 (76.5%)	390 (83.3%)		
Stage III/IV	188 (20.1%)	110 (23.5%)	78 (16.7%)		
Smoking index				1.551	0.213
High	455 (48.6%)	369 (78.8%)	353 (75.4%)		
Low	481 (51.4%)	99 (21.2%)	115 (24.6%)		
Tumor type				33.86	<0.001
LUAD	475 (50.9%)	193 (41.2%)	282 (60.3%)		
LUSC	461 (49.3%)	275 (58.8%)	186 (39.7%)		

Abbreviations: n, number.

stage and risk score) from TCGA (Figure 6G). The calibration curve, which evaluated the conformance of the nomogram, displayed high consistency between the nomogram-predicted probability and actual 1-, 3-, and 5-year OS (Figures 6I–K). The ROC curve showed prediction efficiency of the prognostic model (AUC = 0.693), and the risk score displayed better predictive efficiency than other clinical parameters (Figure 6H).

Pathway enrichment analysis based on the prognosis model

To further understand the relevant pathway mechanism between the two subgroups. KEGG pathway analysis and GSEA were performed on the DEGs of the high-risk groups, and the obtained results suggested that the signaling pathways of the high-risk subgroup were primarily enriched in the cytokine–cytokine receptor interaction pathway, IL-17 signaling pathway, PPAR signaling pathway and so on (Figure 7A). Additionally, GSEA indicated that the top 5 enriched pathways were epithelial mesenchymal transition (*P* adjust < 0.0001), E2F targets (*P* adjust < 0.0001), G2M checkpoint (*P* adjust < 0.0001), MYC targets (*P* adjust < 0.0001) and TNF-α signaling *via* NFKB (*P* adjust < 0.0001); details are presented in Figure 7B.

Tumor immune related and mutation analysis of two subgroups

According to the results of KEGG and GSEA, we found that the risk score was linked to immunity; thus, the tumor immune microenvironment in the two risk categories was compared. The obtained results revealed a lower immune score ($p < 0.001$), stromal score ($p = 0.021$), and ESTIMATE score ($p < 0.001$) and a higher tumor purity ($p < 0.001$) in the high-risk group based on the ESTIMATE algorithm (Figures 8A–D). Additionally, the distribution of 22 infiltrating immune cells in the two risk groups was evaluated based on the CIBERSORT algorithm (Figure 8E), and it indicated a higher proportion of CD4 memory-activated T cells, NK cells, M0 and M1 macrophages and neutrophils in the high-risk group, whereas B cells, CD4 memory resting T cells, and Tregs accounted for more cells in the low-risk group (Figure 8G). We also compared the differential expression of immune checkpoint genes between the two cohorts (Figure 8F), such as PDCD1, TIGIT, CTLA4, and BTLA, which demonstrated remarkably lower mRNA expression in the high-risk group. Furthermore, we explored the top 20 mutated gene mutation profiles between the high- and low-risk groups, as presented in Figures 8H, I. The genetic alteration rate in the high-risk group was higher than that in the low-risk subtype (96.35% vs. 92.01%), and we also found that TP53 had a higher mutation frequency in the high-risk group (71% vs. 61%). TP53 and TTN remained the top two genetic alterations in each group. Missense mutations were the most common form of mutation in the two groups.

Drug sensitivity with prognostic signature

To explore the potential application of personalized drug treatment based on our prognostic model, we investigated the

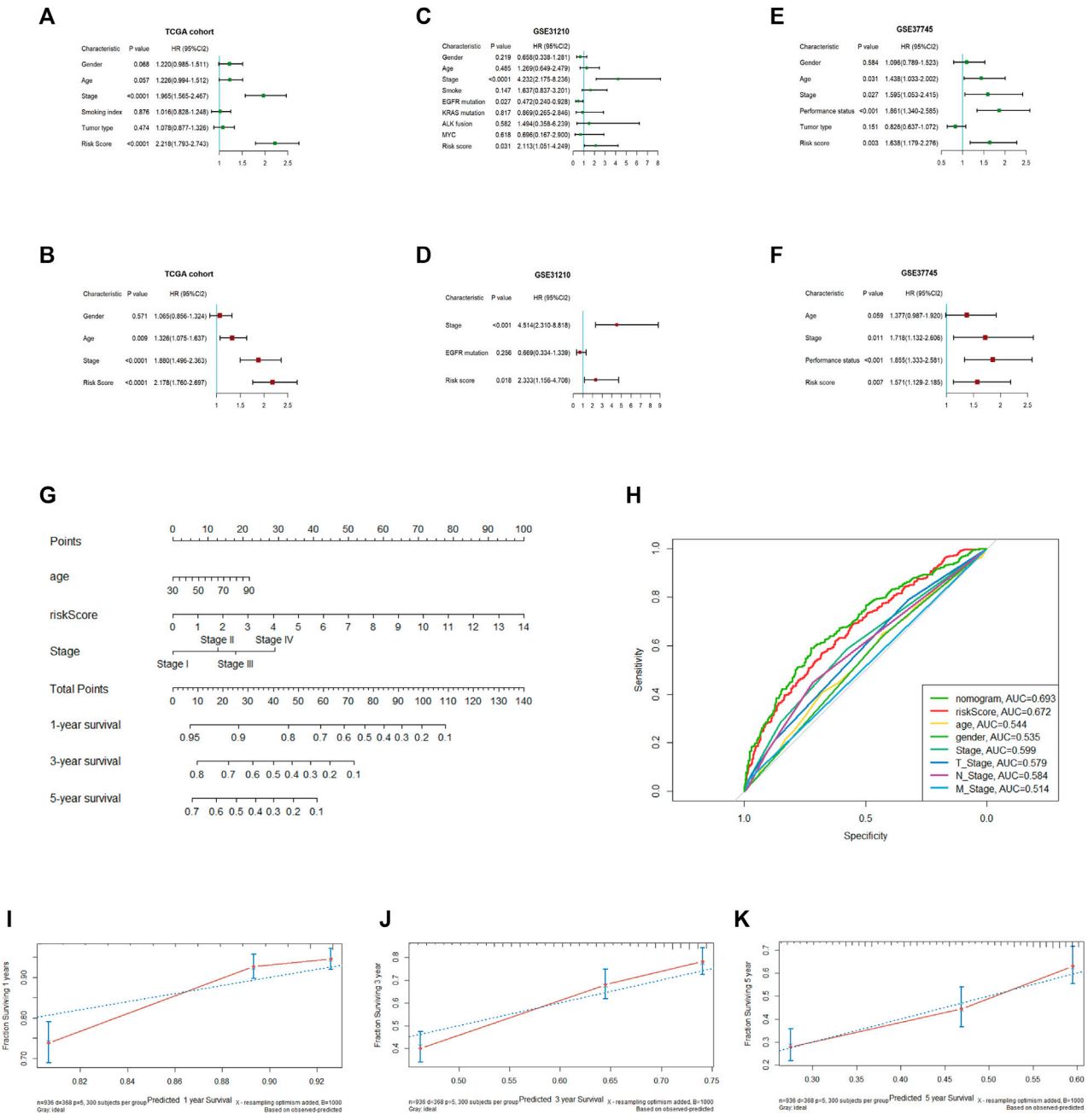

FIGURE 6
Univariate and multivariate Cox regression analyses in the TCGA and validation cohorts and establishment of the nomogram **(A, B)**. Univariate and multivariate Cox regression analyses in TCGA **(C, D)**. Univariate and multivariate Cox regression analyses in GSE31210 **(E, F)**. Univariate, multivariate Cox regression analysis in GSE37745 **(G)**. Establishment of a nomogram predicting OS based on the independent prognostic factors in TCGA **(H)**. ROC curve of the nomogram, risk score and other relevant clinical parameters in TCGA **(I–K)**. Calibration curves of the nomogram prediction of 1-, 3-, and 5-year survival in TCGA.

IC50 values of different drugs between the two sets. Drug sensitivity tests showed lower IC50 values of cisplatin, doxorubicin, docetaxel, paclitaxel, vinblastine and so on in the high-risk group, which indicated that the medication described above may be effective in high-risk patients. The IC50 values of nilotinib, tipifarnib, rapamycin and metformin were lower in the low-risk group, implying that patients in the low-risk group may benefit from these therapies. Details are shown in Figure 9.

Experimental and clinical validation

First, we used the PPI network of the prognostic DEGs from univariate Cox analysis and further visualized it by Cytoscape software (Figure 10A). A total of 7 modules were obtained using MCODE in the PPI network, and two hub genes (EREG and ADH1C) were recognized from two overlapping results between genes of modules and 15 DEGs (Figures 10B, C). Additionally, the

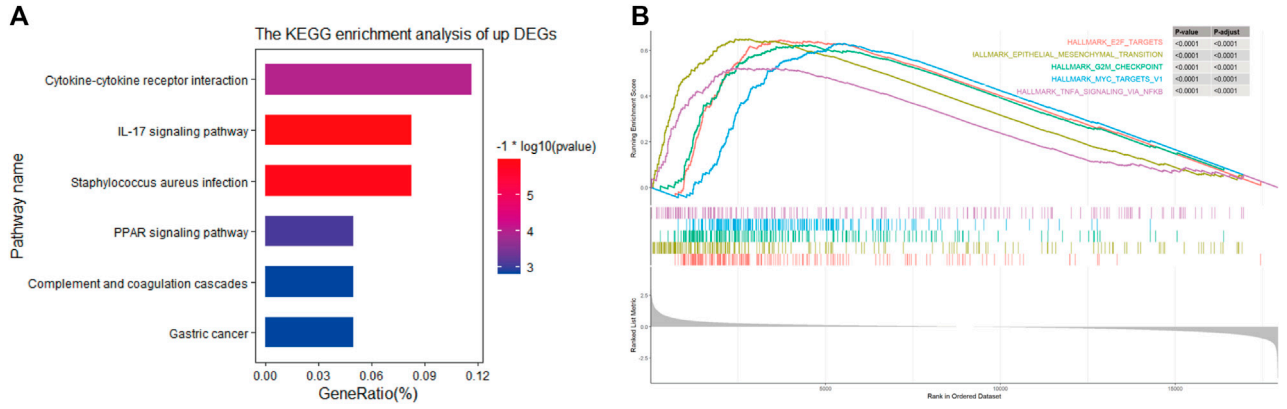

FIGURE 7
(A) KEGG pathways in high-risk group **(B)**. Top 5 Gene Set Enrichment Analysis of gene set of high-risk in TCGA cohort.

variability in survival status and stage was evaluated with differences in hub gene expression. There was a statistically significant higher rate of EREG expression in dead NSCLC patients (*p-value* = 0.042), while a trend toward more ADH1C expression was discovered in surviving patients (Figures 10D1, E1). We also found that EREG was directly proportional to the stage of NSCLC, while the mRNA expression of ADH1C seemed negatively related to the staging system (Figures 10D2, E2). Subsequently, the results of survival analysis showed that EREG was associated with shorter OS and that higher expression of ADHIC was beneficial to survival (*p-value* < 0.05) (Figures 10D3, E3). Similarly, in other datasets ADHIC was related to better survival (*p-value* < 0.05) and the high expression of EREG tends to be worse OS (Supplementary Figure S2).

Moreover, we demonstrated that there was less protein expression of ADH1C in lung tumors than in normal lung tissue based on the HPA database (Figure 10F).

Eventually, PCR experiments were utilized to directly compare the difference in mRNA expression in lung epithelial cells and NSCLC cell lines. EREG demonstrated higher RNA expression in NSCLC than in normal lung epithelial cells, while there was little difference in ADH1C between normal and tumor lung cells, which needs additional experiments for validation (Figures 10G, H).

Discussion

NSCLC diagnosis and treatment have made breakthroughs in the past few decades due to the ongoing discovery of genomic and TME changes in the pathogenesis of lung cancer. The approach has gradually shifted from chemotherapy drugs that broadly attack tumors toward targeted immunotherapy for precision therapy. Further exploration of the tumor immune microenvironment and identification of meaningful biomarkers are expected to provide a new direction for better patient diagnosis and treatment. In our study, through the ESTIMATE algorithm, we first found that the immune score was connected with the survival of NSCLC patients. Then, we divided the patients into two sets based on the optimum critical point of the immune score and mined the differential genes by the "DESeq2" R package. The prognostic gene signature was established by a series of statistical analyses. The external validation of GSE37745 and GSE31210 illustrated the accuracy of our prognostic model. In addition, relative GSEA, tumor immune, mutation and drug sensitivity analyses were performed between the two risk groups. The experimental validation of the hub gene strengthened our results. In general, the results of our research had a certain constructive impact on the predicted prognosis of NSCLC from the perspective of the tumor immune microenvironment (TIME).

The TIME, containing immune-promoting and immunosuppressive cells and molecules, plays a crucial role in the progression and prognosis of tumors. The immune system undergoes three major changes during the development of tumors: immune surveillance, immune balance and immune destruction (Dunn et al., 2004). It presents the characteristic of the two sides; the immune cells originally presented natural antitumor properties in tumor invasion while uncharacteristically changed into a promoting tumor phenotype during tumor progression, which contributes to immune escape and distant metastasis of malignancy. Currently, the characteristics of the TIME, listed as one of ten tumor characteristics (Hanahan and Weinberg, 2011), play a certain role in predicting both clinical prognosis and the efficacy of chemoradiotherapy (Josefowicz et al., 2012). Therefore, it makes significant sense to analyze the types and distribution of immune cells in the TME and generate an efficient immune evaluation system. Previous studies on the TME of pancarcinoma (mainly gastric cancer) have discovered that patients with high TME scores showed a stronger antitumor immune response, were more likely to benefit from immunotherapy and had better survival outcomes (Fatima et al., 2013). In lung cancer, tumor-infiltrating $CD4^+$ T cells play a crucial role in the immune response by allowing $CD8^+$ T cells to enter tumor sites and infect mucous membranes to kill tumors; moreover, they are necessary to inhibit tumor angiogenesis (Borst et al., 2018). Other studies have shown that tumor-associated macrophages (TAMs) in the TME are involved in angiogenesis, tumor migration and metastasis and the antitumor immune response, which is related to tumor progression (Qian and Pollard, 2010).

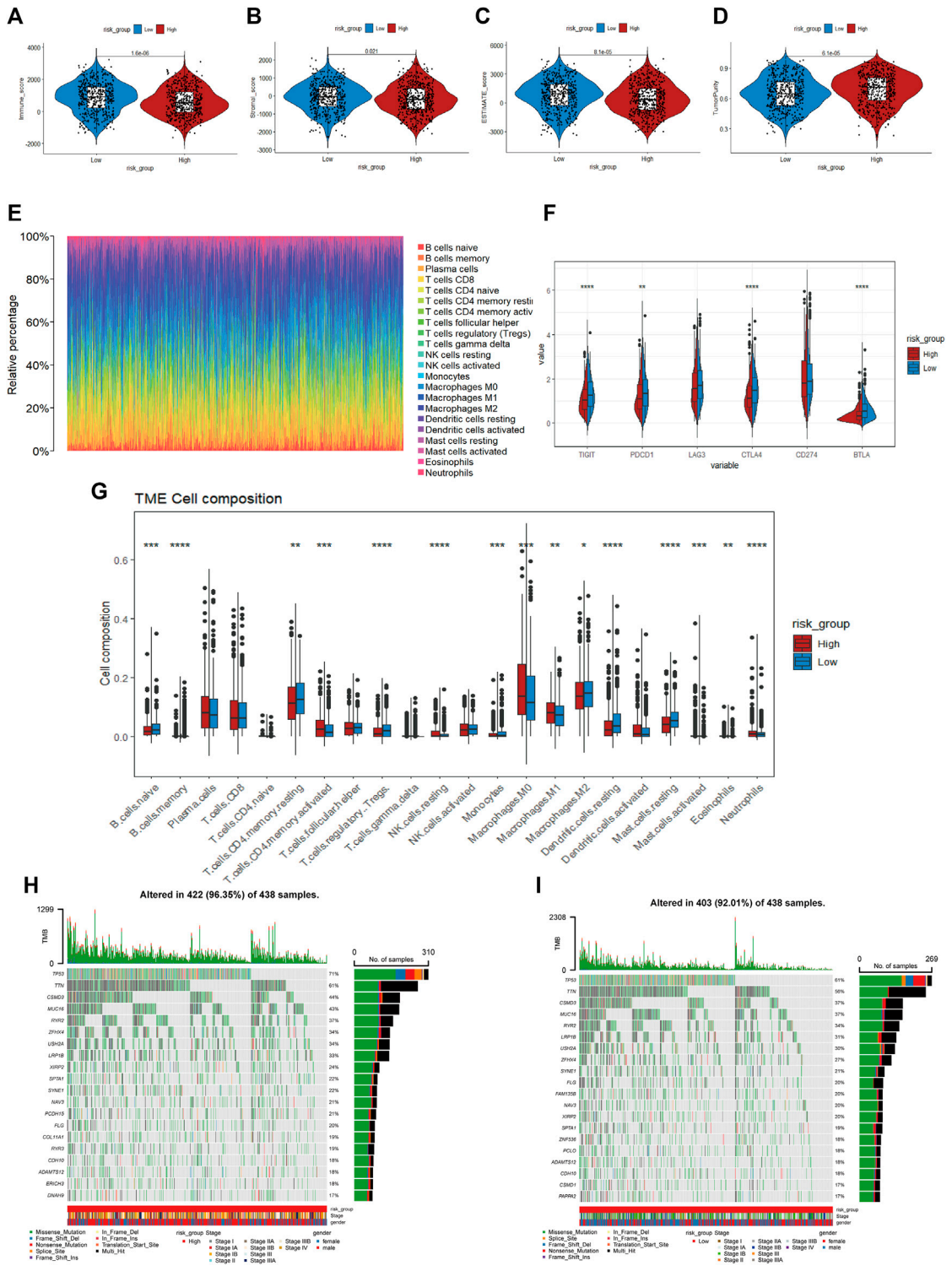

FIGURE 8
(A–D) Immune score, stroma score, ESTIMATE score and tumor purity of the high- and low-risk groups **(E)**. Distribution of infiltration of 22 immune cell types in the two risk groups **(F)** The expression of immune checkpoint genes between the two cohorts **(G)**. The proportions of different immune cells in the high- and low-risk groups **(H, I)**. Mutated gene mutation profiles between the high- and low-risk groups.

Our study applied the ESTIMATE algorithm to NSCLC and found that a high immune score was associated with a better prognosis, which was consistent with previous research.

The gene expression profiles of the two groups with high and low NSCLC immune scores were analyzed and compared, and 1806 DEGs were screened. Subsequently, a 15-gene signature was

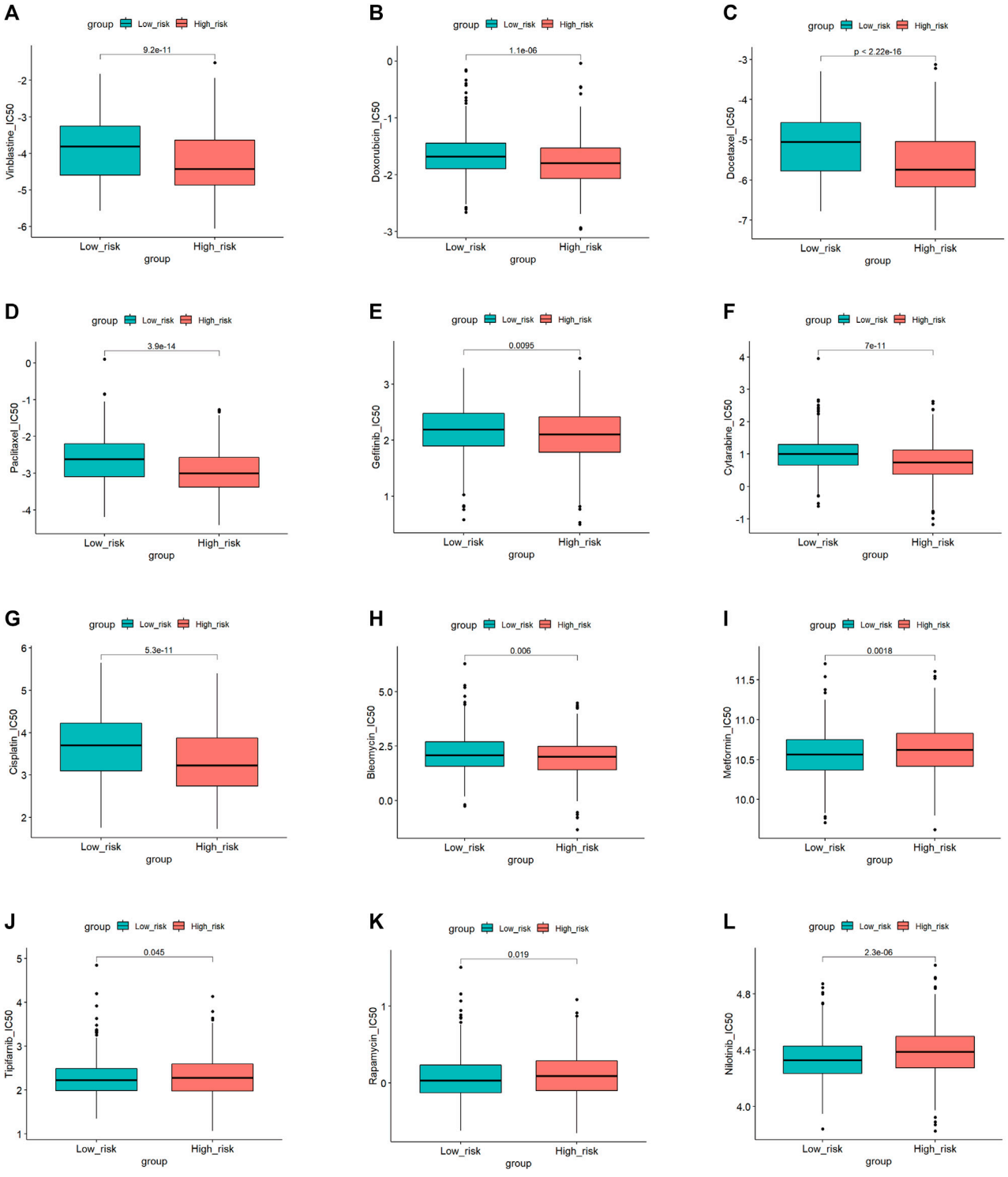

FIGURE 9
Drugs sensitivity in the high and low-risk group.

established through LASSO and Cox analyses, and the risk score of every patient was calculated. To date, a number of gene signatures have been established to predict the survival of NSCLC patients. The research in 2017 identified a tumor immune-associated prognostic gene signature with a precise prediction (AUC = 0.7) in early-stage NSCLC (Li et al., 2017). Liu et al. established a prognostic model that combined molecular biomarkers (TPX2 and MMP12) and several meaningful clinical features and exhibited a higher survival prediction performance (AUC = 0.771) than TNM staging systems in postoperative NSCLC patients (Liu et al., 2018).

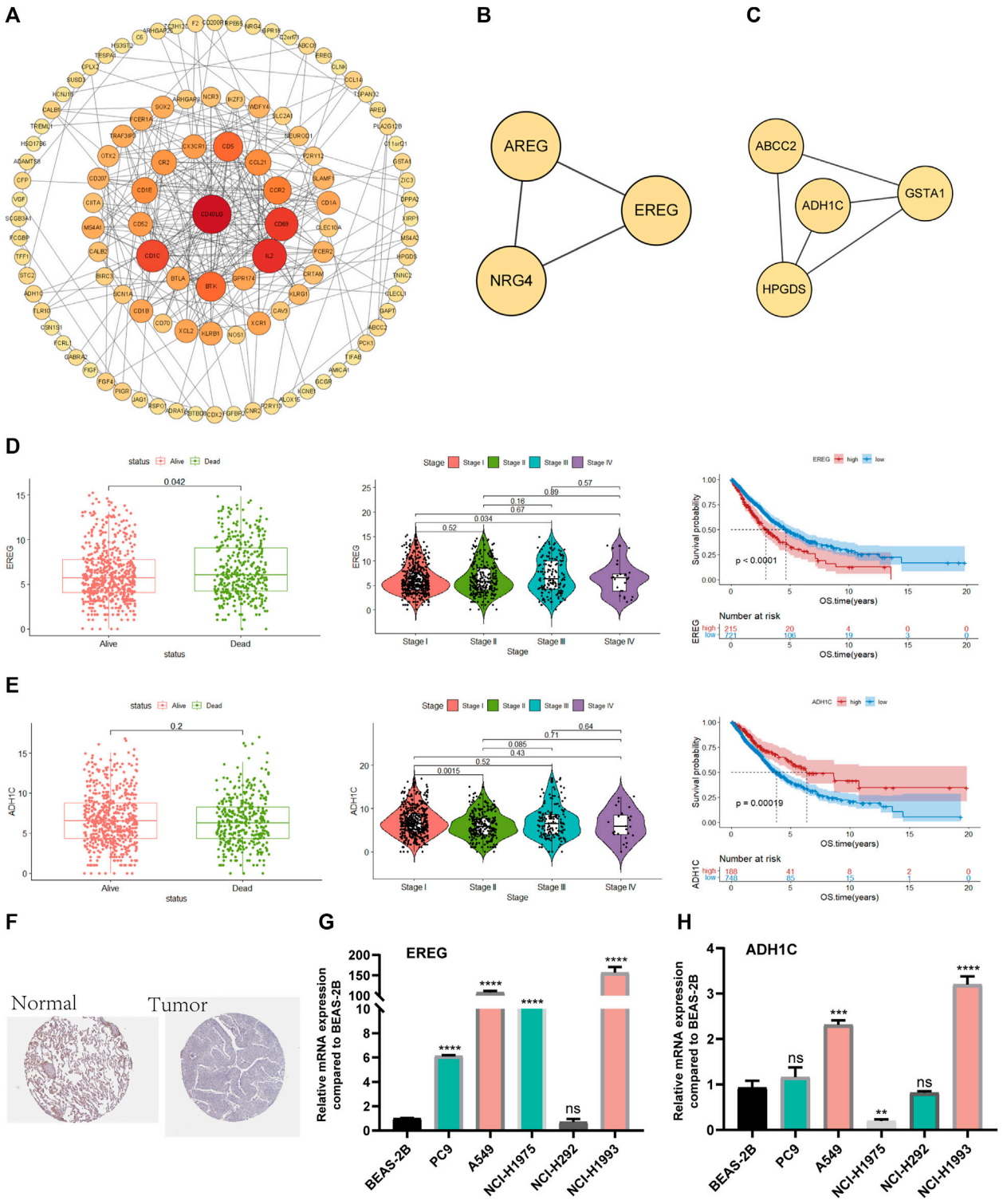

FIGURE 10
Screening and validation of hub genes **(A)**. PPI network among prognostic genes. **(B, C)** Two modules contained many genes in the PPI network **(D)**. The relationship between survival state, stage and mRNA expression levels of EREG, Kaplan–Meier curves of EREG in OS **(E)**. The relationship between survival state, stage and mRNA expression levels of ADH1C, Kaplan–Meier curves of ADH1C in OS **(F)**. ADH1C protein levels in normal lung and NSCLC were visualized by IHC in HPA. **(G, H)** Quantitative real-time PCR analysis of the mRNA expression levels of EREG and ADH1C in NSCLC cell lines and normal lung epithelial cells.

However, they rarely translated into medical practice, which may be due to the following three reasons: 1) the gene signature was trained in a cohort with high variance, 2) mRNA microarray data may be measured using diverse experimental methods, and 3) most gene signatures consist of few typical genes and may neglect other potential reasons that seriously reduce their prediction stability and may result in overfitting. Our study found that a high immune score was associated with a better prognosis in NSCLC, and the subsequently constructed immune-related gene signature showed superior prognostic classification ability than other clinical parameters and was further verified in two other GEO datasets. Our study provides an alternative idea for the development of new targeted drugs. The nomogram, a practical tool for assessing the prognosis of malignant patients, has been recognized to be more effective than traditional TNM staging (Diao et al., 2019). Therefore, we combined the risk score and several clinical parameters to draw a nomogram that predicted 1-, 3-, and 5-year survival and exhibited relatively reliable prediction efficiency. It is worth considering that there were more stage I-III NSCLC patients than advanced stage NSCLC patients in the TCGA cohort. Early-stage NSCLC patients tended to have a good prognosis after surgical treatment, and there were more factors related to prognosis. To a certain extent, the lack of specific treatment, clinical characteristics, laboratory indices, and imaging materials in the databases could influence the model accuracy.

The prognostic model established in our research consisted of 15 prognostic DEGs. Furthermore, we selected key prognostic genes from two overlapping results from PPI and 15 DEGs. Two hub genes (EREG and ADH1C) were recognized. Patients with high mRNA expression of EREG tended to have a poor prognosis, while ADH1C was associated with better survival in TCGA. EREG and ADH1C were further verified through RT–PCR experiments of normal lung epithelium and NSCLC cell lines. Altogether, we determined that EREG and ADH1C likely play significant roles in the process of NSCLC through validation of the TCGA database and RT–PCR assay.

Epiregulin (EREG), a member of the epidermal growth factor family, combines with ErbB receptors and further contributes to proliferation, inflammation and anti-apoptosis in tumor cells (Riese and Cullum, 2014). Additionally, it promotes the progression of various cancers. Research has revealed that patients with positive EREG are associated with a worse prognosis than those with negative EREG in NSCLC (Zhang et al., 2008). Moreover, Chen et al. (Chen et al., 2019) discovered that acquired resistance to 5-FU in colon cancer can be reversed by inhibiting the miR-215-5p-EREG/TYMS axis. A study (Zhang et al., 2022) in 2022 found that EREG enhanced resistance to chemotherapy in NSCLC by increasing the expression of stemness-associated genes. Notably, the expression of EREG in stromal cells is upregulated and activates several downstream signaling pathways, including the MAPK AKT/mTOR and JAK/STAT pathways, in cancer cells by paracrine signaling, promoting their malignant phenotype and accelerating the progression of cancer (Wang et al., 2022). This discovery reinforces our conclusion that EREG plays a crucial role in NSCLC progression by influencing the TIME.

ADH1C is a member of the ADH family that catalyzes the oxidation of ethyl alcohol to acetaldehyde (a carcinogenic metabolite) and plays a crucial role in the etiology of various cancers. The polymorphism of ADH1C may be a crucial factor in the etiology of oral cancer and genetically determine an individual's susceptibility (Brocic et al., 2011). A previous study indicated that patients with positive ADH1C have an increased risk of head and neck cancer (Visapaa et al., 2004). In addition, further studies suggested that ADH1C was not linked to HNC (Peters and McClean, 2005). Similar differences were found for colorectal and breast cancer. Bongaerts et al. (2011) considered that the ADH1C genotype and excessive alcohol intake were associated with an increased risk of CRC, while some researchers have suggested that ADH1C expression is reduced during the progression of CRC from early to advanced stages. ADH1C allele mutations were related to an increased breast cancer risk due to alcohol consumption by comparing postmenopausal breast cancer samples with controls (Benzon Larsen et al., 2010). However, one study suggests that ADH1C polymorphisms may not be connected with breast cancer in Caucasians (Wang et al., 2012). The abovementioned inconsistent conclusions regarding the effect of ADH1C on cancer suggested that the mechanisms related to ADH1C may be complex and remain unclear. A recent study showed that the prognosis of NSCLC patients with high ADH1C expression was associated with longer OS. Our research found that ADH1C may be an antitumor factor whose higher expression is associated with a better prognosis. However, reverse protein and mRNA expression requires further experimental verification.

We further explored the potential pathway mechanism between the two subtypes. It is worth noting that the proliferation, differentiation, metastasis of tumor cells and pathways in cytokines and inflammation were enriched in the high-risk group. For example, epithelial-mesenchymal transition (EMT) indicates the malignant process of tumors, allows tumor cells to invade and metastasize, and promotes chemotherapy resistance (Jolly et al., 2019). E2F is essential to cellular homeostasis and plays a role beyond cell cycle regulation, and its dysregulation may lead to cancer progression, including processes such as apoptosis, metabolism and angiogenesis (Kent and Leone, 2019). Tumor necrosis factor-α (TNF-α) is a proinflammatory cytokine involved in normal inflammatory and immune responses. TNF-α receptors exist on various cell surfaces and are divided into two types (TNFR I and TNFR II). The combination of TNF-α and TNFR usually causes inflammation and the occurrence of tumors (Frances, 2009). TNF-α, as a key regulator of the TME, is well-recognized (Wu and Zhou, 2010). Cytokine interactions accounted for a high proportion in GSEA. Cytokines were the key signaling proteins in the TME. TNF and IL-6 can cause disordered cytokine regulation and promote tumor inflammation. IL-10, IL-4, and TGFβ lead to immunosuppression (Propper and Balkwill, 2022). Cytokines and their receptors have been widely studied as tumor targets or therapeutic strategies. These tumor-related pathways were enriched in the set of high-risk patients, and these pathways were closely related to tumor progression and further verified the accuracy of our study.

The establishment of an immune-related prognostic model in our study was validated from multiangle and multiple databases, and the prognostic gene signature demonstrated good prospects in predicting the prognosis of NSCLC patients. Our study further analyzed mutations and drug sensitivity differences between the two risk groups. The results of differentially mutated genes were convenient for subsequent basic experimental research, and the finding of drug sensitivity had potential guiding meaning for the choice of clinical drug. However, there are still some limitations in

our research. First, the incomplete and lack of specific treatment, clinical characteristics, laboratory indices, and imaging materials in the TCGA databases could influence the model accuracy, and we could not explore the influence of these factors on NSCLC patients. In addition, we believe that functional experiments should be conducted to confirm the molecular mechanism of the hub genes. Finally, it would be best if the prognostic model was verified in prospective or retrospective clinical trials.

Conclusion

In conclusion, we have identified an immune-related 15-gene-based prognostic model that presented an accurate prognostic predictive ability in NSCLC patients. The potential mechanisms and chemotherapy-sensitive analyses were also evaluated between the two risk groups, which could provide the basis for subsequent basic and clinical trials.

Data availability statement

The datasets presented in this study can be found in online databases. This data can be found here: The Cancer Genome Atlas (TCGA) (https://portal.gdc.cancer.gov/) and Gene Expression Omnibus (GEO) (https://www.ncbi.nlm.nih.gov/geo/) databases. The accession numbers can be found in the article.

Author contributions

HZ and RX provided the conception and design, ZJ and SS prepared material, collected analyzed data, JZ and YQ composited the figure, WY edited the tables, ZJ and RX write the original draft. All authors have read and approved the final manuscript.

Acknowledgments

All authors would like to thank the TCGA databases (https://portal.gdc.cancer.gov/) and GEO datasets (https://www.ncbi.nlm.nih.gov/) for data sharing.

Conflict of interest

The authors declare that the research was conducted in the absence of any commercial or financial relationships that could be construed as a potential conflict of interest.

Publisher's note

Supplementary material

The Supplementary Material for this article can be found online at: https://www.frontiersin.org/articles/10.3389/fphar.2023.1153565/full#supplementary-material

References

Anari, F., Ramamurthy, C., and Zibelman, M. (2018). Impact of tumor microenvironment composition on therapeutic responses and clinical outcomes in cancer. *Future Oncol.* 14 (14), 1409–1421. doi:10.2217/fon-2017-0585

Arriagada, R., Dunant, A., Pignon, J. P., Bergman, B., Chabowski, M., Grunenwald, D., et al. (2010). Long-term results of the international adjuvant lung cancer trial evaluating adjuvant Cisplatin-based chemotherapy in resected lung cancer. *J. Clin. Oncol.* 28 (1), 35–42. doi:10.1200/JCO.2009.23.2272

Benzon Larsen, S., Vogel, U., Christensen, J., Hansen, R. D., Wallin, H., Overvad, K., et al. (2010). Interaction between ADH1C Arg(272)Gln and alcohol intake in relation to breast cancer risk suggests that ethanol is the causal factor in alcohol related breast cancer. *Cancer Lett.* 295 (2), 191–197. doi:10.1016/j.canlet.2010.02.023

Binnewies, M., Roberts, E. W., Kersten, K., Chan, V., Fearon, D. F., Merad, M., et al. (2018). Understanding the tumor immune microenvironment (TIME) for effective therapy. *Nat. Med.* 24 (5), 541–550. doi:10.1038/s41591-018-0014-x

Blum, A., Wang, P., and Zenklusen, J. C. (2018). SnapShot: TCGA-analyzed tumors. *Cell* 173 (2), 530. doi:10.1016/j.cell.2018.03.059

Bongaerts, B. W., de Goeij, A. F., Wouters, K. A., van Engeland, M., Gottschalk, R. W., Van Schooten, F. J., et al. (2011). Alcohol consumption, alcohol dehydrogenase 1C (ADH1C) genotype, and risk of colorectal cancer in The Netherlands Cohort Study on diet and cancer. *Alcohol* 45 (3), 217–225. doi:10.1016/j.alcohol.2010.10.003

Borst, J., Ahrends, T., Babala, N., Melief, C. J. M., and Kastenmuller, W. (2018). CD4(+) T cell help in cancer immunology and immunotherapy. *Nat. Rev. Immunol.* 18 (10), 635–647. doi:10.1038/s41577-018-0044-0

Brocic, M., Supic, G., Zeljic, K., Jovic, N., Kozomara, R., Zagorac, S., et al. (2011). Genetic polymorphisms of ADH1C and CYP2E1 and risk of oral squamous cell carcinoma. *Otolaryngology-Head Neck Surg.* 145 (4), 586–593. doi:10.1177/0194599811408778

Chen, S. W., Yue, T. H., Huang, Z. H., Zhu, J., Bu, D. F., Wang, X., et al. (2019). Inhibition of hydrogen sulfide synthesis reverses acquired resistance to 5-FU through miR-215-5p-EREG/TYMS axis in colon cancer cells. *Cancer Lett.* 466, 49–60. doi:10.1016/j.canlet.2019.09.006

Denisenko, T. V., Budkevich, I. N., and Zhivotovsky, B. (2018). Cell death-based treatment of lung adenocarcinoma. *Cell Death Dis.* 9 (2), 117. doi:10.1038/s41419-017-0063-y

Diao, J. D., Wu, C. J., Cui, H. X., Bu, M. W., Yue, D., Wang, X., et al. (2019). Nomogram predicting overall survival of rectal squamous cell carcinomas patients based on the seer database: A population-based strobe cohort study. *Med. Baltim.* 98 (46), e17916. doi:10.1097/MD.0000000000017916

Dunn, G. P., Old, L. J., and Schreiber, R. D. (2004). The three Es of cancer immunoediting. *Annu. Rev. Immunol.* 22, 329–360. doi:10.1146/annurev.immunol.22.012703.104803

Fatima, S. P., Bruno, Z., Igor, S., Roela, R. A., Mangone, F. R. R., Ribeiro, U., Jr, et al. (2013). A gene expression profile related to immune dampening in the tumor microenvironment is associated with poor prognosis in gastric adenocarcinoma. *J. gastroenterology* 48 (49), 1453–1466. doi:10.1007/s00535-013-0904-0

Frances, B. (2009). Tumour necrosis factor and cancer. *Nat. Rev. Cancer* 9 (5), 361–371. doi:10.1038/nrc2628

Hanahan, D., and Weinberg, R. A. (2011). Hallmarks of cancer: The next generation. *Cell* 144 (5), 646–674. doi:10.1016/j.cell.2011.02.013

Herbst, R. S., Morgensztern, D., and Boshoff, C. (2018). The biology and management of non-small cell lung cancer. *Nature* 553 (7689), 446–454. doi:10.1038/nature25183

Hornburg, M., Desbois, M., Lu, S., Guan, Y., Lo, A. A., Kaufman, S., et al. (2021). Single-cell dissection of cellular components and interactions shaping the tumor immune phenotypes in ovarian cancer. *Cancer Cell* 39 (7), 928–944.e6. doi:10.1016/j.ccell.2021.04.004

Hu, M., and Polyak, K. (2008). Microenvironmental regulation of cancer development. *Curr. Opin. Genet. Dev.* 18 (1), 27–34. doi:10.1016/j.gde.2007.12.006

Huang, Q., Zhang, H., Hai, J., Socinski, M. A., Lim, E., Chen, H., et al. (2018). Impact of PD-L1 expression, driver mutations and clinical characteristics on survival after anti-PD-1/PD-L1 immunotherapy versus chemotherapy in non-small-cell lung cancer: A meta-analysis of randomized trials. *Oncoimmunology* 7 (12), e1396403. doi:10.1080/2162402X.2017.1396403

Jolly, M. K., Somarelli, J. A., Sheth, M., Biddle, A., Tripathi, S. C., Armstrong, A. J., et al. (2019). Hybrid epithelial/mesenchymal phenotypes promote metastasis and therapy resistance across carcinomas. *Pharmacol. Ther.* 194, 161–184. doi:10.1016/j.pharmthera.2018.09.007

Josefowicz, S. Z., Lu, L. F., and Rudensky, A. Y. (2012). Regulatory T cells: Mechanisms of differentiation and function. *Annu. Rev. Immunol.* 30, 531–564. doi:10.1146/annurev.immunol.25.022106.141623

Kent, L. N., and Leone, G. (2019). The broken cycle: E2F dysfunction in cancer. *Nat. Rev. Cancer* 19 (6), 326–338. doi:10.1038/s41568-019-0143-7

Li, B., Cui, Y., Diehn, M., and Li, R. (2017). Development and validation of an individualized immune prognostic signature in early-stage nonsquamous non-small cell lung cancer. *JAMA Oncol.* 3 (11), 1529–1537. doi:10.1001/jamaoncol.2017.1609

Liu, L., Shi, M., Wang, Z., Lu, H., Li, C., Tao, Y., et al. (2018). A molecular and staging model predicts survival in patients with resected non-small cell lung cancer. *BMC Cancer* 18 (1), 966. doi:10.1186/s12885-018-4881-9

Lou, X., Zhao, K., Xu, J., Shuai, L., Niu, H., Cao, Z., et al. (2022). CCL8 as a promising prognostic factor in diffuse large B-cell lymphoma via M2 macrophage interactions: A bioinformatic analysis of the tumor microenvironment. *Front. Immunol.* 13, 950213. doi:10.3389/fimmu.2022.950213

Osmani, L., Askin, F., Gabrielson, E., and Li, Q. K. (2018). Current WHO guidelines and the critical role of immunohistochemical markers in the subclassification of non-small cell lung carcinoma (NSCLC): Moving from targeted therapy to immunotherapy. *Semin. Cancer Biol.* 52 (1), 103–109. doi:10.1016/j.semcancer.2017.11.019

Peters, E. S., McClean, M. D., Liu, M., Eisen, E. A., Mueller, N., and Kelsey, K. T. (2005). The ADH1C polymorphism modifies the risk of squamous cell carcinoma of the head and neck associated with alcohol and tobacco use. *Cancer Epidemiol. Biomarkers Prev.* 14 (2), 476–482. doi:10.1158/1055-9965.EPI-04-0431

Propper, D. J., and Balkwill, F. R. (2022). Harnessing cytokines and chemokines for cancer therapy. *Nat. Rev. Clin. Oncol.* 19 (4), 237–253. doi:10.1038/s41571-021-00588-9

Qian, B. Z., and Pollard, J. W. (2010). Macrophage diversity enhances tumor progression and metastasis. *Cell* 141 (1), 39–51. doi:10.1016/j.cell.2010.03.014

Riese, D. J., and Cullum, R. L. (2014). Epiregulin: Roles in normal physiology and cancer. *Seminars Cell & Dev. Biol.* 28, 49–56. doi:10.1016/j.semcdb.2014.03.005

Schulz, M., Salamero-Boix, A., Niesel, K., Alekseeva, T., and Sevenich, L. (2019). Microenvironmental regulation of tumor progression and therapeutic response in brain metastasis. *Front. Immunol.* 10, 1713. doi:10.3389/fimmu.2019.01713

Sung, H., Ferlay, J., Siegel, R. L., Laversanne, M., Soerjomataram, I., Jemal, A., et al. (2021). Global cancer Statistics 2020: GLOBOCAN estimates of incidence and mortality worldwide for 36 cancers in 185 countries. *CA Cancer J. Clin.* 71 (3), 209–249. doi:10.3322/caac.21660

Teng, M. W., Galon, J., Fridman, W. H., and Smyth, M. J. (2015). From mice to humans: Developments in cancer immunoediting. *J. Clin. Invest.* 125 (9), 3338–3346. doi:10.1172/JCI80004

Travis, W. D., Brambilla, E., Nicholson, A. G., Yatabe, Y., Austin, J. H. M., Beasley, M. B., et al. (2015). The 2015 world health organization classification of lung tumors impact of genetic, clinical and radiologic advances since the 2004 classification. *J. Thorac. Oncol.* 10 (9), 1243–1260. doi:10.1097/Jto.0000000000000630

Visapaa, J. P., Gotte, K., Benesova, M., Li, J., Homann, N., Conradt, C., et al. (2004). Increased cancer risk in heavy drinkers with the alcohol dehydrogenase 1C*1 allele, possibly due to salivary acetaldehyde. *Gut* 53 (6), 871–876. doi:10.1136/gut.2003.018994

Wang, C., Long, Q., Fu, Q., Xu, Q., Fu, D., Li, Y., et al. (2022). Targeting epiregulin in the treatment-damaged tumor microenvironment restrains therapeutic resistance. *Oncogene* 41 (45), 4941–4959. doi:10.1038/s41388-022-02476-7

Wang, L., Zhang, Y., Ding, D., He, X., and Zhu, Z. (2012). Lack of association of ADH1C genotype with breast cancer susceptibility in caucasian population: A pooled analysis of case-control studies. *Breast* 21 (4), 435–439. doi:10.1016/j.breast.2012.01.007

Wu, Y., and Zhou, B. P. (2010). TNF-alpha/NF-kappaB/Snail pathway in cancer cell migration and invasion. *Br. J. Cancer* 102 (4), 639–644. doi:10.1038/sj.bjc.6605530

Xu, W. H., Xu, Y., Wang, J., Wan, F. N., Wang, H. K., Cao, D. L., et al. (2019). Prognostic value and immune infiltration of novel signatures in clear cell renal cell carcinoma microenvironment. *Aging (Albany NY)* 11 (17), 6999–7020. doi:10.18632/aging.102233

Yoshihara, K., Shahmoradgoli, M., Martinez, E., Vegesna, R., Kim, H., Torres-Garcia, W., et al. (2013). Inferring tumour purity and stromal and immune cell admixture from expression data. *Nat. Commun.* 4, 2612. doi:10.1038/ncomms3612

Zhang, J., Iwanaga, K., Choi, K. C., Wislez, M., Raso, M. G., Wei, W., et al. (2008). Intratumoral epiregulin is a marker of advanced disease in non-small cell lung cancer patients and confers invasive properties on EGFR-mutant cells. *Cancer Prev. Res.* 1 (3), 201–207. doi:10.1158/1940-6207.Capr-08-0014

Zhang, Y., Qiu, F., Ye, T., Lee, S. H., Xu, J., Jia, L., et al. (2022). Epiregulin increases stemness-associated genes expression and promotes chemoresistance of non-small cell lung cancer via ERK signaling. *Stem Cell Res. Ther.* 13 (1), 197. doi:10.1186/s13287-022-02859-3

frontiers | Frontiers in Pharmacology

TYPE Original Research
PUBLISHED 17 April 2023
DOI 10.3389/fphar.2023.1129544

OPEN ACCESS

EDITED BY
Hongzhou Cai,
Nanjing Medical University, China

REVIEWED BY
Yan Han,
People's Liberation Army General Hospital, China
Jingping Shi,
Nanjing Medical University, China
Binyu Song,
Fourth Military Medical University, China

*CORRESPONDENCE
Zhexuan Li,
lzxuan11733@163.com

RECEIVED 22 December 2022
ACCEPTED 03 April 2023
PUBLISHED 17 April 2023

CITATION
Sun Y, Lei S, Luo X, Jiang C and Li Z (2023), The value of cuproptosis-related differential genes in guiding prognosis and immune status in patients with skin cutaneous melanoma.
Front. Pharmacol. 14:1129544.
doi: 10.3389/fphar.2023.1129544

The value of cuproptosis-related differential genes in guiding prognosis and immune status in patients with skin cutaneous melanoma

Yuming Sun, Shaorong Lei, Xiangyue Luo, Chufeng Jiang and Zhexuan Li*

Department of Plastic and Cosmetic Surgery, Xiangya Hospital, Central South University, Changsha, Hunan, China

Background: Skin cutaneous melanoma (SKCM) is one of the most common cutaneous malignancies, which incidence is increasing. Cuproptosis is a new type of programming cell death recently reported, which may affect the progression of SKCM.

Method: The mRNA expression data of melanoma were obtained from the Gene Expression Omnibus and the Cancer Genome Atlas databases. We constructed a prognostic model according to the cuproptosis-related differential genes in SKCM. Finally, real-time quantitative PCR was performed to verify the expression of cuproptosis-related differential genes in patients with different stages of cutaneous melanoma.

Results: We detected 767 cuproptosis-related differential genes based on 19 cuproptosis-related genes, and screened out 7 differential genes to construct a prognostic model, which including three high-risk differential genes (SNAI2, RAP1GAP, BCHE), and four low-risk differential genes (JSRP1, HAPLN3, HHEX, ERAP2). Kaplan-Meier analysis indicated that SKCM patients with low-risk differential genes signals had better prognosis. The Encyclopedia of Genomes results manifested that cuproptosis-related differential genes are not only involved in T cell receptor signaling channel, natural killer cell mediated cytotoxicity, but also chemokine signaling pathway and B cell receptor signaling pathway. In our risk scoring model, the receiver operating characteristic (ROC) values of the three-time nodes are 0.669 (1-year), 0.669 (3-year) and 0.685 (5-year), respectively. Moreover, the tumor burden mutational and immunology function, cell stemness characteristics and drug sensitivity have significant differences between low-risk group and high-risk group. The mRNA level of SNAI2, RAP1GAP and BCHE in stage III+IV SKCM patients was significantly higher than that in stage I+II patients, while the level of JSRP1, HAPLN3, HHEX and ERAP2 in stage I+II SKCM patients was more remarkable higher than that in stage III+IV SKCM patients.

Conclusion: In summary, we suggest that cuproptosis can not only regulate the tumor immune microenvironment but also affect the prognosis of SKCM patients, and may offer a basic theory for SKCM patients survival studies and clinical decision-making with potentially therapeutic drugs.

KEYWORDS

cuproptosis, prognostic model, skin cutaneous melanoma, bioinformatics, tumor mutational burden (TMB)

Introduction

Skin cutaneous melanoma (SKCM) is the most frequent, malignant and aggressive cutaneous malignancies, which is the result of genetic alterations caused by complex interactions between genetic, environmental and other factors (Andrzej et al., 2001; Xiong et al., 2022). The global incidence of SKCM is increasing rapidly. According to the International Agency for Research on Cancer (IARC), the number of new cases of SKCM worldwide increased from 287,000 to 324,000 between 2018 and 2020 (Bray et al., 2018; Sung et al., 2021). Although the discovery of new targeted drugs and therapeutic targets has improved the treatment effect of SKCM, the annual number of new deaths due to SKCM has decreased, but the number of new deaths of more than 57,000 is still unacceptable (Lorentzen, 2019; Jenkins and Fisher, 2021; Sung et al., 2021). Melanoma cells pose a therapeutic challenge by exploiting their intrinsic resistance to apoptosis against a variety of chemotherapy agents (Hussein et al., 2003; Soengas and Lowe, 2003). The emergence of biological sequencing analysis technology has found that many biomarkers may be related to melanoma (Gogas et al., 2009). The discovery of new biomarkers and the elucidation of their relationship with melanoma are crucial for the early diagnosis and prognosis evaluation of SKCM.

An appropriate amount of copper is an essential element for human survival, and it is mainly involved in pathways required for normal cell development and metabolism (Huang et al., 2022). The function of important metal binding enzymes will be impaired if copper is too little, while excessive amounts can lead to cell death (Martha and Scott, 2022). Recently, Tsvetkov et al. (2022) reported a new mode of cell death that caused by copper, which distinct from apoptosis, pyroptosis, and ferroptosis. Excess copper leads to aggregation of fatty acylated proteins via direct bond to lapidated ingredients in the tricarboxylic acid (TCA) cycle, resulting in loss of iron-sulfur clusterin, proteotoxic stress and eventually cell death (Tsvetkov et al., 2022). The novel mechanism of cuproptosis proposed by Tsvetkov may provide a new way to exploit the unique effects on this metal to kill cancer cells, especially in cancers that are naturally resistant to apoptosis (Martha and Scott, 2022).

We hypothesized that cuproptosis is closely related to the treatment and prognosis of melanoma. In our research, we first constructed a prognostic model based on the Cancer Genome Atlas (TCGA) database and the Gene Expression Omnibus (GEO) database to analyze the cuproptosis-related differential gene data in SKCM.

Materials and methods

Data collection and preparation

The GSE65904 from the Gene Expression Omnibus (https://www.ncbi.nlm.nih.gov/geo/) database which include 214 specimens of SKCM patients were downloaded. Another RNA sequence transcriptome analysis dataset includes 469 melanoma samples that were obtained from TCGA (https://portal.gdc.cancer.gov/projects/TCGA-SKCM). The age, sex, grade, survival time, survival status, tumor stage and other clinical data of SKCM patients were also obtained from TCGA. Additionally, we acquired 19 genes related to cuproptosis from previous studies, including CDKN2A, NLRP3, ATP7A, ATP7B, MTF1, SLC31A1, GLS, PDHA1, DLD, NFE2L2, DBT, DLAT, PDHB, DLST, LIPT1, LIPT2, LIAS and GCSH (Tsvetkov et al., 2022).

Consensus clustering analysis of cuproptosis-related genes to screen the cuproptosis-related differential genes

Based on the SKCM RNA sequence transcriptome in TCGA and GEO, We used the "ConsensusClusterPlus" package to classify SKCM patients into different clusters base on the consensus expression of cuproptosis-related genes (Wilkerson and Hayes, 2010). The cluster variable (k) was increased from 2 to 9 to find the most appropriate K value, and 683 SKCM patients were divided into appropriate clusters according to the expression similarity of 17 cuproptosis-related genes. Kaplan-Meier (KM) survival analysis was applied to parabole the survival times of patients divided into two clusters of melanomas which the "survival" package. The differential genes related to cuproptosis were identified by comparative analysis of the two clusters. The age, sex, and expression of copper death-related genes in 683 SKCM patients were presented using the "pheatmap" package to visualize differences between clinical parameters and taxonomic clusters.

Pathway enrichment analysis and gene set enrichment analysis

In order to clarify the biological function of cuproptosis-related differential genes in SKCM, Gene ontology (GO) is used to analyze biological functions, while enrichment pathways are achieved through the Encyclopedia of Genomes (KEGG).

Cuproptosis-related differential genes prognostic model construction for SKCM

Consensus clustering analysis of cuproptosis-related differential genes. Then, to construct a cuproptosis-related differential genes risk prognostic model, we performed the least absolute shrinkage and selection operator (LASSO) regression analyses for cuproptosis-related differential genes associated with differential prognosis in SKCM patients. We use the R package "glmnet" to establish (LASSO) Cox regression model, which can screen out potential cuproptosis-related differential genes and create a prognosis model for SKCM patients (Engebretsen and Bohlin, 2019).

Validation of risk models

We divided melanoma patients into two groups according to the cuproptosis score in the model: low-risk group and high-risk group. After comparing the difference of overall survival rate between the two groups, the specificity and sensitivity of the risk model were evaluated by the receiver operating characteristic (ROC) curve. Draw ROC curves of each group for 1-year, 3-year and 5-year, respectively.

Independent predictive analysis of the risk models

Univariate and multivariate Cox regression analysis was performed combining the clinical characteristics of melanoma patients and the risk assessment model of cuproptosis-related differential genes. The result of multivariate Cox analysis $p < 0.05$ would be considered as a special prognostic factor for melanoma prognosis.

Analysis of tumor burden mutational and immunological function based on cuproptosis-related differential genes risk score

The nucleotide mutation data related to melanoma patients were collected from TCGA and GEO database. We used the "limma, pheatmap, ggpubr" packages to construct heatmaps and violin plot, which show the differences level of immune cell infiltration and tumor immune microenvironment. Next, in order to predict the tumor purity in TME, ESTIMATE was used to estimate the stromal cells and immune cells in melanoma tissue (Hou et al., 2022). Get the scores of StromalScore, ImmuneScore and ESTIMATEScore of the melanoma tissue, and analyze different groups (high-risk/low-risk groups)with "Limma" packages. Then, utilize the "maftools" package to divide the tumor mutational burden (TMB) in melanoma samples into low-risk groups and high-risk groups base on the predicted model risk score.

Evaluation of drug sensitivity

IC50 represents the half inhibitory concentration of the tested antagonist. To assess the potential clinical utility of cuproptosis-related differential genes in SKCM treatment. We tested each melanoma patient's response to sensitivity to several chemotherapy drugs using the Cancer Drug sensitivity Genomics (GDSC; https://www.cancerrxgene.org/) database and quantified IC50 with the R's "pRRophetic" package. We performed Wilcoxon symbolic rank test to compare IC50 differences between low-risk and high-risk groups of commonly used antitumor agents. Boxplots were drawn using the R package "ggplot2."

TABLE 1 The primers for 7 cuproptosis-related differential genes.

JSRP1	Forward: 5′ TGTCGCTCAACAAGTGCCTG
	Reverse: 5′
	GCCTGGGCCTCGAACTTAG
HAPLN3	Forward: 5′
	TGCGTGTCAAATGGTGGAAG
	Reverse: 5′
	GTAACGCCCATAGTCCTCCAG
SNAI2	Forward: 5′
	CGAACTGGACACACATACAGTG
	Reverse: 5′
	CTGAGGATCTCTGGTTGTGGT
HHEX	Forward: 5′
	ACGCCCTTTTACATCGAGGAC
	Reverse: 5′
	CGTGTAGTCGTTCACCGTC
RAP1GAP	Forward: 5′
	GCCCACAACCAAGGTGAAG
	Reverse: 5′
	CTGGACAACATTAGGGAACTCG
ERAP2	Forward: 5′
	CCAGAGAAACTTACGCCTCAC
	Reverse: 5′
	GCCTGGGTTGGCTCAAAATC
BCHE	Forward: 5′
	GTCAGAGGGATGAACTTGACAG
	Reverse: 5′
	TGAATCGAAGTCTACCAAGAGGT

Clinical specimens and real-time quantitative PCR

Tumor tissue was obtained from patients diagnosed with SKCM who underwent surgery in our hospital between January 2021 and December 2022. All patients signed informed consent prior to use of clinical specimens. The tumor tissues used in this study were approved by the Ethics Committee of Xiangya Hospital, Central South University. Total tissue RNA was extracted with Trizol (Thermo Fisher Scientific) base on the standard protocol. Next, total RNAs were used to synthesize cDNA with HiScript Q RT SuperMix kit (Vazyme, Nanjing, China). Subsequently, Quantitative PCR analyses were conducted with SYBR Green qPCR Master Mix (Bimake). GAPDH was used as an endogenous control. The primer sequences are listed in Table 1.

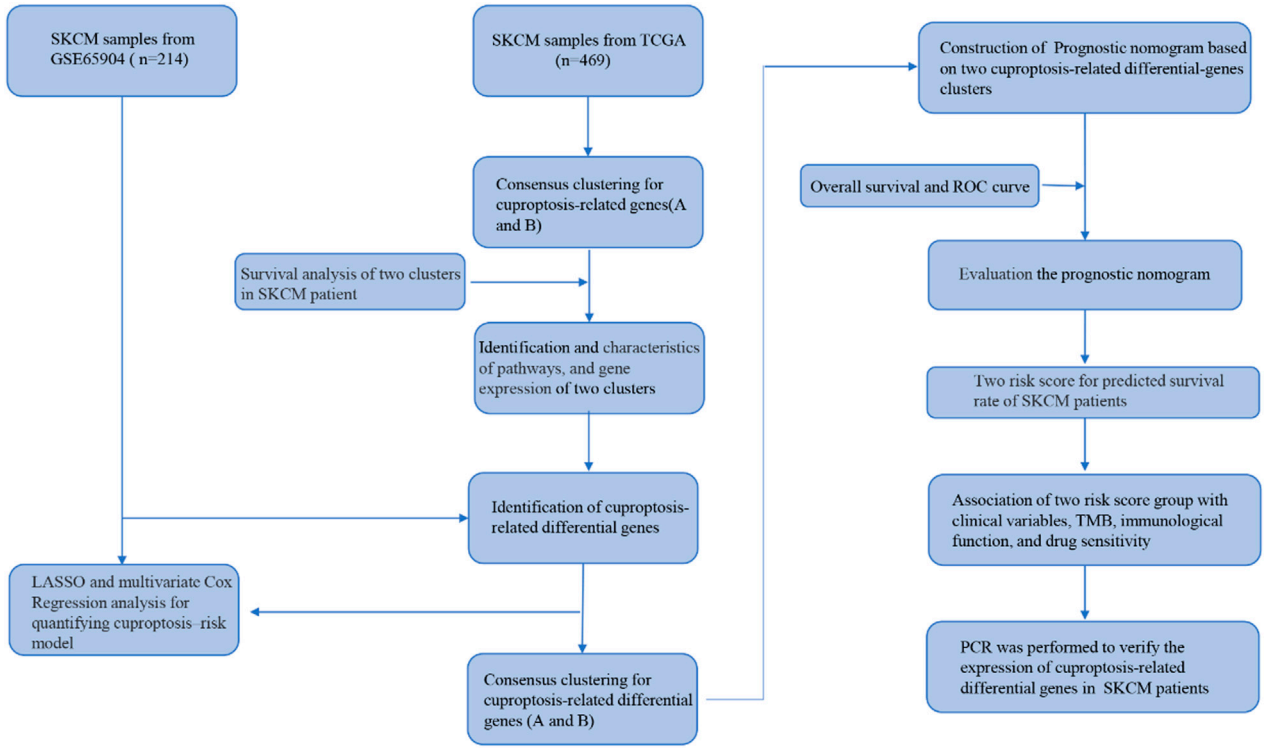

FIGURE 1
A flow chart showing the analysis details.

Statistical analysis

All statistical analyses were performed in R software (version 4.2.1), and values of $p < 0.05$ were considered statistically significant.

Result

The genetic characteristics and transcription changes of cuproptosis-related genes in SKCM

The process of our research is shown in Figure 1. Firstly, based on TCGA database, a total of nineteen cuproptosis-related genes were identified in SKCM transcription group data. The waterfall map showed a mutation of 146 (31.13%) of the 469 SKCM samples. At the same time, the CDKN2A mutation rate was the highest among nineteen cuproptosis-related genes (Figure 2A). Next, we examined the copy number variations (CNV) in these nineteen cuproptosis-related genes and found that the CNV of LIPT2 and NLRP3 increased significantly, while extensive decrease in CNV for DBT, FDX1, CDKN2A, and DLA (Figure 2B). As shown in Figures 2C, D, the position of cuproptosis-related genes in chromosomes. In the survival analysis of the 19 cuproptosis-related genes in melanoma patients, seventeen cuproptosis-related genes have significant differences, while LIPT1 and NLRP3 showed the most significant differences (Supplementary Figure S1). Moreover, we found that LIPT1 and NLRP3 have the strongest correlation with SKCM patient's prognosis through protein-protein interaction (PPI) analysis.

Cuproptosis-related differential genes are identified by consensus clustering

In order to understand the role of cuproptosis in melanoma, we obtained 469 and 214 melanoma patients from TCGA and GEO databases respectively. Then according to the consistency of mRNA expression of cuproptosis-related genes and molecular clustering effects to found the optimal k. We found the k = 2 is the best way to cluster in k = 2 to 9 in OS, and there were significant differences in survival analysis between the two clusters (p = 0.013) (Figures 3A, B). The cuproptosis-related genes between the two clusters showed significant differences in the heatmap (Figure 3C). To assess the signaling pathways associated with cuproptosis-related genes, the functional enrichment of significantly different between the two clusters in KEGG was conducted (Figure 3D). Furthermore, there were significant differences in the relationship between cuproptosis-related genes and immune cells in the two clusters (Supplementary Figure S2).

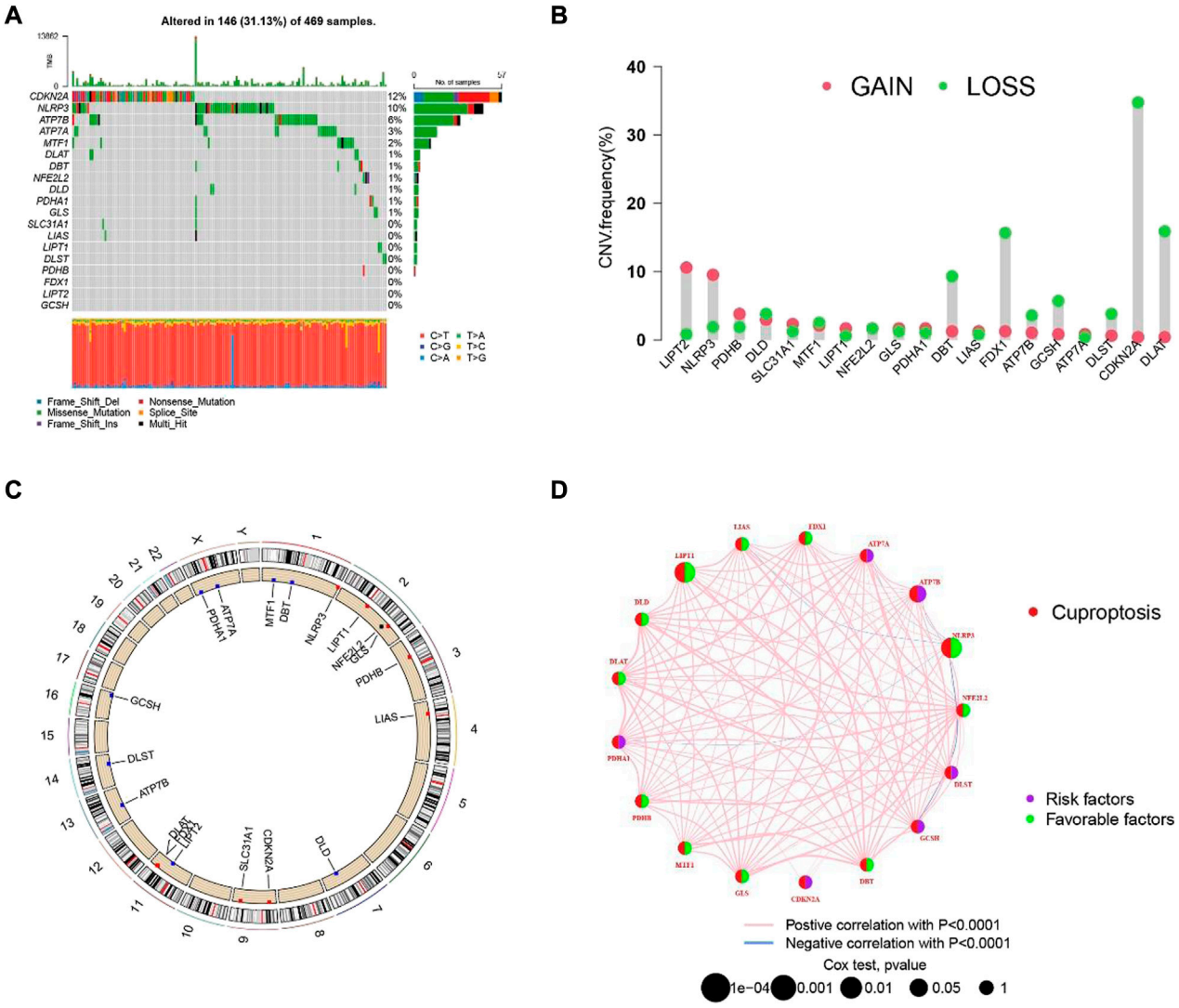

FIGURE 2
The hereditary characteristics and transcription changes of cuproptosis-related genes in melanoma. **(A)** Genetic alteration of cuproptosis-related genes in melanoma. **(B)** Cuproptosis of CNV gain, loss, and non-CNV among cuproptosis-related genes. **(C)** The circus plots show the position of cuproptosis-related genes in chromosomes. **(D)** The PPI network shows the prognosis of cuproptosis-related genes.

Enrichment analysis of cuproptosis-related genes in melanoma

To further understand the downstream reasons, a total of 767 genes was correlated with cuproptosis were identified. Then, we conducted GO and KEGG enrichment analysis for purpose of knowing the potential functions of cuproptosis-related differential genes in SKCM patients. GO analysis shows that the biological process category (BP), the cuproptosis-related differential genes are mainly concentrated in T cell activity, positive regulation of cell, mononuclear cell and leukocyte cell–cell adhesion. From the cell component (CC), we found that these genes were basically involved in the external side of plasma membrane, endocytic vesicle, membrane raft and membrane microdomain. Moreover, In the molecular function (MF) category, they mostly participate in immune regulation and cytokine functions, for instance immune receptor activity and cytokine binding (Figure 4A). In addition, the KEGG results manifested that cuproptosis-related differential genes are mainly involved in T cell receptor signaling pathway, Cytokine–cytokine receptor interaction, chemokine signaling pathway and T cell receptor signaling pathway (Figure 4B).

Construction of a cuproptosis-related differential genes risk prognostic model

According to the consistency of mRNA expression of cuproptosis-related differential genes, Consensus Cluster Plus package was used to consensus clustering analysis. The best stability cluster was K = 2 which was chosen to consensus cluster (Figure 5A). The survival rate between the two clusters

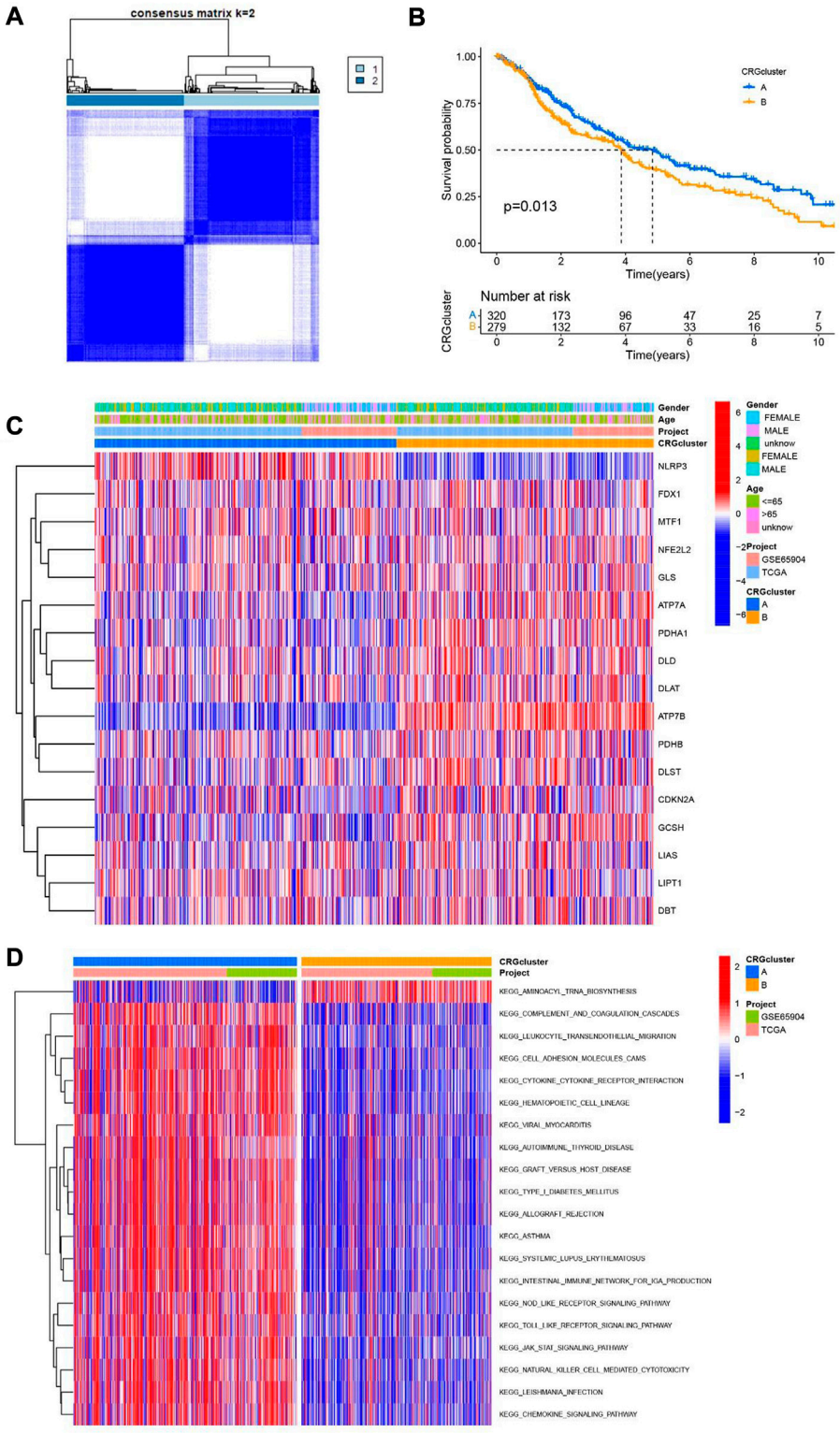

FIGURE 3
Two clusters of cuproptosis-related genes. **(A)** The Consensus matrix heatmap defined two clusters based on the consistency of cuproptosis-related genes expression (K = 2). **(B)** Compare the survival time of two clusters through KM survival analysis. **(C)** Different expression of the two clusters of cuproptosis-related genes clusters. **(D)** KEGG analysis of two clusters of cuproptosis-related genes.

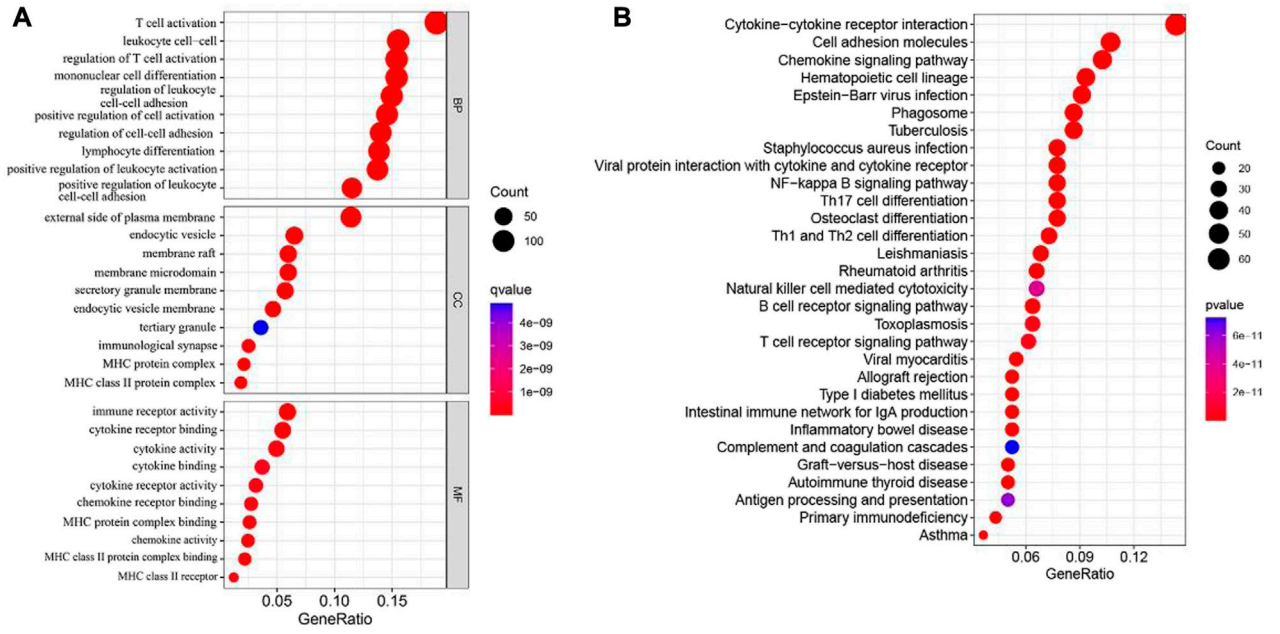

FIGURE 4
GO and KEGG analyses for cuproptosis-related differential genes in melanoma. **(A)** GO analysis. **(B)** KEGG analysis.

showed significant difference in Kaplan Meier curve ($p < 0.001$) (Figure 5B). The heatmap shows that the clinical pathological characteristics between the two clusters are significantly different. Compared with cluster B, most of cuproptosis-related differential genes were higher in cluster A (Figure 5C).

Then, the LASSO algorithm builds a prognostic model based on melanoma patients based on 7 cuproptosis-related differential genes (Figure 6A, Supplementary Figure S3). The Sankey plot shows the distribution of the cuproptosis subgroups, two gene clusters, cuproptosis score, and the survival status of melanoma patients (Figure 6B). Moreover, we also found that the scores of cuproptosis clusters and gene clusters were significantly different ($p < 0.001$) (Figures 6C, D). Finally, the correlation between seven cuproptosis-related differential genes and 17 cuproptosis-related genes was shown in the nomogram (Figure 6E).

Prognostic evaluation of cuproptosis-related differential genes nomogram in SKCM patients

We calculated a risk score for every SKCM patient sample according to the previously obtained model of seven differential genes associated with cuproptosis. Patients are then classified as low risk (risk score below the median risk score) and high risk (risk score above the median risk score) (Figure 7A). It can be observed from the scatter plot of the risk score distribution that with the increase of the risk score, the mortality of the high-risk group also increases, while fewer deaths occur in the low-risk group (Figure 7B). The expression of 7 cuproptosis-related differential genes signals in SKCM was consistent among training group, test group and the all-samples group (Figure 7C). To assess the prognostic prediction of our model for OS status in SKCM patients, we performed K-M survival curve plotting, which showed that the high-risk group had significantly lower OS than the low-risk group in both the training and testing groups (including all samples) ($p < 0.001$; Figure 7D). The ROC curve analysis was performed to assess the accuracy of the prediction model, and the AUC values of the ROC curves of all samples were 0.669(1 year), 0.669(3 years), and 0.685 (5 years), respectively, which were consistent with the results of training group and test group (Figure 7E). These results suggest that these seven genes are associated with cuproptosis and that this model can predict prognosis in SKCM patients.

Evaluation of the clinical utility of cuproptosis-related differential genes nomogram

In order to predict the clinical outcomes in patients of SKCM, a nomogram plot was used to perform quantitavive analysis. As shown in Figure 8A, the calculated risk score increased, the predicted survival rate of SKCM patients decreased. Cuproptosis-related differential genes prognosis model, which is to exert a positive effect in the clinical diagnosis and treatment in SKCM, based on this, to assess the clinical potential applications of this model, we developed a risk score and SKCM patients' clinical characteristics of nomograph, for which to predict the SKCM patients' 1 year, 3 years and

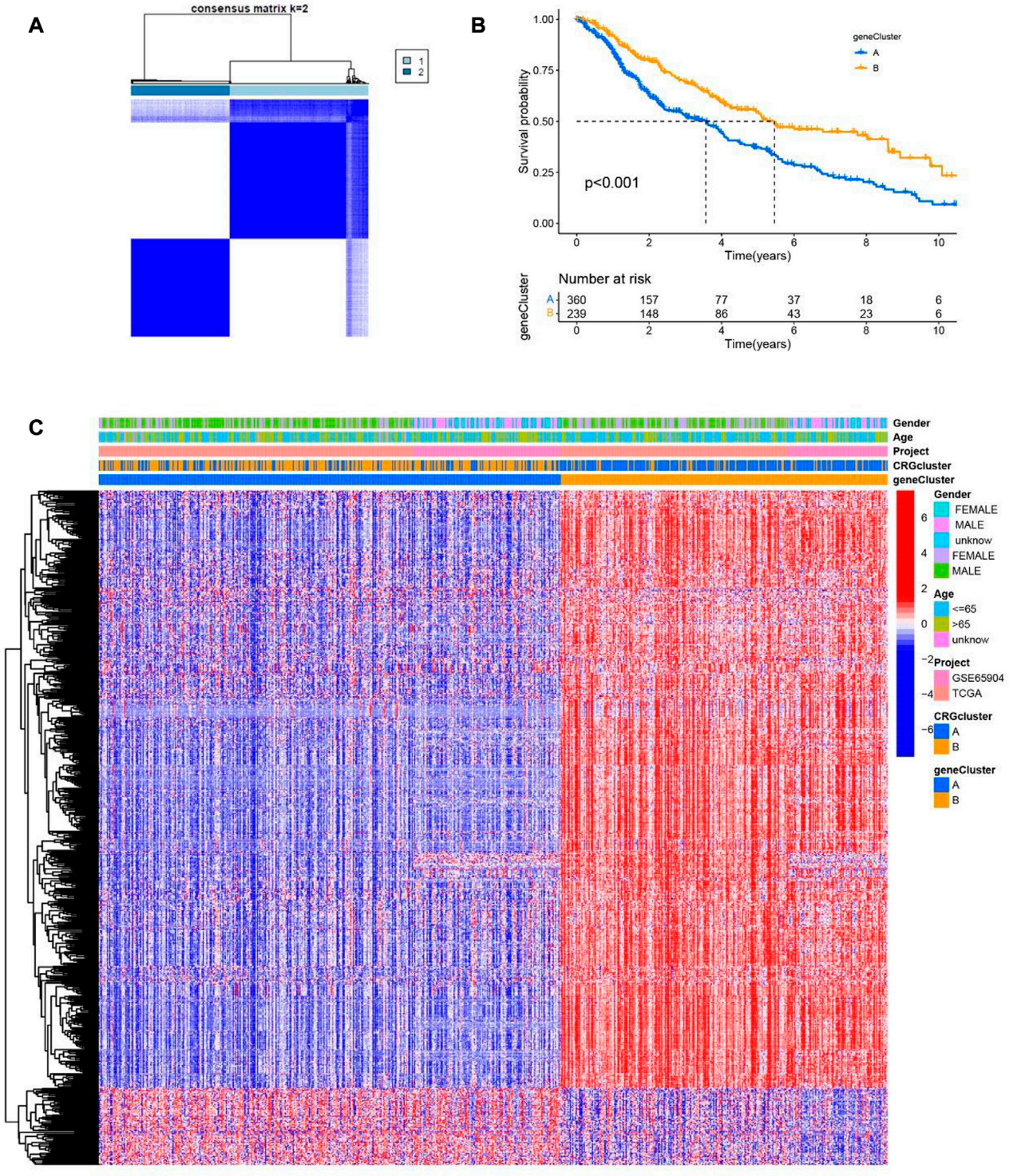

FIGURE 5
Two clusters of cuproptosis-related differential genes. **(A)** The Consensus matrix heatmap defined two clusters based on the consistency of cuproptosis-related differential genes expression (K = 2). **(B)** Compare the survival time of two clusters through KM survival analysis. **(C)** The clinical and pathological information of two cuproptosis-related differential genes clusters are shown in the heatmap.

5 years OS rates. Furthermore, calibration curves were constructed to assess whether he actual observed OS rates were consistent with the nomogram-predicted OS rates. The results showed that 1-, 3-, and 5-year OS predictions between the actual observation group (all samples), training group, and test group were relatively good (Figures 8B–D).

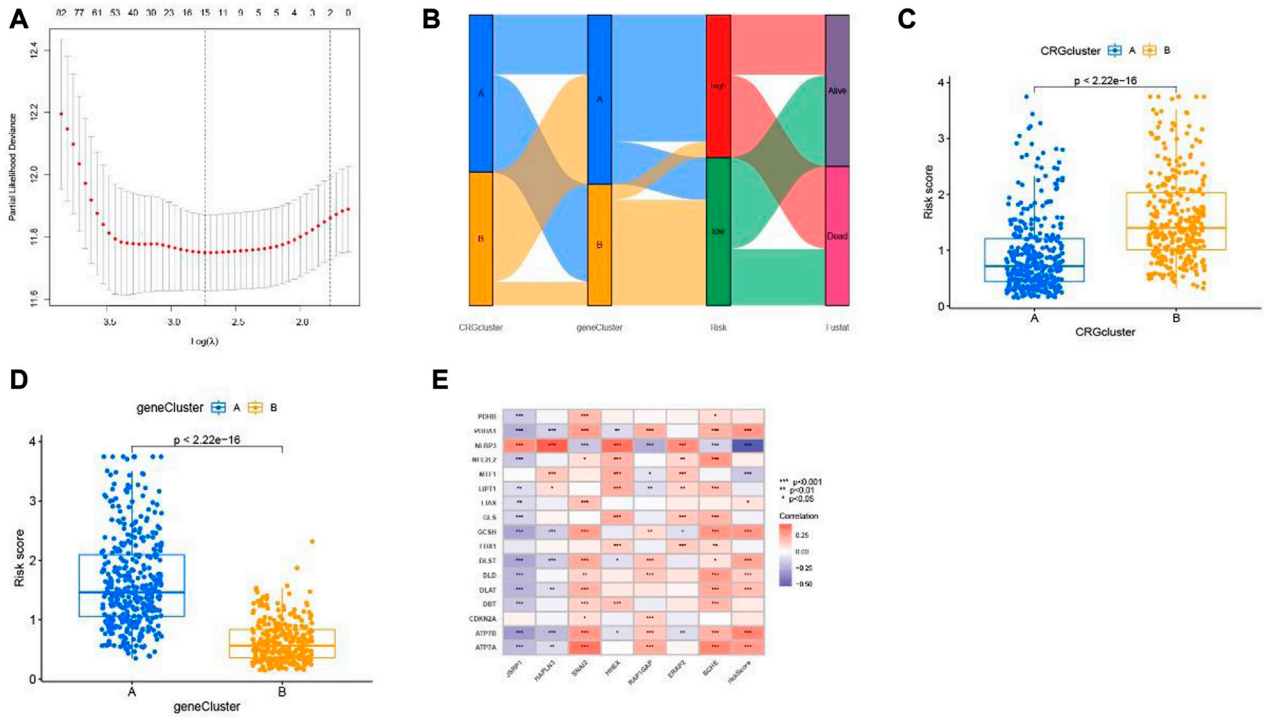

FIGURE 6
Cuproptosis-related differential genes risk prognostic model. **(A)** LASSO Cox regression analysis showed cuproptosis-related differential genes. **(B)** Sankey plot of two risk group anlysis. **(C)** two cuproptosis subtypes and **(D)** two gene clusters. **(E)** Association between cuproptosis-related genes and seven cuproptosis-related differential genes constructed the nomogram.

Tumor burden mutational study and immunological function based on cuproptosis-related differential genes in SKCM samples

Primarily, according to the transcriptional information of melanoma obtained from TCGA and GEO, calculated the tumor mutation burden index of genes low-risk group and in high-risk group respectively. The with the top 20 genes with highest mutation frequency in the low and high-risk group are described in the waterfall diagram. In the high-risk group (Figure 9A), 193 of the 215 samples found mutations; in the other group (Figure 9B), 226 mutations occurred in 241 samples. Among the mutated genes, MUC16, DNAH5, PCLO, TTN, LRP1B, BRAF, ADGRV1, CSMD1, ANK3, DNAH7, PKHD1L1, RP1, MGAM, XIRP2, FAT4, HYDIN, APOB, DSCAM, FLG and USH2A occurred simultaneously between the low- and high-risk groups. TTN, MUC16 and BRAF had the highest mutation frequencies in the two groups, and the mutation frequencies were77%, 71% and 54% in the low-risk group and 66%, 60% and 45% in the high-risk group, respectively. The boxplot showed that the mutation of tumor load was significantly lower in patients with high scores than in patients with low scores (p = 0.019, Figure 9C). We use the Pearson related analysis to confirm the correlation between Risk Score and Tumor Burden Mutational in melanoma patients, and verify the negative correlation between risk score and Tumor Burden Mutational (p = 0.036, R = −0.098, Figure 9D). Next, we explored the correlation between the seven cuproptosis-related differential genes included in the model and immune cells, it was observed that the expression of seven cuproptosis-related differential genes was strongly related to CD8+T cells, T cells CD4 memory activated, Macrophages M0-2. Especially in the expressions of JSRP1 and HAPLN3 are more closely related to immune function (Figure 9E). Then, the Matrix scores, immune scores, and ESTIMATE scores in SKCM samples were evaluated through ESTIMATE methods, and the scores between different groups were compared. We found that the high -risk group was lower than the low -risk group, with significant differences (Figure 9F). Furthermore, we analyzed the relationship between risk score and stemness characteristics in SKCM, and determined that risk score is positively correlated with stemness characteristics (p < 0.001, R = 0.28, Figure 9G).

Drug sensitivity

To explore the possible application of cuproptosis-related differential genes in individualized therapy of SKCM, we explored the connection between IC50 and risk score of drugs in SKCM therapy. Drug sensitivity analysis showed that bryostatin.1, docetaxel, elesclomol, imatinib, sorafenib and thapsigargin were more sensitive in the high-risk group. However, bleomycin, bosutinib, camptothecin, gefitinib, gemcitabine, lenalidomide, metformin, methotrexate, mitomycin. C, nilotinib, rapamycin,

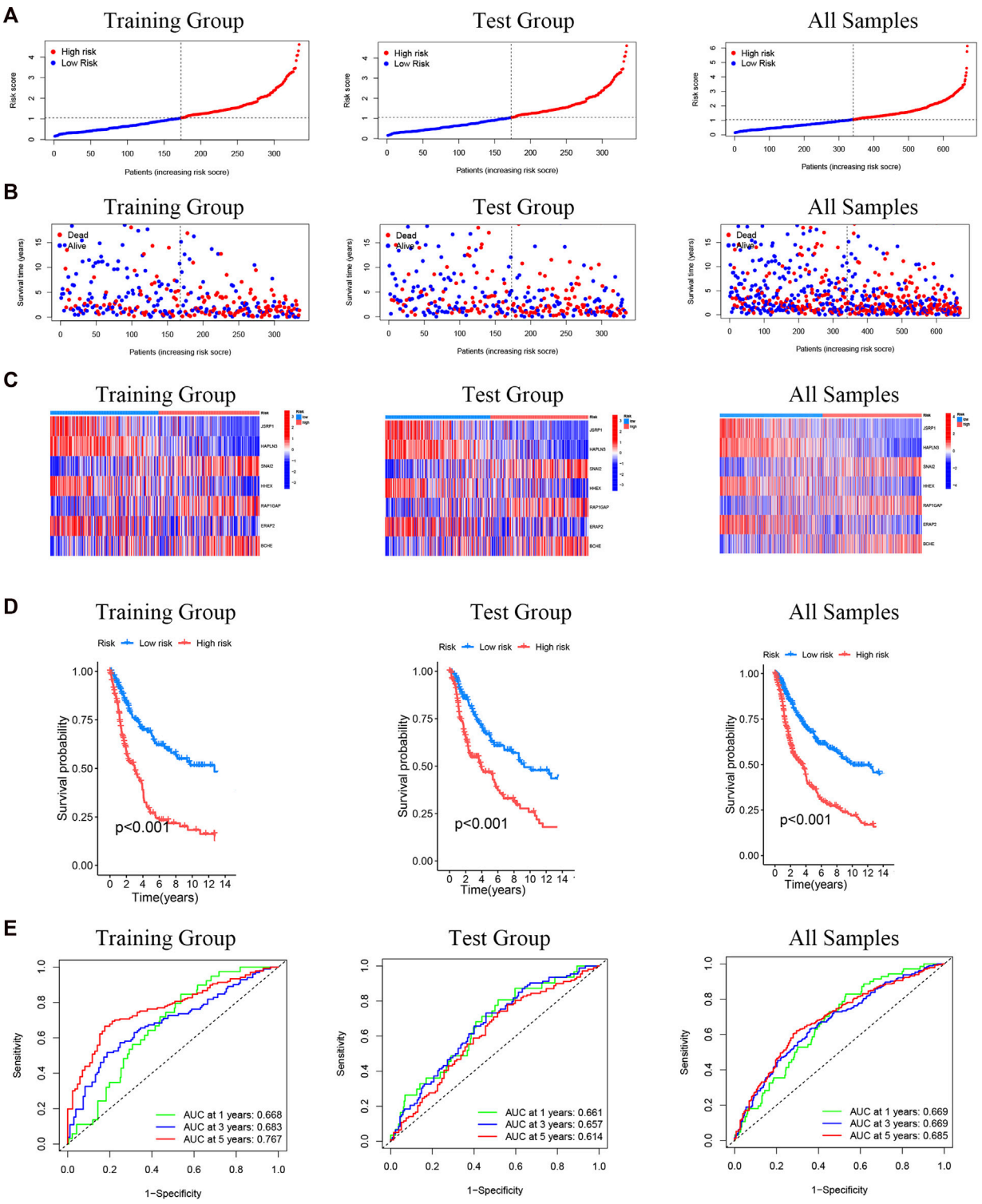

FIGURE 7
Prognostic evaluation of cuproptosis-related differential genes nomogram in melanoma patients. **(A)** Risk score distribution of two risk groups. **(B)** The scatter chart shows the distribution of OS and different risk groups. **(C)** The expression of the seven cuproptosis-related differential genes in the risk model. **(D)** K-M survival curve of melanoma patients in different risk scoring groups. **(E)** ROC curves for training group and test group (including all samples).

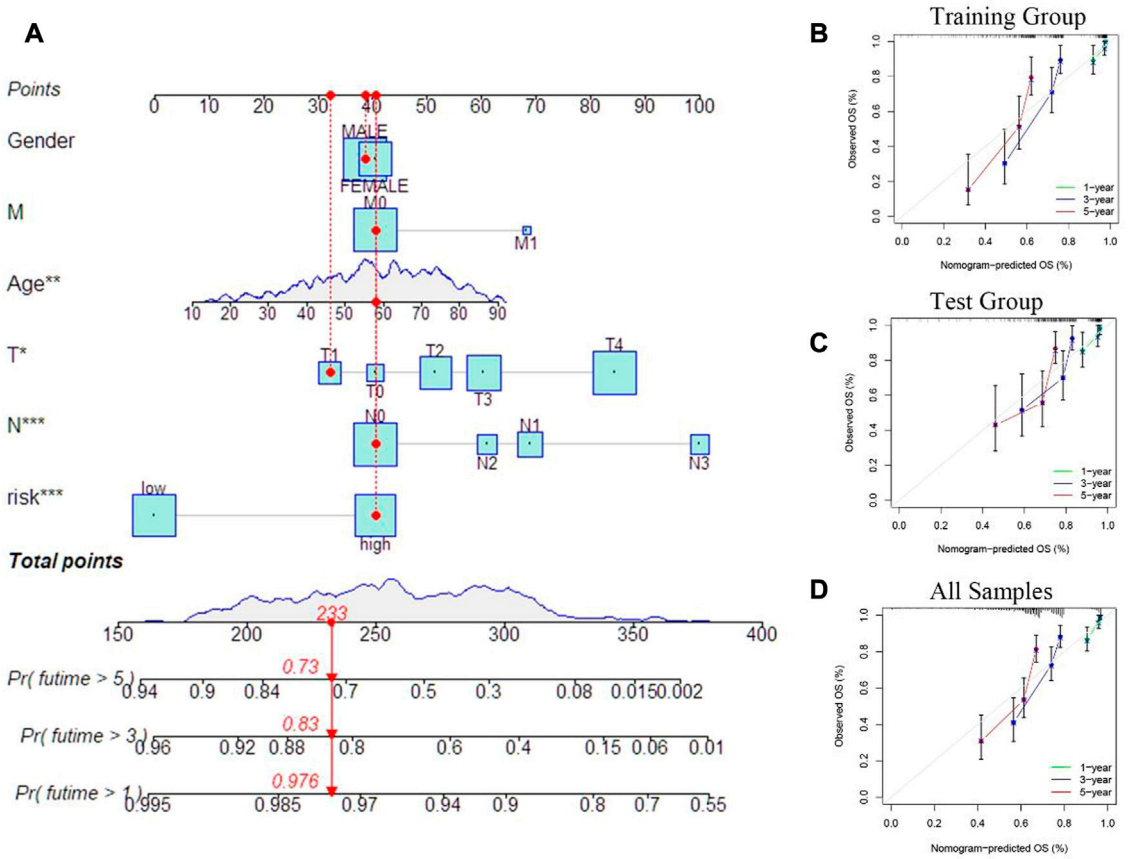

FIGURE 8
Prognostic model evaluation. **(A)** Nomogram with risk score and clinical characteristics of melanoma patients. **(B–D)** Calibration curves show the difference between the 1 -, 3 -, and 5-year operating systems predicted by the training and test groups (including all samples) and the actual operating systems.

vinblastine and vorinostat were more sensitive in the low-risk group (Figure 10).

Verification of expression of the seven cuproptosis-related differential genes

To ulteriorly Validate the expression levels of the seven cuproptosis-related differential genes, we collected specimens from 11 patients with stage I+II melanoma and 9 patients with stage III+IV melanoma. The mRNA expression level of SNAI2, RAP1GAP and BCHE in stage I+II SKCM was strikingly lower than that in stage III+IV SKCM ($p < 0.05$), while the expression of JSRP1, HAPLN3, HHEX and ERAP2 in stage I+II SKCM patients was significantly higher than stablished ($p < 0.05$) (Figure 11).

Discussion

SKCM is one of the deadliest malignancies and prone to metastasis. Although chemotherapy, immunotherapy and molecular therapy are available, the prognosis for SKCM patients remains poor, with a very short median survival time (Donizy et al., 2022; Voglis et al., 2022; Zhang et al., 2022). Although there are a variety of clinical tools to predict the prognosis of patients with SKCM (Weiss et al., 2015), in view of the clinical and biological heterogeneity of primary SKCM, new methods or models that more accurately predict the prognosis of patients with SKCM are still needed. To promote the programmed death of melanoma cells has been the direction of clinicians' efforts. Promoting ferroptosis in melanoma can enhance the sensitivity of melanoma to PD-1 (Guo et al., 2022). Ferroptosis is defined as an iron-dependent and unrestricted form of cell death featured with lipid peroxidation (Dixon Scott et al., 2012). Startlingly, Tsvetkov et al. (2022) recently proposed that copper induces cell death by targeting lipidated TCA cycling proteins, called cuproptosis, which as a novel regulated cell death distinct from apoptosis, necroptosis and ferroptosis (Tang et al., 2022). We conclude that cuproptosis-related genes play a crucial part in the development and prognosis of SKCM.

In our study, we detailedly analyzed the expression of cuproptosis-related differential genes in SKCM and verified them in different stages of SKCM. Their predictive significance in SKCM and their correlation with tumor mutation load and immune function were also analyzed. Firstly, the RNA

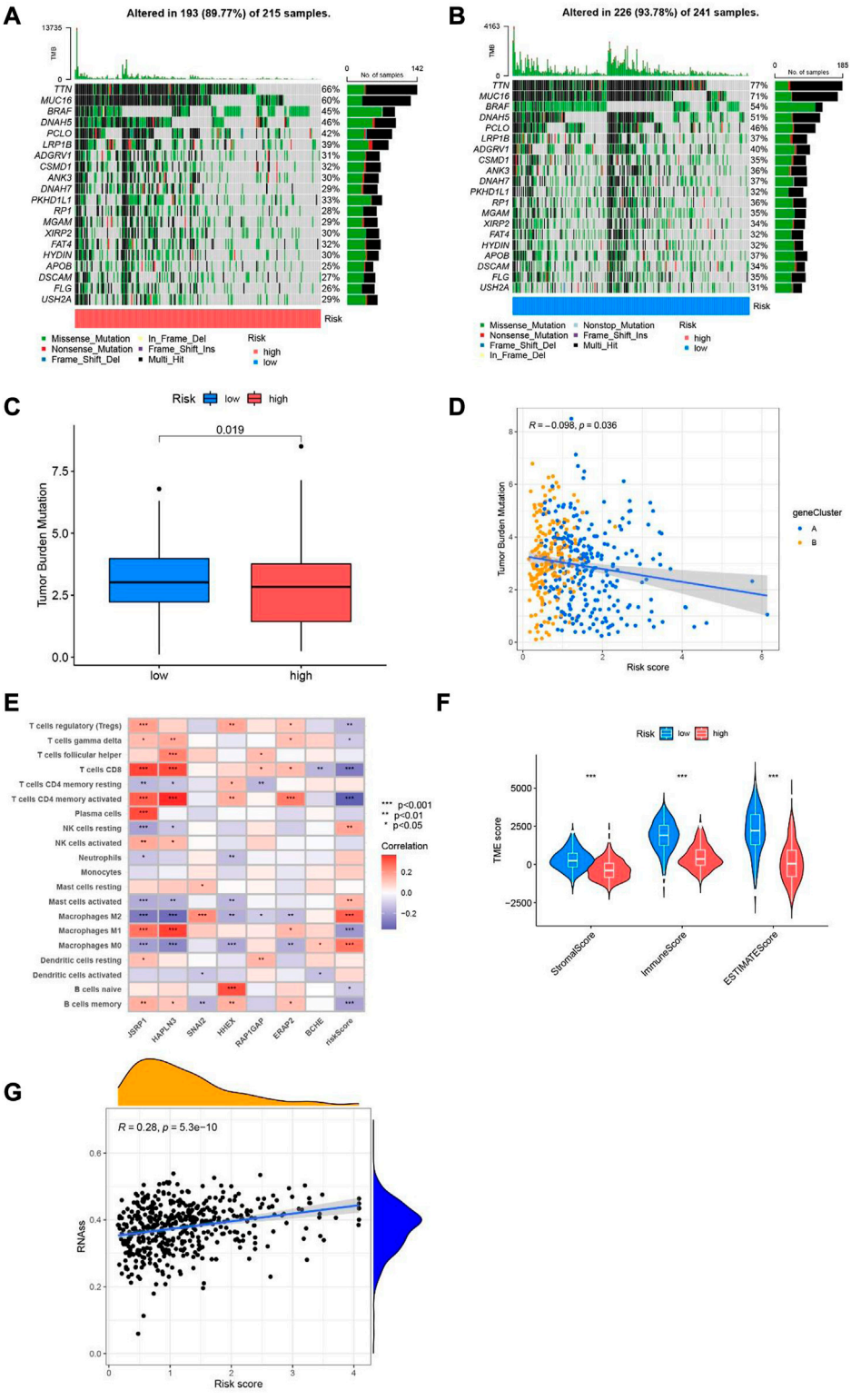

FIGURE 9
Tumor mutation load and immune function in different risk population. **(A)** Waterfall plot of mutant genes in the high-risk group. **(B)** Waterfall plot of mutant genes in the low-risk group. **(C)** boxplot depict the tumor mutational burden of melanoma patients in the two groups. **(D)** The correlation analysis of risk score and tumor burden mutational in melanoma. **(E)** Heatmap of the association of 7 cuproptosis-related differential genes with immune cells. **(F)** Violin diagram of StromalScore, ImmuneScore and ESTIMATEScore compared between low-risk group and high-risk group. **(G)** Relevance analysis between risk score and stemness characteristics.

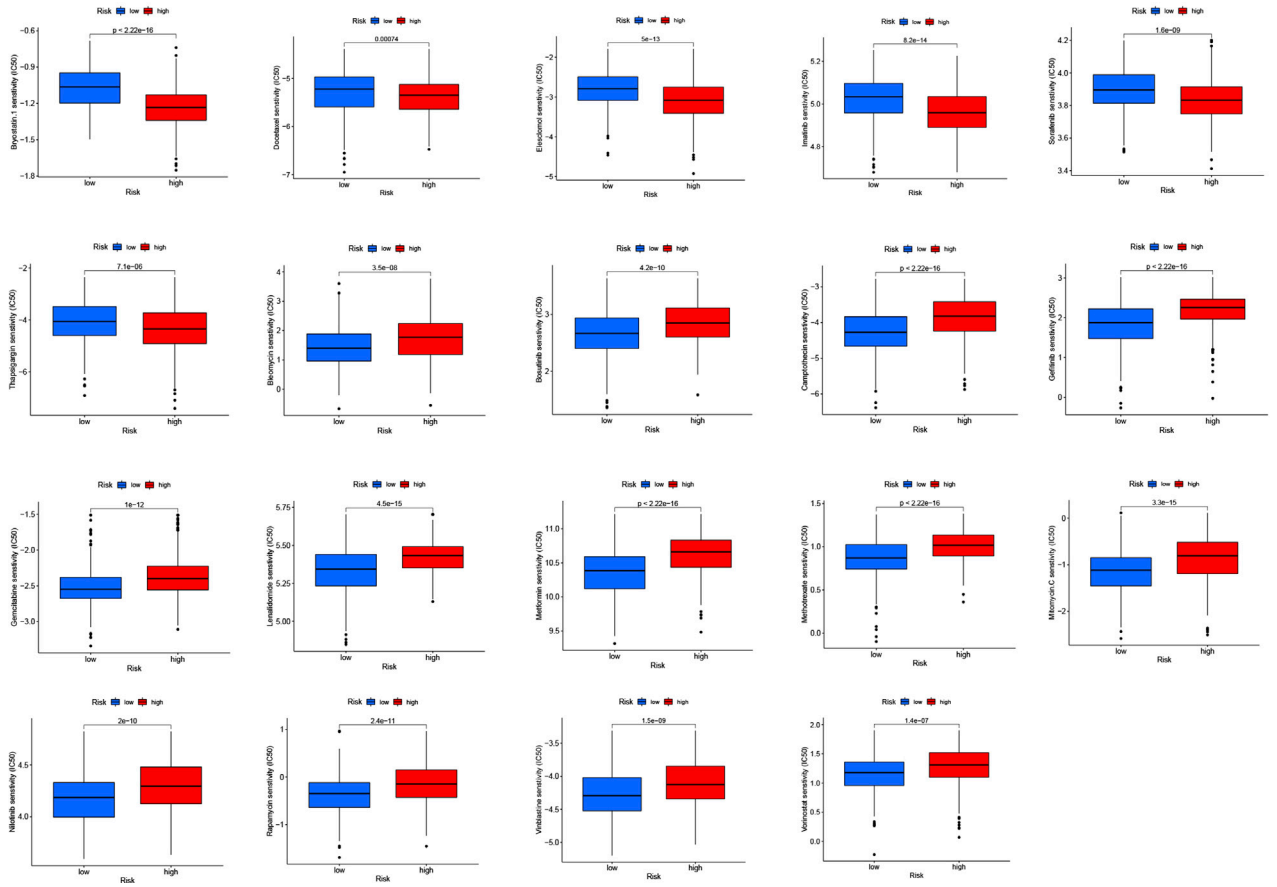

FIGURE 10
Drug susceptibility (IC50) was associated with two risk groups for melanoma.

transcription group data of 469 patients with SKCM was extracted from the TCGA database, and 17 cuproptosis-related genes were selected according to survival analysis of 19 cuproptosis-related genes. Next, RNA transcriptome data for 683 SKCM patients were obtained from GEO and TCGA databases, and 767 cuproptosis-related differential genes related to prognosis of cuproptosis were identified. GO analysis showed that T cell activity, immune receptor activity and external side of plasma membrane were enhanced significantly. Through KEGG pathway analysis, we found that T cell receptor signaling pathway, chemokine signaling pathway, cytokine-cytokine receptor interaction, natural killer cell-mediated cytotoxicity, T cell receptor signaling pathway, B cell receptor signaling pathway and other functions were significantly enhanced. T cell activation is a critical incident both in antiviral and antitumor adaptive immunity (Wang et al., 2022). However, malignant melanoma belongs to the most immunogenic tumor, which can evade T cell recognition by down-regulating tumor associated antigens, defects in antigen processing mechanism, and downregulation of MHC molecules caused by β2-microglobulin mutation, leading to immune evasion (Marzagalli et al., 2019). Moreover, melanoma cells secrete cytokines and chemokines through overactivation of the NF-κB signaling pathway to impede the T-cell targeting of tumor cells (Ellis and Hicklin, 2008; Umansky and Sevko, 2012). NK cells are an important part of initial immunity, which can remove senescent cells and pathogenic microorganisms (Mehta et al., 2018). NK cells are not only more cytotoxic to tumor cells that downregulate MHC expression to evade acquired immunity, but also can directly exert antitumor effects by mobilizing dendritic cells and macrophages and other immune cells or secreting cytokines (Myers and Miller, 2021). At present, new targets and candidate drugs for SKCM immunotherapy are emerging constantly, but most of them are in the early stage, and some of them have unsatisfactory efficacy as monotherapy (Wang et al., 2022). Cuproptosis may play an crucial role in the metastasis and immune escape of melanoma, which could be a new potential target for the therapy of SKCM in the future.

Next, Lasso regression and multi-variable COX regression of 767 cuproptosis-related differential genes were screened out of 7 different differential genes related to cuproptosis. The connection between 7 differential genes and cuproptosis-related genes was verified by relevant analysis. SNAI2 has been implicated in the diseases of melanocytes development and a variety of cancers (Cobaleda et al., 2007). SNAI2 plays a crucial role in regulating T-cell lineages (Pioli et al., 2016) and cancer cell stemness (Chen et al., 2021; Peng et al., 2022), as well as

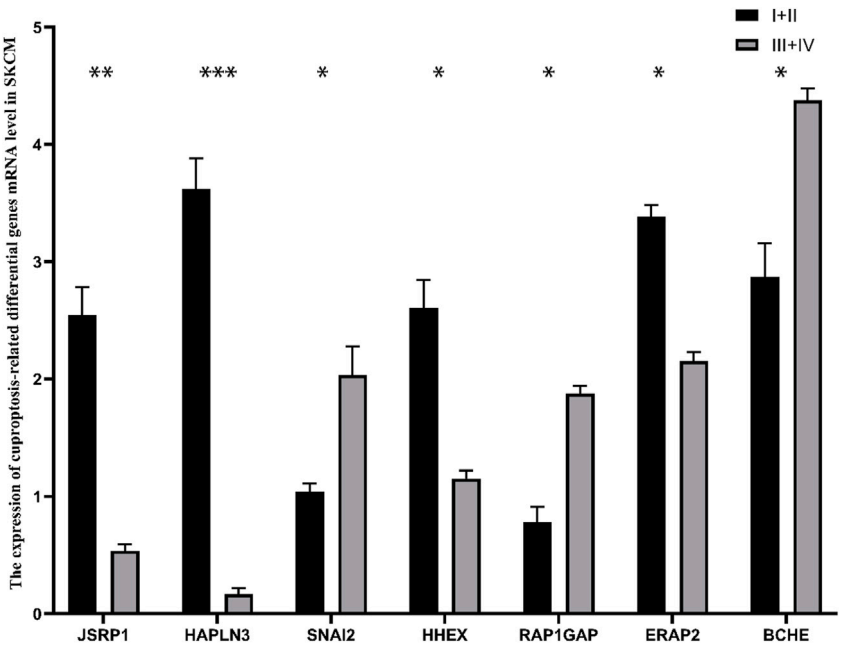

FIGURE 11
The mRNA expression of 7 cuproptosis-related differential genes in patients with different stages of cutaneous melanoma. *$p < 0.05$, **$p < 0.01$, ***$p < 0.001$.

modulating lapatinib resistance in HER2-positive breast cancer (Hamalian et al., 2021) and enhancing 5-fluorouracil sensitivity in colorectal cancer (Findlay et al., 2014). We developed a risk-scoring model for SKCM patients according to seven cuproptosis-related differential genes, using a training set to distinguish between low -risk and high -risk groups. The survival rate of patients in the low-risk group was significantly higher than that in the high-risk group, which was consistent among the training group, test group and all samples group. Importantly, in our risk scoring model, 0.669, 0.669 and 0.685 are ROC values of 1 year, 3 years and 5 years respectively. Indicating that the scoring model can accurately predict the long-term survival outcome of melanoma patients. In addition, we also studied the correlation for the two groups with immune cells, and found that T cells and macrophages were mainly related. This is also consistent with our functional enrichment analysis. Finally, according to the drug sensitivity analysis, we screened 19 drugs with different sensitivities in the two risk groups, which may provide guidance for the treatment of melanoma. Song et al. (2022a), Song et al. (2022b) utilized coagulation and apoptosis related genes to better predict the prognosis and tumor microenvironment of cutaneous melanoma. Although the recent researches on the model of cuproptosis predicting the prognosis of melanoma has shown a good prediction effect, it has not been verified *in vivo* or *in vitro*, and the true prediction effect of the model is still uncertain (Liu et al., 2022; Zhou et al., 2022). We further demonstrated the accuracy and reliability of our model by verifying the expression of seven cuproptosis-related differential genes in different stages cutaneous melanoma patients.

Cuproptosis is a new type of cell death, which may be a breakthrough point for SKCM treatment. However, the research has some limitations. First, the mechanism of cuproptosis in SKCM has not been resolved. In addition, the accurate mechanism between cuproptosis and immune cell infiltration is unclear. Second, the data of our prognosis model comes from the public database, and the lack of additional *in vivo* validation data. Therefore, further basic research and clinical research need to be explored.

Conclusion

In conclusion, we suggest that cuproptosis can not only regulate the tumor immune microenvironment but also affect the prognosis of SKCM patients, and may offer a basic theory for SKCM patients survival studies and clinical decision-making with potentially therapeutic drugs.

Data availability statement

The datasets presented in this study can be found in online repositories. The names of the repository/repositories and accession number(s) can be found in the article/Supplementary Material.

Ethics statement

The studies involving human participants were reviewed and approved by The Ethics Committee of Xiangya Hospital, Central South University. The patients/participants provided their written informed consent to participate in this study.

Author contributions

YS, SL, CJ, and XL participated in performing the research and data analysis. ZL contributed to the research design, writing, and revising of the manuscript. YS, SL, and XL participated in research design and data analysis. All authors read and approved the final manuscript.

Conflict of interest

The authors declare that the research was conducted in the absence of any commercial or financial relationships that could be construed as a potential conflict of interest.

Publisher's note

Supplementary material

The Supplementary Material for this article can be found online at: https://www.frontiersin.org/articles/10.3389/fphar.2023.1129544/full#supplementary-material

References

Andrzej, S., Jacobo, W., Andrew, J. C., Matsuoka, L. Y., Balch, C. M., and Mihm, M. C. (2001). Malignant melanoma. *Arch. Pathol. Lab. Med.* 125 (10), 1295–1306. doi:10.5858/2001-125-1295-mm

Bray, F., Ferlay, J., Soerjomataram, I., Siegel, R. L., Torre, L. A., and Jemal, A. (2018). Global cancer statistics 2018: GLOBOCAN estimates of incidence and mortality worldwide for 36 cancers in 185 countries. *CA Cancer J. Clin.* 68 (6), 394–424. doi:10.3322/caac.21492

Chen, Y., Liang, W., Liu, K., and Shang, Z. (2021). FOXD1 promotes EMT and cell stemness of oral squamous cell carcinoma by transcriptional activation of SNAI2. *Cell. Biosci.* 11 (1), 154. doi:10.1186/s13578-021-00671-9

Cobaleda, C., Perez-Caro, M., Vicente-Duenas, C., and Sanchez-Garcia, I. (2007). Function of the zinc-finger transcription factor SNAI2 in cancer and development. *Annu. Rev. Genet.* 41, 41–61. doi:10.1146/annurev.genet.41.110306.130146

Dixon Scott, J., Lemberg Kathryn, M., Lamprecht Michael, R., Skouta, R., Zaitsev Eleina, M., Gleason Caroline, E., et al. (2012). Ferroptosis: An iron-dependent form of nonapoptotic cell death. *Cell.* 149 (5), 1060–1072. doi:10.1016/j.cell.2012.03.042

Donizy, P., Krzyzinski, M., Markiewicz, A., Karpinski, P., Kotowski, K., Kowalik, A., et al. (2022). Machine learning models demonstrate that clinicopathologic variables are comparable to gene expression prognostic signature in predicting survival in uveal melanoma. *Eur. J. Cancer* 174, 251–260. doi:10.1016/j.ejca.2022.07.031

Ellis, L. M., and Hicklin, D. J. (2008). VEGF-Targeted therapy: Mechanisms of anti-tumour activity. *Nat. Rev. Cancer* 8 (8), 579–591. doi:10.1038/nrc2403

Engebretsen, S., and Bohlin, J. (2019). Statistical predictions with glmnet. *Clin. Epigenetics* 11 (1), 123. doi:10.1186/s13148-019-0730-1

Findlay, V. J., Wang, C., Nogueira, L. M., Hurst, K., Quirk, D., Ethier, S. P., et al. (2014). Camp ER: SNAI2 modulates colorectal cancer 5-fluorouracil sensitivity through miR145 repression. *Mol. Cancer Ther.* 13 (11), 2713–2726. doi:10.1158/1535-7163.MCT-14-0207

Gogas, H., Eggermont, A. M., Hauschild, A., Hersey, P., Mohr, P., Schadendorf, D., et al. (2009). Biomarkers in melanoma. *Ann. Oncol.* 20 (6), vi8–13. doi:10.1093/annonc/mdp251

Guo, W., Wu, Z., Chen, J., Guo, S., You, W., Wang, S., et al. (2022). Nanoparticle delivery of miR-21-3p sensitizes melanoma to anti-PD-1 immunotherapy by promoting ferroptosis. *J. Immunother. Cancer* 10 (6), e004381. doi:10.1136/jitc-2021-004381

Hamalian, S., Guth, R., Runa, F., Sanchez, F., Vickers, E., Agajanian, M., et al. (2021). A SNAI2-PEAK1-INHBA stromal axis drives progression and lapatinib resistance in HER2-positive breast cancer by supporting subpopulations of tumor cells positive for antiapoptotic and stress signaling markers. *Oncogene* 40 (33), 5224–5235. doi:10.1038/s41388-021-01906-2

Hou, D., Tan, J. N., Zhou, S. N., Yang, X., Zhang, Z. H., Zhong, G. Y., et al. (2022). A novel prognostic signature based on cuproptosis-related lncRNA mining in colorectal cancer. *Front. Genet.* 13, 969845. doi:10.3389/fgene.2022.969845

Huang, X., Zhou, S., Toth, J., and Hajdu, A. (2022). Cuproptosis-related gene index: A predictor for pancreatic cancer prognosis, immunotherapy efficacy, and chemosensitivity. *Front. Immunol.* 13, 978865. doi:10.3389/fimmu.2022.978865

Hussein, M. R., Haemel, A. K., and Wood, G. S. (2003). Apoptosis and melanoma: Molecular mechanisms. *J. Pathol.* 199 (3), 275–288. doi:10.1002/path.1300

Jenkins, R. W., and Fisher, D. E. (2021). Treatment of advanced melanoma in 2020 and beyond. *J. Invest. Dermatol* 141 (1), 23–31. doi:10.1016/j.jid.2020.03.943

Liu, J. Y., Liu, L. P., Li, Z., Luo, Y. W., and Liang, F. (2022). The role of cuproptosis-related gene in the classification and prognosis of melanoma. *Front. Immunol.* 13, 986214. doi:10.3389/fimmu.2022.986214

Lorentzen, H. F. (2019). Targeted therapy for malignant melanoma. *Curr. Opin. Pharmacol.* 46, 116–121. doi:10.1016/j.coph.2019.05.010

Martha, A. K., and Scott, J. D. (2022). Copper-induced cell death. *Science* 18 (6586), 1231–1232.

Marzagalli, M., Ebelt, N. D., and Manuel, E. R. (2019). Unraveling the crosstalk between melanoma and immune cells in the tumor microenvironment. *Semin. Cancer Biol.* 59, 236–250. doi:10.1016/j.semcancer.2019.08.002

Mehta, R. S., Randolph, B., Daher, M., and Rezvani, K. (2018). NK cell therapy for hematologic malignancies. *Int. J. Hematol.* 107 (3), 262–270. doi:10.1007/s12185-018-2407-5

Myers, J. A., and Miller, J. S. (2021). Exploring the NK cell platform for cancer immunotherapy. *Nat. Rev. Clin. Oncol.* 18 (2), 85–100. doi:10.1038/s41571-020-0426-7

Peng, L., Fu, J., Chen, Y., Ming, Y., He, H., Zeng, S., et al. (2022). Transcription factor SNAI2 exerts pro-tumorigenic effects on glioma stem cells via PHLPP2-mediated Akt pathway. *Cell. Death Dis.* 13 (6), 516. doi:10.1038/s41419-021-04481-2

Pioli, P. D., Whiteside, S. K., Weis, J. J., and Weis, J. H. (2016). Snai2 and Snai3 transcriptionally regulate cellular fitness and functionality of T cell lineages through distinct gene programs. *Immunobiology* 221 (5), 618–633. doi:10.1016/j.imbio.2016.01.007

Soengas, M. S., and Lowe, S. W. (2003). Apoptosis and melanoma chemoresistance. *Oncogene* 22 (20), 3138–3151. doi:10.1038/sj.onc.1206454

Song, B., Chi, H., Peng, G., Song, Y., Cui, Z., Zhu, Y., et al. (2022). Characterization of coagulation-related gene signature to predict prognosis and tumor immune microenvironment in skin cutaneous melanoma. *Front. Oncol.* 12, 975255. doi:10.3389/fonc.2022.975255

Song, B., Wu, P., Liang, Z., Wang, J., Zheng, Y., Wang, Y., et al. (2022). A novel necroptosis-related gene signature in skin cutaneous melanoma prognosis and tumor microenvironment. *Front. Genet.* 13, 917007. doi:10.3389/fgene.2022.917007

Sung, H., Ferlay, J., Siegel, R. L., Laversanne, M., Soerjomataram, I., Jemal, A., et al. (2021). Global cancer statistics 2020: GLOBOCAN estimates of incidence and mortality worldwide for 36 cancers in 185 countries. *CA Cancer J. Clin.* 71 (3), 209–249. doi:10.3322/caac.21660

Tang, D., Chen, X., and Kroemer, G. (2022). Cuproptosis: A copper-triggered modality of mitochondrial cell death. *Cell. Res.* 32 (5), 417–418. doi:10.1038/s41422-022-00653-7

Tsvetkov, P., Coy, S., Petrova, B., Dreishpoon, M., Verma, A., Abdusamad, M., et al. (2022). Copper induces cell death by targeting lipoylated TCA cycle proteins. *Science* 375 (6586), 1254–1261. doi:10.1126/science.abf0529

Umansky, V., and Sevko, A. (2012). Melanoma-induced immunosuppression and its neutralization. *Semin. Cancer Biol.* 22 (4), 319–326. doi:10.1016/j.semcancer.2012.02.003

Voglis, S., Schaller, V., Muller, T., Gonel, M., Winklhofer, S., Mangana, J., et al. (2022). Maximal surgical tumour load reduction in immune-checkpoint inhibitor naive patients with melanoma brain metastases correlates with prolonged survival. *Eur. J. Cancer* 175, 158–168. doi:10.1016/j.ejca.2022.08.020

Wang, D. R., Wu, X. L., and Sun, Y. L. (2022). Therapeutic targets and biomarkers of tumor immunotherapy: Response versus non-response. *Signal Transduct. Target Ther.* 7 (1), 331. doi:10.1038/s41392-022-01136-2

Weiss, S. A., Hanniford, D., Hernando, E., and Osman, I. (2015). Revisiting determinants of prognosis in cutaneous melanoma. *Cancer* 121 (23), 4108–4123. doi:10.1002/cncr.29634

Wilkerson, M. D., and Hayes, D. N. (2010). ConsensusClusterPlus: A class discovery tool with confidence assessments and item tracking. *Bioinformatics* 26 (12), 1572–1573. doi:10.1093/bioinformatics/btq170

Xiong, K., Qi, M., Stoeger, T., Zhang, J., and Chen, S. (2022). The role of tumor-associated macrophages and soluble mediators in pulmonary metastatic melanoma. *Front. Immunol.* 13, 1000927. doi:10.3389/fimmu.2022.1000927

Zhang, Y., Lan, S., and Wu, D. (2022). Advanced acral melanoma therapies: Current status and future directions. *Curr. Treat. Options Oncol.* 23 (10), 1405–1427. doi:10.1007/s11864-022-01007-6

Zhou, Y., Shu, Q., Fu, Z., Wang, C., Gu, J., Li, J., et al. (2022). A novel risk model based on cuproptosis-related lncRNAs predicted prognosis and indicated immune microenvironment landscape of patients with cutaneous melanoma. *Front. Genet.* 13, 959456. doi:10.3389/fgene.2022.959456

frontiers | Frontiers in Pharmacology

TYPE Review
PUBLISHED 19 April 2023
DOI 10.3389/fphar.2023.1151032

OPEN ACCESS

EDITED BY
Ouyang Chen,
Duke University, United States

REVIEWED BY
Yangqiu Li,
Jinan University, China
Salvador F Aliño,
University of Valencia, Spain

*CORRESPONDENCE
Jishi Wang,
wangjishi9646@163.com

SPECIALTY SECTION
This article was submitted to Pharmacology of Anti-Cancer Drugs, a section of the journal Frontiers in Pharmacology

RECEIVED 25 January 2023
ACCEPTED 24 March 2023
PUBLISHED 19 April 2023

CITATION
Chen Y, Wang J, Zhang F and Liu P (2023), A perspective of immunotherapy for acute myeloid leukemia: Current advances and challenges.
Front. Pharmacol. 14:1151032.
doi: 10.3389/fphar.2023.1151032

A perspective of immunotherapy for acute myeloid leukemia: Current advances and challenges

Ying Chen[1,2], Jishi Wang[1,2]*, Fengqi Zhang[1,2] and Ping Liu[1,2]

[1]Department of Hematology, Affiliated Hospital of Guizhou Medical University, Guiyang, China, [2]Guizhou Province Institute of Hematology, Guizhou Province Laboratory of Hematopoietic Stem Cell Transplantation Centre, Guiyang, China

During the last decade, the underlying pathogenic mechanisms of acute myeloid leukemia (AML) have been the subject of extensive study which has considerably increased our understanding of the disease. However, both resistance to chemotherapy and disease relapse remain the principal obstacles to successful treatment. Because of acute and chronic undesirable effects frequently associated with conventional cytotoxic chemotherapy, consolidation chemotherapy is not feasible, especially for elderly patients, which has attracted a growing body of research to attempt to tackle this problem. Immunotherapies for acute myeloid leukemia, including immune checkpoint inhibitors, monoclonal antibodies, dendritic cell (DC) vaccines, together with T-cell therapy based on engineered antigen receptor have been developed recently. Our review presents the recent progress in immunotherapy for the treatment of AML and discusses effective therapies that have the most potential and major challenges.

KEYWORDS

acute myeloid leukemia, immunotherapy, checkpoint inhibitor, car-t, DC vaccines

Introduction

Acute myeloid leukemia (AML) is a form of leukemia that mostly affects the adult population with most cases occurring in this age group and is diagnosed less frequently in children. First-line chemotherapy has been the mainstay of treatment during the last four decades (Dohner et al., 2010). Despite initial response to first-line treatment and disappearance of symptoms for most patients, only a small fraction achieves prolonged survival due to chemo-resistant relapses. Superior survival has been observed in the patient group undergoing allogeneic hematopoietic stem cell transplantation (allo-HSCT), but these patients only constitute a small fraction of AML cases (Ferrara and Schiffer, 2013; Kadia et al., 2015; Coombs et al., 2016; Short et al., 2018), and the relapse does not seem to decrease with graft-versus-host disease as well as patients with active disease (Vago and Gojo, 2020). Patients who have never achieved complete remission (CR) or relapse within 6 months after achieving a CR have poorer prognosis (De Kouchkovsky et al., 2016).

Immune surveillance is pivotal in suppressing tumor growth and maturation. The immune system can identify the antigens specific to the tumor cells. Nevertheless, the tumor microenvironment fosters immunosuppressive activities and antigen loss that would eventually lead to immune evasion. On the one hand, T-cell surface checkpoint regulators such as cytotoxic T lymphocyte-associated antigen-4 (CTLA-4) and programmed cell death protein 1 (PD-1) have been demonstrated to contribute, at least in part, to these immunosuppressive activities (Gurusamy et al., 2017; Mohme et al., 2017). Enhancement of inhibitory receptors confers robust immune effector response (Deng et al.,

2018). Based on this immunosuppression mechanism, CTLA-4 and PD-1 checkpoint blockade therapies have shown outstanding clinical efficacy in killing tumor cells in several solid organ malignancies (Tang et al., 2017). The continued success of immunotherapy in solid tumors has prompted its use in hematologic malignancies, and PD-1 blockade has shown promising preliminary results in classical Hodgkin lymphoma (cHL) (Hodi et al., 2010; Topalian et al., 2012; Robert et al., 2014; Younes et al., 2016). However, patients with other hematological malignancies, such as AML, have shown fewer encouraging results, underlining the need for future studies in these tumor types. On the other hand, to prevent antigen loss, a novel class of immune therapy strategies has been developed, including specific antibodies, dendritic cell (DC) vaccines, chimeric antigen receptor-engineered T cells (CAR-T), T-cell receptor-engineered T cells (TCR-T). Several antibody-based therapies have become the paradigm for treating acute lymphoblastic leukemia (ALL), and several others are being evaluated in clinical studies. Addition of Rituximab, a CD20-directed cytolytic antibody, to first line chemotherapy has demonstrated enhanced efficacy (Levato and Molica, 2018). Autologous CAR-T cell therapy targeting CD19 has shown striking responses, leading to FDA's approval for the management of precursor B-cell ALL and diffuse large B-cell lymphoma (DLBCL) (Grupp et al., 2013).

Immune checkpoint inhibitors are capable of activating tumor-specific immune cells that are suppressed in the tumor microenvironment (TME). For hematological malignancies such as AML with a maturation and progression pattern different from solid tumors, the mechanisms underlying the activity or inactivity of the immune system may strikingly differ from previous descriptions for solid tumors. Despite the presence of mutual immune evasion pathways, hematological tumors have their unique tolerance mechanisms (Zhang et al., 2009; Zhou et al., 2009; Zhou et al., 2011; Mussai et al., 2013). Moreover, checkpoint blockade has demonstrated greater efficacy in tumors with higher mutation burdens (Ansell et al., 2015; Chalmers et al., 2017; Yarchoan et al., 2017). Characterized by a low mutation burden, AML has only 13 genetic mutations on average in newly diagnosed disease (Cancer Genome Atlas Research et al., 2013), which mean that the immune system has a smaller chance to recognize mutated coding sequences giving rise to neoantigens (Gettinger et al., 2017; Haanen, 2017; Yarchoan et al., 2017). Thus, a better insight into the mechanisms through which immune evasion occurs in AML is fundamental to help evaluate different immunologic strategies for this disease based on study data. In CAR-T therapy, genetically modified immune cells possess new tumor-targeting specificity and efficacy. While the restricted CD19 and CD20 expression profile of ALL patients facilitates successful targeting of these B cell-associated antigens, the heterogeneous tumor antigen expression in a wide array of AML makes it more difficult to select an suitable target antigen (Taussig et al., 2005; Levine et al., 2015). Leukemogenesis has been understood better in recent years (Schwartzman and Tanay, 2015; Greaves, 2016; Ferrando and Lopez-Otin, 2017), and specifically, newly discovered molecular markers have yielded new insight into the pathogenesis of AML. An increasing number of potential markers have been investigated for every immunotherapeutic strategy (Perna et al., 2017; Yang and Wang, 2018). Nevertheless, further clinical research is necessary to ascertain the clinical efficacy.

In the present review, recent advances with regard to immunotherapies for AML will be discussed, various challenges in the field will be looked at, and emerging strategies that may optimize treatment efficacy will be presented.

Checkpoint inhibitor therapy

Targeting immune checkpoints such as CTLA4, PD1 and PD-L1 has produced impressive results across a diverse variety of malignancies including AML through immunoinhibitory signal blockage and $CD8^+$ T-cell activation to initiate a strong antitumor response (Figure 1A).

CTLA-4

CTLA-4 is an immune inhibitor mainly found on the surface of T cells. Through engaging the co-stimulatory protein CD28, ligation of CTLA-4 and CD80/CD86 occurs. CTLA-4 out competes CD28 and exhibits greater affinity in binding CD80 and CD86, which results in inhibiting T cells (Friedman et al., 2016; Byun et al., 2017; Nishino et al., 2017). The higher expression of CTLA-4 on T cells was detected in peripheral blood from patients with newly diagnosed AML (Chen et al., 2020a). As the first immunosuppressive molecule identified, CTLA-4 has provided an optional treatment approach in addition to conventional chemotherapy. Ipilimumab and tremelimumab as CTLA-4 inhibitors were used to treat patients with different cancers in clinical trials and led to prolonged overall survival (Author Anonymous, 2010; Hodi et al., 2010; Kyriakidis et al., 2021), but with limited off-label use in AML. In several clinical studies, favorable anti-leukemic effect, anti-tumor reactivity for relapsed patients and durable responses were reported (Fevery et al., 2007; Davids et al., 2016). Thus, it is suggested that hematological malignancies be treated with the use of CTLA-4 inhibitor. Ipilimumab produced specific potency in treating relapsed AML patients after HSCT (NCT01822509) (Liao et al., 2019; Vago and Gojo, 2020; Penter et al., 2021) and holds promise in affecting local control for the treatment of AML-related extramedullary (Bakst et al., 2020). However, patients with AML have less response to ipilimumab. Moreover, the rational combinations has potential to improve the efficacy of drugs and ipilimumab plus nivolumab have been approved for the management of metastatic melanoma and several other malignancies (Rotte, 2019). Notwithstanding, the two drugs, when used in combination, showed no improving effect on AML (Greiner et al., 2020) and was more likely to cause infectious complications (Spallone et al., 2022). Non-etheless, clinical investigation is ongoing to determine the potent effects of CTLA-4 inhibitor for AML patients (Masarova et al., 2017).

PD-1/PD-L1

As a potent immune checkpoint protein, PD-1 receptor acts like a "brake" on the immune response (Rizvi et al., 2015; Wolchok,

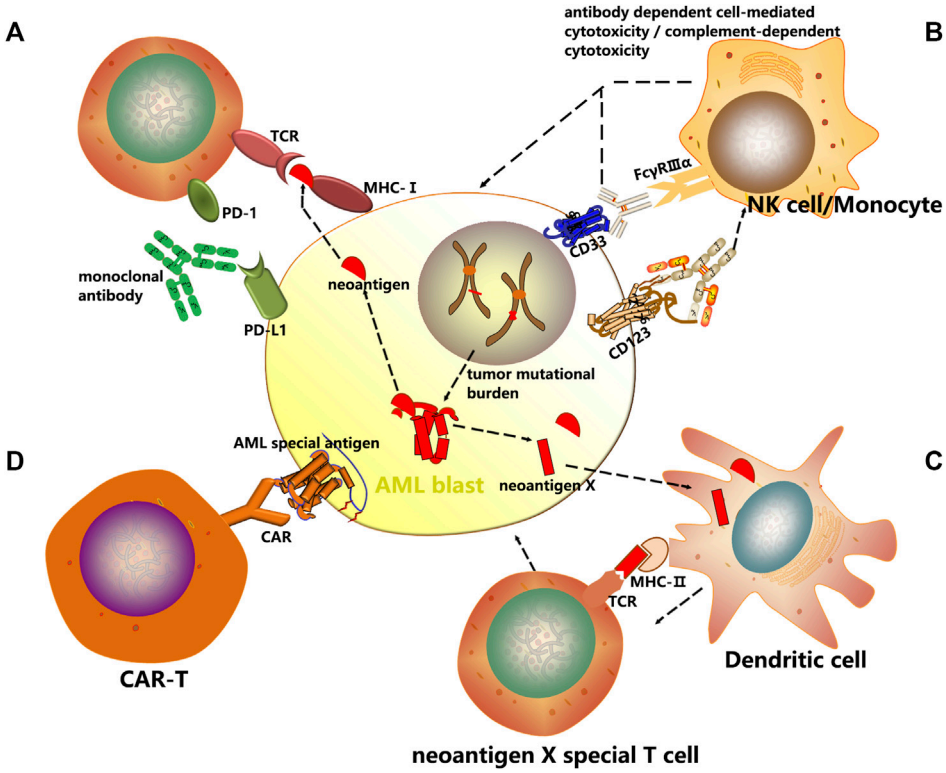

FIGURE 1
Mechanisms of cancer immunotherapy. In this review, several immunotherapeutic strategies have been discussed with an emphasis on AML treatment. **(A)** Checkpoint inhibitors are a new class of immunotherapy that use monoclonal antibodies to modulate inhibitory receptors on T cells to enhance T cell-mediated immune responses. **(B)** The antibody dependent cell mediated cytotoxicity (ADCC) and complement dependent cytotoxicity (CDC) induced by AML surface antigen-directed antibodies, as well as the effect of an internalized antibody-toxin conjugate result in AML cell death. **(C)** Dendritic cells are unique antigen-presenting cells (APC) and comprise the main class of APC. Autologous $CD14^+$ monocytes derived from peripheral blood of cancer patients are differentiated with GM-CSF and IL-4/IL-13 into immature DCs *in vitro*. Thereafter immature DCs are supplied with tumor antigens, that is, whole cell lysates, tumor-associated antigens (TAAs) or neoantigens. These antigen-loaded DCs are further matured and then enhance vaccine-induced immune responses. **(D)** Chimeric antigen receptors (CARs) are genetically modified receptor proteins with both extracellular antigen binding domain and intracellular signaling domain. With their unique structure, particularly effective cytotoxic activity, as well as antigen binding in an MHC-independent fashion is possible.

2015; Im et al., 2016; Gordon et al., 2017; Kamphorst et al., 2017; Kelly, 2017; Eroglu et al., 2018). Blocking this checkpoint by PD-1 inhibitors has resulted in impressive clinical response rates in melanoma (Roboz et al., 2014) and non-small cell lung cancer (Giroux Leprieur et al., 2017), as well as in Hodgkin (Le et al., 2015; Armand et al., 2018) and non-Hodgkin lymphomas (Lesokhin et al., 2016).

AML is characterized by upregulated PD-1 levels expressed on T cells, which is closely related to the treatment and prognosis of the disease (Huang et al., 2019; Tan et al., 2020; Tang et al., 2020). Patients newly diagnosed with AML or those undergoing relapse reported elevated PD-1 levels in peripheral blood (PB) and bone marrow (BM) T cells following front-line treatment, and by contrast, patients in durable remission reported reduced expression levels (Xu et al., 2021a; Brauneck et al., 2021), and TCRβ sequencing revealed clonal expansion in PD-1 positive $CD8^+$ T cells (Feng et al., 2020). The effector function in the BM milieu was reactivated through PD-1, CTLA-4, or TIM3 immune checkpoint pathways (Lamble et al., 2020). PD-L1/PD-L2 are found on the surface of leukemic cells, as demonstrated in several studies (Chen et al., 2008; Berthon et al., 2010). Driver mutations could regulate the expression of inhibitory proteins, for example, PD-L1/PD-L2 overexpression shown in AML cells with NRAS and ASXL1 mutations (You et al., 2022). Similarly, upregulation of PD-L1 was noted in patient cohorts with myelodysplastic syndromes (MDS) harboring TP53 mutations and secondary AML (sAML) (Sallman et al., 2020). Moreover, MDS or AML patients treated with hypomethylating agents (HMA) have also shown elevated PD-1 and PD-L1 expression in peripheral blood mononuclear cells (Yang et al., 2014). The mechanism of immune escape induced by PD-L1 may directly drive Treg cell expansion (Dong et al., 2020). PD-L1 silencing led to significant IFN-γ secretion and proliferation of MiHA-specific CD8+T cells, which was equally effective as PD-1 antibody blockade (van Ens et al., 2020).

Now six PD-1/L1 inhibitors were approved for treatment of lung cancer, melanoma, breast cancer or lymphoma including nivolumab (Opdivo®), pembrolizumab (Keytruda®), atezolizumab (Tecentrip®), avelumab (Bavencio®), durvalumab (Imfinzi®), and cemiplimab (Libtayo®). Immune checkpoint inhibitors (ICIs) confer advantages for solid tumors that are yet to be attained for AML (Chen et al., 2020b). However, the successful therapeutic application of ICIs therapy in solid tumors has inspired its use in hematological

TABLE 1 Current clinical trials using checkpoint inhibitors for immunotherapy of AML.

Trial identifier	Study name	Conditions	Target	Drug name	Clinical phases	Enrollment	Start date	Completion date	Status
NCT02532231	Nivolumab in Acute Myeloid Leukemia (AML) in Remission at High Risk for Relapse	AML	PD-1	Nivolumab	II	30	2015	2022	Active, not recruiting
NCT02275533	Nivolumab in Eliminating Minimal Residual Disease and Preventing Relapse in Patients With Acute Myeloid Leukemia in Remission After Chemotherapy	AML in Remission	PD-1	Nivolumab	II	82	2015	2023	Active, not recruiting
NCT03092674	Azacitidine With or Without Nivolumab or Midostaurin or Decitabine and Cytarabine Alone in Treating Older Patients With Newly Diagnosed Acute Myeloid Leukemia or High-Risk Myelodysplastic Syndrome	AML MDS	PD-1	Nivolumab	II/III	1670	2017	2023	Recruiting
NCT02846376	Single Agent and Combined Inhibition After Allogeneic Stem Cell Transplant	AML MDS	PD-1	Nivolumab Ipilimumab	I	8	2019	2023	Active, not recruiting
NCT03825367	Nivolumab in Combination With 5-azacytidine in Childhood Relapsed/ Refractory AML	AML, Childhood	PD-1	Nivolumab	I/II	26	2019	2024	Recruiting
NCT02397720	Nivolumab and Azacitidine With or Without Ipilimumab in Treating Patients With Refractory Relapsed or Newly Diagnosed Acute Myeloid Leukemia	AML Recurrent AML	PD-1	Nivolumab Ipilimumab	II	182	2015	2022	Recruiting
NCT03600155	Nivolumab and Ipilimumab After Donor Stem Cell Transplant in Treating Participants With High Risk Refractory or Relapsed Acute Myeloid Leukemia	Allo-HSCT Refractory AML	PD-1	Nivolumab Ipilimumab	I	55	2018	2022	Recruiting
NCT02845297	Study of Azacitidine in Combination With Pembrolizumab in Relapsed Refractory Acute Myeloid Leukemia (AML) Patients and in Newly Diagnosed Older (>65 Years) AML Patients	AML	PD-1	Pembrolizumab	II	67	2016	2022	Active, not recruiting
NCT02771197	Lympho depletion and Anti-PD-1 Blockade to Reduce Relapse in AML Patient Not Eligible for Transplant	AML	PD-1	Pembrolizumab	II	20	2016	2023	Active, not recruiting

(Continued on following page)

TABLE 1 (*Continued*) Current clinical trials using checkpoint inhibitors for immunotherapy of AML.

Trial identifier	Study name	Conditions	Target	Drug name	Clinical phases	Enrollment	Start date	Completion date	Status
NCT02768792	High Dose Cytarabine Followed by Pembrolizumab in Relapsed Refractory AML	Relapse AML	PD-1	Pembrolizumab	II	38	2016	2024	Active, not recruiting
NCT03286114	Augmentation of the Graft vs Leukemia Effect Via Checkpoint Blockade With Pembrolizumab	MDS AML ALL	PD-1	Pembrolizumab	I	20	2017	2022	Recruiting
NCT02981914	Pilot Study of Pembrolizumab Treatment for Disease Relapse After Allogeneic Stem Cell Transplantation	AMLetc.	PD-1	Pembrolizumab	I	26	2017	2029	Recruiting
NCT04284787	BLAST MRD AML-2: BLockade of PD-1 Added to Standard Therapy to Target Measurable Residual Disease in Acute Myeloid Leukemia 2- A Randomized Phase 2 Study of Anti-PD-1 Pembrolizumab in Combination With Azacitidine and Venetoclax as Frontline Therapy in Unfit Patients With Acute Myeloid Leukemia	AMLetc.	PD-1	Pembrolizumab	II	76	2020	2023	Recruiting
NCT04372706	RTX-240 Monotherapy and in Combination With Pembrolizumab	Solid Tumor AML Adult	PD-1	Pembrolizumab	I/II	166	2020	2023	Not yet recruiting
NCT04353479	Combined PD1 Inhibitor and Decitabine in Elderly Patients With Relapse and Refractory Acute Myeloid Leukemia	AML	PD-1	Camrelizumab (SHR-1210)	II	29	2020	2022	Not yet recruiting
NCT04722952	PD-1 Inhibitor Combined With Azacytidine and Homoharringtonine, Cytarabine, G-CSF for Refractory or Relapsed AML	Refractory Leukemia Relapse adult AML AML	PD-1	Visilizumab	III	30	2021	2024	Recruiting
NCT02935361	Guadecitabine and Atezolizumab in Treating Patients With Advanced Myelodysplastic Syndrome or Chronic Myelomonocytic Leukemia That Is Refractory or Relapsed	MDS Recurrent AML With MDS	PD-L1	Atezolizumab	I/II	33	2016	2024	Active, not recruiting
NCT03390296	Pfizer Immunotherapy Combinations for Acute Myeloid Leukemia (AML) Multi-Arm Study 1	Recurrent AML Refractory AML	PD-L1	Avelumab	II	138	2017	2024	Active, not recruiting

(Continued on following page)

TABLE 1 (*Continued*) **Current clinical trials using checkpoint inhibitors for immunotherapy of AML.**

Trial identifier	Study name	Conditions	Target	Drug name	Clinical phases	Enrollment	Start date	Completion date	Status
NCT02890329	Ipilimumab and Decitabine in Treating Patients With Relapsed or Refractory Myelodysplastic Syndrome or Acute Myeloid Leukemia	Recurrent AML	CTLA-4	Ipilimumab	I	48	2017	2023	Active, not recruiting

malignancies, and the favorable clinical responses achieved in Hodgkin lymphoma are promising. Currently, PD-1 therapy is only applied for patients with relapsed/refractory AML in clinical trials. An increasing number of investigational studies are in progress to assess the efficacy of the anti-PD-1 inhibitor nivolumab. The relapsed AML patients after allo-HSCT showed good response when treated with nivolumab but paid attention to the clinical signs of graft versus-host disease (GVHD) (Albring et al., 2017; Yao et al., 2021). Another study found that HSCT with prior use of nivolumab and/or ipilimumab appears feasible in patients with AML and cyclophosphamide-based GVHD prevention is associated with improved prognosis (Oran et al., 2020).

As we mentioned earlier, combined strategies produced clinical benefits for the treatment of AML. Daver et al. reported promising preliminary results in a study combining azacitidine and nivolumab for adult cohort with relapsed and refractory AML (n = 51) (Naval Daver et al., 2016; Daver et al., 2018). Another phase II study also demonstrated the safety and efficacy of azacitidine plus nivolumab in patients with AML in first salvage status, with HMA naïvety, or with increased $CD3^+$ BM infiltration as assessed by flow cytometry or IHC (Daver et al., 2019). The combination of the two drugs had an acceptable tolerability and produced a favorable response rate in relapsed AML patients, which is associated with the potential mechanism of adaptive T-cell plasticity and genomic alterations (Abbas et al., 2021). In addition, another clinical trial (NCT02397720) is recruiting patients to determine the therapeutic effect of azacitidine and nivolumab with ipilimumab or without ipilimumab in AML patients who were not responsive or relapsed and newly diagnosed elderly patients (>65 years). In a phase II trial (NCT02464657), the use of three drugs (nivolumab, idarubicin and cytarabine) in combination has been proved efficacious in subjects who were newly diagnosed with AML or at high risk of MDS (Ravandi et al., 2019). Moreover, several clinical studies reported the combined effect of azacitidine and other inhibitors on refractory AML, such as pembrolizumab (Zeidner et al., 2021) and avelumab (Saxena et al., 2021) with encouraging clinical activity. The therapy of pembrolizumab combined with decitabine was clinically feasible in patients who were not responding well or relapsed (NCT02996474) (Goswami et al., 2022). Given the small cohort likely to benefit from ICI therapy, further investigation is necessary to explore the mechanism of action. However, not all combinations can improve rates of durable responses for AML patients. The use of avelumab in combination with decitabine in a phase I clinical trial achieved no clinical benefit in AML patients (Zheng et al., 2021), as well as the combination of ipilimumab and nivolumab (Greiner et al., 2020). Nevertheless, several additional trials are ongoing across the globe to assess the clinical efficacy of ICIs combined with induction chemotherapy or hypomethylating agents for immunotherapy of AML (Table 1).

In addition to CTLA-4 and PD-1/PD-L1, numbers of clinical trials of TIM-3 inhibitors including sabatolimab and TQB2618 for AML are recruiting patients (NCT05426798, NCT03940352, NCT04623216, NCT05367401, NCT03066648). Similarly, TIM-3 inhibitors combined with demethylation drugs (azacitidine or decitabine) is used as the treatment strategy for AML, and one of the clinical trial adopts the combination of spartalizumab (PD-1 inhibitor) and sabatolimab (NCT03066648), which indicates that TIM3 inhibitors will occupy the market in the field of AML in the future.

Monoclonal antibodies therapy

Recent studies have identified numerous candidate AML-associated antigens that can be targeted, including CD33 and CD123. By selectively targeting AML specific antigens, monoclonal antibodies have emerged as effective therapeutic agents that can reduce morbidity and mortality. During treatment of AML, monoclonal antibodies can exert their therapeutic effects through selective drug delivery, cell-mediated and complement-mediated mechanisms, and innate immune enhancement. Besides, antibody-drug conjugation combining chemotherapeutic agents or radioactive particles with monoclonal antibodies is also being evaluated to specifically target cells expressing CD33 or CD123. Despite that the immune system is not activated, they can induce cell injuries which may initiate the innate immune system and activate immune defense (Figure 1B).

Anti-CD33

CD33 is a Siglec receptor protein primarily expressed on leukemic blasts. CD33 expression alone cannot be used as an independent prognostic marker, but low expression of CD33 is often observed in groups with complex karyotypes and translocations, and *FLT3-ITD* or *NPM1* mutations are more prevalent in groups with higher CD33 expression level (Feldman et al., 2005; Pollard et al., 2012; Krupka et al., 2014; Khan et al., 2017). In addition, the endocytosed CD33 makes it a promising target in antibody drug conjugates (ADCs) therapy (Krupka et al., 2014; Laszlo et al., 2016).

The first approved ADC by the FDA is gemtuzumab ozogamycin (GO/Mylotarg) targeting CD33 in 2000 to treat AML (Bross et al., 2001) and was subsequently removed from market due to increased risk of hepatic veno-occlusive disease (VOD) and high mortality (Petersdorf et al., 2013). However, cytotoxic therapy utilizing CD33 has attracted enormous attention because of the remarkable responses in varying patient cohorts receiving GO. New data from a fractionated-dosing schedule for treating newly diagnosed and relapsed/refractory AML led to re-approval of GO (Jen et al., 2018). This was supported by the results that demonstrating decreased number of early deaths, bleeding, low platelet count and VOD while sustaining treatment efficacy (Baron and Wang, 2018). In the phase III ALFA-0701 trial, fractionated doses of GO in combination with daunorubicin and cytarabine (DA) chemotherapy improved event-free survival (EFS) compared to chemotherapy alone (17.3 vs 9.5 months). Moreover, a complete remission (26%) was achieved with GO in relapsed/refractory AML (Lambert et al., 2019). The use of azacitidine and GO in combination in a phase I/II trial for relapsed AML showed good tolerability and achieved a CR of 24% in 12/50 patients (Medeiros et al., 2018). In addition, the renewed knowledge and optimized management regarding VOD risk factors as well as advances in prophylaxis and treatment have promoted the application of GO (Cortes et al., 2020).

ADC linked with pyrrolobenzodiazepine (PBD) dimer is a new strategy for treatment of various cancers (Hartley, 2021). SGN-CD33A is a pyrrolobenzodiazepine (PBD) dimer-based antibody-drug conjugate targeted to CD33. Pre-clinical studies showed that SGN-CD33A was superior to GO in multi-drug resistant AML cell lines as well as in AML patients with poor risk cytogenetics (Kung Sutherland et al., 2013). In an initial phase I study (NCT01902329) designed to assess the safety of the drug, SGN-CD33A used alone resulted in a CR and CRi rate of less than 30% with minimal dose limiting toxicity (DLT) (Stein et al., 2018). SGN-CD33A in combination with a hypomethylating agent yielded a composite CR and CRi rate of 70% (Fathi et al., 2018). In addition, SGN-CD33A in combination with standard 7 + 3 chemotherapy were being assessed in a phase Ib trial (NCT02326584), achieving an encouraging composite CR and CRi rate of 78% (Erba et al., 2016). In this trial, myelosuppression-related side effects were reported in all patients. None of the patients developed VOD, and the 60-day mortality rate was less than 10%. However, due to high mortality rate in the SGN-CD33A-containing arm, the phase III CASCADE trial was discontinued (By The ASCO Post Staff, 2017).

Lintuzumab is a humanized anti-CD33 antibody with a modest single-agent activity against AML. To improve the efficacy, lintuzumab was conjugated to radioactive elements such actinium-225 and bismuth-213. The radio immune conjugates are undergoing clinical investigation in older patients newly diagnosed with AML for whom standard induction treatment is deemed unfit. Actinium-225-lintuzumab was feasible with myelosuppression and no cases of VOD (Finn LE et al., 2017; Rosenblat et al., 2022). Sequential cytarabine and bismuth-213-lintuzumab produced remissions in patients with AML (Rosenblat et al., 2010). Therefore, the conjugate of lintuzumab and actinium-225 or bismuth-213 represents a reasonable treatment option for patients ineligible for intensive chemotherapy.

Anti-CD123

CD123 is a cytokine receptor widely overexpressed in multiple hematologic cancer cells, especially in leukemic stem cells (LSCs). AML cells with FLT3-ITD or NPM1 mutations are correlated with significantly increased levels of CD123 as compared to AML cells with wild-type FLT3 or NPM1 (Ehninger et al., 2014; Cortes et al., 2018; Cruz et al., 2018). Overexpression of CD123 is associated with high-risk disease characteristics in adult and pediatric AML. CD123 as an important biomarker can be potentially targeted in relapsed or refractory AML (Lamble et al., 2022).

CSL360 is a chimeric monoclonal antibody directed against CD123 and is believed to inhibit proliferation of AML cells (Roberts et al., 2008). However, CSL360 was far less efficacious in patients with relapsed/refractory or high risk AML (He et al., 2015). CSL362 (talacotuzumab), another monoclonal antibody directed against CD123, demonstrated promising activity in AML patients (Xie et al., 2017). However, talacotuzumab alone or in combination with other drugs showed limited efficacy but considerable toxicity in AML patients in recent clinical study (Kubasch et al., 2020; Montesinos et al., 2021). Many preclinical trials have studied various CD123 antibodies, such as CD123 antagonistic peptide (Xu et al., 2021b; Xu et al., 2022) and protein-CD123 fusion antibodies (Tahk et al., 2021), which significantly reduced BM infiltration or enhanced the elimination of AML-initiating cells. SL-401 is a cytotoxin that fuses the diphtheria toxin (DT) to the IL3 ligand. It was the first treatment approved by the FDA for the management of blastic plasmacytoid dendritic cell neoplasms (BPDCN) in adult and pediatric patients 2 years and older (Jen et al., 2020), with good tolerability and a predictable and favorable safety profile (Pemmaraju et al., 2022). Clinical trials have shown that treatment with SL-401 was associated with reduced drug resistance and better prognosis in AML patients at high risk for relapse. It is worth noting that a serious adverse reaction induced by SL-401 had caused capillary leak syndrome leading to one death, which was reported among the cohort in remission with MRD (American Society of Hematology, 2016; Lane et al., 2016).

Anti-CD3/CD33 or CD3/CD123 bispecific antibody

Bispecific T-cell-engaging (BiTE) antibodies are composed of dual variable regions that simultaneously bind to CD3 on cytotoxic T lymphocytes and tumor cell antigens on malignant cells, activating the effector function, accompanied by release of cytokines and destruction of tumor cells. By means of this strategy, virtually all T lymphocytes can be recruited and directed against leukemic blasts irrespective of its specificity. The preclinical trial proved that CD3/CD33-directed antibody constructs might be utilized as an alternative treatment in AML (Reusch et al., 2016). AMG 330 has been shown to exhibit strong anti-tumor responses both *in vitro* and in mouse models (Laszlo et al., 2015; Krupka et al., 2016; Jitschin et al., 2018). A clinical trial (NCT02520427) designed to investigate the safety and tolerability of AMG 330 in patients with relapsed/refractory AML is in progress. $CD3^{-}$CD123-BiTE antibody

TABLE 2 Current clinical trials using dendritic cell vaccination for immunotherapy of AML.

Trial identifier	Study name	Conditions	Antigen	Phases	Enrollment	Start date	Completion date	Status
NCT00965224	Efficacy of Dendritic Cell Therapy for Myeloid Leukemia and Myeloma	AML/ CML/MM	WT1	II	50	2010	2014	Unknown
NCT01686334	Efficacy Study of Dendritic Cell Vaccination in Patients With Acute Myeloid Leukemia in Remission	AML	WT1	II	130	2012	2024	Recruiting
NCT04747002	Investigator-initiated Clinical Trial (Phase II) of Cancer Vaccine "Dainippon Sumitomo Phama (DSP)-7888″for Acute Myeloid Leukemia Patients	AML in Remission	WT1	II	100	2020	2024	Recruiting
NCT04284228	Antigen-specific T-cell Therapy for AML or MDS Patients With Relapsed Disease After Allo-HCT	AML MDS	WT1/ PRAME/ Cyclin A1	I/II	22	2020	2023	Recruiting
NCT05000801	Clinical Study of DC-AML Cells in the Treatment of Acute Myeloid Leukemia	AML	WT1/ hTERT/ Survivin	Not Applicable	20	2021	2026	Recruiting
NCT01096602	Blockade of PD-1 in Conjunction With the Dendritic Cell/AML Vaccine Following Chemotherapy Induced Remission	AML	Multiple	II	63	2010	2024	Active, not recruiting
NCT03059485	DC/AML Fusion Cell Vaccine vs. Observation in Patients Who Achieve a Chemotherapy-induced Remission	AML	Multiple	II	75	2017	2025	Recruiting
NCT03697707	Efficacy and Safety of Immunotherapy With Allogeneic Dendritic Cells, DCP-001, in Patients With Acute Myeloid Leukaemia (ADVANCE-II)	AML in Remission	Multiple	II	20	2018	2022	Active, not recruiting
NCT03679650	Dendritic Cell/AML Fusion Cell Vaccine Following Allogeneic Transplantation in AML Patients	AML	Multiple	I	45	2018	2026	Recruiting

is another promising therapy for patients with relapsed/refractory AML (Bonnevaux et al., 2021). Additional early clinical studies are ongoing to investigate $CD3^{-}$CD123-BiTE antibodies, such as XmAb14045 (NCT02730312), and flotetuzumab (MGD006; NCT02152956), a dual-affinity retargeting (DART) molecule.

Dendritic cell vaccines therapy

Cancer vaccines represent a groundbreaking therapeutic approach that employs immune effector cells to eradicate malignant cells. Upon activation of immune signaling, presentation of tumor associated antigens is increased, breaking the tolerance to tumor, and at the same time, immune regulation against autoimmunity is maintained. Dendritic cell (DC)-based vaccines offer the potential of a non-toxic and effective immunotherapeutic strategy. The four most common tumor types can be targeted include melanoma, prostate cancer, glioblastoma and renal cell carcinoma (Germeau et al., 2005; Melero et al., 2014; Anguille et al., 2015; Polyzoidis et al., 2015; Schreibelt et al., 2016). The primary types of cancer vaccines undergoing clinical trials for AML patients are DC-based vaccines (Figure 1C).

WT1 DC vaccine

AML cells have been shown to express the Wilms' tumor 1 (WT1) protein and upregulation of this protein is a predictor of poor prognosis in AML and MDS patients (Bergmann et al., 1997; Brayer et al., 2015). The specific antibody targeting WT1 shows a good inhibitory effect on AML, which prompted the conduct of a clinical trial for relapsed/refractory AML (NCT0458012) (Augsberger et al., 2021). In addition, TCR-T cell therapy or CRISPR-Cas9 genome editing tools has a potential strategy for WT1-exprssing AML (Tawara et al., 2017; Chapuis et al., 2019; Ruggiero et al., 2022). WT1 is one principal protein studied for vaccination potential and is currently in the clinical investigation phase. In a phase I/II trial, Tendeloo et al. assessed the DC-WT1 vaccine in 10 AML patients who achieved CR or PR following chemotherapy and were at a high risk of relapse (Van Tendeloo et al., 2010). Subsequently, the clinical results of 66 cancer patients after DC-WT1 vaccination, including thirty AML patients who were at very high risk of relapse, were reported (Table 2, NCT00965224), which proved that WT1-targeted DC-based vaccination is an effective immunotherapeutic strategy to prevent relapse in AML patients (Anguille et al., 2017). In another phase I/II trial (NCT01051063), 5 elderly AML patients observed clinical benefit after receiving WT1 recombinant protein vaccination

(Kreutmair, 2022). Moreover, clinical trial found the decrease of the regulatory T cells in 8 AML patients following WT1 peptide-loaded DC vaccination (Ogasawara et al., 2022).

Human telomerase reverse transcriptase (hTERT) DC vaccine

Telomerase is a ribonucleoprotein enzyme that positively expressed in most malignant tumor cells and is critical for increasing proliferative potential of cancer cells (Counter et al., 1995; Zhang et al., 1996; Ohyashiki et al., 1997; Stewart and Weinberg, 2000). Telomerase can be used as an important predictor for AML due to its strong expression in AML patients, particularly in high-risk cytogenetic AML subtypes. A phase II clinical trial (NCT00510133) enrolled a total of 22 patients achieving early or subsequent complete remission at intermediate risk or high risk of AML (Khoury et al., 2017). The relapse free survival achieved in this trial is superior to that reported in previous trials, but further clinical validation of these results is needed. Preclinical models confirmed the improved survival outcome and showed that telomerase was upregulated in AML blasts, and reduced telomerase activity thwarts leukemic cell proliferation and disease relapse after chemotherapy (Bruedigam et al., 2014). The TERT gene variability and telomere length affect risk and overall survival in AML (Dratwa et al., 2021). It was reported that diverse short telomere-related somatic mutations promote transformation to MDS/AML (Schratz et al., 2021). If the same results can be obtained from further clinical trials, hTERT-DCs should soon become a form of safe and effective immunotherapy that can be used to extend relapse-free survival for AML patients in complete remission. The approach would provide promising treatment options that bring new hope to AML patients.

DC-AML fusion vaccine

An individualized cancer vaccine strategy was developed by Jacalyn Rosenblatt et al. in which fusion hybrids of autologous dendritic cells and patient-derived AML cells are used to generate antileukemic responses (Rosenblatt et al., 2016). In this phase I/II clinical trial (NCT01096602), a cohort of 17 subjects were responding well to front-line treatment and subsequently received vaccination to target MRD and prevent relapse. The vaccine regimens induced strong T-cell expansion in both PB and BM. Meanwhile, 12 subjects in the cohort undergoing vaccination achieved prolonged survival when followed up to 5 years. These results show that individualized vaccine regimens for AML patients in remission can enhance leukemia-specific T-cell responses and prevent disease relapse.

Cancer vaccines are used to confer protective immunity and enhance tumor antigen-specific T-cell and antibodies. However, clinical outcomes have shown little promise to date. This is largely due to immune suppression in the process of tumor growth, which affects the vaccines' capability to induce strong and systemic immune responses and functionality of immune responses at the tumor site. Therefore, new approaches have been developed, supported by findings demonstrating that human dendritic cells (DCs) can be cultured *in vitro* (Steinman and Banchereau, 2007). The success of DC vaccines generated enormous enthusiasm in DC vaccines employing the latest technology. Major efforts have often directed to the origin of DCs. For example, specific subsets of naturally occurring DCs are superior to monocyte-derived DCs in terms of potency and cost-effectiveness. Results from preliminary trials demonstrated safety and feasibility of next-generation DC vaccines employing naturally occurring DC subsets; furthermore, this approach has resulted in superior efficacy. A phase I trial showed that 12 elderly patients with late-stage AML receiving a DC vaccine generate both cellular and humoral immune response (van de Loosdrecht et al., 2018). A phase I/II trial (NCT01146262) showed DC-vaccines with leukemic apoptotic bodies produced a safety and efficacy for the AML patients (Chevallier et al., 2021). On the other hand, a major impediment with regard to DC vaccination is to pinpoint the right antigen to be vaccinated for maximal T-cell effector function, stimulation of memory T-cells, and reducing the expansion of inhibitory subsets. Normal cancer antigens such as WT1 and hTERT loading to AML patients' DCs are currently under clinical investigation. Another method to improve the immunogenicity of DC is to combine with hypomethylating agents (Nahas et al., 2019) or immune checkpoint inhibitors (Stroopinsky et al., 2021). Future development of cancer vaccines would rely more on multiple antigens or individualized neoantigens to maximize vaccine-based immune responses.

CAR-T cell therapy

CARs, unlike TCRs which interact with HLA molecules, do not need antigen processing or presentation by the HLA peptidome (June et al., 2018), and therefore broadly recognize target antigens independent of HLA background (Figure 1D).

CD19-specific CAR-T cells represent a well-established CAR-T cell therapy with restrictive expression pattern and favorable safety outcome. The promise of anti-CD19 CAR-T cells was immense in ALL, achieving CR in over 90% of B-ALL patients (Davila et al., 2014; Maude et al., 2014). Considering the intense prior treatment: a median of 3 prior intensive chemo regimens with over 1/3 relapsed following allogeneic HSCT, these clinical results are impressive. Anti-CD19 CD28-based CAR-T therapy induced a CR rate of 57% in seven patients with DLBCL with no response to three prior lines of therapy (Locke et al., 2017). The modified CD19 CAR-T cells using the FasT system displayed favorable responses for B-cell ALL in both preclinical study and a phase I trial (NCT03825718) (Yang et al., 2022). CAR-T cell therapy targeting CD19 induces high response rates in B-ALL with central nervous system leukemia (NCT02782351) (Qi et al., 2022). In the context of AML, however, the putative antigens targeted by CAR-T cells must have a restrictive expression pattern to avert destruction of normal myeloid cells. Some targets have been identified in preclinical trials, including natural killer group 2 member D (NKG2D), CD123, CD33, Lewis Y (LeY), CLL-1, etc.

In a phase I study, four patients infused with anti-LeY CAR-T cells were examined to determine the safety and clinical efficacy of adoptive transfer of T cells. The CAR T cells sustained efficacy for up to 10 months post infusion, confirming the feasibility and safety of anti-LeY CAR-T cells in patients with high-risk AML, and

TABLE 3 Current clinical trials using CAR T-cell for immunotherapy of AML.

Trial identifier	Study name	Conditions	Antigen	Phases	Enrollment	Start date	Completion date	Status
NCT04033302	Multi-CAR T-cell Therapy Targeting CD7-positive Malignancies	AML	CD7	I/II	30	2019	2023	Recruiting
NCT04762485	Humanized CD7 CAR T-cell Therapy for r/r CD7$^+$ Acute Leukemia	AML	CD7	I/II	20	2021	2024	Recruiting
NCT05377827	Dose-Escalation and Dose-Expansion Study to Evaluate the Safety and Tolerability of Anti-CD7 Allogeneic CAR T-Cells (WU-CART-007) in Patients With CD7$^+$ Hematologic Malignancies	AMLetc.	CD7	I	48	2022	2025	Not yet recruiting
NCT03896854	CART-19 T-cell in CD19 Positive Relapsed or Refractory Acute Myeloid Leukemia (AML)	AML	CD19	I/II	15	2017	2024	Recruiting
NCT04796441	Clinical Study of Universal CAR-γδT Cell Injection in the Treatment of Patients With Relapsed AML After Transplantation	AML	CD19	Not Applicable	20	2020	2022	Recruiting
NCT04257175	CAR-T CD19 for Acute Myelogenous Leukemia With t 8:21 and CD19 Expression	AML	CD19	II/III	10	2020	2023	Recruiting
NCT05513612	Novel CAR-T Cell Therapy in the Treatment of Hematopoietic and Lymphoid Malignancies	AMLetc.	CD19	I	20	2020	2026	Recruiting
NCT05388305	Universal CAR-γδT Cell Injection in the AML Patients	AML	CD19	Not Applicable	30	2022	2023	Recruiting
NCT01864902	Treatment of Relapsed and/or Chemotherapy Refractory CD33 Positive Acute Myeloid Leukemia by CART-33	Relapsed Refractory AML	CD33	I/II	10	2013	2017	Unknown
NCT02799680	Allogeneic CART-33 for Relapsed/Refractory CD33$^+$ AML	Relapsed Refractory AML	CD33	I	12	2015	2018	Unknown
NCT03971799	Study of Anti-CD33 Chimeric Antigen Receptor-Expressing T Cells (CD33CART) in Children and Young Adults With Relapsed/Refractory Acute Myeloid Leukemia	AML	CD33	I/II	37	2020	2039	Recruiting
NCT05008575	Anti-CD33 CAR NK Cells in the Treatment of Relapsed/Refractory Acute Myeloid Leukemia	AML	CD33	I	27	2021	2023	Recruiting
NCT05105152	PLAT-08: A Study Of SC-DARIC33 CAR T Cells In Pediatric And Young Adults With Relapsed Or Refractory CD33$^+$ AML	AML	CD33	I	18	2021	2039	Recruiting
NCT04835519	Phase I/II Study of Enhanced CD33 CAR T Cells in Subjects With Relapsed or Refractory Acute Myeloid Leukemia	AML	CD33	I/II	25	2022	2024	Recruiting
		Relapse Leukemia						
		Refractory AML						
NCT05445765	Anti-CD33 CAR-T Cells for the Treatment of Relapsed/Refractory CD33$^+$ Acute Myeloid Leukemia	Relapsed/ Refractory AML	CD33	I	10	2022	2024	Not yet recruiting
NCT05473221	Evaluate the Safety and Efficacy of CD33 CAR-T in Patients With R/R AML	AML	CD33	I	20	2022	2025	Not yet recruiting
NCT04351022	CD38-targeted Chimeric Antigen Receptor T-cell (CART) in Relapesd or Refractory Acute Myeloid Leukemia	AML	CD38	I/II	20	2017	2023	Recruiting
NCT05239689	Clinical Study of CD38 CAR-T Cells in the Treatment of Hematological Malignancies	AML	CD38	I	36	2022	2024	Recruiting
NCT05442580	CART-38 in Adult AML and MM Patients	AML	CD38	I	36	2022	2040	Not yet recruiting
		MM						
NCT04662294	CD 70 CAR T for Patients With CD70 Positive Malignant Hematologic Diseases	AML	CD70	I	108	2021	2027	Recruiting

(Continued on following page)

10.3389/fphar.2023.1151032

TABLE 3 (*Continued*) Current clinical trials using CAR T-cell for immunotherapy of AML.

Trial identifier	Study name	Conditions	Antigen	Phases	Enrollment	Start date	Completion date	Status
NCT04692948	TAA6 Cell Injection In The Treatment of Patients With Relapsed/Refractory Acute Myeloid Leukemia	AML	CD276	Not Applicable	5	2019	2023	Recruiting
NCT02159495	Genetically Modified T-cell Immunotherapy in Treating Patients With Relapsed/Recurrent Blastic Plasmacytoid Dendritic Cell Neoplasm	AML	CD123	I	31	2015	2022	Active, not recruiting
NCT03114670	Donor-derived Anti-CD123-CART Cells for Recurred AML After Allo-HSCT	Adult AML	CD123	I	20	2017	2021	Unknown
NCT03190278	Study Evaluating Safety and Efficacy of UCART123 in Patients With Acute Myeloid Leukemia	AML	CD123	I	65	2017	2023	Recruiting
NCT03556982	CART-123 FOR Relapsed/Refractory Acute Myelocytic Leukemia	Relapsed Refractory AML	CD123	II/III	20	2018	2020	Unknown
NCT04265963	CD123-Targeted CAR-T Cell Therapy for Relapsed/Refractory Acute Myeloid Leukemia	AML	CD123	I/II	45	2019	2022	Recruiting
NCT04272125	Safety and Efficacy of CD123-Targeted CAR-T Therapy for Relapsed/Refractory Acute Myeloid Leukemia	AML	CD123	I/II	40	2019	2023	Recruiting
NCT04318678	CD123-Directed Autologous T-Cell Therapy for Acute Myelogenous Leukemia (CATCHAML)	AMLetc.	CD123	I	32	2020	2025	Recruiting
NCT04678336	CD123 Redirected T Cells for AML in Pediatric Subjects	AML in relapse	CD123	I	12	2021	2036	Recruiting
		AML pediatric						
		AML refractory						
NCT04884984	Anti-CLL1 CAR T-cell Therapy in CLL1 Positive Relapsed/Refractory Acute Myeloid Leukemia (AML)	AML	CLL1	I/II	20	2017	2024	Recruiting
NCT05467202	Evaluate the Safety and Efficacy of CLL1 CAR-T in Patients With R/R AML	AML	CLL1	I	20	2022	2025	Not yet recruiting
NCT04219163	Chimeric Antigen Receptor T-cells for The Treatment of AML Expressing CLL-1 Antigen	AML	CLL1	I/II	18	2020	2038	Recruiting
NCT04923919	Clinical Study of Chimeric Antigen Receptor T Lymphocytes (CAR-T) in the Treatment of Myeloid Leukemia	AML	CLL1	I	100	2021	2023	Recruiting
NCT05252572	Clinical Study of CLL1 CAR-T Cells in the Treatment of Hematological Malignancies	AML	CLL1	I	36	2022	2024	Recruiting
NCT05023707	Anti-FLT3 CAR T-cell Therapy in FLT3 Positive Relapsed/Refractory Acute Myeloid Leukemia	AML	FLT3	I/II	5	2021	2025	Recruiting
NCT05432401	TAA05 Injection in the Treatment of Adult Patients With FLT3-positive Relapsed/Refractory Acute Myeloid Leukemia	FLT3-positive Relapsed/ Refractory AML	FLT3	I	18	2022	2025	Recruiting
NCT05445011	Anti-FLT3 CAR-T Cell (TAA05 Cell Injection) in the Treatment of Relapsed/Refractory Acute Myeloid Leukemia	AML	FLT3	I	12	2022	2027	Recruiting
NCT03018405	A Dose Escalation Phase I Study to Assess the Safety and Clinical Activity of Multiple Cancer Indications	MDS/AML/MM	NKG2D	I	146	2016	2021	Unknown
NCT04658004	NKG2D CAR-T Cell Therapy for Patients With Relapsed and/or Refractory Acute Myeloid Leukemia	AML	NKG2D	I	36	2021	2027	Not yet recruiting
NCT04599543	IL3 CAR-T Cell Therapy for Patients With CD123 Positive Relapsed and/or Refractory Acute Myeloid Leukemia	AML	IL3	I	36	2020	2026	Not yet recruiting
NCT05266950	Safety and Efficacy Study of CI-135 CAR-T Cells in Subjects With Relapsed or Refractory Acute Myeloid Leukemia	AML	CI-135	I	7	2021	2023	Recruiting

(Continued on following page)

10.3389/fphar.2023.1151032

TABLE 3 (*Continued*) Current clinical trials using CAR T-cell for immunotherapy of AML.

Trial identifier	Study name	Conditions	Antigen	Phases	Enrollment	Start date	Completion date	Status
NCT04803929	Clinical Study of Anti-ILT3 CAR-T Therapy for R/R AML (M4/M5)	AML	ILT3	I	25	2021	2026	Recruiting
NCT05463640	Evaluate the Safety and Efficacy of ADGRE2 CAR-T in Patients With R/R AML	AML	ADGRE2	I	20	2022	2022	Not yet recruiting
NCT05488132	Administration of Anti-siglec-6 CAR-T Cell Therapy in Relapsed and Refractory Acute Myeloid Leukemia (rr/AML)	Refractory/ Relapse AML	Siglec-6	I/II	20	2022	2025	Recruiting
NCT03795779	CLL1-CD33 cCAR in Patients With Relapsed and/or Refractory, High Risk Hematologic Malignancies	HM	CLL1/ CD33	I	20	2018	2022	Recruiting
		AML						
		MSD						
		CML						
NCT05016063	Dual CD33-CLL1-CAR-T Cells in the Treatment of Relapsed/Refractory Acute Myeloid Leukemia	AML	CD33/ CLL1	I	32	2021	2023	Not yet recruiting
NCT05248685	Optimized Dual CD33/CLL1 CAR T Cells in Subjects With Refractory or Relapsed Acute Myeloid Leukemia	AML	CD33/ CLL1	I	20	2022	2024	Recruiting
NCT05467254	Evaluate the Safety and Efficacy of CLL1+CD33 CAR-T in Patients With R/R AML	AML	CLL1/ CD33	I	20	2022	2025	Not yet recruiting
NCT04010877	Multiple CAR-T Cell Therapy Targeting AML	AML	CLL1, CD33/ CD123	I/II	10	2019	2023	Recruiting
NCT03222674	Multi-CAR T-cell Therapy for Acute Myeloid Leukemia	AML	Multiple	I/II	10	2017	2020	Unknown
NCT03291444	CAR-T Cells Combined With Peptide Specific Dendritic Cell in Relapsed/Refractory Leukemia/MDS	AML	Multiple	I	30	2017	2025	Recruiting
NCT04766840	Donor-derived CAR-T Cells in the Treatment of AML Patients	AML	Multiple	I	9	2021	2023	Not yet recruiting

10.3389/fphar.2023.1151032

demonstrating long-term efficacy (Ritchie et al., 2013). CLL-1 is strongly expressed on AML cells and not detectable on normal HSCs, making it an ideal target in immunotherapy for AML. In a phase I trial that included 10 adult participants with relapsed or refractory AML, chemotherapy coupled with CLL-1 CAR-T cell therapy achieved a CR rate of 70% when followed up to a median period of 173 days, proving that CLL-1 CAR-T cell therapy can mitigate the risk of relapse and improve patient survival (Jin et al., 2022). CLL-1 CAR-T cells with PD-1 knockdown show a successful therapy in patients and represent a feasible immunotherapeutic alternative for treating relapsed or refractory AML (Lin et al., 2021; Ma et al., 2022). Recently, CAR-T cell treatments targeting new potential protein markers (e.g., Siglec-6 and CD70) have been reported. Siglec-6 and CD70 are found on the surface of most AML cells, but are rare or absent in normal BM. Experiments on Siglec-6 and CD70 CAR-T cells in both human and animal models show anti-AML activity and ability to expand and persist (Jetani et al., 2021; Sauer et al., 2021). Based on the CD70 target immunotherapy, the modified CD70-targeted CAR by CD8 non-cleavable hinge method enhance binding capability and expansion, resulting in higher antitumor potency (Leick et al., 2022). Despite the growing number of early-phase studies showing potent antitumor responses of multiple CAR-T cells in recent years, translation into clinical practice and benefits has been slow and challenging. In several early phase clinical trials (Table 3), some adults have received AML CAR-T cell immunotherapy. All NKG2D, CD123, and CD33 have been studied extensively, which are described below.

NKG2D CAR-T

NKG2D ligands are selectively expressed on monoblastic cells in AML, but absent or weakly expressed on myeloblastic cells and chemotherapy-resistant leukemic stem cells in AML, which avoid NK-mediated killing and cause immune evasion (Diermayr et al., 2008; Paczulla et al., 2019). Therefore, inhibitor-mediated activation of surface NKG2D ligands is a useful approach to immunotherapy of AML. Based on this, bispecific FLT3 antibody system (scFv)/NKG2D-CAR T cells have been designed, effectively eradicating AML cells in preclinical study (Li et al., 2022). NKG2D CAR and IL-15 constitutively expressed enhance the efficacy and significantly prolong the mouse survival in the KG-1 AML model.

The safety and lymphodepleting conditioning chemotherapy in participants with AML/MDS or relapsed/refractory multiple myeloma were assessed in a phase I trial (NCT02203825) with dose escalation design (Baumeister et al., 2019). A NKG2D CAR was constructed by human NKG2D linked to CD3ζ signaling domain. Following the treatment, no dose-limiting toxicities, cytokine release syndrome, or neurological toxicities associated with CAR T cells were reported. No autoimmune disorders or serious adverse reactions were found to be associated with NKG2D-based CAR-T cells. NKG2D CAR-T cells were not expanded or persisted in the majority of patients, which is in agreement with murine models in which repeat infusions are needed to eliminate the tumor completely (Barber et al., 2011). As a highly conserved receptor, NKG2D is less likely to elicit immune responses. Additional CAR trials (NCT03018405) assessing multiple infusions and higher doses are underway to further establish the safety profile of NKG2D CAR therapy (Sallman et al., 2018).

CD123 CAR-T

CD123 is a poor prognostic antigen marker found on AML cells and chemo-resistant leukemic stem cells. Anti-CD123 CAR-T therapy was able to eradicate AML blasts in experiments (Arcangeli et al., 2017). Gene-edited CAR-T cells targeting CD123 are primarily directed against AML cells, with tolerable toxicity to normal cells (Sugita et al., 2022).

An early phase I pilot study sponsored by the University of Pennsylvania (NCT02623582) sought to evaluate autologous T lymphocytes containing anti-CD123 linked to TCR/4-1BB domains in AML patients (Tasian, 2018). Five adult subjects with relapsed/refractory AML were given lymphodepleting chemotherapy prior to the CD123 CAR-T cells infusion. However, this trial was eventually terminated because the regimen had induced little anti-leukemic efficacy and on target/off tumor toxicologic effects had been reported. Another phase I trial also reported preliminary results using lentiviral infected T cells to express a CAR targeting CD123 (NCT02159495). CD123-based CAR-T cell treatment induced complete remission in some participants, who became eligible for a second HSCT. Moreover, other drugs such as demethylating agents can augment immune responses and facilitate clearance of tumor cells by CD123-targeting CAR-T cells (El Khawanky et al., 2021). New CD123-directed CAR-T cells were engineered by the rapidly switchable universal CAR-T platform and retain complete anti-AML potency as well as ensuring improved safety of CD123-based immunotherapy in different applications. Currently, a dose-escalating clinical trial is ongoing to assess the therapeutic benefit of this new study drug (NCT04230265) (Loff et al., 2020). Other clinical trials for CD123 CAR-T cells are ongoing including NCT03766126, NCT03114670, NCT03190278, and NCT03631576.

CD33 CAR-T

The CD33 antigen exhibits high expression levels in AML blasts; however, normal myeloid progenitors also express CD33 antigen, limiting its potential as an immunotherapeutic target for AML (Ehninger et al., 2014). An *in vivo* NSG mice model experimenting with AML xenotransplantation has reported significant reduction of leukemic burden and prolonged survival (O'Hear et al., 2015).

Worldwide, several other trials of anti-CD33 CAR T cells for the treatment of AML are underway. A safety test of varying doses of CD33-CAR-T cells in patients with $CD33^+$ AML was conducted by the MD Anderson Cancer Center (MDACC) (NCT03126864). The results found that CAR-T cell production was only possible in cohorts with increased lymphocyte levels and decreased blood cells, but along with systemic inflammatory syndrome and neurotoxic effects

(Tambaro et al., 2021). Chinese PLA General Hospital is conducting an early phase I trial (NCT01864902) and will assess the safety and feasibility of CD33-engineered lymphocyte therapy in patients with AML that is relapsed or not responding to chemotherapy. After initial treatment, one participant with relapsed AML who had previously received an infusion of CD33 CAR T cells had a noticeable decrease in blast count in BM; however these AML blasts subsequently recovered, and relapse occurred 2 months post infusion (Wang et al., 2015). A preclinical experiment evaluated six CD33 CAR constructs using scFv containing CD3ζ domain and showed antileukemia activity, which results in a clinical trial for relapsed/refractory childhood AML (NCT03971799) (Qin et al., 2021). Additional clinical trials with CD33-CAR-T cell strategies are underway (NCT03927261).

To achieve optimal therapeutic effect, the preferred marker in CAR-T treatment should be present in the majority of cancer cells including the subpopulation of cancer stem cells in a substantial percentage of patients. Moreover, to avoid undesired toxicity, the candidate target should not be present on normal tissues or on CAR T cells to avert unwanted self-elimination of CAR T cells. Without a favorable target such as CD19, it is of critical importance to develop a generalizable and combinatorial targeting approach that allows identification of several promising target pairings in AML CAR-T therapy. It was found that AML cells were associated with overexpression of CD33/TIM3 and CLL1/TIM3 as compared to normal tissues when analyzing the density of CD33, CD123, TIM3, among other antigens, on AML bulk and LSCs at initial diagnosis and relapse (Haubner et al., 2019). Like bispecific antibody, CD33/TIM3 or CLL1/TIM3 may serve as viable targets to improve treatment efficiency while limiting toxicity during CAR-T therapy in AML patients. Meanwhile, CD33/CLL-1 is a preferential generic combinatorial immunotarget in pediatric AML (Willier et al., 2021). Moreover, the combination of CAR-T cells and other drugs such as targeted/chemotherapy agents has synergistic effect on AML (El Khawanky et al., 2021; Li et al., 2022). Also, the feasibility of constructing an antigen specific to AML can be considered by removing CD33 from normal cells to overcome resistance to CD33-directed therapy and realize on-target effects with CAR-T cells (Kim et al., 2018).

TCR-T cell therapy

Similar to CAR-T cells, TCR-T cells is belonged to adoptive cell therapy with antigen-specific T cells, and was successfully adopted and transferred in mice in 1986. TCR-T cell therapy targeting New York esophageal squamous cell carcinoma (NY-ESO)-1 has achieved remarkable clinical benefits in the treatment of solid tumors (D'Angelo et al., 2018; Robbins et al., 2011). TCR-T cell specific for MAGE-A4, HA-1H, WT1 are potential strategies for hematological malignancies (Kageyama et al., 2015; Tawara et al., 2017; van Balen et al., 2020; Vasileiou et al., 2021).

In several clinical trials, WT1-specific TCR-T cells has shown strong clinical responses with tolerated safety for AML patients (Tawara, I. et al. S, 2017). Moreover, numerous clinical trials are underway to evaluate other antigen-specific TCR-T cells in AML. Recently, Kang et al. reviewed the update and challenges of TCR-T for AML. TCR-T exhibits a promising tool for AML patients according to the benefit efficacy of clinical trials. However, the toxicity produced in the treatment process and the persistence of *in vivo* TCR-T cells should be the urgent problems of TCR-T immunotherapy.

Conclusion

In this review, we summarized the recent advances for AML immunotherapies and noted the representative emerging strategies. The immunotherapy as a treatment option for AML patients with relapse has shown great promise. However, several limitations to the AML immunotherapy are limited its application in AML. Immune evasion remains a clinical challenge in effectively implementing immunotherapeutic strategies. AML is a complex disorder associated with distinctive genetic features and accumulation of genetic aberrations. The lower level of mutation load in AML would lead to higher chance of immune escape of the immune system and less neoantigen epitopes when compared to melanoma and other types of solid cancers such as lung cancer. Considering reduced mutation load, a core issue around AML requiring further exploration is the extent of immunogenicity. Therefore, clinical success of immune therapy in AML will depend on at least the following efforts: exploiting immune escape mechanism and identifying specific targets.

AML has a distinct pattern of development and progression, and there is a paucity of data on the mechanisms of immune activation or tolerance. The mechanisms underlying antitumor immune responses are well understood and the strategies of immune evasion employed by solid tumors have been studied extensively. Accumulating evidence suggests that certain immune evasion mechanisms are exclusive to AML despite the fact that PD1/L1, among other immune escape pathways, are shared with solid malignancies. Although currently encountering various obstacles, the progress in exploring the mechanisms by which immune surveillance and evasion take place in AML can be attained *via* genetically modified AML models reconstructing the disease. Moreover, integrated data on antigens coupled with analytical platforms to screen out truly AML-specific antigen markers are required. Up till now, transcriptome analyses are mainly used for screening candidate AML targets assuming a direct link between mRNA abundance and protein expression. This complex correlation cannot represent the complete set of proteins expressed by the cell, due to numerous factors such as variations in drug metabolism and mechanisms of post-transcriptional regulation. Therefore, integrative analysis of RNA transcripts and proteins should be performed to complement mRNA or protein expression analysis. In addition, coupling advanced proteomics analytical approaches with plasma membrane proteome enrichment will facilitate direct assessment of surface proteins. In summary, because of the heterogeneous nature of AML, each patient may present distinct cytogenetic aberrations and chromosomal rearrangements that require biomarker-specific individualized treatment. Therefore, tailored treatments combining different forms of immunotherapy with chemotherapy and autologous or allogeneic SCT hold immense promise.

Author contributions

YC wrote the manuscript. JW designed the structure of the paper. FZ drawed the figure and tables. PL proofread the paper. All authors read and approved the final manuscript.

Funding

This work was supported by the National Natural Science Foundation of China (No. 81960032 and 82170168). Science and Technology Program of Guizhou Province Health Committee (No. gzwkj 2019-2-11 and gzwkj 2021-158). Translational Research Grant of NCRCH (2021WWB01).

Conflict of interest

The authors declare that the research was conducted in the absence of any commercial or financial relationships that could be construed as a potential conflict of interest.

Publisher's note

References

Abbas, H. A., Hao, D., Tomczak, K., Barrodia, P., Im, J. S., Reville, P. K., et al. (2021). Single cell T cell landscape and T cell receptor repertoire profiling of AML in context of PD-1 blockade therapy. *Nat. Commun.* 12, 6071. doi:10.1038/s41467-021-26282-z

Albring, J. C., Inselmann, S., Sauer, T., Schliemann, C., Altvater, B., Kailayangiri, S., et al. (2017). PD-1 checkpoint blockade in patients with relapsed AML after allogeneic stem cell transplantation. *Bone Marrow Transplant.* 52, 317–320. doi:10.1038/bmt.2016.274

American Society of Hematology (2016). *Third patient death reported in SL-401 drug trial for patients with BPDCN and AML*. San Diego: ASH Clinical News.

Anguille, S., Smits, E. L., Bryant, C., Van Acker, H. H., Goossens, H., Lion, E., et al. (2015). Dendritic cells as pharmacological tools for cancer immunotherapy. *Pharmacol. Rev.* 67, 731–753. doi:10.1124/pr.114.009456

Anguille, S., Van de Velde, A. L., Smits, E. L., Van Tendeloo, V. F., Juliusson, G., Cools, N., et al. (2017). Dendritic cell vaccination as postremission treatment to prevent or delay relapse in acute myeloid leukemia. *Blood* 130, 1713–1721. doi:10.1182/blood-2017-04-780155

Ansell, S. M., Lesokhin, A. M., Borrello, I., Halwani, A., Scott, E. C., Gutierrez, M., et al. (2015). PD-1 blockade with nivolumab in relapsed or refractory Hodgkin's lymphoma. *N. Engl. J. Med.* 372, 311–319. doi:10.1056/nejmoa1411087

Arcangeli, S., Rotiroti, M. C., Bardelli, M., Simonelli, L., Magnani, C. F., Biondi, A., et al. (2017). Balance of anti-cd123 chimeric antigen receptor binding affinity and density for the targeting of acute myeloid leukemia. *Mol. Ther.* 25, 1933–1945. doi:10.1016/j.ymthe.2017.04.017

Armand, P., Engert, A., Younes, A., Fanale, M., Santoro, A., Zinzani, P. L., et al. (2018). Nivolumab for relapsed/refractory classic Hodgkin lymphoma after failure of autologous hematopoietic cell transplantation: Extended follow-up of the multicohort single-arm phase II CheckMate 205 trial. *J. Clin. Oncol.* 36, 1428–1439. doi:10.1200/JCO.2017.76.0793

Augsberger, C., Hänel, G., Xu, W., Pulko, V., Hanisch, L. J., Augustin, A., et al. (2021). Targeting intracellular WT1 in AML with a novel RMF-peptide-MHC-specific T-cell bispecific antibody. *Blood* 138, 2655–2669. doi:10.1182/blood.2020010477

Author Anonymous (2010). Tremelimumab. *Drugs R&D* 10, 123–132. doi:10.2165/11584530-000000000-00000

Bakst, R., Powers, A., and Yahalom, J. (2020). Diagnostic and therapeutic considerations for extramedullary leukemia. *Curr. Oncol. Rep.* 22, 75. doi:10.1007/s11912-020-00919-6

Barber, A., Meehan, K. R., and Sentman, C. L. (2011). Treatment of multiple myeloma with adoptively transferred chimeric NKG2D receptor-expressing T cells. *Gene Ther.* 18, 509–516. doi:10.1038/gt.2010.174

Baron, J., and Wang, E. S. (2018). Gemtuzumab ozogamicin for the treatment of acute myeloid leukemia. *Expert Rev. Clin. Pharmacol.* 11, 549–559. doi:10.1080/17512433.2018.1478725

Baumeister, S. H., Murad, J., Werner, L., Daley, H., Trebeden-Negre, H., Gicobi, J. K., et al. (2019). Phase I trial of autologous CAR T cells targeting NKG2D ligands in patients with AML/MDS and multiple myeloma. *Cancer Immunol. Res.* 7, 100–112. doi:10.1158/2326-6066.cir-18-0307

Bergmann, L., Miething, C., Maurer, U., Brieger, J., Karakas, T., Weidmann, E., et al. (1997). High levels of Wilms' tumor gene (wt1) mRNA in acute myeloid leukemias are associated with a worse long-term outcome. *Blood* 90, 1217–1225. doi:10.1182/blood.v90.3.1217.1217_1217_1225

Berthon, C., Driss, V., Liu, J., Kuranda, K., Leleu, X., Jouy, N., et al. (2010). In acute myeloid leukemia, B7-H1 (PD-L1) protection of blasts from cytotoxic T cells is induced by TLR ligands and interferon-gamma and can be reversed using MEK inhibitors. *Cancer Immunol. Immunother.* 59, 1839–1849. doi:10.1007/s00262-010-0909-y

Bonnevaux, H., Guerif, S., Albrecht, J., Jouannot, E., De Gallier, T., Beil, C., et al. (2021). Pre-clinical development of a novel CD3-CD123 bispecific T-cell engager using cross-over dual-variable domain (CODV) format for acute myeloid leukemia (AML) treatment. *Oncoimmunology* 10, 1945803. doi:10.1080/2162402X.2021.1945803

Brauneck, F., Haag, F., Woost, R., Wildner, N., Tolosa, E., Rissiek, A., et al. (2021). Increased frequency of TIGIT(+)CD73-CD8(+) T cells with a TOX(+) TCF-1low profile in patients with newly diagnosed and relapsed AML. *Oncoimmunology* 10, 1930391. doi:10.1080/2162402X.2021.1930391

Brayer, J., Lancet, J. E., Powers, J., List, A., Balducci, L., Komrokji, R., et al. (2015). WT1 vaccination in AML and MDS: A pilot trial with synthetic analog peptides. *Am. J. Hematol.* 90, 602–607. doi:10.1002/ajh.24014

Bross, P. F., Beitz, J., Chen, G., Chen, X. H., Duffy, E., Kieffer, L., et al. (2001). Approval summary: Gemtuzumab ozogamicin in relapsed acute myeloid leukemia. *Clin. Cancer Res.* 7, 1490–1496.

Bruedigam, C., Bagger, F. O., Heidel, F. H., Paine Kuhn, C., Guignes, S., Song, A., et al. (2014). Telomerase inhibition effectively targets mouse and human AML stem cells and delays relapse following chemotherapy. *Cell stem Cell* 15, 775–790. doi:10.1016/j.stem.2014.11.010

By The ASCO Post Staff (2017). *Phase III CASCADE trial of vadastuximab talirine in front-line AML discontinued*. Chicago: ASCO Post.

Byun, D. J., Wolchok, J. D., Rosenberg, L. M., and Girotra, M. (2017). Cancer immunotherapy - immune checkpoint blockade and associated endocrinopathies. *Nat. Rev. Endocrinol.* 13, 195–207. doi:10.1038/nrendo.2016.205

Cancer Genome Atlas Research, N., Ley, T. J., Miller, C., Ding, L., Raphael, B. J., Mungall, A. J., et al. (2013). Genomic and epigenomic landscapes of adult de novo acute myeloid leukemia. *N. Engl. J. Med.* 368, 2059–2074. doi:10.1056/NEJMoa1301689

Chalmers, Z. R., Connelly, C. F., Fabrizio, D., Gay, L., Ali, S. M., Ennis, R., et al. (2017). Analysis of 100,000 human cancer genomes reveals the landscape of tumor mutational burden. *Genome Med.* 9, 34. doi:10.1186/s13073-017-0424-2

Chapuis, A. G., Egan, D. N., Bar, M., Schmitt, T. M., McAfee, M. S., Paulson, K. G., et al. (2019). T cell receptor gene therapy targeting WT1 prevents acute myeloid leukemia relapse post-transplant. *Nat. Med.* 25, 1064–1072. doi:10.1038/s41591-019-0472-9

Chen, C., Liang, C., Wang, S., Chio, C. L., Zhang, Y., Zeng, C., et al. (2020). Expression patterns of immune checkpoints in acute myeloid leukemia. *J. Hematol. Oncol.* 13, 28. doi:10.1186/s13045-020-00853-x

Chen, X., Liu, S., Wang, L., Zhang, W., Ji, Y., and Ma, X. (2008). Clinical significance of B7-H1 (PD-L1) expression in human acute leukemia. *Cancer Biol. Ther.* 7, 622–627. doi:10.4161/cbt.7.5.5689

Chen, Y., Tan, J., Huang, S., Huang, X., Huang, J., Chen, J., et al. (2020). Higher frequency of the CTLA-4(+) LAG-3(+) T-cell subset in patients with newly diagnosed acute myeloid leukemia. *Asia-Pacific J. Clin. Oncol.* 16, e12–e18. doi:10.1111/ajco.13236

Chevallier, P., Saiagh, S., Dehame, V., Guillaume, T., Peterlin, P., Bercegeay, S., et al. (2021). A phase I/II feasibility vaccine study by autologous leukemic apoptotic corpse-pulsed dendritic cells for elderly AML patients. *Hum. Vaccines Immunother.* 17, 3511–3514. doi:10.1080/21645515.2021.1943991

Coombs, C. C., Tallman, M. S., and Levine, R. L. (2016). Molecular therapy for acute myeloid leukaemia. *Nat. Rev. Clin. Oncol.* 13, 305–318. doi:10.1038/nrclinonc.2015.210

Cortes, J. E., Tallman, M. S., Schiller, G. J., Trone, D., Gammon, G., Goldberg, S. L., et al. (2018). Phase 2b study of 2 dosing regimens of quizartinib monotherapy in FLT3-ITD-mutated, relapsed or refractory AML. *Blood* 132, 598–607. doi:10.1182/blood-2018-01-821629

Cortes, J. E., de Lima, M., Dombret, H., Estey, E. H., Giralt, S. A., Montesinos, P., et al. (2020). Prevention, recognition, and management of adverse events associated with gemtuzumab ozogamicin use in acute myeloid leukemia. *J. Hematol. Oncol.* 13, 137. doi:10.1186/s13045-020-00975-2

Counter, C. M., Gupta, J., Harley, C. B., Leber, B., and Bacchetti, S. (1995). Telomerase activity in normal leukocytes and in hematologic malignancies. *Blood* 85, 2315–2320. doi:10.1182/blood.v85.9.2315.bloodjournal8592315

Cruz, N. M., Sugita, M., Ewing-Crystal, N., Lam, L., Galetto, R., Gouble, A., et al. (2018). Selection and characterization of antibody clones are critical for accurate flow cytometry-based monitoring of CD123 in acute myeloid leukemia. *Leukemia lymphoma* 59, 978–982. doi:10.1080/10428194.2017.1361023

D'Angelo, S. P., Melchiori, L., Merchant, M. S., Bernstein, D., Glod, J., Kaplan, R., et al. (2018). Antitumor activity associated with prolonged persistence of adoptively transferred NY-ESO-1 (c259)T cells in synovial sarcoma. *Cancer Discov.* 8, 944–957. doi:10.1158/2159-8290.CD-17-1417

Daver, N., Garcia-Manero, G., Basu, S., Boddu, P. C., Alfayez, M., Cortes, J. E., et al. (2018). Efficacy, safety, and biomarkers of response to azacitidine and nivolumab in relapsed/refractory acute myeloid leukemia: A nonrandomized, open-label, phase II study. *Cancer Discov.* 9, 370–383. doi:10.1158/2159-8290.CD-18-0774

Daver, N., Garcia-Manero, G., Basu, S., Boddu, P. C., Alfayez, M., Cortes, J. E., et al. (2019). Efficacy, safety, and biomarkers of response to azacitidine and nivolumab in relapsed/refractory acute myeloid leukemia: A nonrandomized, open-label, phase II study. *Cancer Discov.* 9, 370–383. doi:10.1158/2159-8290.CD-18-0774

Davids, M. S., Kim, H. T., Bachireddy, P., Costello, C., Liguori, R., Savell, A., et al. (2016). Ipilimumab for patients with relapse after allogeneic transplantation. *N. Engl. J. Med.* 375, 143–153. doi:10.1056/NEJMoa1601202

Davila, M. L., Riviere, I., Wang, X., Bartido, S., Park, J., Curran, K., et al. (2014). Efficacy and toxicity management of 19-28z CAR T cell therapy in B cell acute lymphoblastic leukemia. *Sci. Transl. Med.* 6, 224ra225. doi:10.1126/scitranslmed.3008226

De Kouchkovsky, I., and Abdul-Hay, M.' (2016). Acute myeloid leukemia: A comprehensive review and 2016 update. *Blood cancer J.* 6, e441. doi:10.1038/bcj.2016.50

Deng, M., Gui, X., Kim, J., Xie, L., Chen, W., Li, Z., et al. (2018). LILRB4 signalling in leukaemia cells mediates T cell suppression and tumour infiltration. *Nature* 562, 605–609. doi:10.1038/s41586-018-0615-z

Diermayr, S., Himmelreich, H., Durovic, B., Mathys-Schneeberger, A., Siegler, U., Langenkamp, U., et al. (2008). NKG2D ligand expression in AML increases in response to HDAC inhibitor valproic acid and contributes to allorecognition by NK-cell lines with single KIR-HLA class I specificities. *Blood* 111, 1428–1436. doi:10.1182/blood-2007-07-101311

Dohner, H., Estey, E. H., Amadori, S., Appelbaum, F. R., Büchner, T., Burnett, A. K., et al. (2010). Diagnosis and management of acute myeloid leukemia in adults: Recommendations from an international expert panel, on behalf of the European LeukemiaNet. *Blood* 115, 453–474. doi:10.1182/blood-2009-07-235358

Dong, Y., Han, Y., Huang, Y., Jiang, S., Huang, Z., Chen, R., et al. (2020). PD-L1 is expressed and promotes the expansion of regulatory T cells in acute myeloid leukemia. *Front. Immunol.* 11, 1710. doi:10.3389/fimmu.2020.01710

Dratwa, M., Wysoczańska, B., Butrym, A., Łacina, P., Mazur, G., and Bogunia-Kubik, K. (2021). TERT genetic variability and telomere length as factors affecting survival and risk in acute myeloid leukaemia. *Sci. Rep.* 11, 23301. doi:10.1038/s41598-021-02767-1

Ehninger, A., Kramer, M., Röllig, C., Thiede, C., Bornhäuser, M., von Bonin, M., et al. (2014). Distribution and levels of cell surface expression of CD33 and CD123 in acute myeloid leukemia. *Blood Cancer J.* 4, e218. doi:10.1038/bcj.2014.39

El Khawanky, N., Hughes, A., Yu, W., Myburgh, R., Matschulla, T., Taromi, S., et al. (2021). Demethylating therapy increases anti-CD123 CAR T cell cytotoxicity against acute myeloid leukemia. *Nat. Commun.* 12, 6436. doi:10.1038/s41467-021-26683-0

Erba, H. P., Levy, M. Y., Vasu, S., Stein, A. S., Fathi, A. T., Maris, M. B., et al. (2016). A phase 1b study of vadastuximab talirine in combination with 7+3 induction therapy for patients with newly diagnosed acute myeloid leukemia (AML). *Blood* 128 (22), 211. doi:10.1182/blood.v128.22.211.211

Eroglu, Z., Zaretsky, J. M., Hu-Lieskovan, S., Kim, D. W., Algazi, A., Johnson, D. B., et al. (2018). High response rate to PD-1 blockade in desmoplastic melanomas. *Nature* 553, 347–350. doi:10.1038/nature25187

Fathi, A. T., Erba, H. P., Lancet, J. E., Stein, E. M., Ravandi, F., Faderl, S., et al. (2018). A phase 1 trial of vadastuximab talirine combined with hypomethylating agents in patients with CD33-positive AML. *Blood* 132, 1125–1133. doi:10.1182/blood-2018-03-841171

Feldman, E. J., Brandwein, J., Stone, R., Kalaycio, M., Moore, J., O'Connor, J., et al. (2005). Phase III randomized multicenter study of a humanized anti-CD33 monoclonal antibody, lintuzumab, in combination with chemotherapy, versus chemotherapy alone in patients with refractory or first-relapsed acute myeloid leukemia. *J. Clin. Oncol.* 23, 4110–4116. doi:10.1200/jco.2005.09.133

Feng, Z., Fang, Q., Kuang, X., Liu, X., Chen, Y., Ma, D., et al. (2020). Clonal expansion of bone marrow CD8(+) T cells in acute myeloid leukemia patients at new diagnosis and after chemotherapy. *Am. J. Cancer Res.* 10, 3973–3989.

Ferrando, A. A., and Lopez-Otin, C. (2017). Clonal evolution in leukemia. *Nat. Med.* 23, 1135–1145. doi:10.1038/nm.4410

Ferrara, F., and Schiffer, C. A. (2013). Acute myeloid leukaemia in adults. *Lancet* 381, 484–495. doi:10.1016/s0140-6736(12)61727-9

Fevery, S., Billiau, A. D., Sprangers, B., Rutgeerts, O., Lenaerts, C., Goebels, J., et al. (2007). CTLA-4 blockade in murine bone marrow chimeras induces a host-derived antileukemic effect without graft-versus-host disease. *Leukemia* 21, 1451–1459. doi:10.1038/sj.leu.2404720

Finn Le, L. M., Orozco, J. J., Park, J. H., Atallah, E., and Craig, M. (2017). A phase 2 study of actinium-225-lintuzumab in older patients with previously untreated acute myeloid leukemia (AML) unfit for intensive chemotherapy. *Blood* 130 (1), 2638.

Friedman, C. F., Proverbs-Singh, T. A., and Postow, M. A. (2016). Treatment of the immune-related adverse effects of immune checkpoint inhibitors: A review. *JAMA Oncol.* 2, 1346–1353. doi:10.1001/jamaoncol.2016.1051

Germeau, C., Ma, W., Schiavetti, F., Lurquin, C., Henry, E., Vigneron, N., et al. (2005). High frequency of antitumor T cells in the blood of melanoma patients before and after vaccination with tumor antigens. *J. Exp. Med.* 201, 241–248. doi:10.1084/jem.20041379

Gettinger, S., Choi, J., Hastings, K., Truini, A., Datar, I., Sowell, R., et al. (2017). Impaired HLA class I antigen processing and presentation as a mechanism of acquired resistance to immune checkpoint inhibitors in lung cancer. *Cancer Discov.* 7, 1420–1435. doi:10.1158/2159-8290.CD-17-0593

Giroux Leprieur, E., Dumenil, C., Julie, C., Giraud, V., Dumoulin, J., Labrune, S., et al. (2017). Immunotherapy revolutionises non-small-cell lung cancer therapy: Results, perspectives and new challenges. *Eur. J. Cancer* 78, 16–23. doi:10.1016/j.ejca.2016.12.041

Gordon, S. R., Maute, R. L., Dulken, B. W., Hutter, G., George, B. M., McCracken, M. N., et al. (2017). PD-1 expression by tumour-associated macrophages inhibits phagocytosis and tumour immunity. *Nature* 545, 495–499. doi:10.1038/nature22396

Goswami, M., Gui, G., Dillon, L. W., Lindblad, K. E., Thompson, J., Valdez, J., et al. (2022). Pembrolizumab and decitabine for refractory or relapsed acute myeloid leukemia. *J. Immunother. Cancer* 10, e003392. doi:10.1136/jitc-2021-003392

Greaves, M. (2016). Leukaemia 'firsts' in cancer research and treatment. *Nat. Rev. Cancer* 16, 163–172. doi:10.1038/nrc.2016.3

Greiner, J., Götz, M., Hofmann, S., Schrezenmeier, H., Wiesneth, M., Bullinger, L., et al. (2020). Specific T-cell immune responses against colony-forming cells including leukemic progenitor cells of AML patients were increased by immune checkpoint inhibition. *Cancer Immunol. Immunother.* 69, 629–640. doi:10.1007/s00262-020-02490-2

Grupp, S. A., Kalos, M., Barrett, D., Aplenc, R., Porter, D. L., Rheingold, S. R., et al. (2013). Chimeric antigen receptor-modified T cells for acute lymphoid leukemia. *N. Engl. J. Med.* 368, 1509–1518. doi:10.1056/NEJMoa1215134

Gurusamy, D., Clever, D., Eil, R., and Restifo, N. P. (2017). Novel "elements" of immune suppression within the tumor microenvironment. *Cancer Immunol. Res.* 5, 426–433. doi:10.1158/2326-6066.CIR-17-0117

Haanen, J. (2017). Converting cold into hot tumors by combining immunotherapies. *Cell* 170, 1055–1056. doi:10.1016/j.cell.2017.08.031

Hartley, J. A. (2021). Antibody-drug conjugates (ADCs) delivering pyrrolobenzodiazepine (PBD) dimers for cancer therapy. *Expert Opin. Biol. Ther.* 21, 931–943. doi:10.1080/14712598.2020.1776255

Haubner, S., Perna, F., Köhnke, T., Schmidt, C., Berman, S., Augsberger, C., et al. (2019). Coexpression profile of leukemic stem cell markers for combinatorial targeted therapy in AML. *Leukemia* 33, 64–74. doi:10.1038/s41375-018-0180-3

He, S. Z., Busfield, S., Ritchie, D. S., Hertzberg, M. S., Durrant, S., Lewis, I. D., et al. (2015). A Phase 1 study of the safety, pharmacokinetics and anti-leukemic activity of the anti-CD123 monoclonal antibody CSL360 in relapsed, refractory or high-risk acute myeloid leukemia. *Leukemia lymphoma* 56, 1406–1415. doi:10.3109/10428194.2014.956316

Hodi, F. S., O'Day, S. J., McDermott, D. F., Weber, R. W., Sosman, J. A., Haanen, J. B., et al. (2010). Improved survival with ipilimumab in patients with metastatic melanoma. *N. Engl. J. Med.* 363, 711–723. doi:10.1056/nejmoa1003466

Huang, J., Tan, J., Chen, Y., Huang, S., Xu, L., Zhang, Y., et al. (2019). A skewed distribution and increased PD-1+Vβ+CD4+/CD8+ T cells in patients with acute myeloid leukemia. *J. Leukoc. Biol.* 106, 725–732. doi:10.1002/jlb.ma0119-021r

Im, S. J., Hashimoto, M., Gerner, M. Y., Lee, J., Kissick, H. T., Burger, M. C., et al. (2016). Defining CD8+ T cells that provide the proliferative burst after PD-1 therapy. *Nature* 537, 417–421. doi:10.1038/nature19330

Jen, E. Y., Gao, X., Li, L., Zhuang, L., Simpson, N. E., Aryal, B., et al. (2020). FDA approval summary: Tagraxofusp-erzs for treatment of blastic plasmacytoid dendritic cell neoplasm. *Clin. Cancer Res.* 26, 532–536. doi:10.1158/1078-0432.CCR-19-2329

Jen, E. Y., Ko, C. W., Lee, J. E., Del Valle, P. L., Aydanian, A., Jewell, C., et al. (2018). FDA approval: Gemtuzumab ozogamicin for the treatment of adults with newly

diagnosed CD33-positive acute myeloid leukemia. *Clin. Cancer Res.* 24, 3242–3246. doi:10.1158/1078-0432.CCR-17-3179

Jetani, H., Navarro-Bailón, A., Maucher, M., Frenz, S., Verbruggen, C., Yeguas, A., et al. (2021). Siglec-6 is a novel target for CAR T-cell therapy in acute myeloid leukemia. *Blood* 138, 1830–1842. doi:10.1182/blood.2020009192

Jin, X., Zhang, M., Sun, R., Lyu, H., Xiao, X., Zhang, X., et al. (2022). First-in-human phase I study of CLL-1 CAR-T cells in adults with relapsed/refractory acute myeloid leukemia. *J. Hematol. Oncol.* 15, 88. doi:10.1186/s13045-022-01308-1

Jitschin, R., Saul, D., Braun, M., Tohumeken, S., Völkl, S., Kischel, R., et al. (2018). CD33/CD3-bispecific T-cell engaging (BiTE®) antibody construct targets monocytic AML myeloid-derived suppressor cells. *J. Immunother. Cancer* 6, 116. doi:10.1186/s40425-018-0432-9

June, C. H., O'Connor, R. S., Kawalekar, O. U., Ghassemi, S., and Milone, M. C. (2018). CAR T cell immunotherapy for human cancer. *Science* 359, 1361–1365. doi:10.1126/science.aar6711

Kadia, T. M., Ravandi, F., Cortes, J., and Kantarjian, H. (2015). Toward individualized therapy in acute myeloid leukemia: A contemporary review. *JAMA Oncol.* 1, 820–828. doi:10.1001/jamaoncol.2015.0617

Kageyama, S., Ikeda, H., Miyahara, Y., Imai, N., Ishihara, M., Saito, K., et al. (2015). Adoptive transfer of MAGE-A4 T-cell receptor gene-transduced lymphocytes in patients with recurrent esophageal cancer. *Clin. Cancer Res.* 21, 2268–2277. doi:10.1158/1078-0432.CCR-14-1559

Kamphorst, A. O., Wieland, A., Nasti, T., Yang, S., Zhang, R., Barber, D. L., et al. (2017). Rescue of exhausted CD8 T cells by PD-1-targeted therapies is CD28-dependent. *Science* 355, 1423–1427. doi:10.1126/science.aaf0683

Kelly, P. N. (2017). CD28 is a critical target for PD-1 blockade. *Science* 355, 1386. doi:10.1126/science.355.6332.1386-b

Khan, N., Hills, R. K., Virgo, P., Couzens, S., Clark, N., Gilkes, A., et al. (2017). Expression of CD33 is a predictive factor for effect of gemtuzumab ozogamicin at different doses in adult acute myeloid leukaemia. *Leukemia* 31, 1059–1068. doi:10.1038/leu.2016.309

Khoury, H. J., Collins, R. H., Jr, Blum, W., Stiff, P. S., Elias, L., Lebkowski, J. S., et al. (2017). Immune responses and long-term disease recurrence status after telomerase-based dendritic cell immunotherapy in patients with acute myeloid leukemia. *Cancer* 123, 3061–3072. doi:10.1002/cncr.30696

Kim, M. Y., Yu, K. R., Kenderian, S. S., Ruella, M., Chen, S., Shin, T. H., et al. (2018). Genetic inactivation of CD33 in hematopoietic stem cells to enable CAR T cell immunotherapy for acute myeloid leukemia. *Cell* 173, 1439–1453. doi:10.1016/j.cell.2018.05.013

Kreutmair, S. (2022). First-in-human study of WT1 recombinant protein vaccination in elderly patients with AML in remission: A single-center experience. *Cancer Immunol. Immunother.* 71 (12), 2913–2928. doi:10.1007/s00262-022-03202-8

Krupka, C., Kufer, P., Kischel, R., Zugmaier, G., Bögeholz, J., Köhnke, T., et al. (2014). CD33 target validation and sustained depletion of AML blasts in long-term cultures by the bispecific T-cell-engaging antibody AMG 330. *Blood* 123, 356–365. doi:10.1182/blood-2013-08-523548

Krupka, C., Kufer, P., Kischel, R., Zugmaier, G., Lichtenegger, F. S., Köhnke, T., et al. (2016). Blockade of the PD-1/PD-L1 axis augments lysis of AML cells by the CD33/CD3 BiTE antibody construct AMG 330: Reversing a T-cell-induced immune escape mechanism. *Leukemia* 30, 484–491. doi:10.1038/leu.2015.214

Kubasch, A. S., Schulze, F., Giagounidis, A., Götze, K. S., Krönke, J., Sockel, K., et al. (2020). Single agent talacotuzumab demonstrates limited efficacy but considerable toxicity in elderly high-risk MDS or AML patients failing hypomethylating agents. *Leukemia* 34, 1182–1186. doi:10.1038/s41375-019-0645-z

Kung Sutherland, M. S., Walter, R. B., Jeffrey, S. C., Burke, P. J., Yu, C., Kostner, H., et al. (2013). SGN-CD33A: A novel CD33-targeting antibody-drug conjugate using a pyrrolobenzodiazepine dimer is active in models of drug-resistant AML. *Blood* 122, 1455–1463. doi:10.1182/blood-2013-03-491506

Kyriakidis, I., Vasileiou, E., Rossig, C., Roilides, E., Groll, A. H., and Tragiannidis, A. (2021). Invasive fungal diseases in children with hematological malignancies treated with therapies that target cell surface antigens: Monoclonal antibodies, immune checkpoint inhibitors and CAR T-cell therapies. *J. Fungi (Basel)* 7, 186. doi:10.3390/jof7030186

Lambert, J., Pautas, C., Terré, C., Raffoux, E., Turlure, P., Caillot, D., et al. (2019). Gemtuzumab ozogamicin for de novo acute myeloid leukemia: Final efficacy and safety updates from the open-label, phase III ALFA-0701 trial. *Haematologica* 104, 113–119. doi:10.3324/haematol.2018.188888

Lamble, A. J., Eidenschink Brodersen, L., Alonzo, T. A., Wang, J., Pardo, L., Sung, L., et al. (2022). CD123 expression is associated with high-risk disease characteristics in childhood acute myeloid leukemia: A report from the children's oncology group. *J. Clin. Oncol.* 40, 252–261. doi:10.1200/JCO.21.01595

Lamble, A. J., Kosaka, Y., Laderas, T., Maffit, A., Kaempf, A., Brady, L. K., et al. (2020). Reversible suppression of T cell function in the bone marrow microenvironment of acute myeloid leukemia. *Proc. Natl. Acad. Sci. U. S. A.* 117, 14331–14341. doi:10.1073/pnas.1916206117

Lane, A. A., Sweet, K. L., Wang, E. S., Donnellan, W. B., Walter, R. B., Stein, A. S., et al. (2016). Results from ongoing phase 2 trial of SL-401 as consolidation therapy in patients with acute myeloid leukemia (AML) in remission with high relapse risk including minimal residual disease (MRD). *Blood* 128 (22), 215. doi:10.1182/blood.v128.22.215.215

Laszlo, G. S., Gudgeon, C. J., Harrington, K. H., and Walter, R. B. (2015). T-cell ligands modulate the cytolytic activity of the CD33/CD3 BiTE antibody construct, AMG 330. *Blood Cancer J.* 5, e340. doi:10.1038/bcj.2015.68

Laszlo, G. S., Harrington, K. H., Gudgeon, C. J., Beddoe, M. E., Fitzgibbon, M. P., Ries, R. E., et al. (2016). Expression and functional characterization of CD33 transcript variants in human acute myeloid leukemia. *Oncotarget* 7, 43281–43294. doi:10.18632/oncotarget.9674

Le, D. T., Uram, J. N., Wang, H., Bartlett, B., Kemberling, H., Eyring, A., et al. (2015). PD-1 blockade in tumors with mismatch-repair deficiency. *N. Engl. J. Med.* 372, LBA100–2520. doi:10.1200/jco.2015.33.18_suppl.lba100

Leick, M. B., Silva, H., Scarfò, I., Larson, R., Choi, B. D., Bouffard, A. A., et al. (2022). Non-cleavable hinge enhances avidity and expansion of CAR-T cells for acute myeloid leukemia. *Cancer Cell* 40, 494–508.e5. doi:10.1016/j.ccell.2022.04.001

Lesokhin, A. M., Ansell, S. M., Armand, P., Scott, E. C., Halwani, A., Gutierrez, M., et al. (2016). Nivolumab in patients with relapsed or refractory hematologic malignancy: Preliminary results of a phase Ib study. *J. Clin. Oncol.* 34, 2698–2704. doi:10.1200/jco.2015.65.9789

Levato, L., and Molica, S. (2018). Rituximab in the management of acute lymphoblastic leukemia. *Expert Opin. Biol. Ther.* 18, 221–226. doi:10.1080/14712598.2018.1425389

Levine, J. H., Simonds, E. F., Bendall, S. C., Davis, K. L., Amir, E. a. D., Tadmor, M. D., et al. (2015). Data-driven phenotypic dissection of AML reveals progenitor-like cells that correlate with prognosis. *Cell* 162, 184–197. doi:10.1016/j.cell.2015.05.047

Li, K. X., Wu, H. Y., Pan, W. Y., Guo, M. Q., Qiu, D. Z., He, Y. J., et al. (2022). A novel approach for relapsed/refractory FLT3(mut+) acute myeloid leukaemia: Synergistic effect of the combination of bispecific FLT3scFv/nkg2d-CAR T cells and gilteritinib. *Mol. Cancer* 21, 66. doi:10.1186/s12943-022-01541-9

Liao, D., Wang, M., Liao, Y., Li, J., and Niu, T. (2019). A review of efficacy and safety of checkpoint inhibitor for the treatment of acute myeloid leukemia. *Front. Pharmacol.* 10, 609. doi:10.3389/fphar.2019.00609

Lin, G., Zhang, Y., Yu, L., and Wu, D. (2021). Cytotoxic effect of CLL-1 CAR-T cell immunotherapy with PD-1 silencing on relapsed/refractory acute myeloid leukemia. *Mol. Med. Rep.* 23, 208. doi:10.3892/mmr.2021.11847

Locke, F. L., Neelapu, S. S., Bartlett, N. L., Siddiqi, T., Chavez, J. C., Hosing, C. M., et al. (2017). Phase 1 results of ZUMA-1: A multicenter study of kte-C19 anti-CD19 CAR T cell therapy in refractory aggressive lymphoma. *Mol. Ther.* 25, 285–295. doi:10.1016/j.ymthe.2016.10.020

Loff, S., Dietrich, J., Meyer, J. E., Riewaldt, J., Spehr, J., von Bonin, M., et al. (2020). Rapidly switchable universal CAR-T cells for treatment of cd123-positive leukemia. *Mol. Ther. Oncolytics* 17, 408–420. doi:10.1016/j.omto.2020.04.009

Ma, Y. J., Dai, H. P., Cui, Q. Y., Cui, W., Zhu, W. J., Qu, C. J., et al. (2022). Successful application of PD-1 knockdown CLL-1 CAR-T therapy in two AML patients with post-transplant relapse and failure of anti-CD38 CAR-T cell treatment. *Am. J. Cancer Res.* 12, 615–621.

Masarova, L., Kantarjian, H., Garcia-Mannero, G., Ravandi, F., Sharma, P., and Daver, N. (2017). Harnessing the immune system against leukemia: Monoclonal antibodies and checkpoint strategies for AML. *Adv. Exp. Med. Biol.* 995, 73–95. doi:10.1007/978-3-319-53156-4_4

Maude, S. L., Frey, N., Shaw, P. A., Aplenc, R., Barrett, D. M., Bunin, N. J., et al. (2014). Chimeric antigen receptor T cells for sustained remissions in leukemia. *N. Engl. J. Med.* 371, 1507–1517. doi:10.1056/NEJMoa1407222

Medeiros, B. C., Tanaka, T. N., Balaian, L., Bashey, A., Guzdar, A., Li, H., et al. (2018). A phase I/II trial of the combination of azacitidine and gemtuzumab ozogamicin for treatment of relapsed acute myeloid leukemia. *Clin. Lymphoma Myeloma Leuk* 18, 346–352.e5. doi:10.1016/j.clml.2018.02.017

Melero, I., Gaudernack, G., Gerritsen, W., Huber, C., Parmiani, G., Scholl, S., et al. (2014). Therapeutic vaccines for cancer: An overview of clinical trials. *Nat. Rev. Clin. Oncol.* 11, 509–524. doi:10.1038/nrclinonc.2014.111

Mohme, M., Riethdorf, S., and Pantel, K. (2017). Circulating and disseminated tumour cells - mechanisms of immune surveillance and escape. *Nat. Rev. Clin. Oncol.* 14, 155–167. doi:10.1038/nrclinonc.2016.144

Montesinos, P., Roboz, G. J., Bulabois, C. E., Subklewe, M., Platzbecker, U., Ofran, Y., et al. (2021). Safety and efficacy of talacotuzumab plus decitabine or decitabine alone in patients with acute myeloid leukemia not eligible for chemotherapy: Results from a multicenter, randomized, phase 2/3 study. *Leukemia* 35, 62–74. doi:10.1038/s41375-020-0773-5

Mussai, F., De Santo, C., Abu-Dayyeh, I., Booth, S., Quek, L., McEwen-Smith, R. M., et al. (2013). Acute myeloid leukemia creates an arginase-dependent immunosuppressive microenvironment. *Blood* 122, 749–758. doi:10.1182/blood-2013-01-480129

Nahas, M. R., Stroopinsky, D., Rosenblatt, J., Cole, L., Pyzer, A. R., Anastasiadou, E., et al. (2019). Hypomethylating agent alters the immune microenvironment in acute myeloid leukaemia (AML) and enhances the immunogenicity of a dendritic cell/AML vaccine. *Br. J. Haematol.* 185, 679–690. doi:10.1111/bjh.15818

Naval Daver, S. B., Garcia-Manero, G., Cortes, J. E., Ravandi, F., Jabbour, E. J., Hendrickson, S., et al. (2016). Phase IB/II study of nivolumab in combination with azacytidine (AZA) in patients (pts) with relapsed acute myeloid leukemia (AML). *Blood* 128, 763. doi:10.1182/blood.v128.22.763.763

Nishino, M., Ramaiya, N. H., Hatabu, H., and Hodi, F. S. (2017). Monitoring immune-checkpoint blockade: Response evaluation and biomarker development. *Nat. Rev. Clin. Oncol.* 14, 655–668. doi:10.1038/nrclinonc.2017.88

O'Hear, C., Heiber, J. F., Schubert, I., Fey, G., and Geiger, T. L. (2015). Anti-CD33 chimeric antigen receptor targeting of acute myeloid leukemia. *Haematologica* 100, 336–344. doi:10.3324/haematol.2014.112748

Ogasawara, M., Miyashita, M., Yamagishi, Y., and Ota, S. (2022). Wilms' tumor 1 peptide-loaded dendritic cell vaccination in patients with relapsed or refractory acute leukemia. *Ther. Apher. Dial.* 26, 537–547. doi:10.1111/1744-9987.13828

Ohyashiki, J. H., Ohyashiki, K., Iwama, H., Hayashi, S., Toyama, K., and Shay, J. W. (1997). Clinical implications of telomerase activity levels in acute leukemia. *Clin. Cancer Res.* 3, 619–625.

Oran, B., Garcia-Manero, G., Saliba, R. M., Alfayez, M., Al-Atrash, G., Ciurea, S. O., et al. (2020). Posttransplantation cyclophosphamide improves transplantation outcomes in patients with AML/MDS who are treated with checkpoint inhibitors. *Cancer* 126, 2193–2205. doi:10.1002/cncr.32796

Paczulla, A. M., Rothfelder, K., Raffel, S., Konantz, M., Steinbacher, J., Wang, H., et al. (2019). Absence of NKG2D ligands defines leukaemia stem cells and mediates their immune evasion. *Nature* 572, 254–259. doi:10.1038/s41586-019-1410-1

Pemmaraju, N., Sweet, K. L., Stein, A. S., Wang, E. S., Rizzieri, D. A., Vasu, S., et al. (2022). Long-term benefits of tagraxofusp for patients with blastic plasmacytoid dendritic cell neoplasm. *J. Clin. Oncol.* 40, 3032–3036. doi:10.1200/JCO.22.00034

Penter, L., Zhang, Y., Savell, A., Huang, T., Cieri, N., Thrash, E. M., et al. (2021). Molecular and cellular features of CTLA-4 blockade for relapsed myeloid malignancies after transplantation. *Blood* 137, 3212–3217. doi:10.1182/blood.2021010867

Perna, F., Berman, S. H., Soni, R. K., Mansilla-Soto, J., Eyquem, J., Hamieh, M., et al. (2017). Integrating proteomics and transcriptomics for systematic combinatorial chimeric antigen receptor therapy of AML. *Cancer Cell* 32, 506–519.e5. doi:10.1016/j.ccell.2017.09.004

Petersdorf, S. H., Kopecky, K. J., Slovak, M., Willman, C., Nevill, T., Brandwein, J., et al. (2013). A phase 3 study of gemtuzumab ozogamicin during induction and postconsolidation therapy in younger patients with acute myeloid leukemia. *Blood* 121, 4854–4860. doi:10.1182/blood-2013-01-466706

Pollard, J. A., Alonzo, T. A., Loken, M., Gerbing, R. B., Ho, P. A., Bernstein, I. D., et al. (2012). Correlation of CD33 expression level with disease characteristics and response to gemtuzumab ozogamicin containing chemotherapy in childhood AML. *Blood* 119, 3705–3711. doi:10.1182/blood-2011-12-398370

Polyzoidis, S., Tuazon, J., Brazil, L., Beaney, R., Al-Sarraj, S. T., Doey, L., et al. (2015). Active dendritic cell immunotherapy for glioblastoma: Current status and challenges. *Br. J. Neurosurg.* 29, 197–205. doi:10.3109/02688697.2014.994473

Qi, Y., Zhao, M., Hu, Y., Wang, Y., Li, P., Cao, J., et al. (2022). Efficacy and safety of CD19-specific CAR T cell-based therapy in B-cell acute lymphoblastic leukemia patients with CNSL. *Blood* 139, 3376–3386. doi:10.1182/blood.2021013733

Qin, H., Yang, L., Chukinas, J. A., Shah, N., Tarun, S., Pouzolles, M., et al. (2021). Systematic preclinical evaluation of CD33-directed chimeric antigen receptor T cell immunotherapy for acute myeloid leukemia defines optimized construct design. *J. Immunother. Cancer* 9, e003149. doi:10.1136/jitc-2021-003149

Ravandi, F., Assi, R., Daver, N., Benton, C. B., Kadia, T., Thompson, P. A., et al. (2019). Idarubicin, cytarabine, and nivolumab in patients with newly diagnosed acute myeloid leukaemia or high-risk myelodysplastic syndrome: A single-arm, phase 2 study. *Lancet. Haematol.* 6, e480–e488. doi:10.1016/S2352-3026(19)30114-0

Reusch, U., Harrington, K. H., Gudgeon, C. J., Fucek, I., Ellwanger, K., Weichel, M., et al. (2016). Characterization of CD33/CD3 tetravalent bispecific tandem diabodies (TandAbs) for the treatment of acute myeloid leukemia. *Clin. Cancer Res.* 22, 5829–5838. doi:10.1158/1078-0432.CCR-16-0350

Ritchie, D. S., Neeson, P. J., Khot, A., Peinert, S., Tai, T., Tainton, K., et al. (2013). Persistence and efficacy of second generation CAR T cell against the LeY antigen in acute myeloid leukemia. *Mol. Ther. J. Am. Soc. Gene Ther.* 21, 2122–2129. doi:10.1038/mt.2013.154

Rizvi, N. A., Hellmann, M. D., Snyder, A., Kvistborg, P., Makarov, V., Havel, J. J., et al. (2015). Mutational landscape determines sensitivity to PD-1 blockade in non–small cell lung cancer. *Science* 348, 124–128. doi:10.1126/science.aaa1348

Robbins, P. F., Morgan, R. A., Feldman, S. A., Yang, J. C., Sherry, R. M., Dudley, M. E., et al. (2011). Tumor regression in patients with metastatic synovial cell sarcoma and melanoma using genetically engineered lymphocytes reactive with NY-ESO-1. *J. Clin. Oncol.* 29, 917–924. doi:10.1200/JCO.2010.32.2537

Robert, C., Ribas, A., Wolchok, J. D., Hodi, F. S., Hamid, O., Kefford, R., et al. (2014). Anti-programmed-death-receptor-1 treatment with pembrolizumab in ipilimumab-refractory advanced melanoma: A randomised dose-comparison cohort of a phase 1 trial. *Lancet* 384, 1109–1117. doi:10.1016/S0140-6736(14)60958-2

Roberts, A. W., He, S., Bradstock, K. F., Hertzberg, M. S., Durrant, S. T. S., Ritchie, D., et al. (2008). A phase 1 and correlative biological study of CSL360 (anti-CD123 mAb) in AML. *Blood* 112 (11), 2956. doi:10.1182/blood.v112.11.2956.2956

Roboz, G. J., Rosenblat, T., Arellano, M., Gobbi, M., Altman, J. K., Montesinos, P., et al. (2014). International randomized phase III study of elacytarabine versus investigator choice in patients with relapsed/refractory acute myeloid leukemia. *J. Clin. Oncol.* 32, 1919–1926. doi:10.1200/JCO.2013.52.8562

Rosenblat, T. L., McDevitt, M. R., Carrasquillo, J. A., Pandit-Taskar, N., Frattini, M. G., Maslak, P. G., et al. (2022). Treatment of patients with acute myeloid leukemia with the targeted alpha-particle nanogenerator actinium-225-lintuzumab. *Clin. Cancer Res.* 28, 2030–2037. doi:10.1158/1078-0432.CCR-21-3712

Rosenblat, T. L., McDevitt, M. R., Mulford, D. A., Pandit-Taskar, N., Divgi, C. R., Panageas, K. S., et al. (2010). Sequential cytarabine and alpha-particle immunotherapy with bismuth-213-lintuzumab (HuM195) for acute myeloid leukemia. *Clin. Cancer Res.* 16, 5303–5311. doi:10.1158/1078-0432.CCR-10-0382

Rosenblatt, J., Stone, R. M., Uhl, L., Neuberg, D., Joyce, R., Levine, J. D., et al. (2016). Individualized vaccination of AML patients in remission is associated with induction of antileukemia immunity and prolonged remissions. *Sci. Transl. Med.* 8, 368ra171. doi:10.1126/scitranslmed.aag1298

Rotte, A. (2019). Combination of CTLA-4 and PD-1 blockers for treatment of cancer. *J. Exp. Clin. Cancer Res.* 38, 255. doi:10.1186/s13046-019-1259-z

Ruggiero, E., Carnevale, E., Prodeus, A., Magnani, Z. I., Camisa, B., Merelli, I., et al. (2022). CRISPR-based gene disruption and integration of high-avidity, WT1-specific T cell receptors improve antitumor T cell function. *Sci. Transl. Med.* 14, eabg8027. doi:10.1126/scitranslmed.abg8027

Sallman, D. A., Brayer, J., Sagatys, E. M., Lonez, C., Breman, E., Agaugué, S., et al. (2018). NKG2D-based chimeric antigen receptor therapy induced remission in a relapsed/refractory acute myeloid leukemia patient. *Haematologica* 103, e424–e426. doi:10.3324/haematol.2017.186742

Sallman, D. A., McLemore, A. F., Aldrich, A. L., Komrokji, R. S., McGraw, K. L., Dhawan, A., et al. (2020). TP53 mutations in myelodysplastic syndromes and secondary AML confer an immunosuppressive phenotype. *Blood* 136, 2812–2823. doi:10.1182/blood.2020006158

Sauer, T., Parikh, K., Sharma, S., Omer, B., Sedloev, D., Chen, Q., et al. (2021). CD70-specific CAR T cells have potent activity against acute myeloid leukemia without HSC toxicity. *Blood* 138, 318–330. doi:10.1182/blood.2020008221

Saxena, K., Herbrich, S. M., Pemmaraju, N., Kadia, T. M., DiNardo, C. D., Borthakur, G., et al. (2021). A phase 1b/2 study of azacitidine with PD-L1 antibody avelumab in relapsed/refractory acute myeloid leukemia. *Cancer* 127, 3761–3771. doi:10.1002/cncr.33690

Schratz, K. E., Gaysinskaya, V., Cosner, Z. L., DeBoy, E. A., Xiang, Z., Kasch-Semenza, L., et al. (2021). Somatic reversion impacts myelodysplastic syndromes and acute myeloid leukemia evolution in the short telomere disorders. *J. Clin. Investigation* 131, e147598. doi:10.1172/JCI147598

Schreibelt, G., Bol, K. F., Westdorp, H., Wimmers, F., Aarntzen, E. H. J. G., Duiveman-de Boer, T., et al. (2016). Effective clinical responses in metastatic melanoma patients after vaccination with primary myeloid dendritic cells. *Clin. Cancer Res.* 22, 2155–2166. doi:10.1158/1078-0432.CCR-15-2205

Schwartzman, O., and Tanay, A. (2015). Single-cell epigenomics: Techniques and emerging applications. *Nat. Rev. Genet.* 16, 716–726. doi:10.1038/nrg3980

Short, N. J., Rytting, M. E., and Cortes, J. E. (2018). Acute myeloid leukaemia. *Lancet* 392, 593–606. doi:10.1016/s0140-6736(18)31041-9

Spallone, A., Alotaibi, A. S., Jiang, Y., Daver, N., and Kontoyiannis, D. P. (2022). Infectious complications among patients with AML treated with immune checkpoint inhibitors. *Clin. lymphoma, myeloma and leukemia* 22, 305–310. doi:10.1016/j.clml.2021.10.012

Stein, E. M., Walter, R. B., Erba, H. P., Fathi, A. T., Advani, A. S., Lancet, J. E., et al. (2018). A phase 1 trial of vadastuximab talirine as monotherapy in patients with CD33-positive acute myeloid leukemia. *Blood* 131, 387–396. doi:10.1182/blood-2017-06-789800

Steinman, R. M., and Banchereau, J. (2007). Taking dendritic cells into medicine. *Nature* 449, 419–426. doi:10.1038/nature06175

Stewart, S. A., and Weinberg, R. A. (2000). Telomerase and human tumorigenesis. *Seminars Cancer Biol.* 10, 399–406. doi:10.1006/scbi.2000.0339

Stroopinsky, D., Liegel, J., Bhasin, M., Cheloni, G., Thomas, B., Bhasin, S., et al. (2021). Leukemia vaccine overcomes limitations of checkpoint blockade by evoking clonal T cell responses in a murine acute myeloid leukemia model. *Haematologica* 106, 1330–1342. doi:10.3324/haematol.2020.259457

Sugita, M., Galetto, R., Zong, H., Ewing-Crystal, N., Trujillo-Alonso, V., Mencia-Trinchant, N., et al. (2022). Allogeneic TCRαβ deficient CAR T-cells targeting CD123 in acute myeloid leukemia. *Nat. Commun.* 13, 2227. doi:10.1038/s41467-022-29668-9

Tahk, S., Vick, B., Hiller, B., Schmitt, S., Marcinek, A., Perini, E. D., et al. (2021). SIRPα-αCD123 fusion antibodies targeting CD123 in conjunction with CD47 blockade

enhance the clearance of AML-initiating cells. *J. Hematol. Oncol.* 14, 155. doi:10.1186/s13045-021-01163-6

Tambaro, F. P., Singh, H., Jones, E., Rytting, M., Mahadeo, K. M., Thompson, P., et al. (2021). Autologous CD33-CAR-T cells for treatment of relapsed/refractory acute myelogenous leukemia. *Leukemia* 35, 3282–3286. doi:10.1038/s41375-021-01232-2

Tan, J., Yu, Z., Huang, J., Chen, Y., Huang, S., Yao, D., et al. (2020). Increased PD-1+Tim-3+ exhausted T cells in bone marrow may influence the clinical outcome of patients with AML. *Biomark. Res.* 8, 6. doi:10.1186/s40364-020-0185-8

Tang, J., Shalabi, A., and Hubbard-Lucey, V. M. (2017). Comprehensive analysis of the clinical immuno-oncology landscape. *Ann. Oncol.* 29, 84–91. doi:10.1093/annonc/mdx755

Tang, L., Wu, J., Li, C. G., Jiang, H. W., Xu, M., Du, M., et al. (2020). Characterization of immune dysfunction and identification of prognostic immune-related risk factors in acute myeloid leukemia. *Clin. Cancer Res.* 26, 1763–1772. doi:10.1158/1078-0432.CCR-19-3003

Tasian, S. K. (2018). Acute myeloid leukemia chimeric antigen receptor T-cell immunotherapy: How far up the road have we traveled? *Ther. Adv. Hematol.* 9 (6), 135–148. doi:10.1177/2040620718774268

Taussig, D. C., Pearce, D. J., Simpson, C., Rohatiner, A. Z., Lister, T. A., Kelly, G., et al. (2005). Hematopoietic stem cells express multiple myeloid markers: Implications for the origin and targeted therapy of acute myeloid leukemia. *Blood* 106, 4086–4092. doi:10.1182/blood-2005-03-1072

Tawara, I., Kageyama, S., Miyahara, Y., Fujiwara, H., Nishida, T., Akatsuka, Y., et al. (2017). Safety and persistence of WT1-specific T-cell receptor gene-transduced lymphocytes in patients with AML and MDS. *Blood* 130, 1985–1994. doi:10.1182/blood-2017-06-791202

Topalian, S. L., Hodi, F. S., Brahmer, J. R., Gettinger, S. N., Smith, D. C., McDermott, D. F., et al. (2012). Safety, activity, and immune correlates of anti-PD-1 antibody in cancer. *N. Engl. J. Med.* 366, 2443–2454. doi:10.1056/NEJMoa1200690

Vago, L., and Gojo, I. (2020). Immune escape and immunotherapy of acute myeloid leukemia. *J. Clin. Investigation* 130, 1552–1564. doi:10.1172/jci129204

van Balen, P., Jedema, I., van Loenen, M. M., de Boer, R., van Egmond, H. M., Hagedoorn, R. S., et al. (2020). HA-1H T-cell receptor gene transfer to redirect virus-specific T cells for treatment of hematological malignancies after allogeneic stem cell transplantation: A phase 1 clinical study. *Front. Immunol.* 11, 1804. doi:10.3389/fimmu.2020.01804

van de Loosdrecht, A. A., van Wetering, S., Santegoets, S. J. A. M., Singh, S. K., Eeltink, C. M., den Hartog, Y., et al. (2018). A novel allogeneic off-the-shelf dendritic cell vaccine for post-remission treatment of elderly patients with acute myeloid leukemia. *Cancer Immunol. Immunother.* 67, 1505–1518. doi:10.1007/s00262-018-2198-9

van Ens, D., Mousset, C. M., Hutten, T. J. A., van der Waart, A. B., Campillo-Davo, D., van der Heijden, S., et al. (2020). PD-L1 siRNA-mediated silencing in acute myeloid leukemia enhances anti-leukemic T cell reactivity. *Bone Marrow Transplant.* 55, 2308–2318. doi:10.1038/s41409-020-0966-6

Van Tendeloo, V. F., Van de Velde, A., Van Driessche, A., Cools, N., Anguille, S., Ladell, K., et al. (2010). Induction of complete and molecular remissions in acute myeloid leukemia by Wilms' tumor 1 antigen-targeted dendritic cell vaccination. *Proc. Natl. Acad. Sci. U. S. A.* 107, 13824–13829. doi:10.1073/pnas.1008051107

Vasileiou, S., Lulla, P. D., Tzannou, I., Watanabe, A., Kuvalekar, M., Callejas, W. L., et al. (2021). T-cell therapy for lymphoma using nonengineered multiantigen-targeted T cells is safe and produces durable clinical effects. *J. Clin. Oncol.* 39, 1415–1425. doi:10.1200/JCO.20.02224

Wang, Q. S., Wang, Y., Lv, H. y., Han, Q. w., Fan, H., Guo, B., et al. (2015). Treatment of CD33-directed chimeric antigen receptor-modified T cells in one patient with relapsed and refractory acute myeloid leukemia. *Mol. Ther.* 23, 184–191. doi:10.1038/mt.2014.164

Willier, S., Rothämel, P., Hastreiter, M., Wilhelm, J., Stenger, D., Blaeschke, F., et al. (2021). CLEC12A and CD33 coexpression as a preferential target for pediatric AML combinatorial immunotherapy. *Blood* 137, 1037–1049. doi:10.1182/blood.2020006921

Wolchok, J. D. (2015). PD-1 blockers. *Cell* 162, 937. doi:10.1016/j.cell.2015.07.045

Xie, L. H., Biondo, M., Busfield, S. J., Arruda, A., Yang, X., Vairo, G., et al. (2017). CD123 target validation and preclinical evaluation of ADCC activity of anti-CD123 antibody CSL362 in combination with NKs from AML patients in remission. *Blood Cancer J.* 7, e567. doi:10.1038/bcj.2017.52

Xu, L., Liu, L., Yao, D., Zeng, X., Zhang, Y., Lai, J., et al. (2021). PD-1 and TIGIT are highly Co-expressed on CD8(+) T cells in AML patient bone marrow. *Front. Oncol.* 11, 686156. doi:10.3389/fonc.2021.686156

Xu, S., Zhang, M., Fang, X., Hu, X., Xing, H., Yang, Y., et al. (2022). CD123 antagonistic peptides assembled with nanomicelles act as monotherapeutics to combat refractory acute myeloid leukemia. *ACS Appl. Mater. interfaces* 14, 38584–38593. doi:10.1021/acsami.2c11538

Xu, S., Zhang, M., Fang, X., Meng, J., Xing, H., Yan, D., et al. (2021). A novel CD123-targeted therapeutic peptide loaded by micellar delivery system combats refractory acute myeloid leukemia. *J. Hematol. Oncol.* 14, 193. doi:10.1186/s13045-021-01206-y

Yang, H., Bueso-Ramos, C., DiNardo, C., Estecio, M. R., Davanlou, M., Geng, Q. R., et al. (2014). Expression of PD-L1, PD-L2, PD-1 and CTLA4 in myelodysplastic syndromes is enhanced by treatment with hypomethylating agents. *Leukemia* 28, 1280–1288. doi:10.1038/leu.2013.355

Yang, J., He, J., Zhang, X., Li, J., Wang, Z., Zhang, Y., et al. (2022). Next-day manufacture of a novel anti-CD19 CAR-T therapy for B-cell acute lymphoblastic leukemia: First-in-human clinical study. *Blood cancer J.* 12, 104. doi:10.1038/s41408-022-00694-6

Yang, X., and Wang, J. (2018). Precision therapy for acute myeloid leukemia. *J. Hematol. Oncol.* 11, 3. doi:10.1186/s13045-017-0543-7

Yao, S., Jianlin, C., Zhuoqing, Q., Yuhang, L., Jiangwei, H., Guoliang, H., et al. (2021). Case report: Combination therapy with PD-1 blockade for acute myeloid leukemia after allogeneic hematopoietic stem cell transplantation resulted in fatal GVHD. *Front. Immunol.* 12, 639217. doi:10.3389/fimmu.2021.639217

Yarchoan, M., Hopkins, A., and Jaffee, E. M. (2017). Tumor mutational burden and response rate to PD-1 inhibition. *N. Engl. J. Med.* 377, 2500–2501. doi:10.1056/NEJMc1713444

You, X., Liu, F., Binder, M., Vedder, A., Lasho, T., Wen, Z., et al. (2022). Asxl1 loss cooperates with oncogenic Nras in mice to reprogram the immune microenvironment and drive leukemic transformation. *Blood* 139, 1066–1079. doi:10.1182/blood.2021012519

Younes, A., Santoro, A., Shipp, M., Zinzani, P. L., Timmerman, J. M., Ansell, S., et al. (2016). Nivolumab for classical hodgkin's lymphoma after failure of both autologous stem-cell transplantation and brentuximab vedotin: A multicentre, multicohort, single-arm phase 2 trial. *Lancet. Oncol.* 17, 1283–1294. doi:10.1016/S1470-2045(16)30167-X

Zeidner, J. F., Vincent, B. G., Ivanova, A., Moore, D., McKinnon, K. P., Wilkinson, A. D., et al. (2021). Phase II trial of pembrolizumab after high-dose cytarabine in relapsed/refractory acute myeloid leukemia. *Blood Cancer Discov.* 2, 616–629. doi:10.1158/2643-3230.BCD-21-0070

Zhang, L., Gajewski, T. F., and Kline, J. (2009). PD-1/PD-L1 interactions inhibit antitumor immune responses in a murine acute myeloid leukemia model. *Blood* 114, 1545–1552. doi:10.1182/blood-2009-03-206672

Zhang, W., Piatyszek, M. A., Kobayashi, T., Estey, E., Andreeff, M., Deisseroth, A. B., et al. (1996). Telomerase activity in human acute myelogenous leukemia: Inhibition of telomerase activity by differentiation-inducing agents. *Clin. Cancer Res.* 2, 799–803.

Zheng, H., Mineishi, S., Claxton, D., Zhu, J., Zhao, C., Jia, B., et al. (2021). A phase I clinical trial of avelumab in combination with decitabine as first line treatment of unfit patients with acute myeloid leukemia. *Am. J. Hematol.* 96, E46–e50. doi:10.1002/ajh.26043

Zhou, Q., Bucher, C., Munger, M. E., Highfill, S. L., Tolar, J., Munn, D. H., et al. (2009). Depletion of endogenous tumor-associated regulatory T cells improves the efficacy of adoptive cytotoxic T-cell immunotherapy in murine acute myeloid leukemia. *Blood* 114, 3793–3802. doi:10.1182/blood-2009-03-208181

Zhou, Q., Munger, M. E., Veenstra, R. G., Weigel, B. J., Hirashima, M., Munn, D. H., et al. (2011). Coexpression of Tim-3 and PD-1 identifies a CD8+ T-cell exhaustion phenotype in mice with disseminated acute myelogenous leukemia. *Blood* 117, 4501–4510. doi:10.1182/blood-2010-10-310425

frontiers | Frontiers in Pharmacology

TYPE Original Research
PUBLISHED 04 May 2023
DOI 10.3389/fphar.2023.1187700

OPEN ACCESS

EDITED BY
Hongzhou Cai,
Nanjing Medical University, China

REVIEWED BY
Yongbiao Huang,
Tongji hospitai, China
Xu Chen,
Sun Yat-Sen Memorial Hospital, China

*CORRESPONDENCE
Neng Liu,
1991797080@qq.com
Huihuang Li,
lhhuang1994@163.com

RECEIVED 16 March 2023
ACCEPTED 18 April 2023
PUBLISHED 04 May 2023

CITATION
Deng D, Li X, Qi T, Dai Y, Liu N and Li H (2023), A novel platelet risk score for stratifing the tumor immunophenotypes, treatment responses and prognosis in bladder carcinoma: results from real-world cohorts.
Front. Pharmacol. 14:1187700.
doi: 10.3389/fphar.2023.1187700

A novel platelet risk score for stratifing the tumor immunophenotypes, treatment responses and prognosis in bladder carcinoma: results from real-world cohorts

Dingshan Deng[1,2], Xiaowen Li[3], Tiezheng Qi[3], Yuanqing Dai[1,2], Neng Liu[2,4]* and Huihuang Li[1,2]*

[1]Department of Urology, National Clinical Research Center for Geriatric Disorders, Xiangya Hospital, Central South University, Changsha, Hunan, China, [2]National Clinical Research Center for Geriatric Disorders, Xiangya Hospital, Central South University, Changsha, Hunan, China, [3]Xiangya School of Medicine, Central South University, Changsha, Hunan, China, [4]Teaching and Research Section of Clinical Nursing, Xiangya Hospital, Central South University, Changsha, Hunan, China

Background: Although the durable efficacy of immune checkpoint inhibitors (ICIs) in BLCA has been confirmed in numerous studies, not all patients benefit from their application in the clinic. Platelets are increasingly being found to be closely associated with cancer progression and metastasis; however, their comprehensive role in BLCA remains unclear.

Methods: We comprehensively explored platelet expression patterns in BLCA patients using an integrated set of 244 related genes. Correlations between these platelet patterns with tumor microenvironment (TME) subtypes, immune characteristics and immunotherapy efficacies were explored. In addition, a platelet risk score (PRS) was generated for individual prognosis and verified the ability to predict prognosis, precise TME phenotypes, and immunotherapy efficacies.

Results: Genes were clustered into two patterns that represented different TME phenotypes and had the ability to predict immunotherapy efficacy. We constructed a PRS that could predict individual prognosis with satisfactory accuracy using TCGA-BLCA. The results remained consistent when PRS was validated in the GSE32894 and Xiangya cohort. Moreover, we found that our PRS was positively related to tumor-infiltrating lymphocytes (TILs) in the TCGA-BLCA and Xiangya cohort. As expected, patients with higher PRS exhibited more sensitive to immunotherapy than patients with lower PRS. Finally, we discovered that a high PRS indicated a basal subtype of BLCA, whereas a low PRS indicated a luminal subtype.

Conclusion: Platelet-related genes could predict TME phenotypes in BLCA. We constructed a PRS that could predict the TME, prognosis, immunotherapy efficacy, and molecular subtypes in BLCA.

KEYWORDS

platelet, bladder carcinoma, immunotherapy, prognosis, tumor microenvironment

Introduction

Bladder cancer (BLCA) is considered as the 10th commonest malignancy all over the world, leading to approximately 210,000 deaths worldwide annually (Sung et al., 2021). Currently, invasive cystoscopy and tissue biopsy have become the gold standard for BLCA detection and surveillance (Babjuk et al., 2022), and some novel methods show bright prospects, such as urine DNA methylation and urine exosomes assay (Chen et al., 2020; Wei et al., 2022). As for treatment, although neoadjuvant chemotherapy has become the standard of care, the prognoses of advanced BLCAs are still not satisfied due to the insensitivity to this therapy (Patel et al., 2020). Fortunately, urologists found great immunogenicity such as a high tumor mutation burden (TMB) in the BLCA (Patel et al., 2020), which could be coped with immunotherapy, especially including immune checkpoint inhibitors (ICIs) which was considered to have great clinical effect for advanced BLCA (Sharma et al., 2017; Necchi et al., 2018). However, not every patient is sensitive to treatment with ICIs (Bagchi et al., 2021). Therefore, predicting patient response to ICIs is of great significance. The tumor microenvironment (TME) denotes the cancer cells, non-cancerous cells, and their corresponding secreted factors in the tumor (Xiao and Yu, 2021). It can be divided into binary groups according to the appearance of tumor-infiltrating lymphocytes (TILs) (Chen and Mellman, 2017). Inflamed tumors have a high level of TIL infiltration and generally express cytokines that activate immunity, whereas non-inflamed tumors have the opposite characteristics (Chen and Mellman, 2017). Theoretically, ICIs re-invigorated tumor-cytotoxic T cells to inhibit tumor growth in the TME (Duan et al., 2020), thus indicating better efficacy in inflamed tumors. For tumors with limited TILs, patients showed a significantly lower response to ICI treatment (Beer et al., 2017; Quail and Joyce, 2017), while inflamed tumors such as melanoma and renal cell carcinoma show desirable clinical response (Tumeh et al., 2014; McDermott et al., 2018). Thus, discriminating these two phenotypes may contribute to predicting the efficacy of ICIs; in addition, the transformation of non-inflamed tumors into inflamed ones can improve ICI efficacy (Duan et al., 2020).

Platelets, which play a crucial role in coagulation and hemostasis after a mechanical injury to the vasculature, are closely related to cancer progression and metastasis (Schlesinger, 2018). Riess first noted that thrombocytosis was associated with solid tumors over a century ago (Riess, 1872). With the progress of modern biotechnology, recent studies have found that platelets influence TME, cancer progression and metastasis in various ways. Platelets envelop tumor cells by binding to mucins on the surface of cancer cells, which interfere with NK cells' recognition of tumor cells and physically protect them from NK cells' attacks (Goubran et al., 2013). Activated platelets can release VEGFA, PDGF and other pro-angiogenic factors to promote blood vessel formation in TME, thereby promoting tumor growth (De Palma et al., 2017). In addition, platelets can produce TGF-β to inhibit the production of IFN-γ, T cell proliferation and promote tumor cell metastasis (Haemmerle et al., 2018). Thus, platelet-related genes may play key roles in cancer progression and immunity (Haemmerle et al., 2018). Von Willebrand factor (VWF), which plays a vital part in platelet adhesion along the endothelium, is involved in cancer metastasis and inflammation (Patmore et al., 2020). Furthermore, protein tyrosine phosphatase non-receptor type 6 (PTPN6) was found to be a negative regulator of the inflammatory cell death pathways that take part in cancer immunity (Speir et al., 2020). In lung tumor model, peroxiredoxin 6 (PRDX6) contributes to tumor growth, which is associated with JAK2/STAT3 pathway (Yun et al., 2015). However, the comprehensive role of platelet-related genes need to be further explored. In this study, we reported that platelets promote an inflamed TME, and constructed a platelet risk score (PRS) to predict the molecular subtypes, precision immunotherapy, and prognosis in BLCA.

Materials and methods

Data sources

We comprehensively downloaded TCGA-BLCA profiles about gene expression, mutation and clinical data from the UCSC Xena (https://xenabrowser.net/). As for sequencing analysis, we prepared both the count value and the fragments per kilobase per million mapped fragments (FPKM). In particular, we obliterated "invalid data" which lacked sequencing or survival information. Finally, 411 tumor samples were screened from the TCGA-BLCA for further analysis. We captured GSE32894 from the GEO database (https://www.ncbi.nlm.nih.gov/geo/) with the "GEOquery" R package. Our own cohort, the Xiangya cohort (GSE188715) which had a sample size of 56 patients, was developed in our previous study (Li et al., 2021).

Unsupervised clustering

In total, we digged out 244 platelet-related genes from the study by Xie et al. (2021). We adopted consensus clustering with a thousand repetitions. Platelet-related genes were showed in Supplementary Table S1.

Pathway enrichment analysis

We comprehensively captured signatures mainly indicating anti-cancer immunity and ICI therapy efficacy from previous studies (Mariathasan et al., 2018; Braun et al., 2020). Moreover, we obtained other therapeutic signatures with corresponding data from the Drugbank, which wasdescribed detailedly in our published article (Hu et al., 2021). In addition, we collected signatures which could indicate the molecular subtypes of BLCA from the existing documents (Kamoun et al., 2020). Subsequently, the sample-level enrichment scores of those signatures were computed.

To sift out differentially expressed genes (DEGs), we performed differential analysis of gene expression and the threshold was set as the absolute log2 fold change (FC) >1 with adjusted p-value <0.05. Information about the GO knowledgebase, the KEGG database and sets of hallmark genes were sourced by the MSigDB (http://www.gsea-msigdb.org/gsea/index.jsp) and analyzed using GSEA (Liberzon et al., 2015).

Tumor immune microenvironment depiction

The previous study concluded the anti-cancer immunity cycle including 7 key steps and displayed the achievements on the

tracking tumor immunophenotype (TIP, http://biocc.hrbmu.edu.cn/TIP/), where we downloaded relevant data applied in our own analysis (Li et al., 2021). In addition, to calculate relative abundances of diverse immune cell types, we adopted the ssGSEA algorithm with data from the TCGA-BLCA and our Xiangya cohort based on gene sets reported previously (Charoentong et al., 2017).

Development and validation of a platelet risk score

We first constructed a univariable Cox regression model to screen prognostic genes from colletced platelet-related genes. Afterwards, we narrowed down the prognostic genes using the least absolute shrinkage and selector operation (LASSO) with ten-fold cross validation. Finally, 13 genes were selected, and the Cox proportional hazard regression was used to generate a PRS, carried out by the "glmnet" R package:

$$PRS = \Sigma\beta i * RNAi$$

We further validated our PRS in external databases including GSE32894 and Xiangya cohort.

Assessment of molecular subtypes of BLCA

BLCA patients were successfully distinguished by diverse criteria of seven molecular subtypes using "ConsensusMIBC" and "BLCAsubtyping" R packages. In addition, we regrouped these subtypes and renamed them after "basal" and "luminal" subtypes withpublished methods (Kamoun et al., 2020). Previous studies provide a detailed description (Hu et al., 2021; Li et al., 2021).

Statistical analysis

The differences between normally distributed continuous variables were evaluated with the *t*-test. Furthermore, we performed the Wilcoxon rank-sum test. Categorical values were compared using the $\chi 2$ or Fisher's exact test. The Kaplan-Meier method and log-rank tests were used for survival analysis. Pearson's correlation coefficients were used to evaluate correlations among the variables. Time-dependent receiver operating characteristic (ROC) analysis was set up to evaluate the predictive accuracy of our model. *p*-values for DEG and GSEA analyses were adjusted using the false discovery rate method. Two-sided *p* values < 0.05 was set as the criterion of significance. The R version in all our analyses was 4.13.

Result

Platelet regulated patterns in BLCA

To determine whether platelet-related genes were comprehensively regulated by a specific pattern in BLCA, we divided patients in TCGA-BLCA into binary clusters, namely, the platelet cluster1 and platelet cluster2 respectively (Figure 1A, Supplementary Figures S1A–SF). Interestingly, survival analysis results showed that patients in platelet cluster2 displayed better survival outcomes than those in platelet cluster1, with $p = 0.038$ (Figure 1B). Surprisingly, a positive correlation was found between immune activation and cluster1. Further, 2,520 DEGs between these two clusters were finally sifted out (Supplementary Table S2), and then used to generate a volcano plot which indicated that some significant chemokines, including CXCL9, CXCL10, and CXCL11, had increased expression levels in platelet cluster1 (Figure 1C). Further analysis showed that pathways related to cytokines and chemokines were activated in cluster1 (Figure 1D, Supplementary Table S3); hence, we wondered if there was more infiltration of effector immune cells in platelet cluster1. As expected, pathways related to T cells and natural killer (NK) cells were obviously activated (Figures 1E, F, Supplementary Table S2). Furthermore, we performed GSEA for hallmark pathways and observed that the majority of these immune-related pathways were activated in platelet cluster1, including epithelial mesenchymal transition, complement, and apical junction (Figure 1G, Supplementary Table S2), suggesting that platelet cluster1 might represent an immune-activated phenotype relative to platelet cluster2.

Description of immune characteristics between two clusters

To determine if platelet cluster1 represented an inflamed TME phenotype and cluster2 represented a non-inflamed phenotype of BLCA, we further identified the differences between these two clusters in cancer immune cycle. Most steps in the cancer immune cycles showed sensibly higher levels in platelet cluster1 than in cluster2, which indicated a greater level of immune activation and immune cell infiltration in the tumor microenvironment in platelet cluster1 (Figure 2A). We performed ssGSEA and observed that a variety of TILs, such as dendritic cells (DCs), macrophages, T cells of different kinds and neutrophils, were significantly higher in platelet cluster1 than in platelet cluster2 (Figure 2B). Overall, these results suggested that platelet cluster1 had an inflamed phenotype that could be responsive to ICI treatment, whereas platelet cluster2 had a non-inflamed phenotype, which could not respond to ICI treatment. A previous study summarized 21 pathways contributing to the prediction of immunotherapy efficacy (Mariathasan et al., 2018), and we observed that almost all these pathways (such as APM signal, cell cycle, DNA replication and so on) were highly regulated in platelet cluster1 (Figure 2C). What's more, four immune-related signatures were found significantly activated in cluster 1 compared to cluster 2 (Figures 2D–G). These results further support the notion that patients in platelet cluster1 might be responsive to ICI treatment. Unfortunately, the results of unsupervised clustering could hardly explain a single patient's regulation pattern, as it was conducted based on the population. Therefore, we intended to screen out novel genes and construct a risk score.

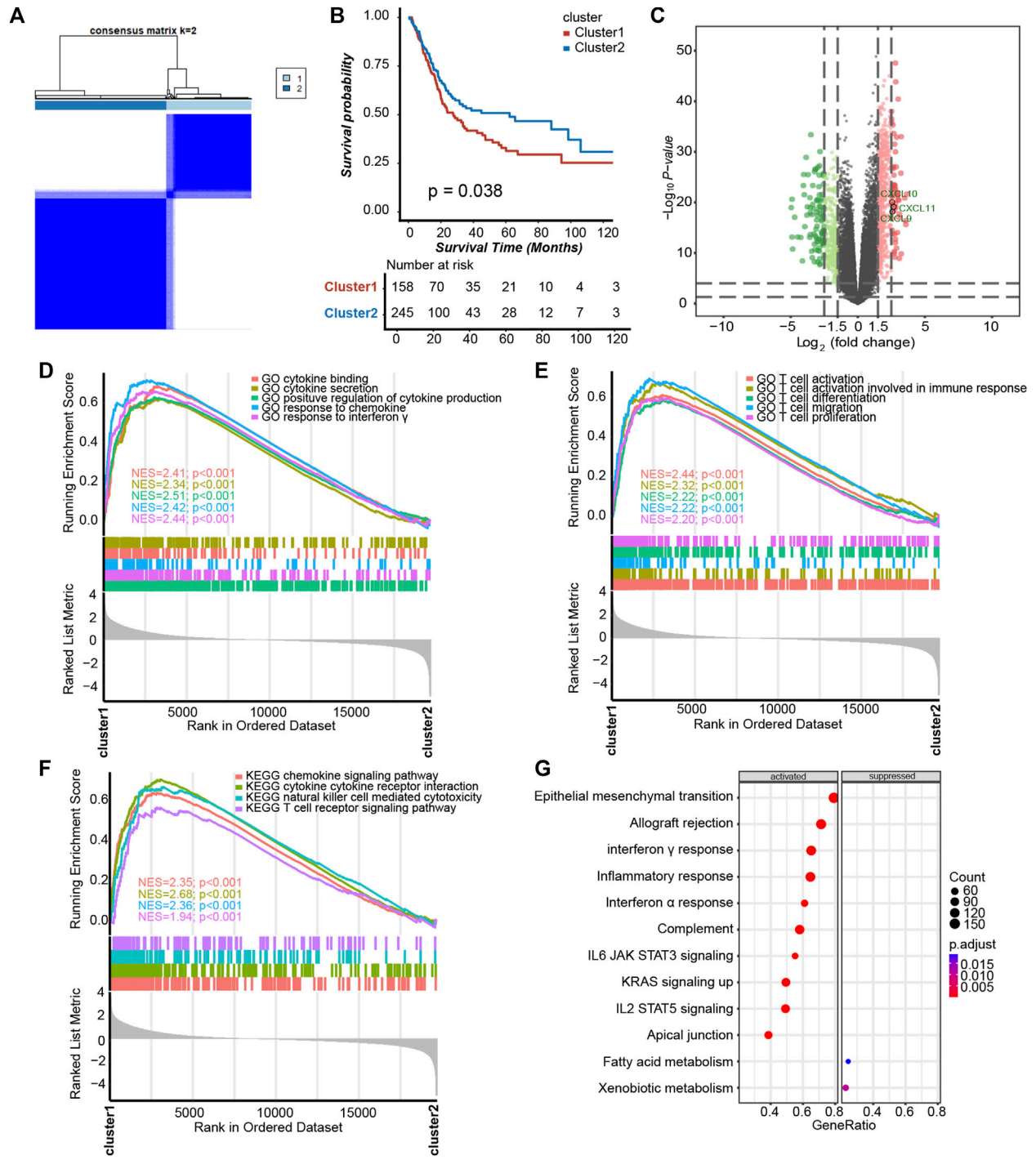

FIGURE 1
Platelet-regulated patterns in BLCA. **(A)** Unsupervised clustering divided 244 platelet-related genes into two clusters, and **(B)** Kaplan–Meier plots revealed that the survival probability of patients exhibited sensibly higher in platelet cluster2 than cluster1. **(C)** The volcano plot showed DEGs between two platelet clusters. **(D)** Cytokine- and chemokine-related pathways in gene ontology (GO) pathways using gene set enrichment analysis (GSEA) analysis. **(E)** GSEA analysis revealed that platelet cluster1 showed significant enrichment of T cell-related pathways in GO pathways. **(F)** T cell-related pathways, chemokine, cytokine and NK cell in Kyoto Encyclopedia of Genes and Genomes (KEGG) pathways using GSEA analysis. **(G)** GSEA of hallmark pathways between two platelet-regulated patterns.

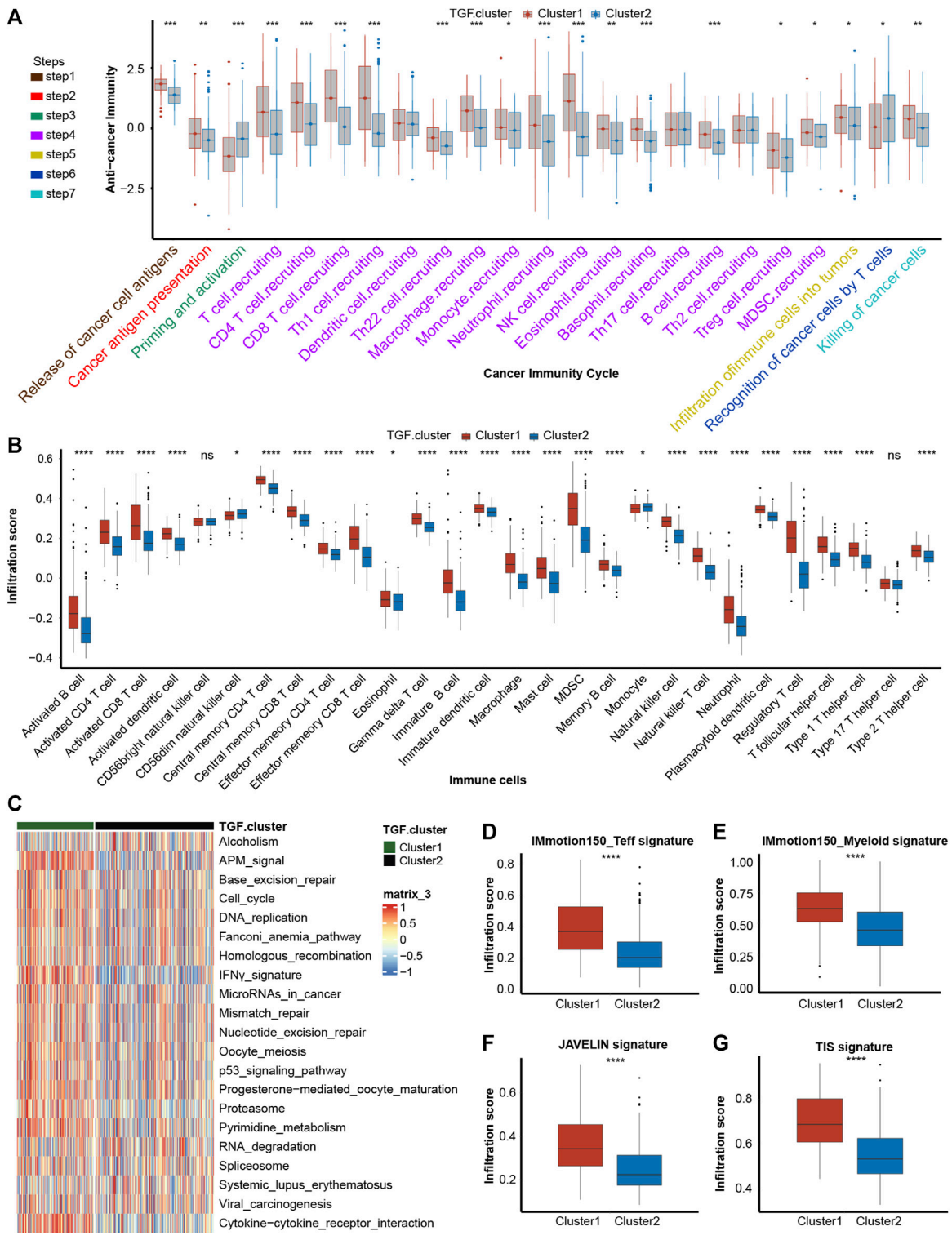

FIGURE 2
Description of immune characteristics between two clusters. **(A)** Differences in each step of tumor immunity cycle between two platelet-regulated patterns. **(B)** Different immune cells infiltration status between two platelet-regulated patterns. **(C)** The heatmap showed that most of twenty-one pathways contributing to immunotherapy efficacy predicting were sensibly upregulated in platelet cluster1. **(D–G)** Box plots showed the estimation and comparison of four immune-related pathways including IMmotion150 Teff signature **(D)**, IMmotion150 Myeloid signature **(E)**, JAVELIN **(F)** and tumor inflammation signature **(G)** between two platelet regulated patterns. The amount of * from one to four means that the corresponding *p*-value is less than 0.05, 0.01, 0.001, 0.0001, respectively. "ns" means that *p* values more than 0.05 and the result is of no significance.

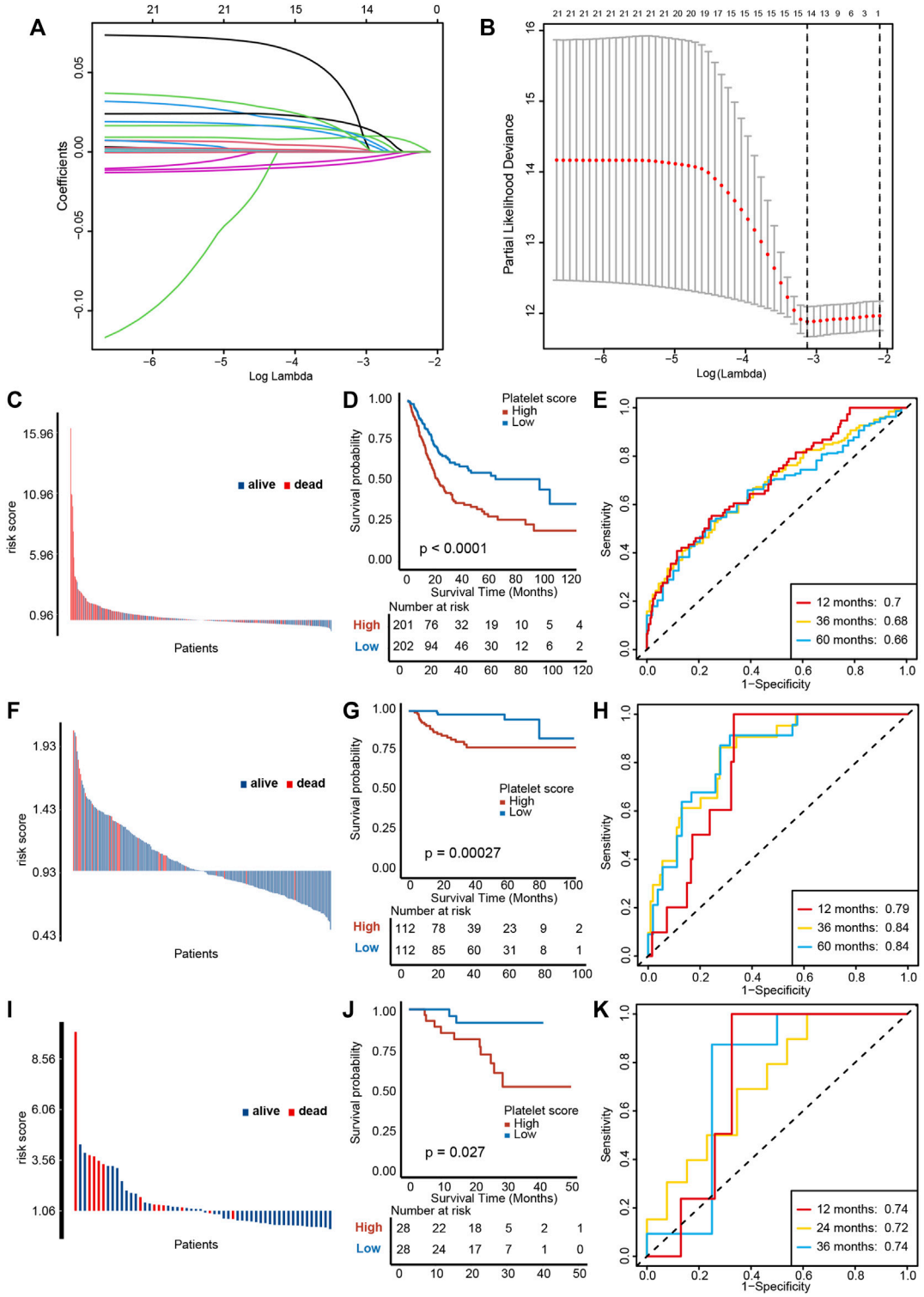

FIGURE 3
Construction and validation of a platelet risk score (PRS) and its clinical significance. **(A)** Results of LASSO regression based on platelet related genes. **(B)** Results of ten-fold cross validation. **(C)** Distribution of patients' survival status demonstrated that patients with high PRS in TCGA-BLCA exhibit poorer overall survival outcomes. **(D)** Kaplan-Meier analysis revealed that higher PRS corresponded to particularly poorer survival outcomes in TCGA-BLCA. **(E)** ROC curves of PRS showed satisfactory predictive accuracy of PRS in TCGA-BLCA cohort. **(F–H)** The validation of PRS prognosis value in GSE32894. **(I–K)** The validation of PRS prognosis value in the Xiangya validation cohort.

10.3389/fphar.2023.1187700

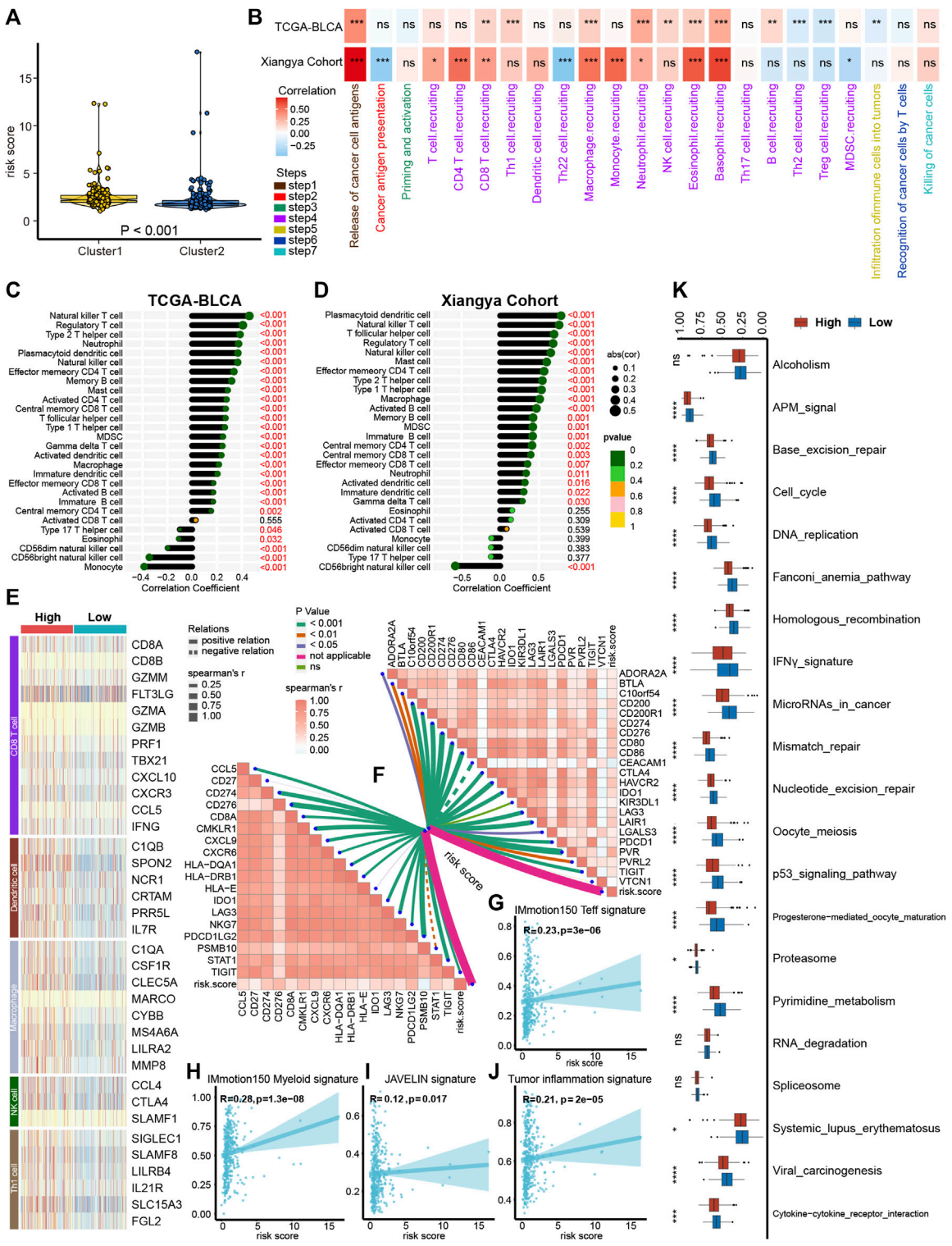

FIGURE 4
Platelet risk score (PRS) for individual patient's immune cell infiltration evaluation. **(A)** The connection between platelet cluster 1/2 and PRS. **(B)** The heatmap showed that in both the TCGA-BLCA and Xiangya cohort, PRS had a positive correlation with most steps of cancer immunity cycle. **(C–D)** PRS had a positive correlation with immune cells infiltration in TCGA-BLCA **(C)** and Xiangya cohort **(D)**. **(E)** The effect genes of five types of tumor-infiltrating immune cells were sensibly upregulated in high PRS group. **(F)** Our PRS had a positive correlation with 22 ICI-relevant genes (right upper) and 18 TIS genes (left bottom). **(G,H)** Our PRS had a positive correlation with IMmotion150 T-effector signature **(G)**, IMmotion150 Myeloid signature **(H)**, JAVELIN signature **(I)**, and tumor inflammation signatures **(J)**. **(K)** Different regulation of immunotherapy related pathways in high and low PRS groups. The amount of * from one to four means that the corresponding *p*-value is less than 0.05, 0.01, 0.001, 0.0001, respectively. "ns" means that *p* values more than 0.05 and the result is of no significance.

Construction and validation of a platelet risk score and its clinical significance

We performed a univariable Cox regression analysis and LASSO with 10-fold cross validation based on 244 platelet-related genes to screen out 14 genes with prognostic value (Figures 3A, B, Supplementary Table S4). In particular, due to KIF26A lacking expression in all other GEO databases, it was removed from these 14 genes. Based on the remaining 13 genes, we constructed a PRS by the Cox proportional hazard regression algorithm. In TCGA-BLCA training cohort, higher PRS corresponded to particularly poorer survival outcomes (Figures 3C, D, $p < 0.0001$), and an area under the curve (AUC) was approximately 0.68, indicating the accuracy of prognostic prediction was satisfactory (Figure 3E). Then, we used the GSE32894 and Xiangya cohort to validate the prognosis value of PRS. In GSE32894, a higher PRS resulted in poorer survival outcomes (Figures 3F, G, $p = 0.00027$), with satisfactory predictive accuracy (Figure 3H, AUCs around 0.82). In the Xiangya cohort, a higher PRS corresponded to shorter survival times and poorer survival outcomes (Figures 3I, J, $p = 0.027$) and the predictive accuracy was also satisfying (Figure 3K, AUC around 0.73). Taken together, these results suggest that our PRS may predict the individual prognosis of patients with BLCA.

We further performed multivariable Cox regression analysis on age, gender, grade, tumor stage, and PRS. We observed that age, tumor stage and PRS were independent risk factors for overall survival (Supplementary Figure S2A). In order to quantifying individual risk assessment, we constructed a nomogram with these three parameters (Supplementary Figure S2B). Supplementary Figure S2C demonstrates the consistence between actual outcomes and the predictive overall survival outcomes, indicating a high accuracy of our nomogram. The corresponding AUCs at 1, 3, and 5 years were 0.74, 0.71, and 0.70, respectively (Supplementary Figures S2D–SF).

Platelet risk score for immune cell infiltration evaluation of individual patient

As demonstrated in Figures 2A, B, platelet cluster1 and cluster2 represent the inflamed and non-inflamed TME phenotypes, respectively. We further analyzed the difference of immune infiltration between platelet cluster 1/2 and PRS and found that platelet cluster1 corresponds to high PRS, while platelet cluster2 corresponds to low PRS (Figure 4A). Therefore, we used the PRS to predict individual TILs infiltration based on the 13 platelet-related genes.

As expected, in the TCGA-BLCA and Xiangya cohort, PRS had a significantly positive correlation with most steps of tumor immune cycle (Figure 4B, Supplementary Table S5). Furthermore, ssGSEA results showed a positive correlation between TILs infiltration and PRS in TCGA-BLCA and Xiangya cohort, including regulatory T cells, type 2 T helper cells, plasmacytoid dendritic cells, and NK cells (Figures 4C, D, Supplementary Table S5). Our previous studies summarized the effector genes of type 1 helper (Th1) cells, $CD8^+$ cells, NK cells, DCs, and macrophages (Hu et al., 2021; Li et al., 2021), and these genes were all positively correlated with high PRS (Figure 4E). Moreover, PRS had a positive correlation with 22 ICI-relevant genes including CTLA4, CD80 and CD86, as well as 18 TIS genes including CCL5, CD27 and STAT1 (Figure 4F, Supplementary Table S6). For the prediction of immunity therapy efficacy, our PRS showed a significantly positive correlation with IMmotion150 Teff signature (Figure 4G, R = 0.23, $p < 0.001$), IMmotion150 Myeloid signature (Figure 4H, R = 0.28, $p < 0.001$), JAVELIN signature (Figure 4I, R = 0.12, $p = 0.017$) and TIS (Figure 4J, R = 0.21, $p < 0.001$). Furthermore, a significant upregulation of all 21 immune therapy-related pathways was observed in the high PRS group (Figure 4K).

PRS for predicting molecular subtypes of BLCA and other therapeutic applications

Different molecular subtypes of BLCA exhibit different responsiveness to immunotherapy treatments; a luminal subtype exhibits longer survival time and lower immunotherapy response rates than a basal subtype (Mariathasan et al., 2018; Kamoun et al., 2020). As demonstrated in Figure 5A, BLCA with high PRS stood for a basal subtype enriched for basal differentiation and epithelial-mesenchymal transition (EMT) differentiation pathways, whereas BLCA with low PRS stood for a luminal subtype enriched for urothelial, Ta, and luminal differentiation pathways, which is in accordance with previous results. What's more, the predictive accuracies of PRS for predicting luminal and basal subtypes were satisfying in both TCGA-BLCA and Xiangya cohort (Figures 5B, C, AUC around 0.85).

In addition to predicting immunotherapy efficacy, our PRS could predict other therapeutic opportunities. The heat map demonstrated that the high PRS group had a significantly higher response to chemotherapy, immunotherapy, and ERBB therapy, whereas the low PRS group had a lower response to antiangiogenic therapy, according to the DrugBank database (Figure 5D). As shown in Figure 5E, immune-inhibited oncogenic pathways were upregulated in the low PRS group, whereas EGFR network and radiotherapy-predicted pathways were upregulated in the high PRS group, which indicated that EGFR and radiotherapy treatment could be more suitable for patients with high PRS and immune-inhibited treatment could bring better outcomes for patients with low PRS. As some immunotherapy cohorts lack survival outcomes, so we constructed platelet signature based 13 genes using ssGSEA algorithm. Then we compared immunotherapy (anti-PD-1/PD-L1) response between high and low signature groups in four immunotherapy cohorts. As expected, in GSE111636 (anti-PD-1), 100% of patients in high signature group showed response to immunotherapy, which was significantly higher than that in low signature group (Figure 5F). In another three cohorts (anti-PD-1, GSE165252 and GSE126044; anti-PD-L1, GSE173839), although without statistical significance, there were more response patients in the high signature group than that in the low signature group (Supplementary Figures S3A–C).

Discussion

Platelets, a type of significant blood cell contributing to coagulation and hemostasis, were found to influence cancer

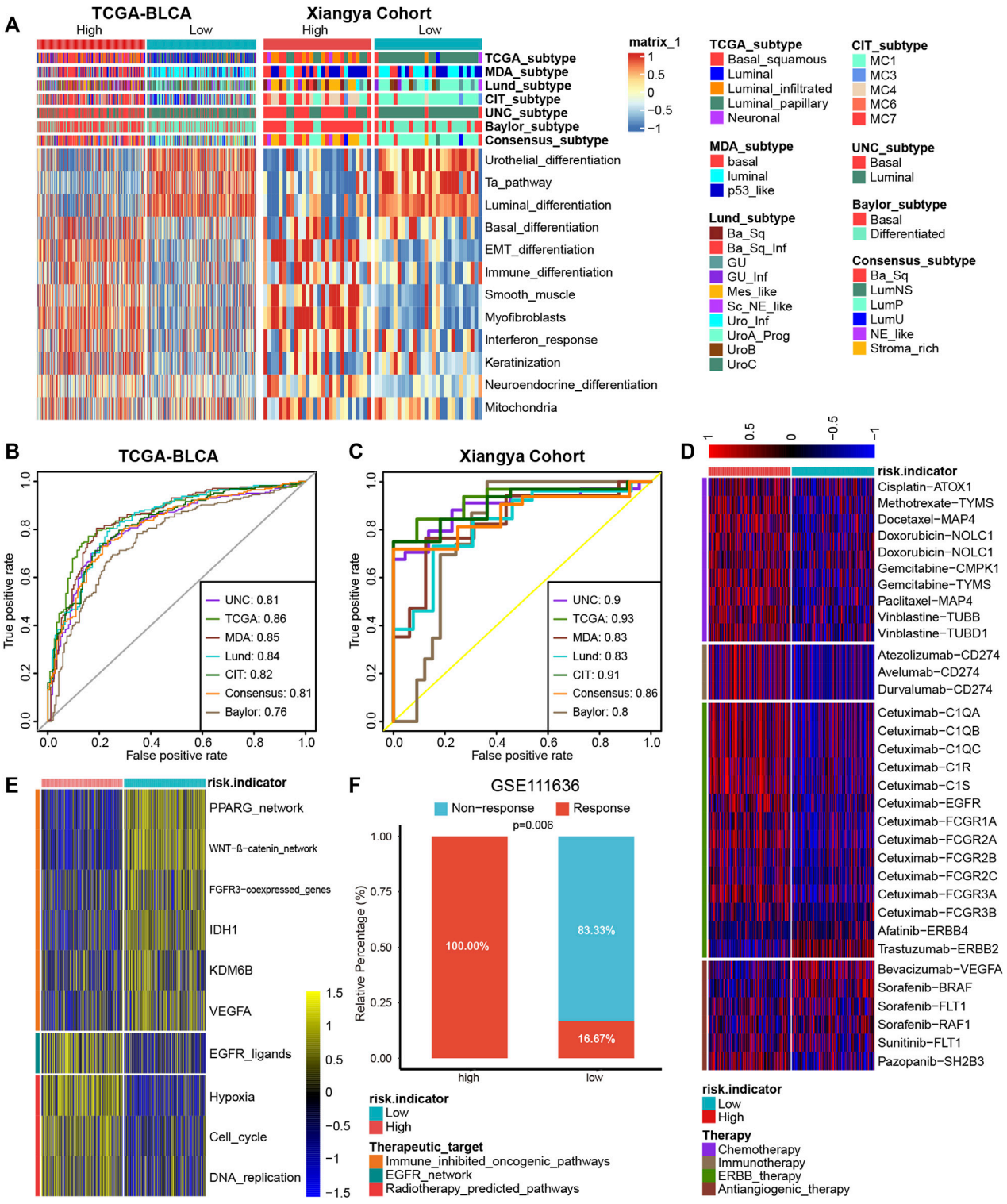

FIGURE 5
PRS for predicting molecular subtypes of BLCA and other therapeutic opportunities. **(A)** BLCA with high PRS stood for a basal subtype and low PRS stood for a luminal subtype in TCGA-BLCA and Xiangya cohort. **(B,C)** The predictive accuracies of PRS for predicting luminal and basal subtypes were satisfying in both TCGA-BLCA and Xiangya cohort. **(D)** As demonstrated in the heatmap, the high and low PRS group had different response to different therapies, according to the DrugBank database. **(E)** The heatmap demonstrated different regulation of the pathways related to different therapies were differently in high and low PRS groups. **(F)** The proportion of patients in the high/low signature group who respond to anti-PD-1 therapy in GSE111636.

progression and metastasis in various ways (Haemmerle et al., 2018). Platelets can aggregate on tumor cells and form a physical barrier to prevent NK cell's attacks (Goubran et al., 2013). Additionally, various growth factors such as TGF-β and PDGF are released by platelets and promote tumor growth by promoting angiogenesis, inducing the expression of tissue factors and other ways (Tesfamariam, 2016; Saito et al., 2018). In BLCA, scientists have found that the platelet-to-lymphocyte ratio has the potential to predict the efficacy of various therapies (Zhang et al., 2015; Wang et al., 2022; Wu et al., 2022). The diagnosis and prognosis predicting values of hemoglobin-to-platelet ratio, platelet-to-leukocyte, platelet volume and platelet distribution width have been also explored in BLCA (Schulz et al., 2017; Tang et al., 2018; Song et al., 2022a). Thus, platelet-related genes are potential targets of cancer therapy. Xie et al. summarized 480 platelet-related genes, the majority of which were reported to take part in tumor development and tumor immune evasion (Xie et al., 2021). Among these genes, α/β-hydrolase domain-containing 6 (AhBHD6) participates in the migration and invasion of non-small cell lung cancer cells (Tang et al., 2020). Type I and II interferons (IFNs) contributes to restricting anti-tumor immunity by $CD^{+}8$ T cell exhaustion (Lukhele et al., 2022). Importantly, the downregulation of the tyrosine kinase Lck/Yes-Related Novel Protein (LYN) was reported to prevent breast tumor invasion and metastasis, and ICI treatment combined with anti-LYN therapy might improve the efficacy of ICIs (Fattet et al., 2020; Vlachostergios, 2021). However, few studies have comprehensively analyzed the relationship between platelet-related genes, cancer immunity, and immunotherapy.

Recently, lots of studies concentrating on a single gene revealed the novel mechanism of TME in BLCA, such as ETV4 and HSF1 (Huang et al., 2022; Zhang et al., 2023). Factually, the relationship between the TME and a group of genes has been also extensively studies. Previously, we used 14 cuproptosis-related genes to generate cuproptosis clusters and observed the correlation between those clusters with TME and immunotherapy in BLCA (Li et al., 2022). Zou et al. generated two programmed cell death clusters, and then comprehensively studied the relationship between those two clusters and prognosis and drug sensitivity in triple-negative breast cancer (Zou et al., 2022). Chen et al. identified three pyroptosis modification patterns and their TME immune characteristics in response to three immune phenotypes (Liu et al., 2022). In BLCA, Song et al. divided patients into four distinct iron metabolism patterns that play vital roles in TME regulation (Song et al., 2022b). These studies could uncover the immune evasion mechanism and are beneficial to precise immunotherapy for patients with BLCA. However, no study has systematically correlated platelet-related genes with the TME, prognosis, and immunotherapy efficacy in BLCA. In this research, we generated two platelet clusters with different survival outcomes, TME phenotypes, and immunotherapy sensitivity. Furthermore, we generated a PRS for individual prognosis and tumor immune infiltration prediction.

BLCA has become the 10th most common malignancy worldwide and poses a huge threat to public health (Sung et al., 2021). Approximately 75% of BLCA cases are non-muscle invasive bladder cancers (NMIBC) with a high recurrence rate (Berdik, 2017; Babjuk et al., 2019). Survival outcomes and response to neoadjuvant chemotherapy are worse when NMIBC develops into muscle invasive bladder cancer (MIBC) (Pietzak et al., 2019). Because BLCA is an immunogenic cancer, ICIs show promising survival benefits in some patients (Sharma et al., 2017; Patel et al., 2020). A clinical trial first found that atezolizumab exhibited good tolerability and durable activity in advanced BLCA. Furthermore, this study was the first to correlate TCGA subtypes with responses to immune checkpoint inhibition (Rosenberg et al., 2016). In addition, nivolumab and pembrolizumab were demonstrated to improve the survival outcomes in advanced BLCA (Sharma et al., 2016; Bellmunt et al., 2017). Nevertheless, we observed that not all patients in these researches were sensitive to ICI treatment, which necessitates the use of biomarkers for predicting ICI efficacy.

Recent studies have found that tumors cannot be separated from the low immune surveillance and drug interference provided by the TME (Binnewies et al., 2018; Crispen and Kusmartsev, 2020). More TILs and an immuno-activated microenvironment can enhance the efficacy of ICI treatment in patients with BLCA (Zou et al., 2021). Thus, discriminating inflamed tumors from non-inflamed tumors could contribute to predicting ICI efficacy, and the transformation of non-inflamed tumors into inflamed ones leads to higher ICI efficacy (Duan et al., 2020). Various studies show the correlation of platelets with prognosis and immunotherapy efficacy in colorectal cancer, triple-negative breast cancer, and other cancer types (Xie et al., 2021; Miao et al., 2022). In the present research, we first constructed a PRS for precise prediction of TME phenotypes, and further validated the result in our cohort. In addition, our PRS could directly predict immunotherapy efficacy and other therapeutic opportunities, which are vital for the treatment of patients with BLCA.

The present research had a few limitations. Firstly, prospective studies are needed to compensate for the limitations of our retrospective data. Secondly, further wet experiments should be performed to investigate the underlying mechanisms in detail. Third, batch effects need to be taken into consideration to validate our findings.

Conclusion

Platelet-related genes predicted TME phenotypes in BLCA. We constructed a PRS that could predict the TME, prognosis, immunotherapy efficacy, and molecular subtypes in BLCA.

Data availability statement

The original contributions presented in the study are included in the article/Supplementary Material, further inquiries can be directed to the corresponding authors.

Author contributions

Conception and design: DD, XL, TQ, YD, NL, and HL. Provision of study materials or patients: XL and TQ. Collection and assembly of data: DD, YD, NL, and HL. Data analysis and interpretation: DD, XL, YD, NL, and HL. Manuscript writing: All authors. Final approval of manuscript: All authors.

Funding

This work was supported by National Natural Science Foundation of China (81902592, 82070785).

Conflict of interest

The authors declare that the research was conducted in the absence of any commercial or financial relationships that could be construed as a potential conflict of interest.

Publisher's note

All claims expressed in this article are solely those of the authors and do not necessarily represent those of their affiliated organizations, or those of the publisher, the editors and the reviewers. Any product that may be evaluated in this article, or claim that may be made by its manufacturer, is not guaranteed or endorsed by the publisher.

Supplementary material

The supplementary material for this article can be found online at: https://www.frontiersin.org/articles/10.3389/fphar.2023.1187700/full#supplementary-material

SUPPLEMENTARY FIGURE S1
Unsupervised clustering generally divided 244 platelet-related genes in the TCGA-BLCA cohort into two clusters.

SUPPLEMENTARY FIGURE S2
Construction of a nomogram. **(A)** Multivariable Cox regression analysis indicated three independent risk factors for overall survival PRS and other clinicopathological factors. **(B)** Details of the nomogram. **(C)** Calibration curves showed the consistence between actual outcomes and the predictive overall survival outcomes. **(D–F)** The corresponding AUCs at 1 **(D)**, 3 **(E)**, and 5 **(F)** years were 0.74, 0.71, and 0.70, respectively.

SUPPLEMENTARY FIGURE S3
The proportion of patients in the high/low signature group who respond to anti-PD-1/PD-L1 therapy in GSE165252 **(A)**, GSE126044 **(B)** and GSE173839 **(C)**, respectively.

References

Babjuk, M., Burger, M., Capoun, O., Cohen, D., Compérat, E. M., Dominguez Escrig, J. L., et al. (2022). European association of Urology guidelines on non-muscle-invasive bladder cancer (Ta, T1, and carcinoma *in situ*). *Eur. Urol.* 81 (1), 75–94. doi:10.1016/j.eururo.2021.08.010

Babjuk, M., Burger, M., Compérat, E. M., Gontero, P., Mostafid, A. H., Palou, J., et al. (2019). European association of Urology guidelines on non-muscle-invasive bladder cancer (TaT1 and carcinoma *in situ*) - 2019 update. *Eur. Urol.* 76 (5), 639–657. doi:10.1016/j.eururo.2019.08.016

Bagchi, S., Yuan, R., and Engleman, E. G. (2021). Immune checkpoint inhibitors for the treatment of cancer: Clinical impact and mechanisms of response and resistance. *Annu. Rev. Pathol.* 16, 223–249. doi:10.1146/annurev-pathol-042020-042741

Beer, T. M., Kwon, E. D., Drake, C. G., Fizazi, K., Logothetis, C., Gravis, G., et al. (2017). Randomized, double-blind, phase III trial of ipilimumab versus placebo in asymptomatic or minimally symptomatic patients with metastatic chemotherapy-naive castration-resistant prostate cancer. *J. Clin. Oncol.* 35 (1), 40–47. doi:10.1200/JCO.2016.69.1584

Bellmunt, J., de Wit, R., Vaughn, D. J., Fradet, Y., Lee, J. L., Fong, L., et al. (2017). Pembrolizumab as second-line therapy for advanced urothelial carcinoma. *N. Engl. J. Med.* 376 (11), 1015–1026. doi:10.1056/NEJMoa1613683

Berdik, C. (2017). Unlocking bladder cancer. *Nature* 551 (7679), S34–S35. doi:10.1038/551S34a

Binnewies, M., Roberts, E. W., Kersten, K., Chan, V., Fearon, D. F., Merad, M., et al. (2018). Understanding the tumor immune microenvironment (TIME) for effective therapy. *Nat. Med.* 24 (5), 541–550. doi:10.1038/s41591-018-0014-x

Braun, D. A., Hou, Y., Bakouny, Z., Ficial, M., Sant' Angelo, M., Forman, J., et al. (2020). Interplay of somatic alterations and immune infiltration modulates response to PD-1 blockade in advanced clear cell renal cell carcinoma. *Nat. Med.* 26 (6), 909–918. doi:10.1038/s41591-020-0839-y

Charoentong, P., Finotello, F., Angelova, M., Mayer, C., Efremova, M., Rieder, D., et al. (2017). Pan-cancer immunogenomic analyses reveal genotype-immunophenotype relationships and predictors of response to checkpoint blockade. *Cell Rep.* 18 (1), 248–262. doi:10.1016/j.celrep.2016.12.019

Chen, D. S., and Mellman, I. (2017). Elements of cancer immunity and the cancer-immune set point. *Nature* 541 (7637), 321–330. doi:10.1038/nature21349

Chen, X., Zhang, J., Ruan, W., Huang, M., Wang, C., Wang, H., et al. (2020). Urine DNA methylation assay enables early detection and recurrence monitoring for bladder cancer. *J. Clin. Invest.* 130 (12), 6278–6289. doi:10.1172/JCI139597

Crispen, P. L., and Kusmartsev, S. (2020). Mechanisms of immune evasion in bladder cancer. *Cancer Immunol. Immunother.* 69 (1), 3–14. doi:10.1007/s00262-019-02443-4

De Palma, M., Biziato, D., and Petrova, T. V. (2017). Microenvironmental regulation of tumour angiogenesis. *Nat. Rev. Cancer* 17 (8), 457–474. doi:10.1038/nrc.2017.51

Duan, Q., Zhang, H., Zheng, J., and Zhang, L. (2020). Turning cold into hot: Firing up the tumor microenvironment. *Trends Cancer* 6 (7), 605–618. doi:10.1016/j.trecan.2020.02.022

Fattet, L., Jung, H. Y., Matsumoto, M. W., Aubol, B. E., Kumar, A., Adams, J. A., et al. (2020). Matrix rigidity controls epithelial-mesenchymal plasticity and tumor metastasis via a mechanoresponsive EPHA2/LYN complex. *Dev. Cell* 54 (3), 302–316. doi:10.1016/j.devcel.2020.05.031

Goubran, H. A., Burnouf, T., Radosevic, M., and El-Ekiaby, M. (2013). The platelet-cancer loop. *Eur. J. Intern Med.* 24 (5), 393–400. doi:10.1016/j.ejim.2013.01.017

Haemmerle, M., Stone, R. L., Menter, D. G., Afshar-Kharghan, V., and Sood, A. K. (2018). The platelet lifeline to cancer: Challenges and opportunities. *Cancer Cell* 33 (6), 965–983. doi:10.1016/j.ccell.2018.03.002

Hu, J., Yu, A., Othmane, B., Qiu, D., Li, H., Li, C., et al. (2021). Siglec15 shapes a non-inflamed tumor microenvironment and predicts the molecular subtype in bladder cancer. *Theranostics* 11 (7), 3089–3108. doi:10.7150/thno.53649

Huang, M., Dong, W., Xie, R., Wu, J., Su, Q., Li, W., et al. (2022). HSF1 facilitates the multistep process of lymphatic metastasis in bladder cancer via a novel PRMT5-WDR5-dependent transcriptional program. *Cancer Commun. (Lond).* 42 (5), 447–470. doi:10.1002/cac2.12284

Kamoun, A., de Reyniès, A., Allory, Y., Sjödahl, G., Robertson, A. G., Seiler, R., et al. (2020). A consensus molecular classification of muscle-invasive bladder cancer. *Eur. Urol.* 77 (4), 420–433. doi:10.1016/j.eururo.2019.09.006

Li, H., Liu, S., Li, C., Xiao, Z., Hu, J., and Zhao, C. (2021). TNF family-based signature predicts prognosis, tumor microenvironment, and molecular subtypes in bladder carcinoma. *Front. Cell Dev. Biol.* 9, 800967. doi:10.3389/fcell.2021.800967

Li, H., Zu, X., Hu, J., Xiao, Z., Cai, Z., Gao, N., et al. (2022). Cuproptosis depicts tumor microenvironment phenotypes and predicts precision immunotherapy and prognosis in bladder carcinoma. *Front. Immunol.* 13, 964393. doi:10.3389/fimmu.2022.964393

Liberzon, A., Birger, C., Thorvaldsdóttir, H., Ghandi, M., Mesirov, J. P., and Tamayo, P. (2015). The Molecular Signatures Database (MSigDB) hallmark gene set collection. *Cell Syst.* 1 (6), 417–425. doi:10.1016/j.cels.2015.12.004

Liu, J., Chen, C., Geng, R., Shao, F., Yang, S., Zhong, Z., et al. (2022). Pyroptosis-related gene expression patterns and corresponding tumor microenvironment infiltration characterization in ovarian cancer. *Comput. Struct. Biotechnol. J.* 20, 5440–5452. doi:10.1016/j.csbj.2022.09.037

Lukhele, S., Rabbo, D. A., Guo, M., Shen, J., Elsaesser, H. J., Quevedo, R., et al. (2022). The transcription factor IRF2 drives interferon-mediated $CD8^+$ T cell exhaustion to restrict anti-tumor immunity. *Immunity* 55 (12), 2369–2385.e10. doi:10.1016/j.immuni.2022.10.020

Mariathasan, S., Turley, S. J., Nickles, D., Castiglioni, A., Yuen, K., Wang, Y., et al. (2018). TGFβ attenuates tumour response to PD-L1 blockade by contributing to exclusion of T cells. *Nature* 554 (7693), 544–548. doi:10.1038/nature25501

McDermott, D. F., Huseni, M. A., Atkins, M. B., Motzer, R. J., Rini, B. I., Escudier, B., et al. (2018). Clinical activity and molecular correlates of response to atezolizumab alone or in combination with bevacizumab versus sunitinib in renal cell carcinoma. *Nat. Med.* 24 (6), 749–757. doi:10.1038/s41591-018-0053-3

Miao, Y., Xu, Z., Feng, W., Zheng, M., Xu, Z., Gao, H., et al. (2022). Platelet infiltration predicts survival in postsurgical colorectal cancer patients. *Int. J. Cancer* 150 (3), 509–520. doi:10.1002/ijc.33816

Necchi, A., Anichini, A., Raggi, D., Briganti, A., Massa, S., Lucianò, R., et al. (2018). Pembrolizumab as neoadjuvant therapy before radical cystectomy in patients with muscle-invasive urothelial bladder carcinoma (PURE-01): An open-label, single-arm, phase II study. *J. Clin. Oncol.* 36 (34), 3353–3360. doi:10.1200/JCO.18.01148

Patel, V. G., Oh, W. K., and Galsky, M. D. (2020). Treatment of muscle-invasive and advanced bladder cancer in 2020. *CA Cancer J. Clin.* 70 (5), 404–423. doi:10.3322/caac.21631

Patmore, S., Dhami, S. P. S., and O'Sullivan, J. M. (2020). Von Willebrand factor and cancer; metastasis and coagulopathies. *J. Thromb. Haemost.* 18 (10), 2444–2456. doi:10.1111/jth.14976

Pietzak, E. J., Zabor, E. C., Bagrodia, A., Armenia, J., Hu, W., Zehir, A., et al. (2019). Genomic differences between "primary" and "secondary" muscle-invasive bladder cancer as a basis for disparate outcomes to cisplatin-based neoadjuvant chemotherapy. *Eur. Urol.* 75 (2), 231–239. doi:10.1016/j.eururo.2018.09.002

Quail, D. F., and Joyce, J. A. (2017). The microenvironmental landscape of brain tumors. *Cancer Cell* 31 (3), 326–341. doi:10.1016/j.ccell.2017.02.009

Riess, L. (1872). Zur pathologischen Anatomie des Blutes. *Arch. Anat. Physiol. Wissensch Med.* 39, 237–249.

Rosenberg, J. E., Hoffman-Censits, J., Powles, T., van der Heijden, M. S., Balar, A. V., Necchi, A., et al. (2016). Atezolizumab in patients with locally advanced and metastatic urothelial carcinoma who have progressed following treatment with platinum-based chemotherapy: A single-arm, multicentre, phase 2 trial. *Lancet* 387 (10031), 1909–1920. doi:10.1016/S0140-6736(16)00561-4

Saito, M., Ichikawa, J., Ando, T., Schoenecker, J. G., Ohba, T., Koyama, K., et al. (2018). Platelet-derived TGF-β induces tissue factor expression via the Smad3 pathway in osteosarcoma cells. *J. Bone Min. Res.* 33 (11), 2048–2058. doi:10.1002/jbmr.3537

Schlesinger, M. (2018). Role of platelets and platelet receptors in cancer metastasis. *J. Hematol. Oncol.* 11 (1), 125. doi:10.1186/s13045-018-0669-2

Schulz, G. B., Grimm, T., Buchner, A., Jokisch, F., Grabbert, M., Schneevoigt, B. S., et al. (2017). Prognostic value of the preoperative platelet-to-leukocyte ratio for oncologic outcomes in patients undergoing radical cystectomy for bladder cancer. *Clin. Genitourin. Cancer* 15 (6), e915–e921. doi:10.1016/j.clgc.2017.05.009

Sharma, P., Callahan, M. K., Bono, P., Kim, J., Spiliopoulou, P., Calvo, E., et al. (2016). Nivolumab monotherapy in recurrent metastatic urothelial carcinoma (CheckMate 032): A multicentre, open-label, two-stage, multi-arm, phase 1/2 trial. *Lancet Oncol.* 17 (11), 1590–1598. doi:10.1016/S1470-2045(16)30496-X

Sharma, P., Retz, M., Siefker-Radtke, A., Baron, A., Necchi, A., Bedke, J., et al. (2017). Nivolumab in metastatic urothelial carcinoma after platinum therapy (CheckMate 275): A multicentre, single-arm, phase 2 trial. *Lancet Oncol.* 18 (3), 312–322. doi:10.1016/S1470-2045(17)30065-7

Song, X., Xin, S., Zhang, Y., Mao, J., Duan, C., Cui, K., et al. (2022b). Identification and quantification of iron metabolism landscape on therapy and prognosis in bladder cancer. *Front. Cell Dev. Biol.* 10, 810272. doi:10.3389/fcell.2022.810272

Song, X., Tian, J., Yang, L., Zhang, Y., Dong, Z., Ding, H., et al. (2022a). Prognostic value of preoperative platelet-related parameters and plasma fibrinogen in patients with non-muscle invasive bladder cancer after transurethral resection of bladder tumor. *Future Oncol.* 18 (26), 2933–2942. doi:10.2217/fon-2022-0223

Speir, M., Nowell, C. J., Chen, A. A., O'Donnell, J. A., Shamie, I. S., Lakin, P. R., et al. (2020). Ptpn6 inhibits caspase-8- and Ripk3/Mlkl-dependent inflammation. *Nat. Immunol.* 21 (1), 54–64. doi:10.1038/s41590-019-0550-7

Sung, H., Ferlay, J., Siegel, R. L., Laversanne, M., Soerjomataram, I., Jemal, A., et al. (2021). Global cancer statistics 2020: GLOBOCAN estimates of incidence and mortality worldwide for 36 cancers in 185 countries. *CA Cancer J. Clin.* 71 (3), 209–249. doi:10.3322/caac.21660

Tang, G., Zhen, Y., Xie, W., Wang, Y., Chen, F., Qin, C., et al. (2018). Preoperative hemoglobin-platelet ratio can significantly predict progression and mortality outcomes in patients with T1G3 bladder cancer undergoing transurethral resection of bladder tumor. *Oncotarget* 9 (26), 18627–18636. doi:10.18632/oncotarget.23896

Tang, Z., Xie, H., Heier, C., Huang, J., Zheng, Q., Eichmann, T. O., et al. (2020). Enhanced monoacylglycerol lipolysis by ABHD6 promotes NSCLC pathogenesis. *EBioMedicine* 53, 102696. doi:10.1016/j.ebiom.2020.102696

Tesfamariam, B. (2016). Involvement of platelets in tumor cell metastasis. *Pharmacol. Ther.* 157, 112–119. doi:10.1016/j.pharmthera.2015.11.005

Tumeh, P. C., Harview, C. L., Yearley, J. H., Shintaku, I. P., Taylor, E. J., Robert, L., et al. (2014). PD-1 blockade induces responses by inhibiting adaptive immune resistance. *Nature* 515 (7528), 568–571. doi:10.1038/nature13954

Vlachostergios, P. J. (2021). Integrin signaling gene alterations and outcomes of cancer patients receiving immune checkpoint inhibitors. *Am. J. Transl. Res.* 13 (11), 12386–12394.

Wang, C., Jin, W., Ma, X., and Dong, Z. (2022). The different predictive value of mean platelet volume-to-lymphocyte ratio for postoperative recurrence between non-muscular invasive bladder cancer patients treated with intravesical chemotherapy and intravesical chemohyperthermia. *Front. Oncol.* 12, 1101830. doi:10.3389/fonc.2022.1101830

Wei, X., Cai, L., Chen, H., Shang, L., Zhao, Y., and Sun, W. (2022). Noninvasive multiplexed analysis of bladder cancer-derived urine exosomes via janus magnetic microspheres. *Anal. Chem.* 94 (51), 18034–18041. doi:10.1021/acs.analchem.2c04408

Wu, R., Li, D., Zhang, F., Bai, Y., Wang, X., and Han, P. (2022). Prognostic value of platelet-to-lymphocyte ratio in non-muscle invasive bladder cancer patients: Intravesical Bacillus calmette-guerin treatment after transurethral resection of bladder tumor. *Front. Surg.* 9, 907485. doi:10.3389/fsurg.2022.907485

Xiao, Y., and Yu, D. (2021). Tumor microenvironment as a therapeutic target in cancer. *Pharmacol. Ther.* 221, 107753. doi:10.1016/j.pharmthera.2020.107753

Xie, J., Zou, Y., Ye, F., Zhao, W., Xie, X., Ou, X., et al. (2021). A novel platelet-related gene signature for predicting the prognosis of triple-negative breast cancer. *Front. Cell Dev. Biol.* 9, 795600. doi:10.3389/fcell.2021.795600

Yun, H. M., Park, K. R., Park, M. H., Kim, D. H., Jo, M. R., Kim, J. Y., et al. (2015). PRDX6 promotes tumor development via the JAK2/STAT3 pathway in a urethane-induced lung tumor model. *Free Radic. Biol. Med.* 80, 136–144. doi:10.1016/j.freeradbiomed.2014.12.022

Zhang, G. M., Zhu, Y., Luo, L., Wan, F. N., Zhu, Y. P., Sun, L. J., et al. (2015). Preoperative lymphocyte-monocyte and platelet-lymphocyte ratios as predictors of overall survival in patients with bladder cancer undergoing radical cystectomy. *Tumour Biol.* 36 (11), 8537–8543. doi:10.1007/s13277-015-3613-x

Zhang, Q., Liu, S., Wang, H., Xiao, K., Lu, J., Chen, S., et al. (2023). ETV4 mediated tumor-associated neutrophil infiltration facilitates lymphangiogenesis and lymphatic metastasis of bladder cancer. *Adv. Sci. (Weinh).* 10, e2205613. doi:10.1002/advs.202205613

Zou, Y., Hu, X., Zheng, S., Yang, A., Li, X., Tang, H., et al. (2021). Discordance of immunotherapy response predictive biomarkers between primary lesions and paired metastases in tumours: A systematic review and meta-analysis. *EBioMedicine* 63, 103137. doi:10.1016/j.ebiom.2020.103137

Zou, Y., Xie, J., Zheng, S., Liu, W., Tang, Y., Tian, W., et al. (2022). Leveraging diverse cell-death patterns to predict the prognosis and drug sensitivity of triple-negative breast cancer patients after surgery. *Int. J. Surg.* 107, 106936. doi:10.1016/j.ijsu.2022.106936

frontiers | Frontiers in Pharmacology

TYPE Original Research
PUBLISHED 08 June 2023
DOI 10.3389/fphar.2023.1202823

OPEN ACCESS

EDITED BY
Ouyang Chen,
Duke University, United States

REVIEWED BY
Jianguo Feng,
Affiliated Hospital of Southwest Medical University, China
Teng Ma,
Capital Medical University, China

*CORRESPONDENCE
Zhijie Xu,
xuzhijie@xiangya.com.cn
Fada Xia,
xiafada@xiangya.com.cn

RECEIVED 13 April 2023
ACCEPTED 30 May 2023
PUBLISHED 08 June 2023

CITATION
Su D, Zhang Z, Xia F, Liang Q, Liu Y, Liu W and Xu Z (2023), ICD-related risk model predicts the prognosis and immunotherapy response of patients with liver cancer.
Front. Pharmacol. 14:1202823.
doi: 10.3389/fphar.2023.1202823

ICD-related risk model predicts the prognosis and immunotherapy response of patients with liver cancer

Duntao Su[1], Zeyu Zhang[1], Fada Xia[1,2]*, Qiuju Liang[3], Yuanhong Liu[3], Wei Liu[4] and Zhijie Xu[4]*

[1]Department of General Surgery, Xiangya Hospital, Central South University, Changsha, Hunan, China, [2]National Clinical Research Center for Geriatric Disorders, Xiangya Hospital, Central South University, Changsha, Hunan, China, [3]Department of Pharmacy, Xiangya Hospital, Central South University, Changsha, Hunan, China, [4]Department of Pathology, Xiangya Hospital, Central South University, Changsha, Hunan, China

Immunogenic cell death (ICD) is a novel cell death mechanism that activates and regulates the immune system against cancer. However, its prognostic value in liver cancer remains unclear. Here, several algorithms such as correlation analysis, Cox regression analysis, and Lasso regression analysis were carried out to evaluate the prognostic value of ICD-related genes in patients with liver cancer. Three ICD-related prognostic genes, the prion protein gene (PRNP), dynamin 1-like gene (DNM1L), and caspase-8 (CASP8), were identified and used to construct a risk signature. Patients with liver cancer were categorized into high- and low-risk groups using the ICD-related signature. Subsequently, a multivariate regression analysis revealed that the signature was an independent risk factor in liver cancer [hazard ratio (HR) = 6.839; 95% confidence interval (CI) = 1.625–78.785]. Patient survival was also predicted using the risk model, with area under the curve values of 0.75, 0.70, and 0.69 for 1-, 3-, and 5-year survival, respectively. Finally, a prognostic nomogram containing the clinical characteristics and risk scores of patients was constructed. The constructed ICD-related signature could serve as a prognostic and immunotherapeutic biomarker in liver cancer.

KEYWORDS

liver cancer, immunogenic cell death, prognosis, signature, tumor immune microenvironment

Introduction

Liver cancer is extremely malignant, and its onset is frequently concealed, with most patients being diagnosed at a late stage. The fatality rate from liver cell cancer has risen steadily over the last few decades (Xu et al., 2022). With the advancement of medical technology, the emergence of novel approaches such as targeted therapy and immunotherapy has considerably increased the survival time of patients with liver cancer (Kalasekar et al., 2021). Sorafenib, for example, remains the only medicine approved for the systemic treatment of advanced hepatocellular carcinoma (HCC), but its efficacy is limited (Li et al., 2021; Wu et al., 2022). As a result, new biological indicators and prediction models are required to accurately predict the immunotherapy response of patients with liver cancer.

Immunogenic cell death (ICD) is a new cell death mechanism that involves the activation and regulation of the immune system against cancer (Zhang et al., 2021). During ICD, dead cells release various substances and antigens to interact with antigen-presenting cells or other immune cells. These immunogenic molecules are called damage-associated molecular patterns (DAMPs). ICD kills cancer cells by triggering specific tumor immune responses (Kim et al., 2021). Notably, Food and Drug Administration-approved ICD-based drugs have been used in treating melanoma and small-cell lung cancer (Markham, 2020; Tzogani et al., 2021). A study demonstrated that disulfiram and copper can synergistically induce ICD in HCC cells by promoting dendritic cell maturation and $CD8^+$ T cell cytotoxicity (Gao et al., 2022). However, there are currently few studies on the prognostic and therapeutic value of ICD signaling in patients with liver cancer. Moreover, a deeper comprehension and investigation of ICD-related molecules can yield novel perspectives and insights regarding the occurrence, treatment, and prognosis of liver cancer.

In this study, we constructed a risk model for liver cancer prognosis based on the differential expression of ICD-related genes. Based on the median cut-off risk score, we divided samples into high-risk and low-risk groups. We also evaluated the risk model's prognostic prediction capacity using an external cohort. The immune status of the two groups was then assessed. Finally, we combined clinicopathological variables with risk score to develop an effective nomogram for predicting samples survival rates. The detailed flowchart can be seen in Supplementary Figure S1. This model could be useful for predicting the immunotherapy response of patients with liver cancer.

Materials and methods

Identification of ICD-related genes

The Cancer Genome Atlas (TCGA, http://cancergenome.nih.gov/), the University of California Santa Cruz (UCSC, http://xena.ucsc.edu), and Xena Browser (TCGA database version: Data Release 31.0, 29 October 2021) served as the primary sources of patients' information in this study. Patients with complete clinical and survival information were included in the study, whereas those with incomplete information were excluded. A total of 39 normal samples and 377 liver cancer samples in the TCGA-HCC datasets were extracted from UCSC databases. The GSE65372 (Zhao et al., 2021a) and GSE25097 (Sung et al., 2012) from Gene Expression Omnibus (GEO, https://www.ncbi.nlm.nih.gov/go/) were used to screen the different genes associated with liver cancer. In addition, 138 ICD-related genes were acquired from Zhang's report (Zhang and Chen, 2022). The overlap of differentially expressed ICD-related genes in TCGA, GSE65372, and GSE25097 datasets was identified.

Construction of the prognostic signature based on ICD-related genes

Lasso regression analysis was performed to select the prognostic ICD-related genes. The risk score was calculated using the formula: risk score = expression of (ICD-related genes 1) × (β1 of ICD-related genes 1) + expression of (ICD-related genes 2) × (β2 of ICD-related genes 2) + expression of (ICD-related genes 3) × (β3 of ICD-related genes 3) (Tibshirani, 1997). To evaluate the diagnostic and predictive value of the signature, the "survminer" and "TimeROC" R packages were used to plot the receiver operating characteristic (ROC) and the Kaplan-Meier curves (Blanche et al., 2013). Univariate and multivariate regression analyses were also used to verify the predictive value of this risk model. The nomogram for estimating the 1-, 3-, and 5-year survival probability of patients with liver cancer was constructed using the "rms" R package. An alluvial plot was used to confirm the predictive value of the signature in patients with clinical and pathological characteristics of liver cancer. In addition, decision curve analysis (DCA) was performed using the "rmda" R package to confirm the clinical significance of the signature.

Immune analysis

To evaluate the effectiveness of immunotherapy, immune checkpoint blockade was predicted using ImmuCellAI (http://bioinfo.life.hust.edu.cn/ImmuCellAI#!/) (Miao et al., 2020). The tumor purity and proportion of infiltrating stromal/immune cells in the high- and low-risk groups were also determined using the CIBERSOFT (Newman et al., 2015) and TIMER (Li et al., 2016) methods.

Gene set enrichment and functional enrichment analyses

Kyoto Encyclopedia of Genes and Genomes (KEGG) (https://metascape.org/gp/index.html#/main/step1) and Gene Ontology (GO) (https://proteomaps.net/) (Subramanian et al., 2005) were used for signaling pathway enrichment and functional annotation analyses, respectively.

Statistical analysis

All statistical evaluations were performed using the R software (version 4.0.1). Nonparametric tests and one-way analysis of variance were used when necessary. Statistical significance was defined as a p-value < 0.05.

Results

Differential expression and gene ontology analysis of ICD-related genes

Due to the lack of additional datasets containing survival information, we included multiple GEO datasets for the analysis of differential genes to improve the robustness of the study findings. We conducted a differential analysis of ICD-related genes using datasets from three databases: GEO65372, GEO25097, and TCGA-HCC. The results were further intersected, and the resulting Venn diagram is shown in Figure 1A. Supplementary Table S1; Figure 1A present detailed information for the Venn diagram. Five ICD-related genes were preliminarily identified. Next, we performed a

10.3389/fphar.2023.1202823

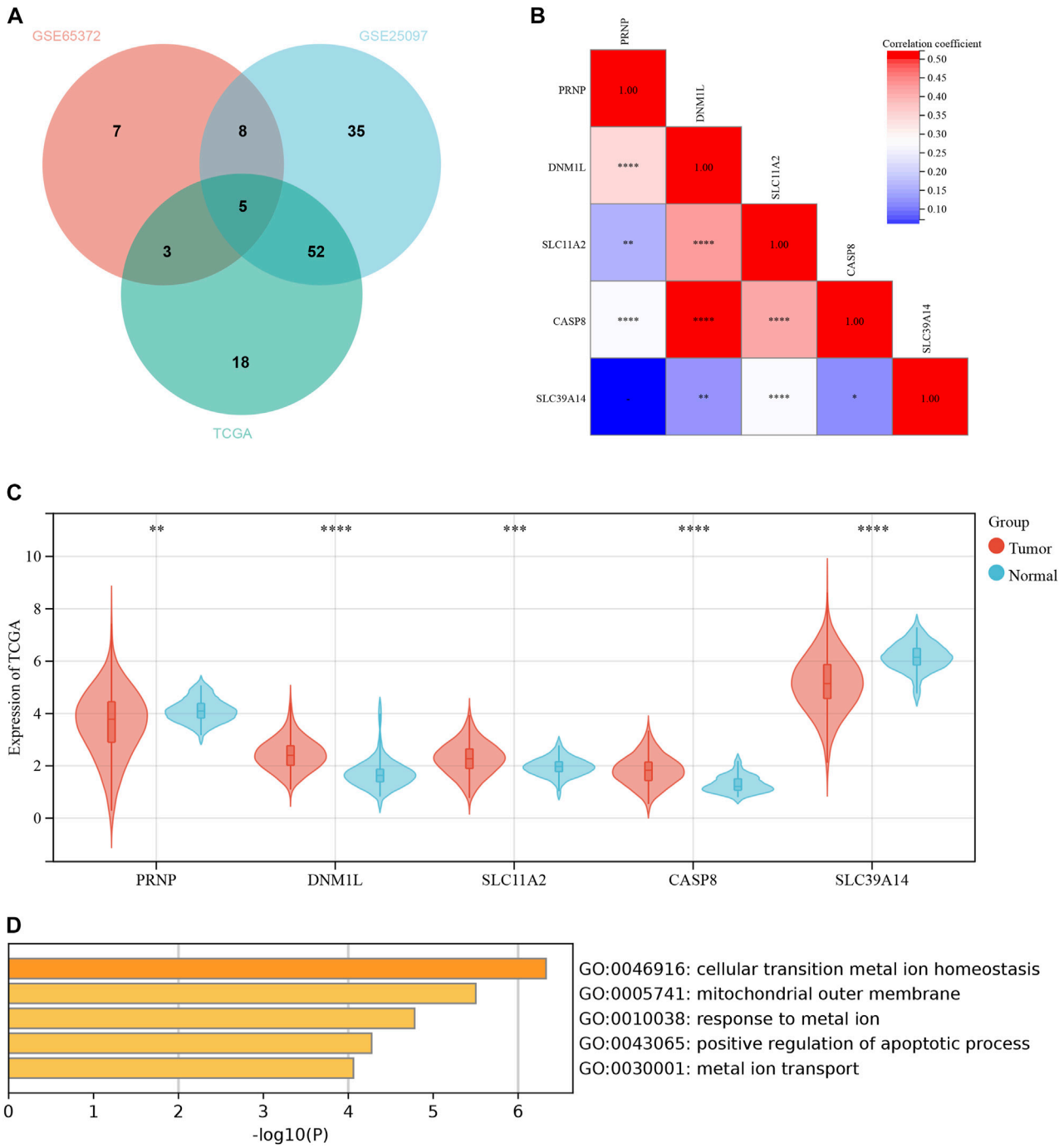

FIGURE 1
Differential expression of ICD-related genes between normal and liver cancer tissues. **(A)** The Venn diagram in GSE65372, GSE25097 and TCGA. **(B)** The heatmap of 5 ICD-related genes in normal and liver cancer tissues. **(C)** The expression of 5 ICD-related genes in normal and liver cancer tissues. **(D)** The GO functional analyses in the 5 ICD-related genes. *$p < 0.05$; **$p < 0.01$; ***$p < 0.001$; ****$p < 0.0001$.

correlation analysis and found that the genes CASP8 and DNM1L had the strongest correlation (Figure 1B). The results of differential expression between tumor and normal tissues are shown in Figure 1C. In the TCGA database, all five genes exhibited significant differences. The GO enrichment analysis indicated that these differentially expressed genes were mainly enriched in cellular transition metal ion homeostasis (Figure 1D).

Establishment and verification of the ICD-related risk signature

Lasso-Cox regression analysis was used to further analyze the differentially expressed genes, and three genes, PRNP, DNM1L, and CASP8 were found to be statistically significant enough to be used to construct a risk model. The results of the Lasso-Cox regression analysis

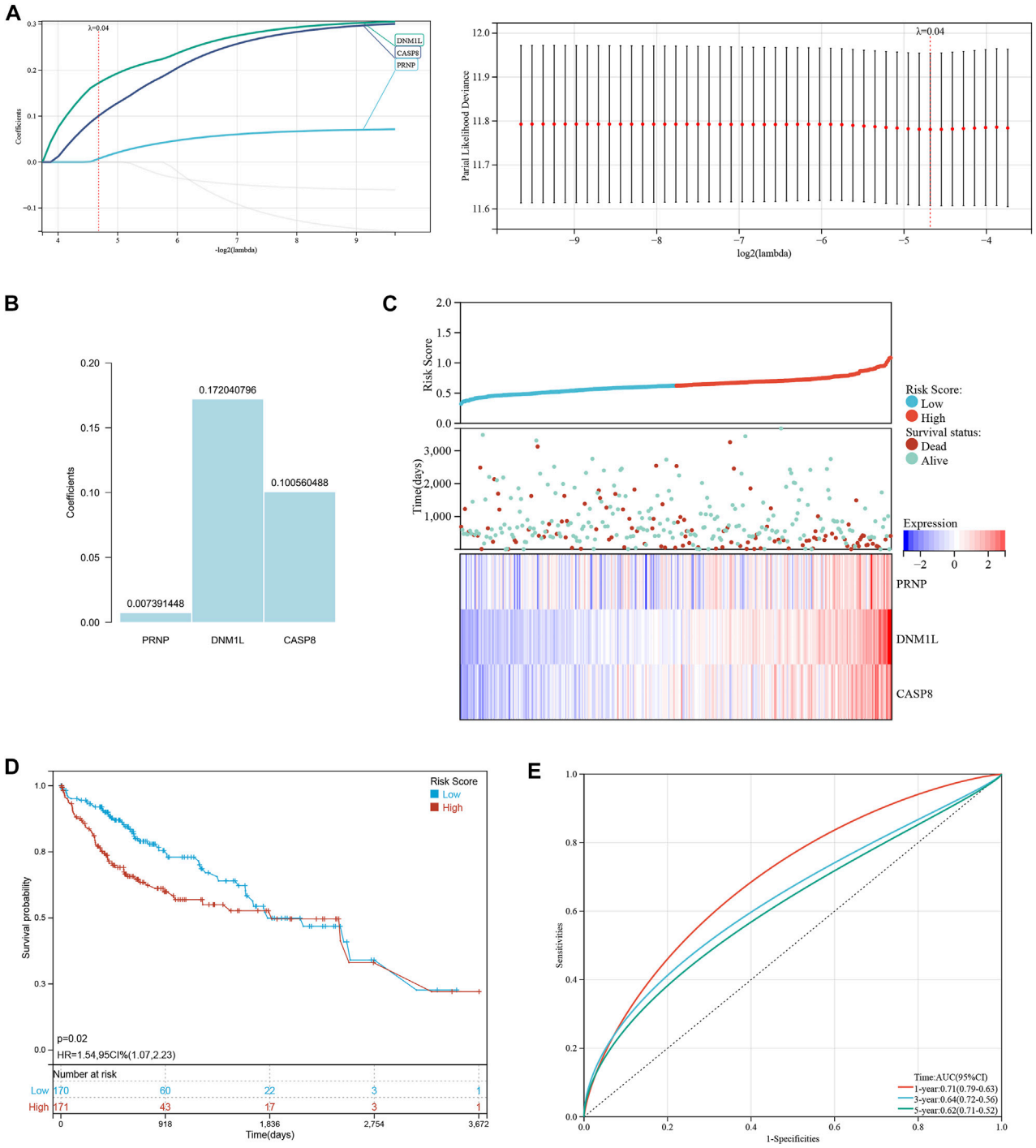

FIGURE 2
Establishment and verification of a risk signature related to ICD-related genes. **(A, B)** The Lasso-Cox regression analysis in ICD-related genes. **(C)** Distribution of risk scores and overall survival status. **(D)** Kaplan-Meier curves for the overall survival of patients in the high- and low-risk groups. **(E)** The time-dependent ROC curves supporting prognostic accuracy of the risk score.

were also used to generate the risk score for each sample. Because the λ value was 0.04, the three ICD-related genes were used to build a risk model. The risk score was calculated as follows: (PRNP) * (0.007391448) + (DNM1L) * (0.172040796) + (CASP8) * (0.100560488) (Figures 2A, B). The distribution of risk scores and overall survival status (Figure 2C) and Kaplan-Meier curve (Figure 2D) demonstrated that the prognosis of patients in the high-risk group was poorer than that of those in the low-risk group. Table 1 displays the clinicopathological characteristics of patients in the high- and low-risk groups. The ROC curve revealed that the risk score had a strong predictive ability, with area under the curve values of 0.71, 0.66, and 0.61 for predicting 1-, 3-, and 5-year survival, respectively (Figure 2E).

TABLE1 Associations between the signature and patient characteristics in high and low risk groups cohort.

Characteristics	High (N = 170)	Low (N = 171)	Total (N = 341)	*p*-value
Age				
Mean ± SD	57.78 ± 14.33	60.40 ± 12.08	59.10 ± 13.30	
Median [min-max]	59.00 [16.00,85.00]	62.00 [20.00,82.00]	61.00 [16.00,85.00]	
gender				0.02
female	64 (18.77%)	44 (12.90%)	108 (31.67%)	
Male	106 (31.09%)	127 (37.24%)	233 (68.33%)	
tumor_stage				0.01
stage i	76 (22.29%)	94 (27.57%)	170 (49.85%)	
stage ii	42 (12.32%)	42 (12.32%)	84 (24.63%)	
stage iii	52 (15.25%)	31 (9.09%)	83 (24.34%)	
stage iv	0 (0.0e+0%)	4 (1.17%)	4 (1.17%)	
pathologic_M				0.25
M0	170 (49.85%)	168 (49.27%)	338 (99.12%)	
M1	0 (0.0e+0%)	3 (0.88%)	3 (0.88%)	
pathologic_N				0.61
N0	167 (48.97%)	170 (49.85%)	337 (98.83%)	
N1	3 (0.88%)	1 (0.29%)	4 (1.17%)	
pathologic_T				0.1
T1+T2	120 (35.19%)	137 (40.18%)	257 (75.37%)	
T3	45 (13.20%)	29 (8.50%)	74 (21.70%)	
T4	5 (1.47%)	5 (1.47%)	10 (2.93%)	

TABLE2 Univariate and multivariate analyses of risk factors in the cohort.

Variables	Univariate analysis		Multivariate analysis	
	HR (95% CI)	*p*-value	HR (95% CI)	*p*-value
Age (years)	1.011 (0.997–1.026)	0.134		
Gender				
Female	1 (ref)			
Male	0.753 (0.517 1.096)	0.138		
T stage				
T1+T2	1 (ref)			
T3	2.357 (1.592 3.490)	<0.001	2.271 (1.531 3.367)	<0.001
T4	4.675 (2.124 10.290)	<0.001	3.881 (1.459 10.328)	0.007
N stage				
N0	1 (ref)			
N1	2.008 (0.494 8.161)	0.330		
M stage				
M0	1 (ref)			
M1	3.894 (1.231 12.320)	0.021	1.536 (0.364 6.486)	0.559
Risk score	8.130 (1.982 33.360)	0.004	6.839 (1.625 28.784)	0.009

To increase the application of the risk model, clinicopathological patient data and risk scores were integrated to construct a nomogram. The multivariate and univariate Cox regression analyses revealed the M stage, T stage, and risk scores were significantly related to prognosis (Table 2). After merging these parameters, a nomogram was developed, and scores were awarded to each patient (Figure 3A). For example, the clinical information of a patient with HCC was stage M1, T3, approximately 30 years of age, and female. Including the risk score, this patient's overall score was 161.04. Figure 3A depicts the 1-, 3-, and 5-year patient survival rates. The calibration curves showed that the nomogram accurately predicted the prognosis of the patients (Figure 3B). In addition,

10.3389/fphar.2023.1202823

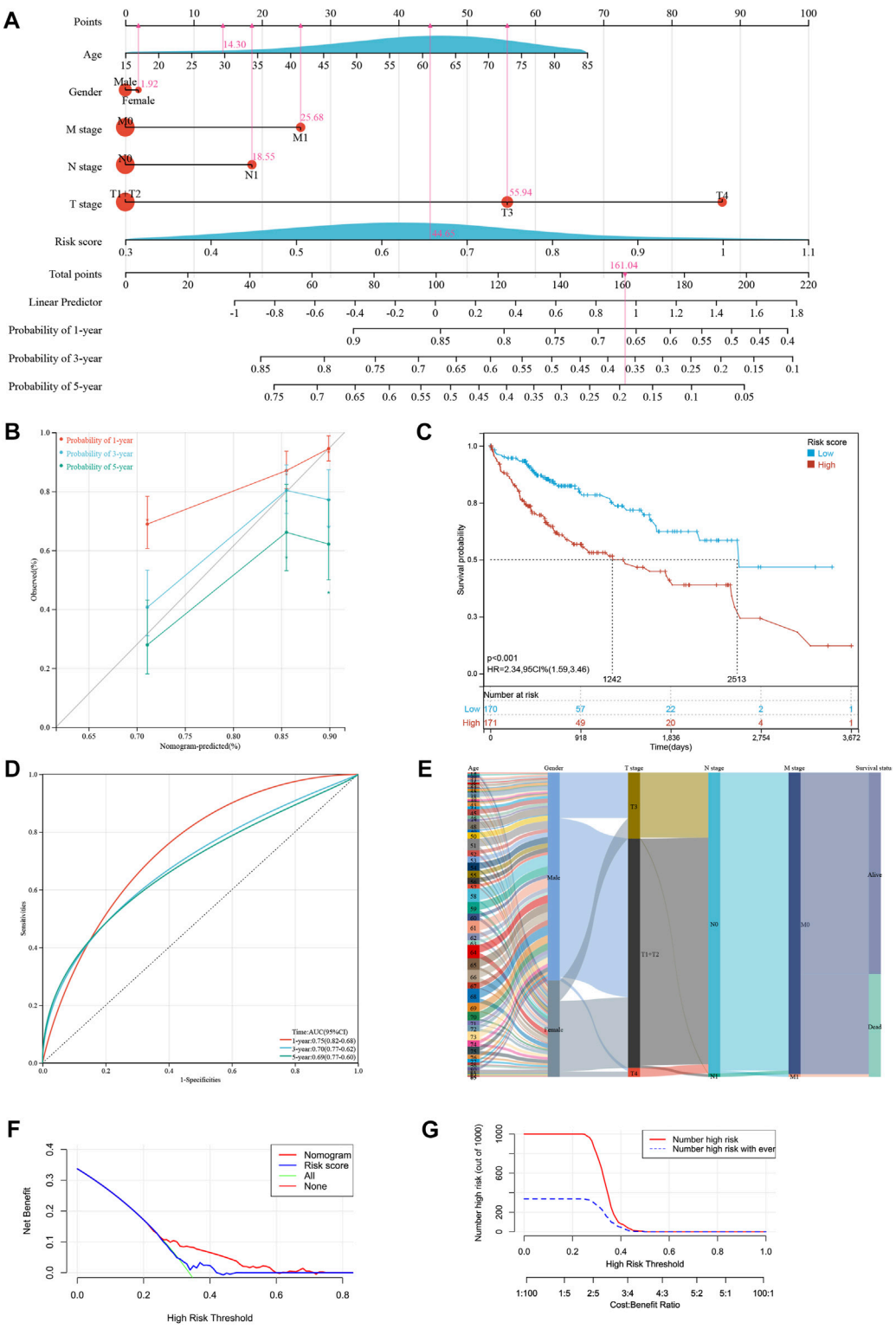

FIGURE 3
Developing a new nomogram with clinicopathological information **(A)** The nomogram of the risk model. **(B)** The calibration curves of the nomogram of risk model. **(C)** Kaplan-Meier curves for the overall survival of patients in the high- and low-risk groups based on risk model. **(D)** The time-dependent ROC curves supporting prognostic accuracy of the risk score based on risk model. **(E)** Sankey diagram showing the connection degree between the clinicopathological information and survival status. **(F)** The DCA curves of clinical practicability of the nomogram. **(G)** The nomogram provided greater net benefit (NB) than a conventional single clinicopathological characteristic.

10.3389/fphar.2023.1202823

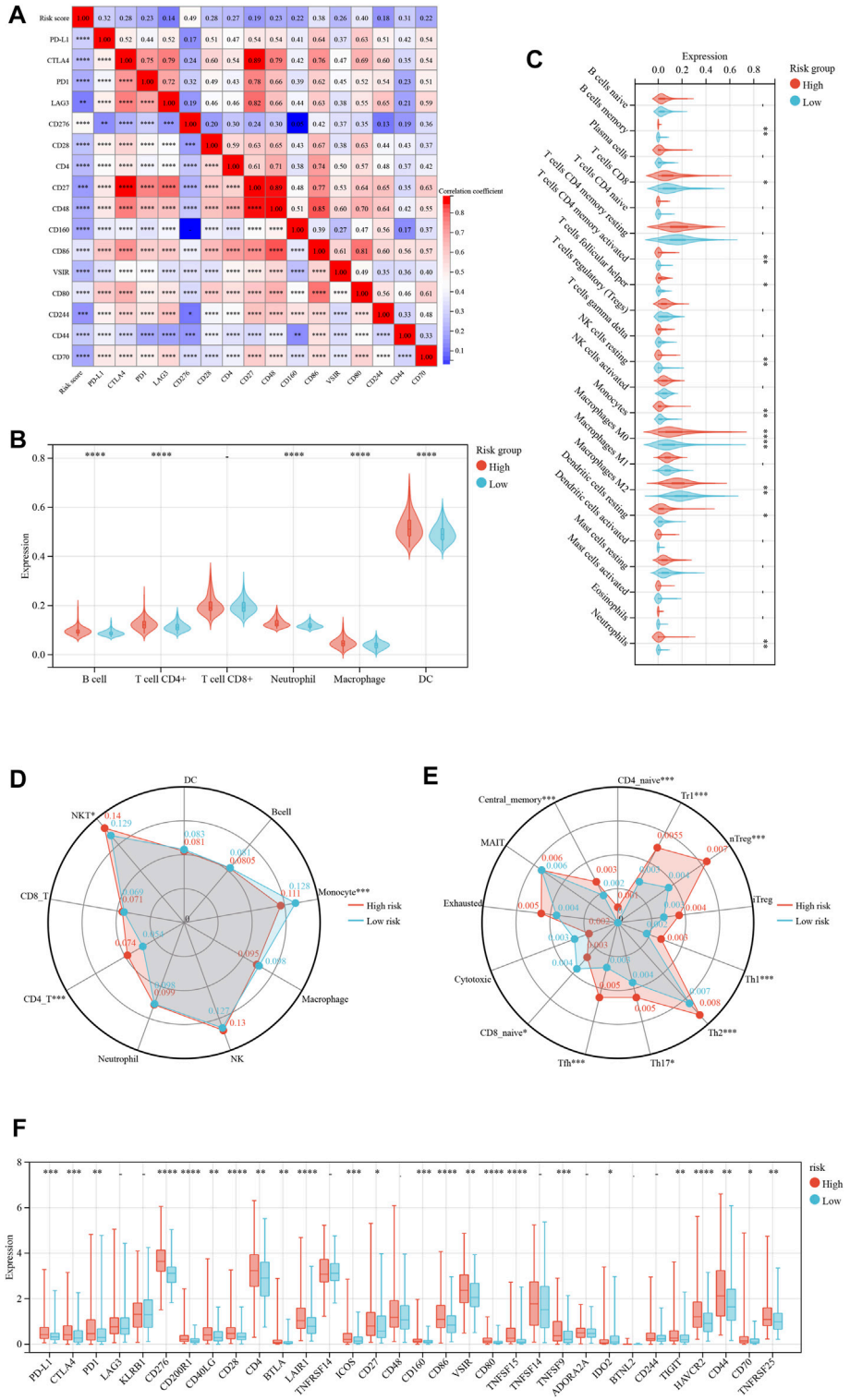

FIGURE 4
Risk model based on immune cell infiltration and clinicopathological factors. **(A)** The correlation hot map between immune check point and risk score. **(B)** The TIMER scores between the low- and high-risk immune cell group. **(C)** The CIBERSOFT scores between the low- and high-risk immune cell group. **(D, E)** The immune cell infiltration between the low- and high-risk group. **(F)** The immune check point of difference expresses between the low- and high-risk group. *$p < 0.05$; **$p < 0.01$; ***$p < 0.001$; ****$p < 0.0001$.

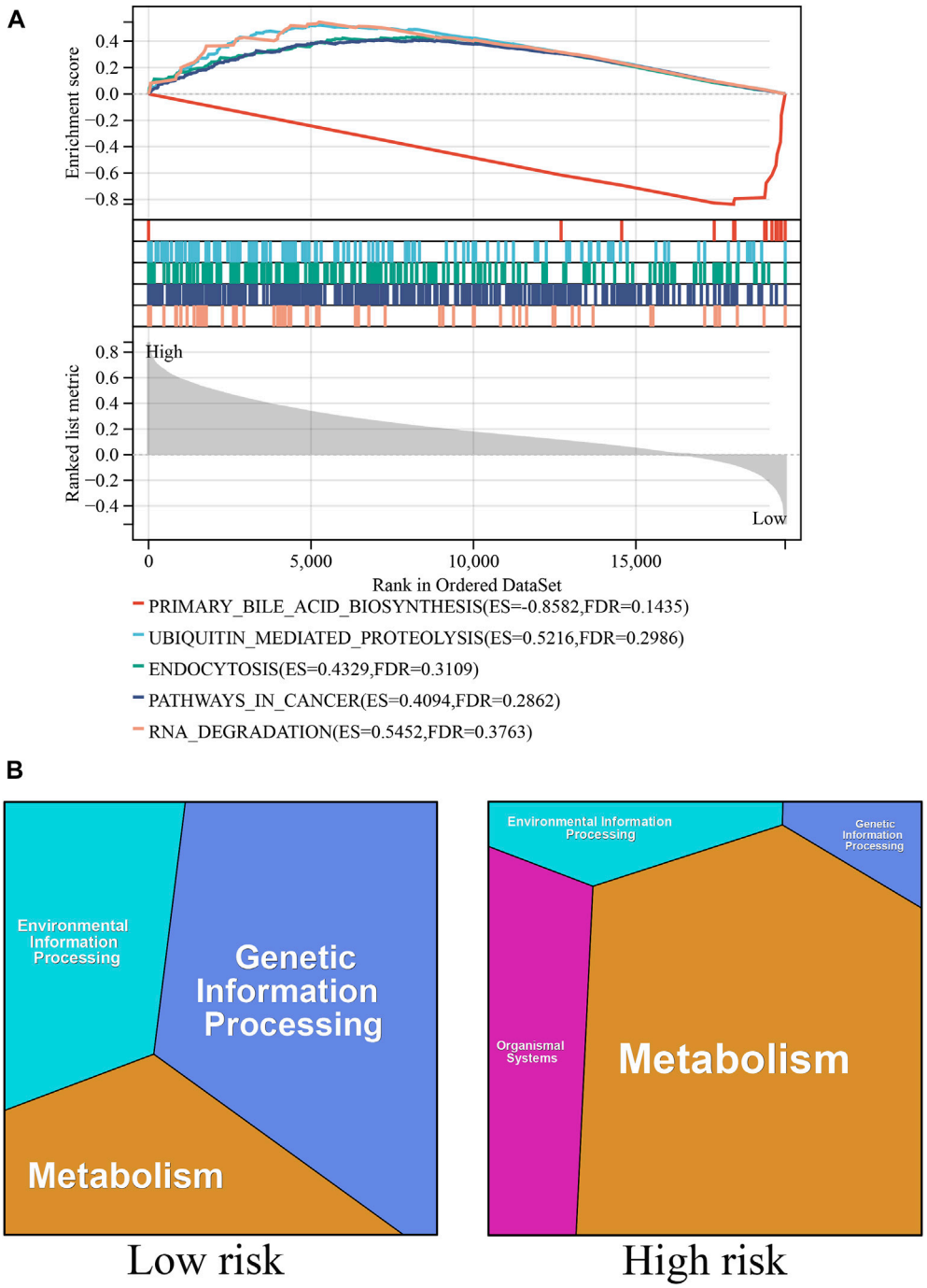

FIGURE 5
Biological pathways associated with ICD-related genes. **(A)** The GSEA functional analyses in the high- and low-risk groups. **(B)** The KEGG functional analyses in the high- and low-risk groups.

Figure 3C depicts the 1-, 3-, and 5-year OS of the patients (HR = 2.34, 95% CI = 1.59–3.46). Figure 3D presents the ROC curve for the nomogram. A high score signified an unfavorable prognosis. Figure 3E depicts the prognosis of patients combined with various influencing factors. DCA curves (Figure 3F) further confirmed the nomogram's clinical applicability. The nomogram provided greater net benefit than a conventional single clinicopathological characteristic (Figure 3G).

The relationship between the ICD-related risk signature and tumor microenvironment

Immunological ICD treatments have yielded favorable clinical outcomes in recent years (Zhu et al., 2020; Dong et al., 2022). Resultantly, we analyzed immunotherapy checkpoints in the high- and low-risk groups. Figure 4A depicts the correlation between various immunotherapy checkpoints. The link between CD27 and

CD48 was the strongest, with a correlation coefficient of 0.89. We analyzed the immune states using several immune scoring methods, such as the TIMER (Figure 4B) and CIBERSOFT algorithm (Figure 4C). The results showed that the expression of multiple immune cells was significantly different between the high- and low-risk groups. Then, we found significant differences in the infiltration of monocytes, CD4-T cells, and NKT **(Natural killer T)** cells between the high- and low-risk groups (Figure 4D). Similarly, we discovered that there were significant differences in the infiltration of CD4 naive, Trl, nTreg, Th1, Th2, Th17, Tfh, CD8 naive, and central memory cells (Figure 4E). By studying the expression of immunotherapy checkpoints in the patients (Figure 4F), we discovered that the majority of immunotherapy checkpoints were significantly expressed at higher levels in the high-risk group than in the low-risk group, suggesting that the patients in the high-risk group might be more responsive to immunotherapy checkpoint-based therapies.

Biological pathways associated with ICD-related genes

GSEA and KEGG functional analyses were performed to explore the biological mechanisms of the ICD-related genes in the high- and low-risk groups (Figures 5A, B). The top GSEA terms indicated the roles of the ICD-related genes in the regulation of primary bile acid production, ubiquitin-mediated proteolysis, endocytosis, cancer pathway, and RNA degradation. The top KEGG terms indicated the roles of ICD-related genes in the regulation of genetic, metabolic, environmental, and organismal systems.

Discussion

The treatment and prognosis of liver cancer have been a major concern for physicians. Despite the development of new antitumor medications, the survival rate of patients with liver cancer remains poor. With the development of the ICD concept, an increasing number of researchers have attempted to induce ICD in liver cancer cells using pharmaceuticals in an effort to treat liver cancer, bringing promise to liver cancer treatment. Several studies have demonstrated that the combination of oxaliplatin and immune checkpoint therapy increases the immunological death of liver cancer cells, resulting in favorable outcomes (Zhu et al., 2020). Other studies have also revealed that cabozantinib induces the death of immune cells and has beneficial therapeutic benefits for patients with liver cancer (Scirocchi et al., 2021). Consequently, computer analysis of the differential expression of ICD-related genes in liver cancer and the development of a prognostic model for liver cancer based on the results of the differential analysis is advantageous in liver cancer treatment and prognosis. In this study, we selected three datasets (GSE65372, GSE25097, and TCGA-HCC) from the GEO and TCGA databases, performed differential analysis, and identified five ICD-related genes with differential expression using a Venn diagram. Then, using the TCGA dataset for validation, we built a prognostic model with three prognosis-related genes. The risk model predicted that the prognosis of patients in the low-risk group was favorable relative to that of patients in the high-risk group. We also found that this model accurately predicted the 1-, 3-, and 5-year survival rates of patients with HCC who underwent surgery. Moreover, the distinct infiltration of immune cells in the high- and low-risk groups may be indicative of distinct immunological microenvironments for various risk models. We then validated the model using the immunohistochemistry public database, further showing the model's usefulness. We expect that the model will have a broader scope for future applications.

We constructed the risk signature using three mRNAs. PRNP serves as an ICD-related gene as well as an autophagy-related gene. Bioinformatics studies have demonstrated that PRNP contributes to the establishment of an HCC-related prognostic signature, which accurately predicts the prognosis of patients with HCC, thereby shedding light on the potential autophagy mechanisms in liver cell cancer (Chen et al., 2021).Kim et al. (2022) found that cellular prion protein encoded by the PRNP gene increases the risk of recurrence and decreases the survival rate of patients with liver cancer after surgery, as was predicted by the model in our study. There have been numerous studies on liver cell cancer and DNM1L. The liver-specific dynamin-related protein 1 (DRP1; gene name: DNM1L) is a key gene that regulates mitochondrial fission. The high expression of DNM1L is indicative of a poor prognosis for patients with HCC. DNM1L overexpression enhances mitochondrial fission in HCC cells, hence promoting the proliferation of HCC cells (Huang et al., 2016). Similarly, studies on mice have indicated that aerobic exercise decreases the expression of DNM1L in liver cell cancer, influences mitochondrial fission, and inhibits the development of liver cell cancer via the PI3K/AKT pathway (Zhao et al., 2021b). Despite the unsatisfactory efficacy of chemotherapy in the treatment of liver cell cancer, studies have demonstrated that inhibiting DNM1L-mediated mitochondrial fission can further promote apoptosis of liver carcinoma cells, thereby providing strong preclinical evidence for the development of mitochondrial autophagy-based combination therapies (Ma et al., 2020). Consistent with our findings, a study discovered that CASP8, a gene associated with pyroptosis, can contribute to the building of a prognostic signature, and the model can be used to predict the survival of patients with liver cell cancer and their response to immunotherapy (Zheng et al., 2021). Similarly, Boege et al. (2017) found that liver cancer cells with low levels of CASP8 expression had lower invasiveness and poor proliferation ability. Resultantly, patients had favorable overall survival performance, which was the same as predicted by the model in our study.

ICD is a specific type of cell death that can interfere with the antitumor functions of the immune system (Ladoire et al., 2016; Deng et al., 2020; Galluzzi et al., 2020). Discovering ICD-related gene biomarkers may be of benefit to patients with HCC. In our study, we developed a risk model based on ICD and predicted patients' prognoses. The risk signature classified all patients into high- and low-risk groups, and we discovered that the prognosis of the patients in the high-risk group was considerably poorer than that of those in the low-risk group. The GO and GSEA and GO analysis revealed that genetic information processing had the highest impact in the low-risk group, whereas metabolism had the highest impact in the high-risk group. The GSEA revealed that the primary bile acid production pathway was significantly enriched, and this may serve as a theoretical foundation for the development of ICD-related therapeutic strategies. In addition, recent studies (Dong et al., 2022) have demonstrated that the combination of immune checkpoint therapy plus ICD treatment is one of the most successful treatment strategies available. Additionally, we discovered significant differences in immune checkpoint markers such as PD-1 and PD-L1 between the high- and low-risk groups, indicating that immune checkpoint therapy combined with ICD

treatment has considerable potential in the development of treatment strategies for liver cell cancer.

Despite major advances in its treatment, the prognosis for liver cancer remains poor due to drug resistance, recurrence, and metastasis. Combination therapy with immune checkpoint inhibitors and vascular endothelial growth factor inhibitors are currently used as first-line treatment for advanced liver cancer. With the development of immune checkpoint inhibitors-based therapies, there is renewed optimism for patients with liver cancer. Due to the dependence of these treatments on the immune milieu of the tumor, it is vital to study the immunological environment of liver cancer to select the most effective treatment (Hao et al., 2021; Oura et al., 2021). Studies have shown that increased levels of infiltrating immune cells in the tumor microenvironment are associated with higher risks (Ding et al., 2022). Consequently, we studied the immunological microenvironment and the infiltration of diverse immune cells. The high-risk group exhibited a greater infiltration of immune cells relative to the low-risk group. A single-cell sequencing study associated elevated levels of Treg cells with liver cell cancer, providing a new direction for the immunological treatment of liver cell cancer based on its immune microenvironment (Zheng et al., 2017). Our data indicate that immune cell infiltration is positively correlated with risk, and the high-risk group had greater immune cell infiltration. This finding may suggest that immunotherapy may be more effective for patients with liver cell cancer who are at high risk for disease progression. Next, we will verify the validity of the three genes through *in vivo* and vitro experiments. More clinical and experimental research are required to increase the generalizability of our survival prediction model in clinical practice in the future.

Conclusion

A risk model based on the ICD-related genes PRNP, DNM1L, and CASP8 was developed to predict the prognosis of liver cancer. This risk model can also predict the immunotherapy response of patients with liver cancer.

Data availability statement

The original contributions presented in the study are included in the article/Supplementary Material, further inquiries can be directed to the corresponding authors.

Ethics statement

Ethical review and approval was not required for the study on human participants in accordance with the local legislation and institutional requirements. Written informed consent for participation was not required for this study in accordance with the national legislation and the institutional requirements.

Author contributions

DS, FX, and ZX: conception and design. ZZ, QL, YL, and WL: data curation. DS, FX, and ZX: writing the manuscript and revision of the manuscript. All authors contributed to the article and approved the submitted version.

Funding

This study is supported by grants from the Science and Technology Innovation Program of Hunan Province (2022RC1210).

Conflict of interest

The authors declare that the research was conducted in the absence of any commercial or financial relationships that could be construed as a potential conflict of interest.

Publisher's note

Supplementary material

The Supplementary Material for this article can be found online at: https://www.frontiersin.org/articles/10.3389/fphar.2023.1202823/full#supplementary-material

References

Blanche, P., Dartigues, J-F., and Jacqmin-Gadda, H. (2013). Estimating and comparing time-dependent areas under receiver operating characteristic curves for censored event times with competing risks. *Stat. Med.* 32 (30), 5381–5397. doi:10.1002/sim.5958

Boege, Y., Malehmir, M., Healy, M. E., Bettermann, K., Lorentzen, A., Vucur, M., et al. (2017). A dual role of caspase-8 in triggering and sensing proliferation-associated DNA damage, a key determinant of liver cancer development. *Cancer Cell.* 32 (3), 342–359. doi:10.1016/j.ccell.2017.08.010

Chen, W., Hu, M-J., Zhong, X-L., Ji, L-H., Wang, J., Zhang, C-F., et al. (2021). Screening of a novel autophagy-related prognostic signature and therapeutic targets in hepatocellular carcinoma. *J. Gastrointest. Oncol.* 12 (6), 2985–2998. doi:10.21037/jgo-21-664

Deng, H., Yang, W., Zhou, Z., Tian, R., Lin, L., Ma, Y., et al. (2020). Targeted scavenging of extracellular ROS relieves suppressive immunogenic cell death. *Nat. Commun.* 11 (1), 4951. doi:10.1038/s41467-020-18745-6

Ding, D., Zhao, Y., Su, Y., Yang, H., Wang, X., and Chen, L. (2022). Prognostic value of antitumor drug targets prediction using integrated bioinformatic analysis for immunogenic cell death-related lncRNA model based on stomach adenocarcinoma characteristics and tumor immune microenvironment. *Front. Pharmacol.* 13, 1022294. doi:10.3389/fphar.2022.1022294

Dong, S., Guo, X., Han, F., He, Z., and Wang, Y. (2022). Emerging role of natural products in cancer immunotherapy. *Acta Pharm. Sin. B* 12 (3), 1163–1185. doi:10.1016/j.apsb.2021.08.020

Galluzzi, L., Vitale, I., Warren, S., Adjemian, S., Agostinis, P., Martinez, A. B., et al. (2020). Consensus guidelines for the definition, detection and interpretation of immunogenic cell death. *J. Immunother. Cancer* 8 (1), e000337. doi:10.1136/jitc-2019-000337

Gao, X., Huang, H., Pan, C., Mei, Z., Yin, S., Zhou, L., et al. (2022). Disulfiram/copper induces immunogenic cell death and enhances CD47 blockade in hepatocellular carcinoma. *Cancers (Basel)* 14 (19), 4715. doi:10.3390/cancers14194715

Hao, X., Sun, G., Zhang, Y., Kong, X., Rong, D., Song, J., et al. (2021). Targeting immune cells in the tumor microenvironment of HCC: New opportunities and challenges. *Front. Cell. Dev. Biol.* 9, 775462. doi:10.3389/fcell.2021.775462

Huang, Q., Zhan, L., Cao, H., Li, J., Lyu, Y., Guo, X., et al. (2016). Increased mitochondrial fission promotes autophagy and hepatocellular carcinoma cell survival through the ROS-modulated coordinated regulation of the NFKB and TP53 pathways. *Autophagy* 12 (6), 999–1014. doi:10.1080/15548627.2016.1166318

Kalasekar, S. M., VanSant-Webb, C. H., and Evason, K. J. (2021). Intratumor heterogeneity in hepatocellular carcinoma: Challenges and opportunities. *Cancers (Basel)* 13 (21), 5524. doi:10.3390/cancers13215524

Kim, M-J., Cho, Y-A., Kim, E., Choe, J-Y., Park, J-W., Lee, J., et al. (2022). Solitary pulmonary capillary hemangioma: CT and PET-CT features with clinicopathologic correlation. *Diagn. (Basel)* 12 (7), 2618. doi:10.3390/diagnostics12112618

Kim, R., Kin, T., Kim, H., Kim, H. R., Jo, H., Hong, J., et al. (2021). Real-world data from a refractory triple-negative breast cancer cohort selected using a clinical data warehouse approach. *Cancers (Basel)* 13 (19), 5835. doi:10.3390/cancers13225835

Ladoire, S., Enot, D., Andre, F., Zitvogel, L., and Kroemer, G. (2016). Immunogenic cell death-related biomarkers: Impact on the survival of breast cancer patients after adjuvant chemotherapy. *Oncoimmunology* 5 (2), e1082706. doi:10.1080/2162402X.2015.1082706

Li, B., Severson, E., Pignon, J-C., Zhao, H., Li, T., Novak, J., et al. (2016). Comprehensive analyses of tumor immunity: Implications for cancer immunotherapy. *Genome Biol.* 17 (1), 174. doi:10.1186/s13059-016-1028-7

Li, Z., Yang, G., Han, L., Wang, R., Gong, C., and Yuan, Y. (2021). Sorafenib and triptolide loaded cancer cell-platelet hybrid membrane-camouflaged liquid crystalline lipid nanoparticles for the treatment of hepatocellular carcinoma. *J. Nanobiotechnology* 19 (1), 360. doi:10.1186/s12951-021-01095-w

Ma, M., Lin, X-H., Liu, H-H., Zhang, R., and Chen, R-X. (2020). Suppression of DRP1-mediated mitophagy increases the apoptosis of hepatocellular carcinoma cells in the setting of chemotherapy. *Oncol. Rep.* 43 (3), 1010–1018. doi:10.3892/or.2020.7476

Markham, A. (2020). Lurbinectedin: First approval. *Drugs* 80 (13), 1345–1353. doi:10.1007/s40265-020-01374-0

Miao, Y-R., Zhang, Q., Lei, Q., Luo, M., Xie, G-Y., Wang, H., et al. (2020). ImmuCellAI: A unique method for comprehensive T-cell subsets abundance prediction and its application in cancer immunotherapy. *Adv. Sci. (Weinh)* 7 (7), 1902880. doi:10.1002/advs.201902880

Newman, A. M., Liu, C. L., Green, M. R., Gentles, A. J., Feng, W., Xu, Y., et al. (2015). Robust enumeration of cell subsets from tissue expression profiles. *Nat. Methods* 12 (5), 453–457. doi:10.1038/nmeth.3337

Oura, K., Morishita, A., Tani, J., and Masaki, T. (2021). Tumor immune microenvironment and immunosuppressive therapy in hepatocellular carcinoma: A review. *Int. J. Mol. Sci.* 22 (11), 5801. doi:10.3390/ijms22115801

Scirocchi, F., Napoletano, C., Pace, A., Rahimi Koshkaki, H., Di Filippo, A., Zizzari, I. G., et al. (2021). Immunogenic cell death and immunomodulatory effects of cabozantinib. *Front. Oncol.* 11, 755433. doi:10.3389/fonc.2021.755433

Subramanian, A., Tamayo, P., Mootha, V. K., Mukherjee, S., Ebert, B. L., Gillette, M. A., et al. (2005). Gene set enrichment analysis: A knowledge-based approach for interpreting genome-wide expression profiles. *Proc. Natl. Acad. Sci. U. S. A.* 102 (43), 15545–15550. doi:10.1073/pnas.0506580102

Sung, W-K., Zheng, H., Li, S., Chen, R., Liu, X., Li, Y., et al. (2012). Genome-wide survey of recurrent HBV integration in hepatocellular carcinoma. *Nat. Genet.* 44 (7), 765–769. doi:10.1038/ng.2295

Tibshirani, R. (1997). The lasso method for variable selection in the Cox model. *Stat. Med.* 16 (4), 385–395. doi:10.1002/(sici)1097-0258(19970228)16:4<385:aid-sim380>3.0.co;2-3

Tzogani, K., Penttilä, K., Lähteenvuo, J., Lapveteläinen, T., Lopez Anglada, L., Prieto, C., et al. (2021). EMA review of belantamab mafodotin (blenrep) for the treatment of adult patients with relapsed/refractory multiple myeloma. *Oncologist* 26 (1), 70–76. doi:10.1002/onco.13592

Wu, W., Xue, X., Chen, Y., Zheng, N., and Wang, J. (2022). Targeting prolyl isomerase Pin1 as a promising strategy to overcome resistance to cancer therapies. *Pharmacol. Res.* 184, 106456. doi:10.1016/j.phrs.2022.106456

Xu, X-F., Yang, X-K., Song, Y., Chen, B-J., Yu, X., Xu, T., et al. (2022). Dysregulation of non-coding RNAs mediates cisplatin resistance in hepatocellular carcinoma and therapeutic strategies. *Pharmacol. Res.* 176, 105906. doi:10.1016/j.phrs.2021.105906

Zhang, X., Lu, Y., Jia, D., Qiu, W., Ma, X., Zhang, X., et al. (2021). Acidic microenvironment responsive polymeric MOF-based nanoparticles induce immunogenic cell death for combined cancer therapy. *J. Nanobiotechnology* 19 (1), 455. doi:10.1186/s12951-021-01217-4

Zhang, Y., and Chen, Y. (2022). Stratification from heterogeneity of the cell-death signal enables prognosis prediction and immune microenvironment characterization in esophageal squamous cell carcinoma. *Front. Cell. Dev. Biol.* 10, 855404. doi:10.3389/fcell.2022.855404

Zhao, T., Guo, B-J., Xiao, C-L., Chen, J-J., Lü, C., Fang, F-F., et al. (2021). Aerobic exercise suppresses hepatocellular carcinoma by downregulating dynamin-related protein 1 through PI3K/AKT pathway. *J. Integr. Med.* 19 (5), 418–427. doi:10.1016/j.joim.2021.08.003

Zhao, Y., Yang, B., Chen, D., Zhou, X., Wang, M., Jiang, J., et al. (2021). Combined identification of ARID1A, CSMD1, and SENP3 as effective prognostic biomarkers for hepatocellular carcinoma. *Aging (Albany NY)* 13 (3), 4696–4712. doi:10.18632/aging.202586

Zheng, C., Zheng, L., Yoo, J-K., Guo, H., Zhang, Y., Guo, X., et al. (2017). Landscape of infiltrating T cells in liver cancer revealed by single-cell sequencing. *Cell.* 169 (7), 1342–1356. doi:10.1016/j.cell.2017.05.035

Zheng, S., Xie, X., Guo, X., Wu, Y., Chen, G., Chen, X., et al. (2021). Identification of a pyroptosis-related gene signature for predicting overall survival and response to immunotherapy in hepatocellular carcinoma. *Front. Genet.* 12, 789296. doi:10.3389/fgene.2021.789296

Zhu, H., Shan, Y., Ge, K., Lu, J., Kong, W., and Jia, C. (2020). Oxaliplatin induces immunogenic cell death in hepatocellular carcinoma cells and synergizes with immune checkpoint blockade therapy. *Cell. Oncol. (Dordr)* 43 (6), 1203–1214. doi:10.1007/s13402-020-00552-2

frontiers | Frontiers in Pharmacology

TYPE Original Research
PUBLISHED 22 June 2023
DOI 10.3389/fphar.2023.1222512

OPEN ACCESS

EDITED BY
Hongzhou Cai,
Nanjing Medical University, China

REVIEWED BY
Dechao Feng,
Sichuan University, China
Huaide Qiu,
Nanjing Normal University of Special Education, China
Wanzun Lin,
Fudan University, China

*CORRESPONDENCE
Dingshan Deng,
dds15116217256@163.com
Bolong Liu,
2674918171@qq.com

RECEIVED 14 May 2023
ACCEPTED 13 June 2023
PUBLISHED 22 June 2023

CITATION
Li Z, Yao Y, Qi T, Wu Z, Deng D and Liu B (2023), ACSM6 overexpression indicates a non-inflammatory tumor microenvironment and predicts treatment response in bladder cancer: results from multiple real-world cohorts. *Front. Pharmacol.* 14:1222512. doi: 10.3389/fphar.2023.1222512

ACSM6 overexpression indicates a non-inflammatory tumor microenvironment and predicts treatment response in bladder cancer: results from multiple real-world cohorts

Zhiwei Li[1], Yiyan Yao[2], Tiezheng Qi[2], Zuowei Wu[3], Dingshan Deng[4,5]* and Bolong Liu[4,5,6]*

[1]The Second Affiliated Hospital, Department of Urology, Hengyang Medical School, Unversity of South China, Hengyang, Hunan, China, [2]Xiangya School of Medicine, Central South University, Changsha, Hunan, China, [3]Department of Interventional Radiology, Third Xiangya Hospital, Central South University, Changsha, China, [4]Department of Urology, National Clinical Research Center for Geriatric Disorders, Xiangya Hospital, Central South University, Changsha, Hunan, China, [5]National Clinical Research Center for Geriatric Disorders, Xiangya Hospital, Central South University, Changsha, Hunan, China, [6]The First Affiliated Hospital, Department of Andrology, Hengyang Medical School, University of South China, Hengyang, China

Background: ACSMs play critical roles in lipid metabolism; however, their immunological function within the tumor microenvironment (TME) remains unclear, especially that of ACSM6. In this study, we investigate the latent effect of ACSM6 on bladder cancer (BLCA).

Methods: Several real-world cohorts, including the Xiangya (in-house), The Cancer Genome Atlas (TCGA-BLCA), and IMvigor210 cohorts, with TCGA-BLCA cohort serving as the discovery cohort were compared. We investigated the potential immunological effects of ACSM6 in regulating the BLCA tumor microenvironment by analyzing its correlation with immunomodulators, anti-cancer immune cycles, immune checkpoints, tumor-infiltrating immune cells, and the T-cell inflamed score (TIS). Additionally, we assessed the precision of ACSM6 in predicting BLCA molecular subtypes and responses to several treatments using ROC analysis. To ensure the robustness of our findings, all results were confirmed in two independent external cohorts: the IMvigor210 and Xiangya cohorts.

Results: ACSM6 expression was markedly upregulated in BLCA. Our analysis suggests that ACSM6 might have significant impact to promote the formation of a non-inflamed tumor microenvironment because of its negative correlation with immunomodulators, anticancer immune cycles, immune checkpoints, tumor-infiltrating immune cells, and the T-cell inflamed score (TIS). Additionally, high ACSM6 expression levels in BLCA may predict the luminal subtype, which is typically associated with resistance to chemotherapy, neoadjuvant chemotherapy, and radiotherapy. These findings were consistent across both the IMvigor210 and Xiangya cohorts.

Conclusion: ACSM6 has the potential to serve as a valuable predictor of the tumor microenvironment phenotypes and treatment outcomes in BLCA, thereby contributing to more precise treatment.

KEYWORDS

ACSM6, bladder cancer, tumor microenvironment, immunotherapy, chemothearpy bladder cancer, chemotherapy

Introduction

According to GLOBOCAN's 2020 estimates, bladder cancer (BLCA) accounts for approximately 573,278 new cases and 212,536 fatalities worldwide, making it the 10th most frequently diagnosed cancer (Sung et al., 2021). Urothelium carcinoma is the main histological type of BLCA and non-muscle invasive BC (NMIBC) patients account for about 75% of BLCA cases, with obvious heterogeneity and the risk of recurrence and progression to muscle invasive BC (MIBC) (van Rhijn et al., 2009). Therefore, despite the high 5-year survival rate of NMIBC (>90%), most patients have to accept long-term cystoscope monitoring and multiple treatment interventions, resulting in lower quality of life (Catto et al., 2021) and huge medical burden, so BLCA is considered to be the most expensive malignant tumor (Svatek et al., 2014).

Although chemotherapy is commonly used as the first course of treatment for advanced or metastatic BLCA, the discouraging objective response rate and consequent poor five-year survival rate indicate the need for alternative therapies (Liu et al., 2022). Currently, the FDA has only approved FGFR3 inhibitors, PD-1/PD-L1-based immune checkpoint inhibitors, and antibody-drug conjugates for the immunological treatment of BLCA, which are especially suitable for platinum-resistant or non-platinum locally advanced or metastatic urothelial cancer. Recent studies suggest that precision therapy may offer superior efficacy compared with either treatment alone (Morales-Barrera et al., 2020; Chang et al., 2021; Grivas et al., 2021). Considering the limitations of chemotherapeutic drugs and surgery (Feng et al., 2020; Feng et al., 2022a; Feng et al., 2022b), precise and personalized treatment based on biomarkers is also becoming increasingly important for urinary system tumors (Hu et al., 2021a; Hu et al., 2021b; Hu et al., 2022; Cai et al., 2023).

Liposomal coenzyme A synthetase is an enzyme that catalyzes the activation of fatty acids and participates in the 1st step of fatty acid metabolism, which is divided into four categories containing medium-chain acyl-CoA synthetase (ACSM). Primarily, ACSMs are located on human chromosome 16p12, which contains six members: ACSM1–ACSM6. However, the connection between the ACSM family and cancer has rarely been reported, especially for ACSM6.

Through multi-omics analysis, we identified ACSM6 as a novel target for BLCA immunotherapy. We conducted a comprehensive investigation to examine the association between ACSM6 and the tumor microenvironment (TME) in BLCA. Our findings revealed that ACSM6 shaped the non-inflammatory TME in BLCA and enabled the prediction of BLCA molecular subtypes.

Methods

Data acquisition and preprocessing of three real-world cohorts

We retrieved BLCA mRNA data using the mRNA expression data (FPKM) values and related clinicopathological messages from TCGA (https://portal.gdc.cancer.gov/). The cohort consisted of 410 BLCA samples and 19 normal urothelial tissue samples. Before analysis, the FPKM values in the TCGA cohort were converted to transcripts per kilobase million (TPM).

The cohort used for validation included patients who underwent surgical treatment for BLCA at Xiangya Hospital. The Xiangya cohort comprised 57 BLCA samples and 13 normal bladder epithelial tissue samples. Data from this cohort were uploaded to the GEO database (GSE188715) (Hu et al., 2021a; Hu et al., 2021b).

The IMvigor210 cohort comprised of patients with BLCA who underwent anti-PD-1 therapy as part of an immunotherapy study. The mRNA expression data and corresponding clinicopathological information were obtained under the Creative Commons 3.0 License (Mariathasan et al., 2018).

Describing the immunological features of BLCA TME

Anticancer immunity has a lot to do with the cancer immune cycle, the expression of immunomodulatory factors, the level of infiltration of tumor-infiltrating lymphocytes (TILs), and the expression of inhibitory immune checkpoints in the TME. We collected 122 immunomodulatory factors from previous studies and compared differentially expressed immunomodulatory factors, including chemokines, immunostimulatory factors, receptors, and MHC, in the low and high ACSM6 groups (Charoentong et al., 2017; Hu et al., 2021a; Hu et al., 2021b; Liu et al., 2021; Hu et al., 2022; Cai et al., 2023). Subsequently, we investigated the impact of ACSM6 on the cancer immune cycle, which comprises seven crucial steps that determine how the tumor cells take effect in BLCA (Chen and Mellman, 2013). Consequently, we employed five distinct algorithms: TIMER, CIBERSORT-ABS, xCell, quanTlseq, and MCP-counter, to calculate the correlation between the level of TIL infiltration and the expression of ACSM6 in the TME (Newman et al., 2015; Becht et al., 2016; Li et al., 2016; Xu et al., 2018; Finotello et al., 2019; Li et al., 2020). Additionally, we studied the relation between ACSM6 and the corresponding effector genes of the TILs. Furthermore, we examined the correlation between ACSM6 expression and 22 common immune checkpoint inhibitors (ICIs), such as PD-1, PD-L1, CTLA-4, and LAG-3 (Auslander et al., 2018). Finally, we examined the TIS in the

TME, its related effector genes, and its effect on the clinical response to immune checkpoint blockade (ICB) (Ayers et al., 2017).

Predicting BLCA molecular subtypes and treatment response

Owing to the high heterogeneity of BLCA, the treatment response and prognosis of different types are different. There are several molecular classification systems for BLCA, including TCGA, Baylor, UNC, Lund, CIT, MDA and Consensus classification systems (Sassoli et al., 2019). In this study, we used the BLCA subtyping R software package and Consensus MIBC to predict the molecular subtype system and describe the correlation between ACSM6 expression and specific markers of the molecular subtypes. The accuracy of ACSM6 in predicting BLCA molecular subtypes was evaluated using ROC curves. We also evaluated differences in neoadjuvant chemotherapy-related mutations between the high and low ACSM6 groups. Additionally, we explored the prognosis of several treatments such as immunotherapy, targeted therapy, and radiotherapy. Finally, we collected and analyzed drug target genes from the Drug Bank database.

Statistical analysis

We calculated Pearson's or Spearman's coefficients to identify correlations between variables. The *t*-test was used to compare the differences between binary groups for normally distributed variables, whereas the chi-square test or Fisher's exact test was used for categorical variables. Statistical significance was determined using a two-sided *p*-value of <0.05. We evaluated the accuracy of the molecular subtype prediction using ROC curves. Statistical analyses and visualizations were conducted using R software version 4.2.2.

Result

The immunological function of ACSM6 in pan-cancer analysis

The immunological role of ACSM6 was determined and the cancer types most affected by ACSM6 were screened using pan-cancer analysis. Figure 1A shows the relationship between ACSM6 expression and immunomodulatory factors in various cancer types. We found that in most cancers, ACSM6 was positively correlated with a variety of immunomodulatory factors. However, in BLCA, ACSM6 was negatively correlated with a variety of immunomodulatory factors, including chemokines, receptors, MHC, immunosuppressants, and immunoactivators. Subsequently, we examined the correlation between ACSM6 expression and several pivotal immune checkpoints. Notably, negative associations were observed between ACSM6 and four immune checkpoints in BLCA: CTLA-4, PD-L1, PD-1, and LAG-3 (Figures 1B–E). Furthermore, we found that ACSM6 was inversely related to the ESTIMATE, immune, and matrix scores in BLCA (Figures 2A–C). In summary, ACSM6 is a potential biomarker for predicting tumor microenvironment status in BLCA. In BLCA, high ACSM6 expression may lead to a non-inflammatory TME because of decreased immunomodulatory factors, immune cells, immune checkpoints, and stromal cells in the TME.

ACSM6 is related to the non-inflammatory tumor microenvironment of BLCA

ACSM6 was highly expressed in the Xiangya cohort (Figure 3A) and was negatively correlated with multiple immunomodulatory factors (Figure 3B). Most chemokines, including CCL24, CCL26, CXCL9, CXCL10, and CCL8, were significantly reduced in the high ACSM6 group, and immune activators, including TNESF9, TNFRSF18, and TNFRSF8, were negatively correlated with ACSM6. Vast major steps in the tumor immune cycle in the high ACSM6 group were downregulated, including cancer cell antigen release, immune cell activation and recruitment, and cancer cell killing (Figure 3C).

To further verify the relation between ACSM6 and TILs in the TME, we used five independent algorithms to calculate the infiltration levels of TILs. Results showed that ACSM6 expression negatively had to do with the infiltration levels of NK cells, $CD8^+$ T cells, macrophages, Th1 cells, and dendritic cells (Figure 3D). Additionally, ACSM6 negatively correlated with TIL effector genes, including NK cells, $CD8^+$ T cells, macrophages, dendritic cell-related genes, and Th1 cells (Figure 3E). Furthermore, the relationship between ACSM6 and immune checkpoint inhibitors in the TME was explored, which showed that ACSM6 negatively had to do with the most common immune checkpoint inhibitors, including C10orf54, CD86, CTLA4, HAVCR2, LAG-3, and PVR (Figure 3F). Additionally, ACSM6 negatively had to do with the TIS and its related TIS effector genes (Figures 4A, B). Collectively, these results demonstrate that ACSM6 promotes a non-inflammatory TME in BLCA.

ACSM6 predicts molecular subtypes and drug sensitivity

Notably BLCA is a highly heterogeneous tumor and different molecular subtypes exhibit different sensitivities to different treatment regimens. Consequently, we distinguished the expression of ACSM6 among the BLCA molecular subtypes in TCGA. As shown in Figure 4C, patients with low ACSM6 expression developed the basal subtype, which characterized in EMT differentiation, basal differentiation, keratinization, and immune differentiation. Conversely, people with high ACSM6 expression were classified into the luminal/differentiated subtype, exhibiting Ta pathway and urothelial and supraluminal differentiation. Furthermore, ROC analysis was employed to evaluate the predictive precision of ACSM6 for molecular subtypes, with the area under the ROC curve ranging from 0.81 to 0.95 (Figure 4D).

Additional investigation of the association between ACSM6 and neoadjuvant chemotherapy (NAC) revealed that the low expression group of ACSM6 better turned to carry mutations related to NAC,

10.3389/fphar.2023.1222512

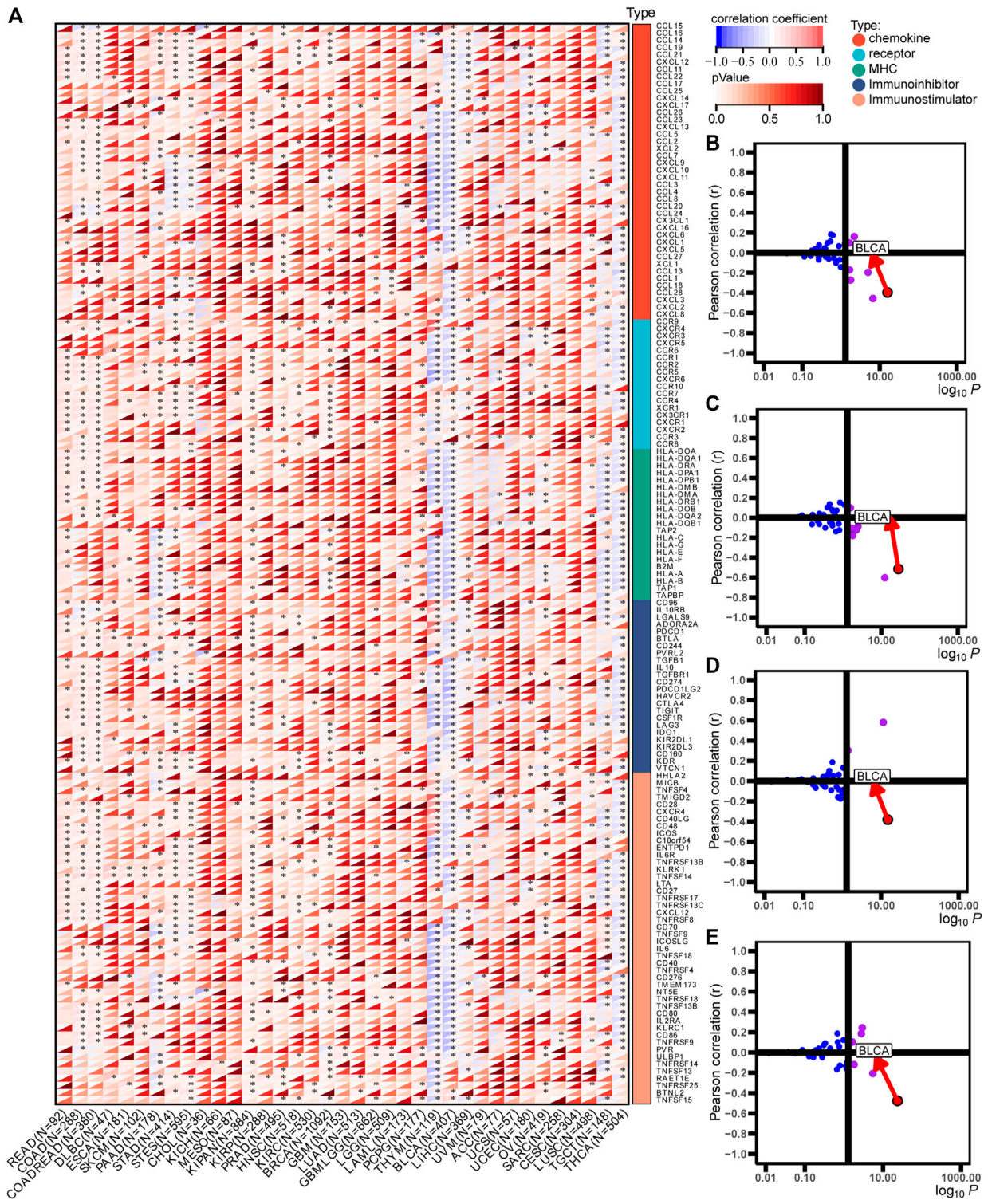

FIGURE 1
Immunological characteristics in pan-cancers correlated with ACSM6. **(A)** Correlation of ACSM6 with immunomodulators, including chemokines, receptors, MHC, and immunostimulators. **(B–E)** Correlation of ACSM6 expression with PD-L1, CTLA-4, PD-1, and LAG-3.

such as ERBB2 (15%), RB1 (26%) and ATM (10%). Additionally, the high expression group of ACSM6 had higher mutation rates in ATM (16%), RB1 (9%), and ERBB2 (8%) (Figure 4E). Importantly, RB1 chemotherapy-related mutations were significantly higher in the low ACSM6 group, indicating that tumors with low ACSM6 expression were more likely to be sensitive to NAC. In addition, in the low ACSM6 group, the radiotherapy prediction pathway and EGFR ligand enrichment scores were higher

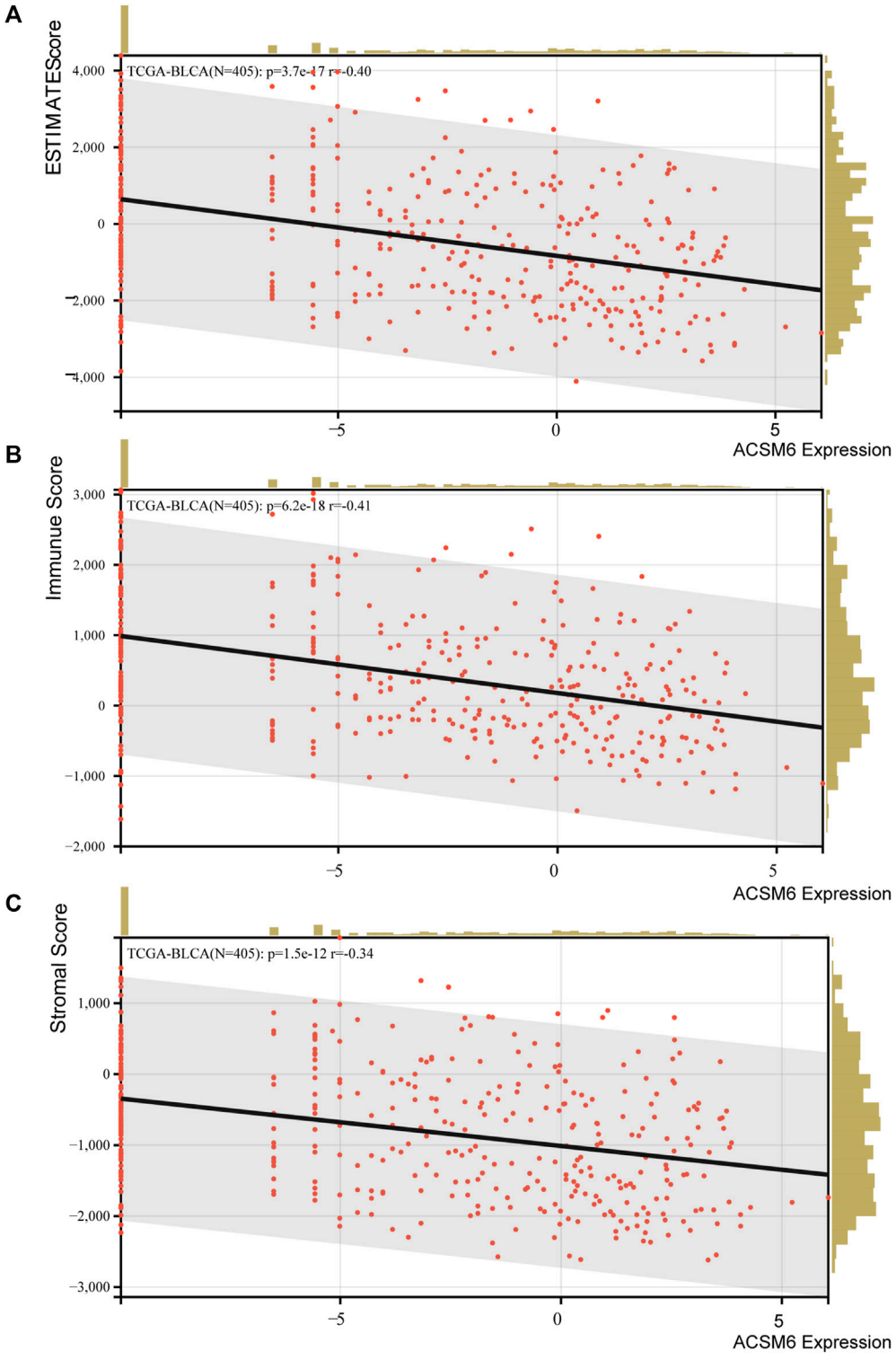

FIGURE 2
(A–C) Correlation between ACSM6 expression and TME scores, including ESTIMATE, immune, and stromal scores.

(Figure 4F). Furthermore, the high ACSM6 group exhibited significantly higher enrichment scores for some immunosuppressive and carcinogenic pathways, including IDH1, WNT-β-catenin pathway, and PPARG co-expressed genes, suggesting the presence of a non-inflammatory TME in BLCA. Moreover, we utilized the Drug Bank database to identify the sensitivity of different groups to various therapies. Our results indicated that the low ACSM6 group was more responsive to

10.3389/fphar.2023.1222512

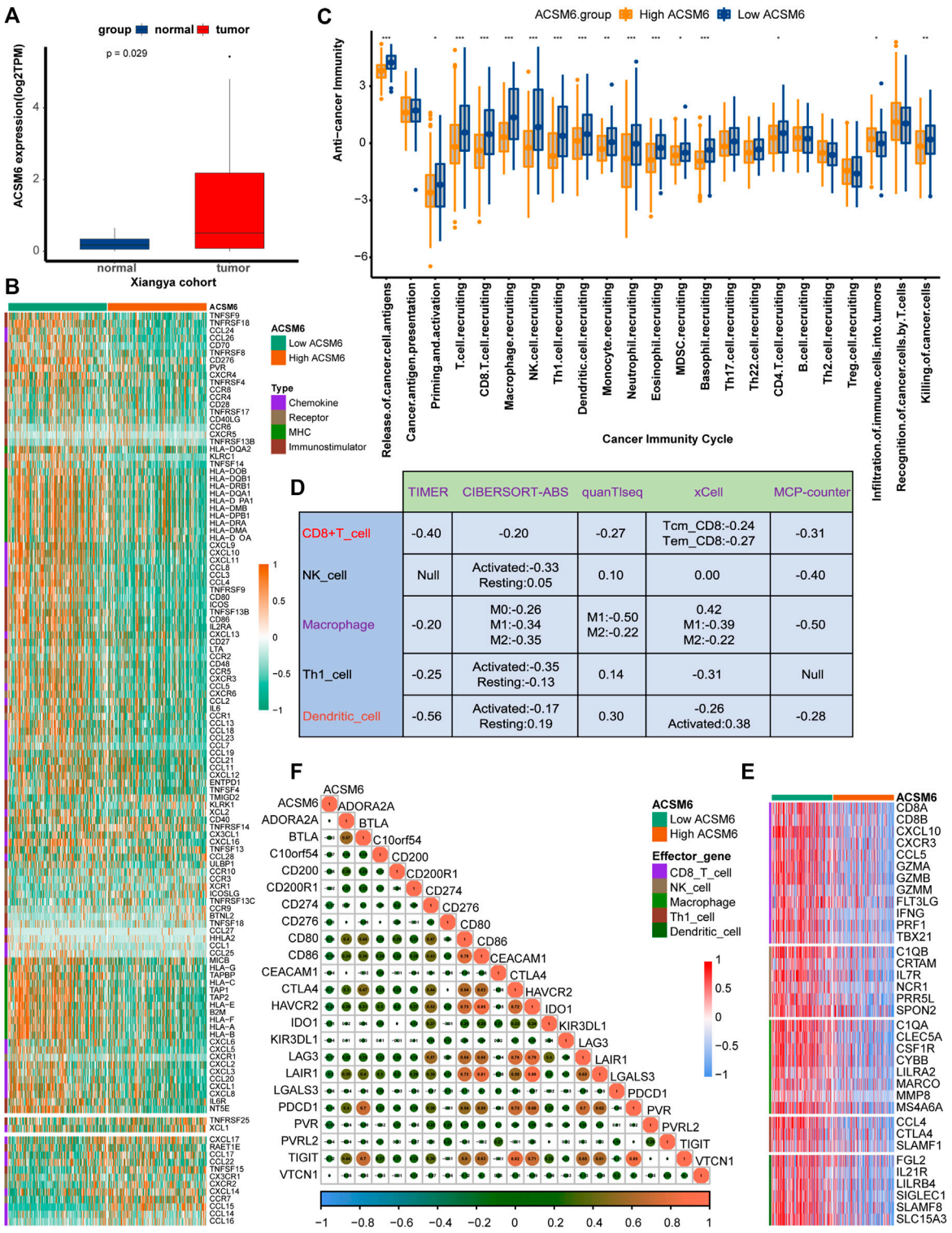

FIGURE 3
In BLCA, the tumor immune microenvironment correlates with ACSM6 expression. **(A)** ACSM6 was highly expressed in the Xiangya cohort. **(B)** ACSM6 expression is different in different tissues in BLCA. **(C)** ACSM6 expression is different in various steps of the anti-tumor immune cycle. **(D)** ACSM6 expression correlates with infiltration levels of five tumor-infiltrating immune cell types (TIICs), as measured by various algorithms. **(E)** High- and low-ACSM6 tissues in BLCA show differential expression of effector genes of the five TIICs mentioned above. **(F)** ACSM6 expression correlates with 20 inhibitory immune checkpoints in BLCA.

10.3389/fphar.2023.1222512

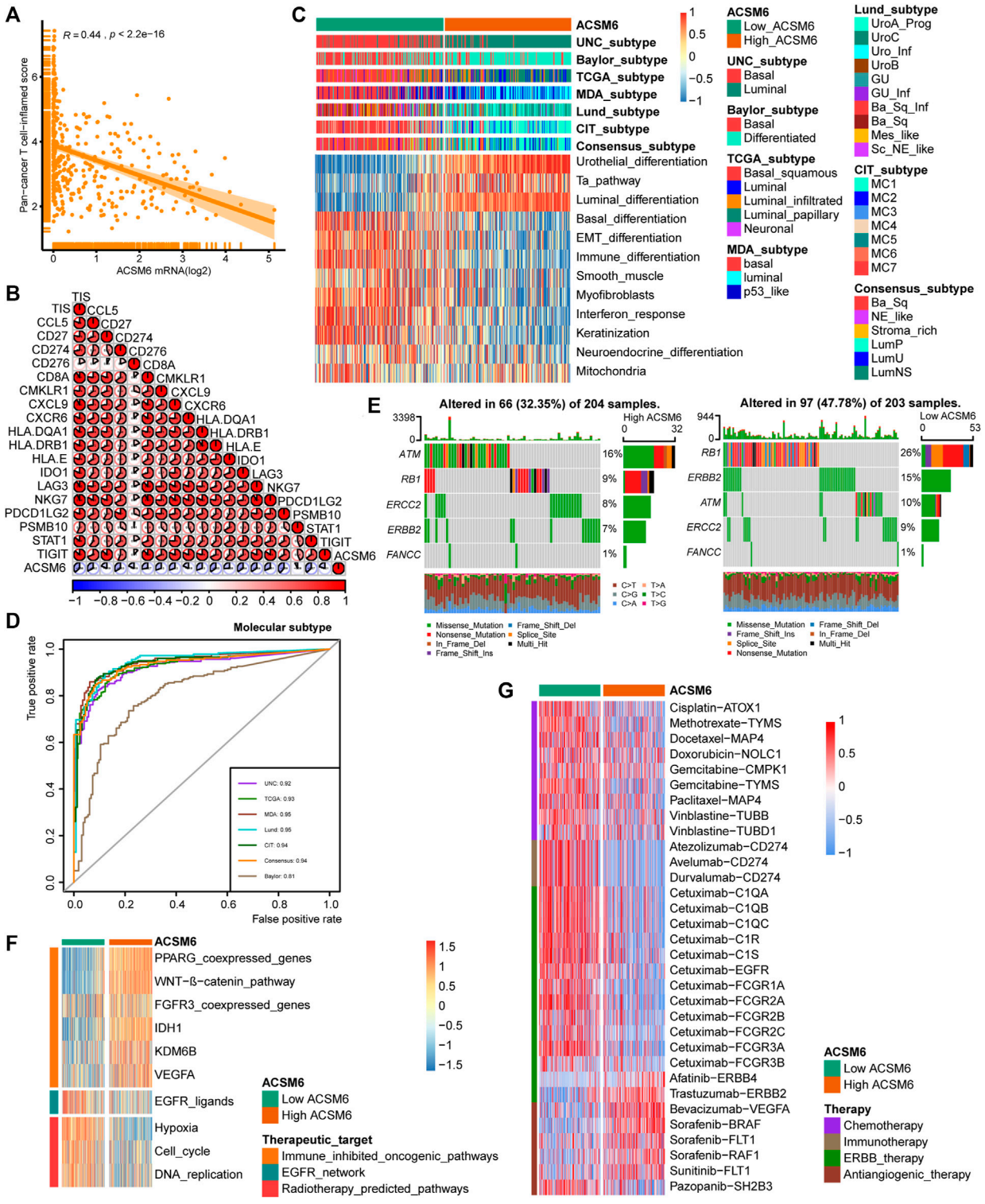

FIGURE 4
In BLCA, ACSM6 expression predicts molecular subtype and response to multiple therapies. **(A, B)** ACSM6 expression correlates with tumor immune subtype and their corresponding effector genes. **(C)** ACSM6 expression correlates with molecular subtypes as defined by seven different subtyping systems. **(D)** ROC analysis demonstrates the prediction accuracy of ACSM6 for molecular subtypes using different systems. **(E)** Mutational profiles of neoadjuvant chemotherapy-related genes differ between low- and high-ACSM6 tissues. **(F)** ACSM6 expression correlates with enrichment scores of therapeutic signatures. **(G)** ACSM6 expression correlates with drug-target genes for various therapies.

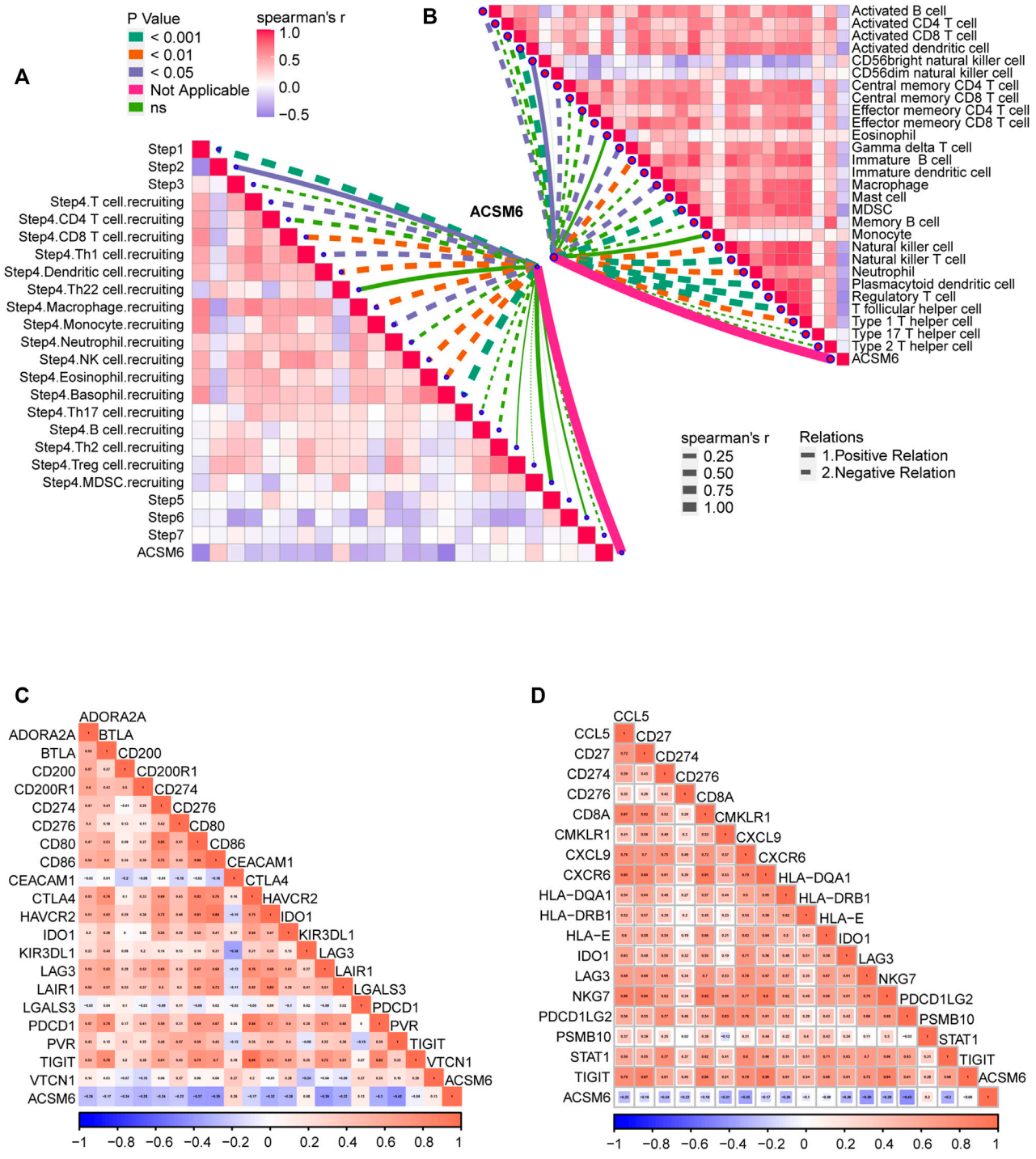

FIGURE 5
Validation of the prediction accuracy of ACSM6 for molecular subtypes and response to therapies in the Xiangya Cohort. **(A)** ACSM6 expression correlates with different steps of the anti-cancer immune cycle. **(B)** ACSM6 expression correlates with multiple ssGSEA immune cells. **(C)** ACSM6 expression correlates with 20 immune checkpoints. **(D)** ACSM6 expression correlates with TIS-related genes.

immunotherapy and ERBB therapy, while the high ACSM6 group was more responsive to anti-angiogenesis therapy (Figure 4G). Overall, patients with low ACSM6 expression could be treated with adjuvant chemotherapy, neoadjuvant chemotherapy, immunotherapy, or ERBB.

Validation of ACSM6 in Xiangya cohort

We performed additional analyses to explore the clinical significance of ACSM6 expression in the Xiangya cohort. ACSM6 was negatively associated with multiple key steps in the

10.3389/fphar.2023.1222512

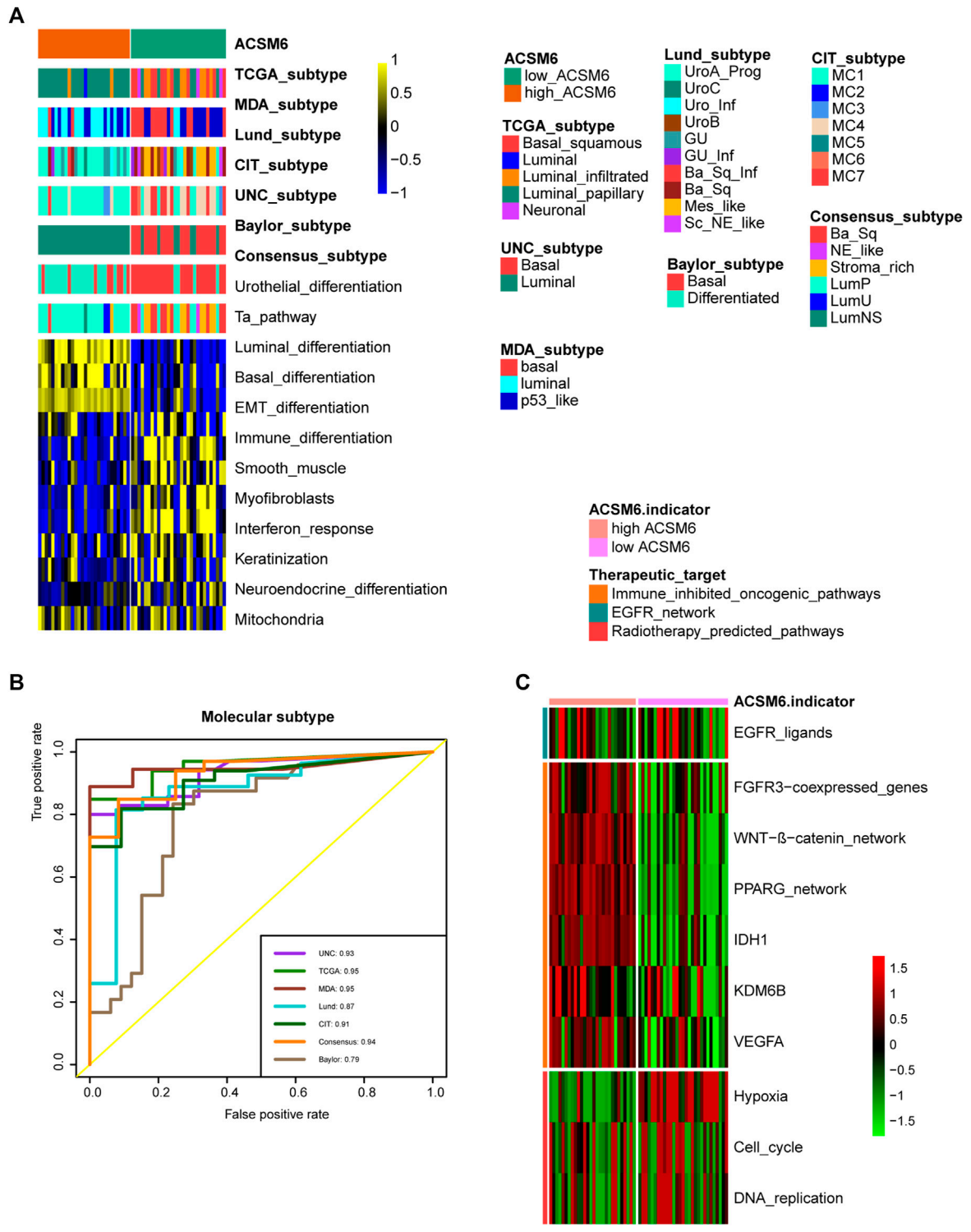

FIGURE 6
ACSM6 expression correlates with TIS-related effector genes. **(A)** ACSM6 expression correlates with seven different molecular subtyping systems. **(B)** The molecular subtype prediction accuracy of ACSM6 is evaluated. **(C)** ACSM6 expression correlates with enrichment scores of therapeutic signatures.

anticancer immune cycle, particularly the release of cancer cell antigens and the recruitment of immune cells (Figure 5A). Similarly, ACSM6 was negatively associated with various ssGSEA immune cells including activated dendritic cells, macrophages, natural killer cells, regulatory T cells, and T follicular helper cells (Figure 5B). Subsequently, ACSM6 levels were negatively associated

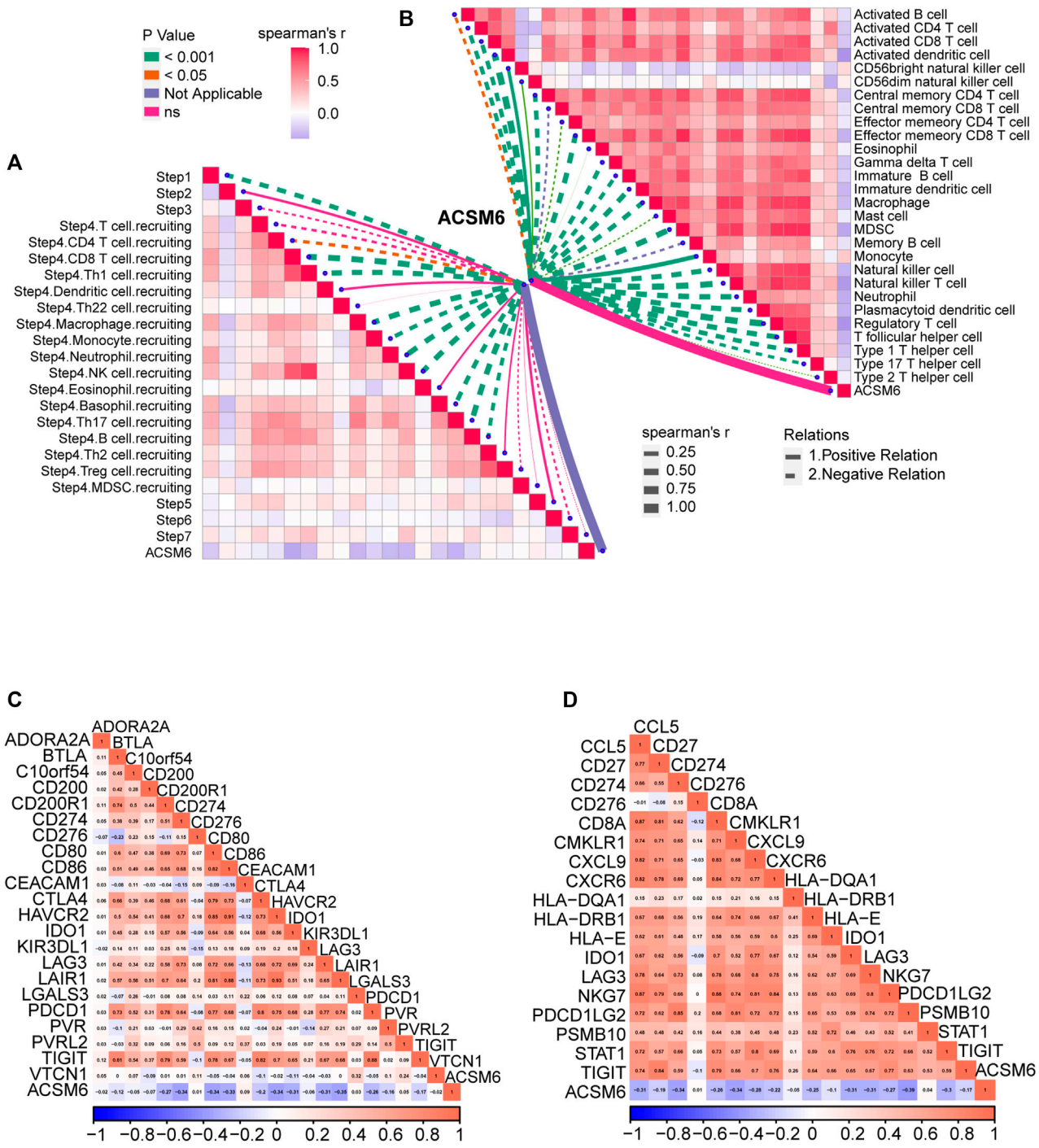

FIGURE 7
Validation of prediction for low immune infiltration and molecular subtypes by ACSM6 in the IMvigor210 cohort. **(A)** ACSM6 expression correlates with different steps of the anti-cancer immune cycle. **(B)** ACSM6 expression correlates with several immune-related cells. **(C)** ACSM6 expression correlates with immune checkpoint inhibitors effector genes. **(D)** ACSM6 expression correlates with TIS-related genes.

with immune checkpoints in the Xiangya cohort (Figure 5C). Additionally, it was confirmed that ACSM6 was negatively related to the expression of effector genes in T cell activation scores, including CXCL9, LAG-3, and PDCD1LG2 (Figure 5D). In good line with the prediction of BLCA subtypes by TCGA, the high ACSM6 group in the Xiangya cohort better turned to be the luminal subtype, while the low ACSM6 group better turned to be the basal subtype (Figure 6A). Furthermore, ACSM6 exhibited higher accuracy in predicting the BLCA molecular subtypes (Figure 6B). Notably, the high ACSM6 group better turned

10.3389/fphar.2023.1222512

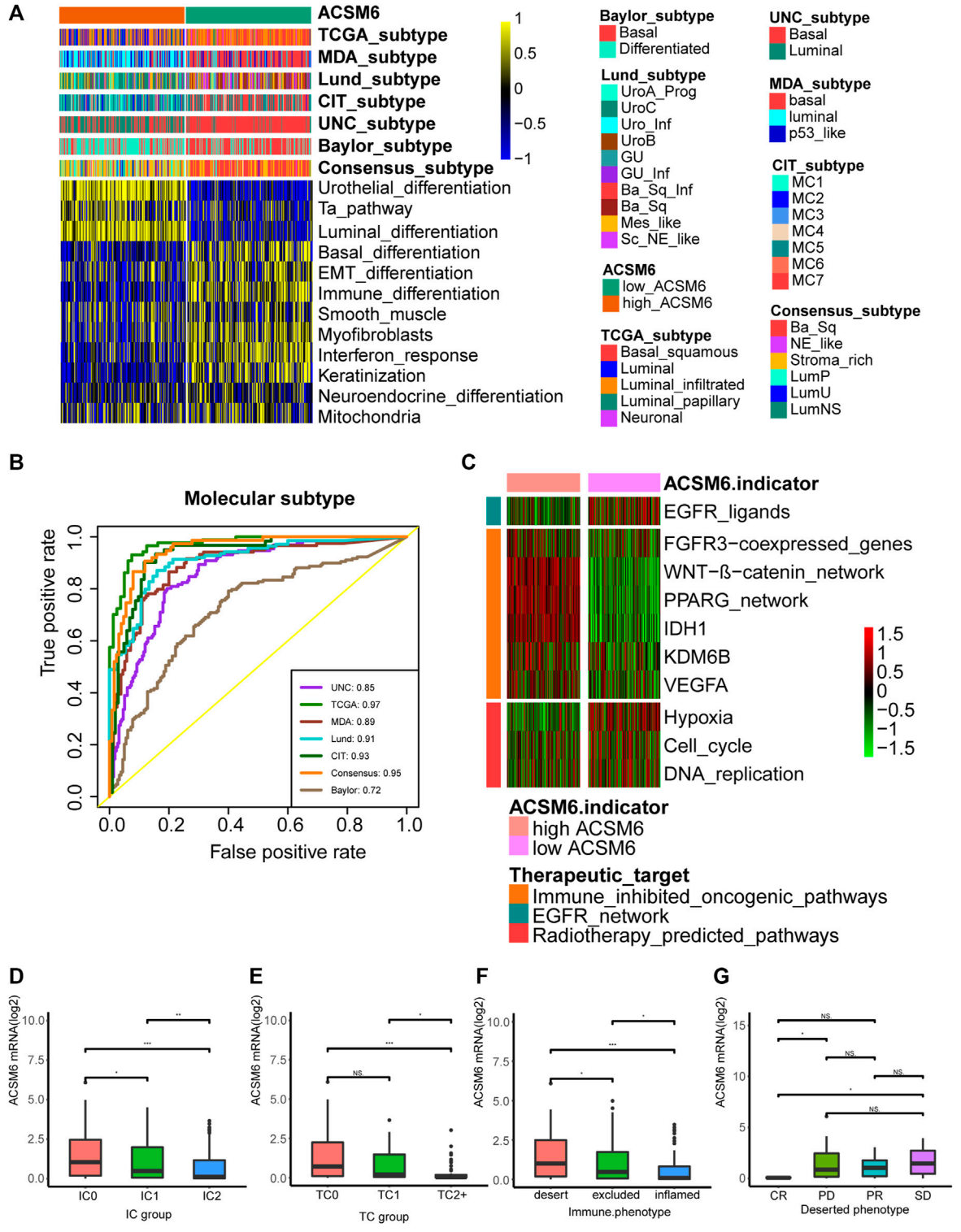

FIGURE 8
Correlations between ACSM6 and seven molecular subtype systems, three immune phenotypes and the clinical response of tumor immunotherapy in the desert group. **(A, B)** ACSM6 expression correlates with seven different molecular subtyping systems, and its prediction accuracy is evaluated by ROC analysis. **(C)** ACSM6 expression correlates with enrichment scores of therapeutic signatures. **(D)** ACSM6 expression shows differential expression in different immune checkpoint groups. **(E)** ACSM6 expression shows differential expression in different IC groups. **(F)** ACSM6 expression shows differential expression in three immune phenotypes: the desert, excluded, and inflamed. **(G)** ACSM6 expression correlates with the clinical response of tumor immunotherapy in the desert group.

to be effected by immunosuppressive tumor therapy (Figure 6C).

ACSM6 predicts the clinical efficacy of ICB

We investigated the predictive value of ACSM6 for the clinical response to ICB in the IMvigor210 cohort. In the Xiangya cohort, we observed a negative correlation between ACSM6 expression and several critical steps in the cancer immune cycle, which was consistent with our findings (Figure 7A), suggesting that when ACSM6 is highly expressed, TIL infiltration in TME is downregulated (Figure 7B). Additionally, a negative correlation was observed between ACSM6 expression and the expression of several ICI and TIS genes (Figures 7C, D). Furthermore, high ACSM6 expression predicted the luminal subtype of BLCA, which was in line with the findings in TCGA cohort (Figure 8A). The area under the ROC curve for predicting molecular subtypes was between 0.72 and 0.97 (Figure 8B). In addition, we found that the enrichment score for the radiotherapy prediction pathway in the low ACSM6 group was higher (Figure 8C).

We conducted immunohistochemistry (IHC) on the IMvigor210 cohort to identify PD-L1 expression in immune and cancer cells. We classified the immune and cancer cells into three groups based on their PD-L1 expression levels. We observed significant ACSM6 expression in the TC0 and IC0 groups (Figures 8D, E). In addition, ACSM6 was highly expressed in the non-inflammatory TME compared to that in the inflammatory TME (Figure 8F). Furthermore, we compared ACSM6 expression in different ICB clinical responses. In spite of lower ACSM6 expression in patients with complete remission (CR) in the non-inflammatory TME, ACSM6 expression was higher in patients with progressive disease (PD), stable disease (SD), and partial remission (PR). However, no significant differences were observed between these groups (Figure 8G).

Discussion

This study found that ACSM6 may act as a potential molecular biomarker for assessing the tumor microenvironment status in various types of cancer, particularly in BLCA and thymoma, and may lead to the formation of a non-inflammatory TME in BLCA. Moreover, ACSM6 can be used to predict the BLCA molecular subtypes. Low ACSM6 expression was observed in the basal subtype and exhibited higher sensitivity to ICB immune infiltration levels. Furthermore, patients with low ACSM6 expression were likely to respond better to neoadjuvant chemotherapy, adjuvant chemotherapy, and ERBB treatment.

ACSM6 is a member 6 of the acyl-CoA synthase middle-chain family; as a new member, no related research has been conducted. However, ACSM3, which belongs to the same family, has been found to be associated with tumor progression. The expression of ACSM3 is significantly reduced in hepatocellular carcinoma tissues and is associated with the late stage and poor survival rates of hepatocellular carcinoma (Boomgaarden et al., 2009). Overexpression of ACSM3 is able to weaken the migration and invasion of hepatocellular carcinoma cells (Ruan et al., 2017; Ruan et al., 2021). ACSM3 also has been reported to suppresses the pathogenesis of high-grade serous ovarian carcinoma via promoting AMPK activity (Yang et al., 2022). In addition, krüppel-like factor 10 can upregulate ACSM3 via the PI3K/Akt signaling pathway to inhibit the malignant progression of melanoma (Zhao et al., 2022). These reports indicate that ACSM3 has a high probability of inhibiting tumors. ACSM1 (Guo et al., 2022) and ACSM5 (Ruan et al., 2021) have been reported to be associated with the progression of prostate and thyroid cancers, respectively. ACSM1 is usually used as a molecular marker of apocrine carcinoma of the breast (Celis et al., 2009). ACSM4 is associated with poor prognosis of triple-negative breast cancer (Alsaleem et al., 2020). However, there are few related studies.

This study has some limitations. First, all results were from bioinformatics analyses, and no *in vivo* or *in vitro* experiments were conducted to investigate the possible mechanisms. Second, although our results were robust in the Xiangya cohort, the small sample size (57 patients) cannot be ignored. Third, grouping into high- and low-expression categories was based on the median ACSM6 mRNA expression, which might have certain limitations, and an ideal cutoff value was not identified. Therefore, this must be verified using additional tumor tissue data and experiments.

Conclusion

Our study showed that the presence of ACSM6 plays the promotion to the development of a non-inflammatory TME in BLCA, which in turn results in resistance to tumor immunotherapy. ACSM6 may be a predictor of BLCA molecular subtypes, suggesting a better prognosis treatment.

Data availability statement

The original contributions presented in the study are included in the article/Supplementary Material, further inquiries can be directed to the corresponding authors.

Author contributions

DD and ZL: conceptualization, resources, supervision, writing-review and editing. YY and BL: conceptualization, methodology, software, formal analysis, writing-original draft. ZW and TQ: data curation, software, validation, writing-original draft. All authors: manuscript writing. All authors contributed to the article and approved the submitted version.

Acknowledgments

We sincerely thank all the participants in the study.

Conflict of interest

The authors declare that the research was conducted in the absence of any commercial or financial relationships that could be construed as a potential conflict of interest.

Publisher's note

All claims expressed in this article are solely those of the authors and do not necessarily represent those of their affiliated organizations, or those of the publisher, the editors and the reviewers. Any product that may be evaluated in this article, or claim that may be made by its manufacturer, is not guaranteed or endorsed by the publisher.

Supplementary material

The Supplementary Material for this article can be found online at: https://www.frontiersin.org/articles/10.3389/fphar.2023.1222512/full#supplementary-material

References

Alsaleem, M. A., Ball, G., Toss, M. S., Raafat, S., Aleskandarany, M., Joseph, C., et al. (2020). A novel prognostic two-gene signature for triple negative breast cancer. *Mod. Pathol.* 33 (11), 2208–2220. doi:10.1038/s41379-020-0563-7

Auslander, N., Zhang, G., Lee, J. S., Frederick, D. T., Miao, B., Moll, T., et al. (2018). Robust prediction of response to immune checkpoint blockade therapy in metastatic melanoma. *Nat. Med.* 24 (10), 1545–1549. doi:10.1038/s41591-018-0157-9

Ayers, M., Lunceford, J., Nebozhyn, M., Murphy, E., Loboda, A., Kaufman, D. R., et al. (2017). IFN-γ-related mRNA profile predicts clinical response to PD-1 blockade. *J. Clin. Invest.* 127 (8), 2930–2940. doi:10.1172/JCI91190

Becht, E., Giraldo, N. A., Lacroix, L., Buttard, B., Elarouci, N., Petitprez, F., et al. (2016). Erratum to: Estimating the population abundance of tissue-infiltrating immune and stromal cell populations using gene expression. *Genome Biol.* 17 (1), 249. doi:10.1186/s13059-016-1113-y

Boomgaarden, I., Vock, C., Klapper, M., and Döring, F. (2009). Comparative analyses of disease risk genes belonging to the acyl-CoA synthetase medium-chain (ACSM) family in human liver and cell lines. *Biochem. Genet.* 47 (9-10), 739–748. doi:10.1007/s10528-009-9273-z

Cai, Z., Chen, J., Yu, Z., Li, H., Liu, Z., Deng, D., et al. (2023). BCAT2 shapes a noninflamed tumor microenvironment and induces resistance to anti-PD-1/PD-L1 immunotherapy by negatively regulating proinflammatory chemokines and anticancer immunity. *Adv. Sci. (Weinh)* 10 (8), e2207155. doi:10.1002/advs.202207155

Catto, J. W. F., Downing, A., Mason, S., Wright, P., Absolom, K., Bottomley, S., et al. (2021). Quality of life after bladder cancer: A cross-sectional survey of patient-reported outcomes. *Eur. Urol.* 79 (5), 621–632. doi:10.1016/j.eururo.2021.01.032

Celis, J. E., Cabezón, T., Moreira, J. M. A., Gromov, P., Gromova, I., Timmermans-Wielenga, V., et al. (2009). Molecular characterization of apocrine carcinoma of the breast: Validation of an apocrine protein signature in a well-defined cohort. *Mol. Oncol.* 3 (3), 220–237. doi:10.1016/j.molonc.2009.01.005

Chang, E., Weinstock, C., Zhang, L., Charlab, R., Dorff, S. E., Gong, Y., et al. (2021). FDA approval summary: Enfortumab vedotin for locally advanced or metastatic urothelial carcinoma. *Clin. Cancer Res.* 27 (4), 922–927. doi:10.1158/1078-0432.CCR-20-2275

Charoentong, P., Finotello, F., Angelova, M., Mayer, C., Efremova, M., Rieder, D., et al. (2017). Pan-cancer immunogenomic analyses reveal genotype-immunophenotype relationships and predictors of response to checkpoint blockade. *Cell. Rep.* 18 (1), 248–262. doi:10.1016/j.celrep.2016.12.019

Chen, D. S., and Mellman, I. (2013). Oncology meets immunology: The cancer-immunity cycle. *Immunity* 39 (1), 1–10. doi:10.1016/j.immuni.2013.07.012

Feng, D., Liu, S., Li, D., Han, P., and Wei, W. (2020). Analysis of conventional versus advanced pelvic floor muscle training in the management of urinary incontinence after radical prostatectomy: A systematic review and meta-analysis of randomized controlled trials. *Transl. Androl. Urol.* 9 (5), 2031–2045. doi:10.21037/tau-20-615

Feng, D., Shi, X., Zhang, F., Xiong, Q., Wei, Q., and Yang, L. (2022a). Mitochondria dysfunction-mediated molecular subtypes and gene prognostic index for prostate cancer patients undergoing radical prostatectomy or radiotherapy. *Front. Oncol.* 12, 858479. doi:10.3389/fonc.2022.858479

Feng, D., Tang, C., Liu, S., Yang, Y., Han, P., and Wei, W. (2022b). Current management strategy of treating patients with erectile dysfunction after radical prostatectomy: A systematic review and meta-analysis. *Int. J. Impot. Res.* 34 (1), 18–36. doi:10.1038/s41443-020-00364-w

Finotello, F., Mayer, C., Plattner, C., Laschober, G., Rieder, D., Hackl, H., et al. (2019). Molecular and pharmacological modulators of the tumor immune contexture revealed by deconvolution of RNA-seq data. *Genome Med.* 11 (1), 34. doi:10.1186/s13073-019-0638-6

Grivas, P., Agarwal, N., Pal, S., Kalebasty, A. R., Sridhar, S. S., Smith, J., et al. (2021). Avelumab first-line maintenance in locally advanced or metastatic urothelial carcinoma: Applying clinical trial findings to clinical practice. *Cancer Treat. Rev.* 97, 102187. doi:10.1016/j.ctrv.2021.102187

Guo, Y., Ren, C., Huang, W., Yang, W., and Bao, Y. (2022). Oncogenic ACSM1 in prostate cancer is through metabolic and extracellular matrix-receptor interaction signaling pathways. *Am. J. Cancer Res.* 12 (4), 1824–1842.

Hu, J., Chen, J., Ou, Z., Chen, H., Liu, Z., Chen, M., et al. (2022). Neoadjuvant immunotherapy, chemotherapy, and combination therapy in muscle-invasive bladder cancer: A multi-center real-world retrospective study. *Cell. Rep. Med.* 3 (11), 100785. doi:10.1016/j.xcrm.2022.100785

Hu, J., Othmane, B., Yu, A., Li, H., Cai, Z., Chen, X., et al. (2021a). 5mC regulator-mediated molecular subtypes depict the hallmarks of the tumor microenvironment and guide precision medicine in bladder cancer. *BMC Med.* 19 (1), 289. doi:10.1186/s12916-021-02163-6

Hu, J., Yu, A., Othmane, B., Qiu, D., Li, H., Li, C., et al. (2021b). Siglec15 shapes a non-inflamed tumor microenvironment and predicts the molecular subtype in bladder cancer. *Theranostics* 11 (7), 3089–3108. doi:10.7150/thno.53649

Li, B., Severson, E., Pignon, J. C., Zhao, H., Li, T., Novak, J., et al. (2016). Comprehensive analyses of tumor immunity: Implications for cancer immunotherapy. *Genome Biol.* 17 (1), 174. doi:10.1186/s13059-016-1028-7

Li, T., Fu, J., Zeng, Z., Cohen, D., Li, J., Chen, Q., et al. (2020). TIMER2.0 for analysis of tumor-infiltrating immune cells. *Nucleic Acids Res.* 48 (W1), W509–W514. doi:10.1093/nar/gkaa407

Liu, S., Chen, X., and Lin, T. (2022). Emerging strategies for the improvement of chemotherapy in bladder cancer: Current knowledge and future perspectives. *J. Adv. Res.* 39, 187–202. doi:10.1016/j.jare.2021.11.010

Liu, Z., Tang, Q., Qi, T., Othmane, B., Yang, Z., Chen, J., et al. (2021). A robust hypoxia risk score predicts the clinical outcomes and tumor microenvironment immune characters in bladder cancer. *Front. Immunol.* 12, 725223. doi:10.3389/fimmu.2021.725223

Mariathasan, S., Turley, S. J., Nickles, D., Castiglioni, A., Yuen, K., Wang, Y., et al. (2018). TGFβ attenuates tumour response to PD-L1 blockade by contributing to exclusion of T cells. *Nature* 554 (7693), 544–548. doi:10.1038/nature25501

Morales-Barrera, R., Suárez, C., González, M., Valverde, C., Serra, E., Mateo, J., et al. (2020). The future of bladder cancer therapy: Optimizing the inhibition of the fibroblast growth factor receptor. *Cancer Treat. Rev.* 86, 102000. doi:10.1016/j.ctrv.2020.102000

Newman, A. M., Liu, C. L., Green, M. R., Gentles, A. J., Feng, W., Xu, Y., et al. (2015). Robust enumeration of cell subsets from tissue expression profiles. *Nat. Methods* 12 (5), 453–457. doi:10.1038/nmeth.3337

Ruan, H. Y., Yang, C., Tao, X. M., He, J., Wang, T., Wang, H., et al. (2017). Downregulation of ACSM3 promotes metastasis and predicts poor prognosis in hepatocellular carcinoma. *Am. J. Cancer Res.* 7 (3), 543–553.

Ruan, X., Tian, M., Kang, N., Ma, W., Zeng, Y., Zhuang, G., et al. (2021). Genome-wide identification of m6A-associated functional SNPs as potential functional variants for thyroid cancer. *Am. J. Cancer Res.* 11 (11), 5402–5414.

Sassoli, C., Pierucci, F., Zecchi-Orlandini, S., and Meacci, E. (2019). Sphingosine 1-phosphate (S1P)/S1P receptor signaling and mechanotransduction: Implications for

intrinsic tissue repair/regeneration. *Int. J. Mol. Sci.* 20 (22), 5545. doi:10.3390/ijms20225545

Sung, H., Ferlay, J., Siegel, R. L., Laversanne, M., Soerjomataram, I., Jemal, A., et al. (2021). Global cancer statistics 2020: GLOBOCAN estimates of incidence and mortality worldwide for 36 cancers in 185 countries. *CA Cancer J. Clin.* 71 (3), 209–249. doi:10.3322/caac.21660

Svatek, R. S., Hollenbeck, B. K., Holmäng, S., Lee, R., Kim, S. P., Stenzl, A., et al. (2014). The economics of bladder cancer: Costs and considerations of caring for this disease. *Eur. Urol.* 66 (2), 253–262. doi:10.1016/j.eururo.2014.01.006

van Rhijn, B. W. G., Burger, M., Lotan, Y., Solsona, E., Stief, C. G., Sylvester, R. J., et al. (2009). Recurrence and progression of disease in non-muscle-invasive bladder cancer: From epidemiology to treatment strategy. *Eur. Urol.* 56 (3), 430–442. doi:10.1016/j.eururo.2009.06.028

Xu, L., Deng, C., Pang, B., Zhang, X., Liu, W., Liao, G., et al. (2018). Tip: A web server for resolving tumor immunophenotype profiling. *Cancer Res.* 78 (23), 6575–6580. doi:10.1158/0008-5472.CAN-18-0689

Yang, X., Wu, G., Zhang, Q., Chen, X., Li, J., Han, Q., et al. (2022). ACSM3 suppresses the pathogenesis of high-grade serous ovarian carcinoma via promoting AMPK activity. *Cell. Oncol. (Dordr).* 45 (1), 151–161. doi:10.1007/s13402-021-00658-1

Zhao, Z., Zhan, Y., Jing, L., and Zhai, H. (2022). KLF10 upregulates ACSM3 via the PI3K/Akt signaling pathway to inhibit the malignant progression of melanoma. *Oncol. Lett.* 23 (6), 175. doi:10.3892/ol.2022.13295

frontiers | Frontiers in Pharmacology

TYPE Original Research
PUBLISHED 13 July 2023
DOI 10.3389/fphar.2023.1192434

OPEN ACCESS

EDITED BY
Ouyang Chen,
Duke University, United States

REVIEWED BY
Yien Che Tsai,
National Cancer Institute at Frederick (NIH), United States
Wei Yang,
Cedars Sinai Medical Center, United States

*CORRESPONDENCE
Chenggui Zhang,
chenggui1214@pku.edu.cn
Zhe Yang,
sdslyyyz@sina.com

†These authors share first authorship

RECEIVED 23 March 2023
ACCEPTED 19 June 2023
PUBLISHED 13 July 2023

CITATION
Li J, Zhang W, Ma X, Wei Y, Zhou F, Li J, Zhang C and Yang Z (2023), Cuproptosis/ferroptosis-related gene signature is correlated with immune infiltration and predict the prognosis for patients with breast cancer.
Front. Pharmacol. 14:1192434.
doi: 10.3389/fphar.2023.1192434

Cuproptosis/ferroptosis-related gene signature is correlated with immune infiltration and predict the prognosis for patients with breast cancer

Jixian Li[1†], Wentao Zhang[2,3†], Xiaoqing Ma[4], Yanjun Wei[5], Fengge Zhou[3], Jianan Li[1], Chenggui Zhang[6*] and Zhe Yang[1,3*]

[1]Shandong Provincial Hospital, Shandong University, Jinan, Shandong, China, [2]Shandong Provincial Hospital, Shandong First Medical University, Jinan, Shandong, China, [3]Tumor Research and Therapy Center, Shandong Provincial Hospital Affiliated to Shandong First Medical University, Jinan, Shandong, China, [4]Radiotherapy and Minimally Invasive Group I, The Second Affiliated Hospital of Shandong First Medical University, Taian, Shandong, China, [5]Department of Radiation Oncology, Weifang People's Hospital, Weifang, China, [6]Department of Orthopedics, Shandong Provincial Hospital Affiliated to Shandong First Medical University, Jinan, Shandong, China

Background: Breast invasive carcinoma (BRCA) is a malignant tumor with high morbidity and mortality, and the prognosis is still unsatisfactory. Both ferroptosis and cuproptosis are apoptosis-independent cell deaths caused by the imbalance of corresponding metal components in cells and can affect the proliferation rate of cancer cells. The aim in this study was to develop a prognostic model of cuproptosis/ferroptosis-related genes (CFRGs) to predict survival in BRCA patients.

Methods: Transcriptomic and clinical data for breast cancer patients were obtained from The Cancer Genome Atlas (TCGA) and Gene Expression Omnibus (GEO) databases. Cuproptosis and ferroptosis scores were determined for the BRCA samples from the TCGA cohort using Gene Set Variation Analysis (GSVA), followed by weighted gene coexpression network analysis (WGCNA) to screen out the CFRGs. The intersection of the differentially expressed genes grouped by high and low was determined using X-tile. Univariate Cox regression and least absolute shrinkage and selection operator (LASSO) were used in the TGCA cohort to identify the CFRG-related signature. In addition, the relationship between risk scores and immune infiltration levels was investigated using various algorithms, and model genes were analyzed in terms of single-cell sequencing. Finally, the expression of the signature genes was validated with quantitative real-time PCR (qRT–PCR) and immunohistochemistry (IHC).

Results: A total of 5 CFRGs (ANKRD52, HOXC10, KNOP1, SGPP1, TRIM45) were identified and were used to construct proportional hazards regression models. The high-risk groups in the training and validation sets had significantly worse survival rates. Tumor mutational burden (TMB) was positively correlated with the risk score. Conversely, Tumor Immune Dysfunction and Exclusion (TIDE) and tumor purity were inversely associated with risk scores. In addition, the infiltration degree of antitumor immune cells and the expression of immune checkpoints were lower in the high-risk group. In addition, risk scores and mTOR, Hif-1, ErbB,

MAPK, PI3K/AKT, TGF-β and other pathway signals were correlated with progression.

Conclusion: We can accurately predict the survival of patients through the constructed CFRG-related prognostic model. In addition, we can also predict patient immunotherapy and immune cell infiltration.

KEYWORDS

cuproptosis, ferroptosis, BRCA, prognosis, immune

Introduction

Breast cancer is the most common cancer in women worldwide (Dumas et al., 2020) and seriously endangers women's lives and health. There were approximately 2.3 million new cases and 685,000 deaths in 2020 (Lei et al., 2021). Breast cancer is a significantly heterogeneous cancer (Yeo and Guan, 2017), and with the continuous development of treatments in the form of surgery, chemotherapy, radiotherapy, targeted therapy, endocrine therapy, etc. (Singh et al., 2021), the survival of breast invasive carcinoma (BRCA) patients has improved. However, some patients still face the risk of recurrence and death. Currently known clinical, pathological and molecular features cannot accurately predict the prognosis of patients; thus, we still urgently need new prognostic markers to evaluate the prognosis of patients and to guide treatment.

Cuproptosis (Tang et al., 2022) and ferroptosis (Dixon et al., 2012) are novel cell death modes that do not depend on apoptotic pathways. The main cause of ferroptosis is the continuous generation of lipid reactive oxygen species (ROS) caused by excessive intracellular iron (Wang et al., 2022). Once ROS levels exceeds the ROS ability to resist oxygen, the ROS will produce oxidative stress, which will damage mitochondria, the endoplasmic reticulum and nucleic acids in cells and finally lead to cell death. Studies have shown that abnormal regulation of ferroptosis is closely related to the occurrence of various human diseases, including ischemic organ damage (Yan et al., 2020), neurodegeneration (Jakaria et al., 2021) and tumors (Mou et al., 2019). However, induction of ferroptosis can prevent malignant progression of tumors in patients, inhibit conventional therapy-resistant cells, and enhance the effectiveness of immunotherapy (Xu et al., 2021). Interestingly, Suppressor of fused homolog (SUFU) inhibits ferroptosis sensitivity in breast cancer cells through the Hippo/YAP pathway (Fang et al., 2022). Cuprotosis is the latest form of programmed cell death to be discovered. Maintaining an adequate amount of copper plays an important role in maintaining function and homeostasis in all living organisms. Excess copper will interact with fatty acylated components in the tricarboxylic acid (TCA) cycle, resulting in abnormal aggregation of fatty acylated proteins and loss of Fe-S cluster proteins (Tsvetkov et al., 2022), at which point proteotoxic oxidative stress is activated, causing cells to undergo "copper toxicity," which in turn leads to cell death (Li S-R. et al., 2022). In addition, this inhibition of the TCA cycle can affect ferroptosis. Thus, through the TCA cycle, both cuproptosis and ferroptosis can be affected (Gao et al., 2019).

In this study, we innovatively linked cuproptosis and ferroptosis. The CFRGs that can predict OS in BRCA patients were screened out by means of bioinformatics, and a proportional hazards regression model was constructed. Based on this model, we can effectively predict the prognosis of patients and help them personalize their treatments.

Material and methods

Data resources

The necessary data were acquired from The Cancer Genome Atlas (TCGA) (https://portal.gdc.cancer.gov/), comprising of RNA-sequencing (RNA-seq) data, clinical information, and simple nucleotide variation data from a total of 1182 BRCA patients. Fragments per kilobase million (FPKM) was selected for mRNA expression profiling. We also acquired RNA-seq data and clinical information from the National Center for Biotechnology Information (NCBI) Gene Expression Omnibus (GEO) database (https://www.ncbi.nlm.nih.gov/geo/, ID: GSE20685, GSE42568, GSE58812). Specifically, GSE20685 contained RNA-seq and clinical data of 327 breast cancer samples, GSE42568 contained RNA-seq and clinical data of 104 breast cancer samples and 17 normal breast samples, and GSE58812 contained RNA-seq and clinical data of 107 breast cancer samples. To ensure uniformity, the mRNA expression data in the TCGA and GEO databases were transformed into transcripts per million (TPM) data by log2 transformation. We downloaded a total of 65 ferroptosis-related genes from the Molecular Signatures Database (MSigDB, http://www.gsea-msigdb.org/gsea/msigdb/) and an additional 19 cuproptosis-related genes from the literature (Tsvetkov et al., 2022) (Ren et al., 2021) (Tao et al., 2021) (Selvaraj et al., 2005).

CFRG identification based on GSVA and WGCNA

GSVA is an algorithm used to analyze gene expression data and functional annotation. It can display the differences in samples on different gene sets by calculating gene set scores. The algorithm does not require standardization and is very fast, so it is widely used in biomedical research. A GSVA of the GSE42568 samples was performed on ferroptosis and cuproptosis genomes to obtain ferroptosis and cuproptosis scores, respectively. The hub genes were screened by weighted gene coexpression network analysis (WGCNA) based on their scores. Scale-free and average connectivity analyses were performed on modules with different power values using the PickSoftThreshold function to set the soft threshold power to 5. Then, the corresponding dissimilarity matrix (1-TOM) and topological overlap matrix (TOM) were obtained. Pearson correlation analysis was performed on coexpression modules with cuproptosis and ferroptosis scores after TOM.

X-tile software is a software designed by Yale University to calculate the optimal cutoff value for survival curves. We calculated the optimal cutoff values for the cuproptosis score and ferroptosis score in the TCGA cohort with this software and divided the scores into high- and low-score groups, respectively. Subgroups with both high and low scores for both cuproptosis and ferroptosis were selected. According to specific criteria ($|log2FC| \geq 1$ and FDR<0.05), the "DeSeq2" R package was used to screen out the high and low subgroup differentially expressed genes (DEGs), and then the DEGs were cross-referenced with the genes screened by WGCNA, and the final genes were identified as CFRGs.

Establishment and validation of the CFRGs prognostic model

After screening out CFRGs related to prognosis, we used five machine learning methods—decision tree, random forest, least absolute shrinkage and selection operator (LASSO), extreme gradient boosting (XGBoost) and gradient boosting decision tree (GBDT)—to evaluate the survival weights of the CFRGs. GSE42568 was used as the training set, and the first 30 genes were selected to construct the LASSO Cox model. With the median risk score as the critical value, the model was divided into a high-risk group and a low-risk group. The overall survival (OS) of the high and low risk groups was analyzed using the KM curve. Subsequently, Kaplan–Meier (KM) analysis was performed on the high- and low-risk groups using the "survival" and "survminer" R packages, and 1-, 3-, and 5-year receiver operating characteristic (ROC) analyses were performed with the "timeROC" R package to evaluate the sensitivity of the model. Finally, the TCGA and GEO cohorts (GSE20685, GSE58812) were used as the validation set, and the obtained prognoses were selected for validation. In addition, we constructed a nomogram by combining the risk score and clinical data.

Analysis of signature and immune-related markers

We used seven algorithms from the Tumor Immune Estimation Resource (TIMER) database, including TIMER, CIBERSORT, CIBERSORT-ASB, QUANTISEQ, MCPCOUNTER, XCELL, and EPIC, to analyze signatures and immunity. In addition, we evaluated the differences in immune cell infiltration and immune function between high-risk and low-risk subgroups using the single-sample gene set enrichment analysis (ssGSEA) algorithm. Furthermore, differences between high- and low-risk groups in immune therapy biomarkers were also analyzed through TIDE (http://tide.dfci.harvard.edu/)), TMB, and immune checkpoint.

Characterization of OCFRGs (optimal cuproptosis/ferroptosis related genes) by single-cell RNA sequencing

Single-cell RNA-seq data for 12 samples were obtained from the GSE149655 dataset in the GEO database. The sequencing data were analyzed using the "Seurat" R package, and low-viability cells were removed. Using the CreateSeuratObject function, and based on specified criteria, low-quality cells were further removed (min.cells<3, min. features<50, percent. mt < 50). The filtered single-cell RNA sequencing (scRNA-seq) data were then normalized, and 1,500 genes with large coefficients of variation between cells were generated and subsequently subjected to principal component analysis (PCA) for dimensionality reduction of the scRNA-seq data. The top 4 PCs were selected for cell clustering analysis using the distributed stochastic neighbor embedding (t-SNE) algorithm. Through the DEGs of each cluster, the cell clusters were tool annotated. Finally, we analyzed the expression levels of OCFRGs in different clusters.

Enrichment analysis of GSEA and GSVA

DEGs in high-risk and low-risk subgroups were screened and GSEA was performed using the GSEA software (https://www.gsea-msigdb.org/gsea/index.jsp). In addition, GSVA was used to perform GSVA on high-risk and low-risk subgroups using the "GSVA" R package. We collected some pathways closely related to the occurrence and development of tumors from the literature, including Hippo, Wnt, MAPK, PI3K/AKT, TGF-β, NF-kB, Notch, AMPK, JAK-STAT, PD-1/PD-L1, mTOR, Ras, TNF, HIF-1, ErbB, Nrf2, as well as functions and pathways related to cuproptosis and ferroptosis, including GLUTATHIONE PEROXIDASE ACTIVITY, P53 SIGNALING PATHWAY, GLUTATHIONE METABOLIC PROCESS, LIPID HOMEOSTASIS, PENTOSE PHOSPHATE PATHWAY, TRICARBOXYLIC ACID CYCLE, MITOCHONDRIAL TRICARBOXYLIC ACID CYCLE ENZYME COMPLEX, TRICARBOXYLIC ACID CYCLE ENZYME COMPLEX, REGULATION OF OXIDATIVE STRESS INDUCED CELL DEATH, RESPONSE TO OXIDATIVE STRESS, CELL MIGRATION INVOLVED IN SPROUTING ANGIOGENESIS, IRON METABOLISM. We used GSVA to calculate the enrichment score for each pathway and evaluate the correlation between risk score and sex enrichment score.

Risk subtype analysis of drug sensitivity

In order to assess the sensitivity of high and low risk groups to drugs, we used the "pRRophetic" R package to analyze the RNA-seq data of BRCA based on the Genomics of Drug Sensitibity in Cancer (GDSC) database. The level of half maximal inhibitory concentration (IC50) reflects the patient's sensitivity to drugs.

Immunohistochemistry validation of the protein expression levels of OCFRGs

Five breast invasive ductal carcinoma tissue chips were purchased from Shanghai Outdo Biotech Company (Shanghai, China). Each tissue chip includes 45 cancer tissues and 45 paracancerous tissues. ANKRD52 (rabbit polyclonal, catalog number: GTX32443, Genetex), HOXC10 (rabbit polyclonal, catalog number: ab153904, Abcam),

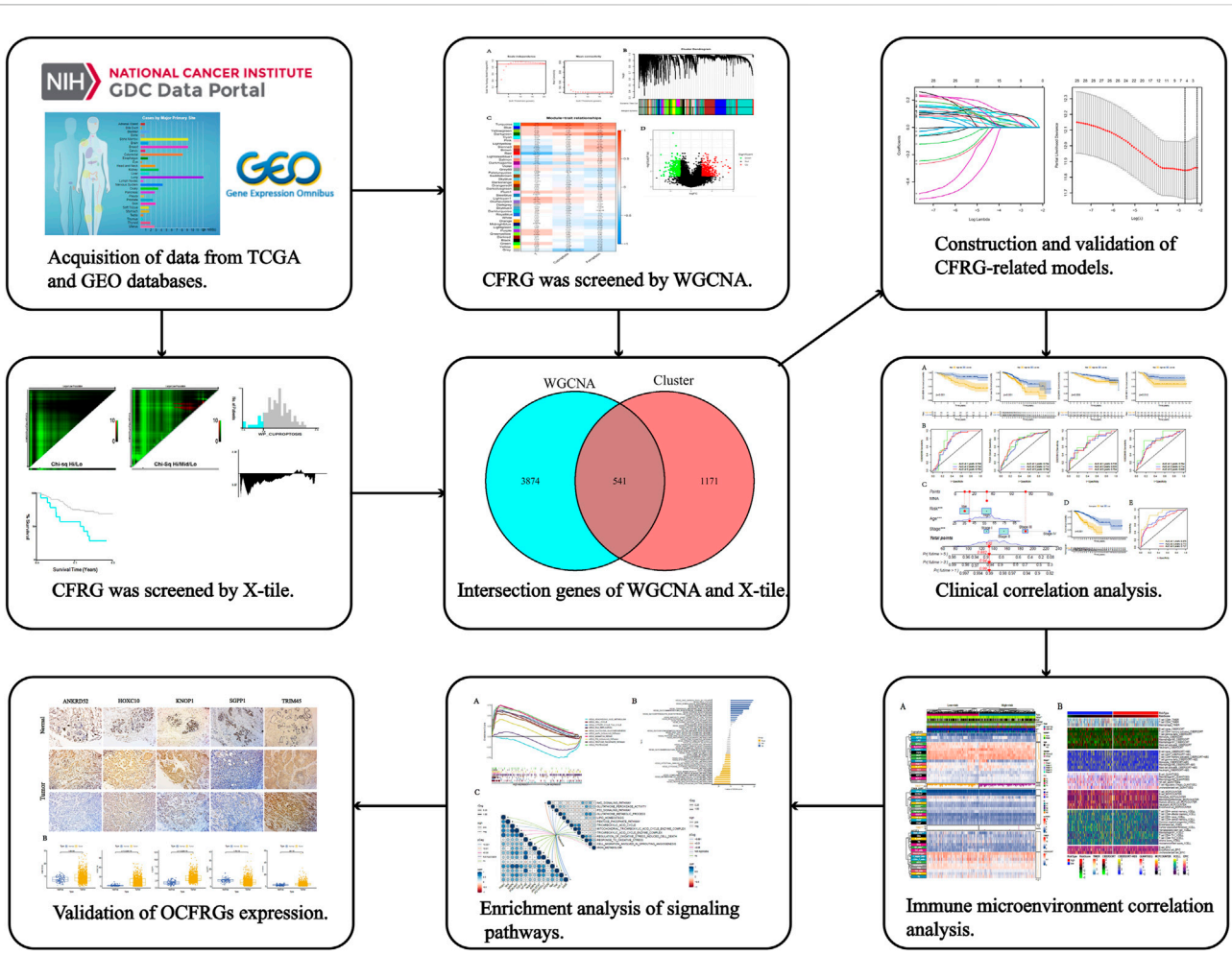

FIGURE 1
The workflow of the research. The figure shows the process of constructing and analyzing the DFRG-related signature.

KNOP1 (rabbit polyclonal, catalog number: ab126512, Abcam), SGPP1 (rabbit polyclonal, catalog number: ab126512, Abcam): ab126512, Abcam) and TRIM45 (rabbit polyclonal, catalog number: TA505920, origene). The results of the immunohistochemical staining were scored. Semiquantitative scoring was performed according to the staining intensity and the percentage of positive cells: No staining, pale yellow (light yellow particles), medium (brown yellow particles), and heavy (dark brown particles) were scored as 0, 1, 2, and 3, respectively. According to the percentage of positively stained cells in the total number of cells, 0% was scored as 0, 5%–25% was scored as 1; 26%–50% was scored as 2; 51%–75% was scored as 3; and >75% was scored as 4 points. The final score was the sum of the staining intensity and the percentage of positive cells. The sum of the staining intensity and the percentage of positive cells was less than 6 for the low expression group and ≥6 for the high expression group. Five 400x high-power fields were randomly selected for each sepction, the staining intensity and percentage of positive cells were scored in each field, and the average value was calculated. The immunohistochemical staining results were microscopically adjudicated by two pathologists in an independent, double-blind manner.

Quantitative real-time PCR

Normal breast epithelial MCF-10A cells and three human breast cancer cell lines, SK-BR-3, MDA-MB-231, and MCF-7, were obtained from the Central Laboratory of Shandong Provincial Hospital. Total RNA was extracted using TRIzol reagent (Invitrogen, United States). Complementary DNA (cDNA) was synthesized using the PrimeScript RT kit (Takara). Supplementary Table S2 shows the primer sequences for Quantitative real-time PCR analysis of OCFRGs.

Western blotting

Cells were lysed in cold Radioimmunoprecipitation assay (RIPA) buffer. The same amount of protein was subjected to SDS-PAGE, and then transferred to PVDF (polyvinylidene fluoride) membrane. Block with nonfat dry milk containing TBST for 1 h. The primary antibody (Western blot and IHC universal primary antibody) was diluted according to the instructions and incubated overnight at 4°C. After washing with TBST, the secondary antibody was added and incubated for 1 h at

10.3389/fphar.2023.1192434

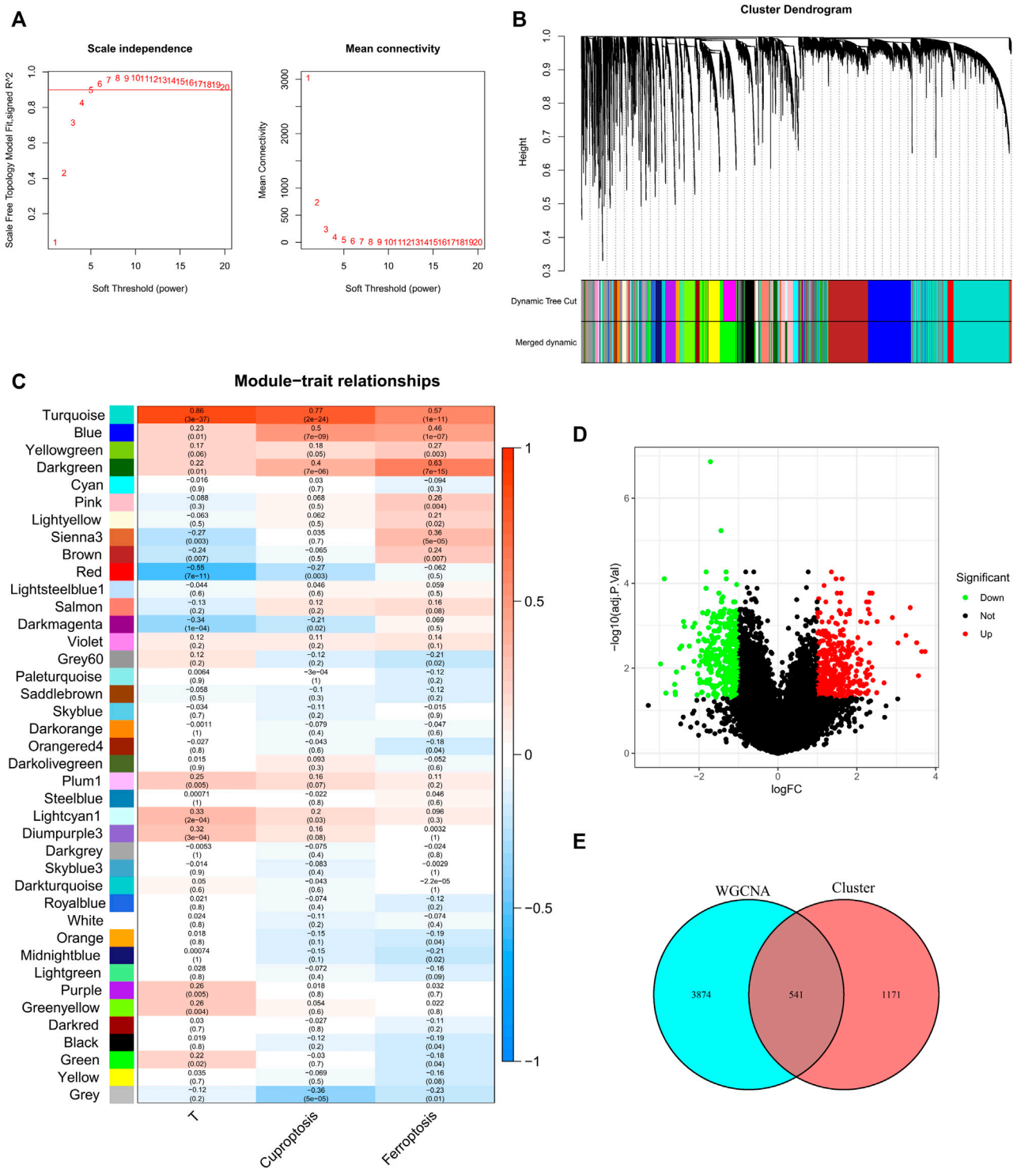

FIGURE 2
Discovery of prognostic CFRGs by WGCNA and Score grouping. **(A)** The distribution and trends of scale free topology model fit and mean connectivity along with soft threshold. **(B)** The clustering of gens among different modules by the dynamic tree cut and merged dynamic method. The gray modules represent unclassified genes. **(C)** Average correlation between multiple modules and tumor development, cuproptosis and ferroptosis. The color of the cell indicates the strength of the correlation, and the number in parentheses idicates the *p*-value for the correlation test. **(D)** According to specific criteria ($p < 0.05$, $|Log2FC| \geq 1$), 1712 DEGs wew screened for high and low score groups of cuproptosis and ferroptosis. **(E)** 541 CFRGs were obtained from WGCNA and high and low score groups.

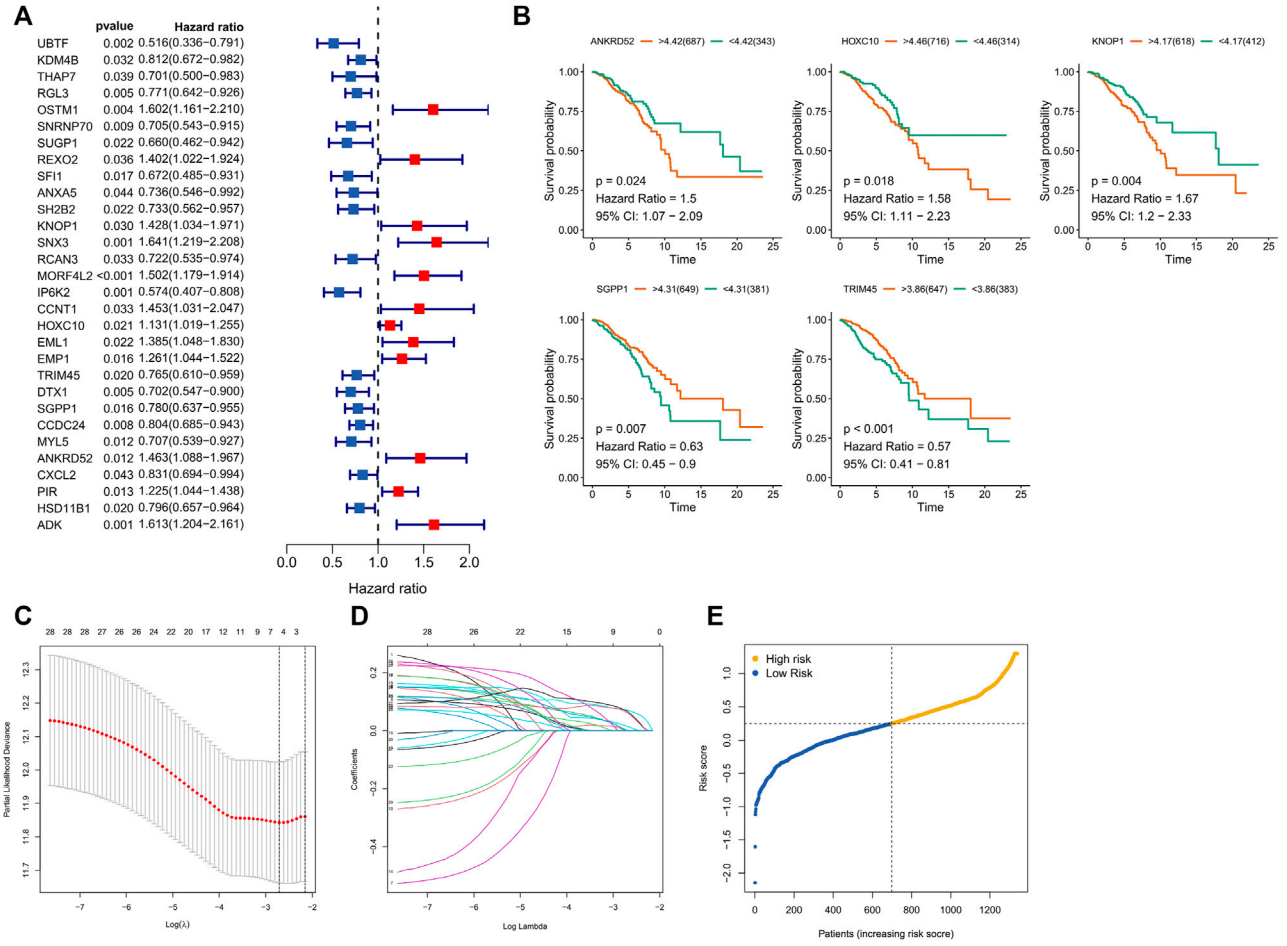

FIGURE 3
Screening and Models Construction of OCFRGs. **(A)** Forest plot of univariate Cox regression analysis (only showing the top 30 CFRGs related to survival). **(B)** Differences in survival between samples with high and low expression of OCFRGs ($p < 0.05$). **(C)** Selecting the best value of lambda through LASSO regression. **(D)** LASSO coefficient configuration of 5 OCFRGs. **(E)** Distribution of patients based on the median risk score in the training set.

room temperature. After washing the membrane, it was developed using enhanced chemiluminescence (ECL) chromogenic solution.

Statistical analysis

The bioinformatics analysis, statistical analysis, and machine learning aspects of this study were all performed with R software (version 4.0.1). Statistical tests included the Pearson chi-square test and Wilcoxon rank-sum test. Kaplan-Meier analysis was used to assess OS in both groups of patients. $p < 0.05$ was considered to be statistically significant.

Results

Identification of cuproptosis/ferroptosis-related genes

The specific process of this study is shown in Figure 1, which includes the acquisition of data, the acquisition of cuproptosis and ferroptosis-related genes, the construction and validation of the signature, the analysis of clinical data, the analysis of immune cell infiltration levels, and the analysis of pathways and functions.

We used the pickSoftThreshold function in the WGCNA R package to automatically select a soft threshold of 5 (Figure 2A). Multiple gene modules were divided by the dynamic cutting method, and the mergeCloseModules function was used to perform cluster analysis on each module into fewer modules and mark them with different colors (Figure 2B). To determine the correlation of coexpression modules with genetic differences between normal and tumor samples that may contribute to tumor development, cuprotosis score and ferroptosis score, we used Pearson correlation analysis, and the results showed that the module "turquoise" had the strongest correlation (R (Turmor) = 0.86, R (cuproptosis) = 0.77, R (ferroptosis) = 0.57) (Figure 2C).

X-tile software was used to determine the optimal cutoff values for the survival curves of the cuproptosis and ferroptosis scores in the TCGA BRCA cohort (Supplementary Figure S1). Patients with high cuproptosis and ferroptosis scores and patients with low cuproptosis and ferroptosis scores were divided into two groups,

10.3389/fphar.2023.1192434

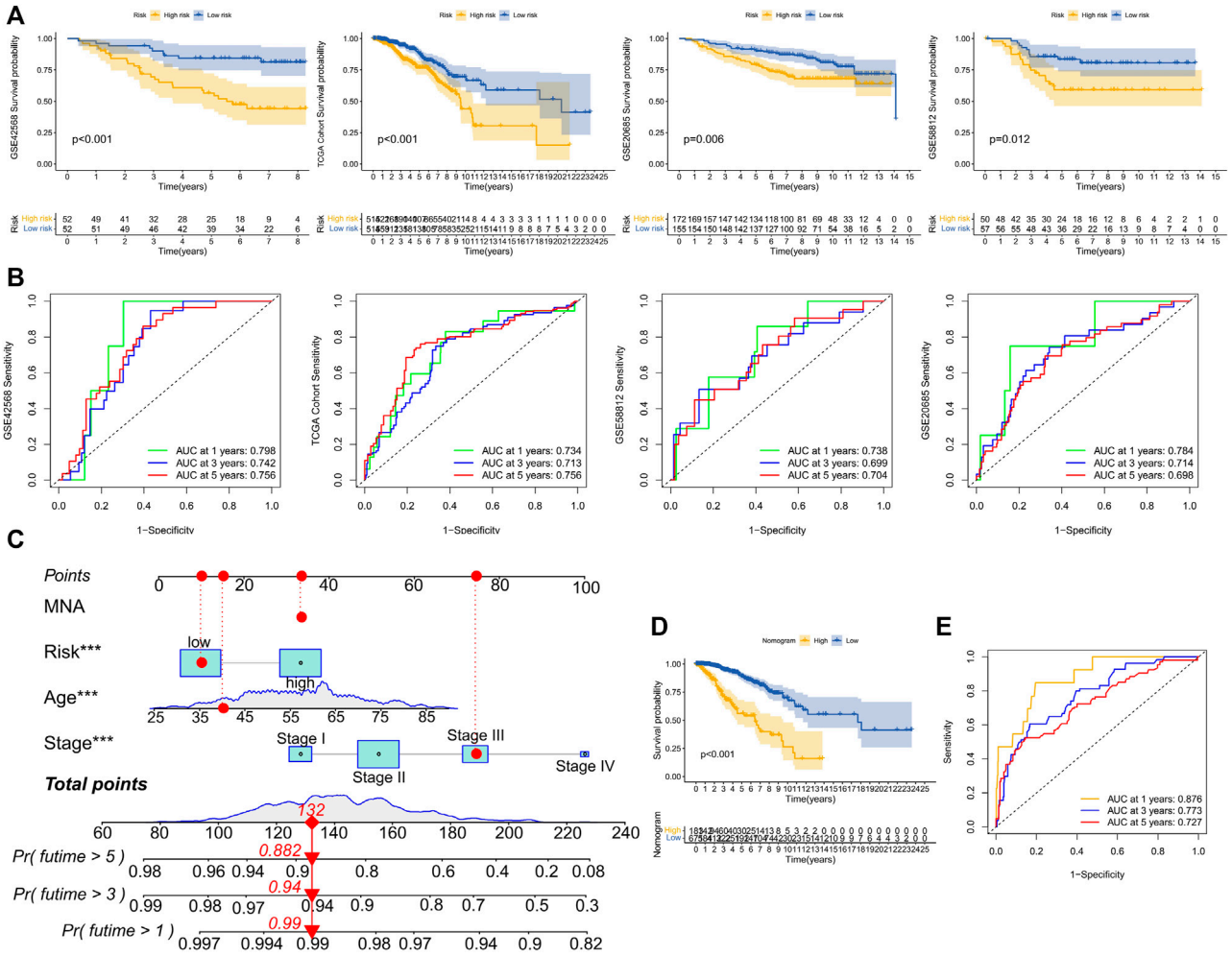

FIGURE 4
Performance evaluation of model prognosis and construction of nomogram. **(A)** KM curve shows the difference between high and low-risk groups in OS for GSE42568, TCGA cohort, GSE20685, and GSE58812. **(B)** ROC curves show the predictive efficiency of risk scores for GSE42568, TCGA cohort, GSE20685, and GSE58812 at 1, 3, and 5 years. **(C)** Column chart of overall survival prediction at 1 year, 3 years, and 5 years. The red line shows an example of how to predict prognosis. **(D)** The difference in survival between high and low-score groups in nomogram. **(E)** The predictive.

and DEGs were screened out with |log2FC| ≥ 1 and FDR<0.05 as criteria (Figure 2D). By analyzing the intersection of the genes screened by means of DEGs and WGCNA, a total of 541 CFRGs were identified (Figure 2E).

Establishment and validation of the CFRG prognostic model

Survival-related CFRGs were screened by using Cox regression analysis (Figure 3A). The survival-related weights of the CFRGs were evaluated using five machine learning algorithms, including decision tree, random forest, LASSO, XGBoost, and GBDT. The top 30 CFRGs with average scores (Supplementary Table S1) were selected to screen genes and to construct models by means of LASSO Cox regression analysis. According to the best λ value, 5 prognostic genes (Figure 3B) were selected and signature was constructed (Figure 3C,D). Calculation of the risk score was conducted as follows:

$$\text{Risk Score} = (0.4024^{*}\text{ANKRD52 exp.}) + (0.1025^{*}\text{HOXC10 exp.}) + (0.2146^{*}\text{KNOP1 exp.}) + (-0.3069^{*}\text{SGPP1 exp.}) + (-0.4003^{*}\text{TRIM45 exp.})$$

Based on the median training set risk score, BRCA patients were divided into high- and low-risk groups and further analyzed (Figure 3F). In the training and validation sets, the KM curve showed that the OS (Overall survival) in the high-risk group was lower than that in the low-risk group (Figure 4A), which was statistically significant ($p < 0.05$). The ROC curve of the training set showed that the AUCs at 1 year, 3 years, and 5 years were 0.76, 0.726, and 0.728, respectively. The AUC of the TCGA cohort was 0.734, 0.713, and 0.756, and that of GSE58812 was 0.784, 0.714, and 0.698. This indicates that our model has reliable predictive performance. We constructed a nomogram, in which Age ($p <$

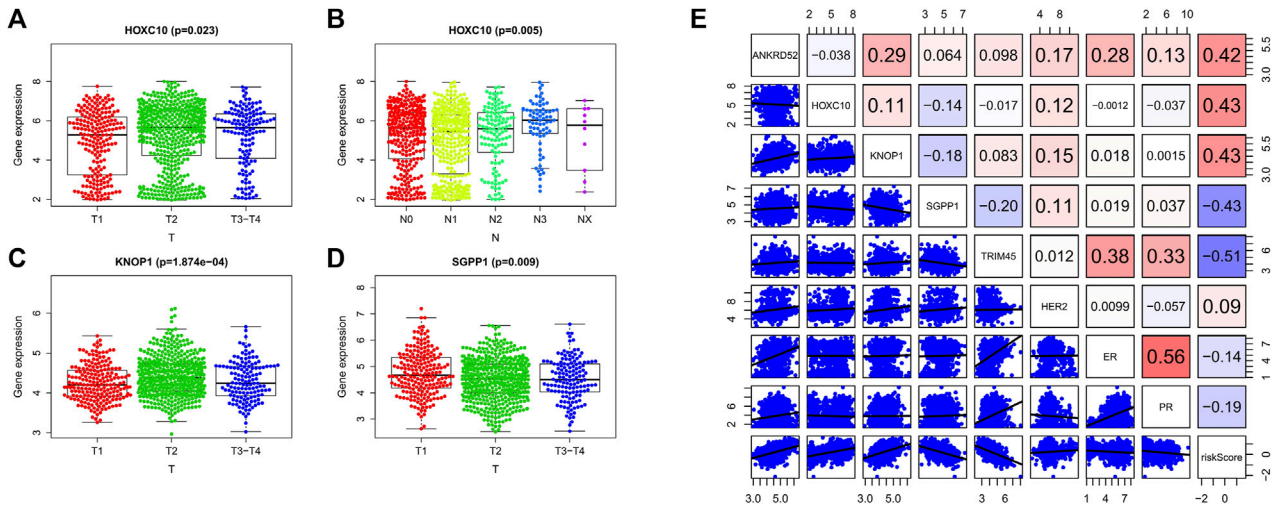

FIGURE 5
Clinical analysis of the model. **(A–D)** By Kruskal–Wallis test, the expression differences of OCFRGs (ANKRD52, HOXC10, KNOP1, SGPP1, TRIM45) in T stage and N stage were analyzed. **(E)** By calculating the Pearson correlation coefficient, the correlation between OCFRGs and the risk score and clinical indicators ER, PR, HER2 of breast cancer were analyzed.

0.001), Stage ($p < 0.001$), and risk score ($p < 0.01$) were all statistically significant (Figure 4C). In the nomogram, the OS of high-scoring patients was significantly lower than that of low-scoring patients (Figure 4D), which was statistically significant ($p < 0.05$). The column chart had good predictive performance with AUCs of 0.876, 0.773, and 0.727 at 1, 3, and 5 years, respectively.

Clinical analysis of the signature

We analyzed the relationship between OCFRGs (ANKRD52, HOXC10, KNOP1, SGPP1, TRIM45) and clinical data. The results showed that the expression level of HOXC10 differed significantly in different T and N stages and was statistically significant. In addition, the higher the expression level of HOXC10, the later the T stage and N stage of the patient (see Figures 5A,B). The expression levels of KNOP1 and SGPP1 also differed significantly in different T stages (see Figures 5C,D) and were statistically significant. We also analyzed the correlation between the expression levels of OCFRGs, risk score, and the expression levels of ER, PR, and HER2 (see Figure 5E). The results showed that the expression level of ANKRD52 was positively correlated with ER (R = 0.28). TRIM45 was also positively correlated with ER (R = 0.38) and PR (R = 0.33). There were also differences in stage, T stage, and M stage between the high-risk and low-risk groups (Figure 6A).

Analysis of risk subtypes and immune markers

We analyzed the relationship between several immune-related markers and the risk subtypes. The results showed that the expression of numerous immune checkpoints was different between high and low-risk groups (Figure 6A), especially CD274 (PDL1, Programmed Cell Death 1 Ligand 1). Additionally, TMB (tumor mutational burden) and TIDE (tumor immune dysfunction and exclusion) are considered important immune therapy markers. Our study found that TMB and TIDE were also different between high and low-risk groups. The results based on the ssGSEA algorithm showed that the expression levels of Mast cells, B cells, NK cells, and Neutrophils also differed between high and low-risk groups. Moreover, according to the results from TIMER database (Figure 6B), all immune-related markers had different expression levels between the high and low-risk groups. It is worth noting that all of the immune-related analyses had statistical significance ($p < 0.05$).

In terms of immune cell infiltration, the expression of OCFRGs was mainly correlated with the infiltration levels of neutrophils and regulatory T cells (Tregs). The expression of ANKRD52 was negatively correlated with the infiltration level of activated dendritic cells (aDCs) (R = −1.4, $p < 0.001$, Figure 6C), and the expression level of HOXC10 was negatively correlated with the infiltration level of Tregs (R = −0.076, $p = 0.014$, Figure 6D). The expression level of KNOP1 was negatively correlated with the infiltration level of neutrophils (R = −0.22, $p < 0.001$, Figure 6E), and the expression level of SGPP1 was positively correlated with the infiltration level of neutrophils (R = 0.34, $p < 0.001$, Figure 6F). The expression level of TRIM45 was positively correlated with the infiltration level of Tregs (R = −0.34, $p < 0.001$, Figure 6G).

Overview of the scRNA-Seq data generated from BRCA

We obtained 14592 cells from 12 samples of GSE168410. A total of 1,418 cells were obtained by screening the total cells according to the intracellular gene features, the percentage of chromosomal genes, etc. Afterward, the top 10 genes with large coefficients of variation were labeled. Latitude reduction was

10.3389/fphar.2023.1192434

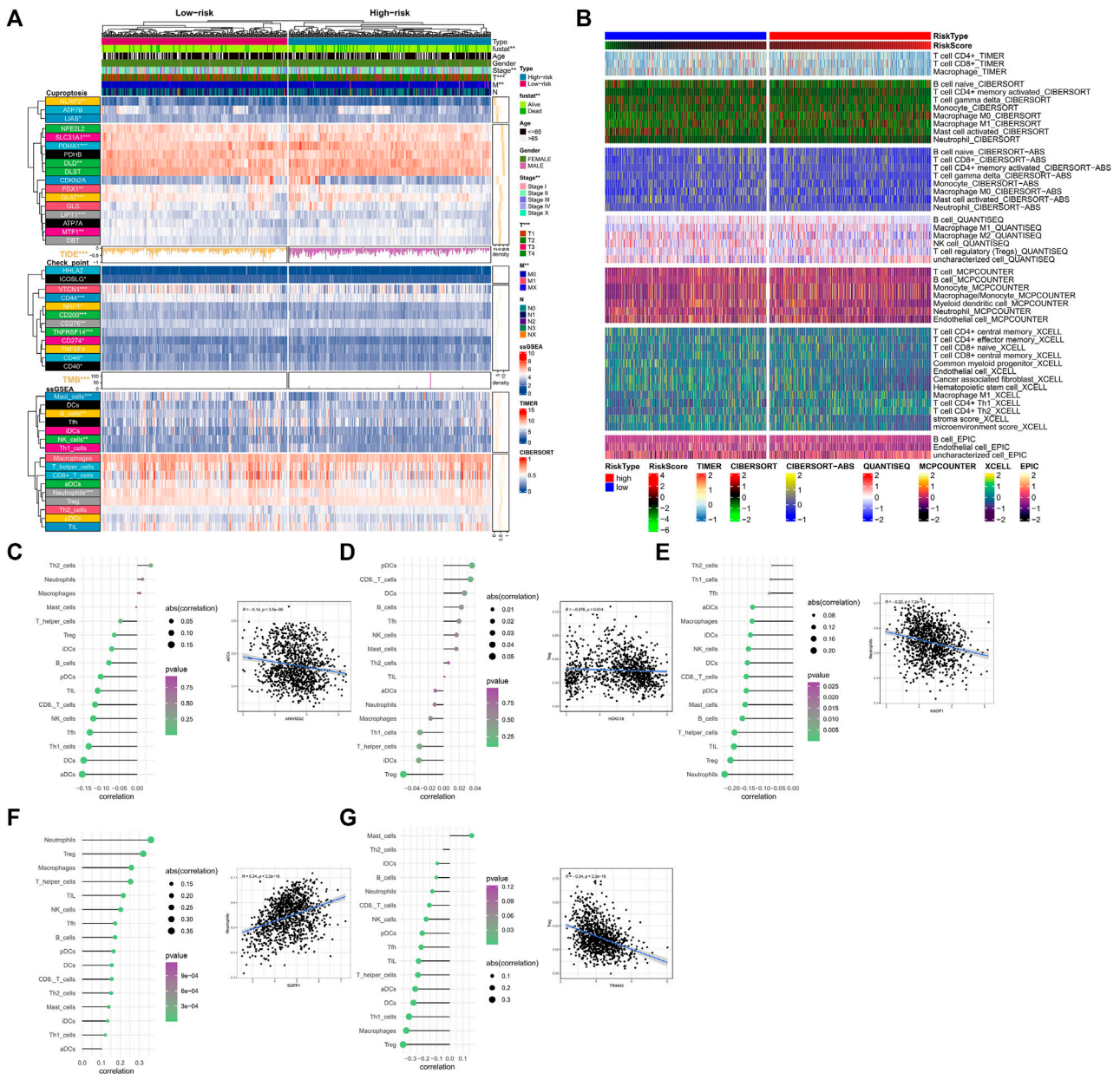

FIGURE 6
Analysis of immune cell infiltration related to the signature. **(A)** Differences in clinical data, CRGs, TMB, TIDE scores, check point and ssGSEA results between high and low-risk groups. TIDE Scores and TMB are presented in the form of a bar chart and density plot respectively. **(B)** The differences in the abundance of immune cell infiltration algorithms in TIMER2.0 database including TIMER, CIBERSORT, CIBERSORT-ABS, MCPCOUNTER, XCELLL and EPIC between the high-risk and low-risk groups (the heatmap shows the results with statistical differences). **(C–G)** The correlation between OCFRGs and immune infiltration level. The color represents the significance, with greener colors indicate higher significance. The size of the circles represents the correlation coefficient.

performed using PCA (Figure 7A). The first 4 PCs were retained for further t-SNE, and 13 cell subsets were obtained (Figure 7B). The top 5 genes in each cluster were visualized with a heatmap (Supplementary Figure S3). We used tools to annotate the cell subsets, namely, fibroblasts, tissue stem cells, epithelial cells, monocytes, endothelial cells, chondrocytes, and T cells (Figure 7C). To investigate the expression of marker genes in different cells, we visualized them with t-SNE and violin plots (Figures 7D,E). OCFRGs were highly expressed in epithelial cells; HOXC10, KNOP1, and SGPP1 were highly expressed in fibroblasts; and only SGPP1 was highly expressed in monocytes.

Analysis of function and signaling pathways

The biological functions of high- and low-risk groups were analyzed using GSEA software, which revealed that certain

10.3389/fphar.2023.1192434

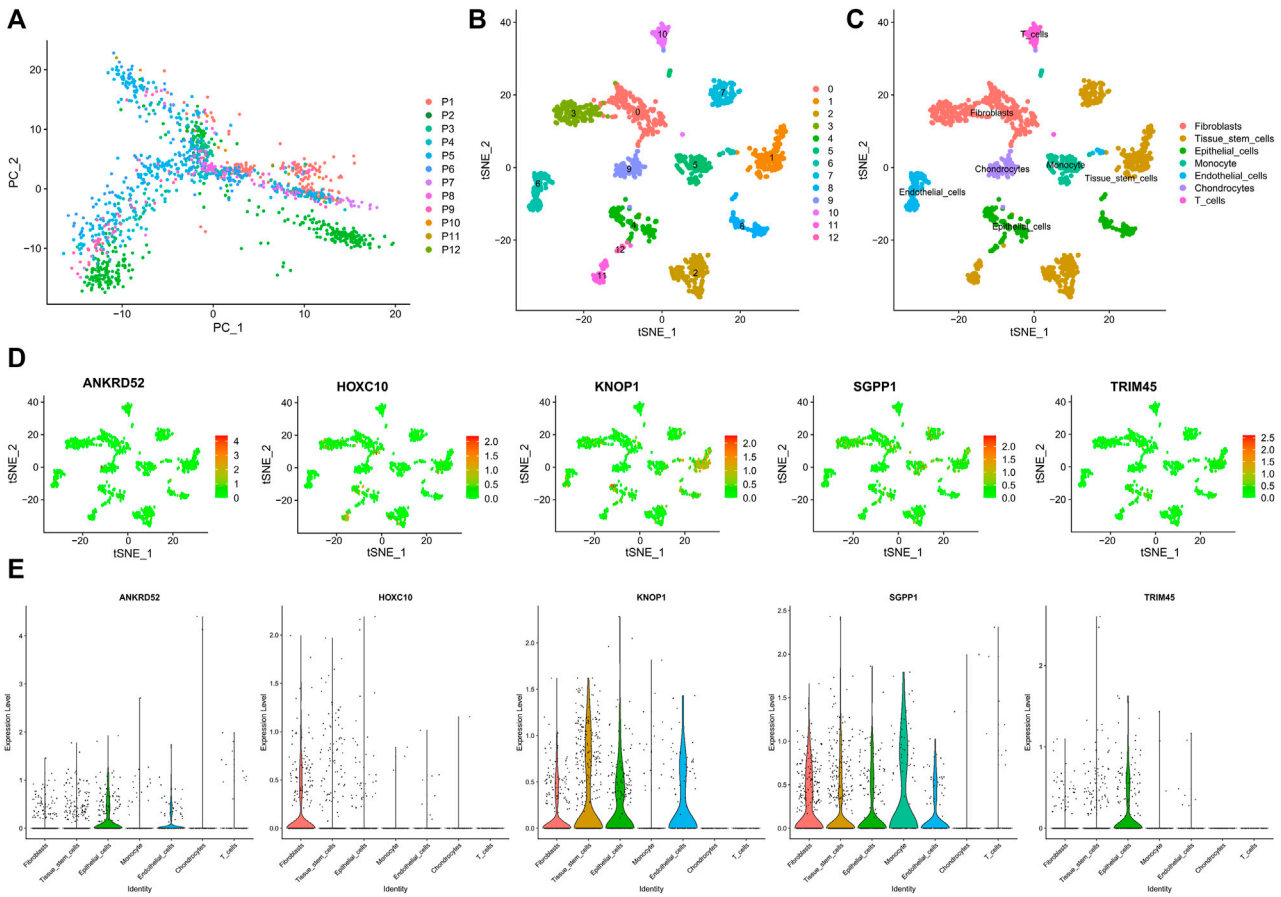

FIGURE 7
Verification of OCFRGs through sc-RNA seq. **(A)** PCA of scRNA-seq data for preliminary dimensionality reduction. **(B,C)** tSNE plots of cells generated from brest cancer tissue. The plots are colored by cell cluster, and the cells are clustered into seven sub-clusters. Each dot represents a breast cance cell. **(D)** The expression of signature genes in BRCA visualized in tSNE. **(E)** Violin plots depicting the expression of signature genes in clusters of BRCA. The y-axis shows the normalized read count. t-SNE:t-distributed stochastic neighbor embedding.

functions such as CELL CYCLE, CITRATE CYCLE/TCA CYCLE, DNA REPLICATION, GLYCOLYSIS/GLUCONEOGENESIS, MISMATCH REPAIR, PENTOSE PHOSPHATE PATHWAY, and PROTEASOME were more active in the high-risk group. On the other hand, the low-risk group exhibited significant enrichment in ARACHIDONIC ACID METABOLISM, MAPK SIGNALING PATHWAY, and P53 SIGNALING PATHWAY (Figure 8A). Additionally, GSVA analysis (Figure 8B) indicated that CELL CYCLE, HOMOLOGOUS RECOMBINATION, MISMATCH REPAIR, and DNA REPLICATION were more enriched in the high-risk group, whereas INTESTINAL IMMUNE NETWORK FOR IGA PRODUCTION, CYTOKINE CYTOKINE RECEPTOR INTERACTION, TYROSINE METABOLISM, and ARACHIDONIC ACID METABOLISM evidenced more enrichment in the low-risk group. Remarkably, several signaling pathways, including mTOR, HIF-1, and ErbB, were significantly activated in the high-risk group, whereas other signaling pathways such as MAPK, PI3K/AKT, TGF-β, and Ras were significantly inhibited (Figure 8C). Furthermore, the scores for cuproptosis/ferroptosis-related functional pathways, including Nrf2 SIGNALING PATHWAY, P53 SIGNALING PATHWAY, TRICARBOXYLIC ACID CYCLE, and REGULATION OF OXIDATIVE STRESS INDUCED CELL DEATH, were positively correlated with the risk score. In contrast, the scores for GLUTATHIONE PEROXIDASE ACTIVITY, GLUTATHIONE METABOLIC PROCESS, and IRON METABOLISM were negatively correlated with the risk score. All the aforementioned analyses exhibited statistical significance ($p < 0.05$).

Drug sensitivity analysis between high and low risk groups

Elesclomol is a potent copper ionophore that promotes cuproptosis. Our analysis shows that the IC50 of various anticancer drugs including elesclomol is different in the high- and low-risk groups, and the IC50 values of high-risk groups are generally higher than those of low-risk groups (Figure 9A–L).

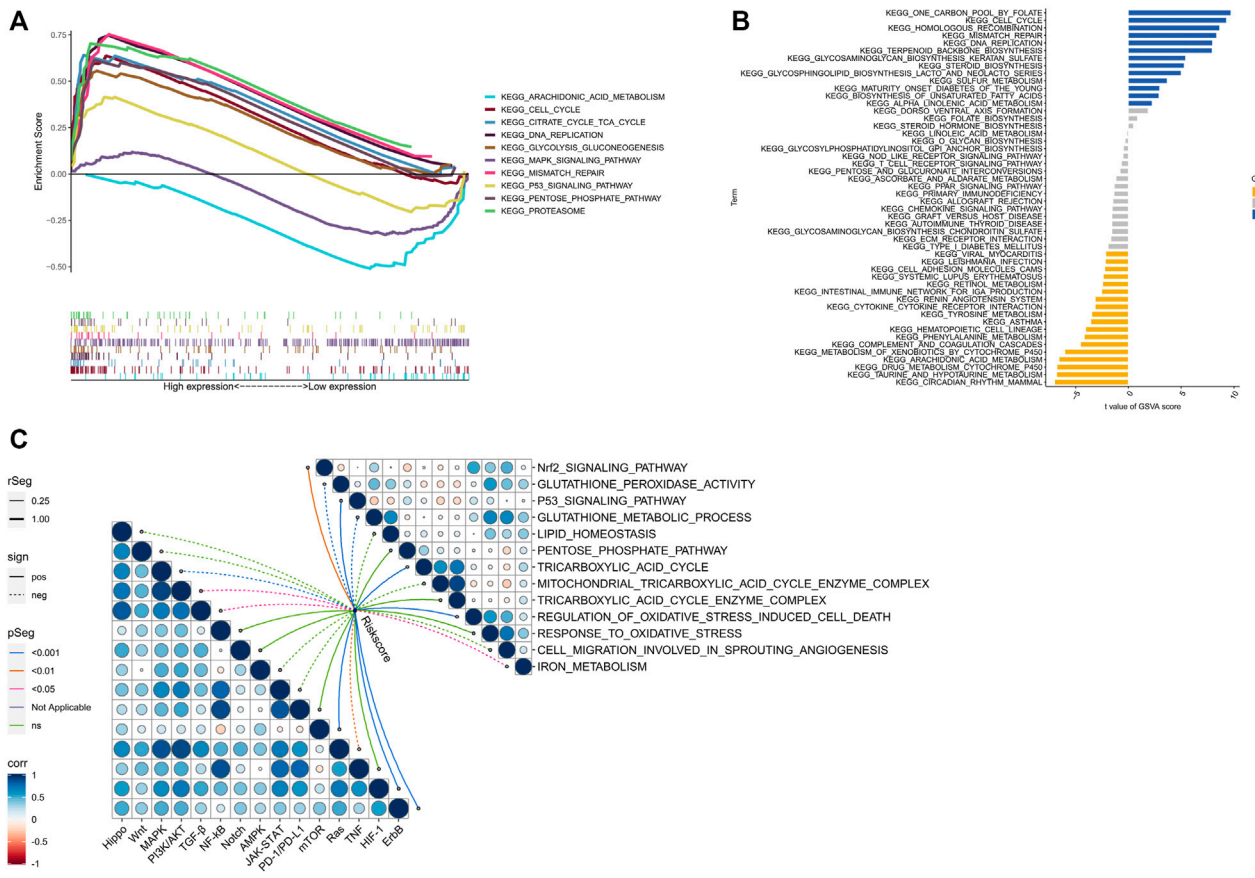

FIGURE 8
Biological functions. **(A)** Significantly enriched pathwways in the high-risk and low-risk groups. The extremum located on the left side idicates a psotive association between risk scores and pathway activity, and *vice versa*. **(B)** There is a significant difference in pathways between high-risk and low-risk groups. Blue bars represent a positive correlation between risk scores and pathway aactivity, while yellow bars indicate the opposite. **(C)** The correlation between riskscore and tumor important pathways, as well as cuproptosis/ferroptosis-related functions.

Experimental verification of the expression of OCFRGs

To explore the differences in the protein expression of OCFRGs in normal tissues and adjacent tissues, we detected the expression levels of ANKRD52, HOXC10, KNOP1, SGPP1, and TRIM45 in tissues by using immunohistochemical staining. The results of ANKRD52 level expressed that the HOXC10, KNOP1, and TRIM45 in the tumor tissue were higher in the paracancerous tissue, and the opposite was true for SGPP1 (Figure 10A). qRT-PCR results showed that ANKRD52, HOXC10, KNOP1, and TRIM45 were significantly higher in MCF-10A cells than other cell lines, while SGPP1 was the opposite (Figure 10B). The results of Western blotting also verified the results of the database (Figure 10C).

Discussion

Cuproptosis was recently defined as a distinct type of regulated cell death that occurs via a novel mechanism directly involving the TCA cycle of mitochondrial metabolism. Conversely, Ferroptosis, characterized by iron dependence, lipid peroxidation, and sensitivity to lipophilic antioxidants, is a well-researched regulated cell death. Literature suggests a relationship between Ferroptosis and TCA cycle with dysregulation of the TCA cycle leading to the occurrence of Ferroptosis. Additionally, TCA cycle metabolites serve as crucial sources of peroxide production, playing a role in the occurrence of Ferroptosis (Yang et al., 2022). Moreover, Gao et al. (Gao et al., 2019) demonstrated the reduction of Ferroptosis by inhibiting the mitochondrial TCA cycle.

According to the World Health Organization, in 2018 alone, 26,000 women worldwide were diagnosed with breast cancer. In the United States and China, the incidence and death rates of breast cancer vary among different ethnicities and races. White American women have an incidence rate of 133.7 per 100,000, while Chinese women have an incidence rate of 29.18 per 100,000. The death rates are 19.7 and 6.59 per 100,000 for White American and Chinese women, respectively (Giaquinto et al., 2022). Due to the high degree of heterogeneity of breast cancer based on genetic status and molecular subtypes, there are significant prognostic differences among patients with various subtypes. Therefore, the discovery of new prognostic biomarkers or models to guide clinical diagnosis and treatment is essential.

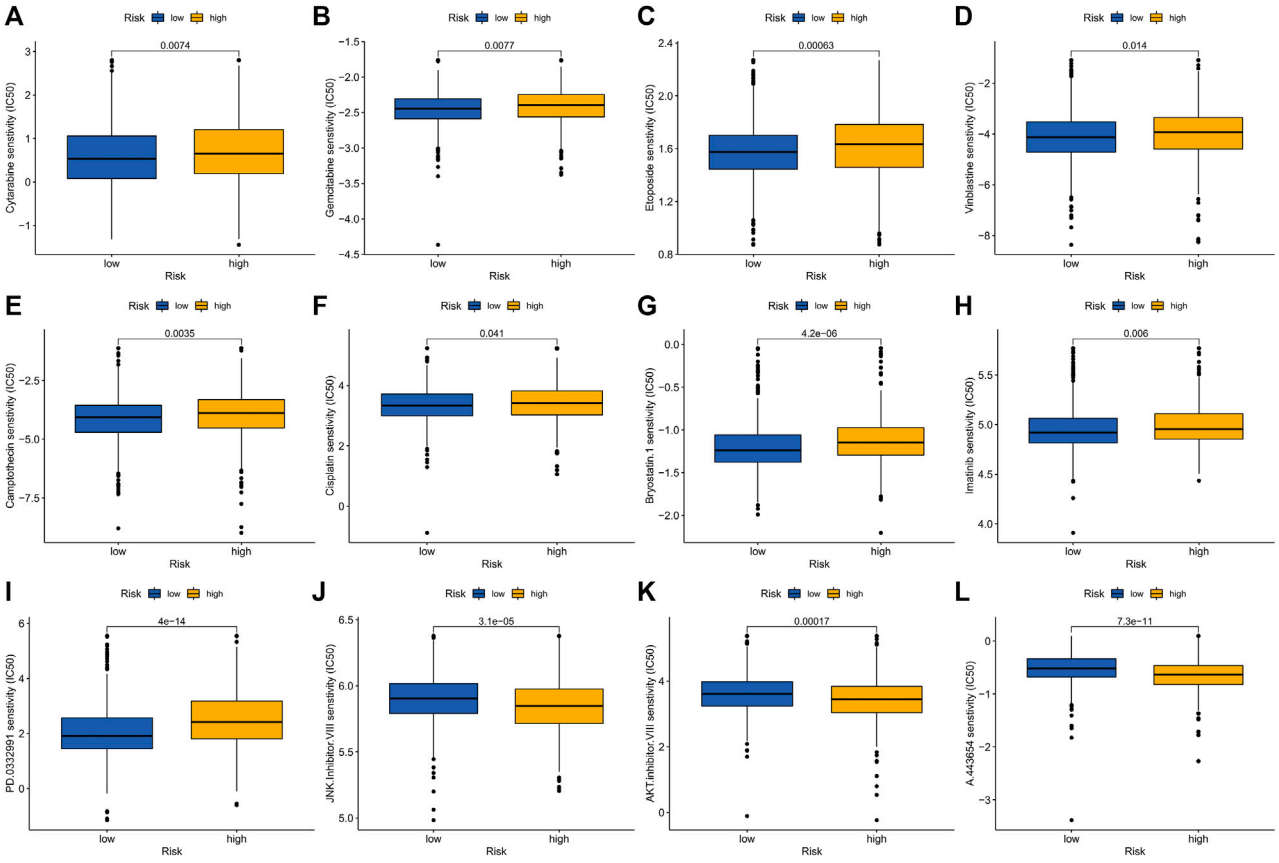

FIGURE 9
Drug sensitivity in patients in high and low risk groups. **(A)** Cytarabine, **(B)** Gemcitabine, **(C)** Epotoside, **(D)** Vinblastine, **(E)** Camptothecin, **(F)** Cisplatin, **(G)** Bryostatin.1, **(H)** Imatinib, **(I)** PD.0332991 (Palbociclib), **(J)** JNK. inhibitor.VIII, **(K)** AKT. Inhibitor.VII and **(L)** A.443654.

Currently, cuproptosis, a recently discovered cell death mechanism, has been studied in BRCA through the use of bioinformatics approaches (Li Z. et al., 2022; Sha et al., 2022; Zou et al., 2022). However, this study innovatively links cuproptosis and ferroptosis to construct a robust prognostic model for BRCA. In this study, we screened CFRGs obtained from GCTA and GEO databases using WGCNA and X-tile. Next, LASSO was implemented to select the optimal lambda value and five OCFRGs- ANKRD52, HOXC10, KNOP1, SGPP1, and TRIM45 were selected to build the model. These genes may play an important role in the regulation of cuproptosis and ferroptosis, or have a direct impact on the copper and iron metabolism of cells. ANKRD52 is reported to function as a tumor metastasis suppressor in lung adenocarcinoma. In addition to being a member of the PP6 holoenzyme, ANKRD52 inhibits tumor progression through PP6c-mediated dephosphorylation of PAK1 (Lee et al., 2021). ANKRD52 is reported to function as a tumor metastasis suppressor in lung adenocarcinoma. However, t Our study has identified a strong correlation between significantly elevated ANKRD52 expression levels in the BRCA and a poor prognosis. ANKRD52 showed a positive correlation with critical clinical indicators including ER, PR, and HER2, and had a high-risk score in our built model. Furthermore, we found that ANKRD52 expression was inversely correlated with the infiltration of Th1 cells, a subtype of antitumor immune cells.

Previous studies have confirmed that HOXC10 participates in the development and progression of breast cancer and affects the prognosis of breast cancer patients. The overexpression of HOXC10 in breast cancer is related to drug resistance to chemotherapy (Sadik et al., 2016) and a positive correlation between immune cell infiltration and poor prognosis in BRCAs (Zhang et al., 2022). Methylation of the HOXC10 promoter, resulting in transcriptional repression, has been shown to contribute to resistance to endocrine therapy in estrogen receptor-positive breast cancer (Pathiraja et al., 2014) In addition, studies have demonstrated that HOXC10 can promote tumor growth in BRCA by upregulating the level of IL-6 to activate the JAK2/STAT3 signal transduction pathway (Shen et al., 2022). HOXC10 expression is dysregulated in various cancers, acting as a carcinogenic driver associated with poor prognosis (Bao et al., 2014). In this study, highly expressed HOXC10 in breast cancer tissues and cells have been associated with high-risk scores, correlated with lymph node infiltration at the time of tumor detection, and positively associated with the infiltration of antitumor immune cells such as $CD8^+$ T cells, NK cells, and DCs.

Studies have shown that the expression of SGPP1 is low in colorectal cancer and is correlated with tumor proliferation, migration, and invasion. Similarly, low expression of SGPP1 in triple-negative breast cancer strongly correlates with poor prognosis

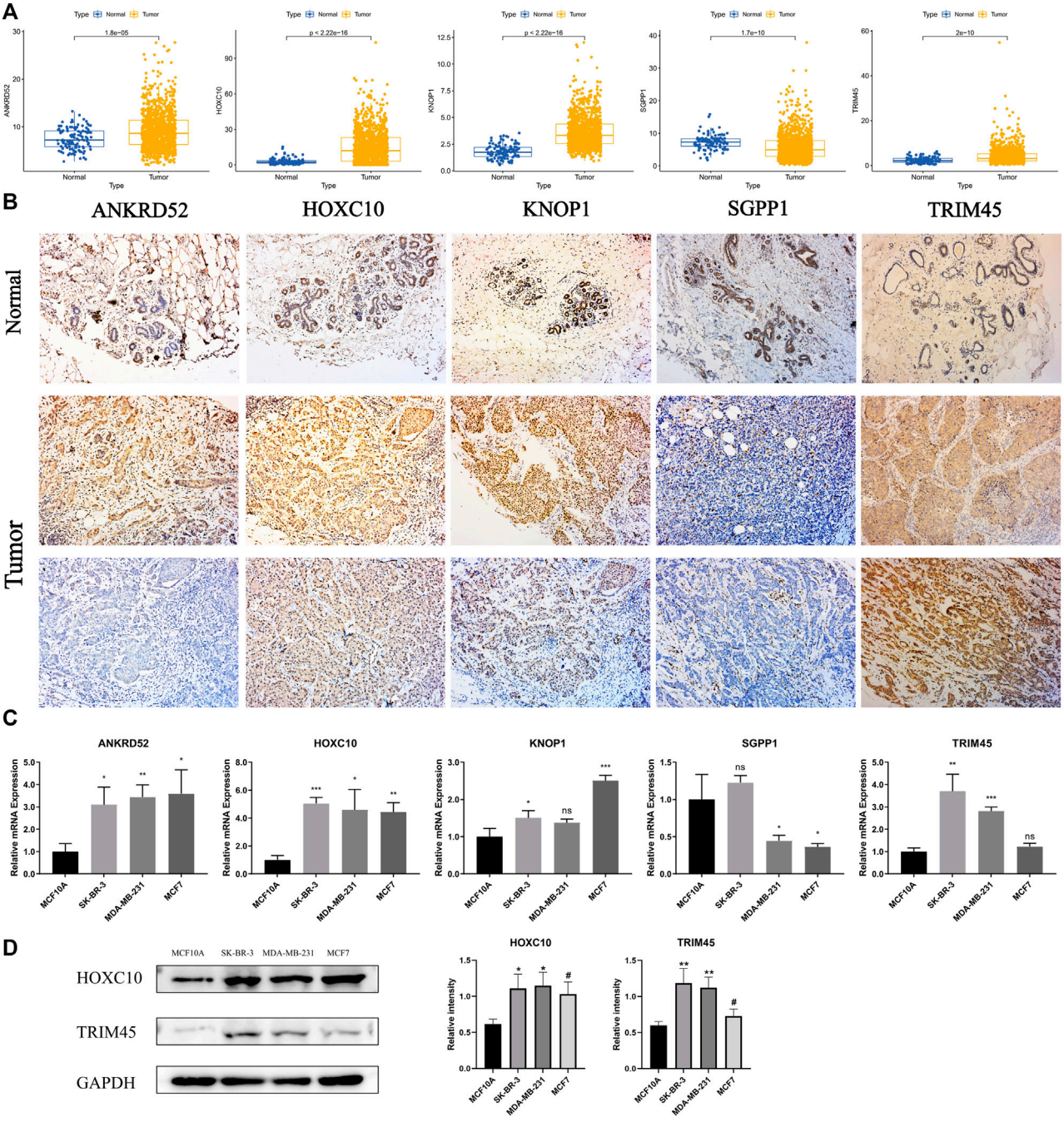

FIGURE 10
THe mRNA and Immunohistochemistry of OCFRGs expression. **(A)** Differences in mRNA levels of OCFRGs between normal and various tumor cells. **(B)** Immunohistochemical staining OCFRGs in BRCA and adjacent tissues. **(C)** Pcr verified the expression levels of OCFRGs in normal and tumor cells. **(D)** Western blotting verified the expression levels of OCFRGs in normal and tumor cells.

(Nema and Kumar, 2021). In addition, our study found that SGPP1 expression in breast cancer was associated with neutrophils, macrophages, $CD4^+$ and $CD8^+$ cells. Likewise, TRIM45 also acts as a tumor suppressor in brain tumors (Zhang et al., 2017) and non-small cell lung cancer (Peng et al., 2020). In this study, we found that the expression of TRIM45 in tumor tissues is higher than that in normal tissues, which correlated with a better prognosis. Furthermore, TRIM45 was highly positively correlated with clinical indicators ER and PR in breast cancer. However, research on KNOP1 in tumors is inadequate; therefore, more in-depth studies need to be conducted.

Single-cell RNA sequencing (scRNA-seq) analysis indicated that fibroblasts have high expression levels of HOXC10, KNOP1, and SGPP1. Cancer-associated fibroblasts (CAFs) are a significant constituent of the tumor microenvironment (TME) and have heterogeneous functions in cancer. Recent studies have demonstrated that targeted CAF therapy, combined with

immunotherapy or chemotherapy, produces optimal therapeutic outcomes. For instance, the elevated expression of HOXC10, KNOP1, and SGPP1 in BRCA indicates that targeted CAF therapy, along with other treatments, might be more effective.

In this study, we developed a LASSO Cox model using the previously mentioned five OCFRGs, which successfully distinguished breast cancer patients into high-risk and low-risk groups. The model's effectiveness was validated in three additional datasets, CGA Cohort, SE20685, and GSE58812, and its diagnostic efficiency was confirmed with a ROC curve analysis. Additionally, the model showed remarkable predictive utility for patient prognosis as a nomogram. Immune checkpoints and TMB are reliable immunotherapy markers. Our investigation of immune checkpoints and TMB in high- and low-risk groups revealed that the expression levels of immune checkpoints, including VTCN1, CD200R1, TNFRSF14, NRP1, TNFRSF4, CD40, CD200, CD44, TNFRSF25, CD48, and CD40LG, decreased in the BRCA high-risk group. Moreover, the risk score and TMB were positively correlated, with TIDE being lower in the high-risk group compared to the low-risk group. As such, the use of immune checkpoint inhibitors (ICIs) may enhance efficacy in high-risk BRCA. Previous research has demonstrated that ferritin therapy modifies tumor immunity (Wang et al., 2019), leading to immune cells within the tumor microenvironment (TME) to initiate lipid peroxidation and undergo ferroptosis, which can influence their function and survival. (Zuo et al., 2021). The use of ferroptosis inducers is a promising approach to augment the effectiveness of immune checkpoint inhibitor (ICI) therapy (Gao et al., 2022). In this study, the TIMER database was utilized to quantify immune cell infiltration in BRCA patients within the TCGA cohort. Our results indicated that Th1 and Th2 cells were higher within the high-risk group, whereas $CD4^+$ T cells, $CD8^+$ T cells, B cells, endothelial cells, and macrophages were lower.

Functional analysis revealed that genes within the high-risk group were primarily enriched in glycolysis, gluconeogenesis, the pentose phosphate pathway, and the cell cycle, whereas the MAPK signaling pathway was inhibited. Of these metabolic processes, glycolysis and gluconeogenesis are potential targets for cancer treatment. Additionally, the pentose phosphate pathway, which is a branch of glycolysis, plays a critical role in combating oxidative stress and assisting glycolytic cancer cells meet anabolic demands (Bao et al., 2014). The cell cycle is related to tumor cell proliferation, and heightened cell cycle activity in tumor cells inhibits antitumor activity. (Evan and Vousden, 2001). Moreover, the risk score was positively associated with mTOR, Hif-1, and ErbB pathways, among others, and negatively correlated with MAPK, PI3K/AKT, TGF-β, and Ras signaling pathways, among others. These results can aid in the investigation of the link between BRCA patients and signaling pathways within high- and low-risk groups. Some studies indicate that ferroptosis and cupperptosis may be targeted to treat tumors (Wang et al., 2021; Oliveri, 2022). Moreover, the risk score was positively associated with mTOR, Hif-1, and ErbB pathways, among others, and negatively correlated with MAPK, PI3K/AKT, TGF-β, and Ras signaling pathways, among others. These results can aid in the investigation of the link between BRCA patients and signaling pathways within high- and low-risk groups. Some studies indicate that ferroptosis and cupperptosis may be targeted to treat tumors.

In summary, we have systematically examined and discussed the molecular changes, intracellular pathways, and immune cell infiltration characteristics associated with cupperptosis and ferroptosis in breast cancer (BRCA) in our study. After utilizing bioinformatics techniques, we selected five OCFRGs (ANKRD52, HOXC10, KNOP1, SGPP1, and TRIM45), verified their differential expression in tumor and non-tumor biological tissue samples at both the cellular and tissue level, and then analyzed their relationship with tumor staging, cellular infiltration, and clinical indicators. The prognostic model we developed was able to reliably predict patient prognosis. Cell pathways closely related to ferroptosis and cupperptosis, such as glycolysis, gluconeogenesis, and the pentose phosphate pathway, were distinguished by the model as high-risk groups. The scoring model may offer guidance for clinical decision-making and precision treatment for BRCA patients.

Conclusion

In conclusion, in this study we combined machine learning and bioinformatics methods to establish a prognostic model for 5 OCFRGs in BRCA. Based on this model, the prognosis in BRCA patients can be accurately predicted. In addition, the degree of immune infiltration and immune resistance in patients were also predicted. Our model guides clinicians in choosing the optimal treatment strategy to personalize treatment.

Data availability statement

Publicly available datasets were analyzed in this study. This data can be found here: TCGA-BRCA, GSE20685, GSE42568, GSE58812.

Author contributions

JL and WZ contributed equally to this work. WZ, JL, ZY, CZ, XM, FZ, and YW contributed to developing the idea for this study. WZ, JL, and YW participated in the data analysis for the article; JL, contributed to the data processing; and WZ wrote the manuscript. WZ and CZ collaboratively conducted the laboratory work. The final manuscript was read and approved by all authors.

Funding

National Natural Science Foundation of China (Project No. 82202701) and Natural Science Foundation of Shandong Province (Grant No. ZR202111300384).

Acknowledgments

We are grateful to the researchers who provided the database data; their contributions are great.

Conflict of interest

The authors declare that the research was conducted in the absence of any commercial or financial relationships that could be construed as a potential conflict of interest.

Publisher's note

All claims expressed in this article are solely those of the authors and do not necessarily represent those of their affiliated organizations, or those of the publisher, the editors and the reviewers. Any product that may be evaluated in this article, or claim that may be made by its manufacturer, is not guaranteed or endorsed by the publisher.

Supplementary material

The Supplementary Material for this article can be found online at: https://www.frontiersin.org/articles/10.3389/fphar.2023.1192434/full#supplementary-material

References

Bao, Y., Chen, Z., Guo, Y., Feng, Y., Li, Z., Han, W., et al. (2014). Tumor suppressor microRNA-27a in colorectal carcinogenesis and progression by targeting SGPP1 and Smad2. *PLoS One* 9 (8), e105991. doi:10.1371/journal.pone.0105991

Dixon, S. J., Lemberg, K. M., Lamprecht, M. R., Skouta, R., Zaitsev, E. M., Gleason, C. E., et al. (2012). Ferroptosis: An iron-dependent form of nonapoptotic cell death. *Cell* 149 (5), 1060–1072. doi:10.1016/j.cell.2012.03.042

Dumas, A., Vaz Luis, I., Bovagnet, T., El Mouhebb, M., Di Meglio, A., Pinto, S., et al. (2020). Impact of breast cancer treatment on employment: Results of a multicenter prospective cohort study (CANTO). *J. Clin. Oncol.* 38 (7), 734–743. doi:10.1200/JCO.19.01726

Evan, G. I., and Vousden, K. H. (2001). Proliferation, cell cycle and apoptosis in cancer. *Nature* 411 (6835), 342–348. doi:10.1038/35077213

Fang, K., Du, S., Shen, D., Xiong, Z., Jiang, K., Liang, D., et al. (2022). SUFU suppresses ferroptosis sensitivity in breast cancer cells via Hippo/YAP pathway. *iScience* 25 (7), 104618. doi:10.1016/j.isci.2022.104618

Gao, M., Yi, J., Zhu, J., Minikes, A. M., Monian, P., Thompson, C. B., et al. (2019). Role of mitochondria in ferroptosis. *Mol. Cell* 73 (2), 354–363.e3. doi:10.1016/j.molcel.2018.10.042

Gao, W., Wang, X., Zhou, Y., Wang, X., and Yu, Y. (2022). Autophagy, ferroptosis, pyroptosis, and necroptosis in tumor immunotherapy. *Signal Transduct. Target Ther.* 7 (1), 196. doi:10.1038/s41392-022-01046-3

Giaquinto, A. N., Sung, H., Miller, K. D., Kramer, J. L., Newman, L. A., Minihan, A., et al. (2022). Breast cancer statistics, 2022. *CA Cancer J. Clin.* 72 (6), 524–541. doi:10.3322/caac.21754

Jakaria, M., Belaidi, A. A., Bush, A. I., and Ayton, S. (2021). Ferroptosis as a mechanism of neurodegeneration in Alzheimer's disease. *J. Neurochem.* 159 (5), 804–825. doi:10.1111/jnc.15519

Lee, T-F., Liu, Y-P., Lin, Y-F., Hsu, C-F., Lin, H., Chang, W-C., et al. (2021). TAZ negatively regulates the novel tumor suppressor ANKRD52 and promotes PAK1 dephosphorylation in lung adenocarcinomas. *Biochim. Biophys. Acta Mol. Cell Res.* 1868 (2), 118891. doi:10.1016/j.bbamcr.2020.118891

Lei, S., Zheng, R., Zhang, S., Wang, S., Chen, R., Sun, K., et al. (2021). Global patterns of breast cancer incidence and mortality: A population-based cancer registry data analysis from 2000 to 2020. *Cancer Commun. (Lond)* 41 (11), 1183–1194. doi:10.1002/cac2.12207

Li, S-R., Bu, L-L., and Cai, L. (2022a). Cuproptosis: Lipoylated TCA cycle proteins-mediated novel cell death pathway. *Signal Transduct. Target Ther.* 7 (1), 158. doi:10.1038/s41392-022-01014-x

Li, Z., Zhang, H., Wang, X., Wang, Q., Xue, J., Shi, Y., et al. (2022b). Identification of cuproptosis-related subtypes, characterization of tumor microenvironment infiltration, and development of a prognosis model in breast cancer. *Front. Immunol.* 13, 996836. doi:10.3389/fimmu.2022.996836

Mou, Y., Wang, J., Wu, J., He, D., Zhang, C., Duan, C., et al. (2019). Ferroptosis, a new form of cell death: Opportunities and challenges in cancer. *J. Hematol. Oncol.* 12 (1), 34. doi:10.1186/s13045-019-0720-y

Nema, R., and Kumar, A. (2021). Sphingosine-1-Phosphate catabolizing enzymes predict better prognosis in triple-negative breast cancer patients and correlates with tumor-infiltrating immune cells. *Front. Mol. Biosci.* 8, 697922. doi:10.3389/fmolb.2021.697922

Oliveri, V. (2022). Selective targeting of cancer cells by copper ionophores: An overview. *Front. Mol. Biosci.* 9, 841814. doi:10.3389/fmolb.2022.841814

Pathiraja, T. N., Nayak, S. R., Xi, Y., Jiang, S., Garee, J. P., Edwards, D. P., et al. (2014). Epigenetic reprogramming of HOXC10 in endocrine-resistant breast cancer. *Sci. Transl. Med.* 6 (229), 229ra41. doi:10.1126/scitranslmed.3008326

Peng, X., Wen, Y., Zha, L., Zhuang, J., Lin, L., Li, X., et al. (2020). TRIM45 suppresses the development of non-small cell lung cancer. *Curr. Mol. Med.* 20 (4), 299–306. doi:10.2174/1566524019666191017143833

Ren, X., Li, Y., Zhou, Y., Hu, W., Yang, C., Jing, Q., et al. (2021). Overcoming the compensatory elevation of NRF2 renders hepatocellular carcinoma cells more vulnerable to disulfiram/copper-induced ferroptosis. *Redox Biol.* 46, 102122. doi:10.1016/j.redox.2021.102122

Sadik, H., Korangath, P., Nguyen, N. K., Gyorffy, B., Kumar, R., Hedayati, M., et al. (2016). HOXC10 expression supports the development of chemotherapy resistance by fine tuning DNA repair in breast cancer cells. *Cancer Res.* 76 (15), 4443–4456. doi:10.1158/0008-5472.CAN-16-0774

Selvaraj, A., Balamurugan, K., Yepiskoposyan, H., Zhou, H., Egli, D., Georgiev, O., et al. (2005). Metal-responsive transcription factor (MTF-1) handles both extremes, copper load and copper starvation, by activating different genes. *Genes Dev.* 19 (8), 891–896. doi:10.1101/gad.1301805

Sha, S., Si, L., Wu, X., Chen, Y., Xiong, H., Xu, Y., et al. (2022). Prognostic analysis of cuproptosis-related gene in triple-negative breast cancer. *Front. Immunol.* 13, 922780. doi:10.3389/fimmu.2022.922780

Shen, J., Wang, M., Li, F., Yan, H., and Zhou, J. (2022). Homeodomain-containing gene 10 contributed to breast cancer malignant behaviors by activating Interleukin-6/Janus kinase 2/Signal transducer and activator of transcription 3 pathway. *Bioengineered* 13 (1), 1335–1345. doi:10.1080/21655979.2021.2016088

Singh, D. D., Verma, R., Tripathi, S. K., Sahu, R., Trivedi, P., and Yadav, D. K. (2021). Breast cancer transcriptional regulatory network reprogramming by using the CRISPR/Cas9 system: An oncogenetics perspective. *Curr. Top. Med. Chem.* 21 (31), 2800–2813. doi:10.2174/1568026621666210902120754

Tang, D., Chen, X., and Kroemer, G. (2022). Cuproptosis: A copper-triggered modality of mitochondrial cell death. *Cell Res.* 32 (5), 417–418. doi:10.1038/s41422-022-00653-7

Tao, X., Wan, X., Wu, D., Song, E., and Song, Y. (2021). A tandem activation of NLRP3 inflammasome induced by copper oxide nanoparticles and dissolved copper ion in J774A.1 macrophage. *J. Hazard Mater* 411, 125134. doi:10.1016/j.jhazmat.2021.125134

Tsvetkov, P., Coy, S., Petrova, B., Dreishpoon, M., Verma, A., Abdusamad, M., et al. (2022). Copper induces cell death by targeting lipoylated TCA cycle proteins. *Science* 375 (6586), 1254–1261. doi:10.1126/science.abf0529

Wang, H., Cheng, Y., Mao, C., Liu, S., Xiao, D., Huang, J., et al. (2021). Emerging mechanisms and targeted therapy of ferroptosis in cancer. *Mol. Ther.* 29 (7), 2185–2208. doi:10.1016/j.ymthe.2021.03.022

Wang, S., Wei, W., Ma, N., Qu, Y., and Liu, Q. (2022). Molecular mechanisms of ferroptosis and its role in prostate cancer therapy. *Crit. Rev. Oncol. Hematol.* 176, 103732. doi:10.1016/j.critrevonc.2022.103732

Wang, W., Liu, Z., Zhou, X., Guo, Z., Zhang, J., Zhu, P., et al. (2019). Ferritin nanoparticle-based SpyTag/SpyCatcher-enabled click vaccine for tumor immunotherapy. *Nanomedicine* 16, 69–78. doi:10.1016/j.nano.2018.11.009

Xu, H., Ye, D., Ren, M., Zhang, H., and Bi, F. (2021). Ferroptosis in the tumor microenvironment: Perspectives for immunotherapy. *Trends Mol. Med.* 27 (9), 856–867. doi:10.1016/j.molmed.2021.06.014

Yan, H-F., Tuo, Q-Z., Yin, Q-Z., and Lei, P. (2020). The pathological role of ferroptosis in ischemia/reperfusion-related injury. *Zool. Res.* 41 (3), 220–230. doi:10.24272/j.issn.2095-8137.2020.042

Yang, J., Zhou, Y., Li, Y., Hu, W., Yuan, C., Chen, S., et al. (2022). Functional deficiency of succinate dehydrogenase promotes tumorigenesis and development of clear cell renal cell carcinoma through weakening of ferroptosis. *Bioengineered* 13 (4), 11187–11207. doi:10.1080/21655979.2022.2062537

Yeo, S. K., and Guan, J. L. (2017). Breast cancer: Multiple subtypes within a tumor? *Trends Cancer* 3 (11), 753–760. doi:10.1016/j.trecan.2017.09.001

Zhang, J., Zhang, C., Cui, J., Ou, J., Han, J., Qin, Y., et al. (2017). TRIM45 functions as a tumor suppressor in the brain via its E3 ligase activity by stabilizing p53 through K63-linked ubiquitination. *Cell Death Dis.* 8 (5), e2831. doi:10.1038/cddis.2017.149

Zhang, X., Zheng, Y., Liu, X., Wang, K., Zhao, H., Yin, Y., et al. (2022). The expression of *HOXC10* is correlated with tumor-infiltrating immune cells in basal-like breast cancer and serves as a prognostic biomarker. *Ann. Transl. Med.* 10 (2), 81. doi:10.21037/atm-21-6611

Zou, Y., Xie, J., Zheng, S., Liu, W., Tang, Y., Tian, W., et al. (2022). Leveraging diverse cell-death patterns to predict the prognosis and drug sensitivity of triple-negative breast cancer patients after surgery. *Int. J. Surg.* 107, 106936. doi:10.1016/j.ijsu.2022.106936

Zuo, T., Fang, T., Zhang, J., Yang, J., Xu, R., Wang, Z., et al. (2021). pH-sensitive molecular-switch-containing polymer nanoparticle for breast cancer therapy with ferritinophagy-cascade ferroptosis and tumor immune activation. *Adv. Healthc. Mater* 10 (21), e2100683. doi:10.1002/adhm.202100683

frontiers | Frontiers in Pharmacology

TYPE Original Research
PUBLISHED 19 July 2023
DOI 10.3389/fphar.2023.1217213

OPEN ACCESS

EDITED BY
Lin Qi,
Central South University, China

REVIEWED BY
Sufang Zhou,
Guangxi Medical University, China
Jingwei Zhang,
Wuhan University, China

*CORRESPONDENCE
Diang Chen,
cdacscscs@qq.com

†These authors share first authorship

RECEIVED 05 May 2023
ACCEPTED 30 June 2023
PUBLISHED 19 July 2023

CITATION
Li H, Xu H, Guo H, Du K and Chen D (2023), Integrative analysis illustrates the role of PCDH7 in lung cancer development, cisplatin resistance, and immunotherapy resistance: an underlying target.
Front. Pharmacol. 14:1217213.
doi: 10.3389/fphar.2023.1217213

Integrative analysis illustrates the role of PCDH7 in lung cancer development, cisplatin resistance, and immunotherapy resistance: an underlying target

Huakang Li†, Haoran Xu†, Hong Guo†, Kangming Du and Diang Chen*

Hospital of Chengdu University of Traditional Chinese Medicine, Chengdu, Sichuan, China

Background: Cisplatin resistance is a common clinical problem in lung cancer. However, the underlying mechanisms have not yet been fully elucidated, highlighting the importance of searching for biological targets.

Methods: Bioinformatics analysis is completed through downloaded public data (GSE21656, GSE108214, and TCGA) and specific R packages. The evaluation of cell proliferation ability is completed through CCK8 assay, colony formation, and EdU assay. The evaluation of cell invasion and migration ability is completed through transwell and wound-healing assays. In addition, we evaluated cell cisplatin sensitivity by calculating IC_{50}.

Results: Here, we found that PCDH7 may be involved in cisplatin resistance in lung cancer through public database analysis (GSE21656 and GSE108214). Then, a series of *in vitro* experiments was performed, which verified the cancer-promoting role of PCDH7 in NSCLC. Moreover, the results of IC_{50} detection showed that PCDH7 might be associated with cisplatin resistance of NSCLC. Next, we investigated the single-cell pattern, biological function, and immune analysis of PCDH7. Importantly, we noticed PCDH7 may regulate epithelial–mesenchymal transition activity, and the local infiltration of $CD8^+$ T and activated NK cells. Furthermore, we noticed that patients with high PCDH7 expression might be more sensitive to bortezomib, docetaxel, and gemcitabine, and resistant to immunotherapy. Finally, a prognosis model based on three PCDH7-derived genes (*GPX8*, *BCAR3*, and *TNS4*) was constructed through a machine learning algorithm, which has good prediction ability on NSCLC patients' survival.

Conclusion: Our research has improved the regulatory framework for cisplatin resistance in NSCLC and can provide direction for subsequent related research, especially regarding PCDH7.

KEYWORDS

lung cancer, cisplatin resistance, PCDH7, immunotherapy, target

Introduction

Lung cancer is a malignant tumor originating from the lung epithelium and is widely distributed worldwide (Nasim et al., 2019). The onset of lung cancer is extremely complex and is the result of a combination of multiple factors (Mao et al., 2016). From a pathological perspective, lung cancer can be divided into different subtypes, with non-small-cell lung cancer (NSCLC) being the most prominent (Herbst et al., 2018). Surgical intervention remains the first choice for lung cancer, but with the progress of related surgeries, the 5-year survival rate of lung cancer remains poor (Pallis and Syrigos, 2013). The advent of tyrosine kinase inhibitors (TKIs) targeting epidermal growth factor receptor (EGFR) mutations and anaplastic lymphoma kinase (ALK) rearrangements has considerably improved patient survival and the quality of life. Moreover, therapies targeting other genomic alterations, such as ROS1 rearrangements and BRAF, MET, and RET mutations, have emerged (Goldstraw et al., 2016). However, despite these advances, challenges persist. Resistance to first-line TKIs commonly develops, leading to disease progression. Novel strategies like combination therapies and next-generation TKIs are being explored to overcome resistance (Camidge et al., 2012). On one hand, the early symptoms of lung cancer are relatively hidden, and some patients have already lost the opportunity for surgery at the initial diagnosis (Nooreldeen and Bach, 2021). On the other hand, lung cancer has a unique biological specificity, which makes finding specific targets from the perspective of molecular biology helpful for clinical transformation.

Cisplatin is a first-line drug for the treatment of many solid tumors, and it is a heavy metal complex that can inhibit the process of DNA replication (Dasari and Tchounwou, 2014; Ghosh, 2019). Cisplatin combined with specific chemotherapy drugs has achieved a certain efficacy in lung cancer, but it is still limited by multiple adverse reactions and acquired drug resistance (Kryczka et al., 2021). Based on this finding, some researchers have begun to explore the molecular biological mechanisms that affect cisplatin resistance (Galluzzi et al., 2012). Lin et al. noticed that autophagy is involved in cisplatin resistance in pharyngeal squamous cell carcinoma, and this process is induced by RAB3B in extrachromosomal circular DNA (Lin et al., 2022). In addition, researchers found that CAMK2G phosphorylated ITPKB by ROS in ovarian cancer, leading to resistance to cisplatin (Li et al., 2022). Ni et al. discovered that the combination of shikonin and cisplatin promotes ferroptosis by upregulating HMOX1, further overcoming cisplatin resistance in ovarian cancer (Ni et al., 2023). In lung cancer, Xiao et al. demonstrated that RAP1 can activate NF-κB signaling and mediate cisplatin resistance of NSCLC (Xiao et al., 2017). Interestingly, Ray et al. revealed that nicotine may affect cisplatin resistance in lung cancer, indicating the importance of lifestyle interventions for patients (Ray et al., 2022). Wu et al. found that the exosome miR-193a can lead to cisplatin resistance of NSCLC by targeting LRRC1 (Wu et al., 2020). Consequently, exploring the factors and potential targets that affect cisplatin resistance from a molecular biology perspective is of great significance.

As sequencing technology developed, massive second-generation sequencing data have been generated and are publicly available, providing great convenience for researchers (Ren et al., 2020; Zhang et al., 2021a; Zhang et al., 2021b; Zhang et al., 2022). Here, we found that PCDH7 may be involved in cisplatin resistance in lung cancer through public database analysis (GSE21656 and GSE108214). Then, a series of *in vitro* experiments was performed, which verified the cancer-promoting role of PCDH7 in NSCLC. Moreover, the results of IC_{50} detection showed that PCDH7 might be associated with cisplatin resistance of NSCLC. Next, we investigated the single-cell pattern, biological function, and immune analysis of PCDH7. Moreover, we noticed that high PCDH7 expression might be more sensitive to bortezomib, docetaxel, and gemcitabine. Finally, a prognosis model based on three PCDH7-derived genes was constructed (*GPX8*, *BCAR3*, and *TNS4*), which has a good prediction ability on NSCLC patients' survival.

Methods

Collection of public data

For The Cancer Genome Atlas (TCGA) database, we downloaded the original transcriptome data from TCGA–GDC (TCGA–LUAD and –LUSC projects; STAR-Counts form). Before conducting the analysis, we merged and organized the downloaded raw transcriptional data into an expression matrix. A human genome reference document is used for ENSG number annotation. Meanwhile, we performed mean taking on duplicate genes, and genes with an average expression of less than 0.05 were deleted. The clinical formation was also obtained from the TCGA–GDC (bcr-xml form). For the Gene Expression Omnibus database, the data from GSE21656 and GSE108214 were selected, which provided the next-sequence data from cisplatin-resistant and wild-type lung cancer cells (Sun et al., 2012; Sarin et al., 2018). The probe annotation of GSE21656 was conducted using GPL6244, and GSE108214, using GPL17077. The baseline information on HNSCC patients from TCGA database is shown in Table 1.

Bioinformatics analysis

The limma package was applied for differentially expressed gene (DEG) analysis with specific thresholds (Ritchie et al., 2015). By integrating patient expression profiles and prognostic data, univariate Cox regression analysis was utilized to identify the genes remarkably correlated with patient survival with a $p < 0.05$. Pathway enrichment was explored using the gene set enrichment analysis (GSEA) algorithm (Subramanian et al., 2005). The Gene Ontology (GO), Hallmark, and Kyoto Encyclopedia of Genes and Genomes (KEGG) gene sets were selected as the reference set. The immune microenvironment was quantified using the CIBERSORT algorithm based on the input expression matrix (Chen et al., 2018). Quantification of immune function was completed using the single-sample GSEA (ssGSEA) algorithm (Hänzelmann et al., 2013). Quantification of the stromal score, immune score, and estimate score was conducted using the ESTIMATE package (Yu et al., 2021a). The response of patients to immunotherapy was quantified using the Tumor Immune Dysfunction and Exclusion (TIDE) algorithm (Fu et al., 2020). The TIDE algorithm gives each patient a TIDE score. Lung cancer patients with TIDE scores more than zero were defined as responders to immunotherapy, and those

TABLE 1 Baseline information on the enrolled patients.

Clinical feature		Number of patients	Percentage (%)
Age	<=65	431	42.0
	>65	567	55.3
	Unknown	28	2.7
Gender	Female	411	40.1
	Male	615	59.9
Stage	Stage I	524	51.1
	Stage II	287	28.0
	Stage III	170	16.6
	Stage IV	33	3.2
	Unknown	12	1.2
T-stage	T1	286	27.9
	T2	576	56.1
	T3	118	11.5
	T4	43	41.9
	Unknown	3	0.3
M-stage	M0	767	74.8
	M1	32	3.1
	Unknown	227	22.1
N-stage	N0	655	63.8
	N1	231	22.5
	N2	115	11.2
	N3	7	0.7
	Unknown	18	1.8

with scores less than zero were the opposite. Quantification of patients on target drugs was realized using the Genomics of Drug Sensitivity in Cancer (GDSC) database (Yang et al., 2013). The machine learning algorithm LASSO regression was utilized to reduce the data dimension (McEligot et al., 2020). The prognosis prediction model was identified using the multivariate Cox regression analysis. For a better clinical application, a nomogram that merges the risk score and clinical features was constructed. The prediction value of one certain continuous variable to survival was performed using the receiver operating characteristic (ROC) curve.

Single-cell analysis

Single-cell analysis is directly completed through an online interactive website—the TISCH project (Sun et al., 2021). GSE148071 was conducted by Wu et al. (2021). In this project, they collected 42 NSCLC samples and characterized the entire tumor ecosystem through single-cell RNA sequencing.

Immunohistochemistry (IHC) and subcellular localization

The IHC image of PCDH7 in lung cancer and para-carcinoma tissue was directly downloaded from The Human Protein Atlas (HPA) project (Colwill and Gräslund, 2011). Subcellular localization of PCDH7 in the HPA project was obtained in the HeLa cells.

Cell culture

The used BEAS-2B, A549, H1299, H522, H460 cells, and A549-Res cell lines (A549 cell line that is resistant to cisplatin) were routinely stored in laboratories. The A549-Res (resistant to cisplatin) cell line was purchased from Shanghai MEIXUAN Biological Science and Technology Co, Ltd. All cells are cultured under normal conditions. The cell culture medium used is 1640-RPMI. According to cell growth, subculture was conducted every 3–4 days.

Quantitative real-time (qRT) PCR

First, total RNA was extracted using the TRIzol reagent and then transcribed into cDNA for further analysis (Pan et al., 2020). The PCR system is a 20-μL system, and PCR detection is performed using SYBR Green. The primer sequence is as follows: PCDH7: F, 5′-GACTCTGGGCGTCTCTGAAG-3'; R, 5′-CTCAACTCCGACTCTGCTCA; GAPDH: F, 5′-CTGGGCTACACTGAGCACC-3'; R, 5′-AAGTGGTCGTTGAGGGCAATG-3'.

Cell transfection

The transfection of control and PCDH7 knockdown plasmids was conducted with Lipofectamine 2000 based on standard procedures (Pan et al., 2020). The target sequence is as follows: sh#1: 5′-GGAGGCTTCTAAGCCAAAT-3′, sh#2: 5′-GGACCATTTACTCCACAAT-3′, sh#3: 5′-CCACCGTGGTCCTTAACAT-3'.

Cell proliferation

The proliferation ability of A549 and H1299 cells was evaluated using the CCK8, colony formation, and EdU assays, according to standard procedures (Pan et al., 2020).

Transwell and wound-healing assays

The invasion and migration ability of A549 and H1299 cells were evaluated using the transwell and wound-healing assays, according to standard procedures (Pan et al., 2020).

IC_{50} detection of cisplatin

The detection of cisplatin was performed according to the procedures of Heinze et al. (2021).

In vivo experiments

For tumor inoculation, each nude mouse was subcutaneously injected with 10×10^5 cells. The mice were then monitored for 4 weeks for tumor development. At the end of the experiment, the mice were euthanized, and tumors were excised, weighed, and photographed.

Data statistics

For all the analyses based on public data, R software version 4.0.4 was used. Moreover, SPSS and GraphPad Prism 8 software were also used for data statistics of the experimental data. Generally, the comparison with a p-value <0.05 was regarded as significant. Different testing methods were chosen based on statistical requirements for variables that meet different data distributions.

Results

The brief process of this study is shown in Figure 1. Here, we found that PCDH7 may be involved in cisplatin resistance in lung cancer through public database analysis (GSE21656 and GSE108214). Then, a series of *in vitro* experiments was performed, which verified the cancer-promoting role of PCDH7 in NSCLC. Moreover, the results of IC_{50} detection showed that PCDH7 might be associated with cisplatin resistance of NSCLC. Next, we investigated the single-cell pattern, biological function, and immune analysis of PCDH7. Moreover, we noticed that patients with high PCDH7 expression might be more sensitive to bortezomib, docetaxel, and gemcitabine but resistant to immunotherapy. Finally, a prognosis model based on three PCDH7-derived genes was constructed (*GPX8*, *BCAR3*, and *TNS4*), which has a good prediction ability on NSCLC patients' survival.

Identification of the genes involved in cisplatin resistance in lung cancer cells

Through careful search, we found two datasets from the GEO database. The GSE21656 provided the transcriptional profile derived from cisplatin-resistant and wild-type H460 lung cancer cells. GSE108214 provided the transcriptional profile derived from cisplatin-resistant and wild-type A549 lung cancer cells. The data preprocessing process is shown in Supplementary Figures S1A, B. The DEG analysis identified 70 upregulated and 106 downregulated genes in cisplatin-resistant cells of the GSE21656 cohort (Figure 2A, H460). For the GSE108214 cohort, 1,430 upregulated and 1,280 downregulated genes were identified in cisplatin-resistant A549 cells (Figure 2B). Through intersection processing, we found that 16 genes showed consistent downregulation in drug-resistant cells in the GSE21656 and GSE108214 cohorts: *NTS*, *TMPRSS15*, *TMEM27*, *MCAM*, *IGFBP3*, *S100A16*, *GALC*, *CDH11*, *DCLK1*, *MYO5C*, *CPVL*, *SEMA5A*, *ANO3*, *AQP3*, *IFITM2*, and *PCDH7*; in total, 11 genes showed consistent upregulation in drug-resistant cells in the GSE21656 and GSE108214 cohorts: *PKIA*, *CDH2*, *CALB2*, *CDK14*, *VAV3*, *KCNK1*, *COL12A1*, *ANO5*, *SNAP25*, *CP*, and *TPM2* (Figure 2C). Then, we compared the expression level of these common genes in NSCLC and para-carcinoma tissue. We noticed most of these genes had a significant difference in the expression level between tumor and normal tissues, revealing their underlying role in cancer development (Figure 2D). The results of univariate Cox regression showed that the genes *PCDH7*, *TPM2*, *S100A16*, *CDH2*, *ANO3*, *CALB2*, *COL12A1*, *PKIA*, and *MCAM* were remarkably correlated with NSCLC patient survival (Figure 2E, *PCDH7*: HR = 1.138; *TPM2*: HR = 1.148; *S100A16*: HR = 1.133; *CDH2*: HR = 1.109; *ANO3*: HR = 1.197; *CALB2*: HR = 1.063; *COL12A1*: HR = 1.065; *PKIA*, HR = 1.085; *MCAM*, HR = 1.115). Among these genes, *PCDH7* has the most significant p-value and was consequently selected for the following analysis. In the TCGA–LUAD cohort (lung adenocarcinoma), patients with high expression of *PCDH7* appear to have a poor prognosis (Figures 2F–H, overall survival, $p = 0.003$; disease-free survival, $p = 0.002$; progression-free survival, $p = 0.003$). However, this effect does not

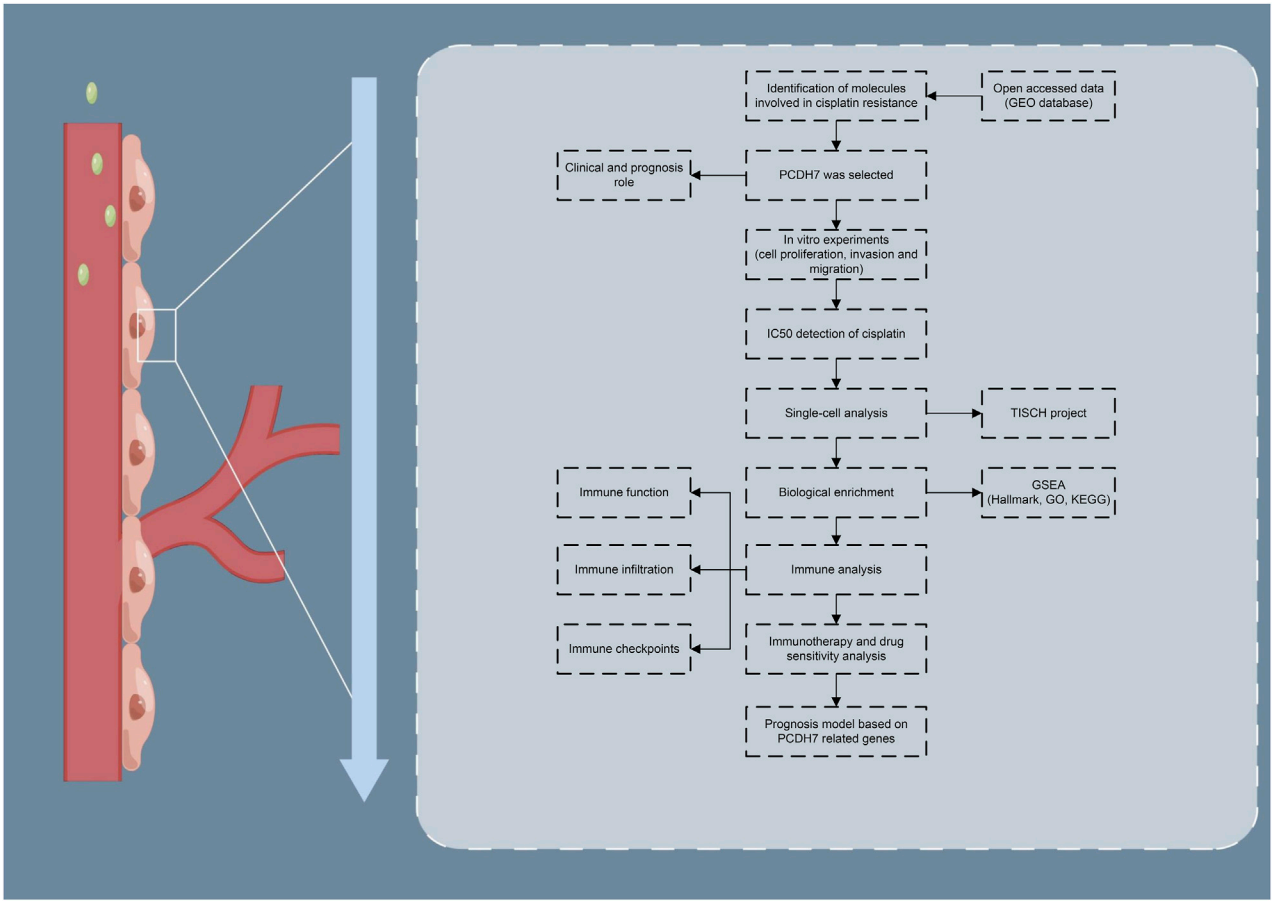

FIGURE 1
Flow chart of the whole study.

seem significant in the TCGA–LUSC cohort (lung squamous cell carcinoma) (Figures 2I, J). Furthermore, an association between PCDH7 and worse clinical features was found in a clinical correlation analysis (Figures 3A–D).

PCDH7 enhances the cell malignant phenotypes and cisplatin resistance of NSCLC cells

Subsequently, we tried to identify the biological role of PCDH7 in NSCLC. The results of qRT-PCR indicated that PCDH7 is overexpressed in lung cancer cells compared to normal lung cells (Supplementary Figure S2A). Moreover, the IHC image from the HPA database indicated a higher PCDH7 protein level in NSCLC than the control tissue (Supplementary Figures S3A, B). The inhibition efficiency of three sh-PCDH7 cells was quantified using qRT-PCR (Supplementary Figures S2B, C). In both A549 and H1299 cells, sh-PCDH7#2 showed the best performance and was consequently selected for further experiments. The transwell assay indicated that knockdown of PCDH7 could hamper the invasion and migration ability of NSCLC cells (Figure 3E). The result of the wound-healing assay obtained the same conclusion (Figure 3F). For cell proliferation, the results of the CCK8 assay indicated that inhibition of PCDH7 could reduce the cell proliferation ability of NSCLC cells (Figures 4A, B). In addition, the number and size of cell colonies in cells with PCDH7 knockdown were smaller than those in control cells (Figure 4C). The EdU assay indicated that inhibition of PCDH7 could remarkably inhibit the DNA replication capability of NSCLC cells (Figures 4D, E). *In vivo* experiments showed that PCDH7 knockdown cells formed a lighter tumor than control cells (Figures 4F, G). Then, we detected the IC_{50} concentration of cisplatin in sh-PCDH7 and control cells. The result indicated that cells with sh-PCDH7 had a lower IC_{50} than control cells, indicating that PCDH7 is associated with cisplatin resistance (Figures 5A, B). Moreover, A549 cells with cisplatin resistance had a higher PCDH7 level (Figure 5C).

Expression pattern and biological function of PCDH7 in NSCLC

Based on the public single-cell data from TISCH projects (Wu et al., 2021), we explored the single-cell expression pattern of PCDH7 in NSCLC. The result showed that PCDH7 was mainly

10.3389/fphar.2023.1217213

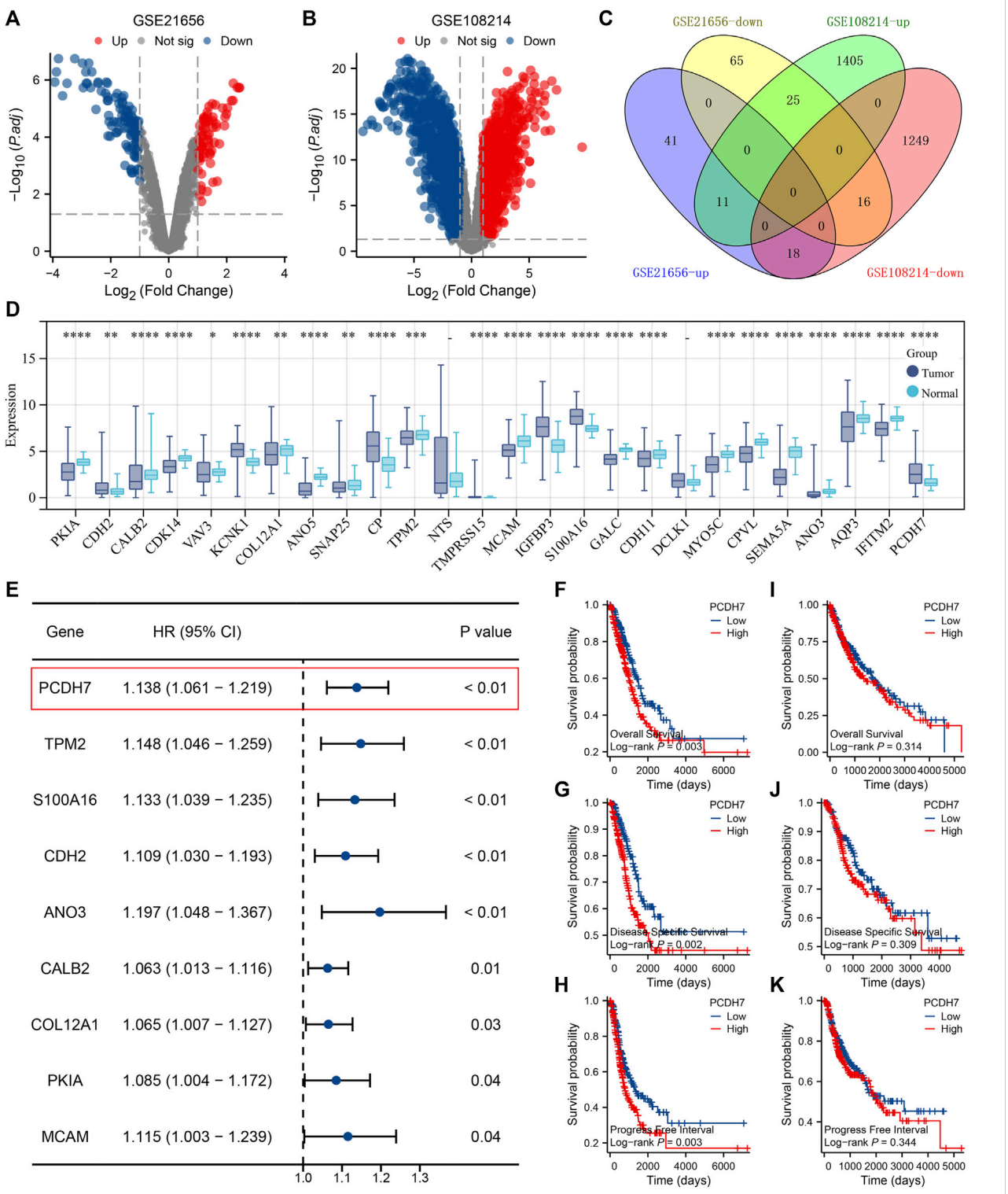

FIGURE 2
Identification of PCDH7 through bioinformatics analysis. Notes: **(A)** DEG analysis between cisplatin-resistant and wild-type cells in GSE21656; **(B)** DEG analysis between cisplatin-resistant and wild-type cells in GSE108214. **(C)** Intersection analysis of the DEGs identified from GSE21656 and GSE108214. **(D)** Expression patterns of intersected genes in NSCLC and para-carcinoma tissues. **(E)** Univariate Cox regression analysis was performed to identify the prognosis-related genes. **(F)** Overall survival difference in patients with high and low PCDH7 expression (TCGA−LUAD). **(G)** Disease-free survival difference in patients with high and low PCDH7 expression levels (TCGA−LUAD). **(H)** Progression-free survival difference in patients with high and low PCDH7 expression levels (TCGA−LUAD). **(I)** Overall survival difference in patients with high and low PCDH7 expression (TCGA−LUSC). **(J)** Disease-free survival difference in patients with high and low PCDH7 expression (TCGA−LUSC). **(K)** Progression-free survival difference in patients with high and low PCDH7 expression (TCGA−LUSC).

10.3389/fphar.2023.1217213

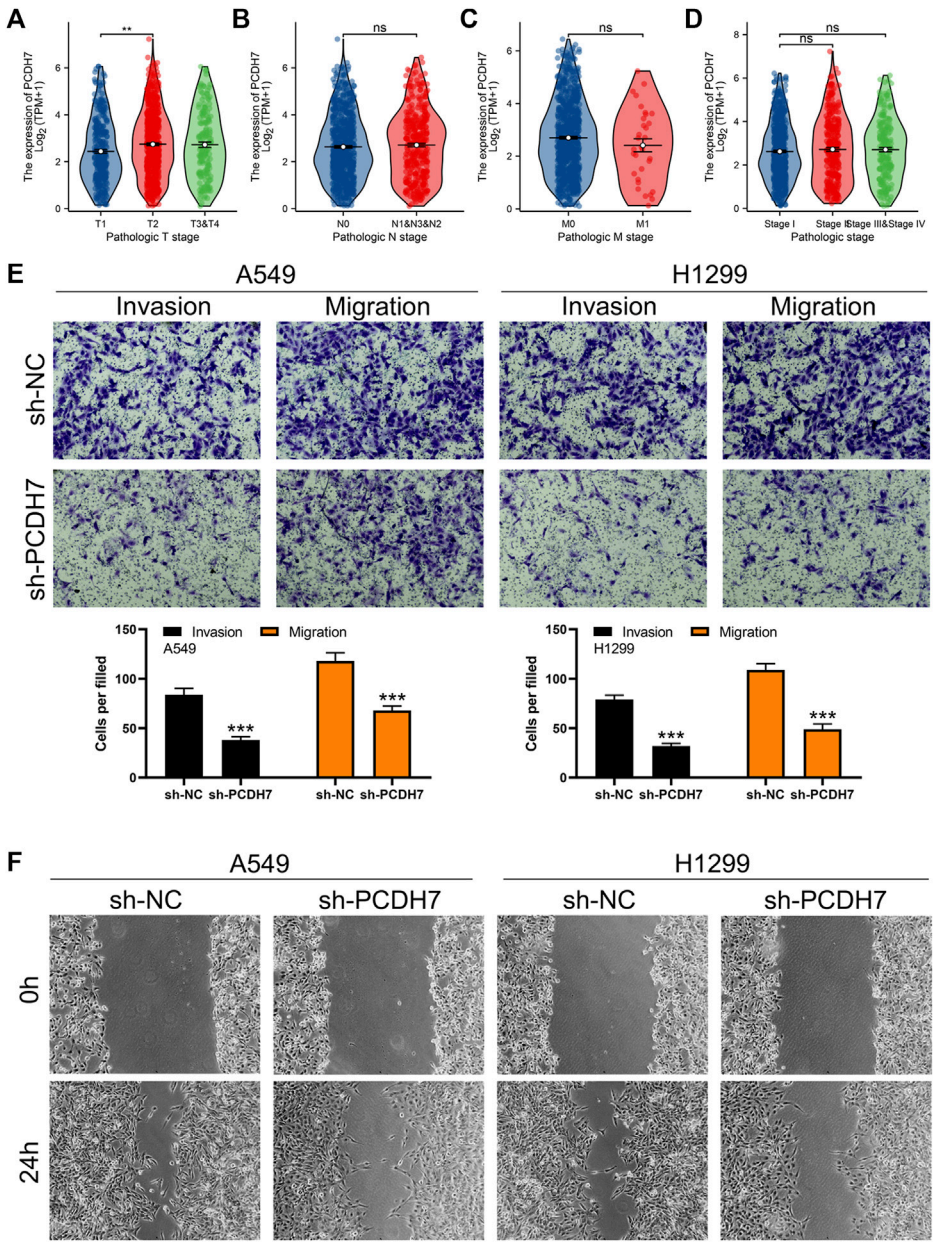

FIGURE 3
PCDH7 promotes the invasion and migration ability of NSCLC. Notes: **(A–D)** expression level of PCDH7 in patients with different clinical features. **(E)** Transwell assay was performed in PCDH7-knockdown and control cells. **(F)** Wound-healing assay was performed in PCDH7-knockdown and control cells.

expressed in malignant cells, fibroblasts, and CD8$^+$ T cells (Figures 5D, E). The GSEA analysis based on the Hallmark set indicated that in the patients with high PCDH7 expression, the top five upregulated terms were epithelial–mesenchymal transition (EMT), apical junction, UV-response, angiogenesis, and TNF-α signaling (Figure 6A). For the GSEA analysis based on the GO set, the top three upregulated terms were all related to the spliceosome-related complex (Figure 6B) and the top three downregulated terms were related to the immunoglobulin complex (Figure 6C). For the GSEA analysis based on the KEGG set, the top three upregulated terms were small-cell lung cancer, focal adhesion, and ECM–receptor interaction, while the top three downregulated terms were ribosome, maturity-onset diabetes of the young, and linolenic acid metabolism (Figures 6D, E). The subcellular localization of PCDH7 in HeLa cells showed that it mainly localized in the plasma membrane (Supplementary Figures S3C, D).

PCDH7 affects the immune microenvironment and therapy response of NSCLC

The heatmap of the level of immune cells quantified by the CIBERSORT algorithm is shown in Figure 7A. Correlation analysis

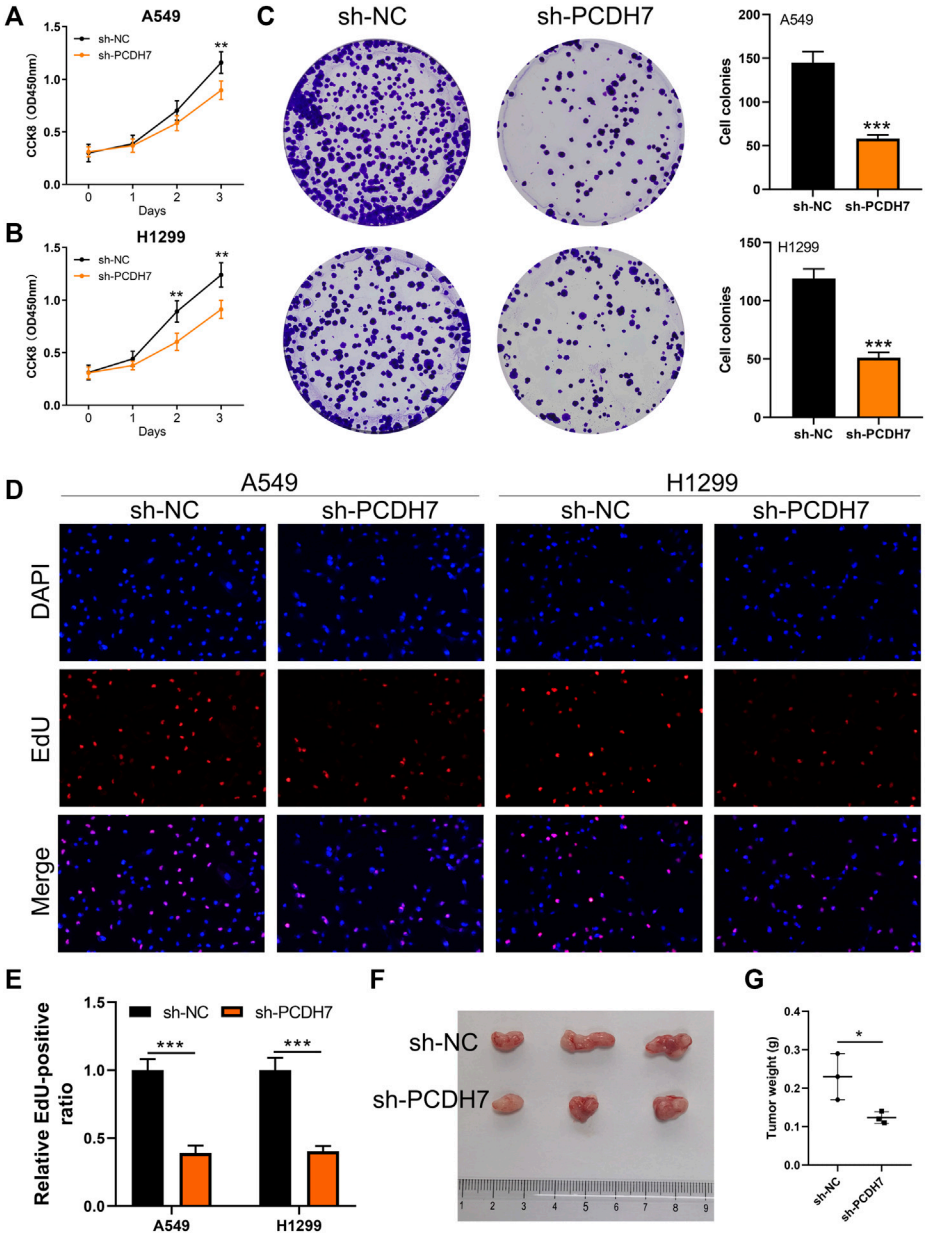

FIGURE 4
PCDH7 promotes the proliferation ability of NSCLC. Notes: **(A, B)** CCK8 assay was performed in PCDH7-knockdown and control cells. **(C)** Colony formation assay was performed in PCDH7-knockdown and control cells. **(D, E)** EdU assay was performed in PCDH7-knockdown and control cells. **(F, G)** Tumor formation experiment in nude mice injected by control and PCDH7-knockdown cells.

indicated that PCDH7 was positively correlated with resting NK cells, M0 macrophages, and neutrophils yet negatively correlated with $CD8^+$ T cells and activated NK cells (Figure 7B). We also noticed a significant difference in several immune-related genes in patients with high and low PCDH7 expression levels (Figure 7C). For the immune function terms quantified by the ssGSEA algorithm, PCDH7 was positively correlated with para-inflammation, CCR, MHC_class_I, and APC_co_inhibition (Figure 7D). Furthermore, we found that PCDH7 was significantly correlated with key immune checkpoints PDCD1LG2 and CD274 (Figures 7E–H). A positive correlation was found between PCDH7 and stromal score, as well as ESTIMATE scores (Figures 8A–C). Moreover, we found that PCDH7 was positively correlated with the TIDE score (Figure 8D, R = 0.330, $p < 0.001$). Correspondingly, 44.6% of patients with low PCDH7 levels tended to respond to immunotherapy, but this percentage reduced to 26.9% in patients with high PCDH7 expression (Figure 8E). Meanwhile, a higher immune exclusion was found in patients with high PCDH7 expression (Figure 8F). The results of drug sensitivity indicated that patients with high PCDH7 expression might be more sensitive to bortezomib, docetaxel, and gemcitabine (Figure 8G).

10.3389/fphar.2023.1217213

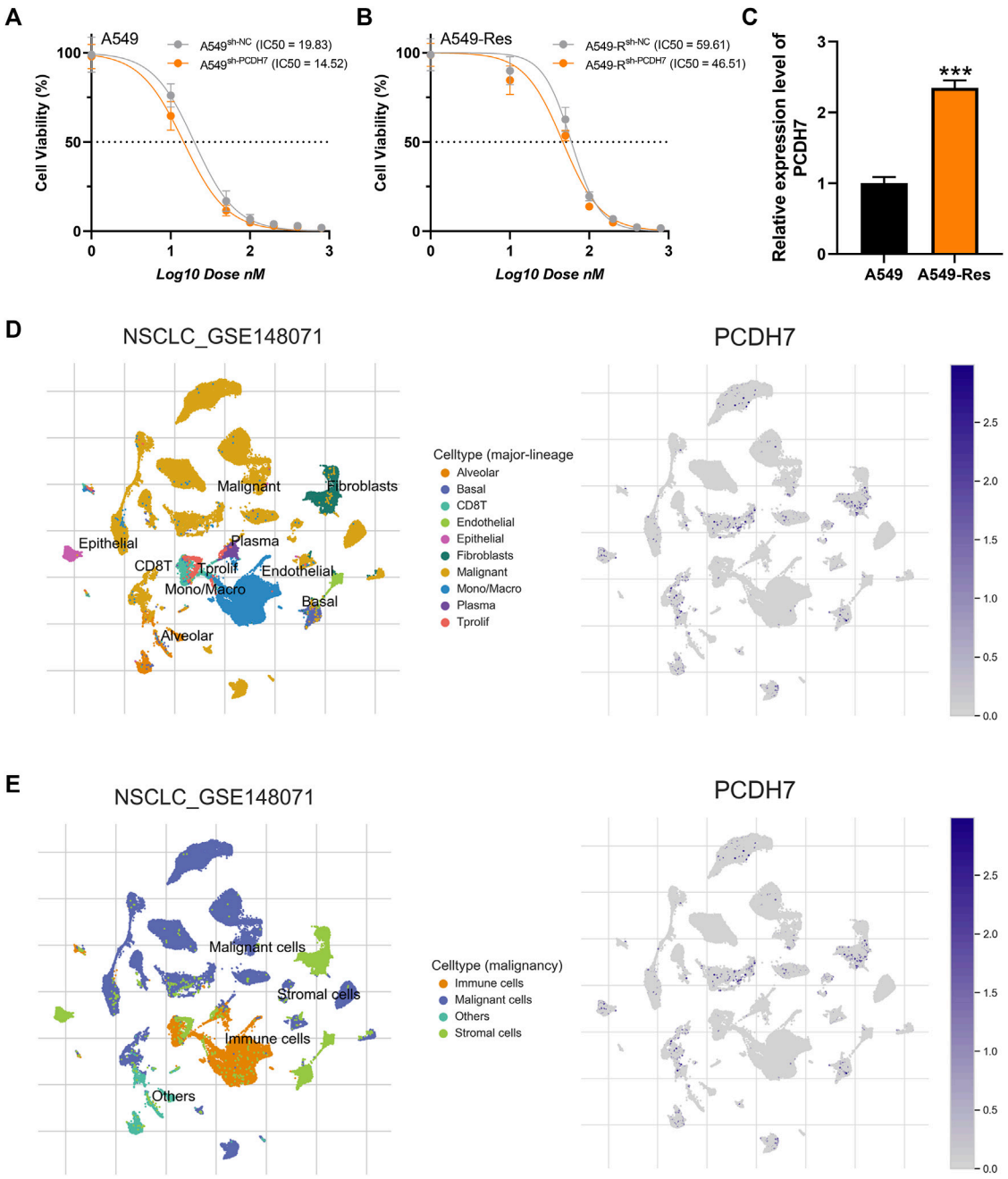

FIGURE 5
PCDH7 affects cisplatin resistance in NSCLC. Notes: **(A, B)** The IC_{50} detection of cisplatin in PCDH7-knockdown and control cells. **(C)** Expression level of PCDH7 in A549- and A549-resistant cells. **(D, E)** Single-cell expression pattern in NSCLC tissue.

Construction of a prognosis model derived from PCDH7 using machine learning algorithms

Then, we tried to construct a prognosis model derived from PCDH7-related genes. The top 100 genes positively and negatively correlated with PCDH7 are shown in Figures 9A, B. Then, univariate Cox regression analysis was performed to identify the prognosis-related genes (Figure 9C; Supplementary File S1). LASSO regression analysis was conducted to reduce data dimensions (Figures 9D, E). Then, three PCDH7-related molecules were identified for a prognosis model: Risk score = GPX8 * 0.107 + BCAR3 * 0.184 + TNS4 * 0.05 (Figure 9F). The KM curve in the training cohort demonstrated a shorter survival rate of patients with a high risk score than those with a low risk score (Figure 10A, HR = 3.96, $p < 0.001$). The AUC values of 1-, 3-, and 5-year ROC curves were 0.750, 0.745, and 0.688, respectively, indicating a good prediction ability of our prognosis model (Figures 10B–D). This effect was also found in the validation cohort (Figures 10E–H, HR = 3.36, $p < 0.001$; AUC values of 1-, 3-, and 5-year ROC curves were 0.724, 0.733, and 0.673,

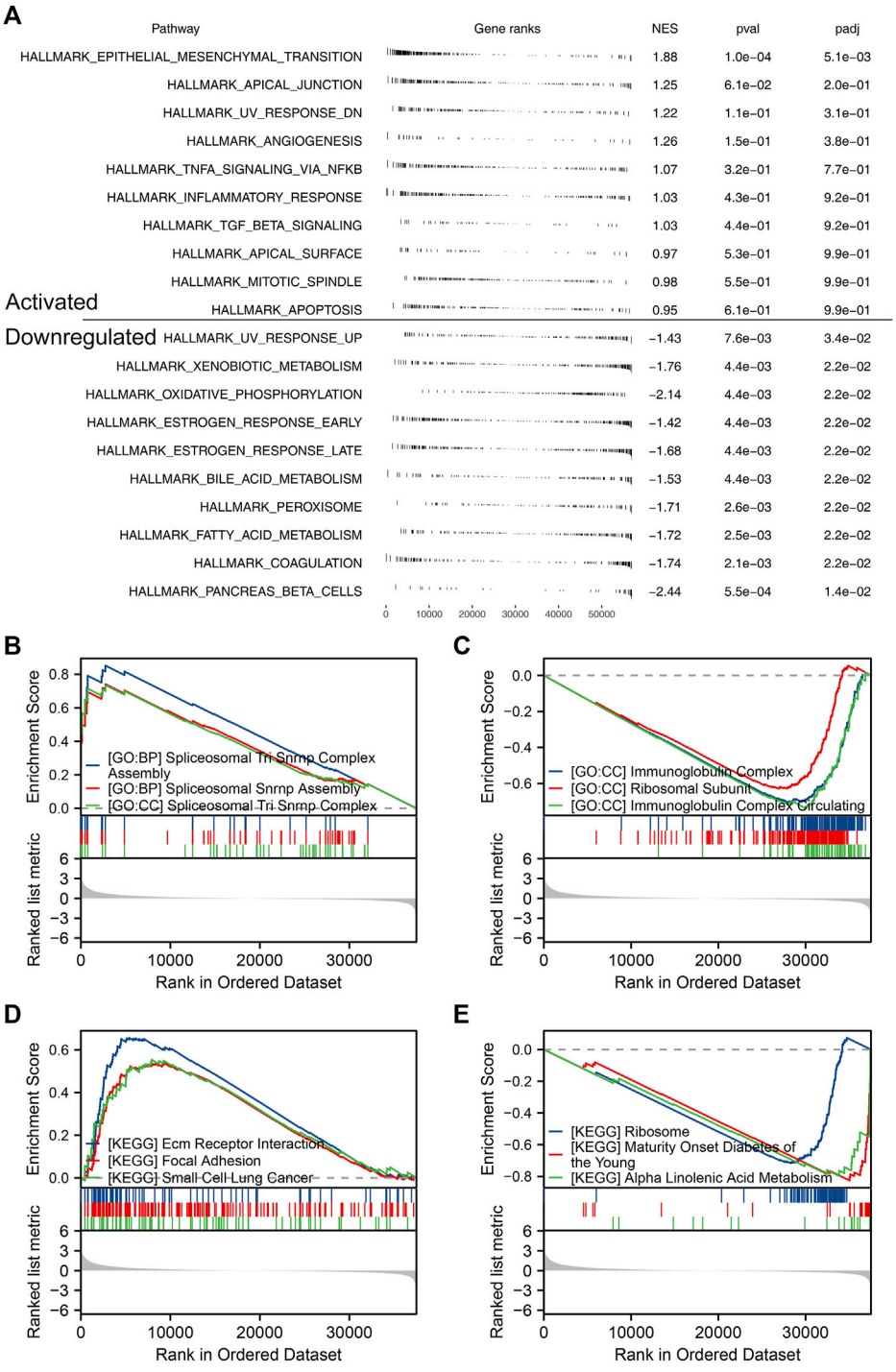

FIGURE 6
Biological enrichment of PCDH7 in NSCLC. Notes: **(A)** GSEA analysis based on the Hallmark gene set in NSCLC patients with high and low PCDH7 expression. **(B)** Top three upregulated terms of GSEA analysis based on the GO gene set in NSCLC patients with high and low PCDH7 expression. **(C)** Top three downregulated terms of GSEA analysis based on the GO gene set in NSCLC patients with high and low PCDH7 expression. **(D)** Top three upregulated terms of GSEA analysis based on the KEGG gene set in NSCLC patients with high and low PCDH7 expression. **(E)** Top three downregulated terms of GSEA analysis based on the KEGG gene set in NSCLC patients with high and low PCDH7 expression levels.

respectively). A nomogram plot was established to get a better clinical application ability by integrating the risk score and clinical features (Figure 10I). For the 1-, 3-, and 5-year survival, a satisfactory fit was observed between the survival predicted by the nomogram and the actual survival (Figure 10J). Moreover, we noticed that the risk score is an independent marker for patient prognosis, which increases its potential for clinical applications (Figures 10K, L).

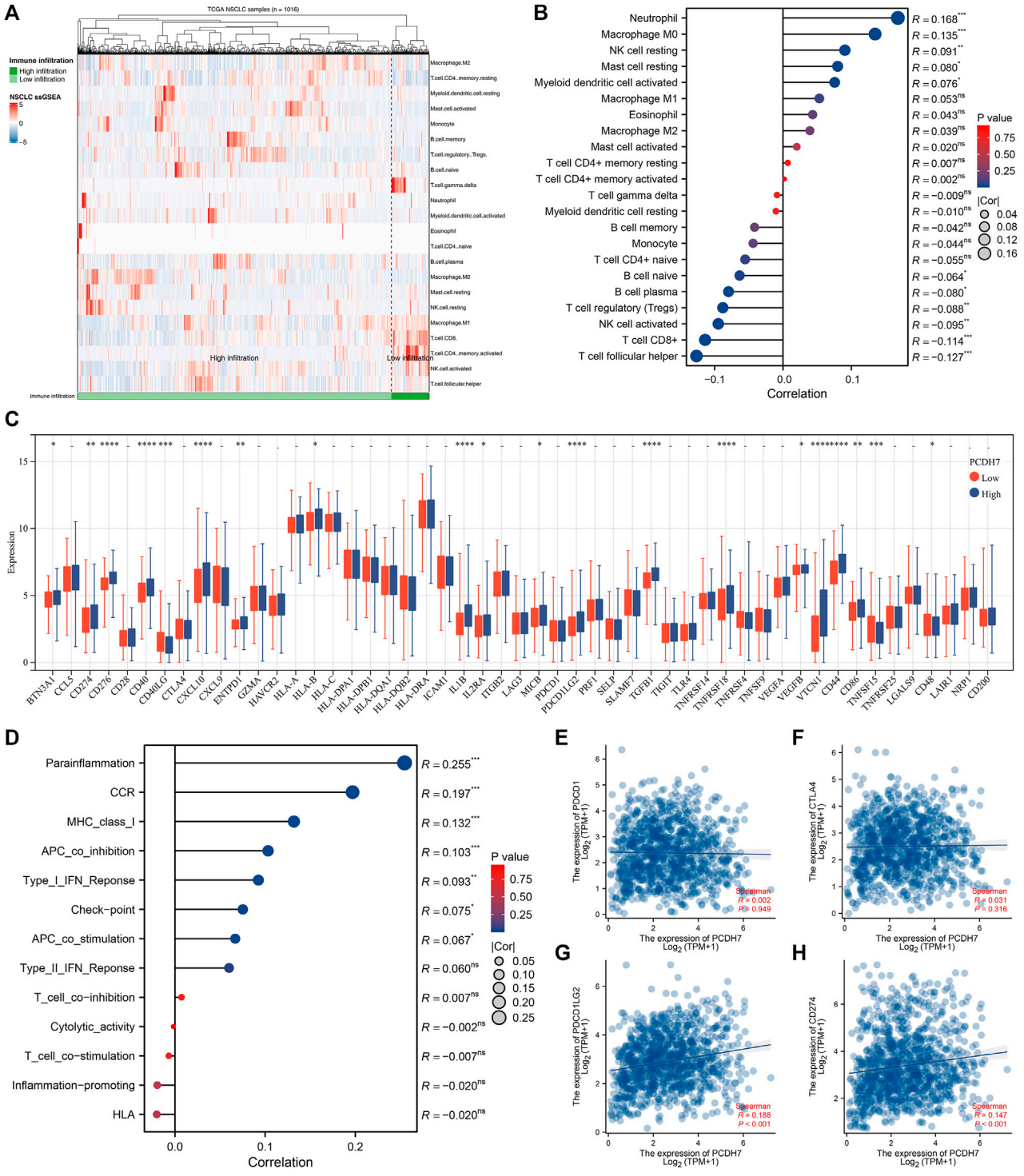

FIGURE 7
Immune-related analysis of PCDH7 in NSCLC. Notes: **(A)** The CIBERSORT algorithm was used to quantify the immune microenvironment of NSCLC. **(B)** Correlation between PCDH7 and quantified immune cells. **(C)** Expression level of immune checkpoint genes in patients with high and low PCDH7 expression. **(D)** Correlation between PCDH7 and quantified immune function. **(E)** Correlation between PCDH7 and PDCD1. **(F)** Correlation between PCDH7 and CTLA4. **(G)** Correlation between PCDH7 and PDCD1LG2. **(H)** Correlation between PCDH7 and CD274.

Discussion

Despite the rapid development of medical management and technology, it is undeniable that lung cancer, especially NSCLC, remains a thorny public health issue (de Sousa and Carvalho, 2018; Bade and Dela Cruz, 2020). Early-stage lung cancer patients can rely on early surgery, but surgical intervention in late-stage patients often has poor results (Hirsch et al., 2017). Early-stage lung cancer can

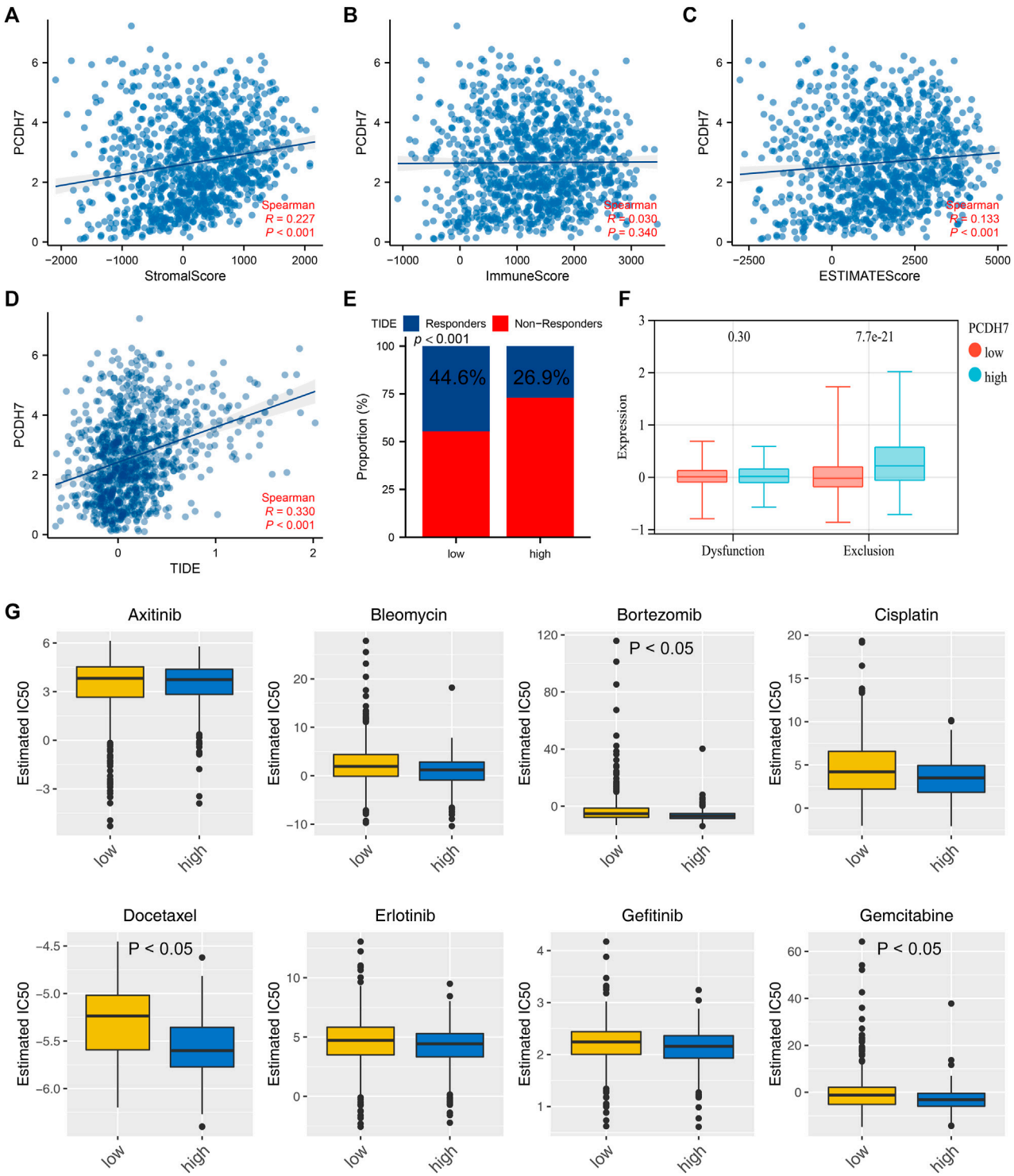

FIGURE 8
PCDH7 affects the sensitivity of immunotherapy and specific chemotherapy in NSCLC. Notes: **(A)** Correlation between PCDH7 and stromal score quantified by the ESTIMATE package. **(B)** Correlation between PCDH7 and immune score quantified by the ESTIMATE package. **(C)** Correlation between PCDH7 and ESTIMATE score quantified by the ESTIMATE package. **(D)** Correlation between PCDH7 and the TIDE score. **(E)** Percentage of immunotherapy responders and non-responders in patients with high and low PCDH7 expression. **(F)** Immune dysfunction and exclusion level in patients with high and low PCDH7 expression. **(G)** Drug sensitivity analysis of patients with high and low PCDH7 expression.

achieve a good prognosis and even clinical cure through multidisciplinary comprehensive treatment. However, many patients already have disease progression at the initial diagnosis, which is an important factor affecting their prognosis (Wang et al., 2019). For unresectable advanced NSCLC patients, platinum-containing dual-drug chemotherapy remains the first-line

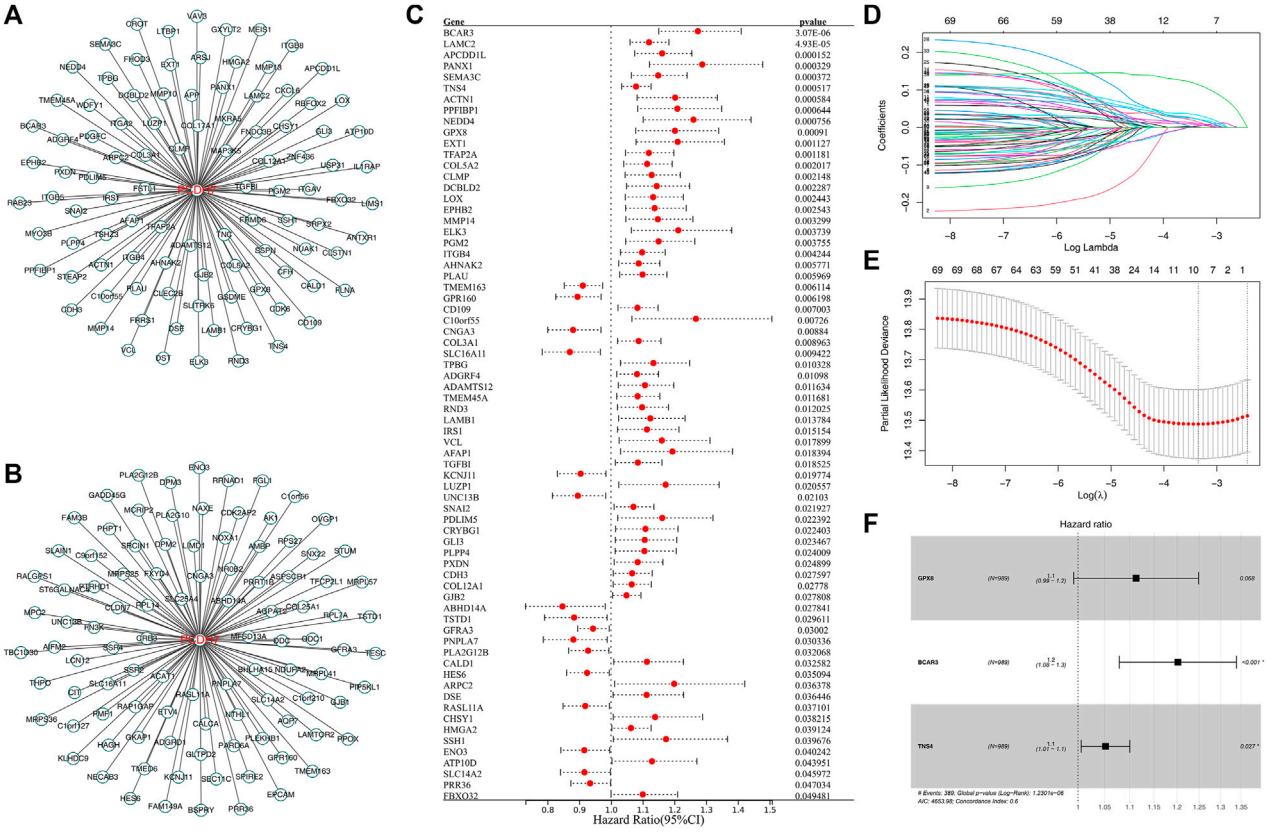

FIGURE 9
Construction of a prognosis model based on PCDH7-derived molecules. Notes: **(A)** Top 100 genes positively correlated with PCDH7. **(B)** Top 100 genes negatively correlated with PCDH7. **(C)** Univariate Cox regression analysis of PCDH7-derived molecules. **(D, E)** LASSO regression analysis. **(F)** Multivariate Cox regression analysis was performed to construct the prognosis model.

treatment strategy (Rossi and Di Maio, 2016). Therefore, cisplatin is extremely important in the treatment of advanced lung cancer.

In recent years, NSCLC has made great progress in both immune and targeted therapies, and these advances have also promoted the development of precision therapy (Imyanitov et al., 2021). Subsequently, the development of targeted drugs and their molecular therapeutic mechanisms have received attention. However, due to the limitations of high cost and off-target effects of precise medical treatment for tumors, the combination therapy of traditional chemotherapy is still indispensable in clinical treatment (Planchard et al., 2018). Currently, the issue of chemotherapy drug resistance has become a significant obstacle to the treatment of NSCLC. Cisplatin is the main chemotherapy drug for NSCLC, which can damage tumor DNA, inhibit tumor cell mitosis, and thus disrupt a series of biological functions of DNA (Makovec, 2019). The resistance mechanism of cisplatin is very complex, and its resistance is often related to "drug pump" proteins, molecular detoxification, DNA damage repair, and activation of certain pathways (Amable, 2016). Some previous studies have begun to focus on the mechanism of cisplatin resistance and potential intervention targets (Wang et al., 2021; Kouba et al., 2022; Shi et al., 2022). Here, we found that PCDH7 may be involved in cisplatin resistance in lung cancer through public database analysis (GSE21656 and GSE108214). Then, a series of *in vitro* experiments was performed, which verified the cancer-promoting role of PCDH7 in NSCLC. Moreover, the results of IC_{50} detection showed that PCDH7 might be associated with cisplatin resistance of NSCLC. Next, we investigated the single-cell pattern, biological function, and immune analysis of PCDH7. Moreover, we noticed that patients with high PCDH7 expression might be more sensitive to bortezomib, docetaxel, and gemcitabine but resistant to immunotherapy. Finally, a prognosis model based on three PCDH7-derived genes was constructed (*GPX8*, *BCAR3*, and *TNS4*), which has a good prediction ability on NSCLC patient survival.

PCDH7, known as protocadherin 7, is a subfamily of the cadherin superfamily (Yoshida et al., 1998). PCDH7 has been reported to play a biological role in various cancer types. For instance, Liu et al. discovered that PCDH7 can affect the chemotherapy response of colon cancer, which is regulated by ferroptosis and autophagy (Liu et al., 2022). Wu et al. found that AQP8 could inhibit cancer progression by downregulating PI3K/AKT signaling (Wu et al., 2018). Shishodia et al. found that prostate cancer has a higher level of PCDH7 and could enhance MEK signaling (Shishodia et al., 2019). Wang et al. found that the PCDH7 could be regulated by the circDVL1/miR-412-3p axis and promote renal cancer development (Wang et al., 2022). We found that PCDH7 significantly enhances lung cancer development and is associated with cisplatin resistance, which provides the direction for the potential drug development targeting PCDH7.

10.3389/fphar.2023.1217213

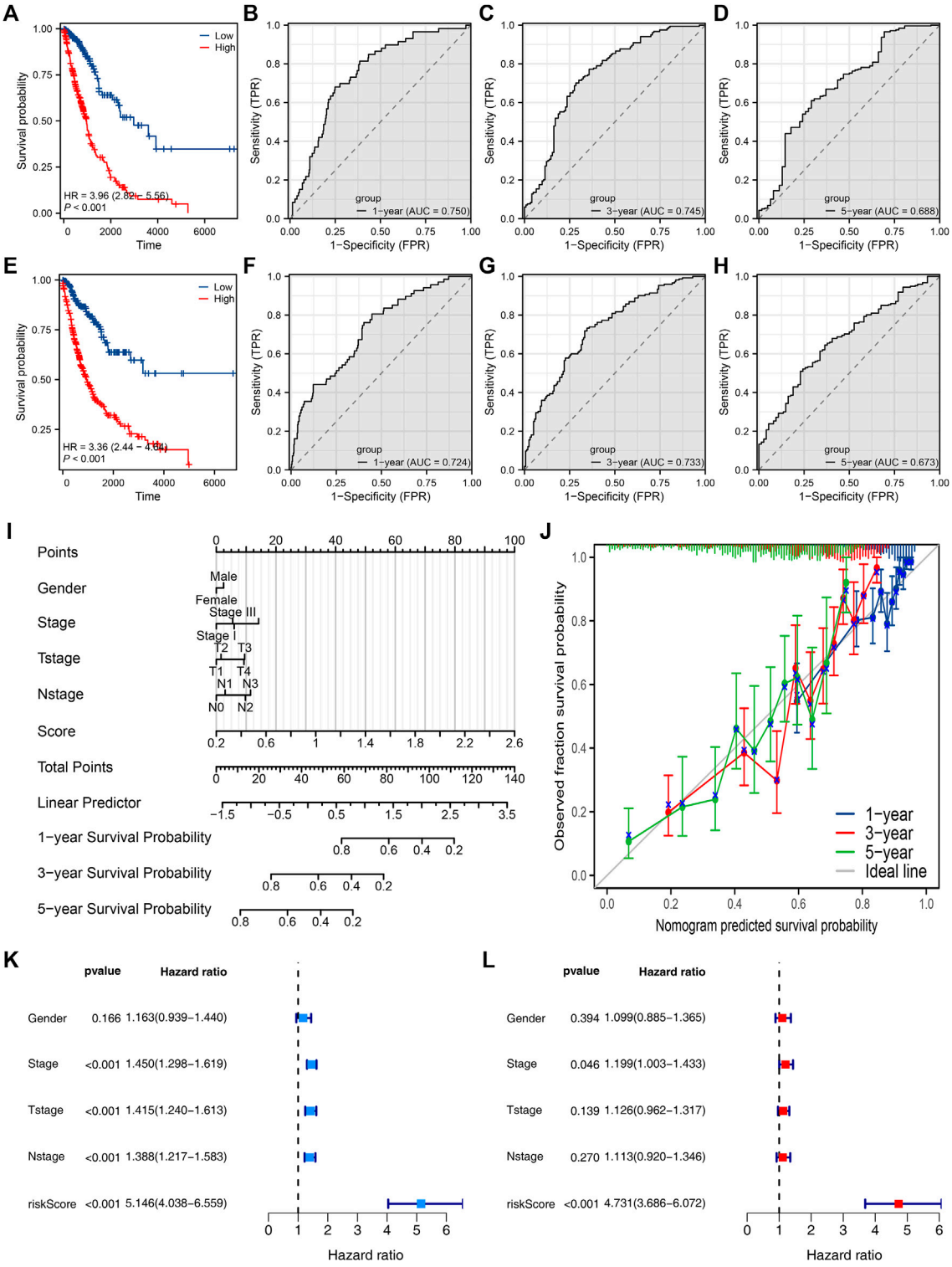

FIGURE 10
Evaluation of the prognosis model and nomogram plot. Notes: **(A)** KM survival curves of high- and low-risk patients in the training cohort; **(B–D)** ROC curves of 1-, 3-, and 5-year survival in the training cohort; **(E)** KM survival curves of high- and low-risk patients in the validation cohort; **(F–H)** ROC curves of 1-, 3-, and 5-year survival in the validation cohort. **(I)** Nomogram plot constructed by combining the risk score and clinical features. **(J)** Calibration curves were used to evaluate the fit between the nomogram-predicted survival and the actual survival. **(K, L)** Univariate and multivariate analyses of the prognosis model.

We noticed that the EMT pathway was the most enriched biological term in patients with high PCDH7 expression, which indicates the role PCDH7 may exert through EMT mediation. Shen et al. noticed that when EMT activity is reversed, the malignancy and resistance to cisplatin in cisplatin-resistant lung cancer cell lines decrease (Shen et al., 2019). The research result also indirectly highlights the effectiveness of our analysis. Meanwhile, other pathways like apical junction, UV-response, angiogenesis, and TNF-α signaling were also found. These pathways may serve as possible mechanisms mediated by PCDH7 and provide direction for future research. Moreover, PCDH7 was negatively correlated with $CD8^+$ T cells and activated NK cells. These two types of cells act as killer cells to suppress cancer in general solid tumors, especially in lung cancer (Guillerey, 2020; Reina-Campos et al., 2021). Therefore, the recruitment of PCDH7 to peripheral cells in the microenvironment of NSCLC may also be the potential mechanism of its role.

With the arrival of the era of biological big data, the rapidly developing bioinformatics has greatly helped relevant researchers (Yu et al., 2021b; Ren et al., 2021). This study identified the potential role of PCDH7 in NSCLC through high-quality data analysis and validated it through further biological experiments. However, some limitations cannot be ignored. First, through specific bioinformatics algorithms, we explored the potential mechanisms by which PCDH7 works through TCGA's big data. However, bioinformatics results are difficult to truly indicate the actual organizational microenvironment. Therefore, the potential bias generated may reduce the credibility of the conclusion. Second, the vast majority of patients obtained from TCGA are from the Western population. Considering the biological differences between different ethnic groups, the credibility of our results in Asian and African American populations will decrease.

Data availability statement

The original contributions presented in the study are included in the article/Supplementary Materials; further inquiries can be directed to the corresponding author.

Author contributions

HL, HX, and HG performed the analysis. HL and KD wrote the manuscript. DC designed this work. All authors contributed to the article and approved the submitted version.

Conflict of interest

The authors declare that the research was conducted in the absence of any commercial or financial relationships that could be construed as a potential conflict of interest.

Publisher's note

All claims expressed in this article are solely those of the authors and do not necessarily represent those of their affiliated organizations, or those of the publisher, the editors, and the reviewers. Any product that may be evaluated in this article, or claim that may be made by its manufacturer, is not guaranteed or endorsed by the publisher.

Supplementary material

The Supplementary Material for this article can be found online at: https://www.frontiersin.org/articles/10.3389/fphar.2023.1217213/full#supplementary-material

SUPPLEMENTARY FIGURE S1
Data preprocessing process of GSE21656 and GSE108214.

SUPPLEMENTARY FIGURE S2
Results of qRT-PCR. Notes: **(A)**: RNA level of PCDH7 in normal and lung cancer cell lines; **(B, C)**: knockdown efficiency of PCDH7 in A549 and H1299 cells.

SUPPLEMENTARY FIGURE S3
IHC and subcellular localization of PCDH7. Notes: **(A)**: IHC of PCDH7 in normal lung tissue; **(B)**: IHC of PCDH7 in lung cancer tissue; **(C)**: subcellular localization of PCDH7 (HPA database, U2OS).

References

Amable, L. (2016). Cisplatin resistance and opportunities for precision medicine. *Pharmacol. Res.* 106, 27–36. PubMed PMID: 26804248. Epub 2016/01/26. eng. doi:10.1016/j.phrs.2016.01.001

Bade, B. C., and Dela Cruz, C. S. (2020). Lung cancer 2020: Epidemiology, etiology, and prevention. *Clin. Chest Med.* 41 (1), 1–24. PubMed PMID: 32008623. Epub 2020/02/06. eng. doi:10.1016/j.ccm.2019.10.001

Camidge, D. R., Bang, Y. J., Kwak, E. L., Iafrate, A. J., Varella-Garcia, M., Fox, S. B., et al. (2012). Activity and safety of crizotinib in patients with ALK-positive non-small-cell lung cancer: Updated results from a phase 1 study. *Lancet Oncol.* 13 (10), 1011–1019. PubMed PMID: 22954507. Pubmed Central PMCID: PMC3936578. Epub 2012/09/08. eng. doi:10.1016/S1470-2045(12)70344-3

Chen, B., Khodadoust, M. S., Liu, C. L., Newman, A. M., and Alizadeh, A. A. (2018). Profiling tumor infiltrating immune cells with CIBERSORT. *Methods Mol. Biol. Clift. NJ)* 1711, 243–259. PubMed PMID: 29344893. Pubmed Central PMCID: PMC5895181. Epub 2018/01/19. eng. doi:10.1007/978-1-4939-7493-1_12

Colwill, K., and Gräslund, S. (2011). A roadmap to generate renewable protein binders to the human proteome. *Nat. methods* 8 (7), 551–558. PubMed PMID: 21572409. Epub 2011/05/17. eng. doi:10.1038/nmeth.1607

Dasari, S., and Tchounwou, P. B. (2014). Cisplatin in cancer therapy: Molecular mechanisms of action. *Eur. J. Pharmacol.* 740, 364–378. PubMed PMID: 25058905. Pubmed Central PMCID: PMC4146684. Epub 2014/07/25. eng. doi:10.1016/j.ejphar.2014.07.025

de Sousa, V. M. L., and Carvalho, L. (2018). Heterogeneity in lung cancer. *Pathobiology J. Immunopathol. Mol. Cell. Biol.* 85 (1-2), 96–107. PubMed PMID: 29635240. Epub 2018/04/11. eng. doi:10.1159/000487440

Fu, J., Li, K., Zhang, W., Wan, C., Zhang, J., Jiang, P., et al. (2020). Large-scale public data reuse to model immunotherapy response and resistance. *Genome Med.* 12 (1), 21. PubMed PMID: 32102694. Pubmed Central PMCID: PMC7045518. Epub 2020/02/28. eng. doi:10.1186/s13073-020-0721-z

Galluzzi, L., Senovilla, L., Vitale, I., Michels, J., Martins, I., Kepp, O., et al. (2012). Molecular mechanisms of cisplatin resistance. *Oncogene* 31 (15), 1869–1883. PubMed PMID: 21892204. Epub 2011/09/06. eng. doi:10.1038/onc.2011.384

Ghosh, S. (2019). Cisplatin: The first metal based anticancer drug. *Bioorg. Chem.* 88, 102925. PubMed PMID: 31003078. Epub 2019/04/20. eng. doi:10.1016/j.bioorg.2019.102925

Goldstraw, P., Chansky, K., Crowley, J., Rami-Porta, R., Asamura, H., Eberhardt, W. E., et al. (2016). The IASLC lung cancer staging project: Proposals for revision of the TNM stage groupings in the forthcoming (eighth) edition of the TNM classification for lung cancer. *J. Thorac. Oncol.* 11 (1), 39–51. PubMed PMID: 26762738. Epub 2016/01/15. eng. doi:10.1016/j.jtho.2015.09.009

Guillerey, C. (2020). NK cells in the tumor microenvironment. *Adv. Exp. Med. Biol.* 1273, 69–90. PubMed PMID: 33119876. Epub 2020/10/30. eng. doi:10.1007/978-3-030-49270-0_4

Hänzelmann, S., Castelo, R., and Guinney, J. (2013). Gsva: Gene set variation analysis for microarray and RNA-seq data. *BMC Bioinforma.* 14, 7. PubMed PMID: 23323831. Pubmed Central PMCID: PMC3618321. Epub 2013/01/18. eng. doi:10.1186/1471-2105-14-7

Heinze, K., Hölzer, M., Ungelenk, M., Gerth, M., Thomale, J., Heller, R., et al. (2021). RUNX3 transcript variants have distinct roles in ovarian carcinoma and differently influence platinum sensitivity and angiogenesis. *Cancers* 13 (3), 476. PubMed PMID: 33530588. Pubmed Central PMCID: PMC7866085. Epub 2021/02/04. eng. doi:10.3390/cancers13030476

Herbst, R. S., Morgensztern, D., and Boshoff, C. (2018). The biology and management of non-small cell lung cancer. *Nature* 553 (7689), 446–454. PubMed PMID: 29364287. Epub 2018/01/25. eng. doi:10.1038/nature25183

Hirsch, F. R., Scagliotti, G. V., Mulshine, J. L., Kwon, R., Curran, W. J., Jr., Wu, Y. L., et al. (2017). Lung cancer: Current therapies and new targeted treatments. *Lancet (London, Engl.* 389 (10066), 299–311. PubMed PMID: 27574741. Epub 2016/08/31. eng. doi:10.1016/S0140-6736(16)30958-8

Imyanitov, E. N., Iyevleva, A. G., and Levchenko, E. V. (2021). Molecular testing and targeted therapy for non-small cell lung cancer: Current status and perspectives. *Crit. Rev. oncology/hematology* 157, 103194. PubMed PMID: 33316418. Epub 2020/12/15. eng. doi:10.1016/j.critrevonc.2020.103194

Kouba, S., Hague, F., Ahidouch, A., and Ouadid-Ahidouch, H. (2022). Crosstalk between Ca(2+) signaling and cancer stemness: The link to cisplatin resistance. *Int. J. Mol. Sci.* 23 (18), 10687. PubMed PMID: 36142596. Pubmed Central PMCID: PMC9503744. Epub 2022/09/24. eng. doi:10.3390/ijms231810687

Kryczka, J., Kryczka, J., Czarnecka-Chrebelska, K. H., and Brzeziańska-Lasota, E. (2021). Molecular mechanisms of chemoresistance induced by cisplatin in NSCLC cancer therapy. *Int. J. Mol. Sci.* 22 (16), 8885. PubMed PMID: 34445588. Pubmed Central PMCID: PMC8396273. Epub 2021/08/28. eng. doi:10.3390/ijms22168885

Li, J., Zheng, C., Wang, M., Umano, A. D., Dai, Q., Zhang, C., et al. (2022). ROS-regulated phosphorylation of ITPKB by CAMK2G drives cisplatin resistance in ovarian cancer. *Oncogene* 41 (8), 1114–1128. PubMed PMID: 35039634. Epub 2022/01/19. eng. doi:10.1038/s41388-021-02149-x

Lin, C., Chen, Y., Zhang, F., Liu, B., Xie, C., and Song, Y. (2022). Encoding gene RAB3B exists in linear chromosomal and circular extrachromosomal DNA and contributes to cisplatin resistance of hypopharyngeal squamous cell carcinoma via inducing autophagy. *Cell death Dis.* 13 (2), 171. PubMed PMID: 35194030. Pubmed Central PMCID: PMC8863882. Epub 2022/02/24. eng. doi:10.1038/s41419-022-04627-w

Liu, Z., Xu, Y., Liu, X., and Wang, B. (2022). PCDH7 knockdown potentiates colon cancer cells to chemotherapy via inducing ferroptosis and changes in autophagy through restraining MEK1/2/ERK/c-Fos axis. *Biochem. Cell Biol. = Biochimie Biol. Cell.* 100 (6), 445–457. PubMed PMID: 35926236. Epub 2022/08/05. eng. doi:10.1139/bcb-2021-0513

Makovec, T. (2019). Cisplatin and beyond: Molecular mechanisms of action and drug resistance development in cancer chemotherapy. *Radiology Oncol.* 53 (2), 148–158. PubMed PMID: 30956230. Pubmed Central PMCID: PMC6572495. Epub 2019/04/09. eng. doi:10.2478/raon-2019-0018

Mao, Y., Yang, D., He, J., and Krasna, M. J. (2016). Epidemiology of lung cancer. *Surg. Oncol. Clin. N. Am.* 25 (3), 439–445. PubMed PMID: 27261907. Epub 2016/06/05. eng. doi:10.1016/j.soc.2016.02.001

McEligot, A. J., Poynor, V., Sharma, R., and Panangadan, A. (2020). Logistic LASSO regression for dietary intakes and breast cancer. *Nutrients* 12 (9), 2652. PubMed PMID: 32878103. Pubmed Central PMCID: PMC7551912. Epub 2020/09/04. eng. doi:10.3390/nu12092652

Nasim, F., Sabath, B. F., and Eapen, G. A. (2019). Lung cancer. *Med. Clin. N. Am.* 103 (3), 463–473. PubMed PMID: 30955514. Epub 2019/04/09. eng. doi:10.1016/j.mcna.2018.12.006

Ni, M., Zhou, J., Zhu, Z., Xu, Q., Yin, Z., Wang, Y., et al. (2023). Shikonin and cisplatin synergistically overcome cisplatin resistance of ovarian cancer by inducing ferroptosis via upregulation of HMOX1 to promote Fe(2+) accumulation. *Phytomedicine Int. J. phytotherapy Phytopharm.* 112, 154701. PubMed PMID: 36773431. Epub 2023/02/12. eng. doi:10.1016/j.phymed.2023.154701

Nooreldeen, R., and Bach, H. (2021). Current and future development in lung cancer diagnosis. *Int. J. Mol. Sci.* 22 (16), 8661. PubMed PMID: 34445366. Pubmed Central PMCID: PMC8395394. Epub 2021/08/28. eng. doi:10.3390/ijms22168661

Pallis, A. G., and Syrigos, K. N. (2013). Lung cancer in never smokers: Disease characteristics and risk factors. *Crit. Rev. oncology/hematology* 88 (3), 494–503. PubMed PMID: 23921082. Epub 2013/08/08. eng. doi:10.1016/j.critrevonc.2013.06.011

Pan, J., Fang, S., Tian, H., Zhou, C., Zhao, X., Tian, H., et al. (2020). lncRNA JPX/miR-33a-5p/Twist1 axis regulates tumorigenesis and metastasis of lung cancer by activating Wnt/β-catenin signaling. *Mol. cancer* 19 (1), 9. PubMed PMID: 31941509. Pubmed Central PMCID: PMC6961326. Epub 2020/01/17. eng. doi:10.1186/s12943-020-1133-9

Planchard, D., Popat, S., Kerr, K., Novello, S., Smit, E. F., Faivre-Finn, C., et al. (2018). Metastatic non-small cell lung cancer: ESMO clinical practice guidelines for diagnosis, treatment and follow-up. *Ann. Oncol.* 29 (4), iv192–iv237. PubMed PMID: 30285222. Epub 2018/10/05. eng. doi:10.1093/annonc/mdy275

Ray, R., Al Khashali, H., Haddad, B., Wareham, J., Coleman, K. L., Alomari, D., et al. (2022). Regulation of cisplatin resistance in lung cancer cells by nicotine, BDNF, and a β-adrenergic receptor blocker. *Int. J. Mol. Sci.* 23 (21), 12829. PubMed PMID: 36361620. Pubmed Central PMCID: PMC9657603. Epub 2022/11/12. eng. doi:10.3390/ijms232112829

Reina-Campos, M., Scharping, N. E., and Goldrath, A. W. (2021). CD8(+) T cell metabolism in infection and cancer. *Nat. Rev. Immunol.* 21 (11), 718–738. PubMed PMID: 33981085. Pubmed Central PMCID: PMC8806153. Epub 2021/05/14. eng. doi:10.1038/s41577-021-00537-8

Ren, X., Liang, S., Li, Y., Ji, Y., Li, L., Qin, C., et al. (2021). ENAM gene associated with T classification and inhibits proliferation in renal clear cell carcinoma. *Aging* 13 (5), 7035–7051. PubMed PMID: 33539322. Pubmed Central PMCID: PMC7993715. Epub 2021/02/05. eng. doi:10.18632/aging.202558

Ren, X., Zhang, T., Chen, X., Wei, X., Tian, Y., Li, G., et al. (2020). Early-life exposure to bisphenol A and reproductive-related outcomes in rodent models: A systematic review and meta-analysis. *Aging* 12 (18), 18099–18126. PubMed PMID: 32996894. Pubmed Central PMCID: PMC7585097. Epub 2020/10/01. eng. doi:10.18632/aging.103620

Ritchie, M. E., Phipson, B., Wu, D., Hu, Y., Law, C. W., Shi, W., et al. (2015). Limma powers differential expression analyses for RNA-sequencing and microarray studies. *Nucleic acids Res.* 43 (7), e47. PubMed PMID: 25605792. Pubmed Central PMCID: PMC4402510. Epub 2015/01/22. eng. doi:10.1093/nar/gkv007

Rossi, A., and Di Maio, M. (2016). Platinum-based chemotherapy in advanced non-small-cell lung cancer: Optimal number of treatment cycles. *Expert Rev. anticancer Ther.* 16 (6), 653–660. PubMed PMID: 27010977. Epub 2016/03/25. eng. doi:10.1586/14737140.2016.1170596

Sarin, N., Engel, F., Rothweiler, F., Cinatl, J., Michaelis, M., Frötschl, R., et al. (2018). Key players of cisplatin resistance: Towards a systems Pharmacology approach. *Int. J. Mol. Sci.* 19 (3), 767. PubMed PMID: 29518977. Pubmed Central PMCID: PMC5877628. Epub 2018/03/10. eng. doi:10.3390/ijms19030767

Shen, M., Xu, Z., Xu, W., Jiang, K., Zhang, F., Ding, Q., et al. (2019). Inhibition of ATM reverses EMT and decreases metastatic potential of cisplatin-resistant lung cancer cells through JAK/STAT3/PD-L1 pathway. *J. Exp. Clin. cancer Res. CR* 38 (1), 149. PubMed PMID: 30961670. Pubmed Central PMCID: PMC6454747. Epub 2019/04/10. eng. doi:10.1186/s13046-019-1161-8

Shi, Z. D., Hao, L., Han, X. X., Wu, Z. X., Pang, K., Dong, Y., et al. (2022). Targeting HNRNPU to overcome cisplatin resistance in bladder cancer. *Mol. cancer* 21 (1), 37. PubMed PMID: 35130920. Pubmed Central PMCID: PMC8819945. Epub 2022/02/09. eng. doi:10.1186/s12943-022-01517-9

Shishodia, G., Koul, S., and Koul, H. K. (2019). Protocadherin 7 is overexpressed in castration resistant prostate cancer and promotes aberrant MEK and AKT signaling. *Prostate* 79 (15), 1739–1751. PubMed PMID: 31449679. Epub 2019/08/27. eng. doi:10.1002/pros.23898

Subramanian, A., Tamayo, P., Mootha, V. K., Mukherjee, S., Ebert, B. L., Gillette, M. A., et al. (2005). Gene set enrichment analysis: A knowledge-based approach for interpreting genome-wide expression profiles. *Proc. Natl. Acad. Sci. U. S. A.* 102 (43), 15545–15550. PubMed PMID: 16199517. Pubmed Central PMCID: PMC1239896. Epub 2005/10/04. eng. doi:10.1073/pnas.0506580102

Sun, D., Wang, J., Han, Y., Dong, X., Ge, J., Zheng, R., et al. (2021). Tisch: A comprehensive web resource enabling interactive single-cell transcriptome visualization of tumor microenvironment. *Nucleic acids Res.* 49 (1), D1420–D1430. PubMed PMID: 33179754. Pubmed Central PMCID: PMC7778907. Epub 2020/11/13. eng. doi:10.1093/nar/gkaa1020

Sun, Y., Zheng, S., Torossian, A., Speirs, C. K., Schleicher, S., Giacalone, N. J., et al. (2012). Role of insulin-like growth factor-1 signaling pathway in cisplatin-resistant lung cancer cells. *Int. J. Radiat. Oncol. Biol. Phys.* 82 (3), e563–e572. PubMed PMID: 22197230. Pubmed Central PMCID: PMC3271860. Epub 2011/12/27. eng. doi:10.1016/j.ijrobp.2011.06.1999

Wang, H., Lu, Y., Wang, M., Wu, Y., Wang, X., and Li, Y. (2021). Roles of E3 ubiquitin ligases in gastric cancer carcinogenesis and their effects on cisplatin resistance. *J. Mol. Med. (Berlin, Ger.* 99 (2), 193–212. PubMed PMID: 33392633. Epub 2021/01/05. eng. doi:10.1007/s00109-020-02015-5

Wang, S., Zimmermann, S., Parikh, K., Mansfield, A. S., and Adjei, A. A. (2019). Current diagnosis and management of small-cell lung cancer. *Mayo Clin. Proc.* 94 (8), 1599–1622. PubMed PMID: 31378235. Epub 2019/08/06. eng. doi:10.1016/j.mayocp.2019.01.034

Wang, Y., Zhang, Y., Su, X., Qiu, Q., Yuan, Y., Weng, C., et al. (2022). Circular RNA circDVL1 inhibits clear cell renal cell carcinoma progression through the miR-412-3p/PCDH7 axis. *Int. J. Biol. Sci.* 18 (4), 1491–1507. PubMed PMID: 35280687. Pubmed Central PMCID: PMC8898370. Epub 2022/03/15. eng. doi:10.7150/ijbs.69351

Wu, F., Fan, J., He, Y., Xiong, A., Yu, J., Li, Y., et al. (2021). Single-cell profiling of tumor heterogeneity and the microenvironment in advanced non-small cell lung cancer. *Nat. Commun.* 12 (1), 2540. PubMed PMID: 33953163. Pubmed Central PMCID: PMC8100173. Epub 2021/05/07. eng. doi:10.1038/s41467-021-22801-0

Wu, H., Mu, X., Liu, L., Wu, H., Hu, X., Chen, L., et al. (2020). Bone marrow mesenchymal stem cells-derived exosomal microRNA-193a reduces cisplatin resistance of non-small cell lung cancer cells via targeting LRRC1. *Cell death Dis.* 11 (9), 801. PubMed PMID: 32978367. Pubmed Central PMCID: PMC7519084. Epub 2020/09/27. eng. doi:10.1038/s41419-020-02962-4

Wu, Q., Yang, Z. F., Wang, K. J., Feng, X. Y., Lv, Z. J., Li, Y., et al. (2018). AQP8 inhibits colorectal cancer growth and metastasis by down-regulating PI3K/AKT signaling and PCDH7 expression. *Am. J. cancer Res.* 8 (2), 266–279. PubMed PMID: 29511597. Pubmed Central PMCID: PMC5835694. Epub 2018/03/08. eng.

Xiao, L., Lan, X., Shi, X., Zhao, K., Wang, D., Wang, X., et al. (2017). Cytoplasmic RAP1 mediates cisplatin resistance of non-small cell lung cancer. *Cell death Dis.* 8 (5), e2803. PubMed PMID: 28518145. Pubmed Central PMCID: PMC5520727. Epub 2017/05/19. eng. doi:10.1038/cddis.2017.210

Yang, W., Soares, J., Greninger, P., Edelman, E. J., Lightfoot, H., Forbes, S., et al. (2013). Genomics of drug sensitivity in cancer (GDSC): A resource for therapeutic biomarker discovery in cancer cells. *Nucleic acids Res.* 41, D955–D961. PubMed PMID: 23180760. Pubmed Central PMCID: PMC3531057. Epub 2012/11/28. eng. doi:10.1093/nar/gks1111

Yoshida, K., Yoshitomo-Nakagawa, K., Seki, N., Sasaki, M., and Sugano, S. (1998). Cloning, expression analysis, and chromosomal localization of BH-protocadherin (PCDH7), a novel member of the cadherin superfamily. *Genomics* 49 (3), 458–461. PubMed PMID: 9615233. Epub 1998/06/06. eng. doi:10.1006/geno.1998.5271

Yu, L., Ding, Y., Wan, T., Deng, T., Huang, H., and Liu, J. (2021a). Significance of CD47 and its association with tumor immune microenvironment heterogeneity in ovarian cancer. *Front. Immunol.* 12, 768115. PubMed PMID: 34966389. Pubmed Central PMCID: PMC8710451. Epub 2021/12/31. eng. doi:10.3389/fimmu.2021.768115

Yu, L., Shen, H., Ren, X., Wang, A., Zhu, S., Zheng, Y., et al. (2021b). Multi-omics analysis reveals the interaction between the complement system and the coagulation cascade in the development of endometriosis. *Sci. Rep.* 11 (1), 11926. PubMed PMID: 34099740. Pubmed Central PMCID: PMC8185094. Epub 2021/06/09. eng. doi:10.1038/s41598-021-90112-x

Zhang, X., Lu, Z., Ren, X., Chen, X., Zhou, X., Zhou, X., et al. (2021a). Genetic comprehension of organophosphate flame retardants, an emerging threat to prostate cancer. *Ecotoxicol. Environ. Saf.* 223, 112589. PubMed PMID: 34358932. Epub 2021/08/07. eng. doi:10.1016/j.ecoenv.2021.112589

Zhang, X., Ren, X., Zhang, T., Zhou, X., Chen, X., Lu, H., et al. (2022). Iron oxide nanoparticles cause surface coating- and core chemistry-dependent endothelial cell ferroptosis. *Nanotoxicology* 14 (4), 829–843. doi:10.1080/17435390.2022.2154176

Zhang, X., Zhang, T., Ren, X., Chen, X., Wang, S., and Qin, C. (2021b). Pyrethroids toxicity to male reproductive system and offspring as a function of oxidative stress induction: Rodent studies. *Front. Endocrinol.* 12, 656106. PubMed PMID: 34122335. Pubmed Central PMCID: PMC8190395. Epub 2021/06/15. eng. doi:10.3389/fendo.2021.656106

frontiers | Frontiers in Oncology

TYPE Original Research
PUBLISHED 21 July 2023
DOI 10.3389/fonc.2023.1222716

OPEN ACCESS

EDITED BY
Lin Qi,
Second Xiangya Hospital, Central South University, China

REVIEWED BY
Dan Wang,
Hubei University of Science and Technology, China
He Huang,
The Third Affiliated Hospital of Sun Yat-sen University, China
Mengle Peng,
Henan Provincial Third People's Hospital, China

*CORRESPONDENCE
Gang Xiong
xionggang_xw@sina.com

†These authors have contributed equally to this work

RECEIVED 15 May 2023
ACCEPTED 22 June 2023
PUBLISHED 21 July 2023

CITATION
Dong D, Zhang S, Jiang B, Wei W, Wang C, Yang Q, Yan T, Chen M, Zheng L, Shao W and Xiong G (2023) Correlation analysis of MRD positivity in patients with completely resected stage I-IIIA non-small cell lung cancer: a cohort study.
Front. Oncol. 13:1222716.
doi: 10.3389/fonc.2023.1222716

Correlation analysis of MRD positivity in patients with completely resected stage I-IIIA non-small cell lung cancer: a cohort study

Daling Dong[1†], Shixin Zhang[1†], Bin Jiang[1], Wei Wei[1], Chao Wang[1], Qian Yang[1], Tingzhi Yan[1], Min Chen[1], Liken Zheng[2], Weikang Shao[2] and Gang Xiong[1*]

[1]Department of Cardiothoracic Surgery, Guiqian International Hospital, Guiyang, China, [2]Genecast Biotechnology Co., Ltd., Wuxi, China

Background: The primary objective of this study is to thoroughly investigate the intricate correlation between postoperative molecular residual disease (MRD) status in individuals diagnosed with stage I-IIIA non-small cell lung cancer (NSCLC) and clinicopathological features, gene mutations, the tumour immune microenvironment and treatment effects.

Methods: The retrospective collection and analysis were carried out on the clinical data of ninety individuals diagnosed with stage I-IIIA NSCLC who underwent radical resection of lung cancer at our medical facility between January 2021 and March 2022. The comprehensive investigation encompassed an evaluation of multiple aspects including the MRD status, demographic information, clinicopathological characteristics, results from genetic testing, the tumor immune microenvironment, and treatment effects.

Results: No significant associations were observed between postoperative MRD status and variables such as gender, age, smoking history, pathological type, and gene mutations. However, a statistically significant correlation was found between MRD positivity and T (tumor diameter > 3 cm) as well as N (lymph node metastasis) stages (p values of 0.004 and 0.003, respectively). It was observed that higher proportions of micropapillary and solid pathological subtypes within lung adenocarcinoma were associated with increased rates of MRD-positivity after surgery (p = 0.007;0.005). MRD positivity demonstrated a correlation with the presence of vascular invasion (p = 0.0002). For the expression of programmed cell death ligand 1 (PD-L1), tumour positive score (TPS) ≥ 1% and combined positive score (CPS) ≥ 5 were correlated with postoperative MRD status (p value distribution was 0.0391 and 0.0153). In terms of ctDNA elimination, among patients identified as having postoperative MRD and lacking gene mutations, postoperative adjuvant targeted therapy demonstrated superiority over chemotherapy (p = 0.027).

Conclusion: Postoperative ctDNA-MRD status in NSCLC patients exhibits correlations with the size of the primary tumor, lymph node metastasis,

pathological subtype of lung adenocarcinoma, presence of vascular invasion, as well as TPS and CPS values for PD-L1 expression; in postoperative patients with MRD, the effectiveness of adjuvant EGFR-TKI targeted therapy exceeds that of chemotherapy, as evidenced by the elimination of ctDNA.

KEYWORDS

molecular residual disease, liquid biopsy, non-small cell lung cancer, adjuvant therapy, clinicopathological features, immune markers

1 Introduction

In China, Lung cancer holds the unenviable distinction of being the most prevalent malignancy and remains the primary contributor to cancer-related mortality. This devastating disease accounts for a staggering 40% of global deaths attributed to lung cancer, further emphasizing its significant impact on public health. Non-small cell lung cancer (NSCLC) comprises roughly85% of lung cancers, with its predominant pathological subtypes being lung adenocarcinoma and lung squamous cell carcinoma (1, 2). Surgery is one of the main treatments for patients with stage I-IIIA NSCLC. For patients with stage IA and low-risk stage IB NSCLC, regular follow-up and imaging examinations are recommended as the main means of tumour monitoring (3). Adjuvant therapy, encompassing various modalities such as chemotherapy, targeted therapy, immunotherapy, and more, plays a crucial role in the management of postoperative patients with high-risk stage IB and II-IIIA NSCLC. It is crucial to ensure regular clinical follow-ups and imaging assessments during and after the treatment process (4). Despite standardized treatment, there are still patients with stage I-IIIA NSCLC who encounter tumor relapse following surgical intervention (5). Traditional imaging examinations such as computed tomography (CT), as the main means of postoperative tumour monitoring in NSCLC, have certain limitations, such as difficulty in detecting residual or recurring small tumour lesions, and lag behind in the evaluation of chemotherapy efficacy and drug resistance. Detecting small tumour lesions early after radical surgery for NSCLC, prognosticating the likelihood of disease recurrence, and guiding postoperative refined and individualized treatment are the main challenges in the postoperative management of NSCLC.

Circulating tumour DNA (ctDNA) pertains to fragments of tumor-derived DNA present in the bloodstream. These fragments encompass both the phenotype and genetic characteristics of tumour cells, such as gene mutation information, including mutations, deletions, insertions, and rearrangements (6, 7). In recent years, from the perspective of evaluating tumour burden, ctDNA has been used in NSCLC research to evaluate minimal residual disease (MRD). A study of stage I-IIIA NSCLC found that MRD detection based on postoperative plasma ctDNA identify tumour recurrence and metastasis earlier than can imaging. In addition, postoperative ctDNA-MRD-positive patients have a worse prognosis than ctDNA-MRD-negative patients. In addition, it is possible to dynamically monitor postoperative MRD and formulate personalized, precise treatment and/or follow-up plans based on MRD status and abundance changes (8–13). The above studies suggest that MRD detection based on plasma ctDNA serves as a valuable and informative reference for guiding the postoperative management of NSCLC patients and has broad application prospects. However, in the realm of lung cancer, MRD research is still in its nascent stages. Significant heterogeneity exists among studies regarding the definitions and methodologies employed to investigate MRD., and the findings cannot be fully generalized; therefore, relevant research is currently at the preliminary exploration stage of “crossing the river by feeling the stones”.

At the Forum on the 18th China Lung Cancer Summit in 2021, an expert consensus was reached on lung cancer MRD: Lung cancer MRD refers to residual cancer that traditional imaging (including positron emission tomography/CT, PET/CT) or laboratory methods cannot detect after treatment. However, consistent detection of MRD can be achieved through the utilization of liquid biopsy techniques *via* ctDNA (abundance ≥ 0.02%), including lung cancer driver genes or other class I/II gene variants, representing the possibility of lung cancer persistence and clinical progression (14). In a recent extensive prospective study conducted across multiple medical centers, it was conclusively shown that ctDNA can serve as a reliable biomarker for prognosticating and detecting MRD within a span of one month following surgical intervention, and the relative contribution of ctDNA-MRD status in multivariate Cox analysis in predicting recurrence-free survival (RFS) surpasses the cumulative impact of clinical variables, including s TNM stage (15). However, there is no detailed literature report on whether the MRD status of NSCLC patients after radical surgery is related to clinicopathological characteristics, gene mutations, tumour immune biomarkers and other factors.

Abbreviations: ACI, Acinar predominant adenocarcinoma; CPS, Combined positive score; CT, Computed tomography; ctDNA, Circulating tumor DNA; cfDNA, Cell-free DNA; HLA, Human leukocyte antigen; LUAD, lung Adenocarcinoma; LUSC, Lung Squamous Cells; LPA, lepidic predominant adenocarcinoma; MPA, micropapillary predominant adenocarcinomaPAP, papillary predominant adenocarcinom; MAF, minimum allele frequency; MRD, molecular residual disease; NSCLC, Non-small cell lung cancer; NGS, Next Generation Sequencing; PCR, Polymerase Chain Reaction; SNV, Single nucleotide variants.

In this study, we retrospectively conducted a comprehensive analysis of a cohort comprising 90 individuals diagnosed with stage I-IIIA NSCLC who had undergone radical surgery in our hospital. The peripheral blood of the patients was analysed by next-generation sequencing (NGS) technology covering 769 cancer-related genes, and the correlation between ctDNA-MRD status and clinicopathological features, gene mutations, the tumour immune microenvironment and treatment efficacy was analysed. By examining these variables collectively, we aimed to investigate the relationship among MRD status, clinicopathological characteristics and treatment prognosis in NSCLC patients.

2 Methods

2.1 Patients and samples

Patients with stage I-IIIA disease (AJCC8th edition) who underwent radical surgery (lobectomy + systematic lymph node dissection) for NSCLC from January 2021 to March 2022 at the Department of Thoracic and Cardiovascular Surgery of Guiqian International General Hospital and agreed to undergo MRD testing were included. Patients with a prior history of neoplastic disease, neoadjuvant therapy, multiple primary lung cancers, compound carcinoma, and germline mutations were excluded. For eligible patients, the excised pathological tissue was fixed in formalin solution and subsequently embedded in paraffin for the purpose of sectioning following surgery. Subsequently, the peripheral blood of each patient was collected for MRD detection 1 month after the operation. If the sample was MRD positive, adjuvant therapy was administered considering the gene test results, and the peripheral blood of the patient was collected again 3 months after the end of the adjuvant treatment for MRD detection. If the patient's peripheral blood MRD test was negative 1 month after surgery, adjuvant therapy was administered based on the stage, and peripheral blood was collected 6 months after surgery for MRD detection regardless of whether the patient received adjuvant therapy. The requirements for pathological tissue sections of patients were as follows: tumour positive score (TPS) ≥10%, area of necrotic tissue ≤50%, and section thickness of 5-10 μm. Streck blood tubes were used for peripheral blood collection, and each blood collection volume was at least 10 ml. Tissue and blood samples were sent to Genecast Biotechnology Co., Ltd. (Wuxi,China) for DNA isolation, library preparation, and NGS. Regular follow-up visits were scheduled for all patients at three-month intervals post-operation. The follow-up protocol encompassed a comprehensive evaluation, including a review of medical history, physical examination, chest CT scan, and abdominal B-ultrasound, as well as yearly cranial MRI and whole-body bone scans. Prior approval for this study was obtained from the Ethics Committee of Guiqian International General Hospital, and written informed consent was obtained from all participating patients, ensuring adherence to ethical guidelines and patient autonomy.

2.2 DNA extraction from tissue and blood samples

The extraction of genomic DNA from tissue slices was performed using the TIANamp Genomic DNA Kit (TIANGEN, China) following established protocols. After centrifugation, TGuide S32 Magnetic Blood DNA Kit-T5C and TGuide S32 (TIANGEN, China) automatic nucleic acid extractor were employed for extracting genomic DNA from the buffy coat fraction. Similarly, isolation of cell-free DNA (cfDNA) was extracted from the plasma fraction using MagMAX Cell-Free DNA Isolation (ThermoFisher, USA). The quantification of DNA concentration was performed utilizing a Qubit dsDNA HS Assay Kit (Thermo Fisher, USA), and DNA quality was assessed using an Agilent 2100 BioAnalyzer (Agilent, USA). Each tumor tissue or plasma sample yielded a range of 30 to 300 ng of genomic DNA, which was then subjected to shearing using Covaris LE220 to achieve a fragment length of 200 bp. The resulting DNA fragments underwent further processing and were deemed qualified for subsequent library preparation.

2.3 Library preparation and sequencing

A KAPA Hyper PCR-free kit was used to construct a DNA library, and the library was amplified using a KAPA Library Amplification Kit and purified using Agencourt AMPure XP magnetic beads. UMI connectors were added to both ends of the DNA. The quantification of modified library samples was carried out using the AccuGreen High Sensitivity dsDNA Quantification Kit (Biotium, USA), enabling accurate measurement of library sample concentration. Additionally, the size distribution of the libraries was evaluated using an Agilent Bioanalyzer 2100 (Agilent, USA).

The HyperCap Target Enrichment Kit (Roche, Switzerland) was employed to capture the desired genomic regions of interest. The designed hybridization panel covered a region of approximately 2.4 MB in the human genome, covering 769 cancer-related genes. The 769-gene NGS panel was developed and validated in-house by Genecast Biotechnology, a CAP-accredited clinical diagnostic laboratory. The genes included in the panels are curated according to publicly available databases, including The Cancer Genome Atlas (TCGA, https://www.cancer.gov), the Catalogue of Somatic Mutations in Cancer (COSMIC, https://cancer.sanger.ac.uk), OncoKB (https://www.oncokb.org), etc., and proprietary internal datasets. Following hybridization and subsequent washing steps as per the provided instructions, the enriched libraries underwent amplification using KAPA HiFi HotStart ReadyMix. The amplified libraries were then purified using 1X AMPure beads, quantified to determine their concentration, and subjected to sequencing in 150-bp paired-end mode using the Illumina NovaSeq 6000 platform.

2.4 Identification of single-nucleotide variants in tumour tissue

Trimming of aptamers and low-quality bases for sequencing reads was performed using Trimmomatic (v0.36) (16). The obtained high-quality reads were aligned to the human reference genome hg19 using BWA aligner (v0.7.17), followed by Picard (v2.23.0) for classification and masking of duplicates. To identify SNVs and insertions/deletions (InDels), VarDict (version 1.5.1) analysis was employed in this study. Additionally, FreeBayes (version 1.2.0) was utilized to detect complex mutations (17). A typical quality check (QC) was used to filter the raw variant list, for example, variant quality and chain bias. Additionally, variants classified as low complexity and segmental repeat regions defined by ENCODE were removed (18), and variants on a list of recurring sequence-specific errors (SSEs) were developed and validated in-house.

2.5 Filtering of point mutations in tumour tissue

Filtering was performed first if germline or clonal haematopoiesis met any of the following criteria: 1) variant allele frequency (VAF) in peripheral blood lymphocytes (PBLs) not less than 5%; 2) VAF in PBLs less than 5% but greater than 1/5 of the VAF in paired tissue samples; and 3) variants found to have a minimum allele frequency (MAF) no less than 2% in the public gnomAD population database. The remaining somatic mutations were subjected to further quality filtering. The minimum supported reads was 5 (19), and the VAF thresholds were 4% for SNVs and 5% for InDels.

2.6 Monitoring point mutations in plasma samples

To ensure the accuracy and reliability of identified SNVs/InDels, each potential ctDNA mutation candidate underwent rigorous statistical testing against an internal background reference library. We adopted a tumor prior analysis strategy for mutational analysis of plasma samples, whereby somatic SNVs/InDels identified in each tissue sample constituted the baseline for ctDNA detection in corresponding plasma cfDNA samples from the same patient; in the initial tissue sequencing, novel ctDNA mutations that were not detected were excluded from the data analysis. In order to mitigate the influence of technical artifacts, each identified ctDNA mutation candidate underwent a rigorous statistical analysis against an internal background reference library. The background library included more than 1,000 plasma samples as well as matched tissue and peripheral blood cell samples from patients of various stages and cancer types. After the removal of true tumour-derived somatic mutations and clonal haematopoietic (CH) variants by reference to matched tissue and PBL sequences, the remaining artificial variants in the background library were merged at the minor allele level and fitted with anti-γ distribution. Each input plasma sample to be analysed first underwent the same mutation filtering process to remove germline and CH variants, with the remaining candidate somatic mutations statistically tested against a background reference library. To account for the zero-inflation effect, the zero weighted probability that a given variant is a true somatic cell was calculated, by Monte Carlo simulations, combining randomly sampled nonzero VAF values with all zero values. Each VAF in this list was further entered into a binomial test as a probability of success with the parameters observed alt-allele support reads and total support reads. Expected values at the variant level were calculated as the mean of all P values, and a threshold for positive ctDNA mutations was set at $P < 0.05$. The following formula was used to calculate the comprehensive P value at the sample level: Psma pte = C^{km}nPi , where m of the combination coefficient (C) is the total number of variants tracked for this patient and k is the number of positive variants tested by the variant level above. A plasma sample was designated as positive using an integrated P value threshold of $P < 0.01$. The mean VAF for a given positive plasma sample was calculated by dividing the sum of the VAF values of all positive SNV/indel variants by the number of all traceable variants. The haploid genome equivalent (hGE, mutant molecules/ml plasma) used to assess ctDNA concentration was calculated using the following formula:

*mean V AF *cfDN A concertration (ng jml pl amsa }*
o.ooa; *(ng /genome)*

2.7 Identification and monitoring of copy number variation in plasma samples

Copy number variation (CNV) for both tissue and plasma samples were analysed using CNV kit (v0.9.2) software based on paired PBL samples (20). For tissue, a copy number threshold of 4.0 was applied to identify CNV gains, while a threshold of 1.0 was used for CNV losses in the tissue samples. In contrast, for plasma samples, the copy number thresholds were set at 3.0 for CNV gains and 1.2 for CNV losses. In the case of plasma samples, a positive report for CNVs was only assigned if the corresponding gene-level copy number alteration (either an increase or decrease) was also identified in the initial resected baseline tissue sample.

2.8 Detection and monitoring of gene fusions in plasma samples

Gene fusions were identified with FACTERA v1.4.4 and FusionMap (21, 22), and only typical driver fusions involving kinase domains that activate ALK, ROS1, and RET were included in the analysis. Clean plasma cfDNA sequences were mapped to fusion references from corresponding tissue samples. Plasma samples were defined as fusion positive if at least 1 sequencing read exactly matched the reference and spanned the breakpoint.

2.9 Tumour marker-related detection

PD-L1: PD-L1 expression was assessed utilizing a Dako 22C3 kit, a well-established method for analyzing PD-L1 protein levels. The scoring system employed in this study was based on the tumor proportion score (TPS), which represents the percentage of PD-L1 membrane-positive tumor cells within the total number of tumor cells evaluated. (TPS ≥ 1% is positive, TPS < 1% is negative). The combined positive score (CPS) is a metric used to evaluate PD-L1 expression levels. It is calculated by dividing the total number of PD-L1-positive cells (including tumor cells, lymphoid cells, and macrophages) by the total number of visible tumor cells assessed, and then multiplying the result by 100 (CPS ≥ 5 is positive, CPS < 5 is negative).

Tumour mutational burden (TMB): TMB (nonsynonymous mutations per megabase (Mbase) of DNA) was calculated using sequencing data from a panel of 769 cancer-related genes and determined by assessing the number of nonsynonymous somatic mutations per megabase (Mb) of the genome. In this study, quantiles < 25% were considered TMB-L, quantiles ≥ 25% and < 75% were considered TMB-M, and quantiles ≥ 5% were considered TMB-H.

Human leukocyte antigen (HLA): Trimmomatic (V0.39) was used to trim the adaptor of raw read pairs. The obtained high-quality reads were aligned to the human reference genome (HG19, UCSC assembly) using the BWA-MEM aligner (version 0.7.12). Subsequently, the alignment files were processed and analyzed using SAMtools (version 1.3). GATK V2.8 was used to perform markduplicates, and local INDEL rearrangement was performed. The HLA gene region in the markduplicated BAM file was converted to FASTQ format and input into HLA-HD (V1.2.0.1) for HLA allele type analysis (MINMUM_TAG_SIZE, 50; RATE_OF_CHUTING, 0.95). The method involved building an extensive dictionary of HLA alleles. Finally, the HLA allele types were analysed.

2.10 Adjuvant therapy

The adenocarcinoma chemotherapy regimen (AP regimen) was as follows: pemetrexed + platinum (cisplatin/carboplatin); specific dosage: pemetrexed 500 mg/m2 q3w ivgtt, carboplatin 200-400 mg/m2 q3w ivgtt, and cisplatin platinum 50~100 mg/m2 q3w ivgtt, 4-6 cycles. The chemotherapy regimen for squamous cell carcinoma (TP regimen) was a follows: nab-paclitaxel + platinum (cisplatin/carboplatin); specific dosage: nab-paclitaxel 260 mg/m2 q3w ivgtt, carboplatin 200-400 mg/m2 q3w ivgtt, and cisplatin 50~100 mg/m2 q3w ivgtt, 4-6 cycles. Tislelizumab (200 mg q3w ivgtt) was used as the immune checkpoint inhibitor. The choice of targeted therapy was guided by the findings of genetic testing. Based on the specific genetic alterations identified, appropriate targeted therapies were selected. In this study, gefitinib (250 mg once daily, orally) was administered as a first-generation EGFR-TKI, while osimertinib (80 mg once daily, orally) was utilized as a third-generation EGFR-TKI.

2.11 Statistical analyses

The mutation status of lung cancer patients was visualized using ComplexHeatmap, and statistical analysis was performed using RStudio software (version 4.1.2; RStudio Inc). Independent samples t-tests were employed to compare continuous variables, while chi-square tests were utilized to assess differences in categorical variables. In both cases, a significance level of $P < 0.05$ was used as the threshold to determine statistical significance.

3 Results

3.1 Patient characteristics

A cohort comprising 110 patients with stage I-IIIA NSCLC underwent radical surgery and agreed to undergo postoperative ctDNA-MRD detection. Eleven patients with multiple primary lung cancer, 2 patients with compound carcinoma, 5 patients with previous malignant tumour, and 2 patients with germline inheritance were excluded. A total of 90 NSCLC patients met the inclusion criteria for the analysis, of whom 15 (16.67%) were ctDNA-MRD positive and 75 (83.33%) were ctDNA-MRD negative. The median duration of postoperative follow-up was 240 days, with a range from 120 to 360 days. During this period, no radiographic evidence of recurrence was detected in any of the patients included in the study (Figure 1).

Among the 90 patients with NSCLC, the median age was 55 years (ranging from 35 to 75 years). Out of these, there were 39 male patients (43.33%) and 51 female patients (56.67%). There were 78 patients (86.67%) with lung adenocarcinoma and 12 patients (13.33%) with lung squamous cell carcinoma. Postoperative pathological staging revealed 41 patients (45.56%) with stage IA disease, 5 patients (5.56%) with stage IB disease, 1 patient (1.11%) with stage IIA disease, 12 patients (13.33%) with stage IIB disease, and 31 patients (34.44%) with stage IIIA disease. All 12 patients with squamous cell carcinoma received adjuvant therapy (4 patients received the TP regimen, and 8 patients received TP + tislelizumab). Thirty-two patients with adenocarcinoma received adjuvant therapy (20 patients received the AP regimen, 4 patients received oral gefitinib, and 8 patients received oral osimertinib (Supplementary Table S1).

3.2 Correlation between clinicopathological features and postoperative MRD status

MRD-positive patients had a median age of 52 years (range: 46-55 years), whereas MRD-negative patients had a median age of 55 years (range: 35-75 years). There was no statistical significance between age and postoperative MRD status ($t = 1.5364$, $df = 33.012$, p value = 0.1341) (Table 1). Among the MRD-positive patients, 7 (7/15, 46.67%) were female, and 8 (8/15, 53.33%) were male; among the MRD-negative patients, 44 (44/75, 58.67%) were female, and 31

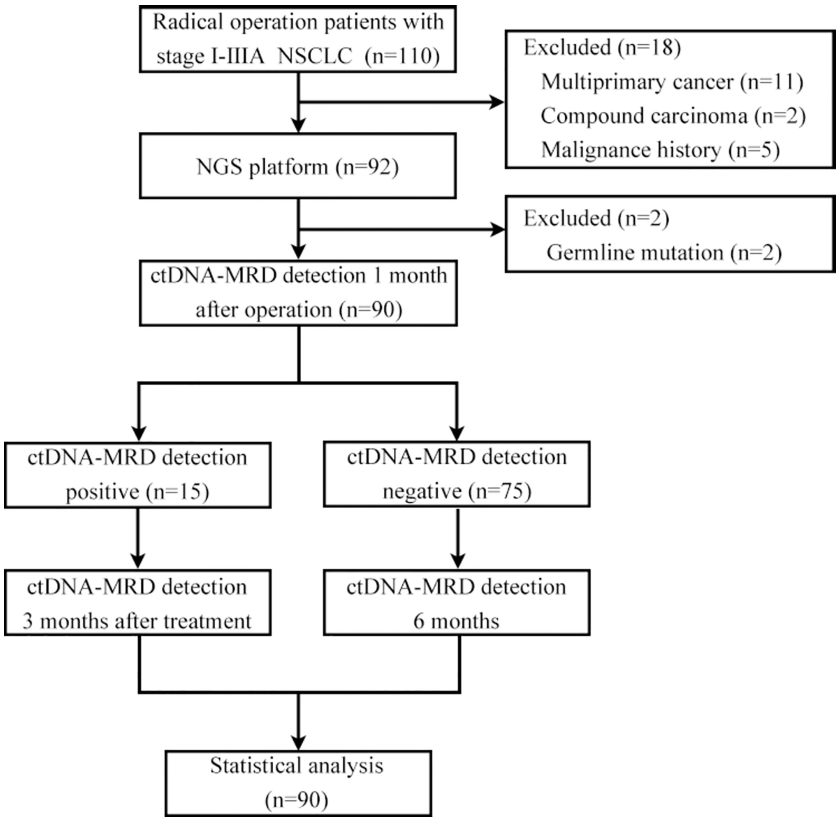

FIGURE 1
Flow chart of patient enrolment.

(31/75, 41.33%) were male. There was no significant difference between sex and postoperative MRD status (X-squared = 0.70769, df = 1, p value = 0.4002) (Table 1). Five MRD-positive patients (5/15, 33.33%) had a smoking history [(smoking index (660 ± 150)], and 13 MRD-negative patients (13/75, 17.33%) had a smoking history [smoking index (940 ± 860)]. The smoking index was not significantly associated with MRD positivity (X-squared = 0.05395, df = 1, p value = 0.8163) (Table 1).

Among the 78 patients with lung adenocarcinoma, 11 (14.10%) had a positive MRD status after the operation, and 67 (85.90%) had a negative MRD status after the operation. Among the 12 patients with squamous cell lung carcinoma, 4 (33.33%) had a positive postoperative MRD status, and 8 (66.67%) had a negative postoperative MRD status. There was no statistical significance between pathological type and postoperative MRD status (X-squared = 0.15624, df = 1, p value = 0.6926) (Table 1).

Among the pathological subtypes of lung adenocarcinoma, there were 16 cases of lepidic predominant adenocarcinoma (LPA) with a negative postoperative MRD status; 41 cases of acinar predominant adenocarcinoma (ACI), including 2 patients (4.88%) with a positive MRD status after surgery and 39 patients (95.12%) with a negative MRD status after surgery; 6 cases of papillary predominant adenocarcinoma (PAP) with a negative postoperative MRD status. There were 4 cases of micropapillary predominant adenocarcinoma (MPA), including 3 patients (75.00%) with a positive postoperative MRD status and 1 patient (25.00%) with a negative postoperative MRD status. There were 11 cases of solid predominant adenocarcinoma with mucin production (SPA), including 6 patients (54.55%) with a positive postoperative MRD status and 5 patients (45.45%) with a negative MRD status. Lung adenocarcinoma patients with higher proportions of SPA and MPA components had a higher rate of postoperative positive MRD status (X-squared = 27.088, df = 5, p value = 0.005) (Table 1). Among the patients with squamous cell carcinoma, 1 case was well differentiated, and the postoperative MRD status of the patient was negative; 8 cases were moderately differentiated, including 2 patients (25.00%) with a positive postoperative MRD status and 6 patients (75.00%) with a negative postoperative MRD status; and 3 cases were poorly differentiated, including 1 patient (33.33%) with a positive MRD status after surgery and 2 patients (66.67%) with a negative MRD status after surgery. There was no significant difference in positive MRD status after surgery among squamous cell carcinoma patients with different tumour differentiation (X-squared = 0.4444, df = 2, p value = 0.800) (Table 1).

We stratified the sample by largest diameter of the lung tumour exceeding 3 cm. There were 61 patients with T ≤ 3 cm, of whom 4 patients (6.56%) had a positive postoperative MRD status and 57 patients (93.44%) had a negative postoperative MRD status. There were 29 patients with T > 3 cm, of whom 11 (37.93%) had a positive postoperative MRD status and 18 (62.07%) had a negative postoperative MRD status. T > 3 cm was positively correlated with positive postoperative MRD status (X-squared = 18.153, df = 3, p value = 0.0004) Table 1).

10.3389/fonc.2023.1222716

TABLE 1 Patient clinical characteristics.

Characteristic	MRD positive	MRD negative	*p* value
Age (years)	52 (46-60)	55 (35-75)	0.1341
Sex			0.4002
Female	7	44	
Male	8	31	
Smoking history			0.8163
YES	5	13	
Smoking index	660 ± 150	940 ± 860	
NO	10	62	
Pathological type			0.6926
LUAD	11	67	
LUSC	4	8	
Pathological subtype (LUAD)			0.007
LPA-based	0	16	
ACI-based	2	39	
PAP-based	0	6	
MPA-based	3	1	
SPA-based	6	5	
Differentiation (LUSC)			0.005
Well Moderate	0 2	1 6	
Poorly	2	2	
TNM staging			0.004
Stage IA	0	41	
Stage IB	0	5	
Stage IIA	0	1	
Stage IIB	3	9	
Stage IIIA	12	19	
Tumour size			0.0040
≤3 cm	4	57	
>3 cm	11	18	
Lymph node metastasis			
LUAD			0.0030
YES	11	16	
NO	0	51	
LUSC			0.0004
YES	4	1	
NO	0	7	
Vascular invasion			0.0002
YES	13	23	

(Continued)

TABLE 1 Continued

Characteristic	MRD positive	MRD negative	*p* value
N0	2	52	
Nerve invasion			0.3636
YES	6	11	
N0	9	64	

LUAD, lung adenocarcinoma; LUSC, lung squamous cells; LPA, lepidic predominant adenocarcinoma; ACI, acinar predominant adenocarcinoma; PAP, papillary predominant adenocarcinoma; MPA, micropapillary predominant adenocarcinoma.

Among the 78 patients with lung adenocarcinoma, 27 had lymph node metastasis, of whom 11 (40.74%) had a positive postoperative MRD status and 16 (59.26%) had a negative postoperative MRD status. Fifty-one patients had no lymph node metastasis, and their postoperative MRD status was negative. Lymph node metastasis was associated with postoperative MRD positivity in lung adenocarcinoma patients (X-squared = 18.153, df = 3, p value = 0.003) (Table 1). Among the 12 patients with squamous cell lung carcinoma, 5 had lymph node metastasis, among whom 4 patients (80.00%) had a positive postoperative MRD status and 1 (20.00%) had a negative postoperative MRD status. Seven patients had no lymph node metastasis, and their postoperative MRD status was negative. Positive postoperative MRD status in patients with squamous cell lung carcinoma was found to be associated with lymph node metastasis (X-squared = 18.153, df = 3, p value = 0.0004) (Table 1).

Of the 36 patients with vascular invasion, 13 (36.11%) had a positive postoperative MRD status, and 23 (63.89%) had a negative postoperative MRD status. Of the 54 patients without vascular invasion, 2 (3.70%) had a positive postoperative MRD status, and 52 (96.30%) had a negative postoperative MRD status. Vascular invasion was associated with positive postoperative MRD status (X-squared = 13.587, df = 1, p value = 0.0002) (Table 1). Of the 17 patients with nerve invasion, 6 (35.30%) had a positive postoperative MRD status, and 11 (64.70%) had a negative postoperative MRD status. Of the 73 patients without nerve invasion, 9 (12.33%) had a positive postoperative MRD status, and 64 (87.67%) had a negative postoperative MRD status. There was no statistical correlation between nerve invasion and postoperative MRD-positive status (X-squared = 4.3802, df = 1, p value = 0.3636) (Table 1).

3.3 Gene mutations associated with postoperative MRD status

Gene mutations detected by NGS in tumour tissue were mainly point mutations, accounting for 88.41% (203 point mutations); fusions and rearrangements accounted for only 11.59% (26 fusions and rearrangements) (Figure 2A). The most frequently mutated genes were EGFR (53%), TP53 (49%), BRAF (13%), NTRK3 (13%), KRAS (11%), ERBB2 (8%), and ALK (7%) (Figure 2B). EGFR, TP53, BRAF, NTRK3, KRAS, ERBB2, and ALK gene mutations were not significantly associated with MRD-positive status (Figures 2B, C; Supplementary Table S2).

3.4 Correlation between immune biomarkers and MRD status

Among MRD-positive patients, 4 patients (26.67%) had a TPS < 1%, and 11 patients (73.33%) had a TPS ≥ 1%; among MRD-negative patients, 58 patients (77.33%) had a TPS < 1%, and 17 patients

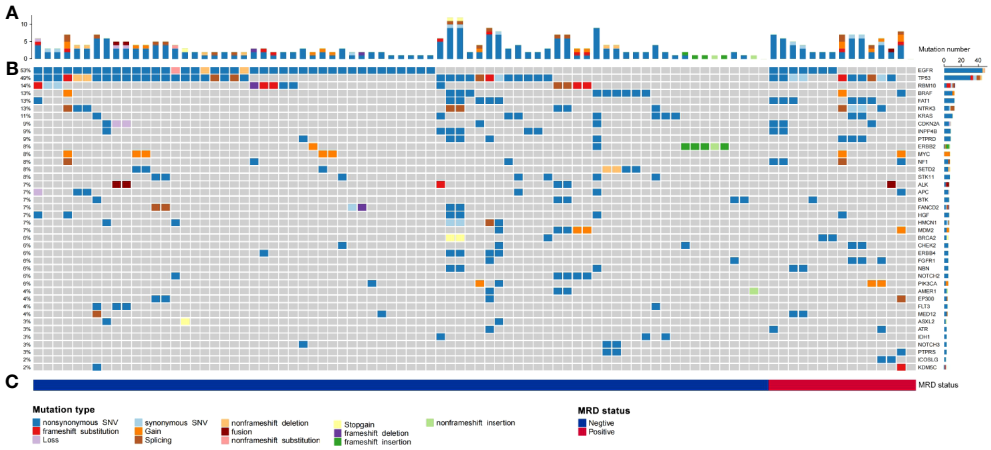

FIGURE 2
Summary of the number of physical mutated genes in tube issue, mutation type, and periodic ctDNA testing in 90 evaluable patients with NSCLC. **(A)** Number of physical mutations in tube issue. **(B)** Candidate driver genes that are frequently mutated in tube issue. **(C)** Patient's mutation type, and MRD status.

(22.67%) had a TPS ≥ 1%. TPS ≥ 1% was significantly associated with postoperative MRD-positive status (X-squared = 4.2558, df = 1, p value = 0.0391) (Figure 3A). Among MRD-positive patients, 5 patients (33.33%) had a CPS < 5, and 10 patients (66.67%) had a CPS ≥ 5; among MRD-negative patients, 59 patients (78.67%) had a CPS < 5, and 16 patients had a CPS ≥ 5. (21.33%). CPS ≥ 5 was significantly associated with postoperative MRD-positive status (X-squared = 0.53321, df = 1, p value = 0.0153) (Figure 3B). Among MRD-positive patients, there were 5 (33.33%) TMB-L patients, 3 (20.00%) TMB-M patients, and 7 TMB-H patients (46.67%); among MRD-negative patients, there were 50 TMB-L patients (66.67%), 15 (20.00%) TMB-M patients, and 10 TMB-H patients (13.33%). No substantial association was observed between TMB and MRD status.(X-squared = 1.8646, df = 2, p value = 0.0636) (Figure 3C). Among MRD-positive patients, 2 (13.33%) were HLA homozygous, 3 (20.00%) were partially HLA homozygous, and 10 (66.67%) were HLA heterozygous; among MRD-negative patients, 4 were HLA homozygous (5.33%), 20 (26.67%) were partially HLA homozygous, and 51 (68.00%) were HLA heterozygous. No significant relationship was identified between HLA expression and postoperative MRD status (X-squared = 4.8062, df = 2, p value = 0.0904) (Figure 3D).

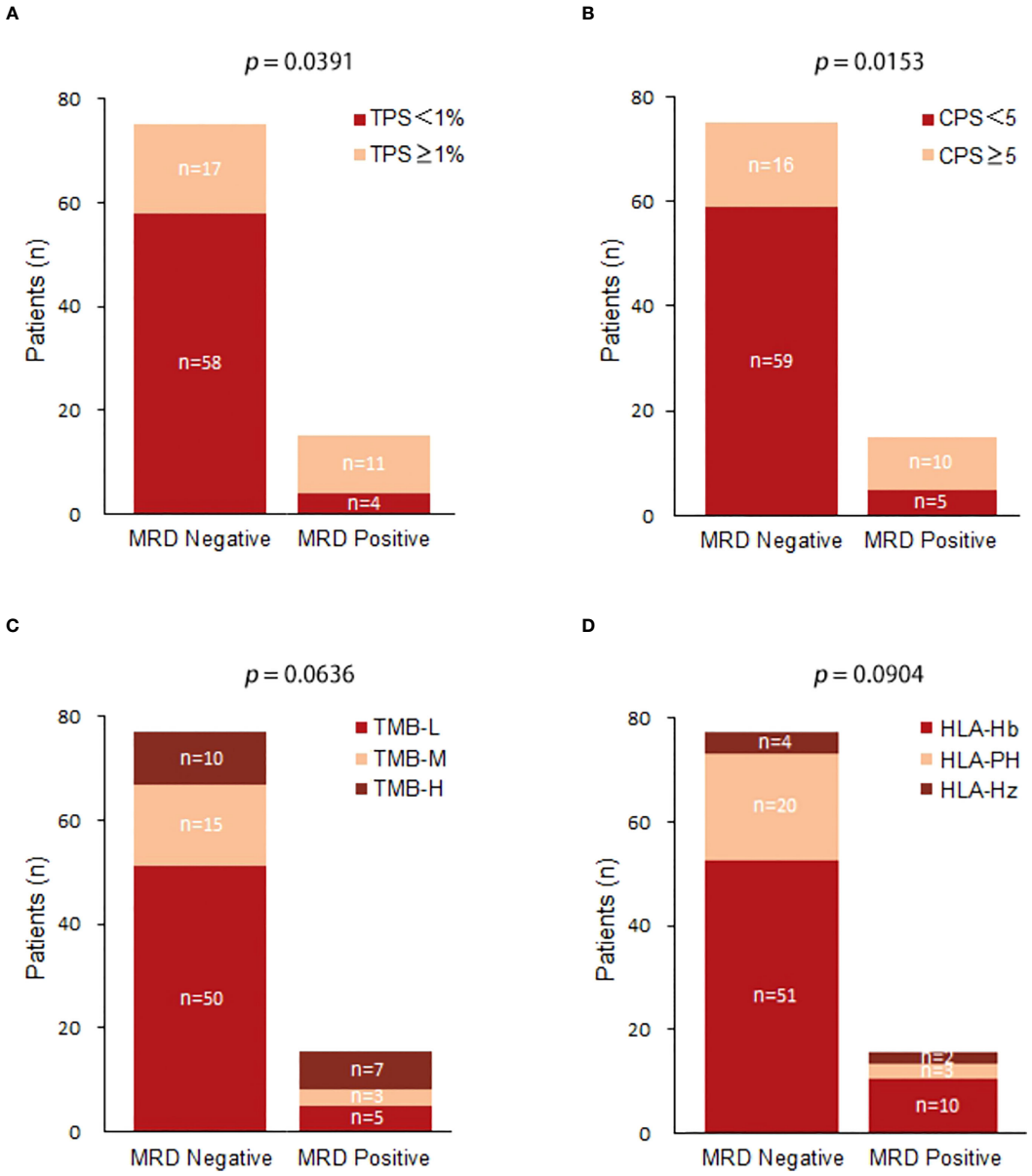

FIGURE 3
(A) Comparison of TPS(Tumor Positive Score) expression between postoperative MRD-positive patients and MRD-negative patients; **(B)** Comparison of CPS(Combined Positive Score) expression between postoperative MRD-positive patients and MRD-negative patients; **(C)** Comparison of TMB expression between postoperative MRD-positive patients and MRD-negative patients.(TMB-L:Tumor Mutational Burden-Low;TMB-M:Tumor Mutational Burden-middle;TMB-H:Tumor Mutational Burden-High); **(D)** Comparison of HLA between postoperative MRD-positive patients and MRD-negative patients.(HLA-Hb : Human leukocyte antigen-;HLA-PH;HLA-HZ).

3.5 MRD status after adjuvant therapy

Of the 11 patients with MRD-positive lung adenocarcinoma, 6 (6/11, 54.55%) were treated with chemotherapy (AP regimen), and 5 (5/11, 45.45%) were treated with EGFR-TKIs (1 with oral gefitinib and 5 cases of oral osimertinib). Among chemotherapy patients, ctDNA abundance decreased after treatment in 5 patients, and ctDNA abundance decreased first and then increased after treatment in 1 patient. The MRD of EGFR-TKI-treated patients became negative (the average treatment time was 126 days). Patients who received postoperative adjuvant EGFR-TKI demonstrated a more effective clearance of ctDNA compared to those who received chemotherapy. (X-squared = 3.2158, df = 1, p value = 0.027) (Figure 4A). All 4 patients with MRD-positive squamous cell carcinoma received chemotherapy + immunotherapy (TP regimen + tislelizumab) after surgery. After treatment, 3 patients were still MRD positive, but ctDNA abundance showed a downwards trend; for 1 patient, MRD status became negative after treatment (Figure 4B).

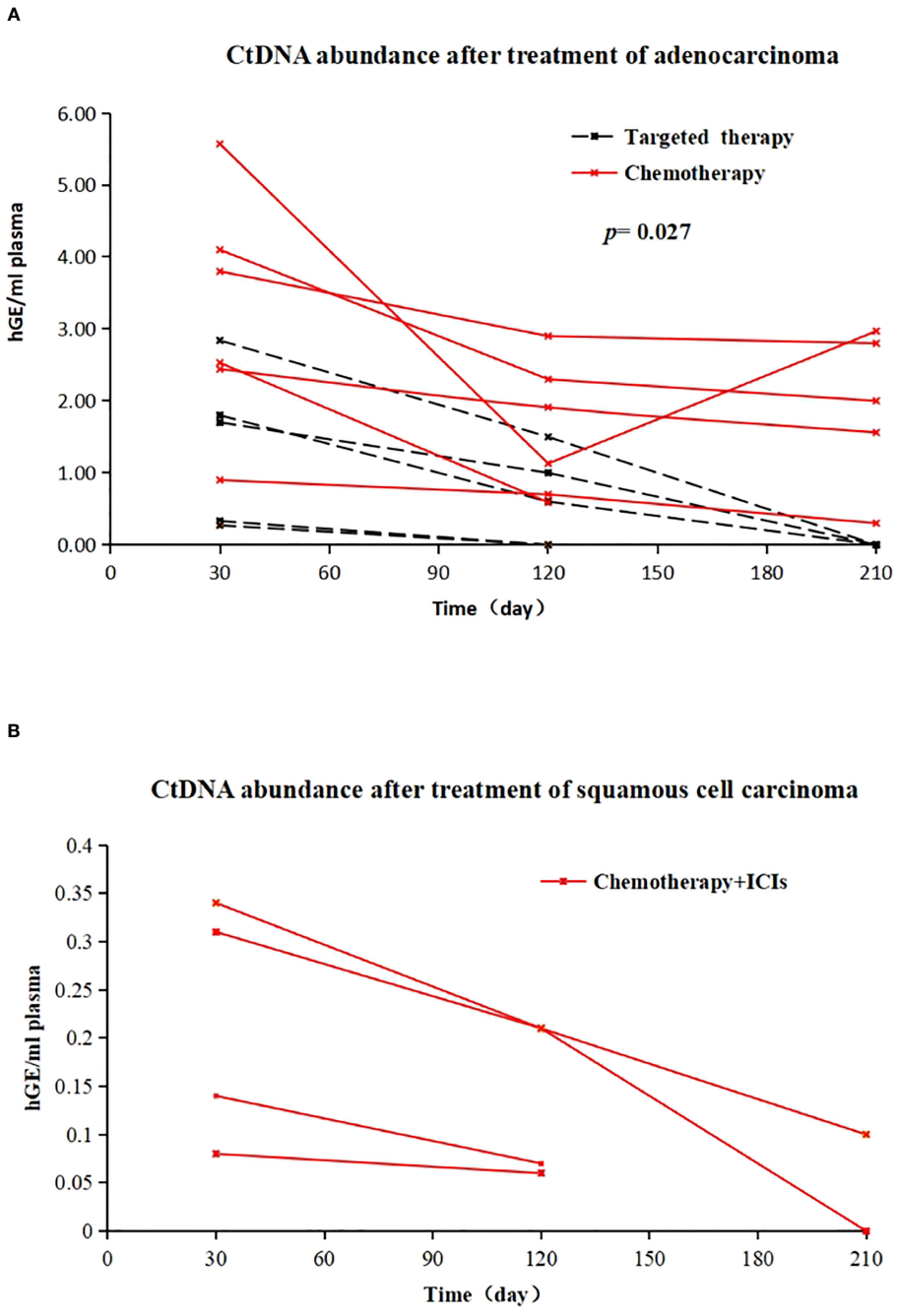

FIGURE 4
(A) Changes in ctDNA abundance after EGFR-TKI treatment (dotted line) and chemotherapy (solid line) in 11 postoperative MRD-positive adenocarcinoma patients; X-axis represents follow-up time, Y-axis represents ctDNA abundance; **(B)** in vivo tumour ctDNA abundance in 4 patients with MRD-positive squamous cell carcinoma treated with chemotherapy + ICIs; X-axis represents follow-up time, Y-axis represents ctDNA abundance.

4 Discussion

With continuous improvements in ctDNA detection technology, postoperative MRD detection has increasingly recognized that liquid biopsy serves as a significant tool for prognostication and assessing treatment response in patients diagnosed with NSCLC (23). For solid tumours, the methods for ctDNA-MRD detection *via* peripheral blood are diverse. Abbosh tracked variations in plasma with tumour-personalized sequencing-focused multidimensional PCR panels. Parikh (24), independent of tumour gene sequencing, established comprehensive genomic and genetic analyses by building a maximized plasma sample bank to identify variant genes in blood. The technical approach by LUNGCA (15) was created on the basis of personalized sequencing, and a negative plasma background reference library was established; each candidate ctDNA mutation was underwent a statistical analysis against an internal reference library. This rigorous assessment was performed to distinguish true somatic mutations from potential confounding germline or CH alterations., in combination with the P value method to determine the MRD status of samples, leading to improved accuracy and reliability in identifying genetic alterations. In this study, the same technical method as that in the LUNGCA study was used to detect ctDNA in peripheral blood, and ctDNA abundance ≥ 0.008% was defined as MRD positive, which is higher than the standard ctDNA abundance ≥ 0.02% required by the expert consensus on MRD in lung cancer. False negatives in MRD interpretations were avoided, which ensured the reliability of the research results.

In the analysis of the basic data of patients, 56.67% of the patients were female, 86.7% of the cancer cases were adenocarcinoma, and 51.3% of the patients had stage I disease, findings that are consistent with the baseline data reported in previous MRD studies (25). This indicates that early-stage female adenocarcinoma is predominant among NSCLC patients currently undergoing surgical treatment. Furthermore, the findings from this investigation indicated no significant associations between postoperative MRD status and patient age, sex, smoking index, or pathological type.

Previous studies have revealed that within the pathological subtypes of lung adenocarcinoma, MPA and SPA types are typically associated with a higher incidence of lymph node metastasis and poorer prognosis (26–29). Our study found that among 78 patients with lung adenocarcinoma, 11 patients (14.10%) had a positive postoperative MRD status; among them, 9 patients had the pathological subtypes MPA and SPA, and the other 2 patients had ACI, but each had 35% micropapillary component and 20% solid component, showing that MPA and SPA were positively correlated with MRD positivity. No significant correlation was observed between the degree of differentiation in squamous cell carcinoma patients and their MRD status., a result that may be due to the small number of squamous cell carcinoma cases. We will supplement these data in a follow-up prospective study.

Our study also revealed a positive correlation between a primary lesion's largest diameter exceeding 3 cm and a postoperative positive MRD status. Previous research has elucidated that in the early stages of lung cancer, nutrients and oxygen are predominantly acquired through diffusion. However, as the tumor volume increases, angiogenesis is induced by the release of vascular endothelial growth factors (VEGFs) to ensure an adequate supply of nutrients (30). The VEGF family includes VEGF-A, VEGF-B, VEGF-C, VEGF-D, VEGF-E, VEGF-F, etc. Among them, VEGF-A plays a pivotal role as a potent regulator of angiogenesis. It exerts control over vascular permeability and facilitates the metastasis of endothelial cells. The close association between VEGF-A and tumor growth and metastasis highlights its significance in tumor progression and dissemination (31). As tumour volume increases, the release of VEGF-A increases, angiogenesis increases, and vascular permeability increases, resulting in an increase in the release of metabolites containing tumour-associated DNA and biologically active micrometastases into the bloodstream (32); these fragments containing tumour genetic material form ctDNA. This is also consistent with the conclusion in this study that tumour size is correlated with postoperative MRD-positive status.

Lymph node metastasis represents an independent prognostic risk factor for patients with lung cancer. The process of lymph node metastasis in lung cancer primarily occurs through two principal mechanisms: the dissemination of tumor cells *via* the lymphatic vessels within the lungs and the induction of lymphangiogenesis by the tumor itself (31, 33). VEGF-C acts as the main driver during lymphangiogenesis, activates the extracellular regulated protein kinases (ERK 1) or ERK2 pathways, plays a significant role in promoting the growth and development of lymphatic endothelial cells (LECs). It facilitates the process of lymphangiogenesis, leading to the formation of new lymphatic vessels surrounding the tumor. Moreover, VEGF-C increases the permeability of peritumoral lymphatic vessels, facilitating nutrient supply and aiding in the growth and progression of the tumor. When multiple lymphatic pathways are established between a tumour and its surroundings, the tumour releases tumour-associated DNA fragments or micrometastases into the blood through lymphatic backflow (34). Furthermore, VEGF-C demonstrates upregulation in numerous cancer cell types and can possess the ability to indirectly trigger infiltration, as well as migration of stromal macrophages in tumours, thereby promoting the metastasis (34, 35). This also explains the positive correlation between lymph node metastasis and postoperative MRD-positive status in this study.

PD-1/PD-L1 plays a crucial role as a coinhibitory signalling pathway that protects cells from autoimmune or inflammatory cell attack in healthy individuals. The correlation between PD-L1 expression and the prognosis of lung cancer patients remains a topic of debate. However, a growing body of research indicates that the PD-1/PD-L1 signaling pathway contributes to oncogene transcription and evasion, ultimately fostering tumor cell survival and proliferation (36). A meta-analysis of 3107 patients with solid tumours by Wu et al. (36) showed that in contrast to patients with negative PD-L1 expression, those exhibiting high PD-L1 expression demonstrated poorer overall survival (OS). Furthermore, the analysis revealed a positive correlation between PD-L1 expression and tumor T stage, with PD-L1 expression being significantly higher in larger-diameter tumors compared to smaller ones. This observation suggests that elevated PD-L1 expression facilitates immune escape by promoting tumor growth and evasion of the immune system. A meta-analysis by Wen et al. (37) included 254 studies with a total of 1819 patients, and the results showed that PD-

L1-positive expression was associated with poorer OS and disease-free survival (DFS) in urothelial carcinoma patients. In this study, among patients with minimal residual disease (MRD), a higher proportion of individuals exhibited PD-L1 tumor proportion score (TPS) ≥ 1% and combined positive score (CPS) ≥ 5, indicating that those with elevated PD-L1 expression experienced a more unfavorable postoperative prognosis.

ADAURA (38) also demonstrated that adjuvant targeted therapy, compared with placebo, after NSCLC surgery has the potential to substantially enhance the DFS outcomes in patients. EVAN (39) showed that in patients with stage IIIA NSCLC with R0 resection and a sensitive EGFR gene mutation, postoperative targeted therapy with erlotinib can benefit patients more than can chemotherapy. This study found that in patients with MRD-positive lung adenocarcinoma, targeted therapy was better than chemotherapy alone for residual ctDNA clearance, which partly provides an explanation for the enhanced DFS and improved prognosis observed in patients undergoing targeted therapy.

Our study has limitations. 1) Given the limited sample size and retrospective nature of this study conducted at a single center, it is important to note that the data may be subject to some degree of skewness. 2) The duration of patient follow-up was relatively brief, and the relationship between MRD status and DFS and OS could not be determined. 3) The effectiveness of postoperative adjuvant therapy for MRD-negative patients still requires evaluation in subsequent studies.

5 Conclusion

In conclusion, our study revealed a correlation between postoperative ctDNA-MRD status in NSCLC patients and various factors including primary tumor size, lymph node metastasis, lung adenocarcinoma subtype, vascular invasion, as well as TPS and CPS for PD-L1 expression. Additionally, among MRD-positive patients, adjuvant EGFR-TKI targeted therapy demonstrated superior clearance of ctDNA compared to chemotherapy. However, further research is needed to validate these findings.

Data availability statement

The original contributions presented in the study are included in the article/Supplementary Material. Further inquiries can be directed to the corresponding author.

Ethics statement

Patients included in this study underwent genetic counselling and signed written informed consent for their data and samples to be used for research purposes. Guiqian International General Hospital Ethics Committee had no objections against this study [project identification codes 2023 Audition No. (01)].

Author contributions

Conceptualization, DD, GX and SZ. Methodology, DD. Formal analysis, WS. Investigation, DD, BJ, WW, QY, TY, MC, LZ and WS. Resources, GX and SZ. Data curation, DD and LZ. Writing—original draft preparation, DD. Writing—review and editing, DD, GX and SZ. Visualization, DD and WS. Supervision, GX and SZ. Project administration, DD. All authors contributed to the article and approved the submitted version.

Conflict of interest

Authors LZ, WS, and GX were employed by the company Genecast Biotechnology Co., Ltd.

The remaining authors declare that the research was conducted in the absence of any commercial or financial relationships that could be construed as a potential conflict of interest.

Publisher's note

Supplementary material

The Supplementary Material for this article can be found online at: https://www.frontiersin.org/articles/10.3389/fonc.2023.1222716/full#supplementary-material

References

1. Zheng R, Zhang S, Zeng H, Wang S, Sun K, Chen R, et al. Cancer incidence and mortality in China, 2016. *J Natl Cancer Center* (2022) 2(1):1–9. doi: 10.1016/j.jncc.2022.02.002

2. Cao W, Chen HD, Yu YW, Li N, Chen WQ. Changing profiles of cancer burden worldwide and in China: a secondary analysis of the global cancer statistics 2020. *Chin Med J (Engl)* (2021) 134(7):783–91. doi: 10.1097/CM9.0000000000001474

3. Gridelli C, Rossi A, Carbone DP, Guarize J, Karachaliou N, Mok T, et al. Non-small-cell lung cancer. *Nat Rev Dis Primers* (2015) 1:15009. doi: 10.1038/nrdp.2015.9

4. Schneider BJ, Ismaila N, Aerts J, Chiles C, Daly ME, Detterbeck FC, et al. Levy b et al: lung cancer surveillance after definitive curative-intent therapy: ASCO guideline. *J Clin Oncol* (2020) 38(7):753–66. doi: 10.1200/JCO.19.02748

5. Yun JK, Lee GD, Choi S, Kim YH, Kim DK, Park SI, et al. Various recurrence dynamics for non-small cell lung cancer depending on pathological stage and histology after surgical resection. *Transl Lung Cancer Res* (2022) 11(7):1327–36. doi: 10.21037/tlcr-21-1028

6. Diaz LAJr., Bardelli A. Liquid biopsies: genotyping circulating tumor DNA. *J Clin Oncol* (2014) 32(6):579–86. doi: 10.1200/JCO.2012.45.2011

7. Chae YK, Oh MS. Detection of minimal residual disease using ctDNA in lung cancer: current evidence and future directions. *J Thorac Oncol* (2019) 14(1):16–24. doi: 10.1016/j.jtho.2018.09.022

8. Chaudhuri AA, Chabon JJ, Lovejoy AF, Newman AM, Stehr H, Azad TD, et al. Zhou l et al: early detection of molecular residual disease in localized lung cancer by circulating tumor DNA profiling. *Cancer Discov* (2017) 7(12):1394–403. doi: 10.1158/2159-8290.CD-17-0716

9. Abbosh C, Birkbak NJ, Wilson GA, Jamal-Hanjani M, Constantin T, Salari R, et al. Rosenthal R et al: phylogenetic ctDNA analysis depicts early-stage lung cancer evolution. *Nature* (2017) 545(7655):446–51. doi: 10.1038/nature22364

10. Ohara S, Suda K, Sakai K, Nishino M, Chiba M, Shimoji M, et al. Hamada a et al: prognostic implications of preoperative versus postoperative circulating tumor DNA in surgically resected lung cancer patients: a pilot study. *Transl Lung Cancer Res* (2020) 9 (5):1915–23. doi: 10.21037/tlcr-20-505

11. Peng M, Huang Q, Yin W, Tan S, Chen C, Liu W, et al. Zou m et al: circulating tumor DNA as a prognostic biomarker in localized non-small cell lung cancer. *Front Oncol* (2020) 10561598. doi: 10.3389/fonc.2020.561598

12. Kuang PP, Li N, Liu Z, Sun TY, Wang SQ, Hu J, et al. Circulating tumor DNA analyses as a potential marker of recurrence and effectiveness of adjuvant chemotherapy for resected non-Small-Cell lung cancer. *Front Oncol* (2020) 10:595650. doi: 10.3389/fonc.2020.595650

13. Chen K, Zhao H, Shi Y, Yang F, Wang LT, Kang G, et al. Perioperative dynamic changes in circulating tumor DNA in patients with lung cancer (DYNAMIC). *Clin Cancer Res* (2019) 25(23):7058–67. doi: 10.1158/1078-0432.CCR-19-1213

14. Wu Yilong LS, Ying C. Zhou qinghua, Wang changli, Wang lvhua, Huang Cheng, han baohui: expert consensus of molecular residual disease for non -small cell lung cancer. *J Evidence-Based Med* (2021) 21(3):129–35.

15. Xia L, Mei J, Kang R, Deng S, Chen Y, Yang Y, et al. Lin Y et al: perioperative ctDNA-based molecular residual disease detection for non-small cell lung cancer: a prospective multicenter cohort study (LUNGCA-1). *Clin Cancer Res* (2022) 28 (15):3308–17. doi: 10.1158/1078-0432.CCR-21-3044

16. Bolger AM, Lohse M, Usadel B. Trimmomatic: a flexible trimmer for illumina sequence data. *Bioinformatics* (2014) 30(15):2114–20. doi: 10.1093/bioinformatics/btu170

17. Lai Z, Markovets A, Ahdesmaki M, Chapman B, Hofmann O, McEwen R, et al. VarDict: a novel and versatile variant caller for next-generation sequencing in cancer research. *Nucleic Acids Res* (2016) 44(11):e108. doi: 10.1093/nar/gkw227

18. Amemiya HM, Kundaje A, Boyle AP. The ENCODE blacklist: identification of problematic regions of the genome. *Sci Rep* (2019) 9(1):9354. doi: 10.1038/s41598-019-45839-z

19. Karczewski KJ, Francioli LC, Tiao G, Cummings BB, Alföldi J, Wang Q, et al. Birnbaum DP et al: the mutational constraint spectrum quantified from variation in 141,456 humans. *Nature* (2020) 581(7809):434–43. doi: 10.1038/s41586-020-2308-7

20. Talevich E, Shain AH, Botton T, Bastian BC. CNVkit: genome-wide copy number detection and visualization from targeted DNA sequencing. *PloS Comput Biol* (2016) 12(4):e1004873. doi: 10.1371/journal.pcbi.1004873

21. Newman AM, Bratman SV, Stehr H, Lee LJ, Liu CL, Diehn M, et al. FACTERA: a practical method for the discovery of genomic rearrangements at breakpoint resolution. *Bioinformatics* (2014) 30(23):3390–3. doi: 10.1093/bioinformatics/btu549

22. Ge H, Liu K, Juan T, Fang F, Newman M, Hoeck W. FusionMap: detecting fusion genes from next-generation sequencing data at base-pair resolution. *Bioinformatics* (2011) 27(14):1922–8. doi: 10.1093/bioinformatics/btr310

23. Qiu B, Guo W, Zhang F, Lv F, Ji Y, Peng Y, et al. Shao y et al: dynamic recurrence risk and adjuvant chemotherapy benefit prediction by ctDNA in resected NSCLC. *Nat Commun* (2021) 12(1):6770.

24. Parikh AR, Van Seventer EE, Siravegna G, Hartwig AV, Jaimovich A, He Y, et al. Miao b et al: minimal residual disease detection using a plasma-only circulating tumor DNA assay in patients with colorectal cancer. *Clin Cancer Res* (2021) 27(20):5586–94. doi: 10.1158/1078-0432.CCR-21-0410

25. Zhang JT, Liu SY, Gao W, Liu SM, Yan HH, Ji L, et al. Lin JT et al: longitudinal undetectable molecular residual disease defines potentially cured population in localized non-small cell lung cancer. *Cancer Discov* (2022) 12(7):1690–701. doi: 10.1158/2159-8290.CD-21-1486

26. Tang Y, He Z, Zhu Q, Qiao G. The 2011 IASLC/ATS/ERS pulmonary adenocarcinoma classification: a landmark in personalized medicine for lung cancer management. *J Thorac Dis* (2014) 6(Suppl 5):S589–596.

27. Wang Y, Zheng D, Luo J, Zhang J, Pompili C, Ujiie H, et al. Risk stratification model for patients with stage I invasive lung adenocarcinoma based on clinical and pathological predictors. *Transl Lung Cancer Res* (2021) 10(5):2205–17. doi: 10.21037/tlcr-21-393

28. Park JK, Kim JJ, Moon SW, Lee KY. Lymph node involvement according to lung adenocarcinoma subtypes: lymph node involvement is influenced by lung adenocarcinoma subtypes. *J Thorac Dis* (2017) 9(10):3903–10. doi: 10.21037/jtd.2017.08.132

29. Zhao Y, Wang R, Shen X, Pan Y, Cheng C, Li Y, et al. Zheng d et al: minor components of micropapillary and solid subtypes in lung adenocarcinoma are predictors of lymph node metastasis and poor prognosis. *Ann Surg Oncol* (2016) 23 (6):2099–105. doi: 10.1245/s10434-015-5043-9

30. Shimoyamada H, Yazawa T, Sato H, Okudela K, Ishii J, Sakaeda M, et al. Woo T et al: early growth response-1 induces and enhances vascular endothelial growth factor-a expression in lung cancer cells. *Am J Pathol* (2010) 177(1):70–83. doi: 10.2353/ajpath.2010.091164

31. Zhao Y, Guo S, Deng J, Shen J, Du F, Wu X, et al. Li X Et al: VEGF/VEGFR-targeted therapy and immunotherapy in non-small cell lung cancer: targeting the tumor microenvironment. *Int J Biol Sci* (2022) 18(9):3845–58. doi: 10.7150/ijbs.70958

32. Ogawa E, Takenaka K, Yanagihara K, Kurozumi M, Manabe T, Wada H, et al. Clinical significance of VEGF-c status in tumour cells and stromal macrophages in non-small cell lung cancer patients. *Br J Cancer* (2004) 91(3):498–503. doi: 10.1038/sj.bjc.6601992

33. Diao X, Guo C, Li S. Lymphatic metastasis in non-small cell lung cancer: recent discoveries and novel therapeutic targets. *Cancer Commun (Lond)* (2022) 42(12):1403–6. doi: 10.1002/cac2.12378

34. Cao R, Ji H, Feng N, Zhang Y, Yang X, Andersson P, et al. Dissing s et al: collaborative interplay between FGF-2 and VEGF-c promotes lymphangiogenesis and metastasis. *Proc Natl Acad Sci USA* (2012) 109(39):15894–9. doi: 10.1073/pnas.1208324109

35. Deng Y, Yang Y, Yao B, Ma L, Wu Q, Yang Z, et al. Paracrine signaling by VEGF-c promotes non-small cell lung cancer cell metastasis *via* recruitment of tumor-associated macrophages. *Exp Cell Res* (2018) 364(2):208–16. doi: 10.1016/j.yexcr.2018.02.005

36. Wu P, Wu D, Li L, Chai Y, Huang J. PD-L1 and survival in solid tumors: a meta-analysis. *PloS One* (2015) 10(6):e0131403. doi: 10.1371/journal.pone.0131403

37. Wen Y, Chen Y, Duan X, Zhu W, Cai C, Deng T, et al. The clinicopathological and prognostic value of PD-L1 in urothelial carcinoma: a meta-analysis. *Clin Exp Med* (2019) 19(4):407–16. doi: 10.1007/s10238-019-00572-9

38. Wu YL, Tsuboi M, He J, John T, Grohe C, Majem M, et al. Kato T et al: osimertinib in resected EGFR-mutated non-Small-Cell lung cancer. *N Engl J Med* (2020) 383(18):1711–23. doi: 10.1056/NEJMoa2027071

39. Yue D, Xu S, Wang Q, Li X, Shen Y, Zhao H, et al. Liu J et al: erlotinib versus vinorelbine plus cisplatin as adjuvant therapy in Chinese patients with stage IIIA EGFR mutation-positive non-small-cell lung cancer (EVAN): a randomised, open-label, phase 2 trial. *Lancet Respir Med* (2018) 6(11):863–73. doi: 10.1016/S2213-2600(18)30277-7

frontiers | Frontiers in Pharmacology

TYPE Original Research
PUBLISHED 31 August 2023
DOI 10.3389/fphar.2023.1212420

OPEN ACCESS

EDITED BY
Ouyang Chen,
Duke University, United States

REVIEWED BY
Tiezheng Qi,
Central South University, China
Weijie Sun,
Anhui Medical University, China

*CORRESPONDENCE
Jun Zhang,
jameszhang2000@zju.edu.cn

†These authors have contributed equally to this work

RECEIVED 26 April 2023
ACCEPTED 09 August 2023
PUBLISHED 31 August 2023

CITATION
Wu C, Yu S, Wang Y, Gao Y, Xie X and Zhang J (2023), Metabolic-suppressed cancer-associated fibroblasts limit the immune environment and survival in colorectal cancer with liver metastasis. *Front. Pharmacol.* 14:1212420. doi: 10.3389/fphar.2023.1212420

Metabolic-suppressed cancer-associated fibroblasts limit the immune environment and survival in colorectal cancer with liver metastasis

Chenghao Wu[1,2†], Shaobo Yu[1,2†], Yanzhong Wang[1,2], Yuzhen Gao[1,2], Xinyou Xie[1,2] and Jun Zhang[1,2*]

[1]Department of Clinical Laboratory, Sir Run Run Shaw Hospital of Zhejiang University School of Medicine, Hangzhou, Zhejiang, China, [2]Key Laboratory of Precision Medicine in Diagnosis and Monitoring Research of Zhejiang Province, Hangzhou, Zhejiang, China

Background: Colorectal cancer liver metastasis is a major risk factor of poor outcomes, necessitating proactive interventions and treatments. Cancer-associated fibroblasts (CAFs) play essential roles in metastasis, with a focus on metabolic reprogramming. However, knowledge about associations between Cancer-associated fibroblasts metabolic phenotypes and immune cell is limited. This study uses single-cell and bulk transcriptomics data to decode roles of metabolism-related subtype of Cancer-associated fibroblasts and immune cells in liver metastasis, developing a CAF-related prognostic model for colorectal cancer liver metastases.

Methods: In this study, Cancer-associated fibroblasts metabolism-related phenotypes were screened using comprehensive datasets from The Cancer Genome Atlas and gene expression omnibus (GEO). Cox regression and Lasso regression were applied to identify prognostic genes related to Cancer-associated fibroblasts, and a model was constructed based on the Cancer-associated fibroblasts subtype gene score. Subsequently, functional, immunological, and clinical analyses were performed.

Results: The study demonstrated the metabotropic heterogeneity of Cancer-associated fibroblasts cells. Cancer-associated fibroblasts cells with varying metabolic states were found to exhibit significant differences in communications with different immune cells. Prognostic features based on Cancer-associated fibroblasts signature scores were found to be useful in determining the prognostic status of colorectal cancer patients with liver metastases. High immune activity and an enrichment of tumor-related pathways were observed in samples with high Cancer-associated fibroblasts signature scores. Furthermore, Cancer-associated fibroblasts signature score could be practical in guiding the selection of chemotherapeutic agents with higher sensitivity.

Conclusion: Our study identified a prognostic signature linked to metabotropic subtype of Cancer-associated fibroblasts. This signature has promising clinical implications in precision therapy for colorectal cancer liver metastases.

KEYWORDS

colorectal cancer liver metastases (CRLM), single cell transcriptome, cancer-associated fibroblasts, metabolism, immunity therapy

Introduction

Liver is the most common site for metastasis of colorectal cancer (CRC), with approximately 50% of CRC patients developing liver metastases (LM) (Hu et al., 2021). Of these patients, 20%–30% have developed liver metastases at the time of initial diagnosis, and there is currently no effective treatment for colorectal cancer with liver metastases. One hallmark of cancer cells is metabolic reprogramming, which involves various metabolic changes that support faster proliferation. Glucose, nucleic acids, and lipids metabolism are all involved in this process (Faubert et al., 2020; Zhang et al., 2021).

The tumor microenvironment (TME) refers to the complex network of cellular and molecular components that surround and interact with tumor cells. It encompasses the intricate interplay between immune cells, such as T cells, B cells, natural killer cells, and macrophages, with tumor and stromal cells. Additionally, the extracellular matrix within the TME provides structural support and influences cellular behavior through dynamic crosstalk with the surrounding cells. The TME also contributes to the metastasis (Lee et al., 2020). Cancer-associated fibroblasts (CAFs) are crucial constituents in the microenvironment of solid tumors (Sahai et al., 2020). Compared to normal fibroblasts (NFs), CAFs exhibit lower contractility and higher ECM remodeling capacity, which secreting more pro-inflammatory mediators, matrix proteins, and immune regulators (Ishii et al., 2016; Lee et al., 2020; Sahai et al., 2020). Additionally, CAFs support tumorigenesis, progression, and metastasis in various ways through their interaction with cancer cells and immune cells.

Cellular metabolic reprogramming is a critical hallmark of malignancy and is most commonly observed in the tumor microenvironment, especially during metastasis. Metabolic reprogramming allows cancer cells to acquire cell-autonomous properties associated with enhanced invasiveness, which facilitate their escape (Faubert et al., 2020). Metabolic reprogramming has been reported to occur not only in tumor cells but also in the TME. Recent evidence has revealed the impact of metabolic interactions between CAFs and tumor cells on tumor metastasis (Faubert et al., 2020). The vast heterogeneity in the functions and sources of CAFs results in the existence of multiple subpopulations, each exhibiting partial functionality. Single-cell RNA sequencing (scRNA-seq), an emerging technology, enables the characterization of the intricate complexity and heterogeneity of distinct CAF subsets across various tumor types (Bartoschek et al., 2018; Friedman et al., 2020). Previous studies of the metastatic process have highlighted the concept of three major CAF subsets that can be dissected by their myofibroblast, inflammatory and/or immunomodulatory, and antigen-presenting activities (Banales et al., 2020; Xing et al., 2021). Nevertheless, the intricate interplay between CAFs and immune cells, as well as the effects of metabolic reprogramming during metastasis, are not yet fully understood, and further study is required to explore more specific CAF subtypes and their functions.

In this study, we identified distinct fibroblast subpopulations based on metabolic analysis at the single-cell level. We identified hub genes that are significantly linked to metabotropic subtypes of cancer associated fibroblasts. Finally, a CAF-related prognostic signature model was created using GEO datasets and demonstrated its roles in predicting outcomes and immunotherapy responses of patients with CRC and colorectal cancer liver metastasis.

Methods

Data source

Single-cell mRNA-sequencing data (Che et al., 2021) were collected from 6 CRC patients, patients numbered COL15, COL 17, and COL18 were patients who received chemotherapy and the others who were not. Bulk RNA-seq datasets GSE41258, GSE39582, GSE103479, GSE38832, GSE192667 and GSE15921 as well as TCGA bulk RNA-seq data with corresponding detailed clinical information were included in our analysis. This study adhered to the guidelines set by the TCGA and GEO databases.

scRNA-seq data processing and analysis

scRNA-Seq data were processed by following Seurat pipelines in R (Hao et al., 2021). Briefly, genes expressed in less than 3 cells, as well as cells expressed less than 250 or more than 3000 genes were filtered out. Cells with high mitochondria and rRNA gene proportions were also excluded. Then, log-normalization was conducted to normalize the data from the 6 samples. The highly variable genes were identified using the FindVariableFeatures function, followed by scaling of all genes. PCA dimensionality reduction was performed to identify anchors. The cells were clustered with a resolution of 0.2. After initial sample integration, cell clustering and annotation, we generated a gene expression and phenotype matrix of 1897 CAF cells from all 111,292 cells.

Metabolism score calculation and CAF subtyping

Metabolic activities of CAFs were evaluated by SCmetabolism packages (Wu et al., 2022). Each CAF cell was scored using the VISION algorithm, and finally the activity scores of the cell in different metabolic pathways were obtained. Second round clustering and subtyping of CAFs cells based on SCmetabolism scores were conducted to identify the heterogeneity of CAFs by Seurat pipelines.

Cell communications analyses

Cell-cell communications based on ligand-receptor interactions were inferred by CellphoneDB (Efremova et al., 2020). To gain more critical cell-cell interactions in the colon cancer tumor microenvironment, we selected receptor-ligand pairs associated with hub genes for further analysis, aiming to explore potential interactions between immune cells. Significantly

differential expressed ligand-receptor pairs ($p < 0.05$) were visualized.

Trajectory analysis

Single-cell trajectories and determination of the continuous process of CAFs were analyzed by Monocle 2.0 package (v 2.10.0) (Jin et al., 2021). Pseudo-temporal analysis was applied to classify cells in pseudo-chronological order using the top 1000 differentially expressed genes in fibroblasts. Subsequently, a branch expression analysis model (BEAM analysis) was used to analyze branch fate-related genes.

Survival analysis using CAFs-related features in bulk RNA-seq datasets

CAFs-associated gene signatures were generated by identifying the marker genes of all CAFs clusters. The activities of these genes in each sample of all CRC datasets were calculated using GSVA. Log-rank test and Cox proportional hazards regression were performed to explore the relationship between CAFs characteristics and patient prognosis, including overall survival (OS) and recurrence-free survival (RFS) rates. Cutoffs for different cell characteristics in different public datasets were determined by the survminer package and used for plotting Kaplan-Meier curves.

Mutation analysis

Mutation data of CRC were obtained from the TCGA, and analyzed using the TCGAbiolinks package (Colaprico et al., 2016). Mutation landscape and lollipop plots were generated using maftools (Mayakonda et al., 2018).

Construction and validation of CAF-related prognostic signatures

We predicted the prognostic characteristics of CRC patients by identifying CAF marker genes from scRNA-seq clusters. Using GSE192667 as training dataset, all CAF marker gene were investigated by univariate Cox regression models for the prognostic evaluation of OS time. Genes with significant prognostic effect ($p < 0.05$) were determined as candidate prognostic genes. The LASSO regression analysis was then used to identify the feature genes and optimize the model to prevent overfitting. Based on the coefficients generated from the LASSO analysis, a risk score was assigned to each colon cancer patient. Finally, we divided all colon cancer patients into high- and low-risk groups based on their risk score by the median. The association between the risk score and OS was assessed using Kaplan-Meier analysis. Heatmaps were generated to visualize the associations between CAF risk scores and candidate genes. The time-dependent prediction accuracy of our model in the training, internal, and external test datasets was evaluated using AUC.

Functional analyses of CAF subtypes

After obtaining differentially expressed genes between CAF subtypes, Metascape (https://Metascape.org) was used for gene set enrichment analysis. To estimate the infiltrating immune cells in the tumor microenvironment, CIBERSORT package was used to infer the relative abundance of immune cells in each sample (Yoshihara et al., 2013). Gene sets of tumor-associated canonical pathways were obtained from previous study (Sanchez-Vega et al., 2018). Activities of these gene sets were generated by single cell gene set enrichment analysis (ssGSEA) for cell state assessment of each tumor sample.

Immunohistochemistry (IHC) staining

Tumor and adjacent tissue samples were fixed in formalin and embedded in paraffin. For IHC staining, sliced samples were deparaffinized and rehydrated. After that, antigen retrieval was performed, and normal goat serum was used for 10 min at room temperature to block non-specific binding site. Each slide was treated with mouse monoclonal anti-human NNMT antibody (1E7, diluted 1:1400) and incubated in 37°C for 40 min. Then, slides were incubated with biotinylated goat anti-mouse antibody for 30 min, and chromogenic reaction was carried out using a diaminobenzidine (DAB) Substrate Kit. Finally, Digital slide scanning system (KF-PRO-005) was used to capture images of IHC. The staining scores of NNMT protein expression were evaluated by two independent pathologists based on their clinical information. The protein expression levels were classified as 0 (no staining), 1+ (weak staining), 2+ (moderate staining), or 3+ (intense staining), and the staining score was calculated by integrating the percentage of positive cells and the respective intensity scores. The staining score ranged from a minimum value of 0 to a maximum value of 300.

Chemotherapy sensitivity and immunotherapy response prediction

Chemosensitivities of high and low CAF score groups were evaluated by oncoPredict (Maeser et al., 2021). Briefly, a ridge regression model with 10-fold cross-validation was built to infer half-maximal inhibitory concentrations (IC_{50}) Value. Pharmacogenomics database Genomics of Cancer Drug Sensitivity (GDSC; https://www.cancerrxgene.org) (Yang et al., 2013) was used to assess the response of CRC patients to chemotherapy. In addition, the Tumor Immune Dysfunction and Exclusion (TIDE) algorithm (Jiang et al., 2018) was implemented to predict immune checkpoint blockade treatment response between the two groups.

Statistical analyses were conducted using R software (v 4.1.0) and data visualizations were generated using appropriate R packages. Non-parametric tests such as the Wilcoxon rank-sum test were used for comparing two groups of continuous variables that did not follow normal distributions, while the Kruskal–Wallis test was used for testing three or more groups. Cox regression was employed to calculate hazard ratios (HR), and Kaplan-Meier

analysis was used for prognostic evaluation. Statistical significance was set at a two-sided p-value of <0.05. Spearman's correlations were determined for correlation analysis ($p < 0.05$, $^{**}p < 0.01$).

Results

Metabolic subtypes of fibroblast in CRC using scRNA-seq data

Six samples obtained from the SMC cohort (GSE178318) were included in our study, which underwent quality control based on cell characteristics and mitochondrial and ribosomal gene expression. Subsequently, dimensionality reduction was performed to classify all cells. T-Distributed Random Neighborhood Embedding (t-SNE) was used to divide the cells into 9 major clusters and 32 more detailed minor clusters (Figure 1A). To further explore the metabolic signature of tumor fibroblasts, we calculated their metabolic signature pathways scores using SCmetabolism and clustered these CAFs based on these scores. Two fibroblast subclusters were identified (Figure 1C), and the important differentially expressed pathways for each cluster were visualized by heatmap for 11 metabolic pathways, including carbohydrate metabolism, energy metabolism, lipid metabolism and other nutrients metabolism (Figure 1D). According to the expression activities of metabolic pathways, two fibroblast subclusters were determined as hypermetabolism CAFs (hyperCAFs) and hypometabolism CAFs (hypoCAFs).

In primary CRC, total CAFs were significantly more abundant than in liver metastases (Figure 1B). Proportions of both CAFs subtypes also were greater in primary tumors than in metastases (Figure 1E). CAF in CRC patients showed significant heterogeneity in different sample, COL12 having a more even proportion in CAFs cells than others (Supplementary Figure S1). However, the proportion of hypoCAFs in other patients was significantly lower than hyperCAFs.

We identified differential expressed genes between clusters (Figure 1F). Hypometabolic CAFs shows higher expression of genes involved in myogenesis and pericyte-associated markers, such as MALAT1. While hypermetabolic CAFs highly expressed THY1, COL1A2, and some metabolism-related genes, such as PLA2G2A and NNMT. We focused on nicotinamide N-methyltransferase (NNMT), which is a cytosolic enzyme that has been identified as a significant metabolic regulator of cancer-associated fibroblasts (Eckert et al., 2019). Our findings were supported by immunohistochemical staining, which revealed that NNMT is predominantly expressed in fibroblasts (Figure 1G). The expression of other metabolism-related genes, including CRABP2, PLA2G2A, OGN, were all highly expressed in hyperCAFs subtypes (Supplementary Figure S2).

Functional heterogeneity, trajectory, cell-cell communication and transcription factors analysis of CAFs in CRC

To describe and explain the functional heterogeneity of the two CAF subpopulations, several sets of genes characterizing the related functions of CAFs were used. Heatmap showed that different metabolic CAF subpopulations were characterized by significant differences in the expression of collagen genes, angiogenesis genes, smooth muscle-related contractile genes, and members of the RAS superfamily (Figure 2A).

Trajectory analysis of CAFs was performed based on the Monocle 2 algorithm to infer the maturation process of CAFs (Figure 2B, Supplementary Figure S3). In particular, we dissected gene patterns involved in CRC cell state transitions. Cell-to-cell communication analysis revealed large-scale interactions between the two CAF subpopulations and other cell types. Hypometabolism CAFs had cellular interactions among hypometabolism CAFs, tumor cells, and endothelial cells (Figure 2C), While hypermetabolism CAFs had the strongest interaction on tumor cells and mast cells (Figure 2C).

We compared different CAF subtypes between CRC and metastasis with genes related to tumor proliferation, metastasis, and progression pathways, to explore whether significant interactions were observed among different cell subsets. The results showed that CAFs, tumor cells, and B cells can participate in a series of functional interactions involving CXCL12 receptor-mediated APP, COPA, and MIF signaling (Figure 2D).

Activity of each transcription factor (TF) and its regulated genes were also inferred in both CAF subtypes. By comparing regulator specificity scores (RSS), we examined key regulators for each cell type and visualized the top 5 regulators (Figures 2E,F). E2F1, RUNX3, and ZNF224 were identified as the top regulators for hypometabolism CAFs, while CREB3L1, NFIB, ARNT, and GTF3A were identified as the top regulators for hypermetabolism CAFs.

Functional and prognostic role of CAF metabolic subtypes signature genes in metastatic CRC

Based on differentially expressed genes (DEG) (Supplementary Table S1) between two CAF subtypes, we performed the functional enrichment analysis using the online gene ontology (GO) enrichment analysis tool Matascape. Highly expressed genes of hypometabolism CAFs were enriched in the regulation of RNA splicing and muscle structure development GO terms, while genes of hypermetabolism CAFs were enriched in the transport of small molecules, cGMP-PKG signaling pathway, and some metabolism-related pathways such as fatty acid degradation (Figures 3A–D).

To investigate the association between CAF subtypes signatures and overall survival (OS) and recurrence-free survival (RFS) of CRC patients, we computed metabolic subtype scores for CAF subtypes by GSVA. Prognostic analysis was performed on all differentially expressed genes (DEGs) across nine publicly available cohorts that were classified into three types according to the metastasis status (i.e., primary tumor cohort, tumor cohort with metastases, and tumor cohort with liver metastases). We conducted a meta-analysis to obtain stable prognostic results for CAF subtypes, and compared our metabolic subtypes with Pan-CAF signatures derived from previous studies (Galbo et al., 2021). Our analysis revealed significant differences between subgroups in hypometabolism CAF scores compared to hypermetabolism CAF scores, in relation to RFS and OS. As a result, we defined hypometabolism CAF-type cells as a class of cells that are specific to colorectal cancer patients with LM.

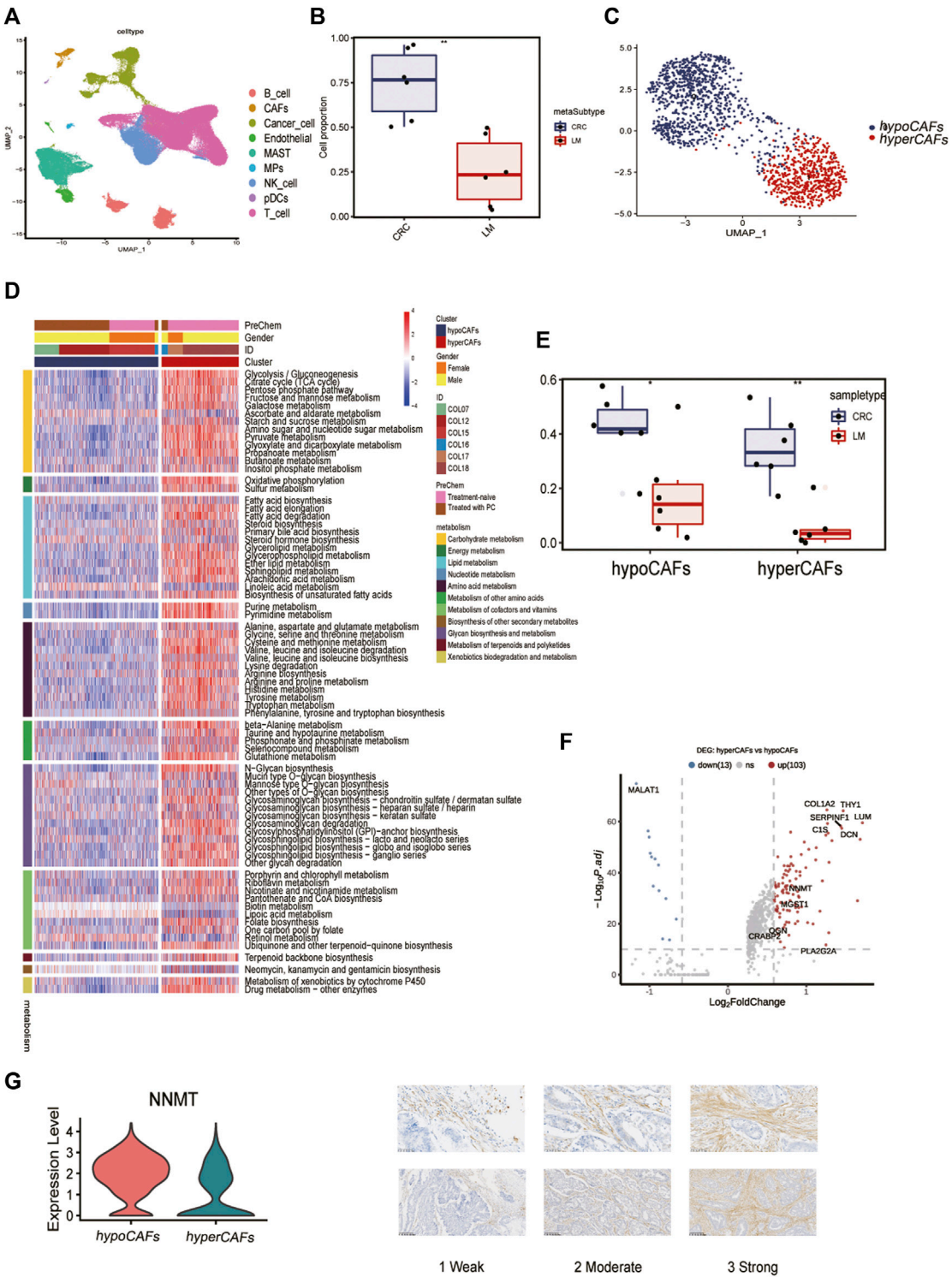

FIGURE 1
Single-cell transcriptome analysis and functions of CAF-related genes. **(A)** Nine cell subsets are shown. **(B)** Boxplot showing the difference between primary and metastatic lesions. **(C)** UMAP plot showing the metabolic grouping of CAF cells. **(D)** Heat map showing differences in 11 metabolic pathways between different metabolic groups. **(E)** Boxplots showing the differences between primary CRC and liver metastases in hypoCAFs and hyperCAFs. **(F)** Volcano plot highlighting the signature genes of different clusters. **(G)** Immunohistochemistry showing NNMT gene expression in fibroblasts.

10.3389/fphar.2023.1212420

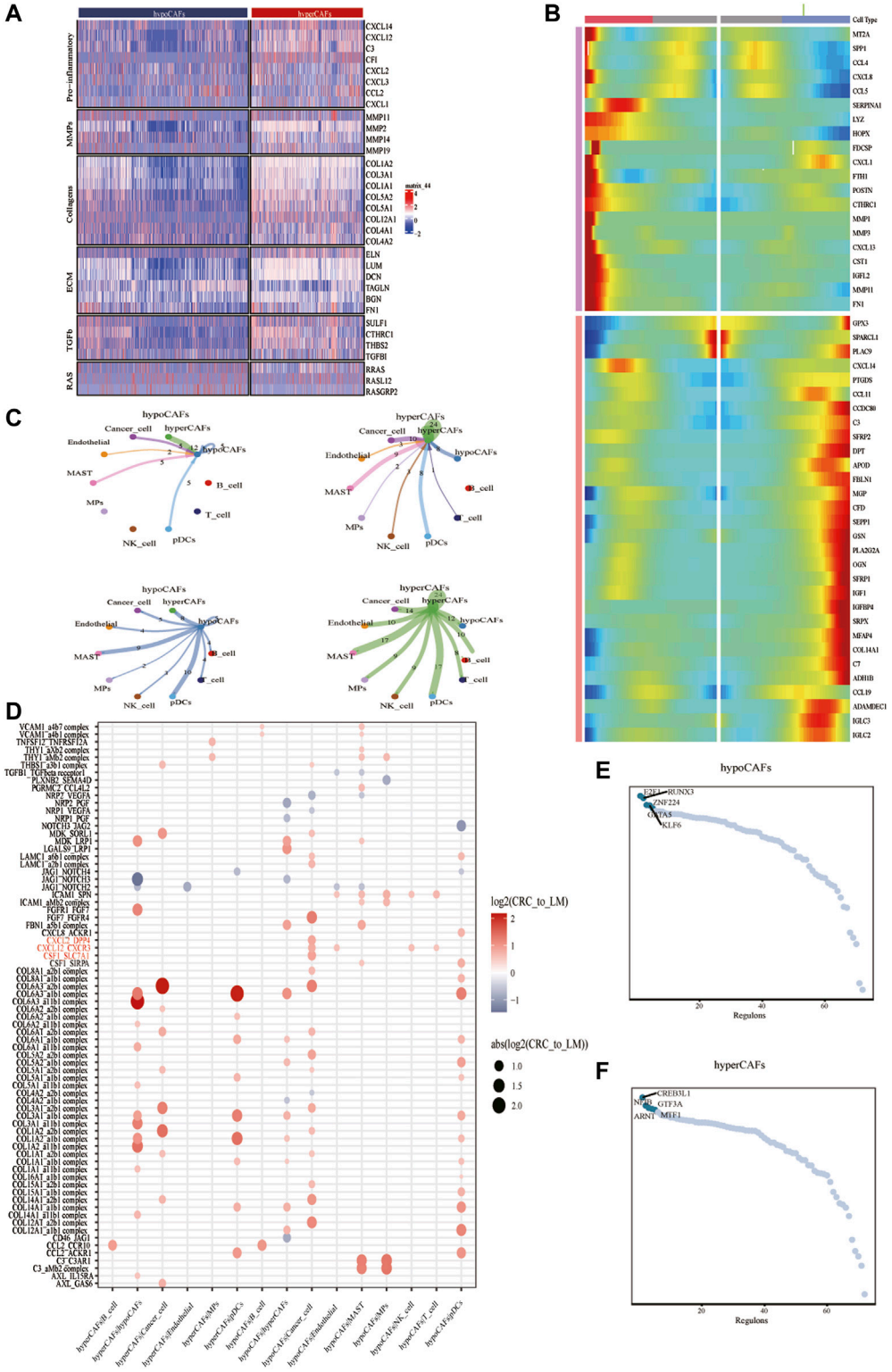

FIGURE 2
Analysis of cellular communication in the TME of CAF cell populations in other different metabolic states. **(A)** Correlations between CAF clustering characteristics and cytokines including chemokines, interleukins, and other cytokines. **(B)** Heat map showing that CAF cells can exhibit two expression patterns after differentiation. **(C)** Shows the number of ligand-receptor pairs between CAF and other subclusters. **(D)** Shows a comparison of specific ligand-receptors between CAF clusters and other subclusters in primary and liver metastases. **(E)** Regulator-specific scores for regulon activity of CAF isoforms.

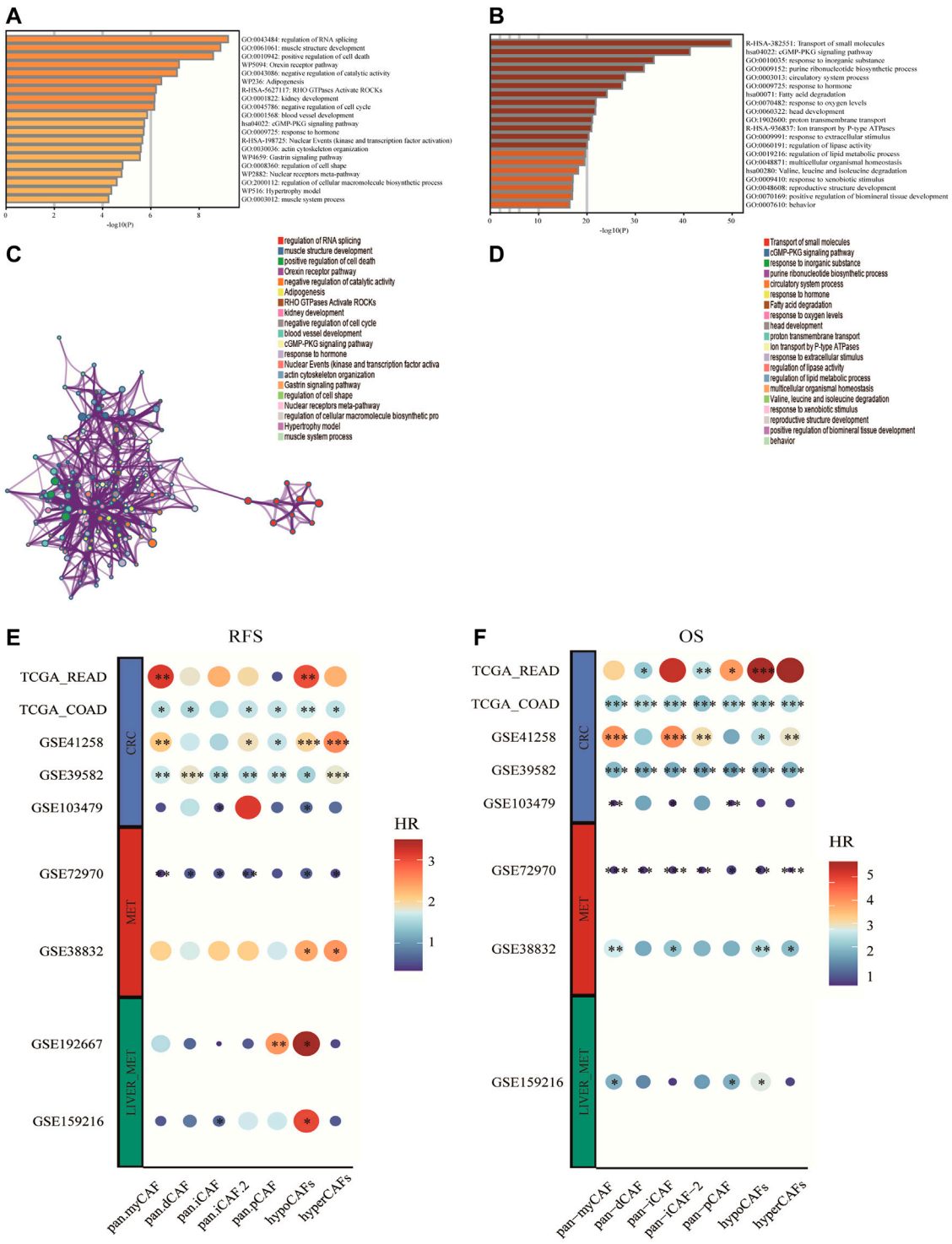

FIGURE 3
Enrichment analysis of CAF cell subgroups and prognosis **(A,B)** Enrichment analysis and corresponding networks of differentially expressed associated genes in CAF subgroups. **(C,D)** Prognosis of CAF cluster (GSVA score). The cut-offs were calculated by the survival R packages. RFS analysis (data from 9 CRC cohorts); B OS analysis (data from 8 CRC cohorts).

Construction and validation of metabolism-CAF score based on metabolism subtypes of CAFs

To explore the prognostic genes associated with hypoCAF, we selected 20 genes based on the univariate Cox regression analysis in the GSE159216 dataset (Figure 4A). These 20 genes underwent Lasso-Cox regression analysis with 10-fold cross-validation to generate the optimal model, which highlighted 13 genes with the smallest partial likelihood deviation and optimal regression efficiency, including TINAGL1, ADIRF, ELP6, CSRP2, PPP1R15A, PABPN1, PHLDA1, ID3, KNOP1, DSTN, PPP1R10, CCDC107, and UBALD2. The risk score was calculated using the formula, and applied to GSE159216, TCGA, and GSE72970 datasets. Results indicated that colorectal cancer patients with high risk score had a higher mortality rate (Figures 4C–E). Heatmap results showed significant differences in the 13 genes expression between two risk score groups.

According to KM curves, patients in the high risk score group had lower survival rates than those in the low risk score group (Figures 5A–C). We also performed time-dependent ROC analysis, with the AUC values of our model in the training set for 1-year, 3-year, and 5-year overall survival being 0.85, 0.78, and 0.80, respectively (Figure Figure5A). In TCGA, the AUC for our 1-, 3-, and 5-year survival models were 0.66, 0.67, and 0.64, respectively, while in the GSE72970 dataset, the AUC values for 1-, 3-, and 5-year survival models were 0.74, 0.75, and 0.74, respectively. Cox regression analysis in three cohorts showed CAF score model would be an independent prognostic marker for CRC with LM (Figure 5G). We developed a nomogram based on CAF score to predict overall survival in CRC patients at 1, 3, and 5 years (Figure 5H). The calibration curves for each time point showed excellent predictive performance.

Biological features of Metabolism-CAF score

We analyzed the correlation between the hypoCAFs signature score and several pathways, the score was negatively correlated with most of the metabolic-related

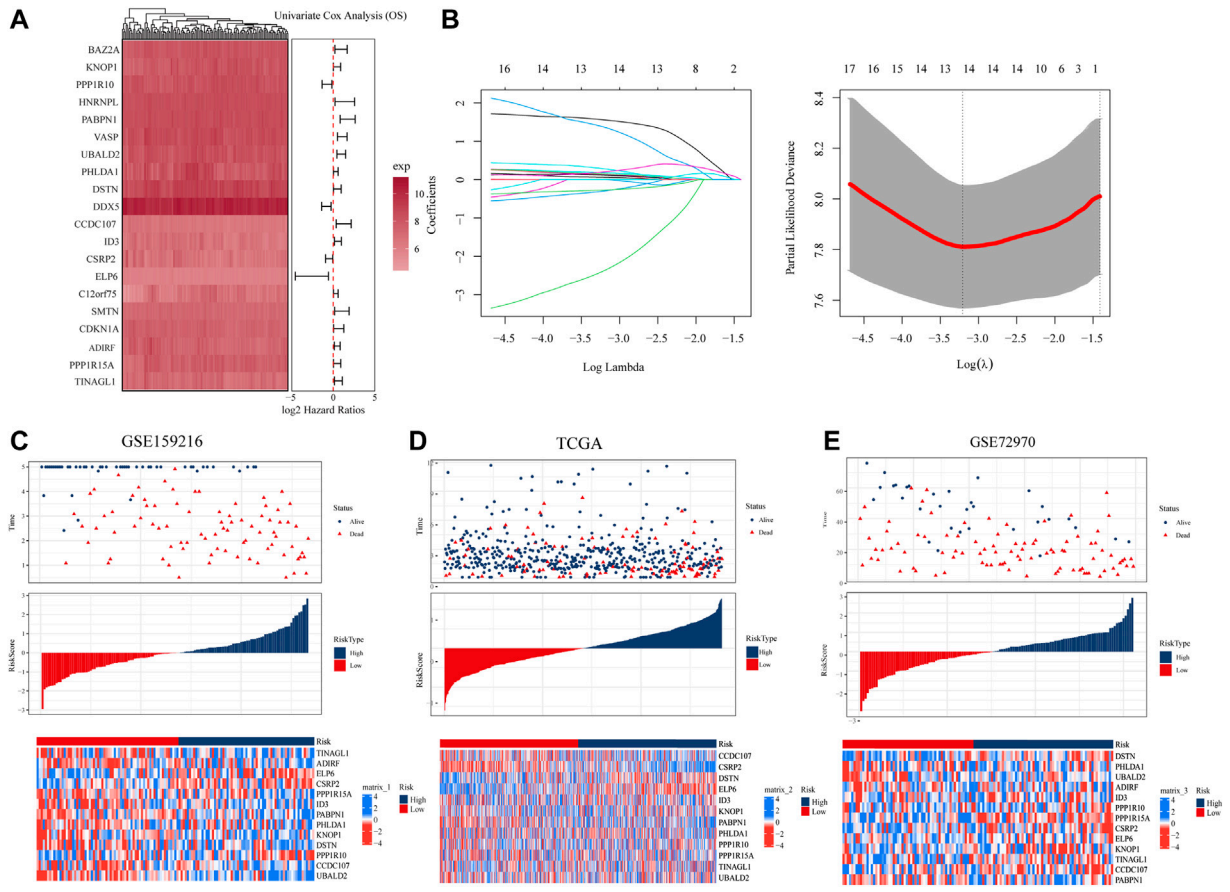

FIGURE 4
Construction and evaluation of prognostic risk model. **(A)** In the GSE159216 dataset, 20 genes were selected for analysis by univariate Cox regression. **(B)** The ten-fold cross-validation and LASSO coefficient distribution used to screen the optimal parameter (lambda) was determined by the optimal lambda. **(C)** Differences in overall survival between high-risk and low-risk groups in the GSE159216 training cohort. **(D)** Difference in overall survival between high-risk and low-risk groups in the TCGA validation cohort. **(E)** Differences in overall survival between high-risk and low-risk groups in the GSE72970 validation cohort.

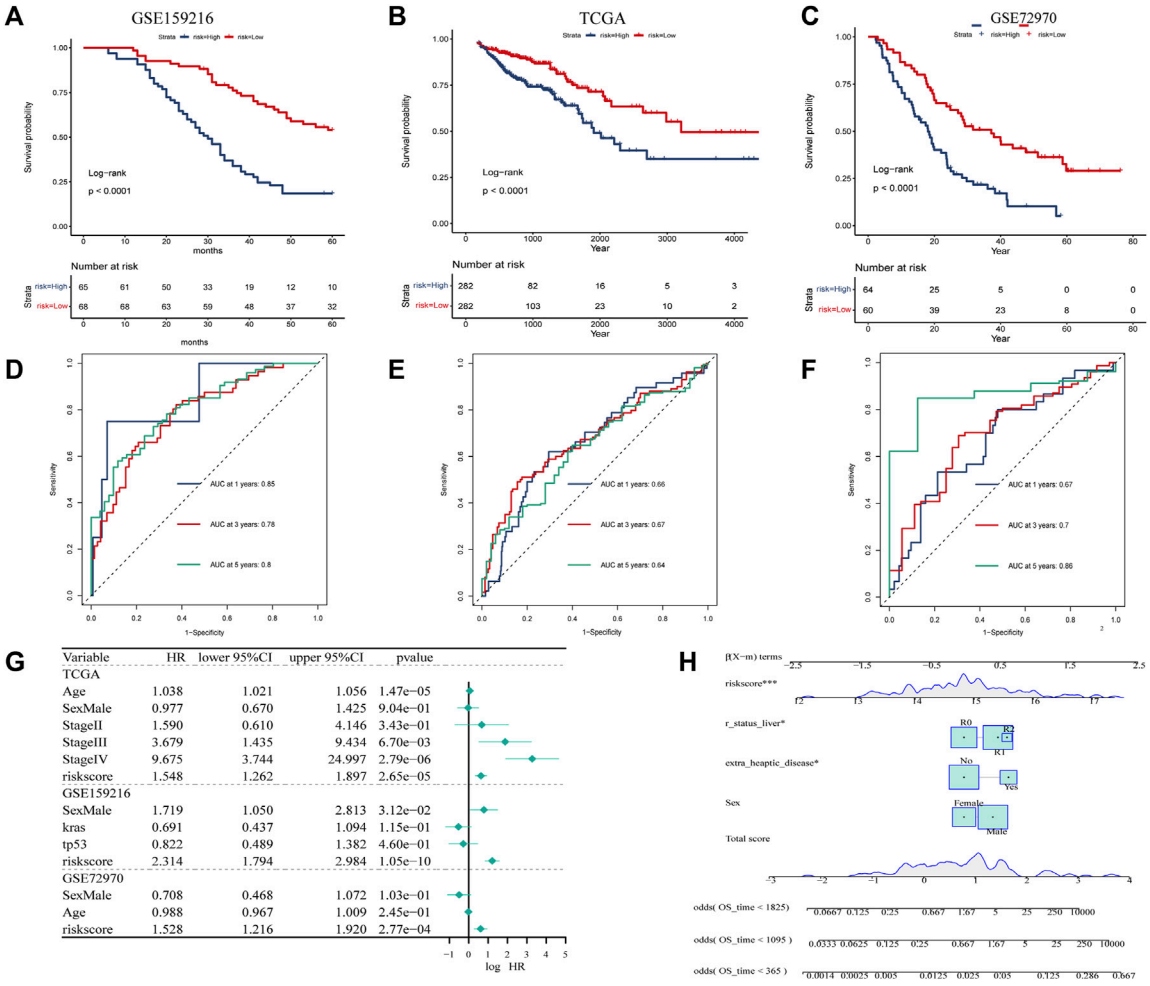

FIGURE 5
Creation of CAF-related prognosis and nomogram. **(A–C)** Kaplan-Meier prognostic analysis of signatures across training, testing, and entire datasets. **(D–F)** Time-dependent ROC signature curves in the training, testing GSE159216, TCGA and GSE72970 datasets. **(G)** Univariate Cox regression in the GSE159216, TCGA and GSE72970 cohorts.

pathways. It was also negatively correlated with some cancer-related pathways such as cell cycle, gene duplication, homologous recombination, and p53 signaling (Figure 6A).

After deconvolution analysis, samples with low CAF scores exhibited high levels of activated memory CD4 T cells and memory B cells, while samples with high CAF scores showed high expression levels of regulatory T cells and resting memory CD4 T cells. To evaluate immune competence, we examined the expression of immune checkpoints (CD274, CTLA4, HAVCR2, IDO1, LAG3) and immune competence factors (CD8A, CXCL10, CXCL9, GZMA, GZMB, IFNG, PRF1, TBX2, and TNF) (Figure 6B). The CAF score demonstrated a negative correlation with 14 out of 75 immunomodulators and 24 immune cells (Figure 6B). Finally, we compared the immune score (Figure 6D), ESTIMATE (Figure 6E), and stroma score (Figure 6F) between samples with high and low CAF scores, and observed that high CAF score samples exhibited elevated matrix and ESTIMATE scores.

Immunotherapy prediction of metabolism-CAF score

To explore the role of CAF score in immunotherapy, we investigated the correlation between risk score and TMB. Our findings revealed that TMB expression was significantly higher in the low-risk subgroup than in the high-risk subgroup (Supplementary Figure S4). Moreover, to gain further insights into the nature of immunity in different risk subgroups, we analyzed genetic mutations. The top 20 genes with the highest mutation rates were identified in both the high-risk and low-risk subgroups (Supplementary Figure S4).

For ICB response prediction, we determined the correlations of CAF scores with TIDE, dysfunction, exclusion, and MSI Expr signature (Figures 7A–D). The results showed that CAF scores were positively associated with TIDE, dysfunction and exclusion, and negatively associated with MSI Expr sig. It was found that CRC patients with lower hypoCAFs scores had a higher possibility

10.3389/fphar.2023.1212420

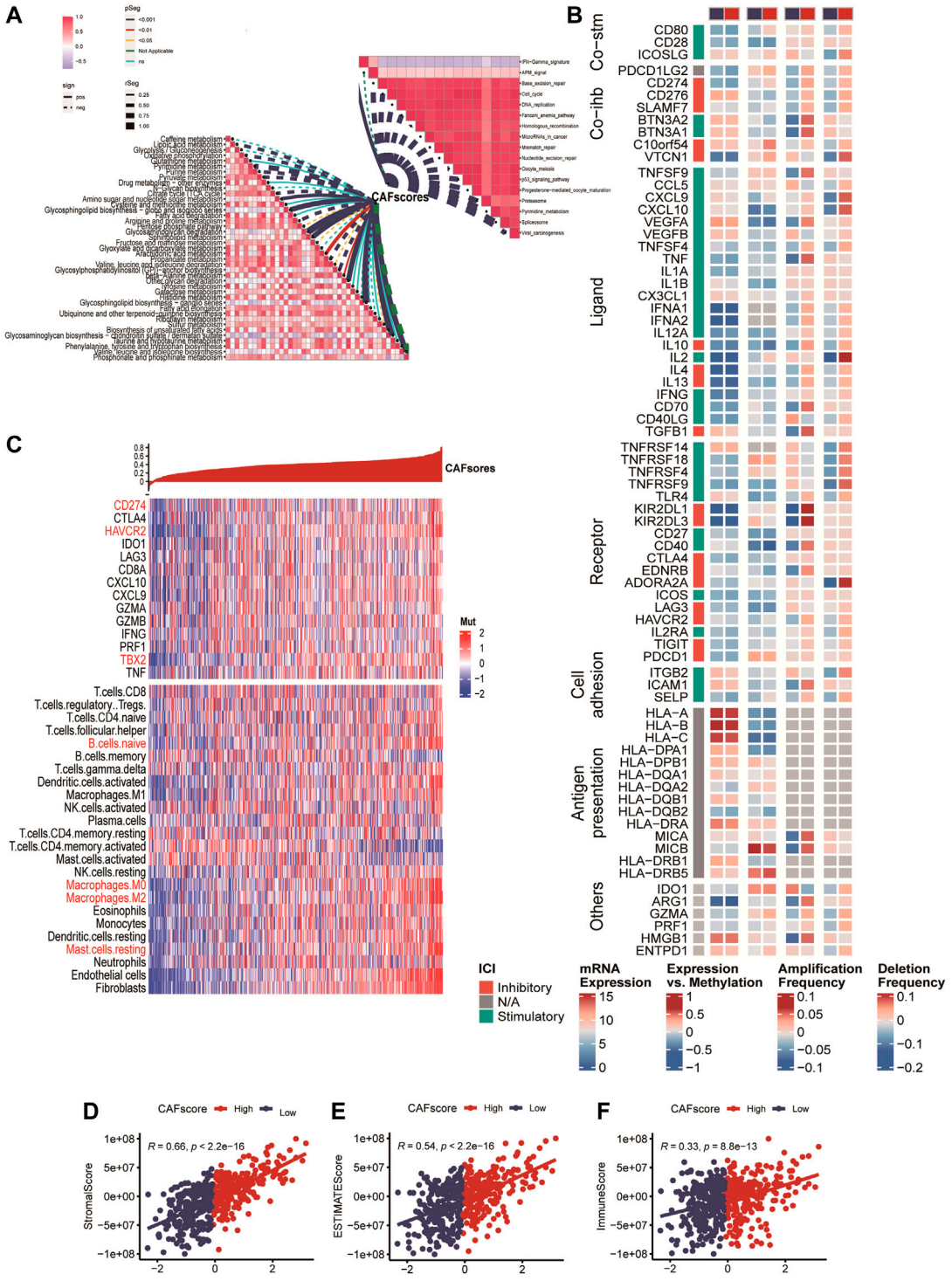

FIGURE 6
Immune analysis of the CAF-related scoring model. **(A)** Correlations between CAF score feature scores and metabolic pathways, immune-related pathways based on GSVA of GO and KEGG terms. **(B)** Multi-omics analysis of 75 immunomodulators between high and low CAF score samples. **(C)** Expression and Pearson correlations of immunity, ESTIMATE, stroma score, tumor purity, TIC, checkpoints and immune competence for each sample are illustrated in a heatmap.

of responding to immunotherapy and may had better prognosis after immunotherapy, indicating that patients with lower CAFs scores were more likely to benefit from immune checkpoint therapy (Wilcoxon test, $p = 0.0001$, Figures 7E–H).

The expressions of five immune checkpoint molecules (PD1, PD-L1, CTLA4, LAG3 and HAVCR2) were compared between groups with high and low CAF score, the results showed that four immune checkpoint molecules (PD1, PD-L1, LAG3, and HAVCR2) were significantly

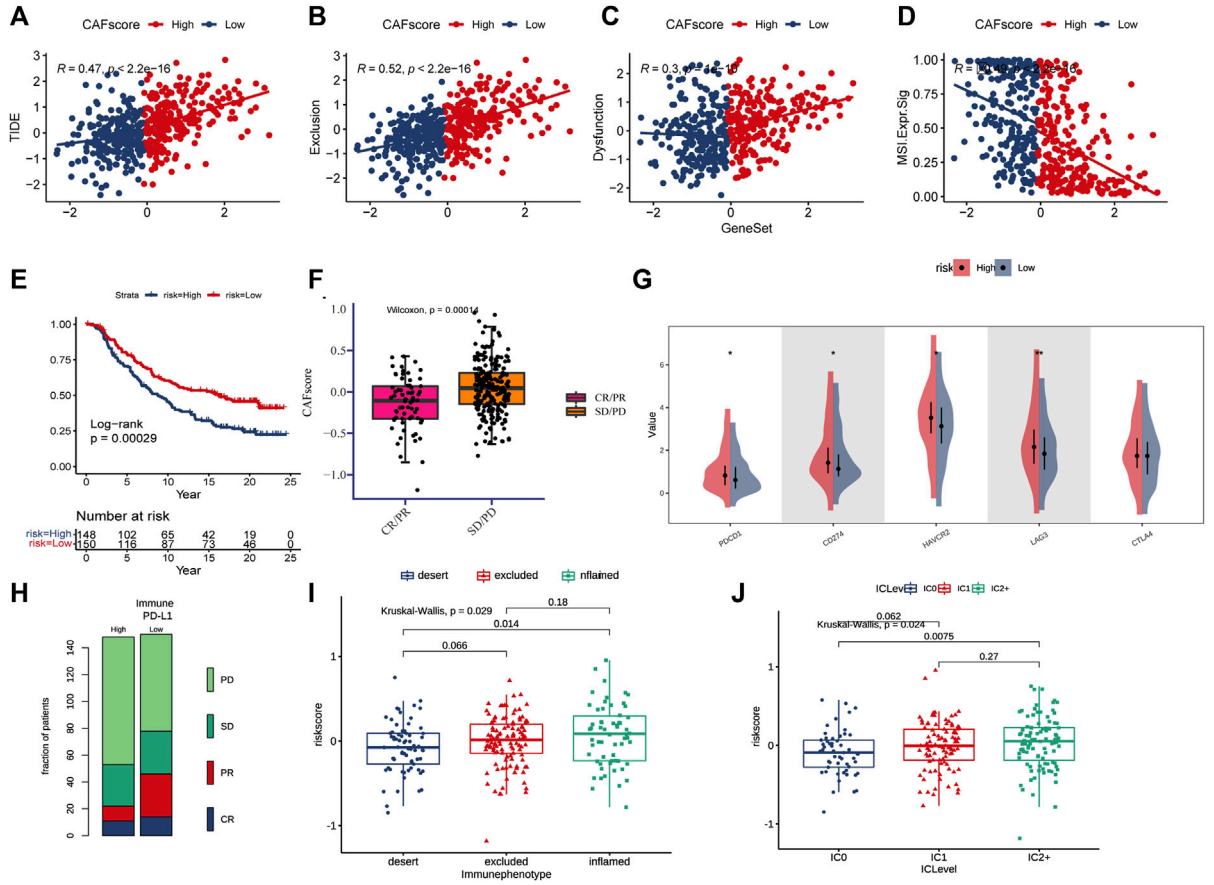

FIGURE 7
CAF score in predicting immunotherapy effect. **(A–D)** Correlations between CAF score and TIDE, dysfunction, exclusion, and MSI expression signatures. **(E)** Kaplan-Meier curve *versus* IMvigor210 survival analysis. **(F)** Wilcoxon test of anti-PD-L1 reactive CAF score variation. **(G)** Expression of 5 immune checkpoint molecules (PDCD1, CD274, CTLA4, LAG3, and HA VCR2) in high and low CAF score groups **(H)** Stacked histogram showing anti-PD-L1 between high and low CAF score difference in reactivity. **(I)** CAF score was tested at three scorch levels using the Kruskal–Wallis test. **(J)** Kruskal–Wallis test of the CAF score of PD-L1 expression on immune cells.

upregulated in the high-risk group (Figure 7G). Furthermore, CAF score was strongly associated with the desert and inflamed immunophenotype (Kruskal–Wallis, $p = 0.0029$, Figure 7I). Our study also found that CAF score was positively correlated with PD-L1 expression in tumor cells and PD-1 expression in immune cells (Figure 7J).

GDSC investigation of metabolism-CAF score

Chemotherapy is the main treatment options for colorectal cancer liver metastases, therefor, whether CAF scores can accurately predict chemotherapy outcomes in colorectal cancer patients was investigated. GDSC is used to predict response to conventional chemotherapy in patients with colorectal cancer liver metastasis. A ridge regression model was built to predict IC_{50} of different drugs. We found that the IC_{50} of cisplatin, gemcitabine and other chemotherapeutics in the high CAF score group were significantly lower than those in the low CAF score group, suggesting that CAF score was positively correlated with chemotherapeutic drug sensitivity of colon cancer liver metastasis. In addition, we used the database to predict small molecule drugs (Figure 8B). The drugs vemurafenib, PLX-4720, dasatinib, and PI-103 were found to be negatively associated with the CAF score, with lower estimated AUC values in samples with high CAF score. These findings suggest that the predicted small-molecule drugs may be more effective in patients with high CAF score.

Discussion

Growing evidence suggests that CAFs are key players in CRC metastasis. Meanwhile, metabolic reprogramming has profound effects on CAFs, thereby regulating cancer progression and metastasis, including glucose, glutamine and fatty acid metabolism (Zhu et al., 2022). A previous scRNA-seq study showed that CAFs identified in PDAC patients have a highly activated metabolic state. The new CAF subtype, called metabolic CAF (meCAF), uses glycolysis as the primary metabolic mode. Although PDAC patients with abundant meCAF have a higher risk of metastases, they have better immunotherapy responses when treated with programmed cell death protein 1 (PD-1) blockade (Wang et al., 2021). Downregulation of metabolism genes in CAFs of PDAC liver metastasis, but not those in

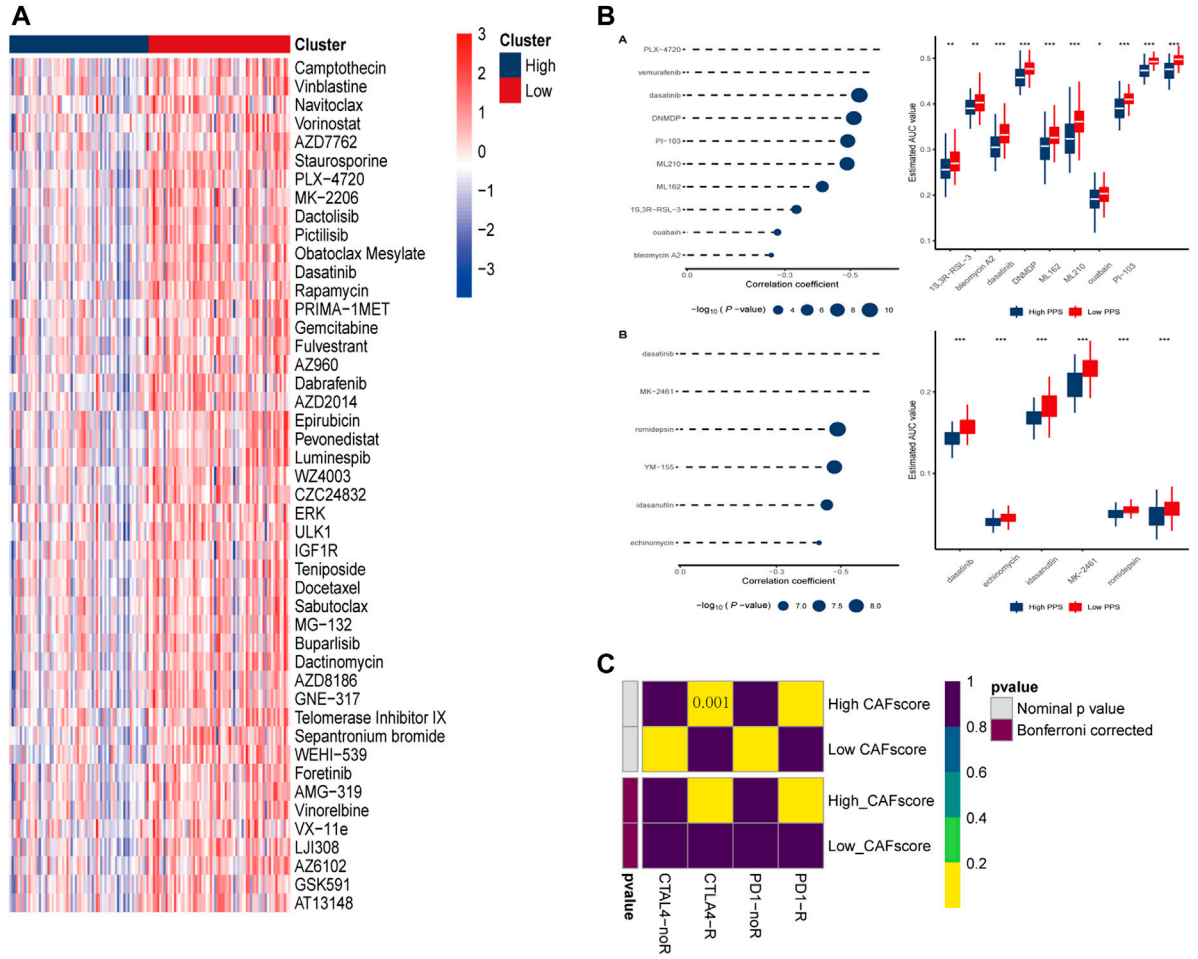

FIGURE 8
Prediction of drug and immune responses. **(A)** Heatmap showing IC_{50} estimates for high and low CAF scores. **(B)** Predicted and estimated AUC values for small molecule drugs in CTRP 2.0 and PRISM databases. **(C)** Immune responses to PD1 and CTLA4 in patients with high and low CAF scores.

lung metastasis, appeared to be regulated by DNA methyltransferase, CAFs metabolism modification may promote PDAC with organ-specific metastatic (Pan et al., 2021). However, the combined effects of fibroblasts with different metabolic status in colorectal cancer liver metastasis are unclear. Studying the role of metabotropic CAF-related gene signatures in the occurrence and development of colorectal cancer liver metastases may contribute to decode the mechanisms of liver metastases and guide appropriate treatment strategies for patients. Cancer-associated fibroblasts are important members of the TME, and previous studies have shown that CAFs with different molecular characteristics were classified into myCAF, pan-dCAF, pan-iCAF, pan-nCAF and pan-pCAF (Galbo et al., 2021). In our study, we identified prognostic CAF populations through single-cell transcriptomes, and these subtypes exhibited distinct activation of metabolism-related pathways, such as glucose metabolism, gluconeogenesis, cysteine and methionine metabolism, etc. In addition, we found that different CAF cells also exhibit extensive interactions with T cells, NK cells, and tumor cells through growth factors and cytokines, thereby promoting tumor progression (Jiang et al., 2021). Cellular communication has shown that the CXCL12-CXCR4/CXCR7 chemokine axis is expressed in hyperCAFs and is significantly expressed in metastases. CXCL12 not only binds to CXCR4, but also to CXCR3 and DPP4 on tumor cells in our study, which is consistent with previous reports (Jiang et al., 2021). Li et al. (Li et al., 2022) pointed out that inflammatory CAFs secrete IL6 and CXCL12 to chemoattract and regulate the function of T cells, which is similar to inflammatory CAFs found in other solid tumors. Costa et al. (Costa et al., 2018) identified differentially expressed secretory molecules, such as CCL11, CXCL12, CXCL13, and CXCL14, in CAF-S1 and CAF-S4 cells in breast cancer. CXCL12 can be produced by hyperCAF, the binding of CXCL12 to tumor cells can inhibit tumor cell apoptosis and change the characteristics of tumor cell adhesion (Augsten et al., 2014; Zhao et al., 2017). HyperCAFs also express the CXCL14, elevated CXCL14 levels in CAFs of clinical specimens are also associated with higher risks for disease recurrence and worse overall survival time in colorectal cancer (Zeng et al., 2013).

Many studies have reported the role of RUNX3 in inhibiting cancer cell migration and tumor growth (Kim et al., 2020). A study reveals that CAF-derived exosomal miR-17-5p promotes an aggressive phenotype in colorectal cancer by initiating a RUNX3/MYC/TGF-β1 positive feedback loop (Zhang et al., 2020). In another study, circMEttL3, which is transcriptionally activated by RUNX3, suppressed CRC development and metastasis by acting as a miR-107 sponge to regulate PER3 signaling

(Zhang et al., 2022). Furthermore, RUNX3 has been shown to promote TRAIL-induced CRC apoptosis (Kim et al., 2019). CREB3L1 is a hypoxia-inducible cytokine (Mellor et al., 2013). Studies have shown that α-SMA-positive CAFs were activated through CREB3L1-mediated IL-1α production, the presence of CAF inhibits thyroid cancer growth and metastasis after CREB3L1 knockdown (Pan et al., 2022).

Cellular communication analysis and hub genes in CAF-related modules suggest the importance of MAST cells in the immune microenvironment remodeled by CAF (Johansson et al., 2010; Derakhshani et al., 2019). Mast cells can generate trypsin, TNF, IL-1, IL-6, and other factors to boost anti-tumor inflammatory responses, stimulate tumor cell apoptosis, and suppress cancer cell invasion (Ribatti and Crivellato, 2011). In prostate cancer, estrogen-induced CAF-derived CXCL12 binds to CXCR4 and enhances mast cell proliferation, migration, and inflammatory cytokine secretion, thus exhibiting oncogenic effects (Ellem et al., 2014). CAF plays a role in immunosuppression through various mechanisms, including collaborating with mast cells to promote the early malignant transformation of benign epithelial cells, and blocking DC maturation and antigen presentation (Cheng et al., 2016; Pereira et al., 2019).

To identify prognostic genes associated with CAFs and improve the clinical utility of the model, we utilized LASSO Cox regression and multivariate Cox regression analyses to identify key CAF-related genes with independent prognostic significance. The resulting risk score prognostic model for sexual symptoms was constructed based on 13 CAF-related genes that exhibited independent prognosis. Then, the model is validated in different GEO cohorts. ROC curve suggested that risk scores derived from genetic signatures were more effective in predicting overall survival at 1-, 3-, and 5-year survival. After performing functional analysis, we observed that several cancer-related pathways and activated cellular crosstalk pathways were enriched in samples with high CAF score. We also investigated the expression levels of immunosuppressive gene markers and found an association between CAF score and immune checkpoint molecules (CXCL9, CTLA4, CD274, TNF, TBX2). Finally, we analyzed chemotherapeutic drug resistance and sensitivity data to predict potential correlation of CAF score and therapeutic effects of chemotherapeutic drugs. These results suggest that the CAF signature is a potential clinical model for the determination of whether a CRC patient are more likely to respond to ICIs or chemotherapeutics.

Moreover, our study identified CD274, HAVCR2, and TBX2 as potential targets for immunotherapy of CRC liver metastasis, as they were found to be increased in samples with high CAF scores. Previous study has reported blocking these immune checkpoints may represent a promising strategy for HCC treatment (Lian et al., 2020). Our results suggest that patients with high CAF scores may have higher sensitivity to some small-molecule drugs. For instance, in a recent clinical trial, the addition of vemurafenib improved the progression-free survival in patients with BRAF-mutant metastatic colorectal cancer treated with irinotecan and cetuximab (Kopetz et al., 2021). While our model showed good predictive performance for the sensitivity of colorectal cancer to cisplatin, it may not be as effective in predicting sensitivity to classical chemotherapeutic agents like oxaliplatin, fluorouracil, and irinotecan. Nonetheless, our findings can guide the selection of chemotherapy drugs for some colorectal cancer patients. In summary, our risk score model provides better prediction of the sensitivity of colorectal cancer patients to immunotherapy and has potential as a reference for selecting appropriate immunotherapy regimens for these patients.

However, there are limitations to our study. First, the data used in this study were obtained from online databases like TCGA and GEO, and further validation study with a larger sample size is required. Second, the findings of this study need to be prospectively validated in a cohort of colorectal cancer liver metastasis patients who receive immunotherapy.

In conclusion, our study indicates that metabolically active CAFs have a stronger communication and interaction with immune and tumor cells compared to metabolically suppressed CAFs. Moreover, hypoCAF score has better prognostic efficacy than hyperCAF score in terms of overall survival and recurrence-free survival of patients with metastatic colorectal cancer. We have developed a metabolic-CAF score model based on hypoCAF score and verified its ability to predict the prognosis of patients with metastatic colorectal cancer. The CAF score can predict the sensitivity of colorectal cancer liver metastasis chemotherapy drugs and is correlated to the prediction of immunotherapy outcomes. Our study provides new ideas and research methods for understanding the metabolic characteristics of CAFs and their role in patients with metastatic colorectal cancer. This study improves the treatment of colorectal cancer metastasis, and further exploration of the mechanism of CAFs can provide a theoretical basis and potential drug targets for CRC patients with metastasis.

Data availability statement

Publicly available datasets were analyzed in this study. This data can be found at the Gene Expression Omnibus (GEO) database (https://www.ncbi.nlm.nih.gov/geo/) - Accession number: GSE178318.

Ethics statement

The studies involving humans were approved by Ethics Committee of Sir Run Run Shaw Hospital (SRRSH) Affiliated to the Zhejiang University School of Medicine. The studies were conducted in accordance with the local legislation and institutional requirements. The participants provided their written informed consent to participate in this study.

Author contributions

Conception and design JZ, YG, and CW; financial support JZ; collection and assembly of data all authors; data analysis and interpretation YG, and CW; manuscript writing YG, SY, and CW, manuscript supervision JZ; All authors contributed to the article and approved the submitted version.

Funding

This work was supported by the National Natural Science Foundation of China (No. 81972012), and Health Bureau Foundation of Zhejiang Province (No. 2022RC185).

Conflict of interest

The authors declare that the research was conducted in the absence of any commercial or financial relationships that could be construed as a potential conflict of interest.

Publisher's note

All claims expressed in this article are solely those of the authors and do not necessarily represent those of their affiliated organizations, or those of the publisher, the editors and the reviewers. Any product that may be evaluated in this article, or claim that may be made by its manufacturer, is not guaranteed or endorsed by the publisher.

Supplementary material

The Supplementary Material for this article can be found online at: https://www.frontiersin.org/articles/10.3389/fphar.2023.1212420/full#supplementary-material

References

Augsten, M., Sjöberg, E., Frings, O., Vorrink, S. U., Frijhoff, J., Olsson, E., et al. (2014). Cancer-associated fibroblasts expressing CXCL14 rely upon NOS1-derived nitric oxide signaling for their tumor-supporting properties. *Cancer Res.* 74 (11), 2999–3010. doi:10.1158/0008-5472.CAN-13-2740

Banales, J. M., Marin, J. J. G., Lamarca, A., Rodrigues, P. M., Khan, S. A., Roberts, L. R., et al. (2020). Cholangiocarcinoma 2020: the next horizon in mechanisms and management. *Nat. Rev. Gastroenterology Hepatology* 17 (9), 557–588. doi:10.1038/s41575-020-0310-z

Bartoschek, M., Oskolkov, N., Bocci, M., Lovrot, J., Larsson, C., Sommarin, M., et al. (2018). Spatially and functionally distinct subclasses of breast cancer-associated fibroblasts revealed by single cell RNA sequencing. *Nat. Commun.* 9, 5150. doi:10.1038/s41467-018-07582-3

Che, L.-H., Liu, J.-W., Huo, J.-P., Luo, R., Xu, R.-M., He, C., et al. (2021). A single-cell atlas of liver metastases of colorectal cancer reveals reprogramming of the tumor microenvironment in response to preoperative chemotherapy. *Cell Discov.* 7 (1), 80. doi:10.1038/s41421-021-00312-y

Cheng, J. T., Deng, Y. N., Yi, H. M., Wang, G. Y., Fu, B. S., Chen, W. J., et al. (2016). Hepatic carcinoma-associated fibroblasts induce Ido-producing regulatory dendritic cells through IL-6-mediated STAT3 activation. *Oncogenesis* 5 (2), e198. doi:10.1038/oncsis.2016.7

Colaprico, A., Silva, T. C., Olsen, C., Garofano, L., Cava, C., Garolini, D., et al. (2016). TCGAbiolinks: an R/bioconductor package for integrative analysis of TCGA data. *Nucleic Acids Res.* 44 (8), e71. doi:10.1093/nar/gkv1507

Costa, A., Kieffer, Y., Scholer-Dahirel, A., Pelon, F., Bourachot, B., Cardon, M., et al. (2018). Fibroblast heterogeneity and immunosuppressive environment in human breast cancer. *Cancer Cell* 33 (3), 463–479. doi:10.1016/j.ccell.2018.01.011

Derakhshani, A., Vahidian, F., Alihasanzadeh, M., Mokhtarzadeh, A., Lotfi Nezhad, P., and Baradaran, B. (2019). Mast cells: a double-edged sword in cancer. *Immunol. Lett.* 209, 28–35. doi:10.1016/j.imlet.2019.03.011

Eckert, M. A., Coscia, F., Chryplewicz, A., Chang, J. W., Hernandez, K. M., Pan, S., et al. (2019). Proteomics reveals NNMT as a master metabolic regulator of cancer-associated fibroblasts. *Nature* 569 (7758), 723–728. doi:10.1038/s41586-019-1173-8

Efremova, M., Vento-Tormo, M., Teichmann, S. A., and Vento-Tormo, R. (2020). CellPhoneDB: inferring cell-cell communication from combined expression of multi-subunit ligand-receptor complexes. *Nat. Protoc.* 15 (4), 1484–1506. doi:10.1038/s41596-020-0292-x

Ellem, S. J., Taylor, R. A., Furic, L., Larsson, O., Frydenberg, M., Pook, D., et al. (2014). A pro-tumourigenic loop at the human prostate tumour interface orchestrated by oestrogen, CXCL12 and mast cell recruitment. *J. Pathology* 234 (1), 86–98. doi:10.1002/path.4386

Faubert, B., Solmonson, A., and DeBerardinis, R. J. (2020). Metabolic reprogramming and cancer progression. *Science* 368 (6487), eaaw5473–+. doi:10.1126/science.aaw5473

Friedman, G., Levi-Galibov, O., David, E., Bornstein, C., Giladi, A., Dadiani, M., et al. (2020). Cancer-associated fibroblast compositions change with breast cancer progression linking the ratio of S100A4(+) and PDPN+ CAFs to clinical outcome. *Nat. Cancer* 1(7), 692–708. doi:10.1038/s43018-020-0082-y

Galbo, P. M., Zang, X., and Zheng, D. (2021). Molecular features of cancer-associated fibroblast subtypes and their implication on cancer pathogenesis, prognosis, and immunotherapy resistance. *Clin. Cancer Res. Official J. Am. Assoc. Cancer Res.* 27 (9), 2636–2647. doi:10.1158/1078-0432.CCR-20-4226

Hao, Y., Hao, S., Andersen-Nissen, E., Mauck, W. M., Zheng, S., Butler, A., et al. (2021). Integrated analysis of multimodal single-cell data. *Cell* 184 (13), 3573–3587.e29. doi:10.1016/j.cell.2021.04.048

Hu, H., Wang, K., Huang, M., Kang, L., Wang, W., Wang, H., et al. (2021). ModifiedFOLFOXIRIWith or without cetuximab as conversion therapy in patients withRAS/BRAFWild-type unresectable liver metastases colorectal cancer: theFOCULMMulticenter PhaseIITrial. *Oncologist* 26 (1), E90–E98. doi:10.1634/theoncologist.2020-0563

Ishii, G., Ochiai, A., and Neri, S. (2016). Phenotypic and functional heterogeneity of cancer-associated fibroblast within the tumor microenvironment. *Adv. Drug Deliv. Rev.* 99, 186–196. doi:10.1016/j.addr.2015.07.007

Jiang, P., Gu, S., Pan, D., Fu, J., Sahu, A., Hu, X., et al. (2018). Signatures of T cell dysfunction and exclusion predict cancer immunotherapy response. *Nat. Med.* 24 (10), 1550–1558. doi:10.1038/s41591-018-0136-1

Jiang, Y.-Q., Wang, Z.-X., Zhong, M., Shen, L.-J., Han, X., Zou, X., et al. (2021). Investigating mechanisms of response or resistance to immune checkpoint inhibitors by analyzing cell-cell communications in tumors before and after programmed cell death-1 (PD-1) targeted therapy: an integrative analysis using single-cell RNA and bulk-RNA sequencing data. *Oncoimmunology* 10 (1), 1908010. doi:10.1080/2162402X.2021.1908010

Jin, S., Guerrero-Juarez, C. F., Zhang, L., Chang, I., Ramos, R., Kuan, C.-H., et al. (2021). Inference and analysis of cell-cell communication using CellChat. *Nat. Commun.* 12 (1), 1088. doi:10.1038/s41467-021-21246-9

Johansson, A., Rudolfsson, S., Hammarsten, P., Halin, S., Pietras, K., Jones, J., et al. (2010). Mast cells are novel independent prognostic markers in prostate cancer and represent a target for therapy. *Am. J. Pathology* 177 (2), 1031–1041. doi:10.2353/ajpath.2010.100070

Kim, B. R., Na, Y. J., Kim, J. L., Jeong, Y. A., Park, S. H., Jo, M. J., et al. (2020). RUNX3 suppresses metastasis and stemness by inhibiting Hedgehog signaling in colorectal cancer. *Cell Death Differ.* 27 (2), 676–694. doi:10.1038/s41418-019-0379-5

Kim, B. R., Park, S. H., Jeong, Y. A., Na, Y. J., Kim, J. L., Jo, M. J., et al. (2019). RUNX3 enhances TRAIL-induced apoptosis by upregulating DR5 in colorectal cancer. *Oncogene* 38 (20), 3903–3918. doi:10.1038/s41388-019-0693-x

Lee, H.-O., Hong, Y., Etlioglu, H. E., Cho, Y. B., Pomelle, V., Van den Bosch, B., et al. (2020). Lineage-dependent gene expression programs influence the immune landscape of colorectal cancer. *Nat. Genet.* 52(6), 594–603. doi:10.1038/s41588-020-0636-z

Li, X., Sun, Z., Peng, G., Xiao, Y., Guo, J., Wu, B., et al. (2022). Single-cell RNA sequencing reveals a pro-invasive cancer-associated fibroblast subgroup associated with poor clinical outcomes in patients with gastric cancer. *Theranostics* 12 (2), 620–638. doi:10.7150/thno.60540

Maeser, D., Gruener, R. F., and Huang, R. S. (2021). oncoPredict: an r package for predicting *in vivo* or cancer patient drug response and biomarkers from cell line screening data. *Briefings Bioinforma.* 22 (6), bbab260. doi:10.1093/bib/bbab260

Mayakonda, A., Lin, D.-C., Assenov, Y., Plass, C., and Koeffler, H. P. (2018). Maftools: efficient and comprehensive analysis of somatic variants in cancer. *Genome Res.* 28 (11), 1747–1756. doi:10.1101/gr.239244.118

Mellor, P., Deibert, L., Calvert, B., Bonham, K., Carlsen, S. A., and Anderson, D. H. (2013). CREB3L1 is a metastasis suppressor that represses expression of genes regulating metastasis, invasion, and angiogenesis. *Mol. Cell. Biol.* 33 (24), 4985–4995. doi:10.1128/MCB.00959-13

Pan, X., Zhou, J., Xiao, Q., Fujiwara, K., Zhang, M., Mo, G., et al. (2021). Cancer-associated fibroblast heterogeneity is associated with organ-specific metastasis in pancreatic ductal adenocarcinoma. *J. Hematol. Oncol.* 14 (1), 184. doi:10.1186/s13045-021-01203-1

Pan, Z., Xu, T., Bao, L., Hu, X., Jin, T., Chen, J., et al. (2022). CREB3L1 promotes tumor growth and metastasis of anaplastic thyroid carcinoma by remodeling the tumor microenvironment. *Mol. Cancer* 21 (1), 190. doi:10.1186/s12943-022-01658-x

Pereira, B. A., Lister, N. L., Hashimoto, K., Teng, L., Flandes-Iparraguirre, M., Eder, A., et al. (2019). Tissue engineered human prostate microtissues reveal key role of mast cell-derived tryptase in potentiating cancer-associated fibroblast (CAF)-induced morphometric transition *in vitro*. *Biomaterials* 197, 72–85. doi:10.1016/j.biomaterials.2018.12.030

Ribatti, D., and Crivellato, E. (2011). Mast cells, angiogenesis and cancer. *Adv. Exp. Med. Biol.* 716, 270–288. doi:10.1007/978-1-4419-9533-9_14

Sahai, E., Astsaturov, I., Cukierman, E., DeNardo, D. G., Egeblad, M., Evans, R. M., et al. (2020). A framework for advancing our understanding of cancer-associated fibroblasts. *Nat. Rev. Cancer* 20 (3), 174–186. doi:10.1038/s41568-019-0238-1

Sanchez-Vega, F., Mina, M., Armenia, J., Chatila, W. K., Luna, A., La, K. C., et al. (2018). Oncogenic signaling pathways in the cancer Genome atlas. *Cell* 173 (2), 321–337.e10. doi:10.1016/j.cell.2018.03.035

Wang, Y., Liang, Y., Xu, H., Zhang, X., Mao, T., Cui, J., et al. (2021). Single-cell analysis of pancreatic ductal adenocarcinoma identifies a novel fibroblast subtype associated with poor prognosis but better immunotherapy response. *Cell Discov.* 7 (1), 36. doi:10.1038/s41421-021-00271-4

Wu, Y., Yang, S., Ma, J., Chen, Z., Song, G., Rao, D., et al. (2022). Spatiotemporal immune landscape of colorectal cancer liver metastasis at single-cell level. *Cancer Discov.* 12 (1), 134–153. doi:10.1158/2159-8290.CD-21-0316

Xing, X., Yang, F., Huang, Q., Guo, H., Li, J., Qiu, M., et al. (2021). Decoding the multicellular ecosystem of lung adenocarcinoma manifested as pulmonary subsolid nodules by single-cell RNA sequencing. *Sci. Adv.* 7 (5), eabd9738. doi:10.1126/sciadv.abd9738

Yang, W., Soares, J., Greninger, P., Edelman, E. J., Lightfoot, H., Forbes, S., et al. (2013). Genomics of drug sensitivity in cancer (GDSC): a resource for therapeutic biomarker discovery in cancer cells. *Nucleic Acids Res.* 41 (Database issue), D955–D961. doi:10.1093/nar/gks1111

Yoshihara, K., Shahmoradgoli, M., Martínez, E., Vegesna, R., Kim, H., Torres-Garcia, W., et al. (2013). Inferring tumour purity and stromal and immune cell admixture from expression data. *Nat. Commun.* 4, 2612. doi:10.1038/ncomms3612

Zeng, J., Yang, X., Cheng, L., Liu, R., Lei, Y., Dong, D., et al. (2013). Chemokine CXCL14 is associated with prognosis in patients with colorectal carcinoma after curative resection. *J. Transl. Med.* 11, 6. doi:10.1186/1479-5876-11-6

Zhang, F., Su, T., and Xiao, M. (2022). RUNX3-regulated circRNA METTL3 inhibits colorectal cancer proliferation and metastasis via miR-107/PER3 axis. *Cell Death Dis.* 13 (6), 550. doi:10.1038/s41419-022-04750-8

Zhang, K.-L., Zhu, W.-W., Wang, S.-H., Gao, C., Pan, J.-J., Du, Z.-G., et al. (2021). Organ-specific cholesterol metabolic aberration fuels liver metastasis of colorectal cancer. *Theranostics* 11 (13), 6560–6572. doi:10.7150/thno.55609

Zhang, Y., Wang, S., Lai, Q., Fang, Y., Wu, C., Liu, Y., et al. (2020). Cancer-associated fibroblasts-derived exosomal miR-17-5p promotes colorectal cancer aggressive phenotype by initiating a RUNX3/MYC/TGF-β1 positive feedback loop. *Cancer Lett.* 491, 22–35. doi:10.1016/j.canlet.2020.07.023

Zhao, L., Ji, G., Le, X., Wang, C., Xu, L., Feng, M., et al. (2017). Long noncoding RNA LINC00092 acts in cancer-associated fibroblasts to drive glycolysis and progression of ovarian cancer. *Cancer Res.* 77 (6), 1369–1382. doi:10.1158/0008-5472.CAN-16-1615

Zhu, Y., Li, X., Wang, L., Hong, X., and Yang, J. (2022). Metabolic reprogramming and crosstalk of cancer-related fibroblasts and immune cells in the tumor microenvironment. *Front. Endocrinol.* 13, 988295. doi:10.3389/fendo.2022.988295

frontiers | Frontiers in Oncology

TYPE Original Research
PUBLISHED 05 September 2023
DOI 10.3389/fonc.2023.1222098

OPEN ACCESS

EDITED BY
Lin Qi,
Central South University, China

REVIEWED BY
Yutao Wang,
Chinese Academy of Medical Sciences and Peking Union Medical College, China
Jianbin Bi,
China Medical University, China

*CORRESPONDENCE
Qitian Mu
muqitian@163.com
Lixia Sheng
fyyshenglixia@nbu.edu.cn
Guifang Ouyang
fyyouyangguifang@nbu.edu.cn

†These authors have contributed equally to this work

RECEIVED 13 May 2023
ACCEPTED 27 July 2023
PUBLISHED 05 September 2023

CITATION
Li T, Lin T, Zhu J, Zhou M, Fan S, Zhou H, Mu Q, Sheng L and Ouyang G (2023) Prognostic and therapeutic implications of iron-related cell death pathways in acute myeloid leukemia. *Front. Oncol.* 13:1222098. doi: 10.3389/fonc.2023.1222098

Prognostic and therapeutic implications of iron-related cell death pathways in acute myeloid leukemia

Tongyu Li[1,2†], Tongtong Lin[3†], Jiahao Zhu[4†], Miao Zhou[1,2], Shufang Fan[1], Hao Zhou[2,5], Qitian Mu[2,5*], Lixia Sheng[1,2*] and Guifang Ouyang[1,2*]

[1]Department of Hematology, The First Affiliated Hospital of Ningbo University, Ningbo, Zhejiang, China, [2]Ningbo Clinical Research Center for Hematologic Malignancies, The First Affiliated Hospital of Ningbo University, Ningbo, Zhejiang, China, [3]Department of Pharmacy, Tsinghua University, Beijing, China, [4]Cixi Biomedical Research Institute, Wenzhou Medical University, Ningbo, Zhejiang, China, [5]Stem Cell Transplantation Laboratory, The First Affiliated Hospital of Ningbo University, Ningbo, Zhejiang, China

Acute myeloid leukemia (AML) is a blood cancer that is diverse in terms of its molecular abnormalities and clinical outcomes. Iron homeostasis and cell death pathways play crucial roles in cancer pathogenesis, including AML. The objective of this study was to examine the clinical significance of genes involved in iron-related cell death and apoptotic pathways in AML, with the intention of providing insights that could have prognostic implications and facilitate the development of targeted therapeutic interventions. Gene expression profiles, clinical information, and molecular alterations were integrated from multiple datasets, including TCGA-LAML and GSE71014. Our analysis identified specific molecular subtypes of acute myeloid leukemia (AML) displaying varying outcomes, patterns of immune cell infiltration, and profiles of drug sensitivity for targeted therapies based on the expression of genes involved in iron-related apoptotic and cell death pathways. We further developed a risk model based on four genes, which demonstrated promising prognostic value in both the training and validation cohorts, indicating the potential of this model for clinical decision-making and risk stratification in AML. Subsequently, Western blot analysis showed that the expression levels of C-Myc and CyclinD1 were significantly reduced after CD4 expression levels were knocked down. The findings underscore the potential of iron-related cell death pathways as prognostic biomarkers and therapeutic targets in AML, paving the way for further research aimed at understanding the molecular mechanisms underlying the correlation between iron balance, apoptosis regulation, and immune modulation in the bone marrow microenvironment.

KEYWORDS

acute myeloid leukemia, iron-related cell death, apoptosis, prognostic biomarkers, targeted therapy

1 Introduction

Acute myeloid leukemia (AML) is a diverse malignancy of the blood that disrupts normal hemopoietic processes and promotes the excessive proliferation of myeloid cells within the bone marrow (1, 2). About 80% of all cases of AML are seen in aged group (3–5). The overall 5-year mortality survival proportion for people with AML is about 24% despite substantial breakthroughs in our knowledge of AML etiology and the introduction of targeted medicines. Because of the wide range of symptoms and reactions to therapy that patients with AML may experience, it is imperative that innovative prognostic biomarkers and therapeutic techniques be developed to better serve this patient population.

Numerous biological functions rely on iron, including DNA synthesis, energy metabolism, and respiration (6, 7). However, increased iron levels may provoke oxidative stress and cell damage by aiding in the creation of reactive oxygen species (ROS) (8). Iron balance, which is the careful regulation of iron availability and utilization in cells, is precisely controlled, and dysregulation of this balance has been associated with the initiation and advancement of various cancers, such as AML (9, 10). Investigation is underway into the viability of ferroptosis and other mechanisms of iron-related cell death as promising therapeutic avenues for cancer treatment (11, 12). The increase of lipid peroxides distinguishes ferroptosis, which is triggered by iron overload, from other forms of cell death such as apoptosis, necrosis, and autophagy (13). The therapeutic benefits of targeting ferroptosis pathways in AML remain to be fully investigated, despite encouraging findings in preclinical research for a variety of malignancies.

Cancer development, metastasis, and resistance to treatment are all tied closely to the immune microenvironment (14, 15). Cancer cells, immune cells, fibroblasts, endothelial cells, and other cell types, as well as extracellular matrix proteins and signaling chemicals, make up this complex. Relapse and medication resistance are factors in AML because the bone marrow microenvironment offers a favorable habitat for leukemia-initiating cells (16, 17). The incursion of immune cells into the bone marrow microenvironment (BME) has been deemed a vital feature affecting cancer advancement and patient prognostication (18). Programmed cell death receptor-1 (PD-1) and its natural ligand programmed cell death ligand-1 (PD-L1) are two examples of immune checkpoint molecules that have been the focus of immunotherapy in recent years, which have produced durable responses in a diverse set of malignancies (19, 20). However, immune checkpoint inhibitors have had little success in treating AML, underlining the need for a deeper insight of the intricate relationship between leukemia cells and the immune system in order to create more potent immunotherapeutic approaches.

Data from high-throughput sequencing projects and computational biology are now often employed in medical studies (21–23). In an effort to comprehend the origins of disease progression, Wang and colleagues leveraged computational biology methodologies, including WGCNA, to identify biomarkers across multiple cancers (24, 25). This investigation endeavors to explore the potential prognostic implication of iron-associated cell death and apoptotic genes in AML and scrutinize their links with the immune status of the BME. By analyzing transcriptomic data from several publicly available AML datasets, we identified differentially expressed iron-related cell death and apoptosis genes associated with patient prognosis. We subsequently utilized unsupervised clustering to separate AML patients into distinct molecular subpopulations based on expression patterns of these genes, and evaluated their connections with clinical response, immune cell infiltration, and drug susceptibility.

Moreover, we probed the plausible interplay between iron-mediated cell death pathways and immune regulation by scrutinizing the expression, methylation, amplification, and deletion patterns of immune regulation-associated genes in the unique AML subtypes. Finally, we established and validated overall clinical outcome risk signature according to the expression of vital differentially expressed genes, to forecast patient survival in AML.

As a result, our discoveries offer novel perspectives on the involvement of iron-mediated cell death pathways in the development of AML and their correlation with the immune - intricacies of the bone marrow microenvironment. Through the delineation of the molecular categories of AML patients based on gene expression related to iron-mediated cell death and apoptosis, we highlight the prognostic potential of these genes and their role in shaping the immune contexture within the BME. Furthermore, our study highlights the complex interplay between iron homeostasis, cell death regulation, and immune regulation, which may have important implications for the development of novel therapeutic strategies in AML.

2 Methods

2.1 Data collection

Three information repositories were collected for this research. Dataset 1 comprised of TCGA combined with GTEx data (malignant = 173, Normal = 70) from the UCSC Xena website (xenabrowser.net) (26). Dataset 2 included TCGA-LAML data (https://portal.gdc.cancer.gov; n=126, eliminating patients who did not survive for more than 30 days.) obtained using the TCGAbiolinks package, with clinical information sourced from TCGA-CDR- Supplemental Table S1.xlsx. Dataset 3 consisted of GSE71014 data (https://www.ncbi.nlm.nih.gov/geo/; n=104, excluding patients with survival times less than 30 days) (27).

The gene set for this study focused on iron-related death and apoptosis genes. Mutation data were downloaded using the TCGAbiolinks package, while CNV and methylation data were obtained from the UCSC Xena website. Unless otherwise specified, all analyses were conducted using the TCGA-LAML dataset, survival-related analyses were performed after excluding patients who had a survival time of fewer than 30 days.

2.2 Determination and analysis of ferroptosis and apoptosis protein-coding genes in AML

First, the limma package was used for differential analysis of AML expression data (log2 (TPM+0.01)) from TCGA combined with GTEx obtained from the UCSC Xena website. Next, the 8,542 differentially expressed genes were intersected with 660 iron death and apoptosis gene sets, resulting in 268 differentially expressed iron death or apoptosis genes. The analysis of the mutation patterns of the 268 genes was conducted using the maftools software package which provides a suite of tools for the comprehensive visualization and statistical exploration of somatic mutation data, and their CNV frequencies were determined. Ultimately, the Kaplan-Meier survival analysis was conducted to evaluate the prognostic implications of the 268 dysregulated genes associated with iron-mediated cell death or apoptosis, identifying 69 prognosis-related key genes ($p<0.05$), consisting of 11 iron death genes and 58 apoptosis genes. The was used to construct a PPI network, which was visualized using Cytoscape software (28).

2.3 Cluster analysis and pathway enrichment

Using the ConsensusClusterPlus package, the 69 prognosis-related genes identified in the TCGA-LAML dataset were subjected to consensus clustering. The optimal number of clusters was determined by analyzing cophenetic, dispersion, and silhouette data. The GSVA package was employed to calculate iron death and apoptosis scores. Differential gene expression between the two clusters and the GSVA-derived 50 hallmark pathway scores were also analyzed. Employing the limma R package, a differential analysis between the two distinct molecular clusters was conducted. The aim of this analysis was to evaluate the gene expression differences between Cluster2 (n=65) and Cluster1 (n=61), and to gain critical insight into the gene expression variations underlying the biological heterogeneity observed in AML patients. By leveraging this analysis, key genes driving the variability between clusters can be identified, paving the way for better prognostic and therapeutic outcomes for patients with AML. The clusterProfiler R package was utilized for the elucidation of KEGG and GO enrichment analysis of the differentially expressed genes, which enabled the identification of the functional pathways associated with these key genes. This analysis has enabled researchers to shed light on the potential biological significance of these genes in the pathogenesis of AML and their probable involvement in the manifestation of the observed heterogeneity within the cancer biology.

2.4 Drug correlation evaluation

The oncoPredits package was utilized to conduct drug sensitivity analysis, which allowed for the measurement of the sensitivity of different molecular subtypes to various drugs. Using the limma package, differential analysis of drug sensitivity results was performed, with the goal of identifying drugs that were differentially responsive in the distinct AML subtypes. Subsequently, the top eight drugs exhibiting the largest differences in upregulation and downregulation between the subtypes were selected for further analysis. The selection of these drugs was based on their potential therapeutic significance in the context of AML. Finally, to summarize the differences in drug response between the two clusters, boxplots were used to compare the selected drugs. This analysis provided novel insights into the potential therapeutic targets of AML subtypes, which is crucial in the development of effective personalized treatment plans.

2.5 ESTIMATE score and bone marrow microenvironment correlation analysishe

ESTIMATE algorithm was applied to calculate the immune and stromal scores for patients belonging to clusters cluster1 and cluster2. The ESTIMATE algorithm, which is based on gene expression signatures, can evaluate the degree of immune infiltration and stromal activation within malignant samples, and can be useful in deciphering the role of the bone marrow microenvironment in AML pathogenesis. Thus, utilizing the ESTIMATE scores, potential differences in the immune context of the different clusters can be assessed, enabling a more comprehensive understanding of the biological heterogeneity underlying AML. Immune checkpoint gene expression, methylation, amplification frequency, and deletion frequency were also analyzed using the IOBR package and various other methods, such as cibersort, EPIC, MCPCounter, and quantiseq.

2.6 LASSO-cox regression analysis and risk model development

A univariate Cox regression analysis was conducted on 342 differentially expressed genes (cluster 2 versus cluster 1) using both the TCGA-LAML and GSE71014 datasets. Analysis was performed to assess the prognostic value of these genes and their association with overall patient survival. Genes having a p-value<0.05 were considered significant. Utilizing this analysis, potential prognostic factors were identified, that can be integrated as part of a personalized treatment protocol for improved disease outcome in AML patients. Applying the LASSO-Cox regression analysis with a 10-fold cross-validation, we evaluated 42 key differentially expressed genes identified during the univariate Cox regression analysis to identify genes with optimal prognostic value. The LASSO-Cox regression approach is a robust method for feature selection, which allows for the identification of the most informative genes in relation to patient survival. The 10-fold cross-validation procedure works to prevent overfitting and helps to identify models that can be suitably generalizable. Consequently, by utilizing this analysis approach, our results allow for an accurate prediction of patient outcomes in AML and are pertinent in developing effective,

patient-specific treatment strategies. The risk score was calculated by multiplying the expression value of each gene with its corresponding coefficient, as shown below:

$$\text{Riskscore} = \sum_{i=1}^{n}[expression\ \ value\ \ of\ \ gene_i * \beta_i] \quad (1)$$

The variable "n" represents the number of genes included in the signature, and the variable "β" denotes the coefficient assigned to each gene obtained from LASSO regression.

2.7 Cell culture

KG-1α and OCI-AML2 cells were cultured in RPMI-1640 media supplemented with 10% fetal bovine serum (FBS) under optimal conditions of 37 degrees Celsius in a humidified 5% CO_2 atmosphere. In accordance with standard practices for cell culture, the cells were split every two to three days to ensure continuous logarithmic growth. These culture conditions offer an optimal environment and nutrient supply to support the growth and maintenance of these cell lines in a manner that is consistent with previous culture methods.

2.8 siRNA transfection

Lipofectamine 3000 (Invitrogen) was used to transfect CD4 siRNA and control siRNA into KG-1α and OCI-AML2 cells. After 6 hours of incubation with the siRNA complexes, the cells were given a fresh supply of media. The cells were collected for examination 48 hours after transfection. The siRNA sequence is as follows: Negative control: Sense: 5′-UUCUCCGAACGUGUCACGUTT-3′, Antisense: 5′-ACGUGACACGUUCGGAGAATT-3′; si-CD4: Sense: 5′- CCCUGAUCAUCAAGAAUCUTT-3′, Antisense: 5′-AGAUUCUUGAUGAUCAGGGTT-3′.

2.9 Western blotting

Total cellular proteins were extracted from transfected cells and the protein concentration was measured using a BCA Protein Assay Kit (Pierce). The extracted proteins were then separated by SDS-PAGE and transferred onto PVDF membranes. To ensure equal quantities of each target protein, membranes were probed with primary antibodies against CD4 (Cat No. 67786-1-Ig; Proteintech), C-Myc (Cat No. 67447-1-Ig; Proteintech), Cyclin D1 (Cat No. 60186-1-Ig; Proteintech), and Vinculin (Cat No. 66305-1-Ig; Proteintech). Following incubation with horseradish peroxidase-conjugated secondary antibodies, the ECL Western Blotting Detection Reagents (GE Healthcare) were used to visualize the membranes and generate chemiluminescent signals. The results of the experiment were analyzed using ImageJ (NIH) and densitometry was applied to measure the thickness of protein bands in the processed images. This rigorous analysis approach allowed for the accurate quantification and comparison of protein samples and resulted in the generation of robust, reliable data.

3 Results

3.1 Identification of differentially expressed iron-related cell death genes

Figure 1 shows the workflow of this study. AML expression data (log2 (TPM+0.01)) from the TCGA combined with GTEx dataset was obtained from the UCSC Xena website. The limma package was utilized to conduct a differential expression analysis. The obtained results were visualized by generating a volcano plot (Figure 2A), which depicts the distribution of differentially expressed genes (DEGs) between malignant (n=173) and normal (n=70) samples. Using the criteria of adj.pvalue< 0.05 & |logFC| > 1.5, the analysis identified a total of 4940 upregulated genes and 3602 downregulated genes. These genes were considered to be significantly differentially expressed, with their potential involvement in the pathogenesis of the condition making them promising targets for further investigation. Overall, the generated results provided crucial insights into the molecular mechanisms underlying the disease, paving the way for the development of more effective diagnostic and therapeutic interventions. The intersection of the 8,542 DEGs and the 660 iron-related cell death and apoptosis genes resulted in 268 differentially expressed iron-related cell death or apoptosis genes (Figure 2B).

3.2 Mutation and copy number variation analysis

Using the maftools package, the mutation status of the 268 differentially expressed iron-related cell death or apoptosis genes was analyzed, and the top 20 genes were displayed in a waterfall plot (Figure 2C). Among all samples, the TP53 gene had the highest mutation frequency (47%), followed by COL2A1 and ERBB3 (11%). Among all mutation types, missense mutation was the most common.

A bar plot shows the CNV frequency of the top 20 mutated genes (Figure 2D). Most genes had both copy number variation (CNV) gain and CNV loss. Only a few genes, such as COL2A1 and AR, existed in only one of these two conditions.

3.3 Prognostic key gene identification and network construction

A Kaplan-Meier survival analysis of the 268 differentially expressed iron-related cell death or apoptosis genes identified 69 prognostic key genes (p< 0.05), including 11 iron-related cell death genes and 58 apoptosis genes. The specific gene list can be found in Supplementary File 1. The construction of a protein-protein interaction (PPI) network was carried out through the use of data obtained from the STRING database, which provides a comprehensive resource for exploring known and predicted PPIs (Figure 2E). The obtained network was used to basic interaction analysis via a visualization method of Cytoscape software. Utilizing

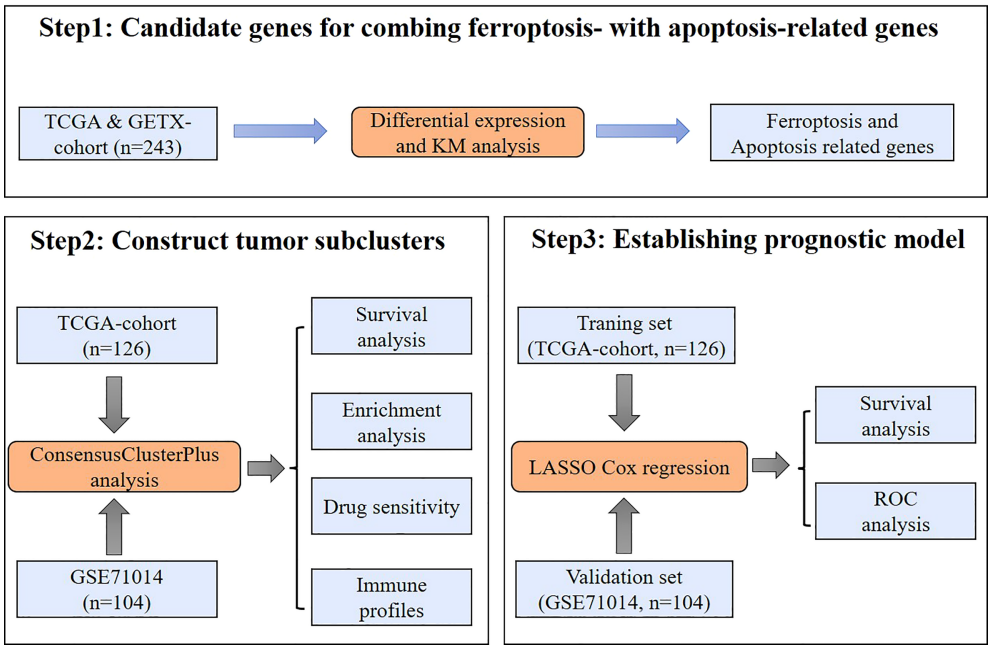

FIGURE 1
Study workflow. A schematic representation of the data collection, analysis, and validation processes used in this study.

these tools and resources, potential biomarkers and therapeutic targets can be identified, aiding in the development of innovative approaches for the treatment of various human malignancies.

3.4 Identify prognostic factors associated with different malignant subtypes

Based on the 69 prognostic key genes identified in Figure 2E, the ConsensusClusterPlus package was used to perform consensus clustering on the TCGA-LAML dataset. We used these genes to construct two different expression patterns in an attempt to compare survival outcomes between the different expression patterns. Patients were divided into two clusters (Figure 3A). The survival curve indicated that patients in cluster 1 were significantly associated with better prognosis (Figure 3B). This finding was validated in the GSE71014 dataset (Figures 3C, D). The GSVA scores reveal significant differences in iron-related cell death and apoptosis pathways between the two distinct expression patterns identified above, with these pathways having higher GSVA scores in Cluster 2 (Figure 3E). The expression levels of the 69 prognostic key genes in different expression patterns are depicted in Figure 3F, showing significant differential expression across both clusters. Finally, the GSVA algorithm was used to compare the enrichment levels of HALLMARK pathways in different expression patterns. The most significantly different pathways are visualized in a heatmap, revealing that pathways such as interferon and inflammatory response are significantly upregulated in Cluster 2 (Figure 3G).

3.5 Functional enrichment and differential expression analysis of AML clusters

A differential expression analysis between the two distinct molecular clusters (Cluster 2: n=65 and Cluster 1: n=61) was carried out by employing the limma package, a widely used tool for the visualization and analysis of differential gene expression data. Subsequently, this analysis enabled a systematic comparison of gene expression levels between the two clusters, facilitating the identification of the genes that were differentially regulated. The approach enabled a deeper understanding of the molecular basis of AML and provides insights into disease mechanisms that could contribute to the development of more efficient therapies. A volcano plot shows 328 upregulated genes and 14 downregulated genes (Figure S1A), with the specific gene list available in Supplementary File 1. In order to select differentially expressed genes (DEGs), particular selection criteria were implemented, requiring an adjusted p-value of less than 0.05 and an absolute log-fold change of greater than 1.5. Subsequently, these DEGs (a total of 342) underwent functional enrichment analysis, which was carried out using the clusterProfiler package, and the results of this analysis are presented in Figures S1B, C.

3.6 Drug efficacy evaluation

To evaluate the efficacy of drugs, the oncoPredits package, which is a powerful tool for predicting drug sensitivity, was employed. This software provides comprehensive analysis of various cancer drugs'

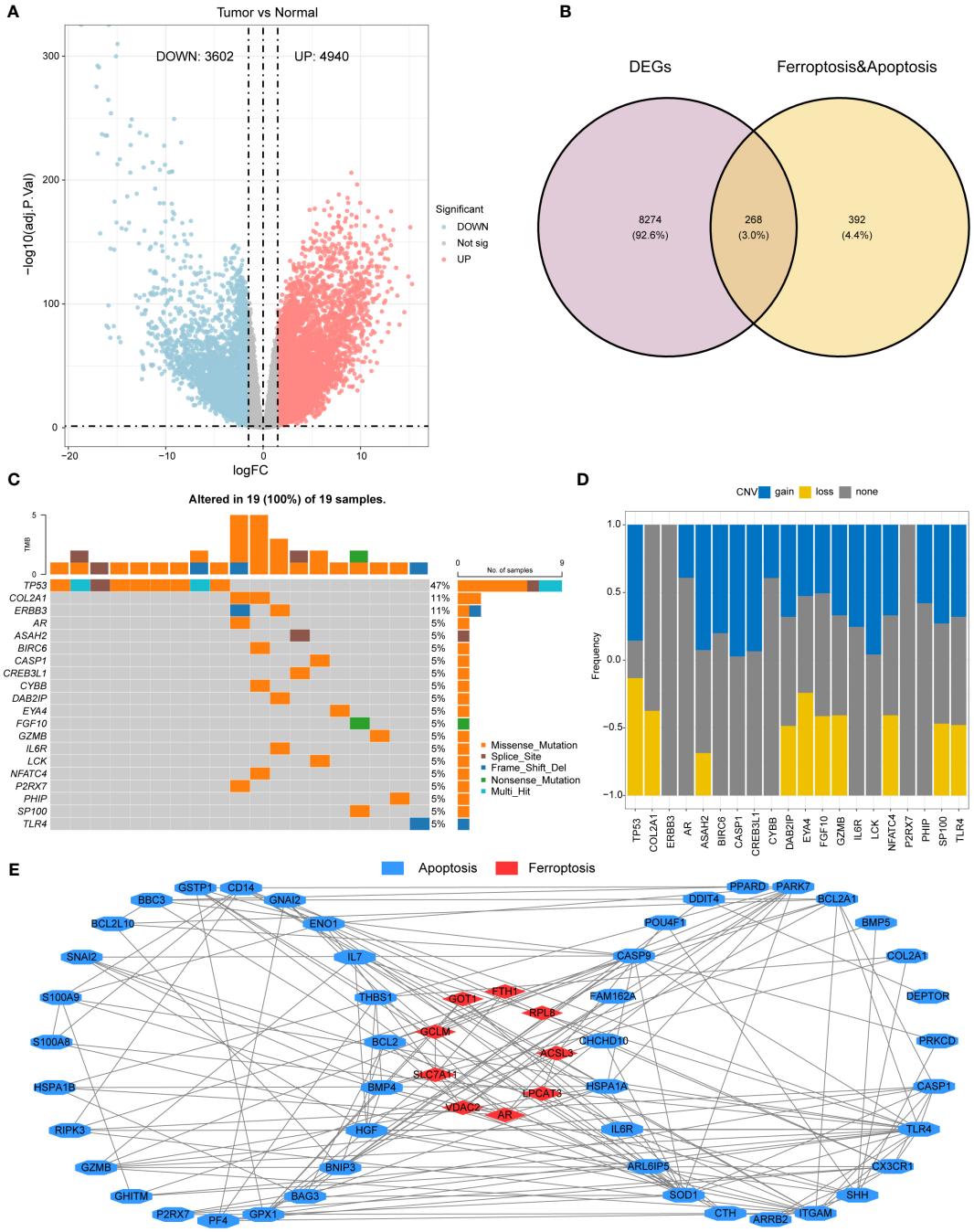

FIGURE 2
Differential gene expression and mutation analysis of iron-related cell death and apoptosis genes **(A)** Volcano plot demonstrating the differentiallyexpressed genes (DEGs) in the AML malignant samples relative to the normal control samples. **(B)** A Venn diagram providing visualization of theoverlap between DEGs and iron-related apoptosis and cellular death genes. **(C)** A waterfall plot illustrating the top 20 mutated genes out of 268DEGs related to iron-mediated apoptosis and cellular death genes. **(D)** A bar plot showing the CNV (copy number variation) frequencies of the top20 mutated genes. **(E)** A protein-protein interaction network was constructed using the STRING database, and visualized in Cytoscape, demonstrating the 69 prognostic key genes.

potential effectiveness based on individual patients' genetic profiles, enabling personalized treatment options and targeted therapeutic approaches to limit side effects. It helps address potential drug resistance and treatment inefficacy, leading to informed decisions and optimal clinical outcomes for patients. Differences in drug sensitivity between the subtypes were analyzed using the limma package, and box plots were created to compare the top 8 most sensitive drugs for each cluster. The top 8 most sensitive drugs for cluster 1 patients were KRAS (G12C) Inhibitor-12_1855, PCI-34051_1621, P22077_1933, WEHI-539_1997, PRIMA-1MET_1131, GSK1904529A_1093, PLX-4720_1036, and insitinib_1510 (Figure 4A). The top 8 most sensitive drugs for cluster 2 patients were Temozolomide_1375, 5-Fluorouracil_1073, Selumetinib_1736,

10.3389/fonc.2023.1222098

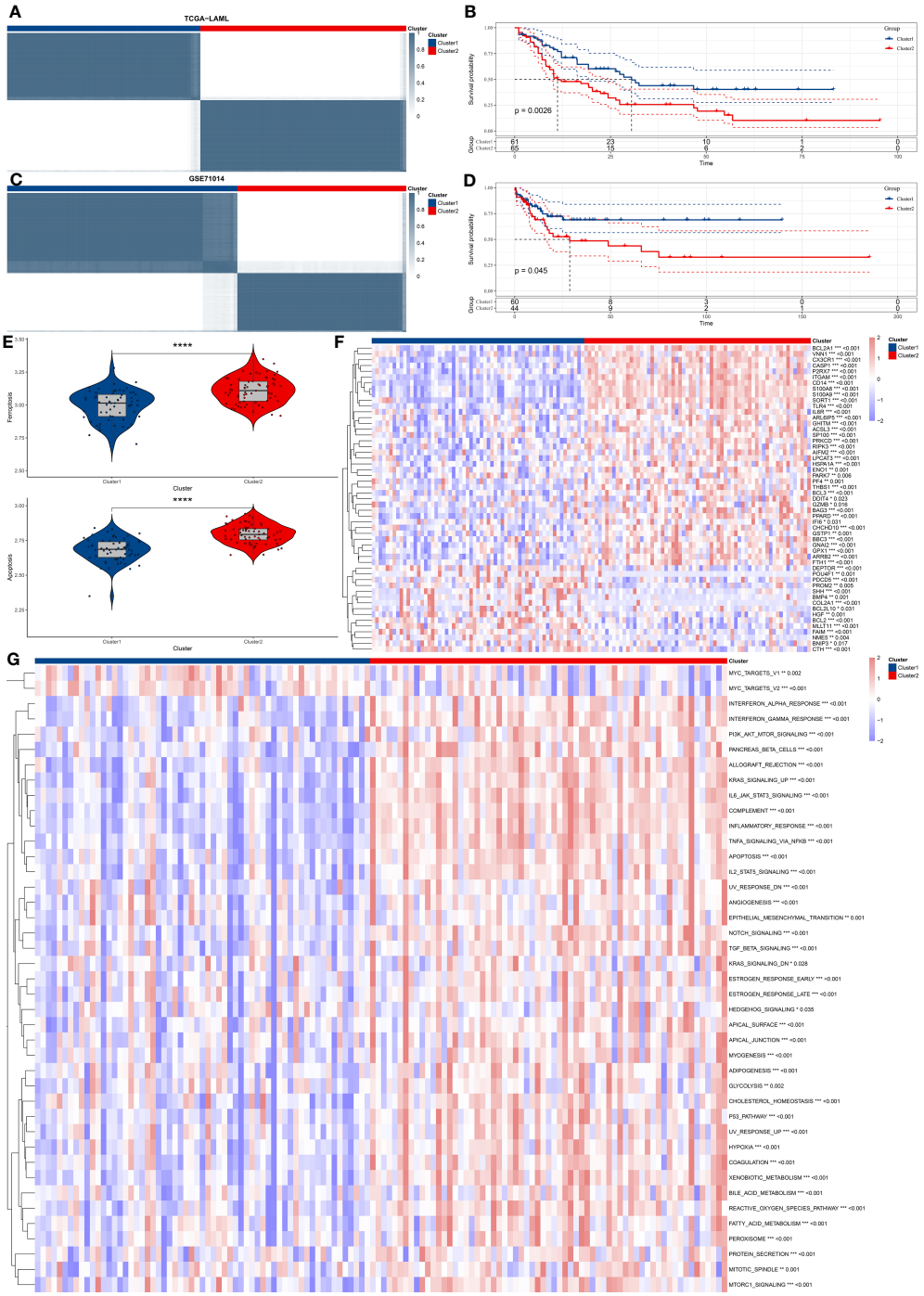

FIGURE 3
Consensus clustering and functional analysis of AML subtypes. **(A)** The figure shows consensus clustering of AML patients based on the gene expression profile of 69 prognostic key genes. **(B)** Kaplan-Meier survival analysis distinguishes two identified clusters, comparing overall survival between the two groups. **(C, D)**. Validation of clustering findings in the GSE71014 dataset. **(E)** GSVA scores show that the iron-related cellular death and apoptosis pathways significantly vary in the two discovered clusters. **(F)** The Heatmap graphically represents differential gene expression levels of 69 prognostic key genes between the two clusters. **(G)** The Heatmap shows differentially activated HALLMARK pathways between the two identified clusters. "*" represents p<0.05,"**" represents p<0.01,"***" represents p<0.001,"****" represents p<0.0001.

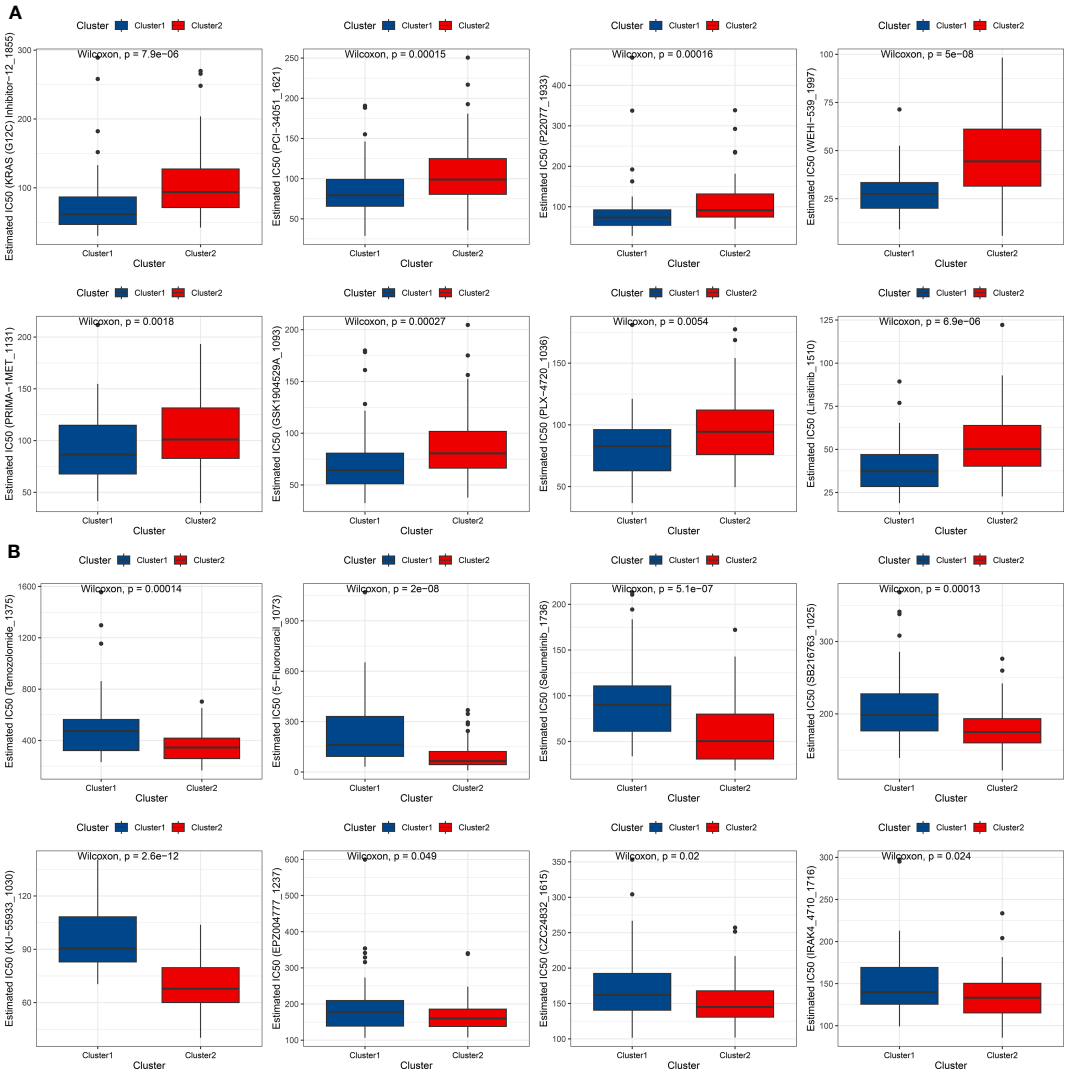

FIGURE 4
Drug sensitivity analysis of AML subtypes. **(A)** Box plot showing the top 8 most sensitive drugs for cluster 1 patients. **(B)** Box plot displaying the top 8 most sensitive drugs for cluster 2 patients.

SB216763_1025, KU-55933_1030, EPZ004777_1237, CZC24832_1615, and IRAK4_4710_1716 (Figure 4B).

3.7 Bone marrow microenvironment and immune infiltration analysis

The bone marrow microenvironment was assessed in patients corresponding to clusters 1 and 2 by utilizing the ESTIMATE algorithm via the IOBR package. The obtained results exhibited that patients in cluster 2 had a significantly higher immune score, stromal score, and ESTIMATE score than did patients in cluster 1, while the tumor purity scores were found to be lower in cluster 2 patients (Figure 5A). Moreover, the expression of the majority of immune checkpoint genes was found to be significantly upregulated in patients of cluster 2 (Figure 5B). In order to further investigate immune infiltration patterns, immune cell infiltration was evaluated, utilizing the IOBR package, and employing several methods such as cibersort, EPIC, MCPCounter, and quantiseq. Heatmaps were employed to visualize distinctive patterns of immune cell infiltration in the bone marrow microenvironment of cluster 1 and cluster 2 patients, with a focus on cell lineages that exhibited statistically significant differences (depicted in Figure 5C). This comprehensive analysis of immune infiltration and microenvironmental variations established significant differential characteristics in different expression patterns, which could provide insights into the underlying mechanisms of tumor initiation, growth, and differentiation.

3.8 Analysis of immune regulatory genes

Heatmaps were used to present the expression levels, methylation levels, amplification frequencies, and deletion frequencies of immune regulatory genes in different expression patterns (Figure 6). There are differential expression levels of

10.3389/fonc.2023.1222098

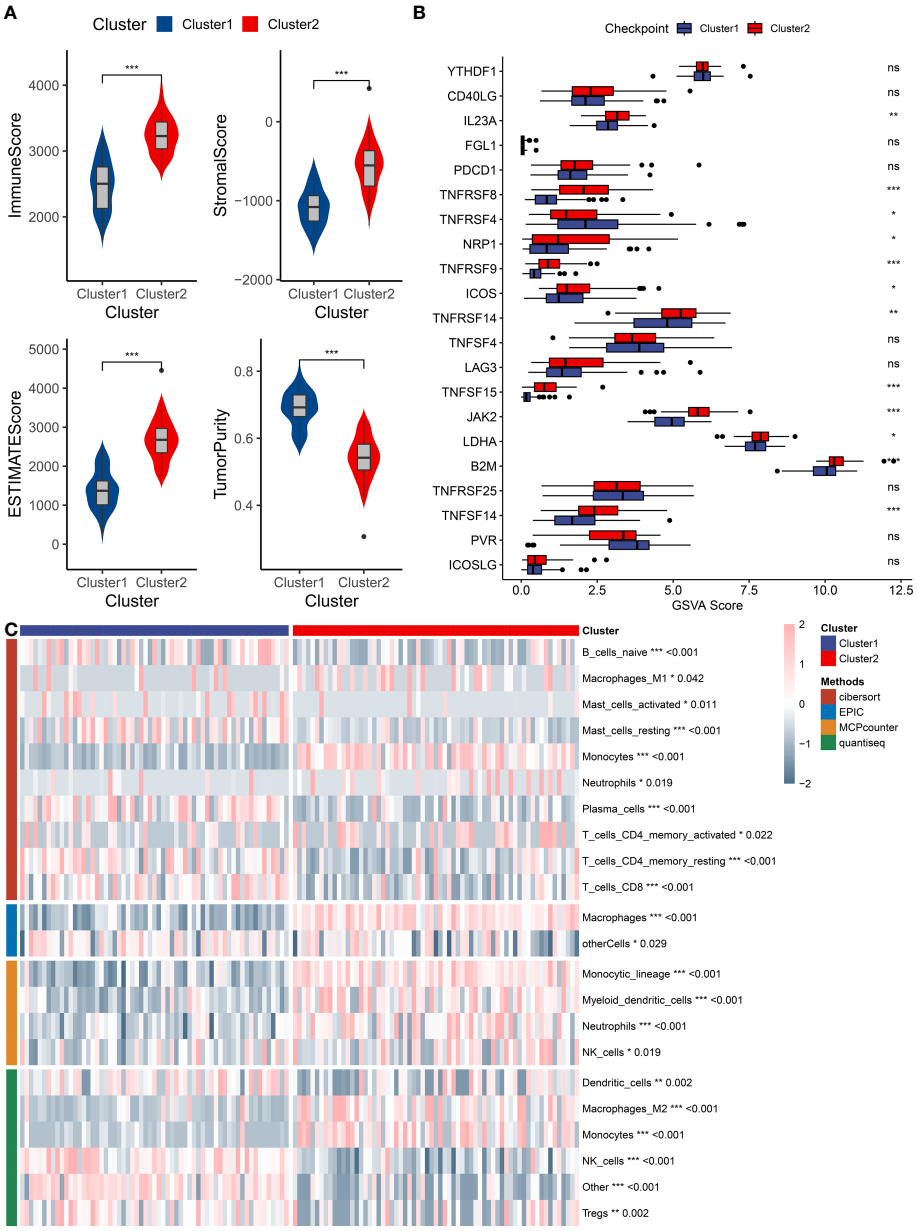

FIGURE 5
Immune infiltration analysis of AML subtypes. **(A)** A box plot compares immune infiltration scores, stromal levels, ESTIMATE scores, and tumor purity between the two identified clusters. **(B)** A box plot represents differential gene expressions of immune checkpoint genes between the two clusters. **(C)** A heatmap displays immune cell infiltration patterns in the bone marrow microenvironment of the two clusters, as analyzed by CIBERSORT, EPIC, MCPCounter, and QuantiSeq algorithms. "*" represents p<0.05,"**" represents p<0.01,"***" represents p<0.001.

antigen presentation-related genes between the two clusters. The two clusters also exhibit differences in the expression/methylation of various immune processes. Moreover, significant variations can be observed in the amplification and deletion frequencies of multiple immune processes between the two clusters. More details on this analysis can be found at https://linkinghub.elsevier.com/retrieve/pii/S1074761318301213.

3.9 Construction of a risk prediction model using differential gene expression data

Using the TCGA-LAML and GSE71014 datasets, 342 differentially expressed genes (cluster 2 vs. cluster 1) were subjected to univariate Cox regression analysis, Selecting genes with p<0.05, and intersecting the results to obtain 42 key

10.3389/fonc.2023.1222098

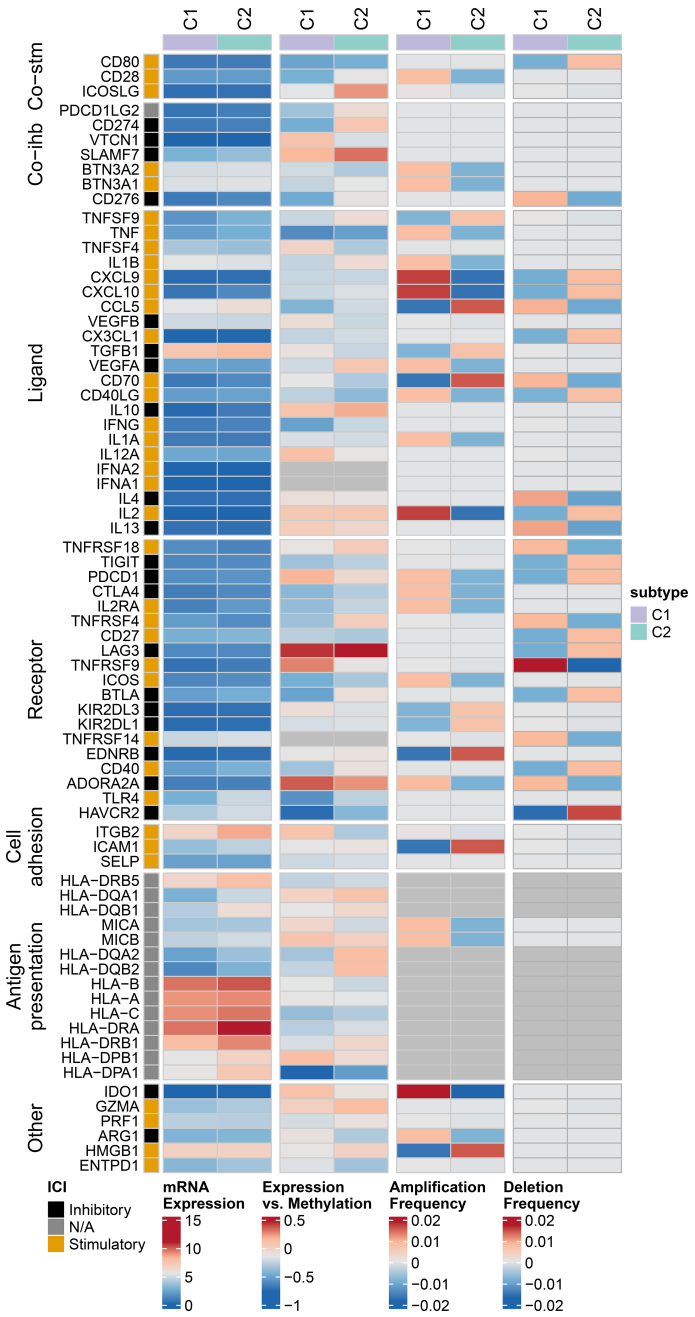

FIGURE 6
Multi-omics analysis of immune regulatory genes in AML subtypes. Heatmap showing expression levels, methylation levels, amplification frequencies, and deletion frequencies of immune regulatory genes in different groups patients.

prognostic differential genes (Supplementary File 1). In the TCGA-LAML dataset, LASSO-Cox regression and ten-fold cross-validation techniques were utilized to screen the 42 differential genes obtained from the above-mentioned results, ultimately resulting in a 4-gene risk model (Figures S2A, B). The scoring system for predicting risk was derived from the following formula: riskScore = 0.047473*VDR + 0.055492*CD4 + 0.093657*LST1 - 0.17468*SIX3.

Scatterplots and dot plots revealed that the probability of death also increased for the patients in the high-risk group (Figures 7A, B). Survival curves for the two groups demonstrated statistically significant differences (Figure 7C), and ROC curves displayed the AUC values of the risk score for predicting different year survival probability, with all values greater than 0.7 (Figures 7D-F). Similar results were obtained in the GSE71014 validation dataset (Figures 8A-F).

3.10 Effects of signature risk gene CD4 in cell cycle in KG-1α and OCI-AML2 cell lines

After constructing prognostic gene models in leukemia, we found that CD4, VDR and LST1 were the most significant prognostic risk

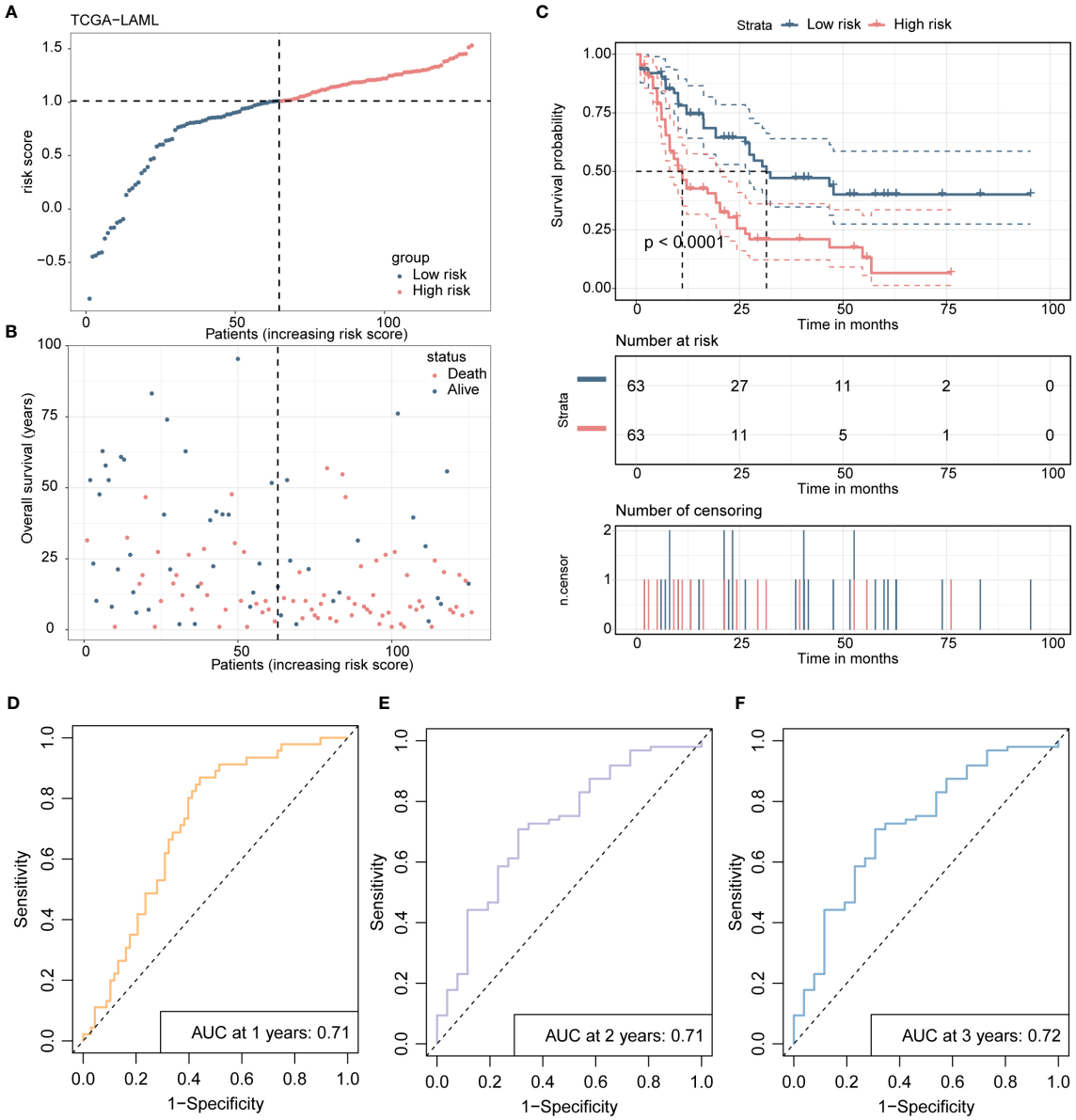

FIGURE 7
Presents the development and validation procedure of a 4-gene risk model in the TCGA-LAML training cohort, as explained below: **(A)** The distribution of risk scores and survival status in the training cohort are visualized using a dot plot. **(B)** The scatter plot showing the relationship between patient survival probability and risk scores is plotted. **(C)** Kaplan-Meier survival analysis is conducted, comparing overall survival between high- and low-risk groups. **(D-F)**. Receiver Operating Characteristic (ROC) curves indicate the prognostic performance of the risk model at 1, 2, and 3 years.

genes. After reviewing the literature and cell experiments, we found that CD4 may have a significant correlation with the cell cycle of leukemia. The results showed that the expression levels of cyclin C-Myc and Cyclin D1 were significantly decreased after CD4 knockdown in KG-1α and OCI-AML2 cell lines (Figures 9A, B). The corresponding statistical data were also shown.

4 Discussion

In this current study, we embarked on a comprehensive investigation to determine the influence of iron-related genes on the initiation, progression, and prognosis of AML. By utilizing sophisticated techniques, we identified distinct molecular subtypes that exhibited variations in immune cell infiltration patterns, prognosis, and drug sensitivity profiles - highlighting the potential of iron-related genes as prognostic biomarkers and therapeutic possibilities for AML. Our findings from this study increase our overall comprehension of the intricate interactions between iron metabolism, regulation of cell death, and immune modulation within the microenvironment.

Our results align with previous studies emphasizing the important role of iron metabolism in the initiation and progression of cancer. These include studies demonstrating the

10.3389/fonc.2023.1222098

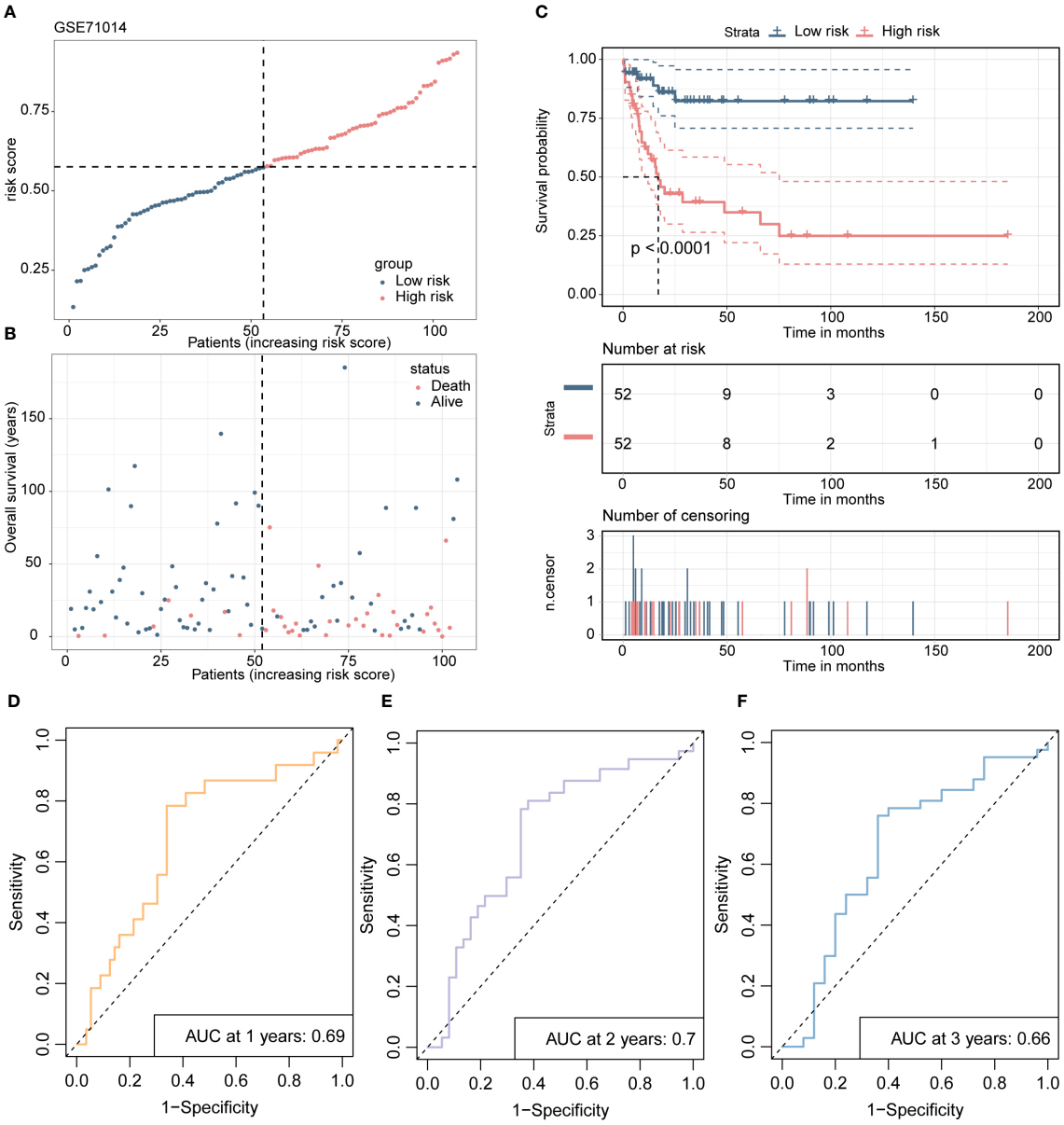

FIGURE 8
The validation process of the 4-gene risk model is presented using the GSE71014 validation cohort. **(A)** The distribution of risk scores and survival status in the validation cohort is displayed through a dot plot. **(B)** A scatter plot is presented to show the correlation between patient survival probability and risk scores. **(C)** Kaplan-Meier survival analysis is conducted to compare overall survival between high- and low-risk groups. **(D-F)**. The ROC curves demonstrate the prognostic performance of the 4-gene risk model for 1, 2, and 3 years in terms of distinguishing between high- and low-risk groups.

participation of iron metabolism in the regulation of tumor angiogenesis, cellular proliferation, and apoptosis, among other mechanisms. Cancer cell proliferation, angiogenesis, metastasis, and therapeutic resistance have all been linked to abnormal iron homeostasis (29, 30). Specifically, iron has been linked to oxidative stress, DNA damage, genomic instability, and tumor promotion, development, and survival (31, 32). ROS are produced when iron oxidizes, and they may be harmful to healthy cells. Furthermore, it is established that iron can also trigger a form of non-apoptotic cell death known as ferroptosis, which is distinguished by lipid peroxidation and the resultant rupture of cellular membranes (33, 34). Building on the conclusions of earlier investigations, we demonstrate that genes involved in iron-related apoptosis and cell death pathways exhibit potential prognostic and therapeutic significance in the context of AML. By utilizing advanced computational tools to perform an in-depth analysis of the differential gene expression patterns in patients corresponding to distinct molecular subtypes of AML, we were able to identify genes involved in iron homeostasis and associated death pathways that are significantly linked with clinical outcomes.

The transcript levels of genes implicated in iron-related cellular demise and apoptotic mechanisms allowed us to identify unique molecular subtypes that were linked with diverse outcomes, immune cell infiltration patterns, and medication sensitivity

10.3389/fonc.2023.1222098

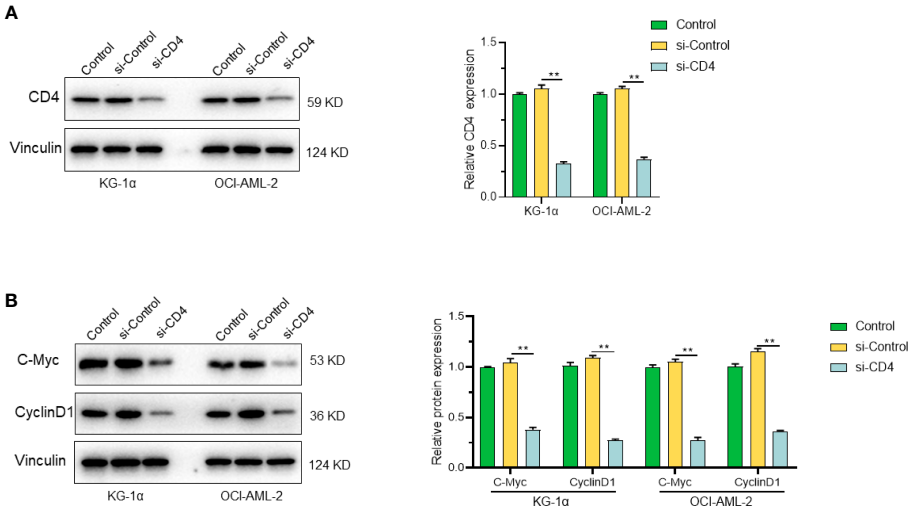

FIGURE 9
CD4 and its role in cell proliferation. **(A)** Expression of CD4 protein in KG-1α and OCI-AML2 cells after CD4 silencing. **(B)** The expression levels of C-Myc and Cyclin D1 were significantly decreased after CD4 knockdown in KG-1α and OCI-AML2 cell lines. "**" represents p<0.01.

profiles. Our findings support the notion that stratifying patients into molecular subtypes has the potential to improve diagnostic precision, allowing for more reliable forecasting of outcomes related to patient response to treatment and disease progression, ultimately culminating in better clinical decision-making (35–37). In our study, we found that patients in cluster 1, characterized by lower expression of iron-related cell death and apoptosis genes, had a better prognosis and were more sensitive to certain targeted therapies. In contrast, patients in cluster 2, with higher expression of these genes, exhibited a poorer prognosis.

One intriguing finding is the correlation between iron-related cell death pathway, which may indicate a connection between iron homeostasis, cell death control, and immunological regulation. Ferroptosis has been recently studied for its impact on tumor immune contexture and its implications for immunotherapy response (38, 39). For instance, damage-associated molecular patterns (DAMPs) released during ferroptosis have been found to stimulate antigen-presenting cells and cytotoxic T cells, therefore eliciting anticancer immune responses (40, 41). However, ferroptosis may also stimulate immunosuppressive processes that aid tumor immune evasion (42, 43), such as MDSC and the activation of immunological checkpoint markers. Together, these lines of evidence suggest that iron-related cell death and apoptosis genes may influence the immunological landscape of AML patients, and our results contribute to this expanding body of research.

In addition to the prognostic implications of iron-related cell death pathways, our study also highlights their potential therapeutic relevance in AML. Our results revealed that there are disparities in the patients' sensitivity to specific targeted therapies based on molecular subtype, such as KRAS (G12C) Inhibitor-12_1855 and PCI-34051_1621, while patients in cluster 2 were more sensitive to other drugs, including Temozolomide_1375 and 5-Fluorouracil_1073. These findings suggest that iron-related cell death and apoptosis gene expression profiles could be used to guide personalized treatment strategies for AML patients, potentially improving therapeutic outcomes.

Our study further utilized Western blotting analysis to demonstrate that CD4 silencing significantly reduced the levels of CD4 protein and cell proliferation markers in AML cells, highlighting the impact of CD4 protein in these cells. Altogether, the evidence suggests that CD4-associated pathways represent a valuable target for leukemia management, which warrants further investigation and exploration. The expression of CD4 protein in T-cell malignancies aids in diagnosing certain types of T-cell leukemia and determining leukocyte differentiation and classification. Moreover, targeting CD4 protein with monoclonal antibodies has shown promising results in T-cell-directed therapies, treating CD4-positive lymphomas, leukemias, and autoimmune diseases.

It is important to note that our study has some limitations. Despite the significant results obtained in our study, the sample size of our datasets is relatively limited, which may hinder the generalization of our findings. Future studies with more extensive cohorts and diverse demographic groups would be considered necessary to test and verify our results, further understanding the potential of iron-related cell death in AML. Finally, our study mainly focuses on gene expression profiles, and other molecular alterations, such as genetic mutations, epigenetic modifications, and post-translational modifications. Furthermore, it is plausible that additional factors impact the regulation of iron-associated cell death pathways in AML, suggesting that further investigations may uncover additional mechanisms contributing to the disease's pathogenesis and prognostic outcomes.

Despite these limitations, our study revealed iron-related cell death pathways in AML pathogenesis and highlights their potential as prognostic biomarkers and therapeutic targets. The results of our study provide a defining impetus for continued research aimed at uncovering the molecular drivers of the intricate relationship between iron homeostasis, cell death regulation, and immune regulation in the

bone marrow microenvironment. Our research has unveiled new avenues for further exploration, with attention directed towards uncovering the molecular mechanisms behind the complex interrelationships between iron homeostasis, immune cell infiltration, and cell death regulation in the bone marrow microenvironment. This, in turn, could catalyze the development of novel therapeutic approaches centered around iron-mediated cellular death pathways in AML and other hematological malignancies.

Our investigation has demonstrated the prognostic and therapeutic importance of iron-related cell death and apoptosis genes in AML, identifying distinct molecular subtypes characterized by different clinical outcomes, immune cell infiltration features, and drug sensitivity profiles. These findings underscore the intricate and multifaceted nature of iron homeostasis, cell death modulation, and immune regulation in the bone marrow microenvironment and suggest that manipulating iron-related cellular death pathways presents a potential therapeutic avenue for managing AML. Further research studies are warranted to authenticate our findings, elucidate the underlying molecular mechanisms, and appraise the clinical utility of iron-associated cell death pathways-based biomarkers and treatments in AML patients.

Data availability statement

The original contributions presented in the study are included in the article/Supplementary Material. Further inquiries can be directed to the corresponding authors.

Ethics statement

The studies involving humans were approved by The First Affiliated Hospital of Ningbo University. The studies were conducted in accordance with the local legislation and institutional requirements. Written informed consent for participation was not required from the participants or the participants' legal guardians/next of kin in accordance with the national legislation and institutional requirements. Ethical approval was not required for the studies on animals in accordance with the local legislation and institutional requirements because only commercially available established cell lines were used.

Author contributions

All the author confirmed their contribution to this research. All authors contributed to the article and approved the submitted version.

Funding

This study received finance support from Ningbo Public Welfare Research Program Project (2022S032).

Conflict of interest

The authors declare that the research was conducted in the absence of any commercial or financial relationships that could be construed as a potential conflict of interest.

Publisher's note

All claims expressed in this article are solely those of the authors and do not necessarily represent those of their affiliated organizations, or those of the publisher, the editors and the reviewers. Any product that may be evaluated in this article, or claim that may be made by its manufacturer, is not guaranteed or endorsed by the publisher.

Supplementary material

The Supplementary Material for this article can be found online at: https://www.frontiersin.org/articles/10.3389/fonc.2023.1222098/full#supplementary-material

SUPPLEMENTARY FIGURE 1
Differential gene expression analysis and functional enrichment analysis of the two AML clusters. **(A)**. A volcano plot presents the differentially expressed genes (DEGs) between patients in cluster 2 and cluster 1. **(B)**. The bar plot displays the significantly enriched KEGG pathways that were identified by clusterProfiler analysis of 342 DEGs. **(C)**. The bar plot demonstrates the significantly enriched biological process, cellular component, and molecular function GO terms, which were identified by clusterProfiler analysis of 342 DEGs.

SUPPLEMENTARY FIGURE 2
Selection of prognostic key genes and development of a 4-gene risk model using LASSO-Cox regression analysis. **(A)** LASSO coefficient profiles of the 42 intersecting prognostic key genes identified in the TCGA-LAML and GSE71014 datasets. **(B)** The selection of tuning parameter (λ) in LASSO-Cox regression analysis was conducted using a robust technique of 10-fold cross-validation.

References

1. Yuan M, Guo X, Li N, Pang H. Silicon oxide-protected nickel nanoparticles as biomass-derived catalysts for urea electro-oxidation. *J Colloid Interface Sci* (2021) 589:56–64. doi: 10.1016/j.jcis.2020.12.100

2. Thiele J, Kvasnicka HM, Orazi A, Gianelli U, Gangat N, Vannucchi AM, et al. The international consensus classification of myeloid neoplasms and acute leukemias: Myeloproliferative neoplasms. *Am J Hematol* (2023) 98(3):544–5. doi: 10.1002/ajh.26821

3. Hanley BP, Yebra-Fernandez E, Palanicawandar R, Olavarria E, Naresh KN. Lineage switch from acute myeloid leukemia to T cell/myeloid mixed phenotype acute leukemia: First report of an adult case. *Am J Hematol* (2018) 93(12):E395–e7. doi: 10.1002/ajh.25283

4. Eisfeld AK, Kohlschmidt J, Mims A, Nicolet D, Walker CJ, Blachly JS, et al. Additional gene mutations may refine the 2017 European LeukemiaNet classification in adult patients with *de novo* acute myeloid leukemia aged <60 years. *Leukemia* (2020) 34(12):3215–27. doi: 10.1038/s41375-020-0872-3

5. Zhang H, Zhang L, Li Y, Gu H, Wang X. SET-CAN fusion gene in acute leukemia and myeloid neoplasms: Report of three cases and a literature review. *Onco Targets Ther* (2020) 13:7665–81. doi: 10.2147/OTT.S258365

6. Mleczko-Sanecka K, Silvestri L. Cell-type-specific insights into iron regulatory processes. *Am J Hematol* (2021) 96(1):110–27. doi: 10.1002/ajh.26001

7. Hilo A, Shahinnia F, Druege U, Franken P, Melzer M, Rutten T, et al. A specific role of iron in promoting meristematic cell division during adventitious root formation. *J Exp Bot* (2017) 68(15):4233–47. doi: 10.1093/jxb/erx248

8. He H, Qiao Y, Zhou Q, Wang Z, Chen X, Liu D, et al. Iron overload damages the endothelial mitochondria via the ROS/ADMA/DDAHII/eNOS/NO pathway. *Oxid Med Cell Longev* (2019) 2019:2340392. doi: 10.1155/2019/2340392

9. Zhao J, Wang Y, Tao L, Chen L. Iron transporters and ferroptosis in Malignant brain tumors. *Front Oncol* (2022) 12:861834. doi: 10.3389/fonc.2022.861834

10. Weber S, Parmon A, Kurrle N, Schnütgen F, Serve H. The Clinical Significance of Iron Overload and Iron Metabolism in Myelodysplastic Syndrome and Acute Myeloid Leukemia. *Front Immunol*. 2021;11:627662. Published 2021 Feb 19. doi:10.3389/fimmu.2020.627662

11. Luo T, Wang Y, Wang J. Ferroptosis assassinates tumor. *J Nanobiotechnology* (2022) 20(1):467. doi: 10.1186/s12951-022-01663-8

12. Yang L, Zhang Y, Wang Y, Jiang P, Liu F, Feng N. Ferredoxin 1 is a cuproptosis-key gene responsible for tumor immunity and drug sensitivity: A pan-cancer analysis. *Front Pharmacol* (2022) 13:938134. doi: 10.3389/fphar.2022.938134

13. Yang X, Park SH, Chang HC, Shapiro JS, Vassilopoulos A, Sawicki KT, et al. Sirtuin 2 regulates cellular iron homeostasis via deacetylation of transcription factor NRF2. *J Clin Invest* (2017) 127(4):1505–16. doi: 10.1172/JCI88574

14. Altorki NK, Markowitz GJ, Gao D, Port JL, Saxena A, Stiles B, et al. The lung microenvironment: an important regulator of tumour growth and metastasis. *Nat Rev Cancer* (2019) 19(1):9–31. doi: 10.1038/s41568-018-0081-9

15. Yu X, Wang X, Yamazaki A, Li X. immune microenvironment-regulated nanoplatforms for the inhibition of tumor growth and metastasis in chemo-immunotherapy. *J Mater Chem B* (2022) 10(19):3637–47. doi: 10.1039/D2TB00337F

16. Xu B, Hu R, Liang Z, Chen T, Chen J, Hu Y, et al. Metabolic regulation of the immune microenvironment in leukemia. *Blood Rev* (2021) 48:100786. doi: 10.1016/j.blre.2020.100786

17. Ladikou EE, Sivaloganathan H, Pepper A, Chevassut T. Acute myeloid leukaemia in its niche: the immune microenvironment in acute myeloid leukaemia. *Curr Oncol Rep* (2020) 22(3):27.

18. van Galen P, Hovestadt V, Wadsworth Ii MH,, et al Single-Cell RNA-Seq Reveals AML Hierarchies Relevant to Disease Progression and Immunity. *Cell*. 2019;176(6):1265-1281.e24. doi:10.1016/j.cell.2019.01.031

19. Zhao T, Li C, Wu Y, Li B, Zhang B. Prognostic value of PD-L1 expression in tumor infiltrating immune cells in cancers: A meta-analysis. *PloS One* (2017) 12(4):e0176822. doi: 10.1371/journal.pone.0176822

20. Chan OS, Kowanetz M, Ng WT, Koeppen H, Chan LK, Yeung RM, et al. Characterization of PD-L1 expression and immune cell infiltration in nasopharyngeal cancer. *Oral Oncol* (2017) 67:52–60. doi: 10.1016/j.oraloncology.2017.02.002

21. Xu Z, Peng B, Liang Q, Chen X, Cai Y, Zeng S, Gao K, Wang X, Yi Q, Gong Z, Yan Y. Construction of a Ferroptosis-Related Nine-lncRNA Signature for Predicting Prognosis and Immune Response in Hepatocellular Carcinoma. *Front Immunol*. 2021 Sep 17;12:719175. doi: 10.3389/fimmu.2021.719175

22. Guo S, Li B, Chen Y, Zou D, Yang S, Zhang Y, Wu N, Sheng L, Huang H, Ouyang G, Mu Q. Hsa_circ_0012152 and Hsa_circ_0001857 Accurately Discriminate Acute Lymphoblastic Leukemia From Acute Myeloid Leukemia. *Front Oncol*. 2020 Sep 2;10:1655. doi: 10.3389/fonc.2020.01655.

23. Bottomly D, Long N, Schultz AR, Kurtz SE, Tognon CE, Johnson K, et al Integrative analysis of drug response and clinical outcome in acute myeloid leukemia. *Cancer Cell*. 2022 Aug 8;40(8):850-864.e9. doi: 10.1016/j.ccell.2022.07.002.

24. Wang Y, Chen L, Ju L, Xiao Y, Wang X. Tumor mutational burden related classifier is predictive of response to PD-L1 blockade in locally advanced and metastatic urothelial carcinoma. *Int Immunopharmacol*. 2020 Oct;87:106818. doi: 10.1016/j.intimp.2020.106818

25. Wang Y, Chen L, Wang G, Cheng S, Qian K, Liu X, Wu CL, Xiao Y, Wang X. Fifteen hub genes associated with progression and prognosis of clear cell renal cell carcinoma identified by coexpression analysis. *J Cell Physiol*. 2019 Jul;234(7):10225-10237. doi: 10.1002/jcp.27692.

26. Wang S, Xiong Y, Zhao L, Gu K, Li Y, Zhao F, et al. UCSCXenaShiny: an R/CRAN package for interactive analysis of UCSC Xena data. *Bioinformatics.B* (2022) 38(2):527–9. doi: 10.1093/bioinformatics/btab561

27. Dong X, Zhang D, Zhang J, Chen X, Zhang Y, Zhang Y, et al. Immune prognostic risk score model in acute myeloid leukemia with normal karyotype. *Oncol Lett* (2020) 20(6):380. doi: 10.3892/ol.2020.12243

28. Szklarczyk D, Morris JH, Cook H, Kuhn M, Wyder S, Simonovic M, et al. The STRING database in 2017: quality-controlled protein-protein association networks, made broadly accessible. *Nucleic Acids Res* (2017) 45(D1):D362–d8. doi: 10.1093/nar/gkw937

29. Moon D, Kim J, Yoon SP. Yeast extract inhibits the proliferation of renal cell carcinoma cells via regulation of iron metabolism. *Mol Med Rep* (2019) 20(4):3933–41. doi: 10.3892/mmr.2019.10593

30. Tasinov O, Kiselova-Kaneva Y, Ivanova D, Pasheva M, Vankova D, Ivanova D. Ferrum phosphoricum D12 treatment affects J774A.1 cell proliferation, transcription levels of iron metabolism, antioxidant defense, and inflammation-related genes. *Homeopathy* (2022) 111(2):113–20.

31. Li J, Zong Q, Liu Y, Xiao X, Zhou J, Zhao Z, et al. Self-catalyzed tumor ferroptosis based on ferrocene conjugated reactive oxygen species generation and a responsive polymer. *Chem Commun (Camb)* (2022) 58(20):3294–7. doi: 10.1039/D1CC06742G

32. Zhou H, Lu X, Du C, Zhou Z, Feng J, Liang Z, et al. Cycloacceleration of reactive oxygen species generation based on exceedingly small magnetic iron oxide nanoparticles for tumor ferroptosis therapy. *Small.B* (2022) 18(35):e2202705. doi: 10.1002/smll.202202705

33. Wei Y, Wang Z, Yang J, Xu R, Deng H, Ma S, et al. Reactive oxygen species / photothermal therapy dual-triggered biomimetic gold nanocages nanoplatform for combination cancer therapy via ferroptosis and tumor-associated macrophage repolarization mechanism. *J Colloid Interface Sci* (2022) 606(Pt 2):1950–65. doi: 10.1016/j.jcis.2021.09.160

34. Huang W, Aabed N, Shah YM. Reactive oxygen species and ferroptosis at the nexus of inflammation and colon cancer. *Antioxid Redox Signal* (2023). doi: 10.1089/ars.2023.0246

35. Yang C, Huang S, Cao F, Zheng Y. Role of ferroptosis-related genes in prognostic prediction and tumor immune microenvironment in colorectal carcinoma. *PeerJ.B* (2021) 9:e11745. doi: 10.7717/peerj.11745

36. Ding L, Long F, An D, Liu J, Zhang G. Construction and validation of molecular subtypes of coronary artery disease based on ferroptosis-related genes. *BMC Cardiovasc Disord* (2022) 22(1):283. doi: 10.1186/s12872-022-02719-1

37. Zhang W, Yao S, Huang H, Zhou H, Zhou H, Wei Q, et al. Molecular subtypes based on ferroptosis-related genes and immune microenvironment infiltration characterization in lung adenocarcinoma. *Oncoimmunology.B* (2021) 10(1):1959977.

38. Liu T, Luo H, Zhang J, Hu X, Zhang J. Molecular identification of an immunity- and Ferroptosis-related gene signature in non-small cell lung Cancer. *BMC Cancer* (2021) 21(1):783. doi: 10.1186/s12885-021-08541-w

39. Zhu J, Chen Q, Gu K, Meng Y, Ji S, Zhao Y, et al. Correlation between ferroptosis-related gene signature and immune landscape, prognosis in breast cancer. *J Immunol Res* (2022) 2022:6871518. doi: 10.1155/2022/6871518

40. Tymoszuk P, Nairz M, Brigo N, Petzer V, Heeke S, Kircher B, et al. Iron supplementation interferes with immune therapy of murine mammary carcinoma by inhibiting anti-tumor T cell function. *Front Oncol* (2020) 10:584477. doi: 10.3389/fonc.2020.584477

41. Sawant A, Schafer CC, Jin TH, Zmijewski J, Tse HM, Roth J, et al. Enhancement of antitumor immunity in lung cancer by targeting myeloid-derived suppressor cell pathways. *Cancer Res* (2013) 73(22):6609–20. doi: 10.1158/0008-5472.CAN-13-0987

42. Ko HJ, Lee JM, Kim YJ, Kim YS, Lee KA, Kang CY. Immunosuppressive myeloid-derived suppressor cells can be converted into immunogenic APCs with the help of activated NKT cells: an alternative cell-based antitumor vaccine. *J Immunol* (2009) 182(4):1818–28. doi: 10.4049/jimmunol.0802430

43. Wang Y, Jia A, Bi Y, Wang Y, Yang Q, Cao Y, et al. Targeting myeloid-derived suppressor cells in cancer immunotherapy. *Cancers (Basel)* (2020) 12(9). doi: 10.3390/cancers12092626

Frontiers in Pharmacology

Explores the interactions between chemicals and living beings

The most cited journal in its field, which advances access to pharmacological discoveries to prevent and treat human disease.

Discover the latest Research Topics

See more →

Frontiers

Avenue du Tribunal-Fédéral 34
1005 Lausanne, Switzerland
frontiersin.org

Contact us

+41 (0)21 510 17 00
frontiersin.org/about/contact